Intermolecular [3+2] Cycloadditions of Imino-isocyanates to Access β-Amino Carbonyl Compounds

Amanda L. Bongers

A thesis submitted to the Faculty of Graduate and Postdoctoral Studies
in partial fulfillment of the requirements for the
Doctor of Philosophy (Ph.D.) degree in chemistry.

Department of Chemistry and Biomolecular Sciences
Ottawa-Carleton Chemistry Institute
Faculty of Science
University of Ottawa

Abstract

In modern synthetic organic chemistry, chemists are driven to develop efficient methods for important C-C and C-N bond formation reactions. The challenge lies with establishing new uses for readily available substrates. In this regard, the synthesis of β-aminocarbonyl compounds from alkenes remains a long-standing challenge. Innovation in reaction discovery often requires finding new reagents, or rare reagents with underappreciated value in synthesis. In Chapter 1, *N*-isocyanates and other heterocumulenes are introduced as versatile amphoteric reagents. Their amphoteric properties are valuable in the discovery of new synthetic approaches, especially in cycloaddition reactions. While *C*-isocyanates are bulk industrial chemicals, the formation and reactivity of *N*-isocyanates remains underexplored.

Chapter 2 describes the development of reactivity with rare imino-isocyanates. This includes methods to access the reagent in situ with a blocking group approach, and the establishment of intermolecular cycloaddition reactivity with a variety of alkenes. This stereospecific reaction provides complex *N,N'*-cyclic azomethine imines, and enables access to β-aminocarbonyl compounds from alkenes. β-Amino amides and esters, pyrazolidinones, and pyrazolones were accessed by reductive derivatization of the aminocarbonylation products. Exploration into the limits of this reactivity gave insight into fundamental properties of imino-isocyanates. This includes the first detection of imino-isocyanates by IR spectroscopy.

A kinetic resolution of the azomethine imines obtained from this alkene aminocarbonylation reaction was then developed, which gave access to enantioenriched β-amino carbonyl compounds (Chapter 3). This was accomplished by Brønsted acid catalysed reduction, with a selectivity factor of 13-43. This was the first example of the enantioselective reduction of azomethine imines, and

represents a new activation mode for reactions of *N,N'*-cyclic azomethine imines. Using this reductive method, both enantiomers of the β-amino amide could be obtained from a racemic azomethine imine in ≥ 97% *ee*.

The discovery of new reactivity of imino-isocyanates with imines in described in Chapter 4, which allowed the synthesis of eight new azomethine imines with the triazolone core. Our initial scope studies revealed different trends with imines than with alkenes, including increased reactivity, which led to investigation of the mechanism of this reaction. In addition, this was shown to be a valuable new approach for the synthesis of triazolones from imines.

Acknowledgements

I wish to thank André for being a patient and kind supervisor, a brilliant chemist, and an exceptional mentor. I am very grateful to have joined your group five years ago. One of your best qualities is turning a negative result into an exciting discovery.

Thank you to my family for their love and support, and for encouraging my interest in science from a young age. A special thanks to my mother, Debbie, for moving my desk outside when I was a child to make homework more enjoyable. Also to my father, Rick, for never doubting me. To Paul, my partner in life, thank you for your unwavering confidence and love. I look forward to exploring the next chapter of our life together.

Dr. Sampada Chitale, thank you for your unbounding kindness and encouragement. Also, thank you for helping me focus on the big picture and teaching me about how chemistry is studied in other cultures. Thank you to Dr. Nicolas Guimond for being an inspiration and role model, and plotting with me to take over the world.

Thank you to the outstanding undergraduate students that I supervised, Patrick Moon and Philippe Lemire, for your fantastic work. Thanks to the many graduate students and post-doctoral associates I have worked and studied with over the years in the Beauchemin group, especially Christian, Tom, Keira, Colin, Kaitlyn, Jing, and Binjie. Also, thanks to the friendly community of graduate students in our department, and those who helped with experiments outside my expertise, and who joined me in the Chemistry Graduate Student Association.

Thank you to Prof. Mike Chong and Dr. Adrien Côté, who encouraged me to pursue a Ph.D. in chemistry. I also want to acknowledge NSERC for generous funding throughout my graduate studies.

Table of Contents

List of Figures

List of Schemes

List of Tables

List of Equations

Glossary of Abbreviations

[M] – generic metal

[O] – generic oxidant

[H] – generic reductant

$[\alpha]_D^{20}$ – specific rotation at 20 °C and 589 nm

°C – degrees Celsius

^{1}H – proton

^{13}C – carbon-13

^{19}F – fluorine-19

A – general Lewis acid

Ac – acetyl

Ar – generic aryl

aq. – aqueous

B3LYP – Becke-3-Lee-Yang-Parr

BG – blocking group

BINOL – 1,1'-bi-2-naphthol

Bn – benzyl

Boc – *tert*-butyloxycarbonyl

Bz – Benzoyl

calcd – calculated

cat – catalyst

cm – centimetre

COD – cyclooctadiene

CSI – chlorosulfonyl isocyanate

Cy – cyclohexyl

DABCO – 1,4-Diazabicyclo[2.2.2]octane

DCC – *N*,*N'*-dicyclohexylcarbodiimide

DCE – 1,2-dichloroethane

DBU – 1,8-Diazabicyclo[5.4.0]undec-7-ene

DDQ – 2,3-dichloro-5,6-dicyano-*p*-benzoquinone

DFT – density functional theory

DHF – dihydrofuran

DMF – *N*,*N*-dimethylformamide

DMSO – dimethyl sulfoxide

DPP – diphenyl phosphoric acid

dr – diastereomeric ratio

e – Euler's number

E – generic electrophile

E – *Ger.*, entgegen

EDG – electron-donating group

ee – enantiomeric excess

EI – electron impact

equiv – stoichiometric equivalent

Eq. – equation

er – enantiomeric ratio

ESI – electrospray ionization

Et – ethyl

EWG – electron-withdrawing group

FMO – frontier molecular orbital

Flu – Fluorenyl

FTIR – Fourier transform infrared

g – gram

G – Gibbs free energy

h – hour

HE – Hantzsch ester

HOMO – highest occupied molecular orbital

HRMS – high-resolution mass spectroscopy

HPLC – high performance liquid chromatography

Hz – Hertz

hν – light; electromagnetic radiation

i-Pr – isopropyl

IR – infrared

J – coupling constant

k – reaction rate constant

K – Kelvin

K_{eq} – equilibrium constant

kcal – kilocalorie

L – generic ligand or levorotatory

LG – generic leaving group

LUMO – lowest unoccupied molecular orbital

m – meta

M – molar (moles per litre)

Markov – Markovnikov

Me – methyl

Mes – mesityl

mg – milligram(s)

min – minute(s)

mmol – milimole(s)

mol – mole

MOM – methoxymethyl

n-Bu – *n*-butyl

n.d. = not determined

NMR – nuclear magnetic resonance

NOE – nuclear Overhauser effect

n.p. = no product

n-Pr – *n*-propyl

Nuc – nucleophile

o – ortho

p – para

PG – protecting group

Ph – phenyl

Phe – phenylalanine

PMP – *para*-methoxyphenyl

ppm – parts per million

pyr – pyridine

R – generic group or gas constant

R – Latin, *rectus*

Ra-Ni – Raney nickel

Rf – retention factor

rt – room temperature

S – *Latin, sinister*

s – selectivity factor

syn – together, same side

T – temperature

t – time

t-Bu – *tert*-butyl

t-BuOH – *tert*-butanol

temp. – temperature

Tf – trifluoromethanesulfonyl

TFA – trifluoroacetic acid

THF – tetrahydrofuran

TLC – thin-layer chromatography

TMS – trimethylsilyl

(*R*)-TRIP – (*R*)-3,3′-Bis(2,4,6-triisopropylphenyl)-1,1′-binaphthyl-2,2′-diyl hydrogenphosphate

Trp – tryptophan

T.S. – transition state

Ts – toluenesulfonyl

UV – ultraviolet

vac – vacuum

X – generic halide, pseudohalide, leaving group, or heteroatom

Y – generic group

Z – *Ger.*, zusammen

Å – angstrom (10^{-10} m)

β – beta

Δ – heat or reflux

δ – chemical shift in parts per million

∠ – angle

π - pi orbital

μm – micrometer

μW – microwave

Chapter 1. Introduction

1.1. The β-Aminocarbonyl Motif

1.1.1. Importance and Prevalence

The β-amino carbonyl is a key structural motif in many biologically active acyclic and (hetero)cyclic compounds, most notably β-amino acid derivatives and β-peptides (Figure 1.1). An additional methylene unit provides proteolytic stability to β-amino carbonyl compounds compared to their natural α-amino carbonyl analogs. This has made the β-amino carbonyl motif abundant in therapeutics, agrochemicals, peptidomimetics, and natural products.[1–5] β-Peptides have also become essential peptidomimetics, and the design of unique foldamer structures has made them exciting subjects in drug discovery and proteomics.[6–8]

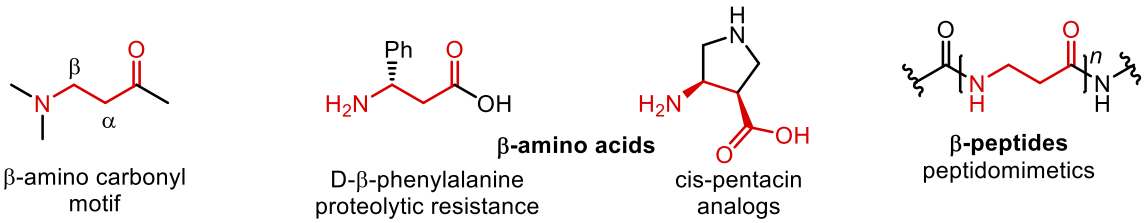

Figure 1.1. The β-amino carbonyl motif (in red).

In particular, the β-amino carbonyl motif is prevalent in biologically important heterocycles. β-Lactams, such as penicillin antibiotics (e.g. Penicillin G),[9,10] and drugs with pyrazolone cores such as metamizole are representative examples (Figure 1.2).[11–13] Pyrazolones are also valuable to the food industry for their use as pesticides.[14–17] The importance of pyrazolones and related heterocycles in medicinal chemistry and agrochemistry has driven intense research towards their synthesis.

In the past decade, there have been significant advances in the use of azomethine imines to access heterocycles with the pyrazolone core. For example, *N,N'*-cyclic azomethine imines have

become increasingly popular substrates in asymmetric catalysis. These dipoles are now established substrates for diastereoselective and enantioselective dipolar cycloadditions with a variety of dipolarophiles,[18–27] and there are also some reports of enantioselective nucleophilic additions.[28–30] Although the scope of this reactivity is broad, the structural complexity of the azomethine imine substrates is very limited. This is due to constraints in their synthesis by traditional methods, and azomethine imines are thus rarely used to synthesize valuable β-amino carbonyl compounds.

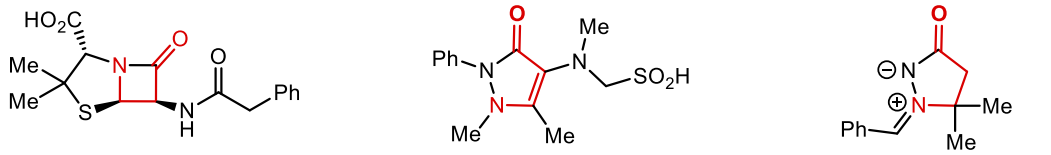

Figure 1.2. Heterocycles containing the β-amino carbonyl motif.

1.1.2. Traditional Synthesis of β-Amino Carbonyl Compounds

The synthesis of β-aminocarbonyl compounds from readily available starting materials is a long-standing challenge, and this is especially true for their asymmetric synthesis.[31,32] Many successful approaches use naturally abundant α-amino acids as starting materials,[33,34] but other methods are needed for unnatural products. In these cases, syntheses typically involve forming either the C-N bond (Mannich) or C-C bond (1,4-addition) (Scheme 1.1).[35–38] These methods are useful if the products are simple and substrates are available, otherwise the precursors can be lengthy to synthesize or difficult to isolate.

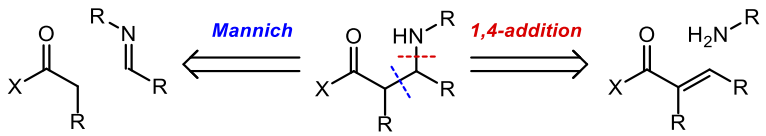

Scheme 1.1. Common disconnections in β-aminocarbonyl synthesis.

These strategies are common in the synthesis of heterocycles containing the β-amino carbonyl motif. For example, the pyrazolidinone core is traditionally synthesized from hydrazine derivatives using a 1,4-addition followed by cyclization (Scheme 1.2). There can be practical problems with this route including sensitivity and chemoselectivity issues, and di-substituted hydrazines can also be difficult to access when the two groups are different. In addition, this route limits substitution at the α and β positions.

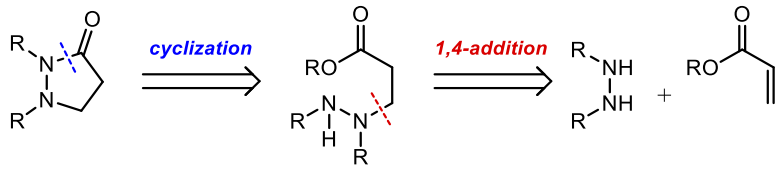

Scheme 1.2. Traditional synthesis of pyrazolidinone, a heterocycle containing the β-amino carbonyl motif.

In contrast to the above methods, current research towards synthesis of β-amino carbonyl compounds has shifted to finding new synthetic routes from readily available starting materials.[39] The following section will discuss the synthesis of this motif by the functionalization of alkenes.

1.2. Synthesis of β-Aminocarbonyl Compounds from Alkenes

The most general and extensively used transformations of C-C multiple bonds are electrophile-nucleophile additions. These reactions have high atom efficiency and convert abundant substrates, such as alkenes, into valuable chemicals through industrial processes. Amination reactions of alkenes are particularly important, and these transformations are under constant study and improvement. However, alkenes are not common substrates in β-aminocarbonyl synthesis. We define such alkene functionalization as *aminocarbonylation*: the addition of a nitrogen and a carbonyl group across the double bond, in analogy to hydroformylation, hydroboration, or oxymercuration (Scheme 1.3). This is not to be confused with other uses of the term

aminocarbonylation, for example in the metal-catalyzed literature where aminocarbonylation (carbamoylation) of aryl halides can be achieved in the presence of CO and amines.[40,41]

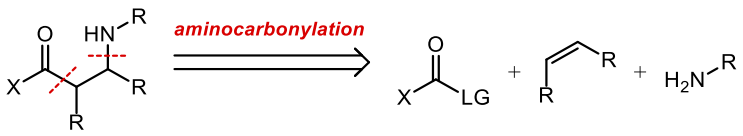

Scheme 1.3. Aminocarbonylation of alkenes: disconnection and synthons.

The difunctionalization of unactivated alkenes requires either high energy input and reactive substrates or catalysis of the reaction. For this reason, intramolecular alkene aminocarbonylation reactions are more common than intermolecular reactions. There are two general strategies for these additions to alkenes: 1) polar additions with clear electrophiles and nucleophiles or 2) organometallic catalysis involving activation of the alkene or the amine with a metal catalyst.[40] Overall, regioselectivity in alkene addition reactions is both kinetically and thermodynamically controlled. Polar additions typically display Markovnikov-type regioselectivity.[42] In stepwise reactions of this type, selectivity is predicted by stability of the carbocation intermediate. In concerted reactions without carbocation intermediates, such as with dipolar reagents, regioselectivity can be difficult to predict unless the transition state is well understood. On the other hand, organometallic catalysis can allow for new control over selectivity. In this section, notable reports on alkene aminocarbonylation using both polar addition and organometallic catalysis are described.

1.2.1. Aminocarbonylation of Alkenes by Palladium Catalysis

Alkene aminocarbonylation has been established in intramolecular systems by palladium (II) catalysis. This involves cyclization of an internal nitrogen nucleophile onto the palladium-coordinated double bond, followed by insertion of carbon monoxide (CO), as shown in Scheme

1.4. It is important to note nomenclature: this is different from palladium-catalyzed alkene carbamoylation, which is often referred to as aminocarbonylation in the literature.[40,41]

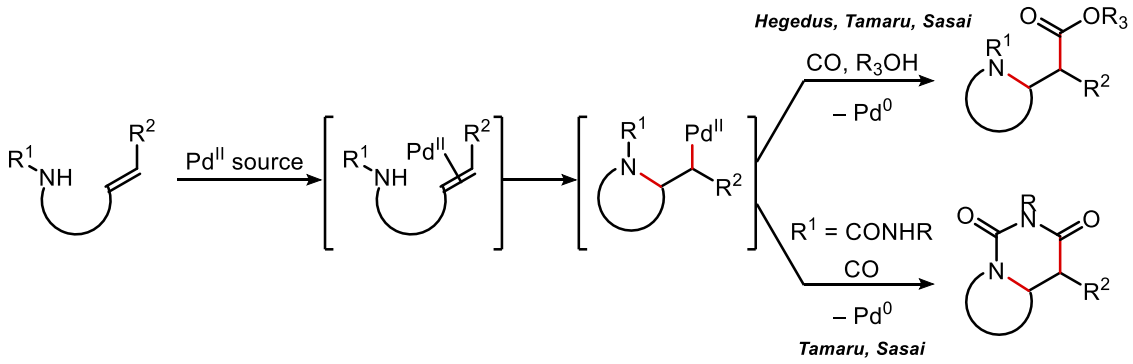

Scheme 1.4. Intramolecular alkene aminocarbonylation with Pd(II).

The first example of metal-catalyzed alkene aminocarbonylation was reported by Hegedus in 1980, in efforts to synthesize functionalized indoles and indolines.[43] They found that stoichiometric Pd(II) promoted intramolecular aminopalladation, and under appropriate conditions CO insertion was favoured over side reactions (including β-hydride elimination and isocyanate formation). The intermediate was trapped with methanol to form β-amino methyl esters. Tamaru later improved upon this reactivity, establishing methods using catalytic Pd(II) with $CuCl_2$ oxidant, and using internal nucleophile traps to make bicyclic heterocycles.[44,45] These methods were used in the synthesis of several natural products.[46–48] More recently, Sasai and coworkers developed enantioselective variants of Pd(II) catalysed alkene aminocarbonylation by using SPRIX ligands, and observed up to 89% ee for their bicyclic urea products.[49,50] However, there are no reports of enantioselective intermolecular alkene aminocarbonylation reactions.

Shortly after their intramolecular studies, Hegedus and coworkers reported preliminary results for the intermolecular aminocarbonylation of alkenes. Building on prior carboacylation work,[51] Hegedus demonstrated palladium-assisted aminoacylation of ethylene with the lithium salts of

indole and skatole in the presence of CO and methanol (Scheme 1.5).[52] The yields of β-*N*-indolyl methyl esters were modest, and intermolecular reactivity with other olefins was not explored.

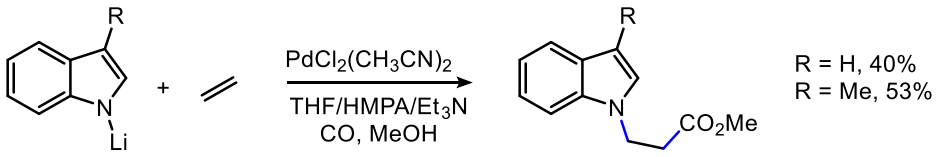

Scheme 1.5. Palladium assisted intermolecular aminocarbonylation of ethylene by Hegedus.

In 2015, Liu reported improved conditions for the aminopalladation of unactivated alkenes and styrenes (Scheme 1.6).[53] Initially, conditions developed for the amination of alkenes were examined, but performed under atmospheric CO. Precipitation of palladium black was observed, likely caused by fast reduction of palladium with CO, which outcompetes the essential aminopalladation step. Fortunately, switching to a hypervalent iodine oxidant allowed formation of the desired β-amino acid, which is trapped in situ with trimethylsilyldiazomethane. This method provides access to a wide range of racemic *N*-substituted β-amino methyl esters.

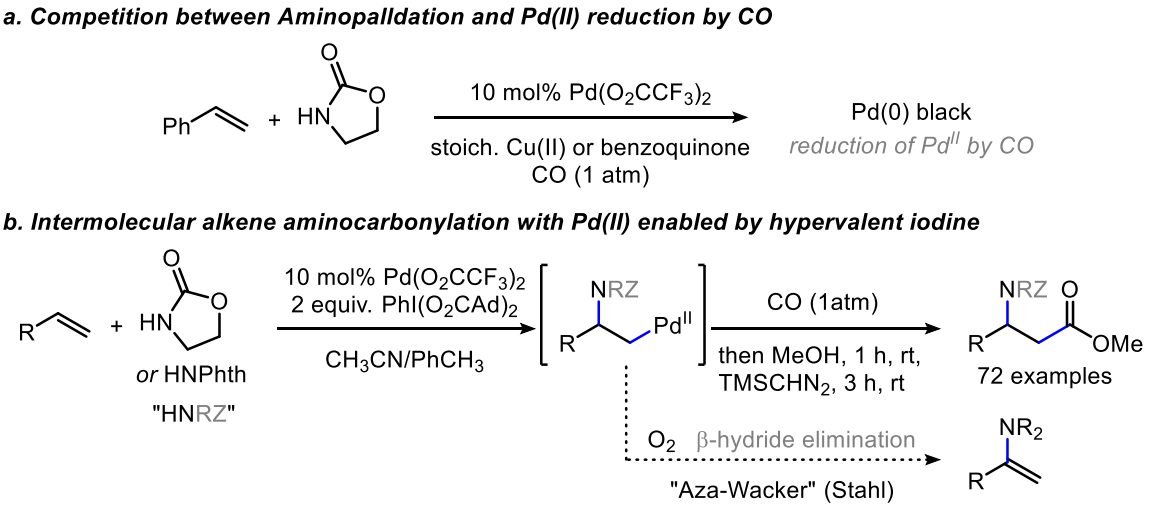

Scheme 1.6. Palladium catalyzed aminocarbonylation of terminal alkenes by Liu.

This body of work shows the growing utility of palladium-catalyzed amination reactions. Challenges with difficult transformations, in this case intermolecular aminopalladation, can be

solved by changing the palladium electronic environment. Also, chemoselectivity can be controlled with palladium catalysis; using CO as a carbonyl source avoids electrophilic alternatives, and the oxidation of palladium with mild reagents prevents amine oxidation seen in non-catalytic processes. However, currently only terminal alkenes are suitable substrates (providing β^3-substituted amino esters), and the reaction is limited to acidic N-H reagents.

1.2.2. Aminocarbonylation of Alkenes by Cycloadditions of Isocyanates

A different strategy for the aminocarbonylation of alkenes is to use an reagent with both nitrogen and carbonyl functionalities in a cycloaddition reaction. In this case, the electrophilic and nucleophilic parts must either prefer not to react with each other (dimerization), or react reversibly, thus masking the reactivity.

The most important example of this reactivity is the formal [2+2] cycloaddition of alkenes with isocyanates to yield β-lactams (Scheme 1.7).[54–56] Strongly nucleophilic alkenes will react with many isocyanates, but unactivated alkenes require the highly electrophilic reagents such as chlorosulfonyl isocyanate (CSI). The promiscuous reactivity of CSI limits functional group tolerance and reacts violently with water.[10,57] In addition, CSI is highly toxic and its cycloadducts can be unstable. Nevertheless, these cycloaddition reactions are valuable to industry for rapidly synthesizing diverse β-lactams, which can be precursors to β-amino acids, agrochemicals, and drugs.[9,10,55]

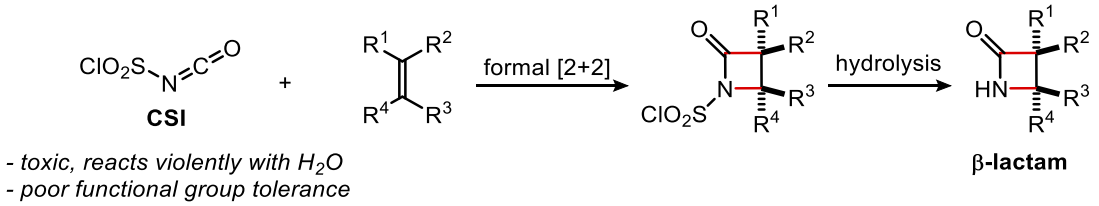

Scheme 1.7. Example of β-lactam synthesis from alkene aminocarbonylation with chlorosulfonyl isocyanate.

Our group's efforts toward alkene aminocarbonylation arose from our early interest in metal-free amination reactions. While exploring intramolecular hydroamination reactions of protected hydrazine derivatives, the group discovered divergent reactivity (Scheme 1.8).[58] When R^1 of the nitrogen protecting group was alkyl or aryl, the desired Cope-type hydroamination reaction gave a pyrrolidinone product.[59,60] However, while attempting an alkene hydroamination reaction with a Boc-protected hydrazide (R^1=O*t*-Bu), an unexpected product was observed. This bicyclic product was the result of an intramolecular alkene aminocarbonylation reaction. The proposed mechanism was thermolysis of the hydrazide with release of *t*-BuOH to produce an amino-isocyanate as the reactive intermediate, which underwent a [3+2] cycloaddition reaction with the alkene. Over the next few years, this discovery was developed into general reactivity, and an article was recently published by our group.[61]

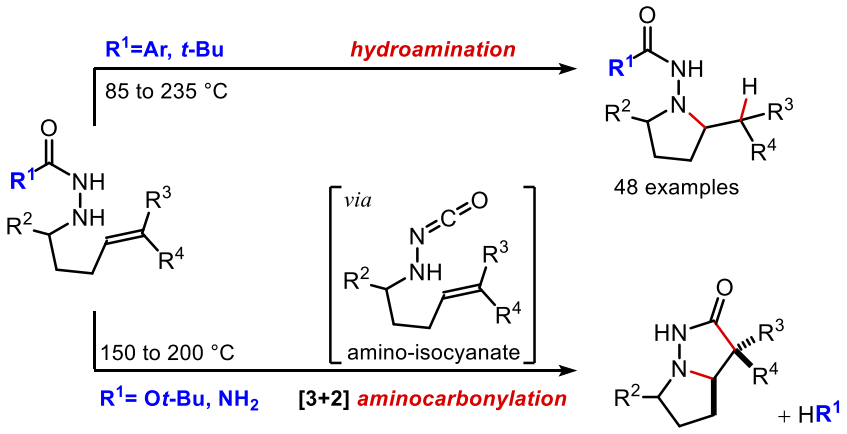

Scheme 1.8. Divergent reactivity: reactions of amino-isocyanates with intramolecular alkenes

Further exploration into intermolecular reactivity was unfruitful, and could only be achieved in one case (Scheme 1.9). After thermolysis of *N*,*N*-dibenzylcarbazate and release of *t*-BuOH, the amino-isocyanate undergoes [3+2] cycloaddition with excess norbornene. This yields a dipole intermediate which undergoes 1,2-benzyl shift to give a pyrazolidinone product. All attempts with other alkenes and alkynes, or mono-benzylated carbazates, yielded no product.[62]

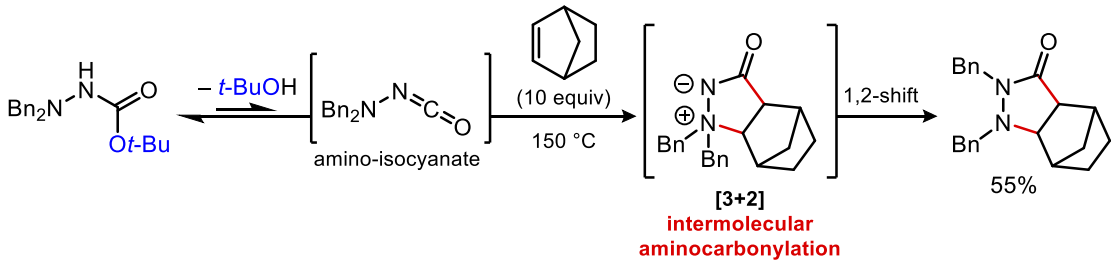

Scheme 1.9. Clavette's only example of intermolecular alkene aminocarbonylation with amino-isocyanates derived from carbazates.

While isocyanates like CSI are bulk industrial chemicals with well-known and useful cycloaddition reactivity, amino-isocyanates are very rare in the literature (see Chapter 1.3.2). This may be attributed to their stability; many isocyanates are stable, but our discovery showed amino-isocyanates to be reactive intermediates, and so their occurrence in the literature may be underreported. Following this discovery, our group became focused on studying amino-isocyanates and imino-isocyanates as reagents for the synthesis of β-amino carbonyl compounds from alkenes. The following chapter overviews the cycloaddition reactivity of these *N*-isocyanates and related amphoteric molecules.

1.3. [3+2] Cycloaddition Reactions of Amphoteric Molecules

Cycloaddition reactions are useful to rapidly control complexity by forming multiple bonds at once, and when selectivity control is important. Cycloaddition reactions provide alternative routes in the synthesis of heterocycles, and can even enable late-stage derivatization. This chapter describes rare examples of amino- and imino-isocyanate [3+2] cycloaddition reactivity, as well as the more well-known 1,3-dipolar cycloadditions of azomethine imines. Both *N*-isocyanates and azomethine imines contain the N-N-CO motif, and can be described as amphoteric: having both nucleophilic and electrophilic centres (Figure 1.3).[63,64]

Figure 1.3. Amphoteric cycloaddition partners containing the N-N-CO motif.

1.3.1. Amphoteric Molecules

Traditionally, the term 'amphoteric' was used to identify chemicals that could act as both an acid and a base. However, it has recently been applied to more types of reactivity, including molecules which act as both electrophiles and nucleophiles.[63,64] This is not to be confused with ambident reactivity, where delocalization of a charge (or lone pair) allows nucleophilic reactivity at two different sites in a molecule. In amphoteric molecules, there exist two functional groups which are typically incompatible, or could react rapidly together (e.g. amino-aldehydes). However, control of the availability or reactivity of each functional group can provide useful bifunctional reactivity. Recent work on this topic has focused on amphoteric reagents with orthogonal reactivity. For example, 1,3-amphoteric aziridine aldehydes can react as electrophilic carbonyls without interference from the internal amine (Scheme 1.10).[64–68] It should also be noted that this definition excludes functional groups such as imines, which can react as both nucleophiles and electrophiles, and compounds such as α-aminoamides, in which the electrophile is quite stable in the presence of the nucleophile.

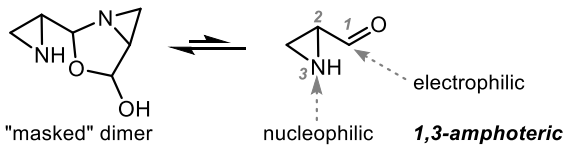

Scheme 1.10. Aziridine aldehydes as 1,3-amphoteric reagents.

The description of reactivity as amphoteric is also useful in cycloaddition chemistry when one partner has dipolar nature. This encompasses cycloaddition reactions of dipoles (i.e. 1,3-dipolar

cycloadditions) and reagents with dipolar nature, such as heteroatom-substituted heterocumulenes. Heterocumulenes are common reaction partners in cycloaddition reactions for heterocyclic synthesis, and can engage in a wide range of reactivity (Figure 1.4). The major classes of reactive heterocumulenes are ketenes, carbodiimides, isocyanates, and isothiocyanates. These compounds are well known for [2+2] cycloaddition reactivity to yield 4-membered heterocycles (eg. β-lactams).

Figure 1.4. Examples of heterocumulenes.

Isocyanates are a class of heterocumulenes that have been particularly useful in heterocyclic synthesis, and the type of reactivity is often dependent on the N-substituent. For example, alkyl or aryl isocyanates are known to dimerize in [2+2] cycloaddition reactions, or react with other π bonds such as carbonyls and imines (Scheme 1.11a). This reactivity is increased when isocyanates have electron-withdrawing N-substituents such as sulfonyl, phosphorous, and carbonyl groups.

Isocyanates and other heterocumulenes also react as dipolarophiles in [3+2] cycloaddition reactions to give 5-membered heterocyclic adducts.[69] For example, isocyanates combine readily with nitrones to provide 1,2,4-oxadiazolidin-5-ones (Scheme 1.11b). This chemistry was recognized and developed by Huisgen in the 1960s.[69–71] In general, the same bond in the heterocumulene that reacts in [2+2] cycloadditions also reacts in the [3+2] cycloaddition (eg. C=C bond in ketenes, C=N bond in isocyanates).[69] However, when an electron-donating group such as a heteroatom is present, heterocumulenes take on 1,3-amphoteric character and can also react as

1,3-dipoles. For example, isocyanates equipped with electron-donating substituents (O, N, S) can undergo dimerization by [3+2] cycloaddition (Scheme 1.11c).

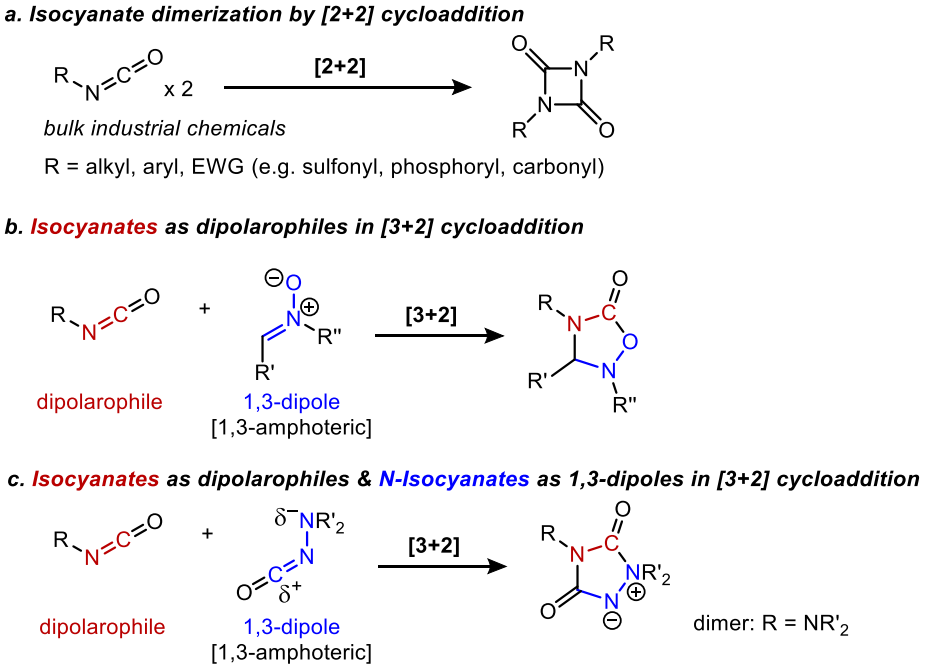

Scheme 1.11. Cycloaddition reactivity of different isocyanates. (a) Isocyanates are well known for 1,2-cycloaddition reactions, like dimerization. In 1,3-cycloadditions, isocyanates can react as (b) dipolarophiles and (c) 1,3-dipoles.

In contrast to common isocyanates, which are bulk industrial chemicals, these heteroatom substituted isocyanates are extremely rare in the literature.[72,73] Over the past 40 years, the fundamental and physical aspects of this reactivity have been studied, but until recently this reactivity has escaped practical use. In the following sections of this chapter, the cycloaddition reactivity of electron rich *N*-isocyanates is described.

1.3.2. Amino-isocyanates

Containing a nucleophilic nitrogen and an electrophilic isocyanate carbon, amino-isocyanates are one example of electron-rich heterocumulenes that can undergo [3+2] cycloaddition reactions (Scheme 1.12).[61,72,74,75] Amino-isocyanates are reactive intermediates and difficult to isolate. In fact, they are known to dimerize at temperatures as low as –40 °C.[72] Since early studies, amino-

isocyanates have been accessed by Curtius rearrangement of carbamoyl azides.[73,76–82] There are also reports of their production upon the heating of carbazates and semicarbazides, with expulsion of a blocking group (BG) in an approach analogous to blocked (masked) isocyanates.[83] The amino-isocyanates were studied in [3+2] cycloaddition reactions with alkyl and aryl isocyanates (Scheme 1.12).

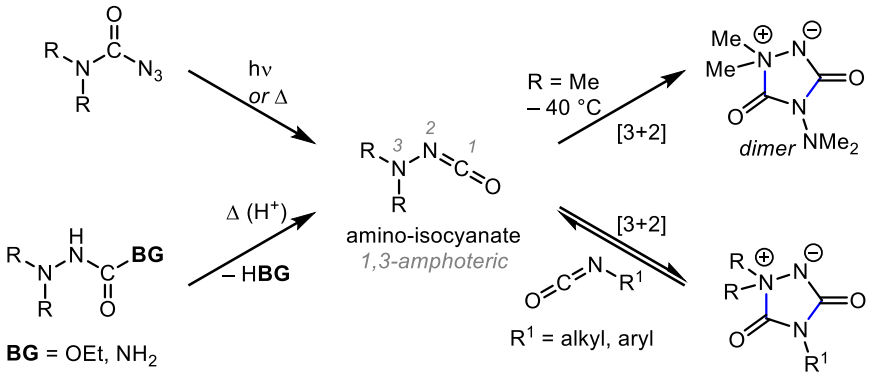

Scheme 1.12. Formation and [3+2] cycloadditions of amino-isocyanates. BG = blocking group.

These [3+2] cycloadditions reactions occur exclusively in one direction. The polarity of the amino-isocyanate, which can be depicted as partial charges, dictates the regiochemistry of the cycloadduct (Figure 1.5).[69] When considering the frontier molecular orbitals in cycloaddition reactions of amino-isocyanates, the dominant interaction will be the HOMO of the amino-isocyanate with the LUMO of the dipolarophile. The lone pair orbital of the amino-group can rotate to be in alignment with the C=N π bond, and will have the largest coefficient in the HOMO.

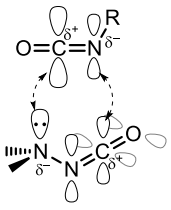

Figure 1.5. Partial charges and orbital geometry for the cycloaddition of amino-isocyanates with isocyanates.

Another way to access amino-isocyanates is through thermal cycloreversion of the dimer cycloadducts.[84–86] When the *C*-isocyanate substituent is bulky (e.g. *t*-Bu), this process can be facile and occur with heating above 60 °C. In these cases, reactions with other dipolarophiles have been shown to compete with dimerization and yield valuable 5-membered heterocycles (Scheme 1.13).

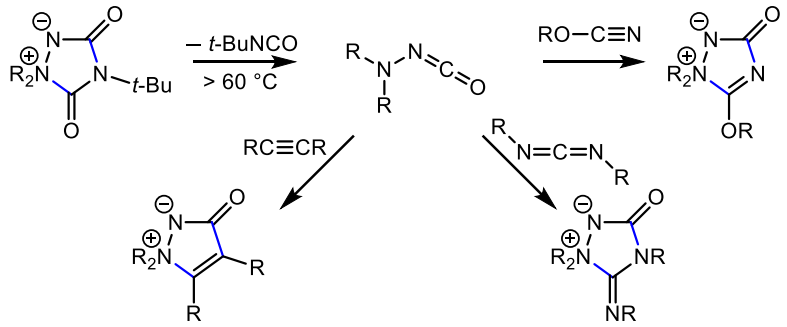

Scheme 1.13. [3+2] Cycloaddition reactions of amino-isocyanates.

In the cycloaddition of dimethylamino-isocyanate with phenylacetylene, Lwowski showed that heating the product at 210 °C caused a 1,2-methyl shift to give a known pyrazolone (Scheme 1.14). Comparison to the pyrazolone, synthesized by the traditional 2-step sequence from dimethylhydrazine confirmed their findings. This example shows the efficiency of amino-isocyanate cycloaddition reactions to access the pyrazolone core, as an alternative approach to traditional methods.

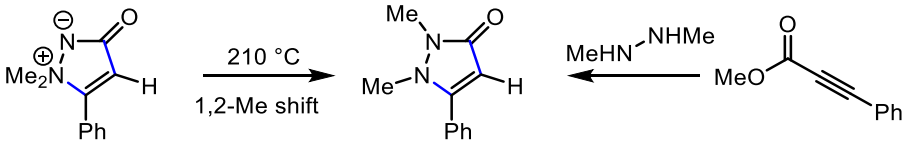

Scheme 1.14. Proof of structure and demonstration of traditional pyrazolone synthesis.

Our group became interested in [3+2] cycloadditions of amino-isocyanates after observing the unexpected intramolecular alkene aminocarbonylation reaction described in Chapter 1.2.2. After this exciting discovery, the group set out to develop *N*-isocyanates as amphoteric reagents for

alkene aminocarbonylation. A key aspect to controlling the amphoteric reactivity was accessing the *N*-isocyanate in situ using a 'blocked' isocyanate approach.[87] This preliminary work with amino-isocyanates gave promising results for intramolecular reactions.[58] However, intermolecular reactivity was very limited, and only the reaction with norbornene provided any product (Scheme 1.15). In addition, the required high temperatures (>150 °C) led mostly to the formation of isocyanate dimers and degradation of the reagent.

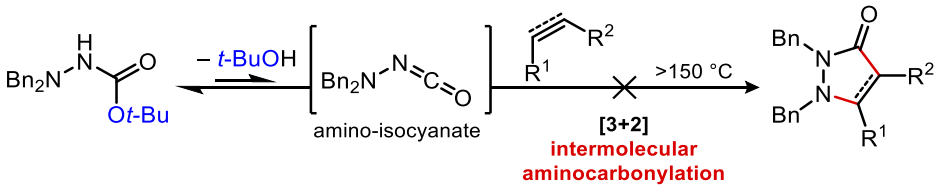

Scheme 1.15. Attempted intermolecular alkene aminocarbonylation with amino-isocyanate.

1.3.3. Imino-isocyanates

Imino-isocyanates are less studied than amino-isocyanates, and these species have not been isolated. They were first studied by Larsen and Jakobsen in 1970.[88] In analogy to prior work on amino-isocyanates from semicarbazides, they studied the two possible C-N fragmentations when heating semicarbazones (Scheme 1.16). They heated cyclohexanone-derived semicarbazones at low or high temperatures, and analyzed the mixtures by mass spectrometry. The 1,2' C-N fragmentation of cyclohexanone semicarbazide occurs at high temperature (>200 °C) to provide isocyanic acid (HNCO) and cyclohexanone hydrazone. The 1,2 C-N fragmentation releases an imino-isocyanate and amine, and this is the favoured process at low temperatures (150-180 °C). It was proposed that 1,2 fragmentation occurs at lower temperatures because the C-N bond has less double bond character, due to resonance with the adjacent C=N bond. They studied and observed similar reactivity with the analogous *N*-phenyl semicarbazone, where the leaving group is aniline.[88]

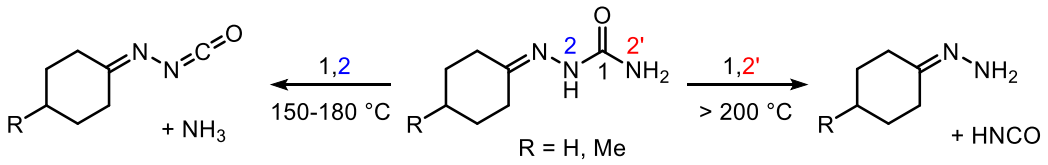

Scheme 1.16. First study of imino-isocyanates generated by thermal fragmentation.

The work by Larsen and Jakobsen was the first example of using a traditional isocyanate "blocking group" approach to access imino-isocyanates. Their interest in fragmentation mechanisms left the cycloaddition reactivity of the imino-isocyanate intermediates unexplored. However, they provided useful methods for imino-isocyanate detection by mass spectrometry, and also discussed degradation of imino-isocyanates to azines. This was followed up by Shah and coworkers, who studied the thermal fragmentation of aldehyde-derived semicarbazones to azines for applications in liquid crystalline materials.[89,90] Their 2000 study showed that semicarbazones are general imino-isocyanate precursors, and they performed mass spectrometry studies similar to those of Larsen and Jakobsen.[90] When an aldehyde-derived semicarbazone was heated to 260 °C, an azine was formed. They proposed a pathway involving generation of the imino-isocyanate intermediate, which undergoes [2+2] dimerization followed by threefold extrusion to give an azine (Scheme 1.17).

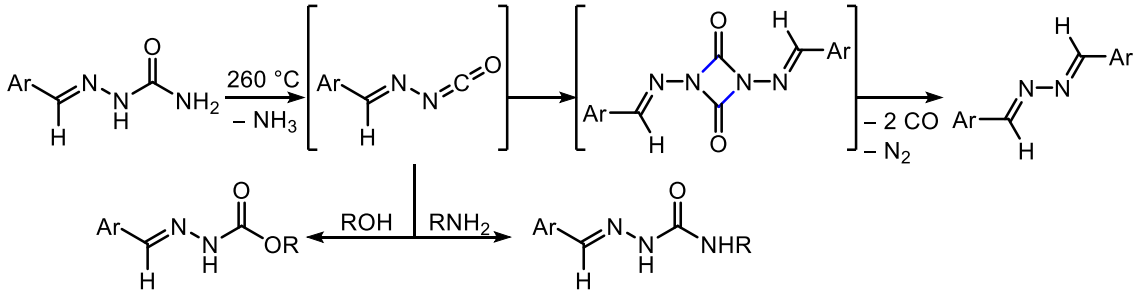

Scheme 1.17. Reactions of aldehyde-derived imino-isocyanates from thermal fragmentation.

The support provided for this mechanism includes detection of CO and N_2 by gas chromatography, NH_3 by litmus test and mass spectrometry, and successful trapping of the imino-

isocyanate with amine or alcohol nucleophiles. Although [2+2] dimerization reactivity is known for *C*-isocyanates, the proposed [2+2] cycloadduct intermediate was not isolated or observed in these studies.

With an adjacent C-N double bond, the π system of the isocyanate is extended in the imino-isocyanate. The 'imino' nitrogen of the imino-isocyanate (sp^2) is also less electron rich than in the amino-isocyanate (sp^3). These factors give imino-isocyanates an advantage in [3+2] cycloaddition reactivity, but there are still only a handful of examples of this in the literature. In these cases, cycloadducts are used as precursors to imino-isocyanates, which are generated in situ by thermal cycloreversion. The first example of this reactivity was reported by Warkentin in 1976 (Scheme 1.18).[91] In this report, 2-hydrazono-Δ^3-1,3,4-oxadiazolines were heated in refluxing chlorobenzene in the presence of a phenyl isocyanate trap. The intermediate imino-isocyanate (also referred to as *N*-isocyanatoimine) underwent [3+2] cycloaddition with phenyl isocyanate to yield a dipole. This dipole can be seen as a type of azomethine imine, which will be discussed later in this chapter. The azomethine imine then reacts in a second [3+2] cycloaddition with another equivalent of phenyl isocyanate.

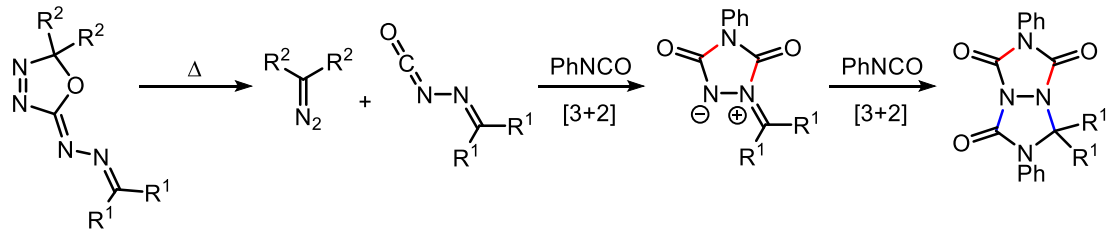

Scheme 1.18. Thermal cycloreversion to access imino-isocyanates, and initial reactivity scope.[91]

Although there have been few studies on the cycloaddition reactivity of imino-isocyanates, the polarity and observed regioselectivity is analogous to cycloadditions of amino-isocyanates described above. However, the geometry of the imino-isocyanate is important, since additional conjugation with the imino C=N bond must be considered. Figure 1.6 shows the transition state

geometry of the imino-isocyanate that should allow for cycloaddition reactivity (in blue), as well as two $n \rightarrow \pi^*$ interactions (in grey) that could stabilize the developing transition state charge. In Chapter 2, a more detailed description of the frontier molecular orbitals involved in imino-isocyanate cycloaddition reactions is provided.

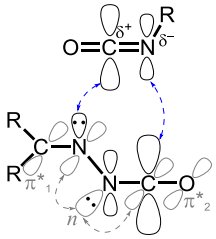

Figure 1.6. Imino-isocyanate transition state geometry and frontier molecular orbital interactions.

In 1982, Jones accidentally synthesized a very bulky dipole when attempting a [4+2] cycloaddition reaction with 1,3-dimesitylbenzo[c]furan and 4-phenyltriazoline-3,5-dione (Scheme 1.19).[92] Upon heating in toluene, this triazoline-derived dipole underwent cycloreversion to release a sterically hindered imino-isocyanate. In this report, Jones studied the reactivity of the proposed imino-isocyanate intermediate, and discovered unprecedented reactivity with alkenes and alkynes. Upon brief reflux in toluene, he observed [3+2] cycloaddition reactions of the imino-isocyanate to give *N,N'*-cyclic azomethine imine products. However, no yields were provided and the characterization of products was incomplete. His observation of reactivity with electron rich alkenes (1,5-cyclooctadiene, styrene, and norbornadiene) suggests that the HOMO of the alkene reacts with the LUMO of the imino-isocyanate. On the other hand, reactivity with N-Ph maleimide could suggest that the HOMO of the imino-isocyanate can also participate in reactivity with electron-deficient alkenes. Presumably, the dipole is too hindered to undergo 1,3-dipolar cycloaddition with phenyl isocyanate present in the mixture.

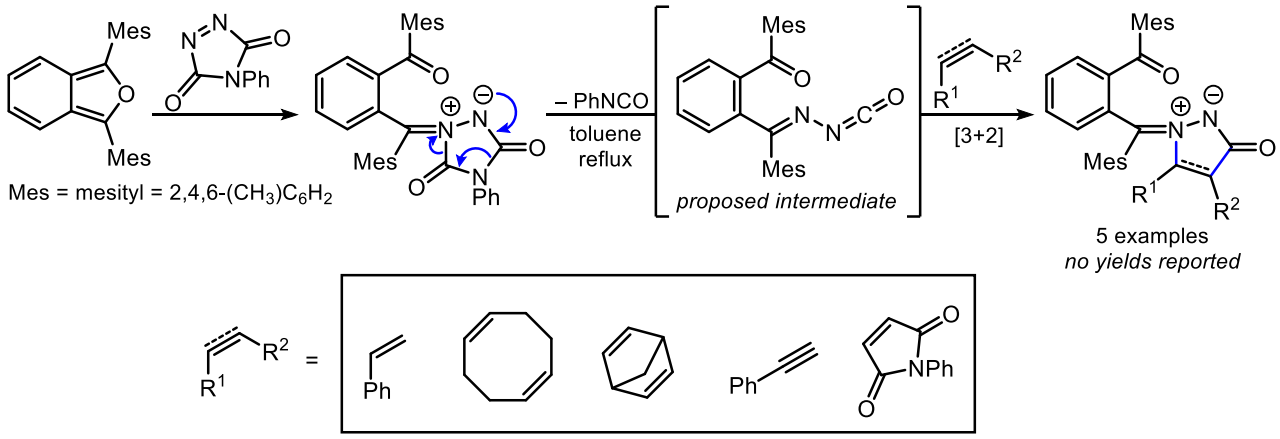

Scheme 1.19. Jones' unexpected discovery of imino-isocyanate reactivity with alkenes and alkynes.

In 1985, Regitz expanded on the reactivity observed by Jones and synthesized 17 dipoles derived from various ketones in 70-91% yield.[93] A bulky dipole was chosen to study imino-isocyanate reactivity, and heating in the presence of methyl isocyanate produced a new cycloadduct and released phenyl isocyanate (Scheme 1.20). The reaction likely occurs through thermal cycloreversion followed by [3+2] cycloaddition of the imino-isocyanate intermediate with methyl isocyanate. The choice of studying a sterically hindered system was important to prevent 1,3-dipolar cycloaddition reaction of the dipole product, which was observed by Regitz for other substrates.

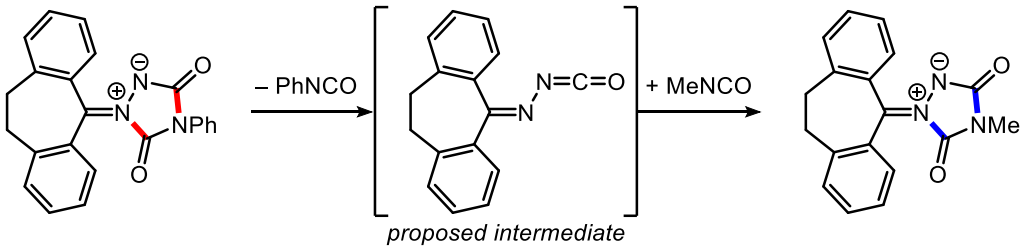

Scheme 1.20. Cycloreversion and cycloaddition reactions of imino-isocyanates.[93]

The seminal work described above shows that imino-isocyanates are reactive heterocumulenes that undergo [3+2] cycloadditions to give dipolar products known as azomethine imines. Unlike the products of amino-isocyanate [3+2] cycloadditions, these azomethine imines cannot undergo

proton or alkyl shift. Thus, they are prone to undergo 1,3-dipolar cycloaddition reactions, as observed by Warkentin and Regitz, unless the dipole is very bulky such as in Jones' study. Although the potential of imino-isocyanates as synthetic tools was demonstrated by Jones, their use in cycloaddition reactions is clearly underdeveloped. This is partly due to the impractical methods used by Jones and Regitz to access sterically hindered imino-isocyanates.

Our group began to explore intramolecular [3+2] cycloaddition reactions of imino-isocyanates after the discovery of amino-isocyanate reactivity described above (Chapter 1.2.2). In the initial exploration of alkene aminocarbonylation with imino-isocyanates, intramolecular reactivity with a readily available *N*-Boc hydrazone containing an internal alkene was first explored. The advantage of switching to study imino-isocyanate reactivity was the simple synthesis of *N*-Boc protected hydrazones compared to alkyl hydrazines. Our group's study relates to the early work by Larsen and Jakobsen, using a "blocking group" approach to access imino-isocyanates by thermolysis, but with a goal of achieving aminocarbonylation of the alkene.

Initial studies with ketone-derived hydrazones showed successful [3+2] cycloaddition with the internal alkene (Scheme 1.21).[62] The presence of a methyl of phenyl group (R) proved sufficient to shield the dipole from the unwanted additional 1,3-dipolar cycloaddition, and the products were obtained in good crude yields. The products of these reactions, bicyclic azomethine imines, proved difficult to isolate. However, this was an exciting example of uncatalyzed alkene aminocarbonylation reactivity, and our group was eager to explore intermolecular systems.

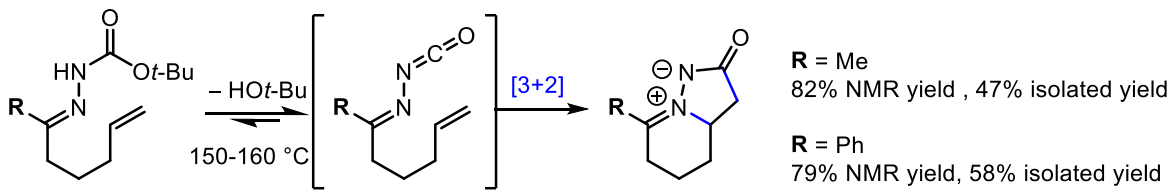

Scheme 1.21. Improved intramolecular imino-isocyanate cycloaddition and isolation of the dipole.

The desired [3+2] reactivity was also observed with aldehyde-derived hydrazones, but the resulting unshielded dipole reacted with a second equivalent of imino-isocyanate (Scheme 1.22).

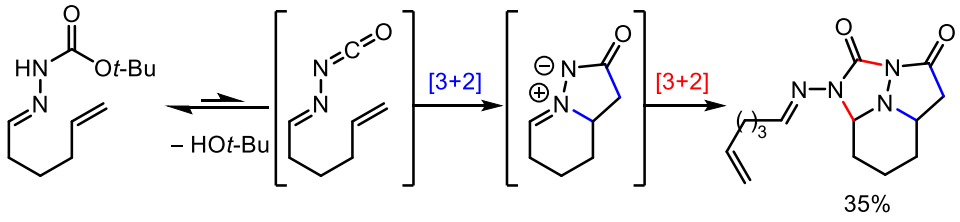

Scheme 1.22. Intramolecular [3+2] cycloaddition of an imino-isocyanate by Clavette.

In an effort to trap the above azomethine imine in situ and prevent side reactions, an intermolecular dipolar cycloaddition was attempted. In this cascade, the expected result was intramolecular aminocarbonylation followed by intermolecular cycloaddition with the dipolarophile, norbornene (Scheme 1.23). Surprisingly, the major product obtained resulted from an initial intermolecular reaction with norbornene, followed by an intramolecular cycloaddition.

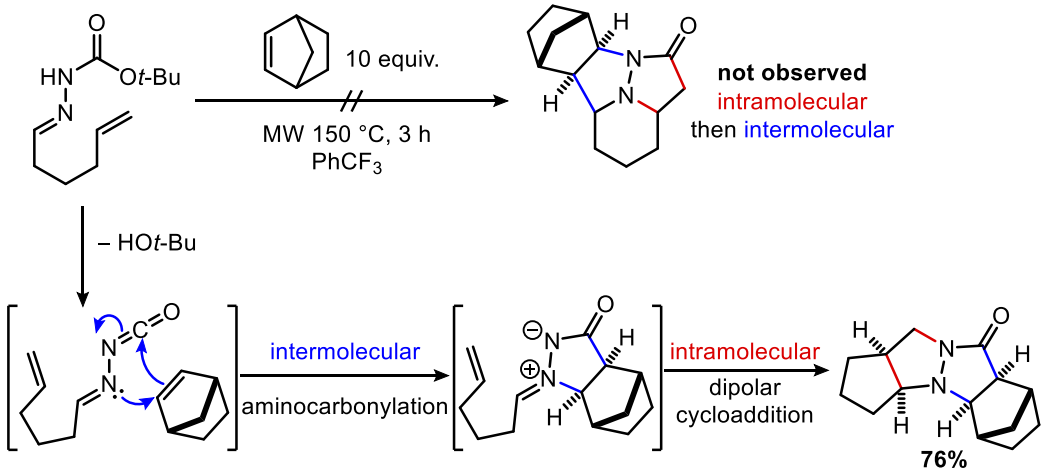

Scheme 1.23. Unexpected reactivity of imino-isocyanates with intramolecular and intermolecular alkenes.

With a simple route in hand to access imino-isocyanates in situ, our group was able to explore the intermolecular [3+2] cycloaddition reactivity first discovered by Jones, described earlier in this chapter. Jones observed the unexpected formation of a hindered imino-isocyanate reagent, and

reported the first intermolecular reactivity of these reagents with alkenes and alkynes. We recognized the potential of this reactivity as an alkene aminocarbonylation strategy, but Jones' report lacked a simple way to access the unique imino-isocyanate that he examined. With the thermolysis approach described for amino-isocyanates, we proposed the use of hydrazones as blocked (masked) *N*-isocyanates (Scheme 1.24). Hydrazones are simple to synthesize from a variety of ketones or aldehydes, and choice of blocking group allows for controlled formation of the reactive imino-isocyanate intermediate.

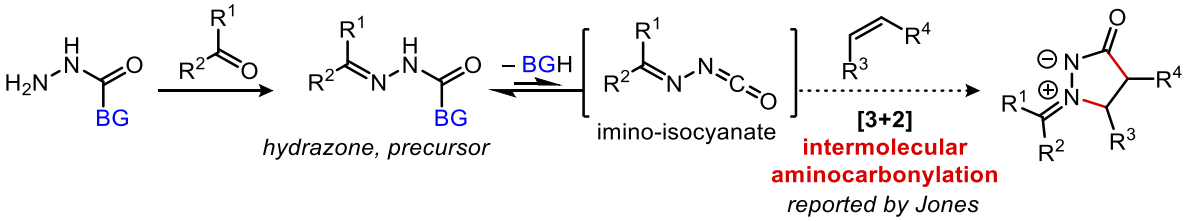

Scheme 1.24. Alkene aminocarbonylation strategy: Cycloaddition of imino-isocyanates with alkenes.

Importantly, the aminocarbonylation products, azomethine imines, are potential precursors to a variety of valuable compounds possessing the β-amino carbonyl motif including complex hydrazines, pyrazolidinones, pyrazolones, and β-amino acid derivatives. The improvement, study and use of the above reactivity is a topic of this thesis. In Chapter 2, optimization of the reactivity, including access to the imino-isocyanate intermediate, will be described in detail.[94] This is followed by the development of the reaction into a robust process for alkene aminocarbonylation, and access to enantioenriched β-aminocarbonyl compounds from alkenes.

1.3.4. Dipolar Cycloadditions of Azomethine Imines

Azomethine imines are a type of 1,3-dipole that are classified as either acyclic, *C,N*-cyclic, or *N,N'*-cyclic (Figure 1.7). These compounds are often formed in situ, although some are stable and isolable. A common feature of azomethine imines is a carbonyl group adjacent to the terminal

nitrogen atom, which is known to lend stability to the dipole. These azomethine imines are another example of 1,3-amphoteric reagents containing the N-N-CO motif, but have different polarities than the *N*-isocyanates.

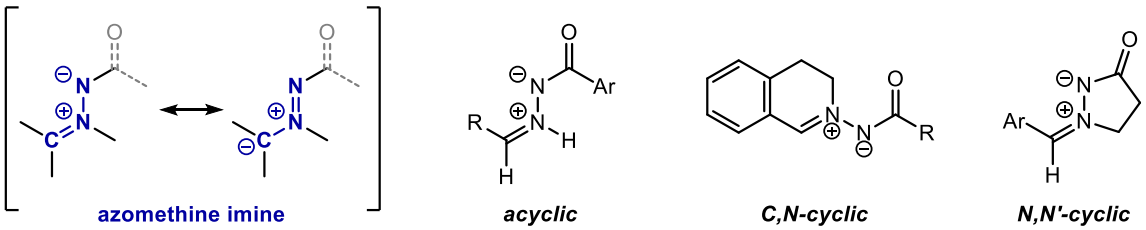

Figure 1.7. Structures of azomethine imines with the N-N-CO motif.

Azomethine imines can react readily with electron-deficient dipolarophiles in 1,3-dipolar cycloaddition reactions. The most common of these are [3+2] cycloaddition reactions with alkenes or alkynes to synthesize 5-membered di-nitrogenated heterocycles, although higher order [3+3] and [4+3] reactivity is also known.[95] In these reactions, the HOMO of the azomethine imine controls the reactivity, similar to a normal-electron-demand Diels-Alder reaction (Figure 1.8). However, inverse-electron-demand reactivity is possible, and the regioselectivity of these cycloadditions can vary depending on the dipolarophile or catalyst.[95]

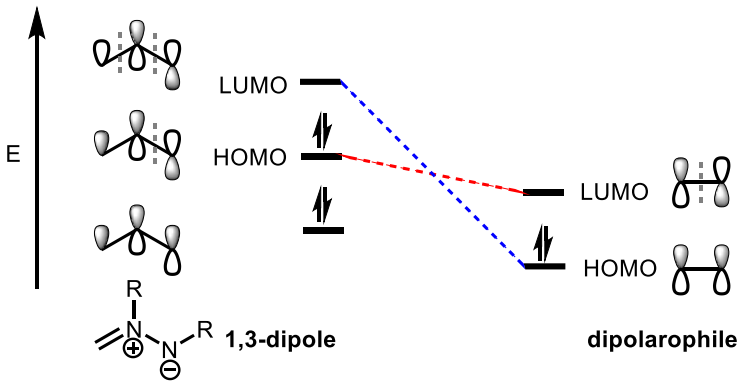

Figure 1.8. Energy and orbital diagram for the 1,3-dipolar cyucloaddition reaction of azomethine imines.

Acyclic azomethine imines are typically unstable and synthesized in situ for 1,3-dipolar cycloadditions. They are accessed by two common routes from hydrazine and carbazate precursors.[95,96] The first route involves the 1,2-prototropy of a mono-substituted hydrazine derivative (Scheme 1.25a), which occurs by heating or with a Lewis or Brønsted acid. The second route implicates the reversible condensation of a 1,2-disubstituted hydrazine onto a carbonyl compound (Scheme 1.25b). Acyclic azomethine imines react in [3+2] cycloadditions with electron deficient dipolarophiles, most often alkenes and alkynes, to give pyrazolidines and pyrazolines.[95,96] In this respect, dipoles accessed by the condensation route are more reactive. In addition, unactivated alkenes are reactive in intramolecular cycloadditions, and recent catalysis work has produced inverse electron demand reactivity with electron-rich dipolarophiles like enol ethers, and cycloadditions with enantioselectivity.[95,97–99]

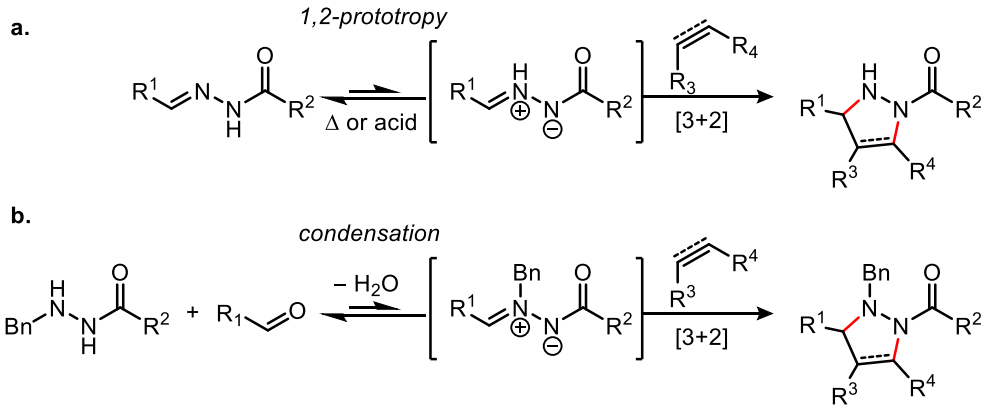

Scheme 1.25. Synthesis and representative [3+2] cycloaddition reactions of acyclic azomethine imines.

C,N-Cyclic azomethine imines react with dipolarophiles in normal or inverse electron demand 1,3-dipolar cycloadditions. When the reaction is a [3+2] cycloaddition, this is a useful route to synthesize a variety of ring-fused pyrazolidones, pyrazolines, and pyrazolones. There are many different dipoles that fit this class, but one popular type is the *N*-iminoisoquinolin-2-ium ylide. These *C,N*-cyclic azomethine imines have an isoquinoline core, and are synthesized by the *N*-

alkylation and cyclization of aryl hydrazone derivatives (Scheme 1.26). These dipoles undergo [3+2] cycloaddition with many types of dipolarophiles, and highly enantioselective variations have been developed by Maruoka,[100–102] Togni,[103] and others (Scheme 1.26).[95]

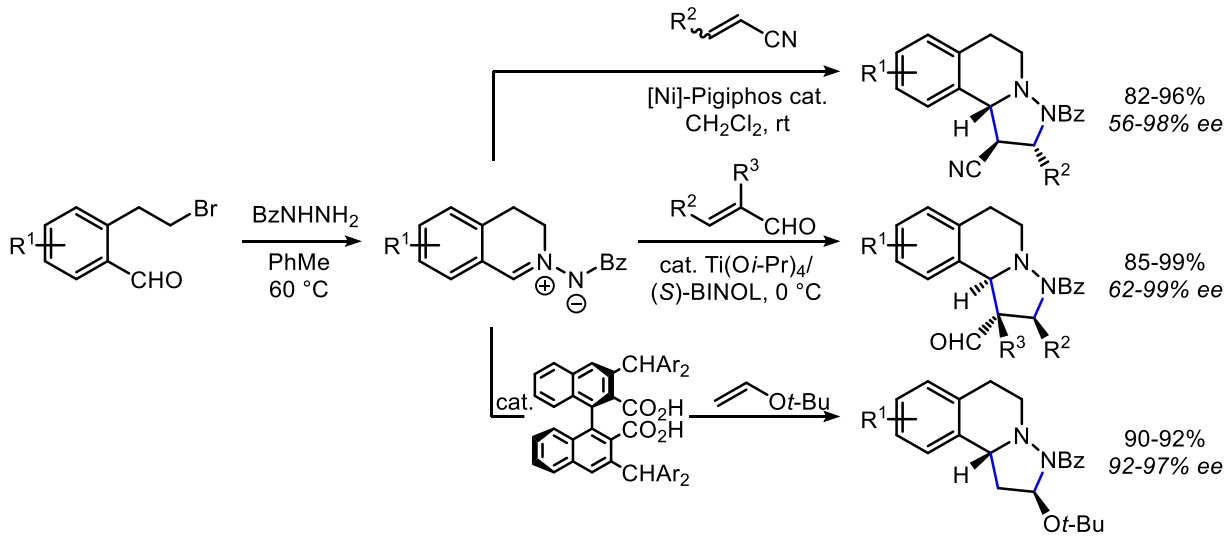

Scheme 1.26. Synthesis and examples of [3+2] cycloaddition reactions with a C,N-Cyclic azomethine imine.

N,N'-Cyclic azomethine imines can be described by their core structure, derived from different 5-membered heterocycles (Figure 1.9), although 4- and 6-membered rings are also known.

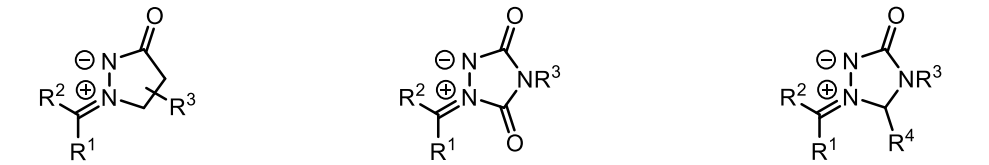

Figure 1.9. N,N'-Cyclic azomethine imines and their derivative heterocycles (in brackets).

Earlier in this chapter triazolidine-3,5-dione derived azomethine imines were presented as products of imino-isocyanate and *C*-isocyanate [3+2] cycloaddition reactions, or from the procedures by Jones & Regitz (Scheme 1.27). These dipoles have been shown to undergo [3+2] cycloadditions with phenyl isocyanate and dimethyl but-2-ynedioate, but this is the extent to which their reactivity was studied (Scheme 1.27). In a report by Wilson, a cyclic azomethine imine

derived from 2,3-dimethylindole and *N*-phenyl triazolinedione was found to be sensitive to water and acid, and was shown to readily undergo hydrolysis under various conditions.[104]

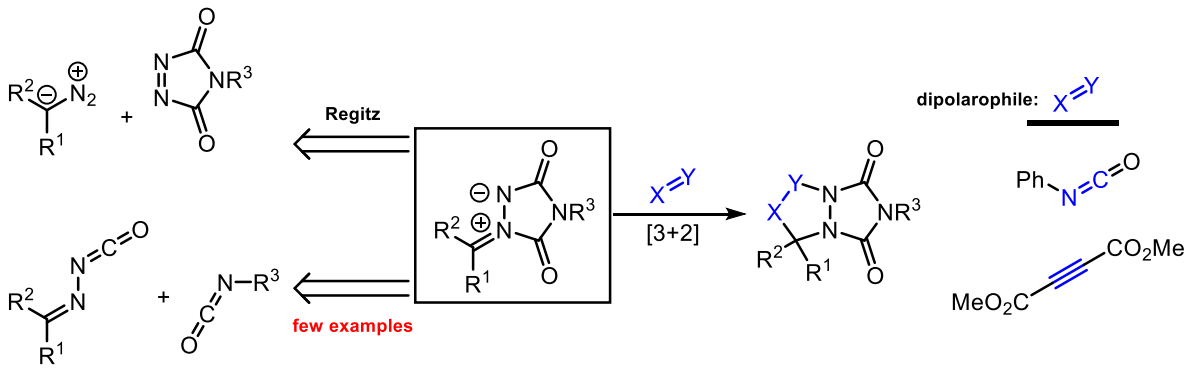

Scheme 1.27. Synthesis and [3+2] reactivity of triazolidine-dione derived N,N'-cyclic azomethine imines.

Pyrazolidin-3-one derived *N,N'*-cyclic azomethine imines are typically stable and isolable, and contain the valuable β-amino carbonyl motif (see Chapter 1.1). Since their first synthesis by Dorn & Otto in 1968,[105] they have been useful to chemists for studying 1,3-dipolar cycloadditions. There are examples of reactivity with many different dipolarophiles, and enantioselective variants of [3+2] cycloadditions with these substrates are now common in the literature (Scheme 1.28).[18-27] These reactions have been catalyzed by metals such as Cu, Ni, Au, and Mg, Lewis bases like phosphines, and also NHCs and Lewis or Brønsted acids. Overall, these *N,N*'-cyclic azomethine imines are extremely popular in the field of asymmetric catalysis.

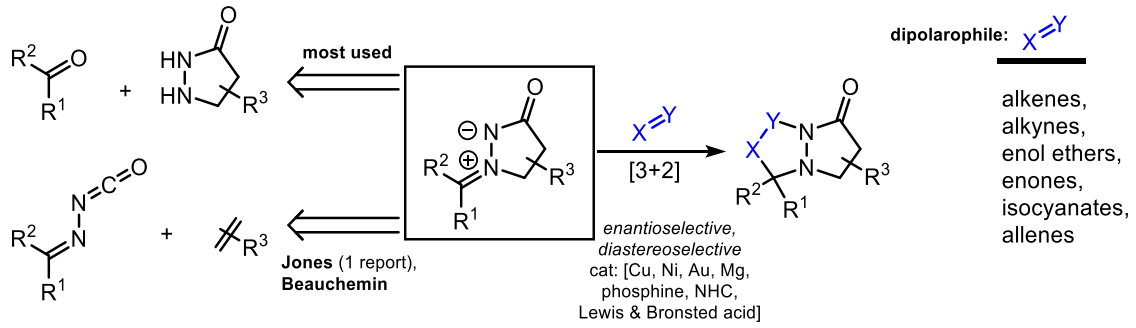

Scheme 1.28. Synthesis and [3+2] reactivity of pyrazolidin-3-one derived N,N'-cyclic azomethine imines.

These *N,N'*-cyclic azomethine imines are almost exclusively synthesized by simple condensation of the pyrazolidinone core onto aldehydes (ketones are generally unreactive in this respect). This reaction works best for electron poor aldehydes, and the complexity is limited by the availability and reactivity of the pyrazolidinone. Structurally complex/substituted pyrazolidinones are usually unavailable or not suitable for this chemistry. Within the >100 publications using these azomethine imines as substrates, only a handful have any substitution other than H or Me on the pyrazolidinone ring (Figure 1.10). This lack of complexity in the structure of these azomethine imines translates to the cycloadducts, where diversity comes only from the dipolarophile. As such, these azomethine imines are rarely used as precursors to valuable β-amino carbonyl compounds.

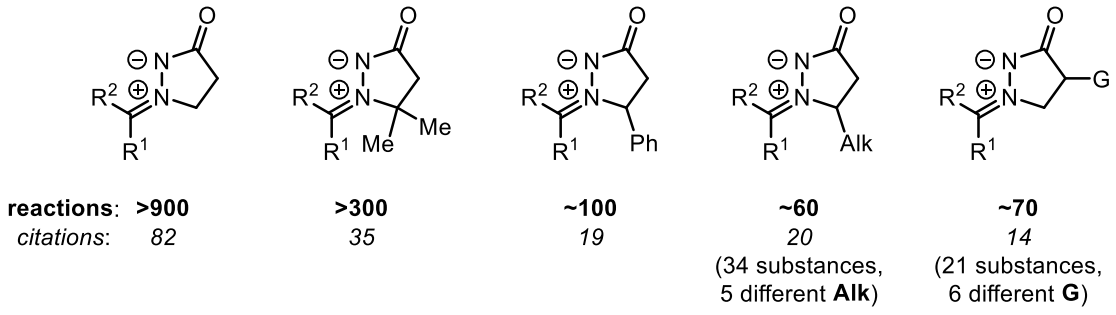

Figure 1.10. Substrates in reactions of pyrazolidin-3-one azomethine imines. Alk = any alkyl group. G = any group, including heteroatom, but not H.

This point is illustrated in a recent article describing a diastereoselective [3+2] cycloadditions of pyrazolidin-3-one azomethine imines with lithium ynolates (Scheme 1.29). Most of the reactivity is performed with 4,5-unsubstituted azomethine imines derived from aryl aldehydes. After the [3+2] cycloaddition, the azomethine imine-derived portion is removed by heating under acidic conditions. This provides a new pyrazolidinone that is more complex than the one from which the starting material was derived. The simple azomethine imine portion is expendable, and used as a chiral auxiliary in stereospecific [3+2] reactions (Scheme 1.29). This example shows that

the synthesis of complex azomethine imines from pyrazolidinone precursors is difficult, especially for enantioenriched compounds.

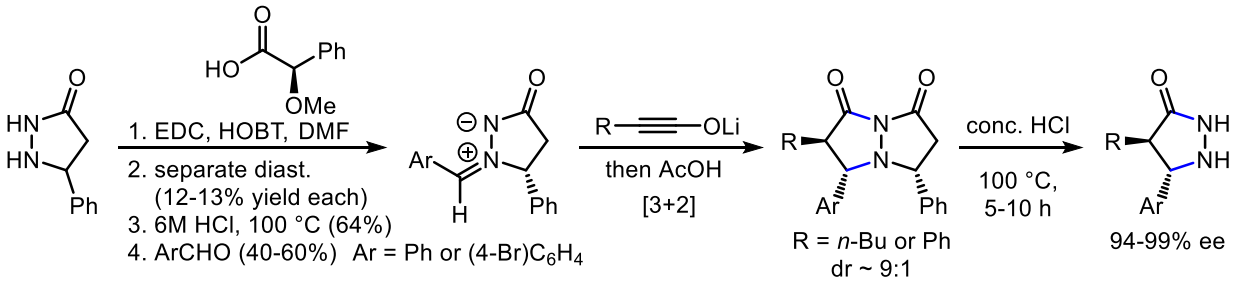

Scheme 1.29. Ready's procedure for the synthesis of enantioenriched 4,5-substituted pyrazoldinin-3-ones, starting from racemic 5-Ph pyrazolidinone, via azomethine imine [3+2] cycloaddition.

In contrast to this approach, our group has been interested in developing a general alkene aminocarbonylation reaction to broaden the scope of accessible pyrazolidinone azomethine imines, and thus make them useful precursors to compounds containing the β-amino carbonyl motif. Herein we will describe this work, including exploration of reactivity of imino-isocyanates in the synthesis of novel azomethine imines with valuable heterocyclic cores.

1.4. References

(1) Steer, D. L.; Lew, R. A.; Perlmutter, P.; Smith, A. I.; Aguilar, M.-I. *Curr. Med. Chem.* **2002**, *9*, 811.
(2) Seebach, D.; Beck, A. K.; Bierbaum, D. J. *Chem. Biodivers.* **2004**, *1*, 1111.
(3) Kuhl, A.; Hahn, M. G.; Dumić, M.; Mittendorf, J. *Amino Acids* **2005**, *29*, 89.
(4) Seebach, D.; Gardiner, J. *Acc. Chem. Res.* **2008**, *41*, 1366.
(5) Cabrele, C.; Martinek, T. A.; Reiser, O.; Berlicki, Ł. *J. Med. Chem.* **2014**, *57*, 9718.
(6) Gellman, S. H. *Acc. Chem. Res.* **1998**, *31*, 173.
(7) Porter, E. A.; Wang, X.; Lee, H.-S.; Weisblum, B.; Gellman, S. H. *Nature* **2000**, *404*, 565.
(8) Checco, J. W.; Lee, E. F.; Evangelista, M.; Sleebs, N. J.; Rogers, K.; Pettikiriarachchi, A.; Kershaw, N. J.; Eddinger, G. A.; Belair, D. G.; Wilson, J. L.; Eller, C. H.; Raines, R. T.; Murphy, W. L.; Smith, B. J.; Gellman, S. H.; Fairlie, W. D. *J. Am. Chem. Soc.* **2015**.
(9) Dhar, D. N.; Dhar, P. *The Chemistry of Chlorosulfonyl Isocyanate*; World Scientific, 2002.
(10) Dener, J. M.; Fantauzzi, P. P.; Kshirsagar, T. A.; Kelly, D. E.; Wolfe, A. B. *Org. Process Res. Dev.* **2001**, *5*, 445.
(11-13) Bondock, S.; Rabie, R.; Etman, H. A.; Fadda, A. A. *Eur. J. Med. Chem*. **2008**, *43*, 2122.; Sujatha, K.; Shanthi, G.; Selvam, N. P.; Manoharan, S.; Perumal, P. T.; Rajendran, M. *Bioorg. Med. Chem. Lett.* **2009**, *19*, 4501.; Watanabe, T.; Yuki, S.; Egawa, M.; Kellner, H. M. *Br. J. Clin. Pharmacol.* **1980**, *10*, 2995.;
(14-17) Maser, H.; Boehner, B.; Forey, W. Eur. Patent Appl. EP 268554, 1988.; Yagi, K.; Numata, A.; Mimori, N.; Miyake, T.; Arai, K.; Ishii, S. *Pestic. Sci.* **1999**, *55*, 161.; Naylan, S. S.; Singh, C. P. Asian J. Chem. **1999**, *11*, 207.

(18-27) Recent examples of azomethine imine asymmetric dipolar cycloadditions: Shintani, R.; Fu, G. C. *J. Am. Chem. Soc.* **2003**, *125*, 10778; Shintani, R.; Hayashi, T. *J. Am. Chem. Soc.* **2006**, *128*, 6330; Suga, H.; Funyu, A.; Kakehi, A. *Org. Lett.* **2007**, *9*, 97; Chan, A.; Scheidt, K. A. *J. Am. Chem. Soc.* **2007**, *129*, 5334; Sibi, M. P.; Rane, D.; Stanley, L. M.; Soeta, T. *Org. Lett.* **2008**, *10*, 2971; Shapiro, N. D.; Shi, Y.; Toste, F. D. *J. Am. Chem. Soc.* **2009**, *131*, 11654; Na, R.; Jing, C.; Xu, Q.; Jiang, H.; Wu, X.; Shi, J.; Zhong, J.; Wang, M.; Benitez, D.; Tkatchouk, E.; Goddard, W. A.; Guo, H.; Kwon, O. *J. Am. Chem. Soc.* **2011**, *133*, 13337; Xu, X.; Qian, Y.; Zavalij, P. Y.; Doyle, M. P. *J. Am. Chem. Soc.* **2013**, *135*, 1244; Zhu, R.-Y.; Wang, C.-S.; Zheng, J.; Shi, F.; Tu, S.-J. *J. Org. Chem.* **2014**, *79*, 9305; Hori, M.; Sakakura, A.; Ishihara, K. *J. Am. Chem. Soc.* **2014**, *136*, 13198.
(28-30) Kawai, H.; Kusuda, A.; Nakamura, S.; Shiro, M.; Shibata, N. *Angew. Chemie Int. Ed.* **2009**, *48*, 6324; Shintani, R.; Soh, Y.-T.; Hayashi, T. *Org. Lett.* **2010**, *12*, 4106; Imaizumi, T.; Yamashita, Y.; Kobayashi, S. *J. Am. Chem. Soc.* **2012**, *134*, 20049.
(31) Juaristi, E.; Soloshonok, V. A. *Enantioselective Synthesis of Beta-Amino Acids, 2nd Edition*; Wiley, 2005.
(32) Kiss, L.; Fülöp, F. *Chem. Rev.* **2014**, *114*, 1116.
(33) Seebach, D.; Beck, A.; Capone, S.; Deniau, G.; Grošelj, U.; Zass, E. *Synthesis* **2009**, 1.
(34) Podlech, J.; Seebach, D. *Angew. Chemie Int. Ed.* **1995**, *34*, 471.
(35) Uraguchi, D.; Terada, M. *J. Am. Chem. Soc.* **2004**, *126*, 5356.
(36) Akiyama, T.; Itoh, J.; Yokota, K.; Fuchibe, K. *Angew. Chem., Int. Ed.* **2004**, *43*, 1566.
(37) Guo, Q.-X.; Liu, H.; Guo, C.; Luo, S.-W.; Gu, Y.; Gong, L.-Z. *J. Am. Chem. Soc.* **2007**, *129*, 3790.
(38) Bandar, J. S.; Lambert, T. H. *J. Am. Chem. Soc.* **2013**, *135*, 11799.
(39) Gerfaud, T.; Chiang, Y. L.; Kreituss, I.; Russak, J. A.; Bode, J. W. *Org. Process Res. Dev.* **2012**, *16*, 687.
(40) Beller, M.; Seayad, J.; Tillack, A.; Jiao, H. *Angew. Chem. Int. Ed.* **2004**, *43*, 3368.
(41) Beccalli, E. M.; Broggini, G.; Martinelli, M.; Sottocornola, S. *Chem. Rev.* **2007**, *107*, 5318.
(42) Gooch, E. E. *J. Chem. Educ.* **2001**, *78*, 1358.
(43) Hegedus, L. S.; Allen, G. F.; Olsen, D. J. *J. Am. Chem. Soc.* **1980**, *102*, 3583.
(44) Tamaru, Y.; Kobayashi, T.; Kawamura, S.; Ochiai, H.; Yoshida, Z. *Tetrahedron Lett.* **1985**, *26*, 4479.
(45) Tamaru, Y.; Hojo, M.; Higashimura, H.; Yoshida, Z. *J. Am. Chem. Soc.* **1988**, *110*, 3994.
(46) Fox, D. N. A.; Lathbury, D.; Mahon, M. F.; Molloy, K. C.; Gallagher, T. *J. Am. Chem. Soc.* **1991**, *113*, 2652.
(47) Ham, W.; Hoon, Y.; Kyenghae, J.; Oh, C.; Lee, K. *Tetrahedron Lett.* **1997**, *38*, 3247.
(48) Szolcsányi, P.; Gracza, T.; Koman, M.; Prónayová, N.; Liptaj, T. *Tetrahedron Asymmetry* **2000**, *11*, 2579.
(49) Shinohara, T.; Arai, M. A.; Wakita, K.; Arai, T.; Sasai, H. *Tetrahedron Lett.* **2003**, *44*, 711.
(50) Tsujihara, T.; Shinohara, T.; Takenaka, K.; Takizawa, S.; Onitsuka, K.; Hatanaka, M.; Sasai, H. *J. Org. Chem.* **2009**, *74*, 9274.
(51) Hegedus, L. S.; Darlington, W. H. *J. Am. Chem. Soc.* **1980**, *102*, 4980.
(52) Hegedus, L. S.; Winton, P. M.; Varaprath, S. *J. Org. Chem.* **1981**, *46*, 2215.
(53) Cheng, J.; Qi, X.; Li, M.; Chen, P.; Liu, G. *J. Am. Chem. Soc.* **2015**, *137*, 2480.
(54-56) Moriconi, E. J.; Kelly, J. F. *J. Org. Chem.* **1968**, *33*, 3036; Rasmussen, J. K.; Hassner, A. *Chem. Rev.* **1976**, *76*, 389; Murthy, K. S. K.; Dhar, D. N. *Synthesis* **1986**, 437.
(57) Nakamura, A. *J. Synth. Org. Chem. Jpn* **1988**, *46*, 1209

(58) Roveda, J. G.; Clavette, C.; Hunt, A. D.; Gorelsky, S. I.; Whipp, C. J.; Beauchemin, A. M. *J. Am. Chem. Soc.* **2009**, *131*, 8740.
(59) Cooper, N. J.; Knight, D. W. *Tetrahedron* **2004**, *60*, 243.
(60) Beauchemin, A. M. *Org. Biomol. Chem.* **2013**, *11*, 7039.
(61) Ivanovich, R. A.; Clavette, C.; Vincent-Rocan, J.-F.; Roveda, J.-G.; Gorelsky, S. I.; Beauchemin, A. M. *Chem. - A Eur. J.* **2016**, *22*, 7906.

(62) Clavette, C. Synthesis of beta-Aminocarbonyl Compounds and Hydrazine Derivatives Using Amino- and Imino-Isocyanates, PhD Thesis, University of Ottawa, 2015.
(63) Yudin, A. K.; Hili, R. *Chem. - A Eur. J.* **2007**, *13*, 6538.
(64-68) Selected examples of amphoteric reactivity: He, Z.; Zajdlik, A.; Yudin, A. K. *Acc. Chem. Res.* **2014**, *47*, 1029.; Hili, R.; Yudin, A. K. *J. Am. Chem. Soc.* **2006**, *128*, 14772.; Li, X.; Yudin, A. K. *J. Am. Chem. Soc.* **2007**, *129*, 14152.; Hili, R.; Yudin, A. K. *Angew. Chem., Int. Ed.* **2008**, *47*, 4188.; Hili, R.; Yudin, A. K. *J. Am. Chem. Soc.* **2009**, *131*, 16404.
(69) Ulrich, H. In *Cycloaddition Reactions of Heterocumulenes*; Academic Press Inc., 1967; p. 374.
(70) Huisgen, R. *Angew. Chemie Int. Ed.* **1963**, *2*, 565.
(71) Seidl, H.; Huisgen, R.; Grashey, R. *Chem. Ber.* **1969**, *102*, 926.
(72) Wentrup, C.; Finnerty, J. J.; Koch, R. *Curr. Org. Chem.* **2011**, *15*, 1745.
(73) Pasinszki, T.; Krebsz, M.; Tarczay, G.; Wentrup, C. *J. Org. Chem.* **2013**, *78*, 11985.
(74) Koch, R.; Finnerty, J. J.; Wentrup, C. *J. Org. Chem.* **2011**, *76*, 6024.
(75) Vincent-Rocan, J.-F.; Beauchemin, A. M. *Synthesis* **2016**, *48*, 3625-3645.
(76-82) Examples of access to amino-isocyanates: Lwowski, W.; DeMauriac, R. *Tetrahedron Lett.* **1964**, *205*, 3285.; Wadsworth, W. S.; Emmons, W. D. *J. Org. Chem.* **1967**, *32*, 1279.; Chupp, J. P.; Alt, G. H. *Tetrahedron Lett.* **1970**, 3155.; Chupp, J. P. *J. Heterocycl. Chem.* **1971**, *8*, 557.; Lwowski, W.; de Mauriac, R. A.; Thompson, M.; Wilde, R. E.; Chen, S.-Y. *J. Org. Chem.* **1975**, *40*, 2608.; Lwowski, W.; Kanemasa, S.; Murray, R. A.; Ramakrishnan, V. T.; Thiruvengadam, T. K.; Yoshida, K.; Subbaraj, A. *J. Org. Chem.* **1986**, *51*, 1719.; Gibson, H. H.; Weissinger, K.; Abashawl, A.; Hall, G.; Lawshae, T.; LeBlanc, K.; Moody, J.; Lwowski, W. *J. Org. Chem.* **1986**, *51*, 3858.
(83) Selected reviews on blocked isocyanates (a) Wicks, D. A.; Wicks Jr., Z. W. *Prog. Org. Coatings* **1999**, *36*, 148. (b) Wicks, D. A.; Wicks Jr., Z. W. *Prog. Org. Coatings* **2001**, *41*, 1. (c) Wicks, D. A.; Wicks Jr., Z. W. *Prog. Org. Coatings* **2001**, *43*, 131.
(84) Lockley, W. J. S.; Ramakrishnan, V. T.; Lwowski, W. *Tetrahedron Lett.* **1974**, *15*, 2621.
(85) Lockley, W. J. S.; Lwowski, W. *Tetrahedron Lett.* **1974**, *15*, 4263.
(86) Reichen, W. *Chem. Rev.* **1978**, *78*, 569.
(87) Vincent-Rocan, J.-F.; Ivanovich, R. A.; Clavette, C.; Leckett, K.; Bejjani, J.; Beauchemin, A. M. *Chem. Sci.* **2016**, *7*, 315.
(88) Larsen, C.; Jakobsen, P. *Acta Chem. Scand.* **1970**, *24*, 1445.
(89) Chudgar, N. K.; Shah, S. N.; Vora, R. A. *Mol. Cryst. Liq. Cryst.* **1991**, *209*, 237.
(90) Shah, S. N.; Chudgar, N. K. *Molecules* **2000**, *5*, 657.
(91) Ramakrishnan, K.; Fulton, J. B.; Warkentin, J. *Tetrahedron* **1976**, *33*, 2685.
(92) Jones, D. W. *J. Chem. Soc. Chem. Commun.* **1982**, 766.
(93) Theis, W.; Bethauser, W.; Regitz, M. *Chem. Ber.* **1985**, *118*, 28.
(94) Clavette, C.; Gan, W.; Bongers, A.; Markiewicz, T.; Toderian, A. B.; Gorelsky, S. I.; Beauchemin, A. M. *J. Am. Chem. Soc.* **2012**, *134*, 16111.
(95) Nájera, C.; Sansano, J. M.; Yus, M. *Org. Biomol. Chem.* **2015**, *13*, 8596.
(96) Schantl, J. G. In *Science of Synthesis - Heteroatom Analogues of Aldehydes and Ketones*; Bellus, D.; Padwa, A., Eds.; Thieme: Stuttgart, New York, 2004; Vol. 27, pp. 731–824.
(97) Shirakawa, S.; Lombardi, P. J.; Leighton, J. L. *J. Am. Chem. Soc.* **2005**, *127*, 9974.
(98) Hashimoto, T.; Takiguchi, Y.; Maruoka, K. *J. Am. Chem. Soc.* **2013**, *135*, 11473.
(99) Hong, X.; Küçük, H. B.; Maji, M. S.; Yang, Y.-F.; Rueping, M.; Houk, K. N. *J. Am. Chem. Soc.* **2014**, *136*, 13769.
(100-102) Hashimoto, T.; Maeda, Y.; Omote, M.; Nakatsu, H.; Maruoka, K. *J. Am. Chem. Soc.* **2010**, *132*, 4076.; Hashimoto, T.; Omote, M.; Maruoka, K. *Angew. Chemie Int. Ed.* **2011**, *50*, 8952.; Hashimoto, T.; Omote, M.; Maruoka, K. *Angew. Chemie Int. Ed.* **2011**, *50*, 3489.
(103) Milosevic, S.; Togni, A. *J. Org. Chem.* **2013**, *78*, 9638.
(104) Wilson, R. M.; Hengge, A. *Tetrahedron Lett.* **1985**, *26*, 3673.
(105) Dorn, H.; Otto, A. *Chem. Ber.* **1968**, *101*, 3287.

Chapter 2. Intermolecular Aminocarbonylation of Alkenes

2.1. Introduction

Since the initial discovery of alkene aminocarbonylation with imino-isocyanates, the Beauchemin group has focused on developing the reactivity into a useful route towards β-amino carbonyl compounds. The key aspect of our approach was to use hydrazones as stable and easily accessible imino-isocyanate precursors. There were few accounts that describe the formation and reactivity of imino-isocyanates (Chapter 1.3), and no reports using hydrazone precursors to access imino-isocyanates for cycloaddition reactivity. The group first studied how the basic structure of the hydrazone, such as the blocking group or the derivative aldehyde or ketone, would affect the overall aminocarbonylation reactivity (Scheme 2.1). Early in this research, optimization of the hydrazone was focused on preventing 1,3-dipolar cycloaddition of the product azomethine imine with the alkene (Scheme 2.1), since excess alkene is required to prevent degradation of the imino-isocyanate by dimerization or trimerization. An initial scan of aldehyde reagents revealed several side reactions of this type, as well as mixtures of diastereomers.

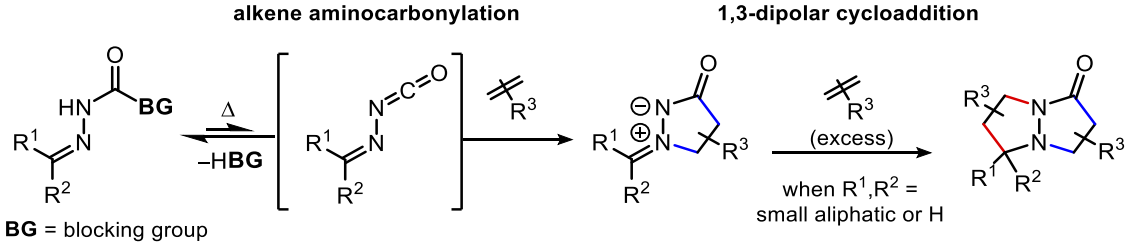

Scheme 2.1. Alkene aminocarbonylation with imino-isocyanate and unwanted dipolar cycloaddition with alkene.

For simplicity and to prevent these side reactions, further studies focused on symmetrical ketones with increasing bulk. Several *N*-Boc hydrazones were evaluated with norbornene in work by Dr. Gan and Dr. Clavette (Scheme 2.2). Hydrazones with small R groups (**1**, Me; **2**, Et) provided the azomethine imine products in 67-70% isolated yield, but complete consumption of hydrazone

was observed owing to competing side-reactions of the imino-isocyanate. Diisopropyl ketone derived hydrazone (**5**) gave 95% yield of the aminocarbonylation product. Presumably, the bulky isopropyl groups assist in shielding the dipole from a second cycloaddition and may also prevent dimerization of the reactive imino-isocyanate.

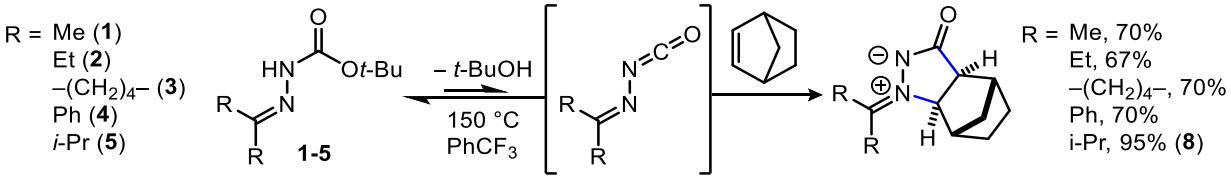

Scheme 2.2. Scope of ketone-derived hydrazones in the aminocarbonylation or norbornene.

The effect of the hydrazone blocking group (BG) was then investigated. There are two steps in the overall aminocarbonylation reaction: 1) generation of the reactive imino-isocyanate by expulsion of the leaving group; 2) cycloaddition of the imino-isocyanate with the alkene. The nature of the blocking group will affect which step is rate determining and the in situ concentration of imino-isocyanate at a given temperature. Drs. Gan and Clavette tested seven blocking groups and a range of temperatures in the reaction of diisopropylketone-derived hydrazones (**5a-g**) with excess norbornene (Table 2.1). In this experiment, all hydrazones are precursors to the same imino-isocyanate and product. At 150 °C, all blocking groups performed comparably. As the reaction temperature was lowered, the different groups had a large effect on the product yield. For example, hydrazone **5d** (BG = OPh) gave 84% yield of azomethine imine at 100 °C, whereas **5b** (BG = OEt) only provided an 8% yield of product was recovered after the reaction. At 80 °C, low yields of product were obtained with all hydrazones. This is attributed to small concentrations of imino-isocyanate at low temperatures and insufficient energy for the intermolecular cycloaddition to occur. The leaving groups OPh (entry 4) and O*t*-Bu (entry 1) were chosen for further investigations of hydrazone structure.

Table 2.1. Survey of leaving groups for a first generation aminocarbonylation reagent.[a]

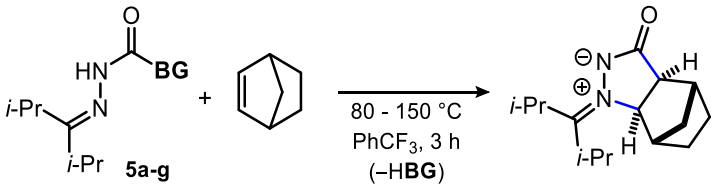

entry	BG	Yields (%)[b]			
		150 °C	120 °C	100 °C	80 °C
1	**5a**: O*t*-Bu	99	69	23	7
2	**5b**: OEt	99	8	0	0
3	**5c**: OCH_2CF_3	82	55	30	9
4	**5d**: OPh	92	85	84	38
5	**5e**: SEt	98	64	46	11
6	**5f**: SPh	90	69	60	31
7	**5g**: N(*i*-Pr)$_2$	90	69	46	13

a) Conditions: hydrazone (5a-g, 1 equiv.) and norbornene (10 equiv.) in $PhCF_3$ (0.05 M) heated in a sealed vial (microwave reactor, 80-150 °C, 3 h). b) NMR yields using 1,3,5-trimethoxybenzene as internal standard.

The first generation of hydrazones (**5a**-**g**) revealed leaving group trends and possible side reactions. The reactivity was optimized for norbornene, which is activated by strain, and these conditions did not give high yields of product with unactivated alkenes (e.g. styrene, 1-hexene, cycloalkenes). This is due to a difficult cycloaddition step, and not an issue with formation of the imino-isocyanate. In this chapter, work towards accessing reactivity with a broad scope of alkenes is presented. This centres around the reactivity of bulky, ketone-derived imino-isocyanate precursors. In parallel to this research, other group members studied improving reactions of aldehyde-derived precursors. Parts of their work is discussed throughout this chapter, and further information can be found in their communication in *Organic Letters*.[1]

Given the novelty of the cycloaddition, the reaction and its transition state were studied computationally. DFT calculations for a simplified model of alkene aminocarbonylation were performed by Dr. Serge Gorelsky (Figure 2.1).[2,3] The transition state (T.S.) calculations were performed on a simple imino-isocyanate with ethylene and norbornene. The transition state was

found to be asynchronous, bond ***a*** is more formed than bond ***b***. In this model, there is a partial positive charge on the alkene at the transition state.

Figure 2.1. Calculated alkene aminocarbonylation transition states (T.S.) of simplified model systems.

2.2. Results and Discussion

Optimization of the imino-isocyanate precursor and blocking group set the stage for exploring the scope of alkene aminocarbonylation. The end goal is the synthesis of complex azomethine imines and their derivative β-amino carbonyl compounds. Early on in this work, we found limits to the scope of reactivity with our first generation reagent **5a**, as well as issues with derivatization described above. This led us to search for an improved reagent, and to the discovery of better reactivity with hydrazones derived from fluorenone (**6a**). In this chapter, development of this new imino-isocyanate precursor will be presented, along with alkene scope and insights into its unique reactivity. Initial work with first generation reagents will also be described. Early contributions from Drs. Gan and Clavette will be noted.

2.2.1. Alkene aminocarbonylation with 1st generation reagent

My research began with assessing the reactivity of reagent **5** with protected allyl alcohols. This reaction would give access to azomethine imines with the β-homoserine motif, and synthesis of this amino acid analog by reductive N-N bond cleavage (Figure 2.2).

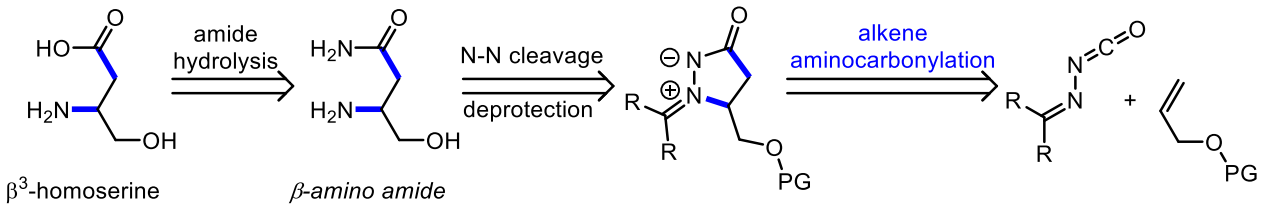

Figure 2.2. Retrosynthetic strategy to access β-homo serine by alkene aminocarbonylation.

We first tested allyl benzyl ether under standard reaction conditions, with the first generation hydrazone reagent **5a** (Table 2.2, entry 1). Unfortunately, this alkene was a poor substrate for the alkene aminocarbonylation reaction. Changing to neat conditions (entry 2), and shortening the reaction time (entry 3) had little effect on the yield of product (**7**). Surprisingly, a significant amount of the anti-Markovnikov regioisomer (***iso*-7**) was observed. Prior to this work, Dr. Clavette observed only small amounts of this regioisomer in reactions with 1-hexene.[2]

Table 2.2. Aminocarbonylation of allyl benzyl ether with reagent **5a** (BG = O*t*-Bu).[a]

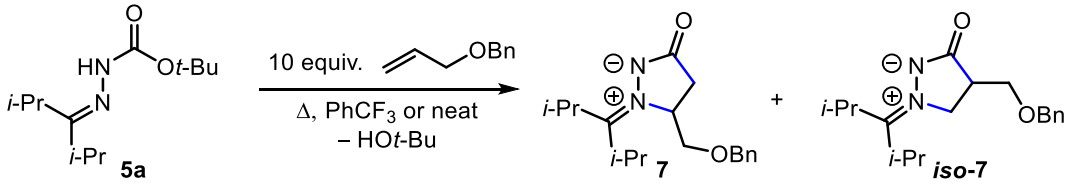

Entry	Solvent	t (h)	T (°C)	Yield (%) **7** [b]	Yield (%) ***iso*-7** [b]	*r* (**7**:***iso*-7**) [c]
1	$PhCF_3$	3	150	12	6	2:1
2	neat	3	150	13	6	2:1
3	neat	1	150	12	5	2:1

a) Conditions: Hydrazone **5a** (0.25 mmol, 1 equiv) and allyl benzyl ether (2.5 mmol, 10 equiv) were combined in a vial and purged with nitrogen. The reaction was heated by microwave irradiation, either neat or in $PhCF_3$ (5 mL). b) NMR yields are reported, determined using 1,3,5-trimethoxybenzene internal standard. c) *r* = ratio of products **7**:***iso*-7**, determined by analysis of the crude ^{1}H NMR spectrum.

The hydrazone reagent with BG = N(*i*-Pr)$_2$ (**5g**) showed slightly similar reactivity under standard conditions (Table 2.3, entry 2). When the reaction was heated to 200 °C, the major product was regioisomer ***iso*-7**, isolated in 15% yield (entry 3). The yields increased slightly under neat conditions at 150 °C, with the best yield of **7** being 16% (entry 4).

Table 2.3. Aminocarbonylation of allyl benzyl ether with reagent **5g** (BG = N(*i*-Pr)$_2$).[a]

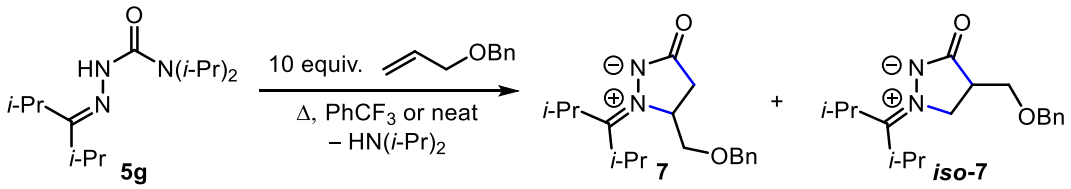

Entry	Solvent	t (h)	T (°C)	Yield (%) **7** [b]	Yield (%) ***iso*-7** [b]	*r* (**7**:***iso*-7**) [c]
1	$PhCF_3$	3	120	-	-	-
2	$PhCF_3$	3	150	12 (7)[d]	6	2:1
3	$PhCF_3$	3	200	3	17 (15)[d]	1:6
4	neat	3	150	16[e]	8[e]	2:1[e]
5	neat	0.2	150	12	7	2:1
6	neat	0.5	200	2	5	1:2

a) Conditions: Hydrazone **5g** (0.25-0.50 mmol, 1 equiv) and allyl benzyl ether (2.5-5.0 mmol, 10 equiv) were combined in a vial and purged with nitrogen. The reaction was heated by microwave irradiation, either neat or in $PhCF_3$ (5 mL). b) NMR yields are reported, determined using 1,3,5-trimethoxybenzene internal standard. c) *r* = ratio of products **7**:***iso*-7**, determined by analysis of the crude ^{1}H NMR spectrum. d) Isolated yields are given in brackets. e) Yields represent an average of two trials.

At this point, it was clear that allyl benzyl ether was a poor substrate for the reaction, as very little product was consistently observed (Scheme 2.3). Under the tested conditions (150-200 °C), the imino-isocyanate is readily available; this is indicated by high yields of cycloadduct that are obtained with norbornene (Table 2.1), and also by degradation of the starting material observed in unsuccessful reactions at these temperatures. This points to the cycloaddition being the limiting step, and the high concentration of the reactive imino-isocyanate generated was degrading instead of undergoing alkene aminocarbonylation. To counteract this, we tested a hydrazone reagent with a poorer leaving group (BG = OEt, **5c**). This would lower the concentration of imino-isocyanate, and possibly create conditions where the alkene aminocarbonylation could take place over long reaction times and without imino-isocyanate degradation.

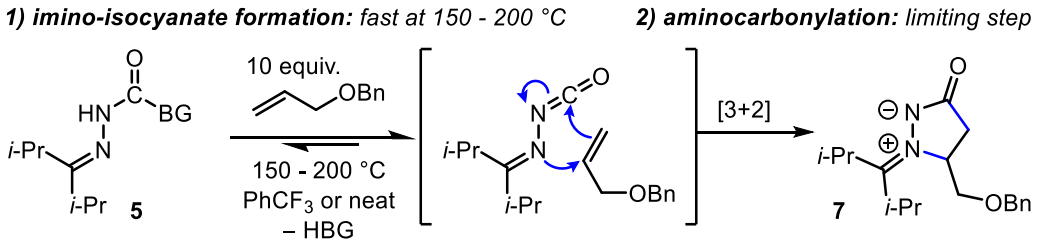

Scheme 2.3. Two steps of the alkene aminocarbonylation reaction from hydrazone precursor ***5****.*

The reaction of reagent **5c** (BG = OEt) with allyl benzyl ether did not improve yields of the desired product over 1 to 6 hours (Table 2.4). We observed recovery of starting material, thanks to controlling the concentration of imino-isocyanate, but this did not lead to increased yield of product or improved regioselectivity.

Table 2.4. Aminocarbonylation of allyl benzyl ether with reagent **5c** (BG = OEt).[a]

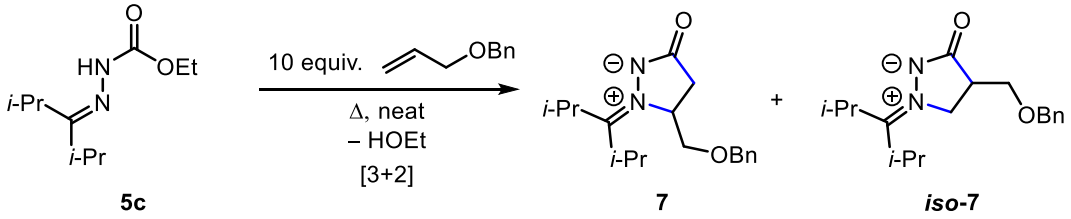

Entry	Solvent	t (h)	T (°C)	Yield (%) **7** [b]	Yield (%) ***iso*-7** [b]	*r* (**7**:***iso*-7**) [c]
1	neat	1	150	3	1	3:1
2	neat	3	150	3	1	3:1
3	neat	6	150	-	-	-
4	neat	0.5	200	2	2	1:1

a) Conditions: Hydrazone **5c** (0.25-0.50 mmol, 1 equiv) and allyl benzyl ether (2.5-5.0 mmol, 10 equiv) were combined in a vial and purged with nitrogen. The reaction was heated neat by microwave irradiation. b) NMR yields are reported, determined using 1,3,5-trimethoxybenzene internal standard. c) *r* = ratio of products **7**:***iso*-7**, determined by analysis of the crude ^{1}H NMR spectrum.

The limited reactivity of allyl benzyl ether with imino-isocyanates is in agreement with the calculated asynchronous transition state described above.[3] This transition state model places a partial positive charge on allyl benzyl ether, and predicts limited reactivity for electron deficient alkenes.

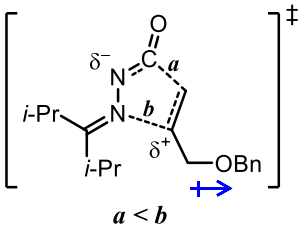

Figure 2.3. Concerted asynchronous transition state model for the aminocarbonylation of allyl benzyl ether.

The observed reactivity trend suggests a rate-limiting transition state involving the HOMO of the alkene and the LUMO of the imino-isocyanate (Figure 2.4). Electron-deficient alkenes like allyl benzyl ether have stabilized HOMO orbitals, which increases the energy gap between this orbital and the imino-isocyanate LUMO. In addition, this rationalizes the anti-Markovnikov regioselectivity observed with this electron deficient alkene, due to a change in the orbital coefficients of the HOMO compared to electron rich alkenes.

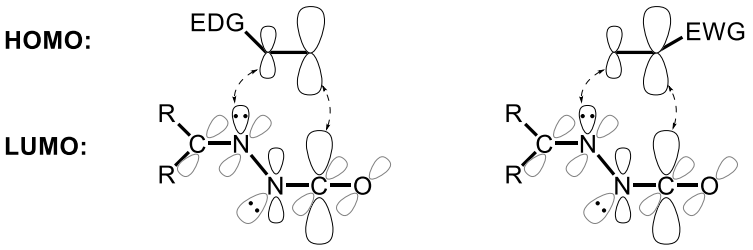

Figure 2.4. FMO Diagram for the cycloaddition of imino-isocyanates (LUMO) with alkenes (HOMO).

In testing the limits of alkene reactivity, we gained valuable insight into cycloaddition reactions of imino-isocyanates. We found that the overall result of the reaction relies on interacting factors such as the blocking group, imino-isocyanate concentration, and alkene reactivity. These principles were taken forward and used to direct our search for a new imino-isocyanate reagent for alkene aminocarbonylation, to access reactivity with less activated alkenes.

An important reason to design a new aminocarbonylation reagent was for the end goal of accessing β-amino acid derivatives. The essential steps to access the desired β-amino acid derivatives are N-N bond cleavage and deprotection of the β-amine (Scheme 2.4). Unfortunately,

the products from the diisopropyl precursor (eg. **8**) were resistant to reductive N-N bond cleavage, likely due to the high steric shielding that was required to prevent unwanted dipolar cycloaddition. Deprotection of the diisopropyl methylene after reductive cleavage was also not feasible. A more versatile reagent was needed in order to access a variety of β-amino carbonyl compounds. Ideally, this would include having a functional group on the nitrogen that could be easily removed by known methods or reduced to provide a built-in protecting group.

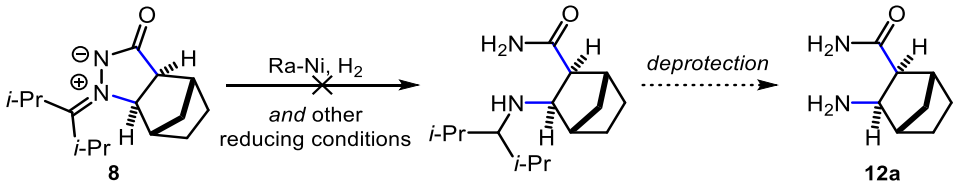

Scheme 2.4. Attempted derivatization of first generation alkene aminocarbonylation products.

2.2.2. Alkene aminocarbonylation with 2nd generation reagent

While the above work was underway, Drs. Gan & Clavette and Thomas Markiewicz were searching for a new imino-isocyanate derived from a symmetrical ketone. Single X-ray crystal structures of diisopropyl- and diphenyl-derived azomethine imines show that the groups are twisted or staggered to each other, which both shields the dipole and creates the steric hindrance that confers resistance to reductive bond cleavage (Figure 2.5).

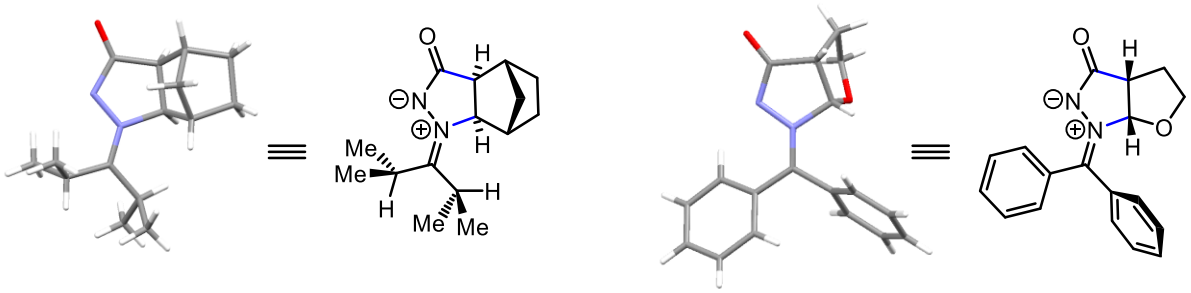

Figure 2.5. Single crystal X-ray structures of bulky ketone-derived azomethine imines.

The new reagent would ideally shield or stabilize the dipole without hindering approach of a reductant. We thought that planar, conjugated systems could allow delocalization of the

developing negative charge on the nitrogen and stabilize the product toward unwanted dipolar cycloaddition. From these criteria the fluorenone-derived hydrazone reagent was discovered. The hydrazone derived from fluorenone (**6a**, BG=OPh) was simple and inexpensive to prepare, and showed excellent reactivity at 120 °C with norbornene, giving **9a** in 99% yield (Scheme 2.5). Dr. Gan also demonstrated the utility of the fluorenyl group in accessing the free β-amino amide from the azomethine imine (Scheme 2.5). With the reagent in hand, we began to explore reactivity of this reagent with less activated alkenes.

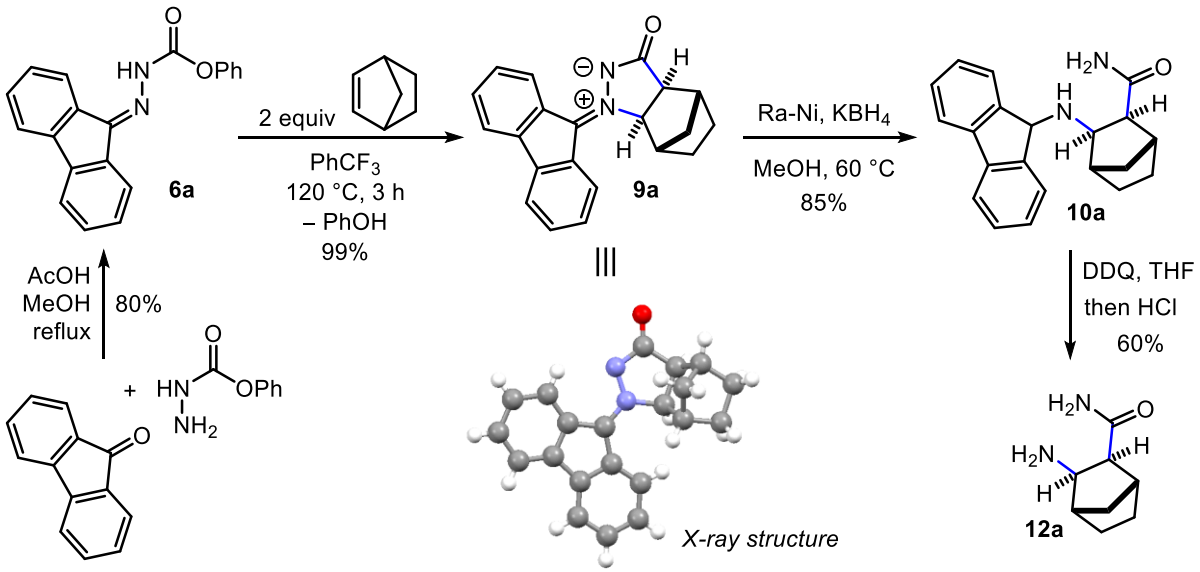

*Scheme 2.5. Synthesis and reactivity of new fluorenone-derived reagent **6a**, including reductive ring opening and deprotection to the free β-amino amide (by Dr. Gan).*

Initial experiments were performed with reagent **6a** and allyl benzyl ether to access product **9b**. Unfortunately, this alkene was still unreactive towards alkene aminocarbonylation (Scheme 2.6). Reagent **6b** (BG = O*t*-Bu) also showed low reactivity with allyl benzyl ether, and a 5:1 mixture of **9b:iso-9b** was observed in 6% combined yield. These results supported the idea that the HOMO of the alkene reacts with the LUMO of the imino-isocyanate.

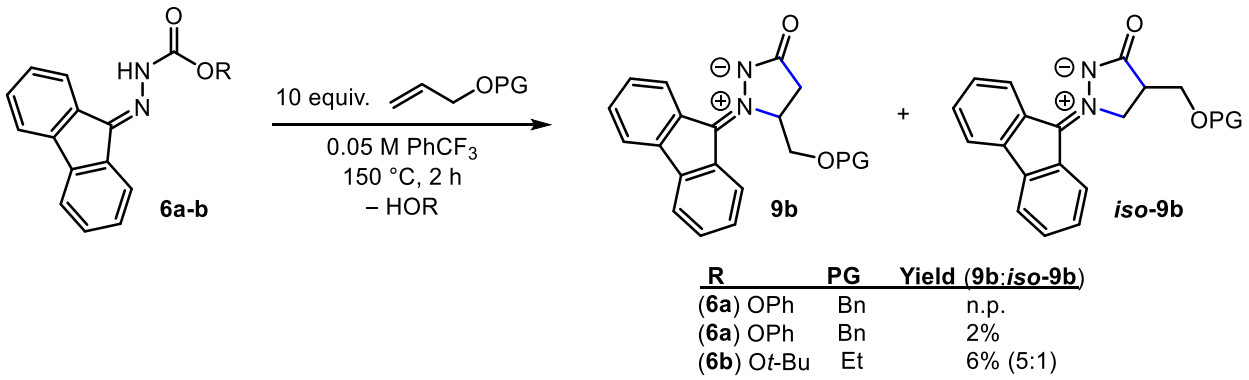

R	PG	Yield (9b:*iso*-9b)
(**6a**) OPh	Bn	n.p.
(**6a**) OPh	Bn	2%
(**6b**) O*t*-Bu	Et	6% (5:1)

Scheme 2.6. Initial test of fluorenone-derived reagents in aminocarbonylation reaction of protected allyl ethers.

Instead, we decided to optimize the reactivity optimization of **6a** with an 'unactivated' alkene, 1-hexene (Table 2.5). Under standard reaction conditions at 150 °C, 73% of the desired product was obtained with high regioselectivity for the Markovnikov isomer **9c** (entry 4). Increasing the reaction concentration (0.1 and 0.5 M) caused a slight decrease in yield and selectivity. When the blocking group was changed to O*t*-Bu (**6b**), the yield of **9c** fell to 38% (entry 5). Importantly, good reactivity was also observed at 100 °C (entry 6, 57% NMR yield, 49% isolated), just under the boiling point of $PhCF_3$ (102 °C). Operating the reaction at 100 °C is desirable, because it allows for conventional heating under reflux conditions, without a sealed vial, and this should lead to more reproducible results.

Table 2.5. Optimization of 1-hexene aminocarbonylation with reagents **6a** and **6b**.[a]

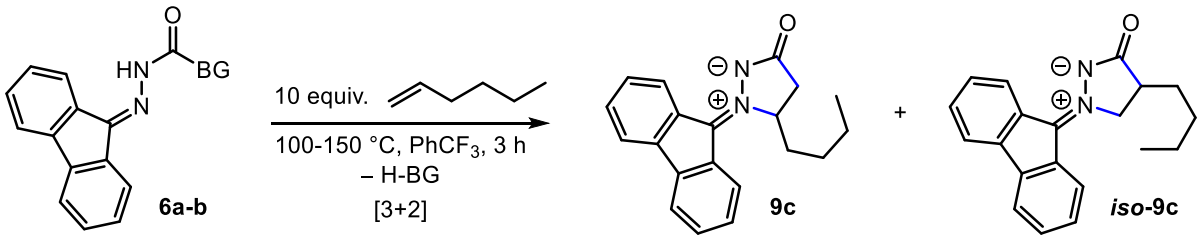

Entry	BG	Concentration (M)	T (°C)	Yield (%) **9c** [b]	Yield (%) ***iso*-9c** [b]
1	OPh (**6a**)	0.50	150	67	3
2	OPh (**6a**)	0.25	150	67	3
3	OPh (**6a**)	0.10	150	67	3
4	OPh (**6a**)	0.05	150	73 (73)[c]	3
5	O*t*-Bu (**6b**)	0.05	150	38	2
6	OPh (**6a**)	0.05	100	57 (49)[c,d]	2

a) Conditions: Hydrazone **6a** or **6b** (0.25 mmol, 1 equiv) and 1-hexene (2.5 mmol, 10 equiv), and $PhCF_3$ (0.5-5 mL) were combined in a vial and purged with nitrogen. The reaction was heated by microwave irradiation. b) NMR yields are reported, determined using 1,3,5-trimethoxybenzene internal standard. c) Isolated yield. d) Gram scale reaction.

Additionally, we observed intact starting material **6a** after reactions at 100 °C. Notably, all starting material was consumed when reactions were performed at or above 120 °C, and in reactions with the 1st generation reagent **5a**. This indicates a beneficial equilibrium between hydrazone precursor and imino-isocyanate at 100 °C, releasing just enough imino-isocyanate for the reaction without concerns of dimerization. Practically, this meant that longer reaction times at 100 °C could be used to increase yields. With these conditions, we moved forward to study the scope of the reaction of reagent **6a**. Presented herein are results from the scope study that I performed, unless otherwise noted.

Table 2.6 shows the scope of aminocarbonylation with aliphatic and cyclic alkenes. The alkenes were first tested under the optimized conditions (100 °C, 3 h, 10 equiv alkene), and variations were tested when low yields were observed. Homoallyl benzyl ether performed better than allyl benzyl ether (see Scheme 2.6), with reduced inductive withdrawing effect on the alkene, and gave **9d** in

39% yield. The yield of **9d** was improved to 52% by increasing the reaction time to 6 hours. Allyl trimethylsilane was an excellent substrate, providing **9e** in 81% isolated yield. This is likely due to stabilization of the partial positive charge on the olefin by the β-silicon atom. Increasing bulk of the aliphatic chain (**9f**,**g**) had a negative impact on the yield. Increasing the reaction time to 16 hours decreased the yield of **9g**, due to a slow degradation of the product. Cyclic alkenes showed an interesting trend with ring size. Under similar conditions, yields were highest for n=1 (cyclopentene; **9h**, 69-76%), lowest for n=2 (**9i**, 10%), and moderate for n=3 (**9j**, 40%) and n=4 (**9k**, 54%). This is attributed to varying conformational effects and changes in strain with the different ring sizes. To obtain a suitable yield of **9i**, the reaction was performed neat in freshly distilled (or newly opened) cyclohexene at 150 °C. On the other hand, norbornene is highly reactive due to high strain. In fact, only one equivalent of norbornene is required to give good yields of **9a**, and short reaction times at 150 °C also provided high yield. Surprisingly, a strained cyclopropene was unreactive, and provided none of the desired product **9m**. Cyclic aliphatic alkenes with electron-withdrawing atoms were poorly reactive, providing either no product (**9n**,**o**) or low yield (**9p**). Disubstituted internal alkenes are also a challenge, and product **9r** was observed in only 3% NMR yield. In our only experiment with a gaseous alkene, ethylene, we observed 6% of **9q** by ^{1}H NMR after only 1 hour at 100 °C. While there is room for improvement, this result is interesting for applications in detecting ethylene gas, which is important in the food supply industry.[4]

Table 2.6. Scope of aliphatic and cyclic alkene aminocarbonylation with reagent **6a**.[a]

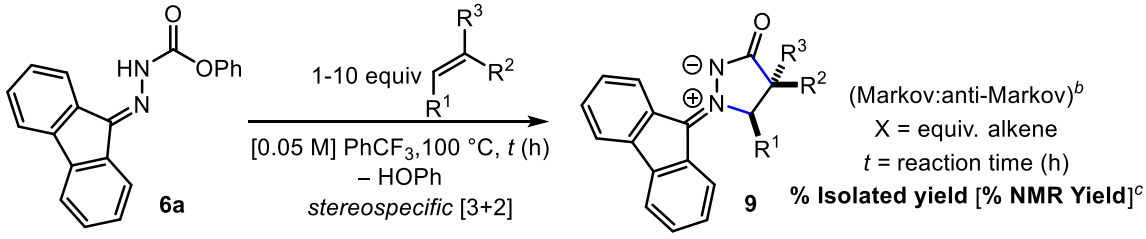

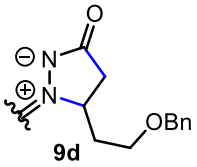

9d
(15:1)
X = 10, *t* = 3 h, **39%**
X = 10, *t* = 6 h, **52%**

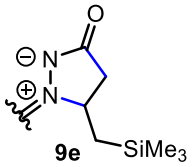

9e
(>100:1)
X = 10, *t* = 3 h, **81%**

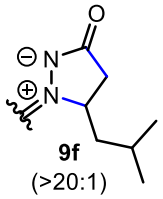

9f
(>20:1)
X = 5, *t* = 3 h, **45%**[d]
X = 10, *t* = 16 h, [**38%**]

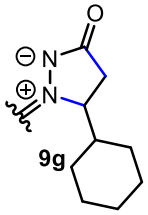

9g
X = 5, *t* = 3 h, **50%**[g]

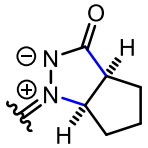

9h
X = >20, *t* = 2 h, **89%**
X = 10, *t* = 3 h, **69%**
X = 10, *t* = 6 h, **76%**

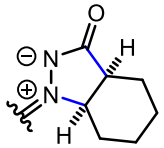

9i
X = ~200, *t* = 3 h, **49%**[d,e]
X = 10, *t* = 3 h, [**10%**]

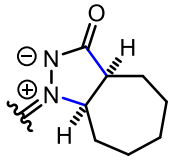

9j
X = 10, *t* = 6 h, **40%**

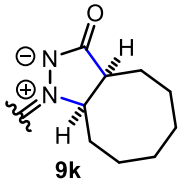

9k
X = 10, *t* = 6 h, **54%**

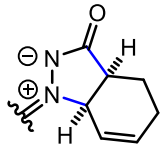

9l
(>10:1)
X = 10, *t* = 3 h, **52%**
X = 10, *t* = 6 h, [**60%**]

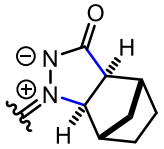

9a
X = 10, *t* = 3 h, **99%**
X = 1, *t* = 3 h, **65%**
X = 2, *t* = 0.2 h, **90%**[d,f]

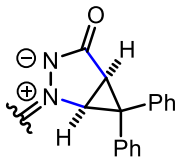

9m
X = 5, *t* = 3 h, **n.p.**

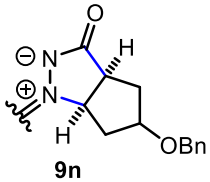

9n
X = 10, *t* = 6 h, **n.p.**

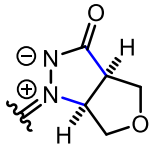

9o
X = 10, *t* = 3 h, **n.p.**

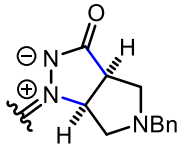

9p
X = 10, *t* = 3 h,
[**38%**]

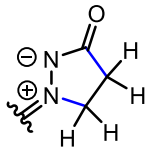

9q
X = (ethylene headspace),
t = 1 h, **4%**

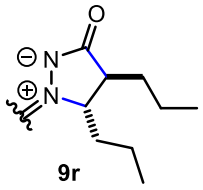

9r
X = 10, *t* = 3 h, [**3%**]

a) Conditions: Hydrazone **6a** (1 equiv) and alkene (1-10 equiv), and $PhCF_3$ (0.05 M) were combined in a vial and purged with nitrogen. The reaction was heated at 100 °C by microwave irradiation or conventional heating. Isolated yields are provided, n.p. = no product. b) Ratio of (Markovnikov : anti-Markovnikov) regioisomers, determined by analysis of crude ^1H NMR spectrum. c) NMR yield, determined using 1,3,5-trimethoxybenzene internal standard. d) 150 °C. e) neat reaction. f) $PhCF_3$ (1.3 M). g) *by Patrick Moon.*

We then explored the reactivity of styrene derivatives, which were poor substrates for the first generation reagent. Since the reactivity with styrenes was new, we first performed a solvent scan using the electron rich styrene derivative *p*-vinyl anisole (Table 2.7). We hoped to find a "greener" alternative to α,α,α-trifluorotoluene ($PhCF_3$), since halogenated solvents are considered environmentally hazardous.[5,6] With "green" solvent TBME, the hydrazone was insoluble in the reaction mixture and no reaction occurred. The reaction mixture was completely soluble in THF, even at room temperature, but the yield of **9s** was only 17%. We also observed low yields when the reaction was performed in acetonitrile or neat, with considerable by-product formation. Other aromatic solvents (toluene, *ortho*-xylene) gave good yields of **9s**, but $PhCF_3$ was still the optimal solvent for the reaction. The optimized conditions in $PhCF_3$ provided **9s** in 74% isolated yield.

Table 2.7. Optimization of *p*-vinyl anisole aminocarbonylation with reagent **6a**.[a]

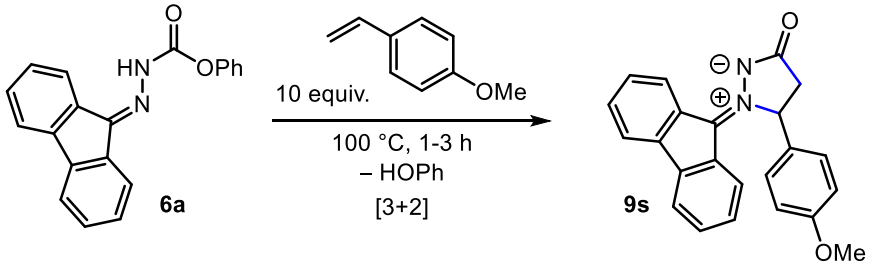

Entry	Solvent	*t* (h)	Yield (%) **9s** [b]	Comment
1	TMBE	3	-	insoluble
2	THF	3	23	soluble
3	MeCN	3	17	by-products
4	neat	3	21	by-products
5	$PhCH_3$	3	57	
6	*o*-xylene	3	53	
7	$PhCF_3$	3	75 (74)[c]	
8	$PhCF_3$	1	58	

a) Conditions: Hydrazone **6a** (0.25 mmol, 1 equiv) and *p*-vinyl anisole (2.5 mmol, 10 equiv), and solvent (5 mL) were combined in a vial and purged with argon. The reaction was heated at 100 °C for 1 or 3 hours. b) NMR yields are reported, determined using 1,3,5-trimethoxybenzene internal standard. c) Isolated yield.

We were able to quickly study the scope of this reaction with various aryl alkenes (Table 2.8). In many cases good reactivity was observed at 100 °C. The amount of *p*-vinyl anisole could be

reduced to 5 equiv, and the reaction time doubled to 6 hours, to obtain a similar yield (entry 1). These conditions were used to examine the effect of the position of the OMe group. In the *para*- and *ortho*-position, the group is electron donating and good yields of **9s** and **9u** are observed (entries 1 & 2). In the *meta*-position, the effect of the methoxy group is only inductive and the yield of **9t** falls to 29%. Styrene itself showed good reactivity (**9v**, 64%), and this reaction could be performed on gram scale, where longer reaction times (6 h) were beneficial to the yield. 4-Methyl and 4-fluoro styrenes also showed good reactivity (entries 5-7). As expected, a low yield of **9y** was observed with the electron deficient 1-(trifluoromethyl)-4-vinylbenzene (entry 8). In this reaction we also isolated 5% of the anti-Markovnikov regioisomer (**iso-9y**). Patrick Moon, an undergraduate student assisting with this project, achieved good yields with bulky naphthalene derivatives by heating at 120 °C (entries 9 & 10). Di-substituted styrene derivatives such as (Z)-prop-1-en-1-ylbenzene also showed low reactivity at 100 and 120 °C. Only after heating at 150 °C could we isolate 39% of **9ab**, although a short reaction time was needed to prevent degradation of the alkene and product. The modest reactivity observed with trans-chalcone (entry 12, **9ac**) was our first observation of reactivity at 100 °C with an electron deficient alkene. Moderate reactivity but poor regioselectivity was observed with indene-type alkenes (entries 13-14, **9ad** & **9ae**). In an excellent example of the reactivity of electron-rich substrates, only one equivalent of vinyl ferrocene reacted at 80 °C (where isocyanate concentration is low) to give 93% of the cycloadduct **9af** (entry 15).

Table 2.8. Scope of styrene derivatives in aminocarbonylation with reagent **6a**.[a]

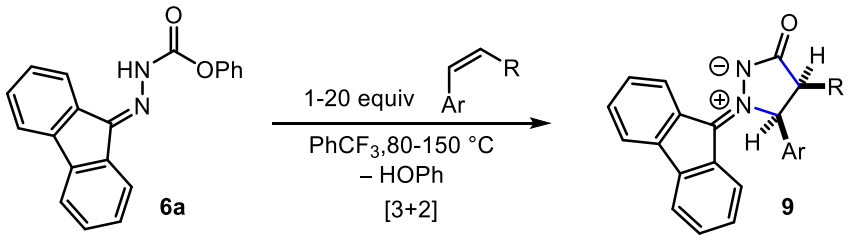

Entry	Alkene (Ar-CH=CH-R)		Equiv	T (C)	t (h)	Yield (%) **9** [b]
1	X =	4-OMe	5	100	6	68 (**9s**)
2		3-OMe	5	"	6	29 (**9t**)
3		2-OMe	5	"	6	72 (**9u**)
4	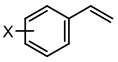	H	5	"	6	64 (**9v**)
5		4-Me	10	"	3	52 (**9w**)
6		4-F	5	120	6	47 (**9x**)
7			10	120	3	54[c] (**9x**)
8		4-CF_3	10	100	6	23[d] (**9y**)
9	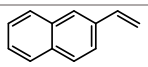		5	120	3	56[c] (**9z**)
10	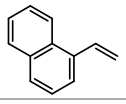		5	120	3	66[c] (**9aa**)
11	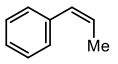		10 10 20	100 120 150	6 3 0.3	[5][e] [12][e] 39 (**9ab**)
12	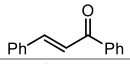		5	100	6	[14][e] (**9ac**)
13		*n*=1	10	120	2	41[c] (**9ad**)[d]
14		*n*=2	10	120	3	31[c] (**9ae**)[d]
15	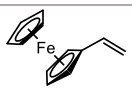		1	80	3	93[c] (**9af**)

a) Conditions: Hydrazone **6a** (1 equiv) and alkene (1-20 equiv), and $PhCF_3$ (0.05-1.0 M) were combined in a vial and purged with nitrogen. The reaction was heated by microwave irradiation or conventional heating. b) Isolated yield. c) Entries 8, 13-15 by Christian Clavette, entries 10, 11 by Patrick Moon. d) **9v**: 5% of regioisomer (***iso*-9v**) was also isolated. **9ad**: Isolated as a 6:1 mixture of regioisomers. **9ae**: 20% of regioisomer (***iso*-9ae**) was also isolated e) NMR yield, determined using 1,3,5-trimethoxybenzene internal standard.

The azomethine imines synthesized from **6a** are valuable precursors to protected β-amino amides (**10**) by reductive N-N cleavage, using the protocol discovered by Dr. Gan. This transformation requires Raney nickel and a borohydride reagent, and no reaction was observed with hydrogen gas as the sole reductant. The fluorenyl group is a known *N*-protecting group, and can be removed by oxidation with DDQ as shown earlier in this Chapter (Figure 2.6). The β-amino

amides (**10**) can be transformed into β-amino esters (**11**) in good yields with known methods (Figure 2.6).[7]

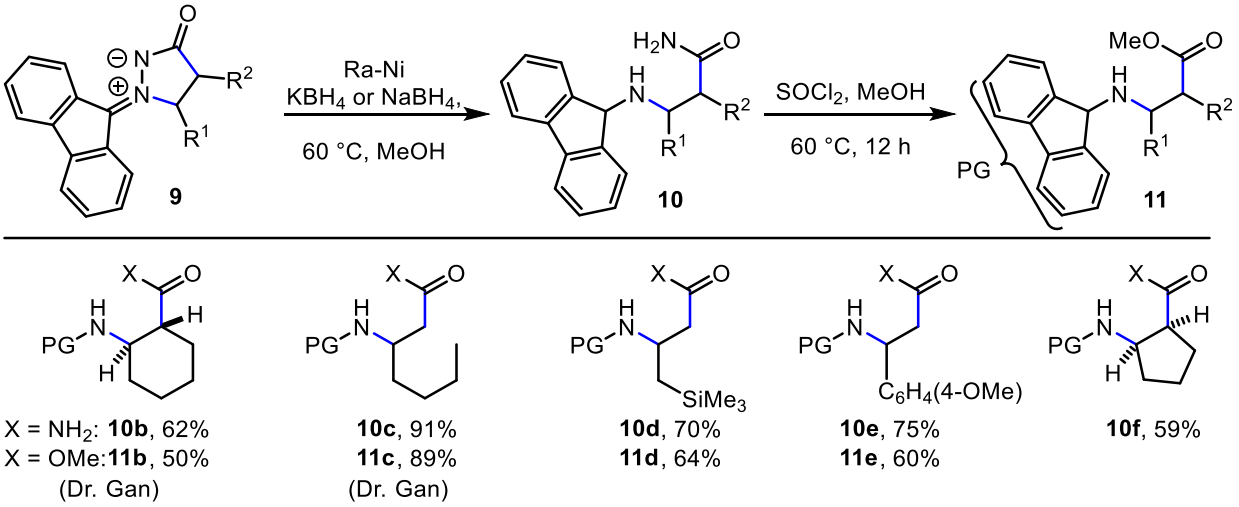

Figure 2.6. Synthesis of β-amino amides and esters from alkene aminocarbonylation products.

Following this work, we set out to develop simpler and milder derivatization methods. First, we sought an alternative to our deprotection reaction (removal of the fluorenyl group), and M. Sc. student Lyanne Betit explored various nitrogen-based nucleophiles in a transimidation approach. The goal was to perform a transimination: addition of a nitrogen nucleophile to the C=N bond of the dipole, then formation of a new C=N bond with the nucleophile to release the free pyrazolidinone **12**. Lyanne discovered the desired reactivity with aqueous hydroxylamine, and this method became the standard procedure in the group. We observed a clean reaction with norbornene-adduct **9a**, with quantitative conversion to give **12a.** Addition of water to the crude reaction mixture causes precipitation of the fluorenone oxime, which is then easily removed by filtration (Scheme 2.7).

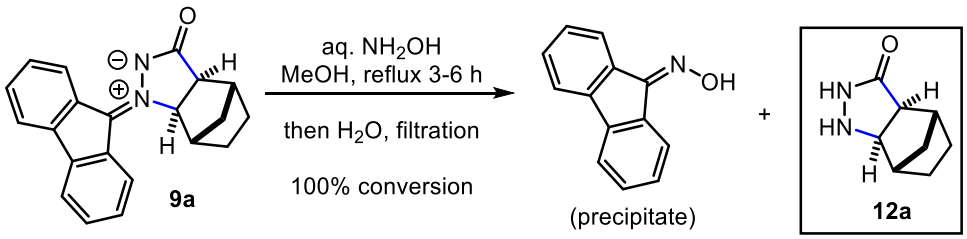

Scheme 2.7. Nucleophilic deprotection (transimination) with hydroxylamine.

Lyanne showed that **12a** can undergo reductive ring opening with Raney nickel and H_2, and Boc protection allowed for straightforward isolation (Scheme 2.8a). I was able to apply this method to access new aldehyde-derived azomethine imines, for which the imino-isocyanate precursors show poor reactivity in aminocarbonylation reactions (Scheme 2.8b).[1] These azomethine imines were used in a kinetic resolution discussed in Chapter 3. Overall, with this transimination protocol we can access a variety of β-amino carbonyl compounds from alkenes.

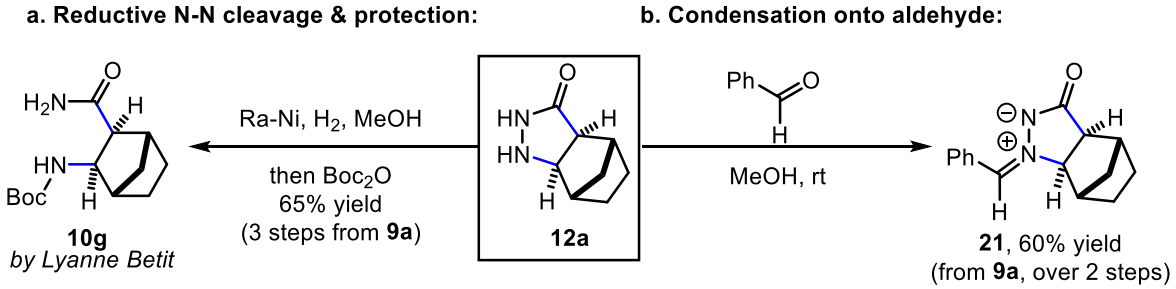

Scheme 2.8. Transformations of free pyrazolone obtained from transimidation deprotection method.

Overall, the fluorenone reagent **6a** provided superior reactivity with alkenes compared to other aminocarbonylation reagents, and enabled a large scope of complex azomethine imines to be synthesized. We attribute this improved reactivity to the geometry of the imino-isocyanate and planarity of the fluorenone system. The imino-isocyanate can exist in various conformations, with the s-cis and s-trans geometries likely being the most stable and important to consider (Figure 2.7). For the cycloaddition to occur, the imino-isocyanate must adopt an s-trans conformation.

Figure 2.7. S-cis and s-trans geometries of the imino-isocyanate.

The planarity observed in single X-ray crystal structures of the fluorenone hydrazone precursor and the azomethine imine product suggests a favourable planar geometry of the imino-isocyanate. This planarity would influence the conformation of the imino-isocyanate, and would favour the less hindered s-trans geometry required for the cycloaddition reaction. The extended π system, made possible by the sp^2 hybridization of the R group, would stabilize fluorenone-derived imino-isocyanate relative to the 1st generation system, wherein the R group has sp^3 hybridization. This is supported by the increased robustness of the fluorenone hydrazone, which could be recovered even after heating for 6 hours at 100 °C. This extension of the imino-isocyanate π system is also expected to lower the energy of the LUMO, decreasing the energy gap with the alkene HOMO. In contrast, the di-isopropyl imino-isocyanate is expected to be more electron rich, have a higher energy LUMO and larger energy gap.

The analysis of single crystal X-ray structures of multiple fluorenone-derived azomethine imines shows co-planarity of the fluorenone with the dipolar pyrazolone core. This is attributed to delocalization of the negative charge into the fluorenyl group (Figure 2.8, **9a**). The availability of this resonance structure, which is stabilized by conjugation to aromatic rings, should lower the energy of the azomethine imine. Evidence for conjugation of the dipole with the fluorenyl group is also found in the ^{1}H NMR spectra of these fluorenone-derived azomethine imines, where a single proton is shifted +1 ppm from the other aromatic protons. These observations are in agreement with our experimental observation that the dipole is both stabilized and shielded against 1,3-dipolar

cycloaddition. This would also lower the energy of the cycloaddition transition state, by resonance stabilization of the partial charges. In addition, this planarity makes the azomethine imine more approachable to nucleophiles, which allowed derivatization.

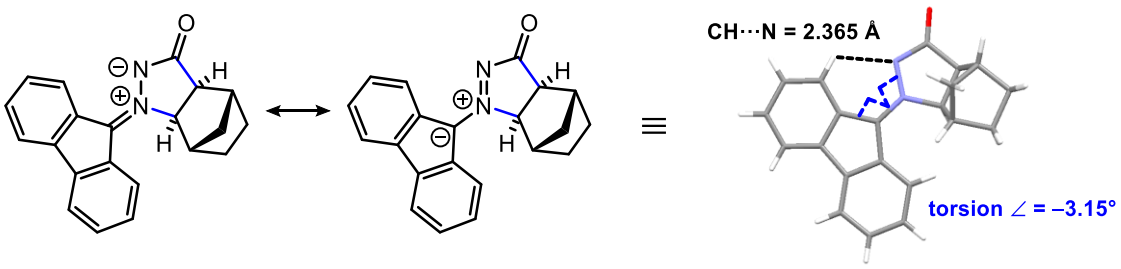

*Figure 2.8. Properties of an azomethine imine product (**9a**) derived from fluorenone.*

To this time, we have not observed reactivity of **6a** with alkynes or allenes. For example, no product was observed in reactions of **6a** with excess 1-hexyne, under various conditions (Figure 2.9). The major product observed in these reactions was the fluorenone azine, a byproduct from imino-isocyanate decomposition. A reaction with copper (I) hexylacetylenide was also unsuccessful.

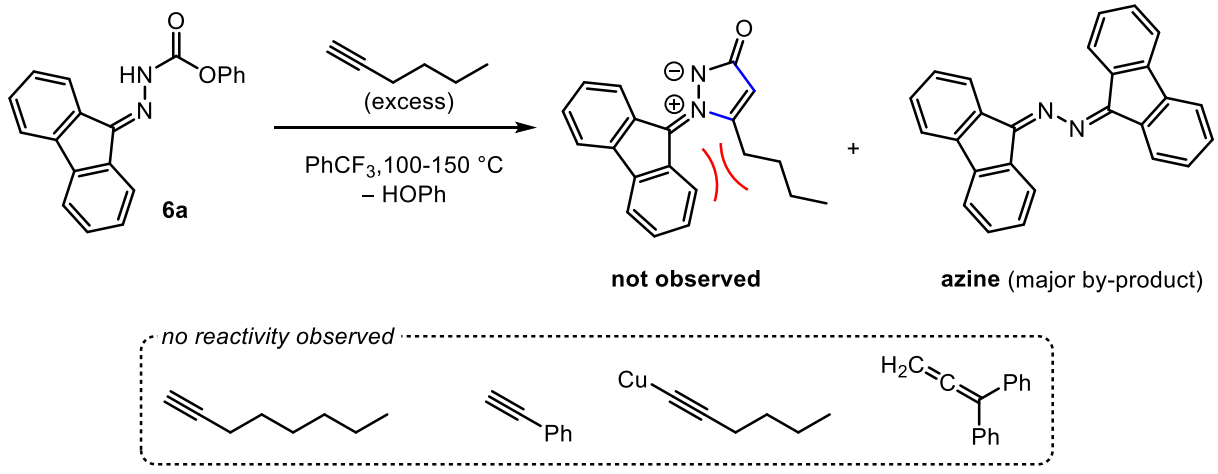

Figure 2.9. No reactivity has been achieved with various alkynes, copper (I) hexylacetylenide, or an allene.

The geometry of the imino-isocyanate that is required for reactivity might be hindering the approach of the alkyne. We expect co-planarity of the pyrazole core and fluorenone group in the

alkyne adduct, due to the aforementioned observation in fluorenone-derived azomethine imines. As a result, the transition state of the cycloaddition reaction with alkynes would be strained and high in energy. In his work, Jones demonstrated successful alkyne aminocarbonylation with a bulky imino-isocyanate at 110 °C. In this case, it is likely that the groups were twisted out of plane, allowing room for approach of the alkyne (Scheme 2.9). There may be other factors that contribute to this reactivity, and the yield of the product was not reported.

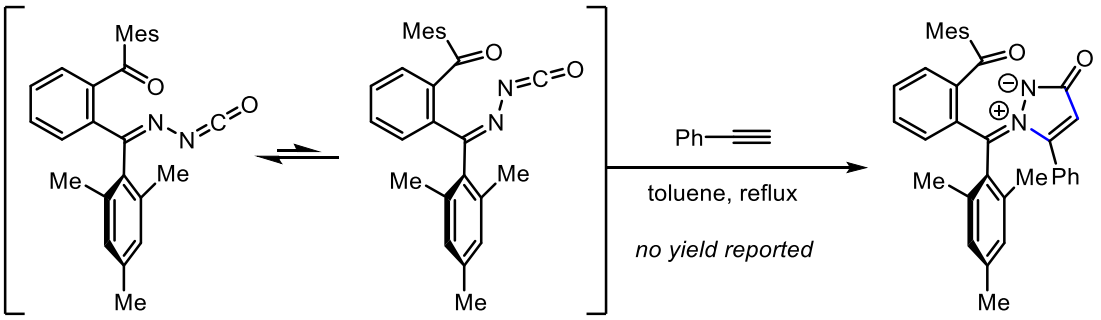

Scheme 2.9. Aminocarbonylation of phenylacetylene with a bulky imino-isocyanate by Jones. R = Ph or alkyl.

To test if strain from forced planarity was the reason we did not observe alkyne reactivity, reactions were also performed with diphenyl precursor **4b**. Unfortunately, these reactions did not yield the desired alkyne aminocarbonylation product (Scheme 2.10).

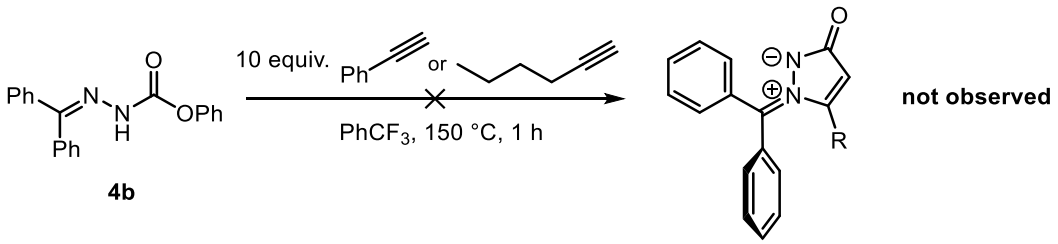

Scheme 2.10. Our attempt to replicate Jones' reactivity with non-planar imino-isocyanate precursor.

We explored more systems similar to the one reported by Jones in an effort design a new imino-isocyanate precursor to enable reactivity with alkynes. Synthesis of imino-isocyanate precursor **13** was first attempted from 4-phenyltriazoline-3,5-dione, using the same method reported by Jones for his mesityl substrate (Scheme 2.11). Using equimolar quantities of reagents and stirring at room

temperature did not provide the dipole product, and a complex mixture of products and starting material was observed. Unfortunately, attempted condensation of *O*-Ph carbazate onto the diketone to access precursor **14** was also unsuccessful.

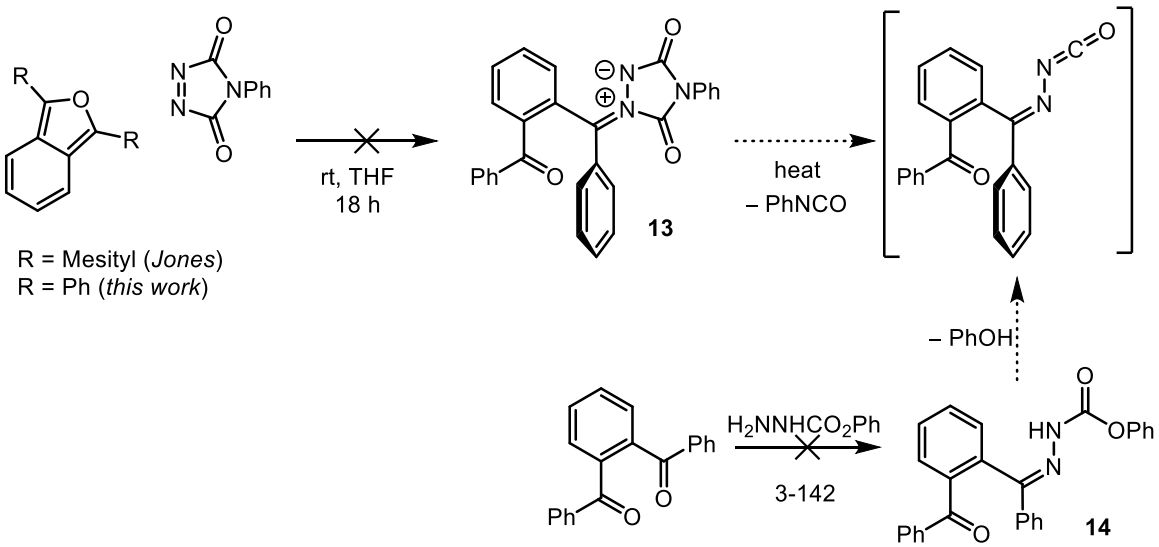

Scheme 2.11. Efforts toward synthesis of a Jones-type aminocarbonylation reagent.

Condensation of *O*-Ph carbazate onto mesitylphenone to access the precursor **15** was also attempted, but the desired hydrazone was not observed (Scheme 2.12). It seems likely that the reagent is too bulky for attack of the carbazate.

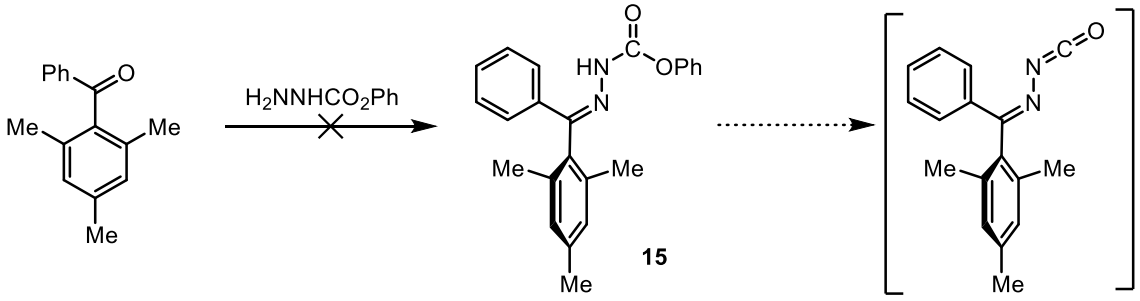

Scheme 2.12. Unsuccessful condensation of carbazate onto mesitylphenone.

The requirement for a bulky imino-isocyanate created challenges in substrate synthesis, and has limited the development of new reagents for aminocarbonylation. A different approach could be taken to find conditions for catalysis of the cycloaddition step. This would allow the use of imino-

isocyanates that are either less reactive or prone to side reactions at higher temperatures (e.g. aldehyde-derived reagents). Catalysis of the cycloaddition reaction would control the concentration of imino-isocyanate, and prevent degradation of the intermediate by dimerization. Also, lower reaction temperatures and fewer equivalents of alkene would prevent 1,3-dipolar cycloaddition addition of the product. Work towards these goals is discussed later in this chapter.

2.2.3. Enol ether aminocarbonylation with 2nd generation reagent

Enol ethers have electron rich C=C bonds, and we were eager to study their aminocarbonylation reactivity as alkyne equivalents. Dihydrofuran and other enol ethers were initially discovered to undergo facile intermolecular aminocarbonylation with first-generation imino-isocyanates.[3] With the new reagent **6a**, Drs. Gan and Clavette also observed reactivity with a small set of enol ethers at 100 °C. Although enol ethers showed excellent reactivity, the scope was limited by decomposition of many enol ethers at 100 °C.

We suspected that imino-isocyanate formation might be rate-determining in reactions with enol ethers, and catalysis of imino-isocyanate formation at lower temperatures could improve the reaction. This hypothesis was tested by M.Sc. student Kaitlyn Lavergne, who found that base catalysis could affect formation of the imino-isocyanate. After testing a variety of bases and conditions in the reaction with dihydrofuran, she found that 3 mol% triethylamine allowed catalysis of the overall reaction at 70 °C (Scheme 2.13). The best yield of **16c** was obtained when dihydrofuran was the limiting reagent, which shows the drastic reactivity difference of enol ethers compared to alkenes.

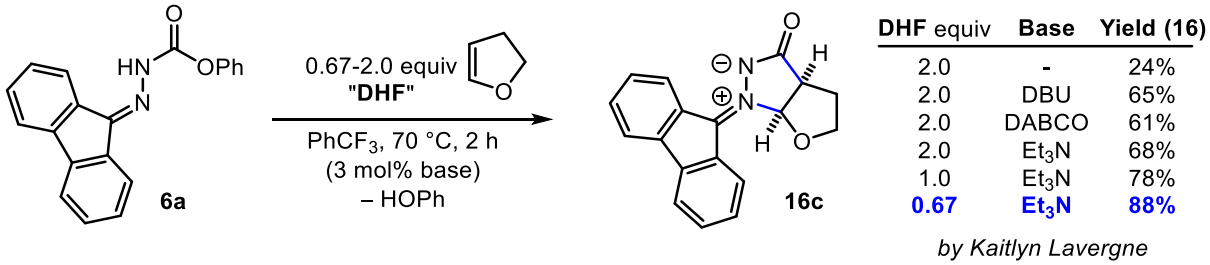

DHF equiv	Base	Yield (16)
2.0	-	24%
2.0	DBU	65%
2.0	DABCO	61%
2.0	Et_3N	68%
1.0	Et_3N	78%
0.67	**Et_3N**	**88%**

by Kaitlyn Lavergne

Scheme 2.13. Optimization of base catalysis conditions for the aminocarbonylation of dihydrofuran.

The base catalysis conditions were used as a tool in exploring the scope of enol ether reactivity. The effect of the base additive was an indicator of enol ether reactivity and was used to determine cases where imino-isocyanate formation was rate determining. The addition of base had no effect on the yield at 100 °C, where imino-isocyanate formation is thermally favoured. For our publication,[8] Kaitlyn and I synthesized 12 azomethine imines (**16a-l**) from enol ethers and **6a**, which gave access to complex azomethine imines with pyrazolone cores (Table 2.9).

Azomethine imines derived from enol ethers are at the right oxidation state to access the pyrazolone core, a family of heterocycles with many uses in pharmaceuticals and agrochemicals.[9-16] Given this homology, we were drawn to explore derivatization methods to convert our products into pyrazolones (**17**). Pyrazolones are typically synthesized from hydrazones and β-ketoesters, and rarely from alkenes. We expected that addition of a nucleophile to the azomethine imine C=N+ bond would trigger aromatization, with cleavage of the C-O bond and loss of the inherent alcohol (Scheme 2.14).

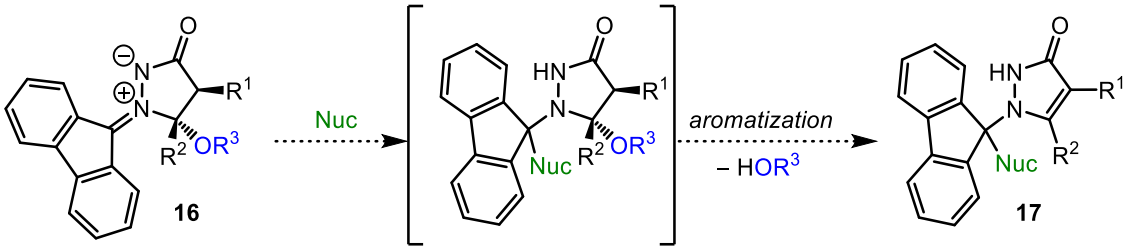

Scheme 2.14. Proposed synthesis of pyrazolones by nucleophile-triggered aromatization of azomethine imines.

Table 2.9. Aminocarbonylation of enol ethers with reagent **6a**.[a]

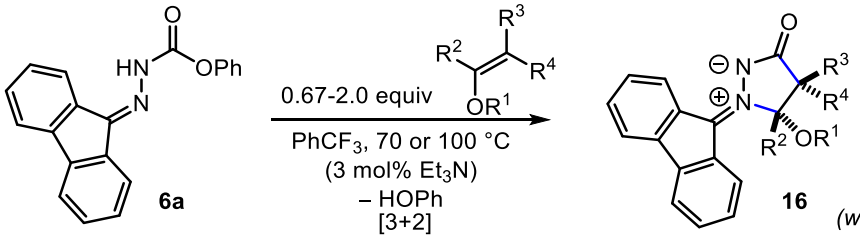

(with Kaitlyn Lavergne)

Entry	Enol ether		Equiv	Catalyst [a]	T (°C)	t (h)	Yield (%) **16** [b]	
1	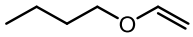		2	-	100	2	**16a**	75
			0.67	Et_3N	70	3		68
2	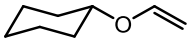		2	-	100	2	**16b**	68
3			2	-	100	2	**16c**	57
4			0.67	Et_3N	70	2.5		95
5			2	-	100	2		77
6			0.67	Et_3N	100	3	**16d**	81
7			0.67	Et_3N	70	2.5		38
8	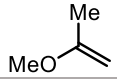		0.68	Et_3N	70	3	**16e**	69
9			2	-	100	2	**16f**	70[c]
10	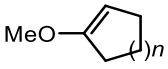	$n = 1$	0.67	-	100	3	**16g**	63
11		$n = 2$	0.67	-	100	3	**16h**	25
12		$n = 3$	0.5	-	100	3	**16i**	57
13	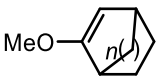	$n = 1$	2	-	100	1	**16j**	98[d]
14				-	40	72		85[d,e]
15		$n = 2$	2.5	-	100	3	**16k**	86[d]
16	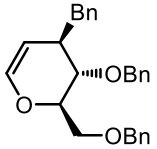		0.67	Et_3N	100	3	**16l**	76[f]

a) Conditions: Hydrazone **6a** (1 equiv) and alkene (0.67-2.0 equiv), and $PhCF_3$ (0.1 M) were combined in a vial and purged with nitrogen, and heated at 70 or 100 C for 1-3 h. In some reactions, Et_3N (3 mol%) was added. b) Isolated yield. c) Enol ether is a mixture of cis/trans, final product is 16:1 *anti*/*syn*. d) Ring junction hydrogens are *anti* to the bridge. e) NMR yield using 1,3,5-trimethoxyebenzene internal standard. f) Ring junction hydrogens are *syn* to the CH_2OBn.

This strategy was first demonstrated using 'hydride' as the nucleophile, in a reduction of the dipole with sodium borohydride. In many cases, only **17** was observed after the reaction and the reduced product could not be isolated. However, bicyclic azomethine imines were slow to aromatize after reduction, and a mixture of products was observed. For example, the reduction of **16j** at room temperature gave a mixture of **18** (44%), desired product **17j** (27%), and an unknown

product in 7% NMR yield (Scheme 2.15). We propose that after the initial reduction, expulsion of the alcohol from intermediate **I** by assistance from the adjacent nitrogen gives a dipole intermediate **II**. This unusual intermediate is either the unknown or gives rise to it. Furthermore, heating **18** in the presence of NH_4Cl causes complete conversion to the unknown.

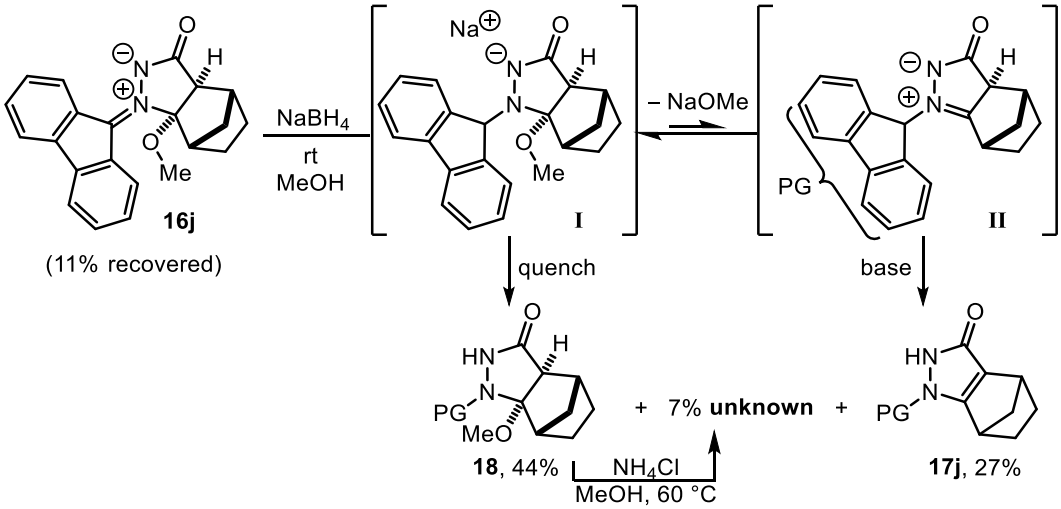

*Scheme 2.15. Mechanism and by-product formation in the reduction of bicyclic azomethine imine **16j**.*

To prevent this unwanted pathway, the reduction and quench were performed at 0 °C, allowing isolation of crude **18**, which could then be treated with catalytic acid to afford the pyrazolone in in high yields. This method was applied to all bicyclic systems, and sometimes cooling to –20 °C was required for the reduction step. Overall, we were able to synthesize a variety of fluorenyl protected pyrazolones **17** in typically excellent yields (Table 2.10). The aminocarbonylation of enol ethers to synthesize pyrazolones represents a new approach that enables more complexity and diversity than traditional methods.

Table 2.10. Synthesis of pyrazolones (**17**) from enol ether aminocarbonylation products (**16**).[a]

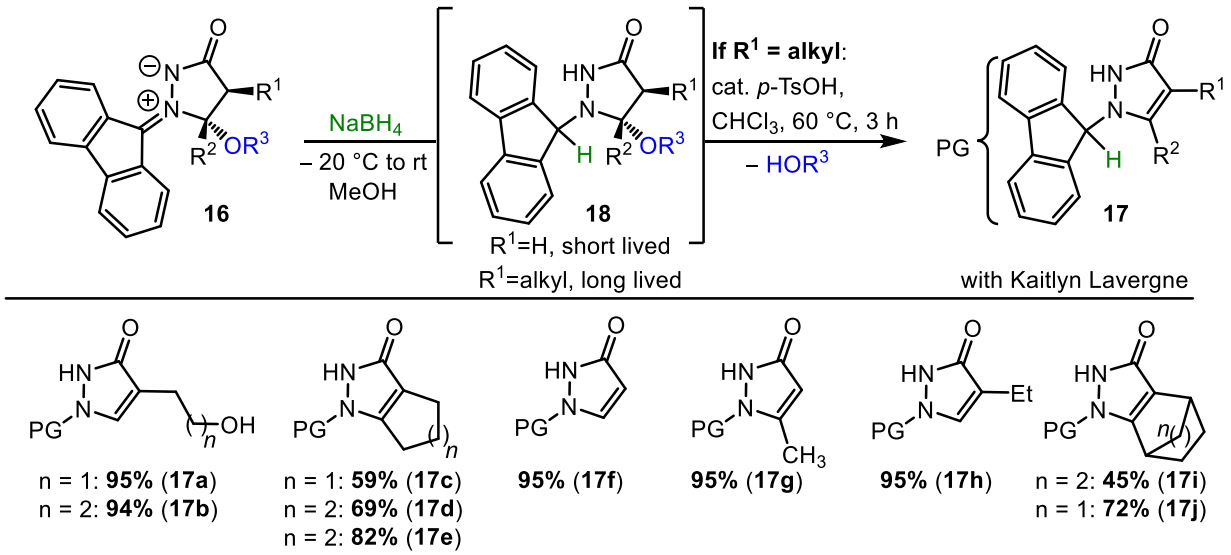

a) Conditions: **16** (1 equiv), $NaBH_4$ (1−5 equiv) in MeOH (0.5 M). If R^1 = H: –20 °C to rt; NH_4Cl quench. If R^1 = alkyl: –20 to 0 °C; NH_4Cl quench; then *p*-TsOH (0.5 mol %), $CHCl_3$ (0.05 M), 60 °C, 3 h.

2.2.4. Mechanistic Studies

Throughout exploring the scope of the alkene aminocarbonylation reaction, we also dedicated time to studying the mechanism and developing evidence to support the proposed intermediacy of the reactive imino-isocyanate. Earlier, we discussed DFT calculations for a model system which showed favourable formation of the imino-isocyanate and were consistent with a concerted [3+2] cycloaddition.[3] We also performed experimental studies to probe the mechanism, which began with examination of by-products. With reagent **6a**, this was simplified by insolubility of many by-products in the reaction solvent, $PhCF_3$. As discussed before, a major by-product pathway discovered in the initial work was a second 1,3-dipolar cycloaddition of the azomethine imine with excess olefin. However, this side reaction was never observed with the fluorenone hydrazone, and this contributes to its success as an aminocarbonylation reagent (Scheme 2.16).

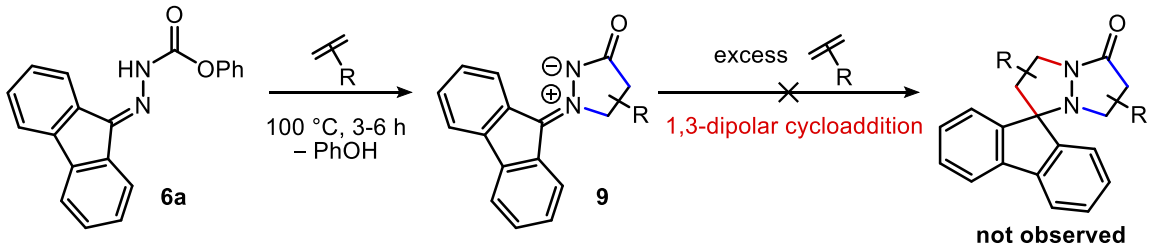

*Scheme 2.16. Unwanted 1,3-dipolar cycloaddition with excess olefin is not observed with **6a**.*

The new major by-product in aminocarbonylation reactions with **6a** is the carbohydrazone **19** (Scheme 2.17), which was found as a precipitate in the reaction mixture. This is formed by the reaction of the imino-isocyanate with trace amounts of water, loss of CO_2, and nucleophilic addition of the resulting free hydrazone onto another equivalent of imino-isocyanate. This precipitate was observed to form early on, and then stay at a consistent amount throughout the reaction. The mechanism provided is also supported by observed formation of gas upon opening the sealed mixture after the reaction. The detrimental effect of water prompted us to use dry $PhCF_3$ from a solvent purification system, which was kept in a sealed flask over molecular sieves.

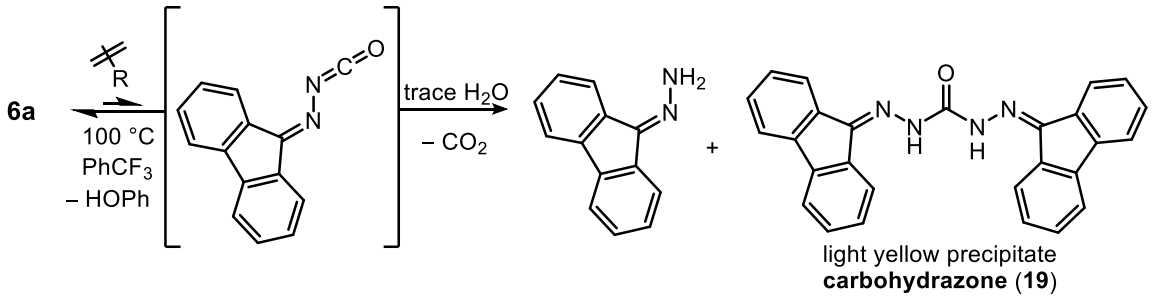

*Scheme 2.17 Carbohydrazone by-product (**19**) formation from imino-isocyanate.*

When the reagent **6a** was heated in the absence of alkene, some precipitate **19** was first observed, followed by the mixture turning dark red. Observation of this red colour was rare in reactions with alkenes, and indicative of poor yields of the product. The red by-product was isolated and determined to be the fluorenone azine, confirmed by single crystal X-ray analysis. Azines are known by-products from the thermolysis of imino-isocyanates, through the [2+2] dimer

intermediate (Scheme 2.18). This by-product provides strong support for the intermediacy of the imino-isocyanate, and supports using an excess of less reactive alkenes to compete with dimerization.

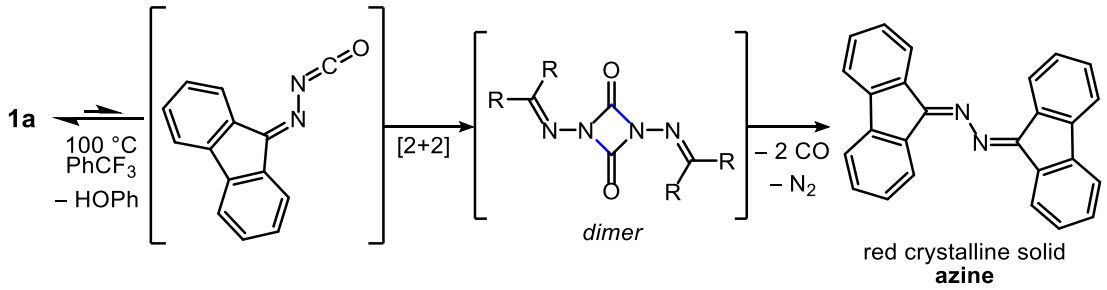

Scheme 2.18. Proposed mechanism for formation of azine by-product via [2+2] dimerization of imino-isocyanate.

Further support for the intermediacy of the imino-isocyanate came from cycloreversion experiments with the second generation reagent. When the azomethine imine adduct of styrene was heated in the presence of norbornene, the norbornene adduct was observed in 30% yield as determined by NMR (Scheme 2.19).

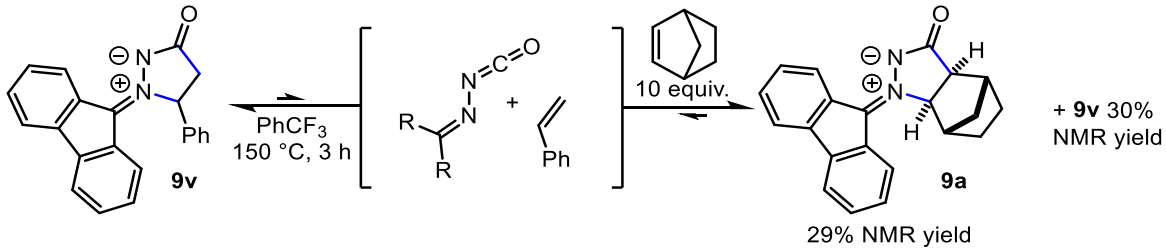

Scheme 2.19. Cycloreversion experiment by Patrick Moon.

We also performed a ^{1}H NMR study to learn more about the equilibrium between the hydrazone **6a** and the imino-isocyanate (Figure 2.10). These experiments had the possibility of allowing visualization of the imino-isocyanate in situ, but the signals from the isocyanate are expected to overlap significantly with the other components in the ^{1}H NMR. However, the concentration of isocyanate can be calculated from the mass balance, using the concentrations of PhOH and **6a** at equilibrium. The experiment began with acquisition of the starting material **6a** in toluene-d_8 at 50

°C (**6a** is insoluble at room temperature, and stable at 50 °C). The mixture was then heated to 90 °C, with an initial acquisition at 30 seconds, then at approximately every 5 min (Figure 2.10).

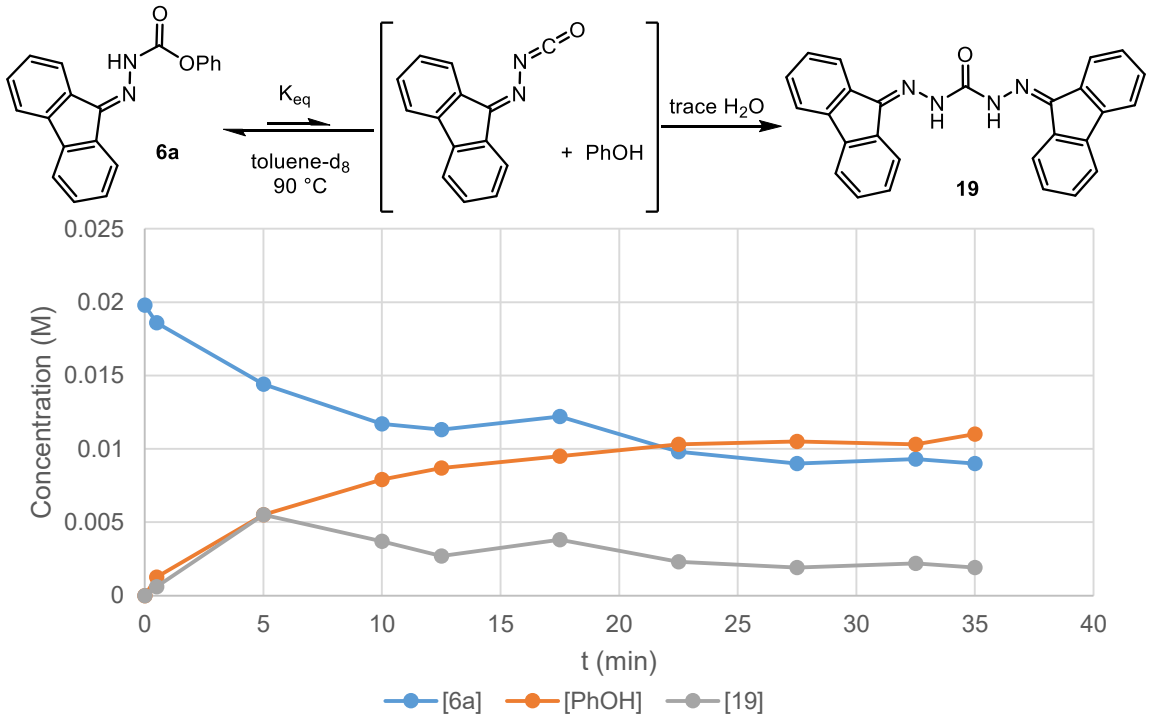

*Figure 2.10. Equilibration study by ^{1}H NMR analysis of **6a** (0.02 M) at 90 °C.*

The mixture reaches an equilibrium, with stable concentrations of hydrazone and PhOH after 20 minutes. A small amount of by-product **19** is observed early in the reaction, caused by an initial reaction of the imino-isocyanate with trace water. The formation of **19** is irreversible at this temperature, and the concentration of **19** is consistent over the reaction time. However, the formation of **19** changes the initial concentrations of 6a and PhOH, and this was taken into account. From the observed equilibrium concentrations of **6a** and PhOH, we can calculate the equilibrium concentration of imino-isocyanate, and determine the equilibrium constant $K_{eq} = 9 \times 10^{-3}$. After the experiment (35 min), the ^{1}H NMR spectrum of the cooled mixture showed **6a** and PhOH, with the disappearance of **19**, which is soluble at 90 °C but not at room temperature, and there was precipitate in the NMR tube. Notably, no azine is observed in this analysis, indicating that imino-

isocyanate dimerization is not occurring at 90 °C or that the dimer is not heated enough to convert to azine. Although this method was not precise or suitable for direct observation of the imino-isocyanate, it may be useful for monitoring reaction progress with alkenes or determining de-blocking temperatures of imino-isocyanate precursors. In order to visualize the imino-isocyanate, we became interested in reaction monitoring with IR spectroscopy.

Reaction monitoring with IR spectroscopy has been a valuable tool to study isocyanate reactivity, such as the kinetics of deblocking (isocyanate release) or polymerization (isocyanate consumption).[17-20] Isocyanates have intense signature peaks in the infrared sp region, typically from 2200-2300 cm^{-1}. In our system we were faced with two challenges: detection of the imino-isocyanate at the low concentration during the reaction, and side-reactions such as dimerization that would occur at high concentration. The study began with the first generation reagent **5a** under base catalysis conditions. The analysis was performed in a glove box to allow control of moisture and oxygen. A flow-IR instrument equipped with an injector was used, which is designed for analysis of liquid solutions and reaction mixtures. First, comparison of the IR spectra of **5a** in toluene (0.05 M) at room temperature, with and without triethylamine, showed no significant differences. The mixture of **5a** and Et_3N was then heated to 90 °C, and samples of the reaction mixture were injected into the detector. In order to detect reactive intermediates, the samples were immediately analyzed before the mixture cooled. Upon heating, the colourless mixture became dark orange, which could indicate formation of a conjugated π system. The first spectrum after 17 min at 90 °C showed a new peak at 2201 cm^{-1} (Figure 2.11).

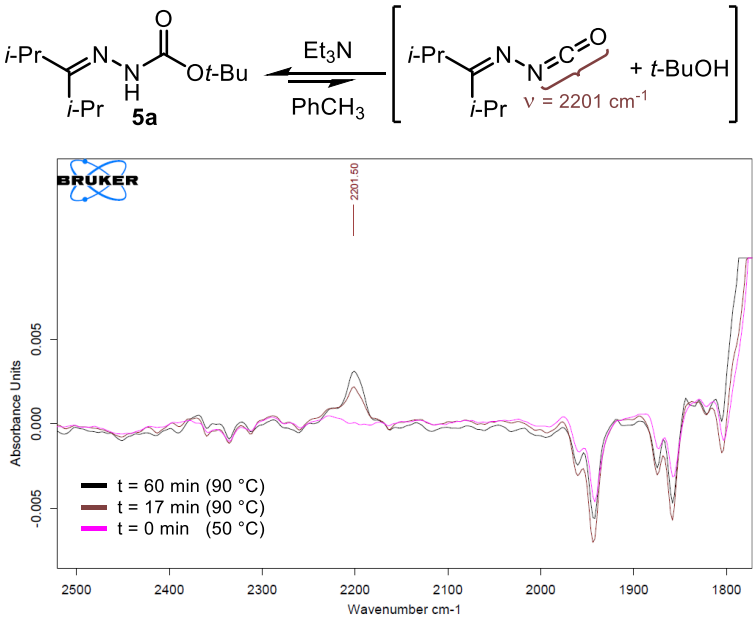

Figure 2.11. IR detection of imino-isocyanate NCO asymmetric stretch at 2201 cm^{-1}.

The peak observed at 2201 cm^{-1} is in good agreement with the reported NCO asymmetric stretch frequency of 2220 cm^{-1} for Me_2N-NCO and 2221 cm^{-1} for N_3-NCO in Argon matrices.[21,22] This peak does not correspond to CO_2 (2337 cm^{-1}) or CO (2138 cm^{-1}), both being possible products of imino-isocyanate degradation. The peak at 2201 cm^{-1} became more prominent in the spectrum recorded at 60 min, which indicates that the imino-isocyanate is stable in the glove box towards dimerization and degradation at 90 °C. Alternatively, this could signify that dimerization is favourably reversible under the conditions.

Next, we studied **6a** under similar conditions but without the added base. Upon heating at 90 °C in toluene, **6a** solubilized to a yellow solution, which then became dark ruby red. After 10 min, analysis of the sample showed a peak appeared at 2191 cm^{-1}, corresponding to the asymmetric NCO stretch of the imino-isocyanate (Figure 2.12). The lower stretching frequency compared to that of **5a** is the result of increased conjugation in this system, and is in agreement with a lower energy LUMO for the imino-isocyanate derived from **6a**. This peak does not appear in any IR

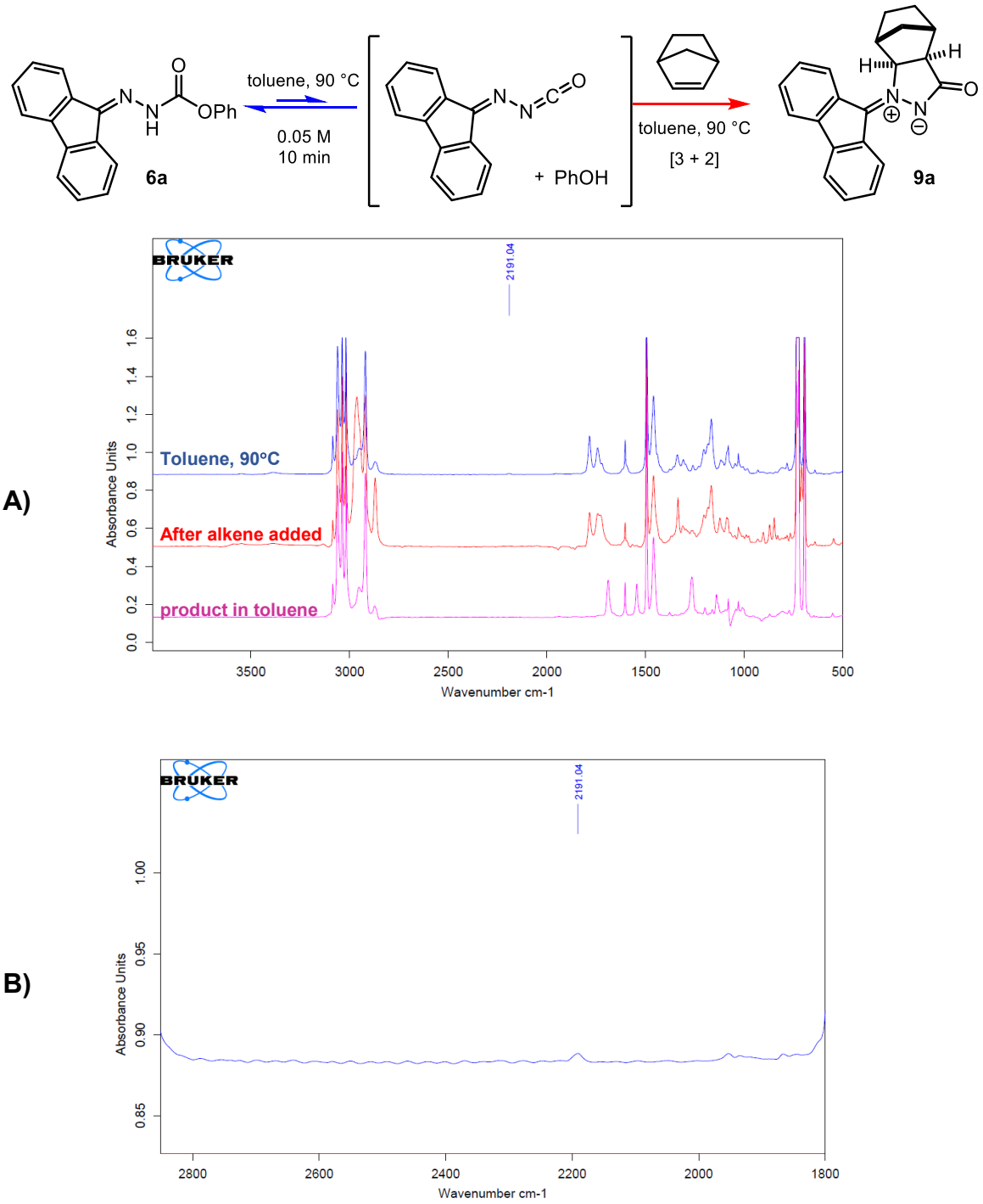

*Figure 2.12. IR Study of **6a**: detection of imino-isocyanate NCO asymmetric stetch at 2191 cm^{-1}. A) Blue line = mixture in toluene at 90 ℃ after 10 min. Red line = Analysis after norbornene added. Pink line = spectrum of azomethine imine product **9a** in toluene. B) Blue spectrum in closer detail.*

spectrum of the hydrazone reagent at room temperature, and also does not match the expected frequency of the azine (1600-1650 cm^{-1}).[23] After 20 minutes, norbornene was added to the reaction mixture. The ruby colour immediately disappeared, and the mixture returned to a pale yellow solution. Prompt analysis of the reaction mixture revealed no peak at 2191 cm^{-1}. Strong peaks corresponding to the azomethine product **9a** were unfortunately not observed, due to a very short reaction time with the norbornene. This IR study provided our first direct evidence for the intermediacy of the imino-isocyanate, and the first characterization of these species by IR. However, attempts to reproduce these results on a less sensitive instrument have failed to show the imino-isocyanate peaks. Still, this has the potential to be a valuable technique for studying the generation of imino-isocyanates and their reactivity.

2.2.5. Exploratory Attempts at Aminocarbonylation Catalysis

Catalysis of the imino-isocyanate alkene aminocarbonylation reaction is an ongoing project and challenge in our group. The reaction involves two steps, and either can be rate determining. We accomplished catalysis of imino-isocyanate formation, but this is ineffective in cases where cycloaddition is the rate-determining step. Unfortunately, there are no examples in the literature for catalysis of *N*-isocyanate cycloaddition reactions. We were interested in strategies such as H-bonding catalysis to assist the cycloaddition step (Figure 2.13), but attempts toward this reactivity have not been successful. Another possibility is using acid catalysis, which aims to make the imino-isocyanate more reactive (Figure 2.13). This has been an effective approach for reactions of *C*-isocyanates.[24,25] However, this could inhibit the cycloaddition step by promoting side-reactions of the imino-isocyanate. Additionally, the nucleophilic nitrogen of the *N*-isocyanate is the likely site of acid binding, and this would also inhibit the reaction.

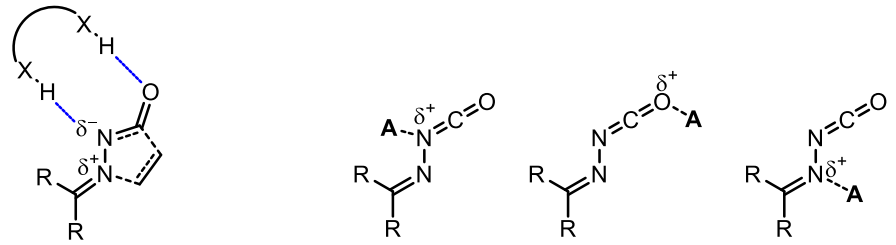

Figure 2.13. Strategies for catalysis of the alkene aminocarbonylation reaction with imino-isocyanates.

A kinetic strategy to make the imino-isocyanate more reactive is to make it less bulky. However, small imino-isocyanates tend to dimerize, and azomethine imine adducts undergo unwanted dipolar cycloadditions. We required a catalytic strategy that would favour the use of small imino-isocyanate precursors, and where the azomethine imine is removed from the reaction mixture. From this thought process, we designed a carbonyl catalyzed alkene aminocarbonylation reaction (Equation 2.1). This involves using a catalytic amount of the aldehyde or ketone portion of the imino-isocyanate.

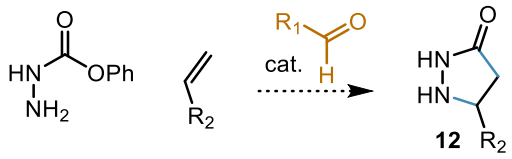

Equation 2.1.

The proposed catalytic cycle is provided in Figure 2.14. The aldehyde catalyst condenses with the carbazate to provide a hydrazone (**20**). Alternatively, and to avoid release of water from the condensation, **20** can be used as the catalyst instead of the parent carbonyl. Under the reaction conditions, imino-isocyanate will be generated with release of PhOH (Step 1). Next, aminocarbonylation of the alkene gives an azomethine imine (Step 2). The azomethine imine is then attacked by carbazate, to provide the free pyrazolidinone (**12**) and regenerate **20** (Step 3). This turn-over step is key to the cycle, and to preventing unwanted 1,3-dipolar cycloaddition of the product with readily available alkene.

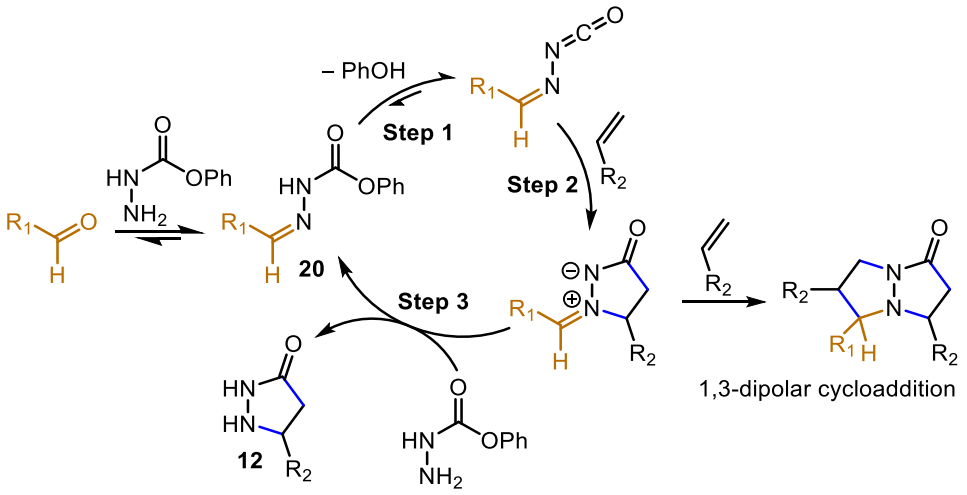

Figure 2.14. Proposed catalytic cycle for carbonyl catalyzed alkene aminocarbonylation

The carbonyl catalysis model has several advantages over the typical reaction. The carbazate is stable up to 120 °C, and will not form the amino-isocyanate (Equation 2.2). Only upon condensation with the carbonyl catalyst will *N*-isocyanate formation be favourable. This controls concentration of the imino-isocyanate during the reaction, which would prevent dimerization. This strategy allows us to use less hindered and kinetically more reactive imino-isocyanates. These less hindered azomethine imine products are also less stable and prone to hydrolysis or nucleophilic attack.

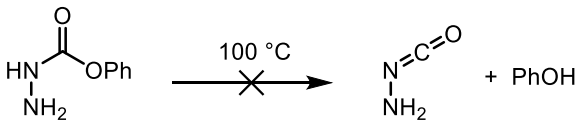

Equation 2.2.

There are some challenges to face with the proposed catalytic cycle. Attack of the carbazate onto the azomethine imine (Step 3) has little precedent and is crucial for turn-over of the catalyst. This step is expected to become more difficult as the reaction progresses, due to consumption of the carbazate and competing nucleophilic reaction with the pyrazolidinone product (**12**). For this reason, the carbazate will need to be used in excess and the alkene will be the limiting reagent. We

chose to explore the aminocarbonylation reaction of norbornene and styrene with various carbonyl catalysts. The background reactions without catalyst were first tested, and no product was observed (Scheme 2.20).

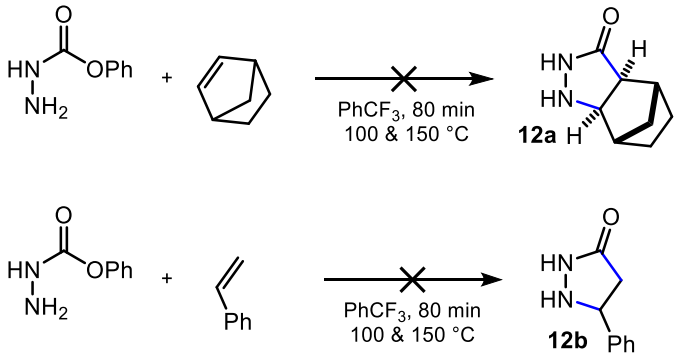

Scheme 2.20. Background reactions (no carbonyl catalyst) for alkene aminocarbonylation.

We performed initial tests of the catalytic reaction by the addition of hydrazones to the reaction of carbazate with norbornene. Unfortunately, no reactivity was observed with 0.2 equivalents of fluorenone hydrazone **6a**, or with the less hindered acetaldehyde hydrazone **20a** (Scheme 2.21). Before making more attempts at the catalytic reaction, the individual steps of the cycle were tested.

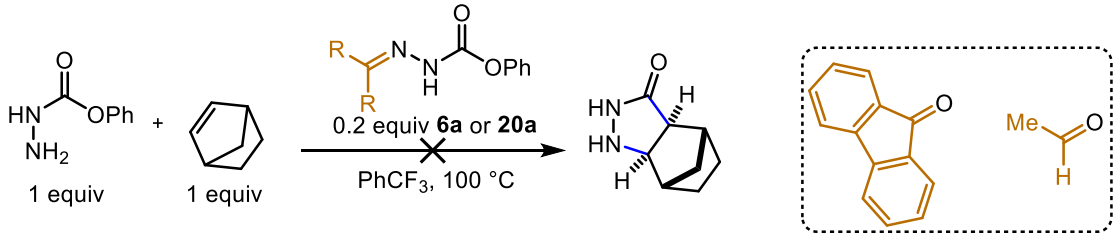

Scheme 2.21. Attempted aminocarbonylation of norbornene with carbonyl catalysts.

First, the turn-over step was examined under the same conditions known for aminocarbonylation reactivity. Aldehyde-derived azomethine imines were heated to 100 °C in the presence of 5 equivalents of carbazate. For the azomethine imine derived from benzaldehyde (**21**), the free pyrazolidinone **12a** was not observed in analysis of the crude mixture by TLC and ^{1}H NMR (Scheme 2.22a). This agrees with our knowledge that aromatic azomethine imines are

bench-stable towards hydrolysis. However, the same reaction with cyclohexanecarbaldehyde-derived azomethine imine (**22**) gave quantitative conversion of the dipole to **12b** (Scheme 2.22b). Analysis of the crude mixture by ^{1}H NMR revealed 39% yield of the expected hydrazone (**20b**) and 42% yield of PhOH (from formation of the imino-isocyanate from **20b**). There remained 4 equivalents of the unreacted carbazate, demonstrating the stability of this reagent under these conditions. We tested if the observed reactivity was due to hydrolysis of **22** by trace water, and not brought about by the carbazate. Subjecting **22** to the conditions without addition of carbazate resulted in no reaction (Scheme 2.22c).

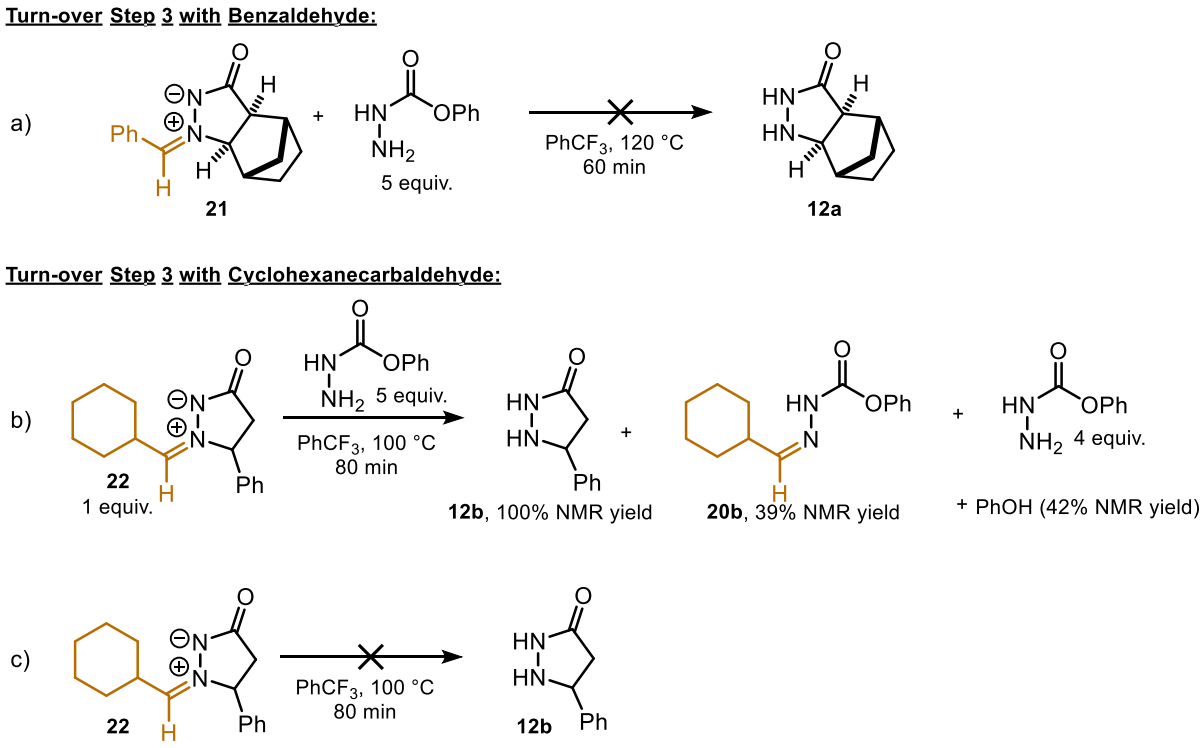

Scheme 2.22. Testing catalytic turn-over (Step 3) with azomethine imines and O-phenyl carbazate.

With the turn-over step working under the reaction conditions, the catalytic reaction was then tested. Norbornene was combined with a slight excess of carbazate and a catalytic amount of hydrazone catalyst **20b** (Scheme 2.23a). At reaction temperatures of 100-150 °C, the desired

product (**12b**) or the azomethine imine (**23**) were not observed. In all cases, the detection of PhOH suggests the formation of imino-isocyanate, and we can conclude that the cycloaddition step is not occurring. The aminocarbonylation reactivity of **20b** with norbornene was tested (Scheme 2.23b), and we found the reagent unable to undergo the cycloaddition at 100 or 120 °C.

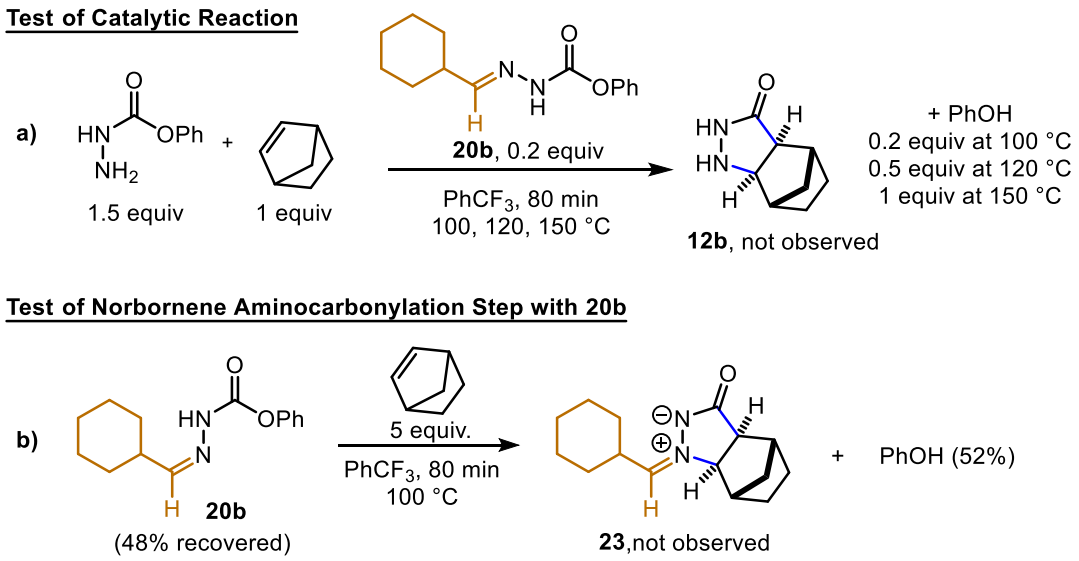

*Scheme 2.23. Unsuccessful catalysis reaction, and the absence of reactivity in the attempted aminocarbonylation reaction of **20b** with norbornene.*

Although many of the individual steps in the cycle have been achieved, the carbonyl catalyzed reaction has not been realized. To continue this work, we must find a carbonyl catalyst which provides good reactivity with norbornene and also allows the required turn-over step. This catalytic strategy could also be revisited with the fluorenone reagent with a base co-catalyst. In this case, the base could assist both with isocyanate formation and the turn-over step.

2.3. Summary and Outlook

Exploring many variations on conditions with the 1st generation aminocarbonylation reagent (**5a**) informed us on reactivity trends, mechanism, and the nature of the cycloaddition transition state as the rate-determining step. This was used to direct the discovery of a 2nd generation reagent derived from fluorenone (**6a**), which showed superior reactivity. We performed a full scope of alkenes, and observed broad reactivity with electron-rich alkenes and other substrates such as 1-hexene, cyclopentene, and various styrenes. Importantly, our method enables access to racemic β-amino amides (**10**) from complex azomethine imines (**9**) via the *N*-fluorenyl protecting group. In Chapter 3, we further demonstrate the value of this alkene aminocarbonylation to accessing enantioenriched β-amino carbonyl compounds, by developing a kinetic resolution of our azomethine imines.

Throughout the scope study, we analysed by-products and discovered pathways for degradation of the imino-isocyanate and the dipole. This knowledge was used to improve reaction conditions and confirm the intermediacy of the imino-isocyanate. The equilibrium between imino-isocyanate and its precursor was also studied by ^{1}H NMR. This work led into an IR study where we demonstrated the direct observation imino-isocyanates from **5a** and **6a** under reaction conditions. To our knowledge, this is the first example of the observation of imino-isocyanates by IR, and this tool could be valuable in the future for studying imino-isocyanate reactivity.

In developing reactivity with enol ethers we discovered imino-isocyanate formation to be rate-determining, which enabled base catalysis of the overall reaction. This was used to expand the scope of enol ethers as alkyne equivalents for aminocarbonylation reactions, and to access new azomethine imines (**16**) and complex pyrazolone cores (**17**). The avenue of carbonyl catalysis of the alkene aminocarbonylation was also explored, including early studies of background reactivity

and turn-over abilities with different catalysts. With these foundations in place, more studies are required to find working catalyst system. If the desired reactivity is discovered, then stereoselective catalysis should be explored by using chiral aldehyde catalysts. This approach would provide a value method to access enantioenriched pyrazolidinones, and their derivative β-aminocarbonyl compounds, from alkenes. However, while searching for a catalyst system for alkene aminocarbonylation, we became interested in other routes to enantioenriched aminocarbonylation products. In the next chapter, a Brønsted acid catalysed kinetic resolution of azomethine imines is described.

2.4. References

(1) Gan, W.; Moon, P. J.; Clavette, C.; Das Neves, N.; Markiewicz, T.; Toderian, A. B.; Beauchemin, A. M. *Org. Lett.* **2013**, *15*, 1890.
(2) Clavette, C. Synthesis of beta-Aminocarbonyl Compounds and Hydrazine Derivatives Using Amino- and Imino-Isocyanates, Thesis, University of Ottawa, 2015.
(3) Clavette, C.; Gan, W.; Bongers, A.; Markiewicz, T.; Toderian, A. B.; Gorelsky, S. I.; Beauchemin, A. M. *J. Am. Chem. Soc.* **2012**, *134*, 16111.
(4) Janssen, S.; Schmitt, K.; Blanke, M.; Bauersfeld, M. L.; Wollenstein, J.; Lang, W. *Philos. Trans. R. Soc. A Math. Phys. Eng. Sci.* **2014**, *372*, 20130311.
(5) DeSimone, J. M. *Science* **2002**, *297*, 799.
(6) Capello, C.; Fischer, U.; Hungerbühler, K. *Green Chem.* **2007**, *9*, 927.
(7) Li, L.-C.; Ren, J.; Liao, T.-G.; Jiang, J.-X.; Zhu, H.-J. *European J. Org. Chem.* **2007**, 1026.
(8) Lavergne, K.; Bongers, A.; Betit, L.; Beauchemin, A.M. *Org. Lett*. **2015**, *17*, 3612.
(9-16) Bondock, S.; Rabie, R.; Etman, H. A.; Fadda, A. A. *Eur. J. Med. Chem*. **2008**, *43*, 2122.; Sujatha, K.; Shanthi, G.; Selvam, N. P.; Manoharan, S.; Perumal, P. T.; Rajendran, M. *Bioorg. Med. Chem. Lett.* **2009**, *19*, 4501.; Kawai, H.; Nakai, H.; Suga, M.; Yuki, S.; Watanabe, T.; Saito, K. I. J. *J. Pharmacol. Exp. Ther.* **1997**, *281*, 921.; Watanabe, T.; Yuki, S.; Egawa, M.; Kellner, H. M. *Br. J. Clin. Pharmacol.* **1980**, *10*, 2995.; Laleu, B.; Gaggini, F.; Orchard, M.; Fioraso-Cartier, L.; Cagnon, L.; Houngninou-Molango, S.; Gradia, A.; Duboux, G.; Merlot, C.; Heitz, F.; Szyndralewiez, C.; Page, P. *J. Med. Chem.* **2010**, *53*, 7715.; Maser, H.; Boehner, B.; Forey, W. Eur. Patent Appl. EP 268554, 1988.; Yagi, K.; Numata, A.; Mimori, N.; Miyake, T.; Arai, K.; Ishii, S. *Pestic. Sci.* **1999**, *55*, 161.; Naylan, S. S.; Singh, C. P. Asian J. Chem. **1999**, *11*, 207.
(17) Unland, M. L. *Science* **1973**, *179*, 567.
(18) Ishida, H. *Fourier Transform Infrared Characterization of Polymers. Volume 36 of Polymer Science and Technology Series*; Ishida, H., Ed.; English.; Springer Science & Business Media: Boston, 1987.
(19) Xu, L.; Li, C.; Ng, K. Y. S. *J. Phys. Chem. A* **2000**, *104*, 3952.
(20) Blocked isocyanates in films: Wicks, D. A.; Wicks Jr., Z. W. *Prog. Org. Coatings* **2001**, *43*, 131.
(21) Pasinszki, T.; Krebsz, M.; Tarczay, G.; Wentrup, C. *J. Org. Chem.* **2013**, *78*, 11985.
(22) Zeng, X.; Beckers, H.; Willner, H. *Angew. Chemie Int. Ed.* **2011**, *50*, 482.
(23) Frederickson, L. D. *Anal. Chem.* **1964**, *36*, 1349.
(24) Alper, H.; Butler, D. C. D. *Chem. Commun.* **1998**, 2575.
(25) Daly, W. H.; Holle, H. J.; Fouad, F. M. *J. Org. Chem.* **1974**, *39*, 1600.

Chapter 3. Kinetic Resolution of Azomethine Imines by Enantioselective Reduction

3.1. Introduction

3.1.1. Overview of Kinetic Resolution

Kinetic resolution is a method used to separate components from a mixture by the selective reaction of one component. This technique is used frequently to separate enantiomers from a racemic mixture, using a chiral enantioenriched reagent or catalyst which results in diastereotopic transition states. In practical terms, a kinetic resolution is efficient when the ratio of the reaction rates of the enantiomers is at least 10.[1] This is defined as the selectivity factor, *s*, or sometimes referred to as the relative rates of the reaction (Equation 3.1). In general, reactions that offer the possibility of recycling the unwanted enantiomer, either dynamically or through separate chemical reactions, are typically more desirable.

$$s = \frac{k_R}{k_S} = e^{\Delta\Delta G^{\ddagger}/RT}$$

Equation 3.1. Kinetic resolution selectivity factor (s), when $k_R > k_S$.

Kinetic resolution is a valuable tool when the racemic process for accessing a compound is efficient and high yielding, or when direct asymmetric catalysis proves challenging. Such is the case with the aminocarbonylation of alkenes to give azomethine imines. In this reaction, there are two steps to control: imino-isocyanate formation and alkene aminocarbonylation; stereoselective intermolecular aminocarbonylation reactions have not been reported.[2] Depending on the imino-isocyanate precursor and alkene, either can be rate-determining. In order to access enantioenriched β-aminocarbonyl compounds from alkenes, we chose to explore the kinetic resolution of azomethine imines. After some investigation, we concentrated on enantioselective reduction for

the kinetic resolution, which is on the pathway toward β-amino amides. This is advantageous compared to typical kinetic resolutions, for example those known for azomethine imines, where the product is an unwanted cycloadduct.[3,4]

3.1.2. Contributions

The following is an unabridged version of the article "*Kinetic Resolution of Azomethine Imines by Enantioselective Reduction*," published in November 2015 in Angewandte Chemie International Edition and reprinted under license from John Wiley and Sons and Copyright Clearance Center (See Appendix I).[5] This includes a detailed Supporting Information (Chapter 6.3) with optimization data and tables, as well as additional unpublished data, provided therein. The development of the catalytic system and reaction conditions was done by myself. Patrick Moon, an undergraduate honours student working under my supervision, synthesized and performed kinetic resolutions of bulky, less reactive azomethine imines (**1f**,**g**,**h**), and found new conditions to improve solubility for these substrates. The article was written by myself with assistance and revisions from my thesis supervisor, Prof. André Beauchemin.

3.1.3. Abstract

Azomethine imines are valuable substrates in asymmetric catalysis, and can be precursors to β-amino carbonyl compounds and complex hydrazines. However, their utility is limited because complex and enantioenriched azomethine imines are often unavailable. Reported herein is a kinetic resolution of *N,N′*-cyclic azomethine imines by enantioselective reduction (*s*=13–43). This resolution was accomplished using a Brønsted acid catalyst, and represents the first example of the asymmetric reduction of azomethine imines. The pyrazolidinone product (up to 86 % *ee*) and the recovered azomethine imine (up to 99 % *ee*) can both be used to access the opposite enantiomers of valuable products.

3.1.4. References

(1) Keith, J. M.; Larrow, J. F.; Jacobsen, E. N. *Adv. Synth. Catal.* **2001**, *343*, 5.
(2) For a recent example of diastereoselective intramolecular alkene aminocarbonylation, see this article and those cited therein: Faulkner, A.; Scott, J. S.; Bower, J. F. .
(3) Suárez, A.; Downey, C. W.; Fu, G. C. *J. Am. Chem. Soc.* **2005**, *127*, 11244.
(4) Wang, M.; Huang, Z.; Xu, J.; Chi, Y. R. *J. Am. Chem. Soc.* **2014**, *136*, 1214.
(5) Bongers, A.; Moon, P. J.; Beauchemin, A. M. *Angew. Chemie Int. Ed.* **2015**, *54*, 15516.

3.2. Article: Kinetic Resolution of Azomethine Imines by Enantioselective Reduction

In the past decade, azomethine imines have been intensely studied in the field of asymmetric catalysis. These versatile compounds are well known as substrates in 1,3-dipolar cycloadditions and nucleophilic additions, as well as directing groups and bifunctional catalysts.[1] In 2003, Shintani and Fu reported the first example of asymmetric catalysis with azomethine imines, where they described the enantioselective cycloaddition of prochiral *N,N′*-cyclic azomethine imines.[2] Since this report, there have been many examples of catalytic stereoselective reactions with *N,N′*-cyclic azomethine imines (**1**; see Scheme 1),[3] thus establishing their value as precursors to pyrazolidinones, hydrazines, and β-aminocarbonyl compounds. However, because of the difficult synthesis of structurally diverse azomethine imines, the scope of these reactions is limited to simple and achiral substrates. While simple azomethine imines can be synthesized by the condensation of pyrazolidinones onto aldehydes, the complex and ketone-derived **1** are typically inaccessible.[4] There are only two reports on the access to enantioenriched **1**, that is, the kinetic resolution of a small scope of substrates (Scheme 1a).[5] In both cases, the selective cycloaddition of one enantiomer provides resolution, but at the cost of half the starting material going to the cycloadduct. These reaction conditions are only amenable to aldehyde-derived azomethine imines, with limited substitutions at C5 and no substitution at C4. Herein, we report a kinetic resolution of the complex ketone- and aldehyde-derived **1** by enantioselective reduction (s=13-43),[6] where both the products and recovered starting materials are valuable enantioenriched compounds containing the β-aminocarbonyl motif.

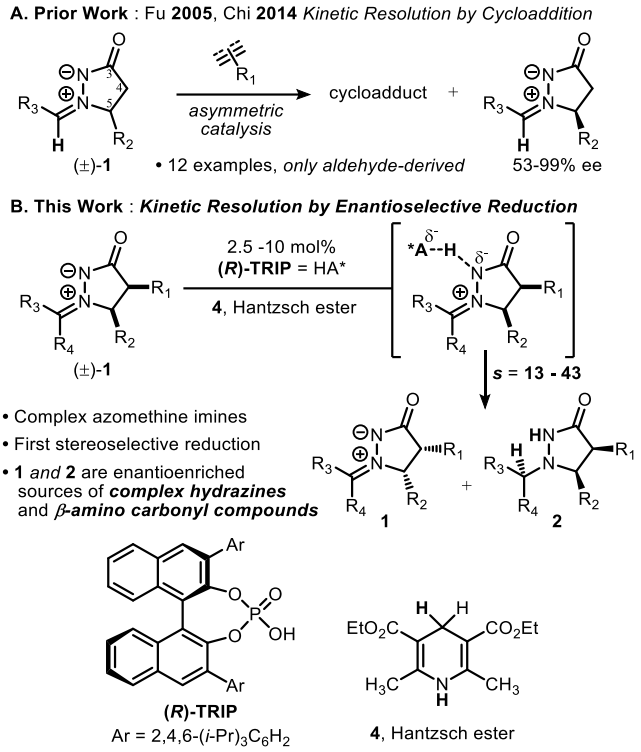

Scheme 1. Access to Enantioenriched Azomethine Imines.

We recently reported a cycloaddition of simple alkenes with imino isocyanates, to give azomethine imines (±)-**1** of unprecedented complexity.[7,8] Because examples of intermolecular alkene aminocarbonylations are rare,[7,9] and enantioselective variants have not been developed,[10] we aimed to find a general kinetic resolution procedure to resolve these azomethine imines. An attractive strategy is enantioselective reduction, to afford two enantioenriched compounds of opposite stereochemistry and differing simply by their oxidation state. This approach would provide access to enantioenriched pyrazolidinones, hydrazines, and β-amino carbonyl compounds. Azomethine imines are commonly reduced with hydrides, but to the best of our knowledge there are no reports of enantioselective reduction.[11] Furthermore, there are only two examples of enantioselective nucleophilic additions to **1**.[3h,i]

We explored several methods for the enantioselective reduction of imines, and became interested in chiral phosphoric acid catalysis.[12,13] We envisioned that the Brønsted acid catalyst

would activate the dipole at the negative nitrogen center, and selectively deliver the hydride to one enantiomer. While chiral phosphoric acids are well-known for the reduction of imines, the binding mode of these catalysts with azomethine imines is unique and has not been shown to provide efficient control of enantioselective 1,2-additions.[14] After testing several chiral phosphoric acid organocatalysts, reducing agents, and reaction conditions (see Tables S1-S4 in the Supporting Information for selected optimization data), we identified (*R*)-TRIP as an excellent catalyst for selective reduction, with the Hantzsch ester (**4**) as a mild reductant (Scheme 1b). We first investigated the use of these reaction conditions with fluorenone-derived azomethine imines [(±)-**1a-h**], which are the products of our alkene aminocarbonylation process.

Table 1. Kinetic Resolutions of Fluorenone-Derived Azomethine Imines by Enantioselective Reduction[a]

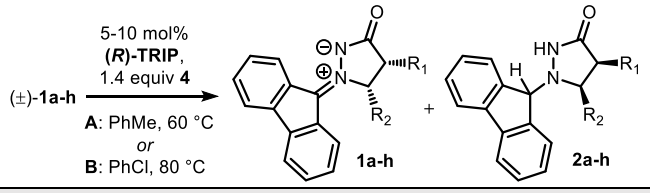

Entry	R_1, R_2	Cond[a]	t (h)	% *C*	*ee* (Yield) [%][b]		*s*[c]
					1	**2**	
1	**1a**: H, Ph	A	6	54	96 (45)	73 (41)	38
2	**1b**: H, 4-(F)C_6H_4	A	6	58	96 (32)	76 (32)	21
3	**1c**: H, 4-(Me)C_6H_4	A	6	57	95 (42)	74 (48)	22
4	**1d**: H, 4-(MeO)C_6H_4	A	16	55	95 (43)	77 (43)	29
5	**1d**	A	5	49	82 (50)	83 (46)	35
6	**1e**: Me, Ph	B	24	54	93 (43)	79 (52)	29
7	**1f**: H, 2-naphthyl	B	24	53	95 (45)	74 (45)	43
8	**1g**: H, 1-naphthyl	B	24	50	82 (48)	81 (45)	26
9	**1h**: H, *c*-C_6H_{11}	B[d]	24	46	72 (47)	83 (38)	26

[a] Azomethine imine (0.1-0.2 mmol, 1 equiv), **4** (1.4 equiv). Conditions A: (*R*)-TRIP (5 mol%) in toluene (0.02-0.04 M) at 60 °C. Conditions B: (*R*)-TRIP (10 mol%) in PhCl (0.01-0.02 M) at 80 °C. Conversion (% *C*) determined from ^{1}H NMR of crude reaction mixture. [b] The *ee* value was determined by HPLC using a Diacel ChiralPak AD-H column. Yield is that of the isolated product [c] Selectivity factor = k_{fast}/k_{slow} [d] 2.0 equiv of **4** were used.

Aldehyde-derived *N,N′*-cyclic azomethine imines [(±)-**1i-l**] showed high reactivity towards the reduction compared to the fluorenone-derived substrates, thus requiring lower catalyst loading and temperatures (Table 2). These kinetic resolutions proceeded selectively at 40-60 °C to provide

enantioenriched azomethine imines (**1i-l**) and pyrazolidinones (**2i-l**) in high yields (entries 1-5). In addition to solving the lack of reactivity observed with some of the substrates in Table 1, this protocol allowed us to assign the absolute configuration of the products (resolved **1i** was compared to previous reports).[5] The benzaldehyde-derived substrates (±)-**1k** and (±)-**1l** were synthesized by a one-pot net transimidation protocol from the fluorenone-derived aminocarbonylation products [Eq. (1)].[15] These azomethine imines were now easily reduced (entries 3-4), compared to the fluorenone-derived precursors (e.g. **1g**, Table 1, entry 8). The resolution of (±)-**1l** was effectively scaled up to 1 mmol, thus affording the azomethine imine in greater than 99% *ee* (Table 2, entry 5). Fortunately, pyrazolidinone **2l** (67% *ee*) produced in this experiment could be recrystallized to 98% *ee* (entry 5). After separation, both **1l** and **2l** underwent reductive ring opening to give the corresponding β-amino amides in good yields with no loss in enantiopurity [Eq. (2)].

Table 2. Kinetic Resolutions of Unsymmetrical Azomethine Imines by Enantioselective Reduction[a]

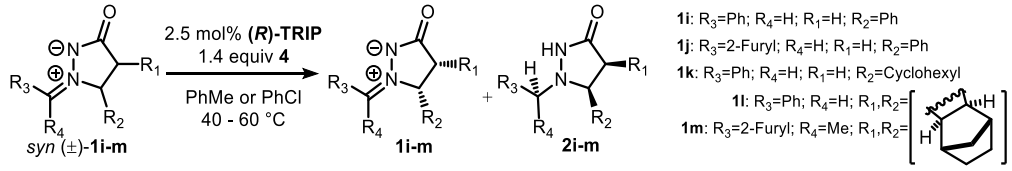

Entry		Solvent	T (°C)	t (h)	% *C*	*ee* (Yield) [%][b]		*s*[c]
						1	**2**	
1	**1i**	PhMe	40	6	57	95 (41)	86 (43)	22
2	**1j**	PhMe	60	6	56	94 (45)	75 (54)	23
3[d]	**1k**	PhCl	60	6	61	93 (35)	76 (41)	13
4	**1l**	PhMe	60	6	63	99 (32)	66 (52)	18
5[e]	**1l**	PhCl	60	4	61	>99 (39)	67 (50) 98 (29)[f]	25
6	**1m**	PhCl	80	24	56	85 (37)	78 (51)[g]	13

[a] Azomethine imine (0.1-0.2 mmol, 1 equiv), **4** (1.4 equiv), (*R*)-TRIP (2.5 mol%) in toluene (0.025 M) or PhCl (0.05 M). Conversion (% *C*) determined from ^{1}H NMR of crude reaction mixture. [b] The *ee* value was determined by HPLC using a Diacel ChiralPak AD-H column. Yield is that of the isolated product [c] Selectivity factor = k_{fast}/k_{slow}. [d] 5 mol% (*R*)-TRIP [e] 1 mmole scale. [f] After recrystallization. [g] Mixture of two diastereomers (2:1), % *ee* of major diastereomer.

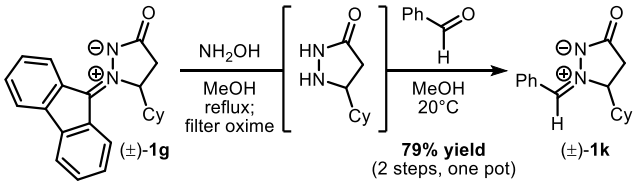

(1)

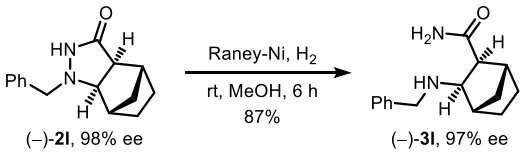

(2)

The proposed pre-transition state complex for selective reduction of **1i** is shown in Figure 1. This model features both Brønsted acid activation of the azomethine imine and Brønsted base activation of the Hantzsch ester by the chiral phosphoric acid.[16] The observed selectivity is rationalized by orienting the large substituent of the azomethine imine (Ph) in the most accessible quadrant.

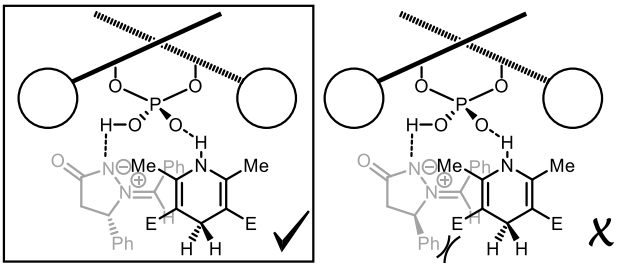

Figure 1. Pre-transition state complexes for stereoselective reduction of azomethine imine (±)-**1i**. E=CO_2Et.

In summary, we developed a kinetic resolution of complex *N,N′*-cyclic azomethine imines (±)-**1** by selective reduction of one enantiomer (*s*=13-43) by using the Brønsted acid organocatalyst (*R*)-TRIP. This protocol demonstrates the first example of stereoselective reduction of azomethine imines. The enantioenriched azomethine imines **1** and pyrazolidinones **2** are both valuable precursors to β-amino carbonyl compounds and complex hydrazine derivatives, as well as attractive substrates for asymmetric synthesis. Combined with our previously reported intermolecular alkene aminocarbonylation reaction to synthesize (±)-**1**,[7] this work provides a versatile approach to enantioenriched compounds possessing the β-aminocarbonyl motif.

Article References

[1] Reviews on azomethine imine synthesis and reactivity: a) C. G. Stuckwisch, *Synthesis* **1973**, *1973*, 469; b) J.G. Schantl, *Science of Synthesis* **2004**, *27*, 731–824; c) S. Tšupova, U. Mäeorg, *Heterocycles* **2014**, *88*, 129; d) G. Qiu, Kuang, Y., Wu, J. *Adv. Synth. Catal.* **2014**, *356*, 3483; e) See also: A. K. Griffith, C. M. Vanos, T. H. Lambert, *J. Am. Chem. Soc.* **2012**, *134*, 18581; f) C. Nájera, J. M. Sansano, M. Yus *Org. Biomol. Chem.* **2015**, *13*, 8596.

[2] R. Shintani, G. C. Fu, *J. Am. Chem. Soc.* **2003**, *125*, 10778.

[3] For examples of catalytic stereoselective reactions of *N,N'*-cyclic azomethine imines see: a) R. Shintani, T. Hayashi, *J. Am. Chem. Soc.* **2006**, *128*, 6330; b) W. Chen, W. Du, Y.-Z. Duan, Y. Wu, S.-Y. Yang, Y.-C. Chen, *Angew. Chem.* **2007**, *119*, 7811-7814; *Angew. Chem. Int. Ed.* **2007**, *46*, 7667-7670; c) H. Suga, A. Funyu, A. Kakehi, *Org. Lett.* **2007**, *9*, 97; d) A. Chan, K. A. Scheidt, *J. Am. Chem. Soc.* **2007**, *129*, 5334; e) M. P. Sibi, D. Rane, L. M. Stanley, T. Soeta, *Org. Lett.* **2008**, *10*, 2971; f) M. Keller, A. S. Sido, P. Pale, J. Sommer, *Chem. - A Eur. J.* **2009**, *15*, 2810; g) N. D. Shapiro, Y. Shi, F. D. Toste, *J. Am. Chem. Soc.* **2009**, *131*, 11654; h) H. Kawai, A. Kusuda, S. Nakamura, M. Shiro, N. Shibata, *Angew. Chem*. **2009**, *121*, 6642-6645; *Angew. Chem. Int. Ed.* **2009**, *48*, 6324-6327; i) R. Shintani, Y.-T. Soh, T. Hayashi, *Org. Lett.* **2010**, *12*, 4106; j) R. Na, C. Jing, Q. Xu, H. Jiang, X. Wu, J. Shi, J. Zhong, M. Wang, D. Benitez, E. Tkatchouk, W. A. Goddard, H. Guo, O. Kwon, *J. Am. Chem. Soc.* **2011**, *133*, 13337; k) T. Imaizumi, Y. Yamashita, S. Kobayashi, *J. Am. Chem. Soc.* **2012**, *134*, 20049; l) X. Xu, Y. Qian, P. Y. Zavalij, M. P. Doyle, *J. Am. Chem. Soc.* **2013**, *135*, 1244; m) X. F. Xu, X. C. Xu, P. Y. Zavalij, M. P. Doyle, *Chem. Commun.* **2013**, *49*, 2762; n) H. Guo, H. Liu, F.-L. Zhu, R. Na, H. Jiang, Y. Wu, L. Zhang, Z. Li, H. Yu, B. Wang, Y. Xiao, X.-P. Hu, M. Wang, *Angew. Chem.* **2013**, *125*, 12873-12877; *Angew. Chem. Int. Ed.* **2013**, *52*, 12641-12645; o) R.-Y. Zhu, C.-S. Wang, J. Zheng, F. Shi, S.-J. Tu, *J. Org. Chem.* **2014**, *79*, 9305; p) M. Hori, A. Sakakura, K. Ishihara, *J. Am. Chem. Soc.* **2014**, *136*, 13198.

[4] a) H. Dorn, A. Otto, *Angew. Chem.* **1968**, *80*, 911-912; *Angew. Chem. Int. Ed.* **1968**, *7*, 214-215; b) S. Zupancic, J. Svete, B. Stanovnik, *J. Heterocycl. Chem.* **1999**, *36*, 607.

[5] a) A. Suárez, C. W. Downey, G. C. Fu, *J. Am. Chem. Soc.* **2005**, *127*, 11244; b) M. Wang, Z. Huang, J. Xu, Y. R. Chi, *J. Am. Chem. Soc.* **2014**, *136*, 1214.

[6] J. M. Keith, J. F. Larrow, E. N. Jacobsen, *Adv. Synth. Catal.* **2001**, *343*, 5.

[7] C. Clavette, W. Gan, A. Bongers, T. Markiewicz, A. B. Toderian, S. I. Gorelsky, A. M. Beauchemin, *J. Am. Chem. Soc.* **2012**, *134*, 16111.

[8] W. Gan, P. J. Moon, C. Clavette, N. Das Neves, T. Markiewicz, A. B. Toderian, A. M. Beauchemin, *Org. Lett.* **2013**, *15*, 1890.

[9] a) R. Graf *Justus Liebigs Ann. Chem.* **1963**, *661*, 111; b) J. K. Rasmussen, A. Hassner, *Chem. Rev.* **1976**, *76*, 389; c) J. Cheng, X. Qi, M. Li, P. Chen, G. Liu, *J. Am. Chem. Soc.* **2015**, *137*, 2480

[10] Sasai has pioneered enantioselective intramolecular alkene aminocarbonylations: a) T. Shinohara, M. A. Arai, K. Wakita, T. Arai, H Sasai, *Tetrahedron Lett.* **2003**, *44*, 711; b) T. Tsujihara, T. Shinohara, K. Takenaka, S. Takizawa, K. Onitsuka, M. Hatanaka, H. Sasai, *J. Org. Chem.* **2009**, *74*, 9274

[11] For Ir-catalyzed reduction of related *N*-iminopyridinium ylides see: C. Y. Legault, A. B. Charette, *J. Am. Chem. Soc.* **2005**, *127*, 8966.

[12] a) S. Hoffmann, A. M. Seayad, B. List, *Angew. Chem.* **2005**, *117*, 7590-7593; *Angew. Chem. Int. Ed.* **2005**, *44*, 7424-7427; b) S. G. Ouellet, J. B. Tuttle, D. W. C. MacMillan, *J. Am. Chem. Soc.* **2005**, *127*, 32; c) M. Rueping, E. Sugiono, C. Azap, T. Theissmann, M. Bolte, *Org. Lett.* **2005**, *7*, 3781.

[13] Selected articles on chiral phosphoric acid catalysts: a) D. Uraguchi, M. Terada, *J. Am. Chem. Soc.* **2004**, *126*, 5356; b) T. Akiyama, J. Itoh, K. Yokota, K. Fuchibe, *Angew. Chem.* **2004**, *116*, 1592-1594; *Angew. Chem. Int. Ed.* **2004**, *43*, 1566-1568; c) T. Akiyama, *Chem. Rev.* **2007**, *107*, 5744; d) K. Kaupmees, N. Tolstoluzhsky, S. Raja, M. Rueping, I. Leito, *Angew. Chem.* **2013**, *125*, 11783-11786; *Angew. Chem. Int. Ed. 52*, 11569-11572; e) D. Parmar, E. Sugiono, S. Raja, M. Rueping, *Chem. Rev.* **2014**, *114*, 9047; f) For a discussion on binding modes see: X. Hong, H. B. Küçük, M. S. Maji, Y.-F. Yang, M. Rueping, K. N. Houk, *J. Am. Chem. Soc.* **2014**, *136*, 13769.

[14] Maruoka showed chiral carboxylic acid catalysts activate acyclic/*C*,*N*-cyclic azomethine imines towards enantioselective nucleophilic addition: a) T. Hashimoto, H. Kimura, Y. Kawamata, K. Maruoka, *Nat.*

Chem. **2011**, *3*, 642; b) T. Hashimoto, M. Omote, K. Maruoka, *Angew. Chem.* **2011**, *123*, 9114-9117; *Angew. Chem. Int. Ed.,* **2011**, *50*, 8952-8955; c) T. Hashimoto, H. Kimura, Y. Kawamata, K. Maruoka, *Angew. Chem.* **2012**, *124*, 7391-7393; *Angew. Chem. Int. Ed.* **2012**, *51*, 7279-7281; d) See also reference 13f. For work with a chiral thiourea, see: e) B.-S. Li, Y. Wang, Z. Jina, Y. R. Chi, *Chem. Sci.* **2015**, *6*, 6008-6012

[15] a) K. Lavergne, A. Bongers, L. Betit, A. M. Beauchemin, *Org. Lett*. **2015**, *17*, 3612; b) L. Betit, M. Sc. Thesis, University of Ottawa, 2015.

[16] K. Saito, Y. Shibata, M. Yamanaka, T. Akiyama, *J. Am. Chem. Soc.* **2013**, *135*, 11740.

3.3. Summary and Outlook

The work presented in this chapter established that the aminocarbonylation reaction of imino-isocyanates with alkenes is a useful approach for accessing β-amino carbonyl motifs. This kinetic resolution of the aminocarbonylation products by Brønsted acid catalysis is the first example of asymmetric reduction of any type of azomethine imine. This method enables the synthesis of enantioenriched β-amino amides in three steps from alkenes, and the reduction strategy gives access to both enantiomers. In addition to the work described in the communication, this kinetic resolution was also attempted with other types of azomethine imines. First, the conditions were tested with a bicyclic azomethine imine (±)-**1n** derived from intramolecular alkene aminocarbonylation (Scheme 3.1). The kinetic resolution proceeded to only 40% conversion after the mixture was heated at 80°C for 24 hours. Fortunately, the product was isolated as a single diastereomer in 86% enantiomeric excess. If this reactivity could be improved, we could develop a new approach to enantioenriched piperidines with the β-amino carbonyl motif.

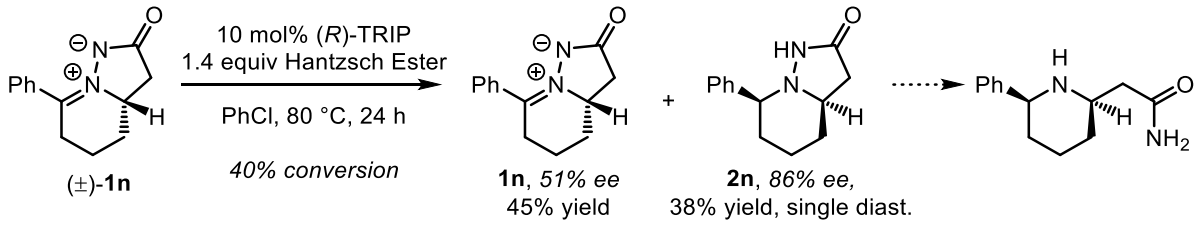

*Scheme 3.1. Kinetic resolution of bicyclic azomethine imine (±)-**1n**.*

Complex, unsymmetrical ketone-derived azomethine imines are difficult to synthesize with available methods. Attempts to synthesize a small variety by condensation methods gave very low yields (see Chapter 6.3.4). In addition, both condensation and aminocarbonylation gave an inseparable mixture of E/Z diastereomers. In general, the attempted kinetic resolutions these ketone-derived azomethine imines proceeded to low conversion over long reaction times, with competitive degradation of the Hantzsch ester. This includes unsuccessful reactions of the analogous 4-membered *N,N'*-cyclic azomethine imines (Scheme 3.2).

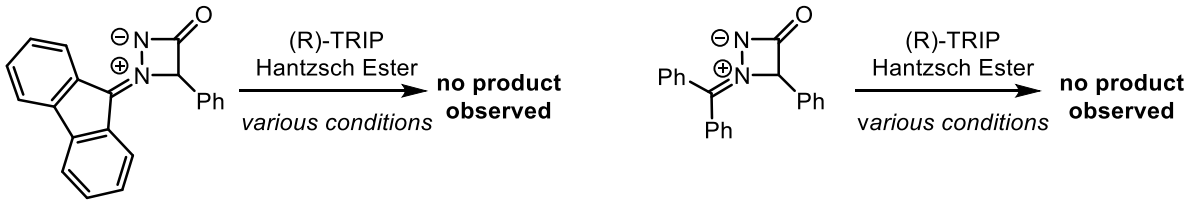

Scheme 3.2. Unsuccessful attempts at the kinetic resolution of 4-membered N,N'-cyclic azomethine imines.

Enantioselective reductions of acyclic azomethine imines were also explored. As described in Chapter 1.3, these azomethine imines can be accessed by 1,2-prototropy of hydrazones or mono-substituted hydrazines, or by the condensation of carbonyl compounds onto 1,2-disubstituted hydrazines. Both methods for in situ access to the dipole were tested under Brønsted acid catalysis conditions, using achiral catalyst diphenylphosphate (DPP) and chiral catalyst (*R*)-TRIP (Chapter 6.3.5, Table 6.8 & Table 6.9). Unfortunately, the desired reduction was only observed in one case, and the selectivity was poor.

Overall, the synthesis of enantioenriched β-amino carbonyl compounds from alkenes is still a challenge, and the activation of azomethine imines with chiral Brønsted acids is still not fully explored. However, at this stage we moved forward to further study the reactivity of imino-isocyanates and discover new cycloaddition partners for the aminocarbonylation reaction.

Chapter 4. Intermolecular Aminocarbonylation of Imines

4.1. Introduction

Our study of the [3+2] cycloaddition reactions of imino-isocyanates with alkenes has proven the value of this approach to access molecules containing the beta-amino carbonyl motif, including azomethine imines, pyrazolones, and enantioenriched β-amino amides. More broadly, this represents a new route to synthesize heterocycles with the N-NCO motif, which exists in many pharmaceuticals and agrochemicals (Figure 4.1).[1–4]

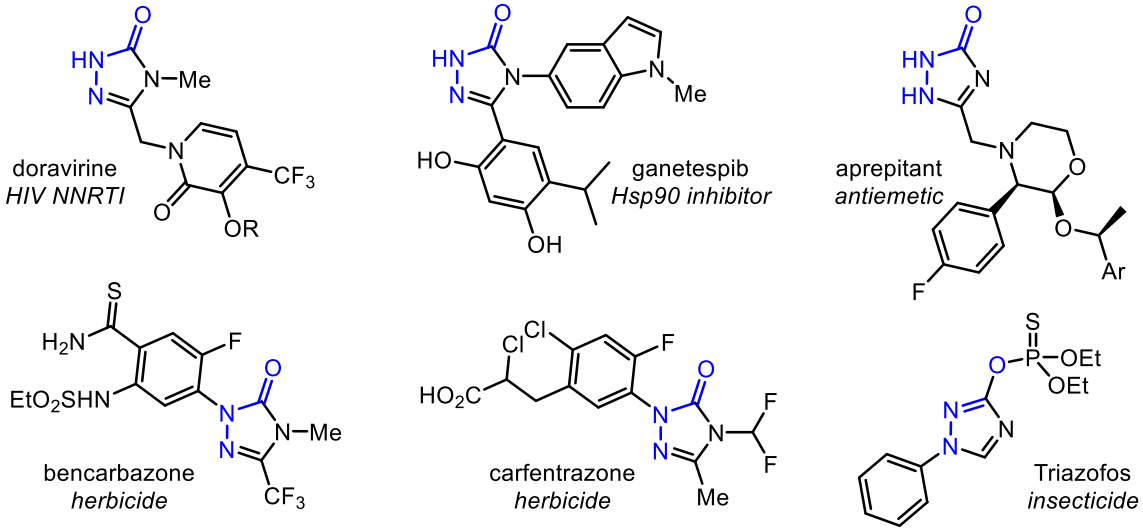

Figure 4.1. Triazolone cores important to pharmaceutical and agrochemical industries (N-N-CO motif in blue).

As part of our research program, we became interested in exploring the reactivity of imino-isocyanates with new substrates, to give access to more diverse azomethine imines and their derivatization products. This led us to study cycloaddition reactions of imines as alternative substrates to alkenes, with the objective to yield azomethine imines containing a triazole core.[5] The use of imino-isocyanates would provide a new disconnection to access these heterocycles, complementary to the traditional route involving *C*-isocyanates and hydrazines (Scheme 4.1).

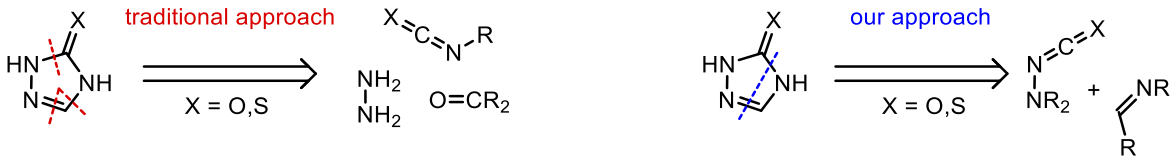

Scheme 4.1. Retrosynthetic analysis for access to the triazlone core by two different approaches.

C-Isocyanates are important building blocks in modular syntheses of heterocycles, including systems containing the N-N-CO motif.[6–10] Advantages of this approach are simplicity and high reactivity, since substitution and condensation reactions of small molecules provide the desired heterocycles. However, there are some practical issues including the toxicity and functional group diversity of *C*-isocyanates, problems with chemoselectivity, and the sensitivity of hydrazines. This traditional synthesis of the heterocycle is also non-convergent, and can add several steps to an overall synthesis of the target. Alternatively, we envisioned the cycloaddition of imino-isocyanates with imines to rapidly assemble the core in a more convergent approach, which improves the efficiency of multistep synthesis. In this strategy, the imino-isocyanate precursor is a less sensitive hydrazine derivative, and a masked electrophilic carbonyl.

As outlined in Chapter 1, cycloaddition reactions of heterocumulenes with various C=N bonds are well known. Carbodiimides and isocyanates are well known to dimerize and react with other heterocumulenes at their C=N bonds in [2+2] reactions,[11] and [3+2] cycloadditions are also possible with 1,3-amphoteric amino-isocyanates.[12–14] These reactions generally occur under mild conditions, and the mechanism (concerted or stepwise) often depends on the reacting partners.[11] Reactions of imines are also known, with an excellent example being the Staudinger synthesis. In this reaction, the heterocumulene, a ketene, reacts in a formal [2+2] cycloaddition with an imine (Scheme 4.2). The reaction was discovered in 1907, but the mechanism has been the subject of a long-standing debate.[15,16] It is now accepted that in solution the stepwise approach shown below

is the favoured pathway. Electron withdrawing R^1 and R^2 substituents can assist the reaction, by increasing electrophilicity of the ketene and stabilizing the zwitterionic intermediate. However, when substituents are bulky the cyclization can become rate determining.

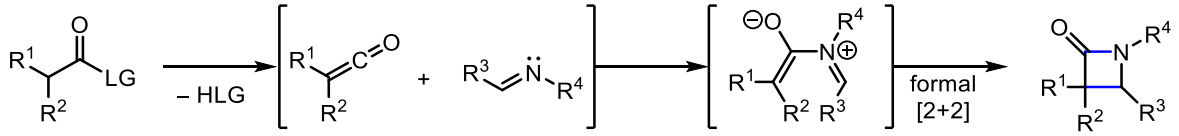

Scheme 4.2. Mechanism of the Staudinger synthesis.

In the context of our work, the Staudinger synthesis has interesting parallels to aminocarbonylation cycloadditions of imino-isocyanates, including the often employed in situ formation of the ketene by loss of a leaving group. We used the large body of literature around this and similar reactions to guide our search for reactivity with imines. In this Chapter, cycloadditions of imines with imino-isocyanates will be presented, which gives access to new azomethine imines having the triazolone core. The comparison of reactivity of imines with alkenes will be discussed, as well as possible mechanisms for the transformation.

4.2. Results and Discussion

4.2.1. Aminocarbonylation of Imines

In our efforts toward cycloaddition reactions with imines, we began by synthesizing and testing a simple imine with the fluorenone reagent (**1a**). We quickly discovered reactivity with *N*-methyl-1-phenylmethanimine (**2a**) under typical alkene aminocarbonylation conditions, and observed the desired product (**3a**) in 22-27% NMR yield (Scheme 4.3). We also observed a by-product in the crude mixture (**4a**), which results from substitution of methylamine onto the imino-isocyanate.

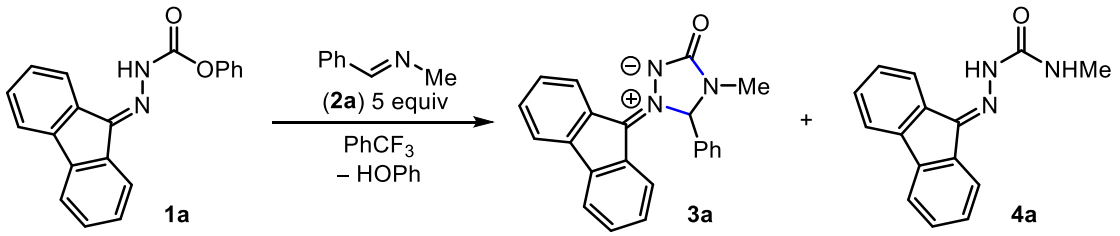

*Scheme 4.3. Initial study of imine cycloaddition reactivity with hydrazone **1**.*

Unfortunately, the presence of excess imine after the reaction caused problems for isolation of **3a** by chromatography. When the crude mixture was loaded onto silica gel, imine **2a** decomposed producing excess methylamine relative to the desired product. This reacted with the desired product, and none of the dipole was isolated from the column. However, the free triazolidinone **5** was isolated, which provided evidence for the formation of the azomethine imine product (Equation 4.1.).

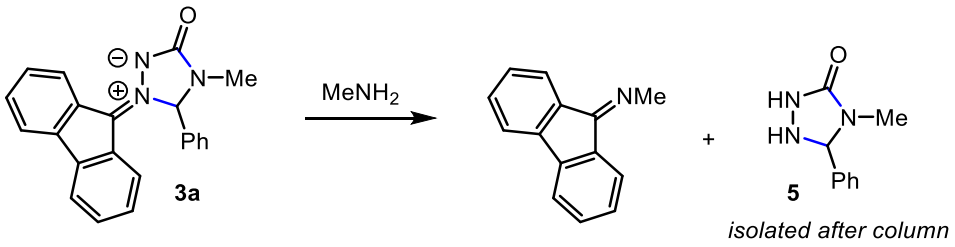

Equation 4.1.

We decided to continue exploring the reactivity of **2a** by screening imino-isocyanate precursors. Only two equivalents of **2a** were used, in order to to prevent the methylamine side reactions described above. We tested a variety of simple unsymmetrical precursors (**1b-g**), under conditions typical for these reagents in alkene aminocarbonylation reactions (Table 4.1).[17] Hydrazones derived from aromatic aldehydes gave only 12-31% of the cycloadduct (entries 1-2,5). Thienyl- and furyl-substituted products were detected in 94% and 52% NMR yields, respectively (entries 3-4). The ketone-derived precursor gave no yield of product (entry 6). While the crude mixtures

with precursors **1b-f** were clean, the reaction with **1g** showed considerable by-product formation in the crude mixture.

Table 4.1. Screening of imino-isocyanate precursors for aminocarbonylation of imine **2a**.

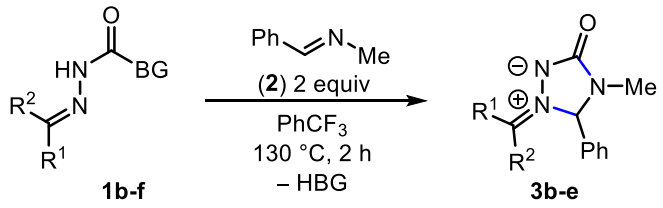

Entry		BG	R^1	R^2	Yield (%) [b]
1	**1b**	OPh	Thienyl	H	94 (**3b**)
2	**1c**	OPh	Furyl	H	52 (**3c**)
3	**1d**	O*t*-Bu	Ph	H	12 (**3d**)
4	**1e**	OPh	Ph	H	31 (**3d**)
5	**1f**	OPh	(4-OMe)C_6H_4	H	30 (**3e**)
6	**1g**	OPh	Furyl	Me	n.p.

a) Conditions: Hydrazone 1**c-h** (0.10 mmol, 1 equiv) and **2** (0.20 mmol, 2 equiv) were combined in a vial and purged with Argon. The reaction was heated to 130 °C by microwave irradiation. b) NMR yields are reported, determined using 1,3,5-trimethoxybenzene internal standard. n.p.= no product observed.

This difference in yield observed with precursors **1b** and **1c** was interesting, and we decided to run a competition experiment to learn more about this reactivity. We combined one equivalent of each hydrazone with one equivalent of **2a**, and heated the reaction for 10 minutes at 130 °C (Scheme 4.4). We expected to see low conversion of the imine, and more of product **3b** from precursor **1b**. However, we observed almost complete consumption of the imine, in a clean reaction with good mass balance. We also observed ca. twice the amount of product **3c** than **3b**. This experiment shows that imines are very reactive substrates for the cycloaddition reaction. It also indicates that precursor **1c** is a better substrate for the reaction at short times, and suggests the lower yield observed after 2 hours is due to degradation of the product.

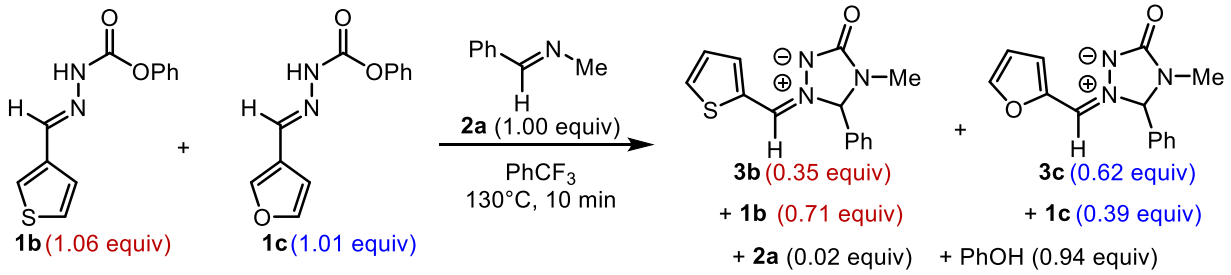

*Scheme 4.4. Competition experiment between imino-isocyanate precursors **1b** and **1c**.*

We further explored the reaction conditions using hydrazone **1c**, and the results are summarized in Table 4.2. Shortening the reaction time from two hours to one hour increased the yield of **3c** from 52 to 78%. This supports the hypothesis that the product is degrading over time under the reaction conditions. The yield is comparable when the temperature is lowered to 120 °C, and the reaction time could be increased to 3 h at this temperature to improve the yield to 81% (entries 3-4). The amount of imine could be reduced to 1.1 equivalents to give 71% yield (entry 5). Additionally, the reaction could be performed under traditional reflux conditions overnight and still provide 64% of **3c** (entry 6).

Table 4.2. Optimization of the aminocarbonylation of imine **2a** with precursor **1c**.[a]

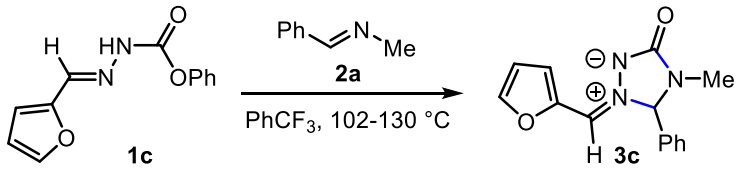

Entry	Equiv **2**	t (h)	T (°C)	Yield (%) **3c** [b]
1	2.0	2	130	52
2	2.0	1	130	78
3	2.0	1	120	72
4	2.0	3	120	81
5	1.1	3	120	71
6	2.0	16	102[c]	64

a) Conditions: **1c** (1.0 equiv.), **2a** (1.1 or 2.0 equiv.), and $PhCF_3$ (0.05 M) were combined in a dry vial, which was sealed and purged with Argon. The mixture was heated by microwave irradiation. b) NMR yields, determined using 1,3,5-trimethyoxybenzene internal standard. c) Conventional heating at reflux in an oil bath.

A single crystal X-ray structure of **3b** was obtained to probe the origin of the increased stability observed for this product (Figure 4.2). The S···N distance is 2.84 Å, which is less than the sum of the van der Waals radii (S + N = 3.35 Å) and within the range of known thienyl S···N non-covalent interactions (2.7-3.0 Å).[17] The presence of a S···N chalcogen bond could explain the improved product stability and yield observed with the thienyl group.[17] The dihedral angles (S-C-C-N-N) of φ_1 = 0.59° and φ_2 = −1.20° position the thienyl group and triazolone core as co-planar, which suggests conjugation of the thienyl group with the dipole.

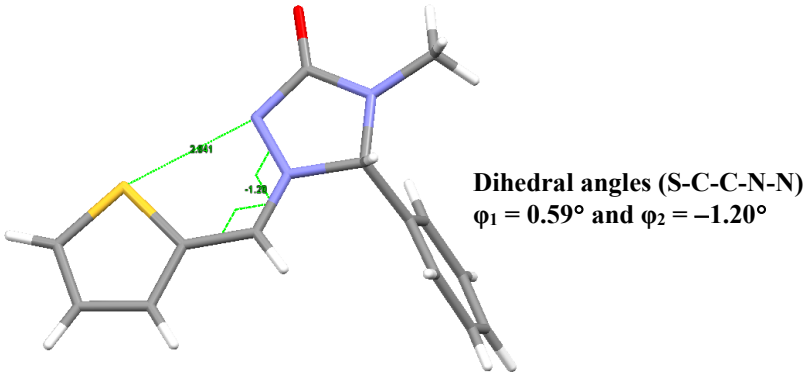

*Figure 4.2. Single crystal X-ray structure of **3b**. Proximity of the thienyl sulfur and N⁻ is shown.*

In crude reaction mixtures we often observed the Z-imine (*Z*-**2a**), which was predicted to be formed from cycloreversion of the product. In the single crystal X-ray structure obtained of **3b**, we observe the methyl group is in plane with the triazolone core, with loss of the starting material imine geometry (Figure 4.2). We expected the product decomposition pathway to involve cycloreversion and slow degradation of the imino-isocyanate over longer reaction times. When the dipole **3b** was heated for 2 hours in benzene-d_6 at the reaction temperature, we observed 43% conversion to a 2:1 mixture of *E*-**2a**:*Z*-**2a** (Scheme 4.5). Importantly, *E*-**2a** was not observed to isomerize under the same conditions, or in the presence of PhOH additive. In practical terms, the *Z*-imine is an indicator for cycloreversion and likely loss of product. If this was observed during

our optimization, we would retest the reaction at shorter times and lower temperatures to improve the yield of cycloadduct.

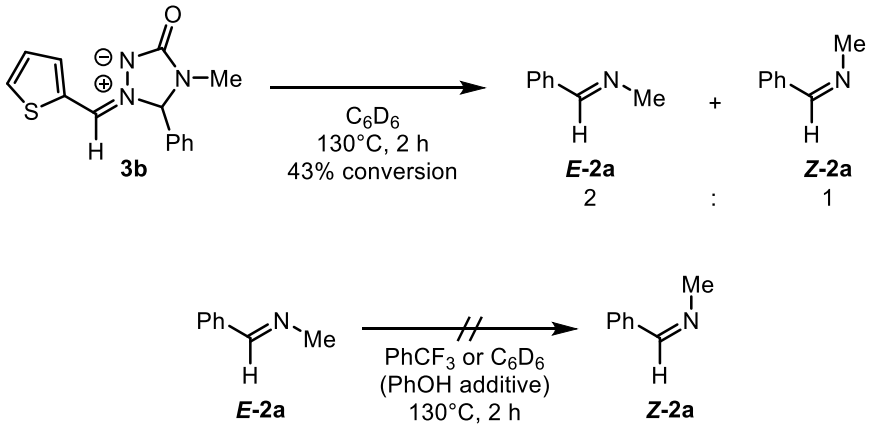

*Scheme 4.5. Cycloreversion of cycloadduct **3b**, and control reaction for imine isomerization.*

With a good understanding of the cycloaddition reaction and by-product pathways, the scope of imines with aldehyde-derived hydrazones was expanded (Table 4.3). The products were found to be sensitive towards silica gel. Isolation was achieved by trituration of the crude mixture in Et_2O, and yields were often higher at larger scale. Imines derived from aromatic aldehydes gave the best reactivity, and using only 1.5-2.0 equiv of the imine was sufficient. Even under optimized conditions, benzaldehyde-derived hydrazone **1d** displayed poor reactivity, related to stability of the product, and isolation of **3d** was not possible without derivatization. The products from hydrazone **1f** were easier to isolate, and 64% yield of **3e** was obtained from the *N*-benzyl imine. Hydrazone **1e** continued to provide the best yields, and the stability of **3f-i** allowed for easy isolation. *N*-Methyl imines with electron-withdrawing groups (product **3f**, 41%) and electron-donating groups (product **3g**, 69% yield) were both well-tolerated. Overall, higher yields were obtained in the presence of *N*-alkyl substituents while an *N*-Ph imine provided **3h** in 39% yield.

Table 4.3. Scope of imine in aminocarbonylation reactions with **1b**,**c**,**e**.[a]

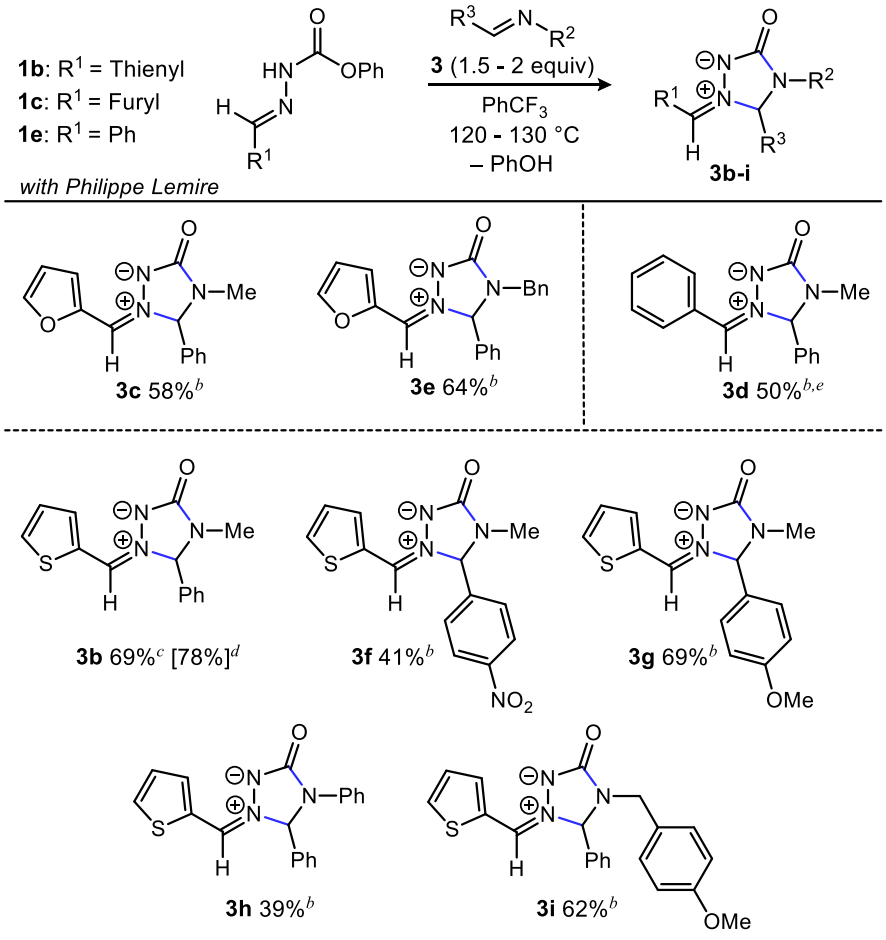

[a]Conditions: **1b-c** or **1e** (1.0 equiv), imine (1.5-2.0 equiv), $PhCF_3$ (0.05-0.10 M), heated (microwave or conventional) to [b]120 °C or [c]130 °C for 1-3 hours in a sealed vial under Argon. Isolated yields are provided. [d][NMR yield] with 1,3,5-trimethoxybenzene internal standard. [e]NMR yield of **3d**=50%. Isolation by reduction of **3d** with $NaBH_4$, isolated yield of ***red*-3d** =39% over 2 steps.

A multicomponent reaction was also performed, where benzaldehyde, benzyl amine, and **1c** were combined in one pot (Equation 4.2). Amines can react with isocyanate precursors at room temperature, but we expected the condensation onto benzaldehyde to be fast and favourable. Molecular sieves were added to remove water produced by the condensation. This reaction yielded 40% of **3e**, with 47% of the substitution product **4b**.

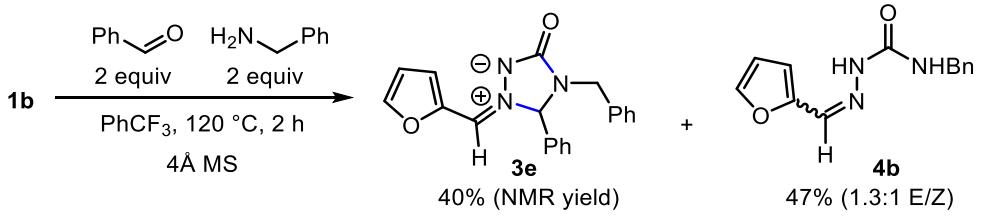

Equation 4.2

Unfortunately, no product was observed in reactions with various ketimines, and there was very low reactivity with a *C,N*-cyclic imine to give **3j** (Scheme 4.6). Cycloaddition with these bulkier imines is likely limited by steric hindrance.

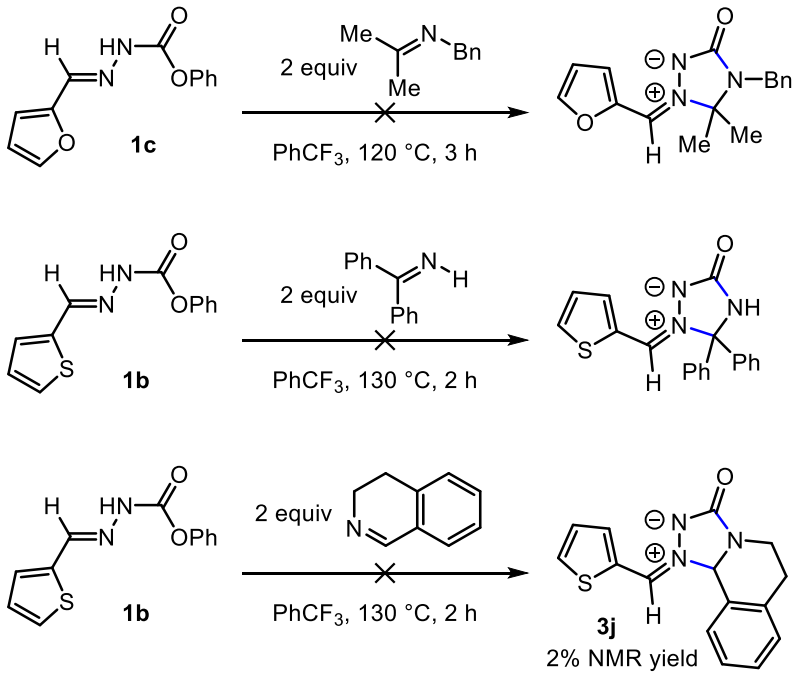

Scheme 4.6. Attempted cycloaddition reactions of ketimines and C,N-cyclic imines.

There are two possible mechanisms for the reaction of imino-isocyanates with imines: 1) Concerted (asynchronous) cycloaddition in direct analogy to alkene reactivity; 2) Stepwise intermolecular and intramolecular nucleophilic additions in analogy to the Staudinger synthesis (Scheme 4.7).

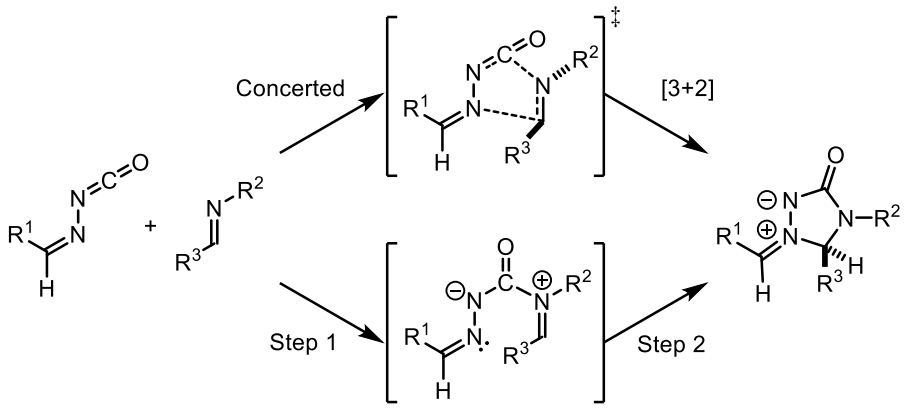

Scheme 4.7. Concerted and stepwise mechanisms for the aminocarbonylation of imines with imino-isocyanates.

One indication that a different mechanism is at work is the increased reactivity we observe with imines compared to alkenes. This is not rationalized when comparing typical features of imines vs. alkenes. The average strengths of C=N (147 kcal) and C=C (146 kcal/mol) bonds are similar,[18] with C=N bonds typically being stronger with substitution. Additionally, the HOMO of the imine is expected to be stabilized compared to an alkene. However, C=N bonds are more polarized, causing imines to be more electrophilic than alkenes. Combined, these factors suggest the stepwise mechanism but could also support a concerted cycloaddition that is more synchronous compared to the reaction of alkenes.

Another difference with imine reactivity, compared to alkenes, is that aldehyde-derived imino-isocyanates perform the best. For example, precursor **1c** yields 53% of cycloadduct with norbornene, and 78% yield of cycloadduct with imine **2a**, under the same conditions.[17] In contrast, the fluorenone reagent gives >95 % yield of norbornene cycloadduct, but only 25% of imine cycloadduct **3a** under equal conditions. This points to steric limitations in reactions of imines with ketone-derived imino-isocyanates which are less important in cycloaddition reactions of alkenes. Steric hindrance would be important in the nucleophilic addition of the imino-isocyanate in the stepwise mechanism (Scheme 4.8). This could help explain the formation of semicarbazone by-

product (**4**) in reactions of the fluorenone precursor, especially under mild conditions (90 °C) where the imine itself is confirmed to be stable towards degradation.

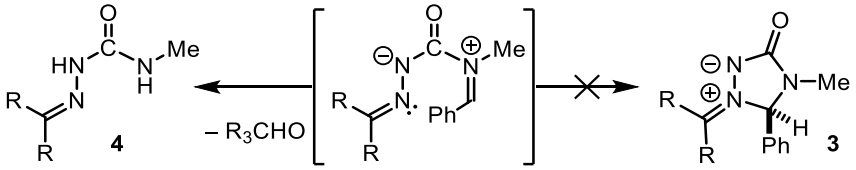

Scheme 4.8. Possible pathway for production of by-product with ketone-derived imino-isocyanate precursors.

4.2.2. Other C=N Bonds

In the study of new imino-isocyanate cycloaddition reactions we also tested C=N bonds of heterocumulenes, which is in line with known reactivity of amino-isocyanates described in Chapter 1. Unfortunately, reactions of **1c** with *C*-isocyanate and carbodiimide substrates were not successful, as shown in Scheme 4.9. From the perspective of the concerted cycloaddition, the heterocumulene HOMO is stabilized compared to alkenes and imines, which could preclude reactivity. From a stepwise approach, *C*-isocyanates are much less nucleophilic than imines, and would be poor substrates for the reaction.

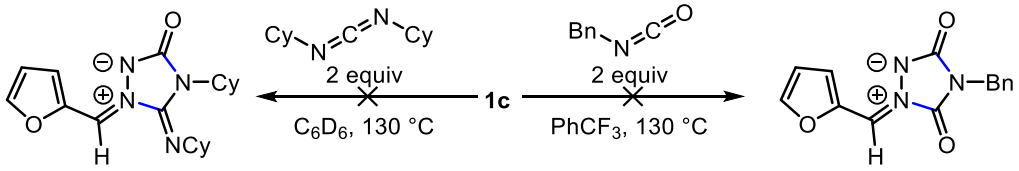

Scheme 4.9. Unsuccessful reactions of imino-isocyanate with dicyclohexyl carbodiimide and benzyl isocyanate.

4.2.3. Derivatization

The azomethine imine products of C=N aminocarbonylation were unknown prior to this work. However, we were confident in their potential as precursors to heterocycles with the triazolone core. As a proof of principle, we performed derivatization of these azomethine imines by simple reduction reactions (Scheme 4.10). From dipole **3c**, the triazolone **6** was isolated in 74% yield

using the transimination method described in Chapter 2. In this reaction, the intermediate triazolidinone (**5**) is generated rapidly at room temperature, followed by aromatization to **6** when the mixture is heated to reflux. The triazolidinone can be also isolated by reduction of the dipole, and **7** was obtained in 89% yield from **3f** using sodium borohydride.

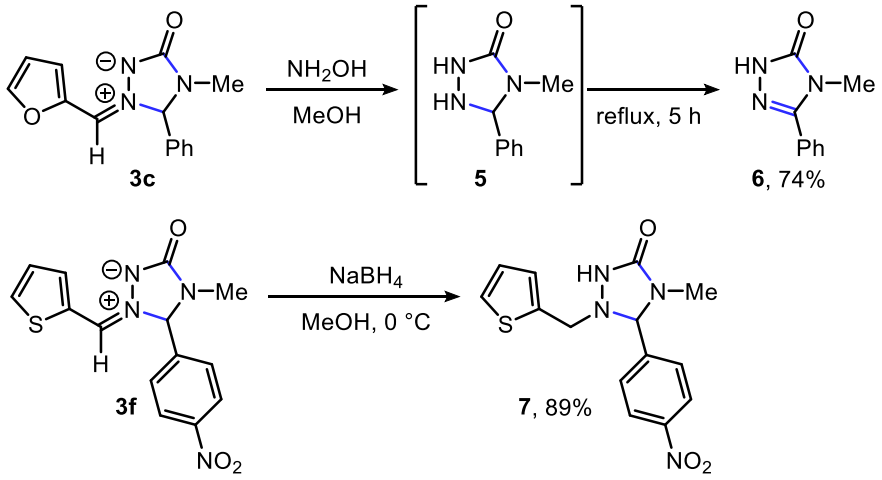

*Scheme 4.10. Derivatization of azomethine imines to triazolones (**6**) and triazolidinones (**7**).*

In the future, we aim to synthesize a known triazolone pharmaceutical or agrochemical using our strategy.[2] For example, this approach could be useful for a new route to the core structure in Doravirine. The state of the art synthesis of this HIV drug involves a linear construction of a hydrazine precursor, which cyclizes to give the core, followed by protection/deptrotection and S_N2 substitution (Scheme 4.11).[3,19] With a cycloaddition approach, the core can be accessed rapidly from an imino-isocyanate and the *N*-methyl imine. This is a more convergent method; the imino-isocyanate precursor (hydrazone) and imine can be synthesized separately (Scheme 4.11). This approach can also be used to test variations on the structure of the drug outside the triazolone core, by the use of various imines.

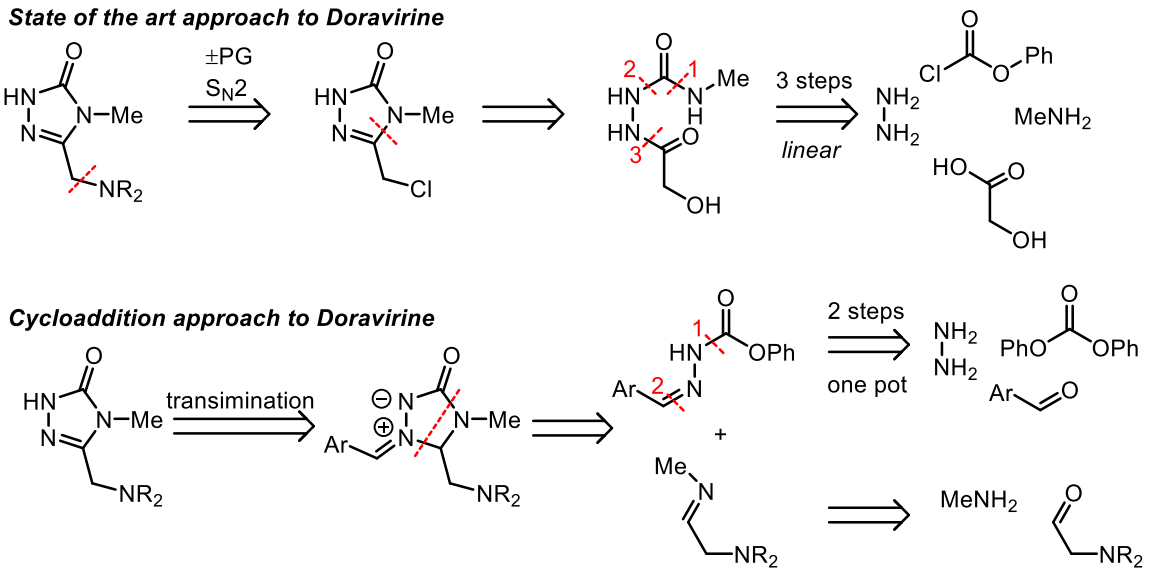

Scheme 4.11. Different approaches to the triazolone core of Doravirine

4.3. Summary and Outlook

In summary, the scope of [3+2] cycloaddition reactions with imino-isocyanates was expanded to include the aromatic imines. This work provides a convergent approach for the synthesis of triazolones, triazolidinones, and new azomethine imines,[5] and shows the potential of amphoteric reagents like imino-isocyanates in the discovery of new disconnections. The mechanism of reactions with imines is still unknown, and there is still a lot to be known about the cycloaddition reactivity of imino-isocyanates. Future work, such as LFER studies, will provide more information. Computational studies of the cycloaddition reaction would be an asset, including potential energy surfaces for stepwise or concerted mechanisms, and HOMO/LUMO interactions of each reaction partner.

In addition to the work presented, this study allowed the discovery of similar reactivity with imino-iso*thio*cyanates. In parallel to studies with imino-isocyanates, our group has developed precursors for imino-isothiocyanates However, they have observed only modest reactivity with alkenes, and were limited two imino-isothiocyanate precursors.[5,20] The discovery of aldimines as

reactive cycloaddition partners stimulated studies on related reactions with imino-isothiocyanates. As a consequence, new reactivity was discovered which enabled the synthesis aldehyde- and ketone-derived thioxo-azomethine imines (**9**) and their triazolium-thione derivatives (**10**) from a variety of imino-isothiocyanate precursors (**8**) (Equation 4.3).[5]

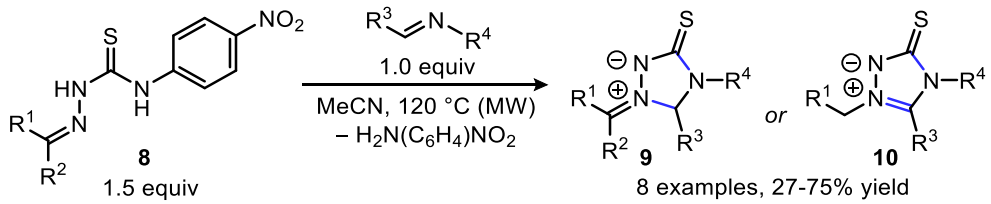

Equation 4.3.

4.4. References

(1) Al-Masoudi, I. A.; Al-Soud, Y. A.; Al-Salihi, N. J.; Al-Masoudi, N. A. *Chem. Heterocycl. Compd.* **2006**, *42*, 1377.
(2) Jayalatha; Palled, M. S.; Chandran, M.; Regi, C.; Bhat, A.; Krishnakumar, K. *World J. Pharm. Pharm. Sci.* **2014**, *3*, 1051.
(3) Gauthier, D. R.; Sherry, B. D.; Cao, Y.; Journet, M.; Humphrey, G.; Itoh, T.; Mangion, I.; Tschaen, D. M. *Org. Lett.* **2015**, *17*, 1353.
(4) Luo, Y.-P.; Jiang, L.-L.; Wang, G.-D.; Chen, Q.; Yang, G.-F. *J. Agric. Food Chem.* **2008**, *56*, 2118.
(5) Bongers, A.; Ranasinghe, I.; Lemire, P.; Perozzo, A.; Vincent-Rocan, J.-F.; Beauchemin, A. M. *Org. Lett.* **2016**, *18*, 3778.
(6) Whitehead, C. W.; Traverso, J. J. *J. Am. Chem. Soc.* **1955**, *77*, 5872.
(7) Kane, J. M. *Synthesis.* **1987**, 912.
(8) Deng, J. Z.; Burgey, C. S. *Tetrahedron Lett.* **2005**, *46*, 7993.
(9) Novikov, M. S.; Khlebnikov, A. F.; Stepanov, A. A.; Kostikov, R. R. *Synthesis* **1994**, 782.
(10) Pore, D. M.; Hegade, P. G.; Mane, M. M.; Patil, J. D. *RSC Adv.* **2013**, *3*, 25723.
(11) Ulrich, H. In *Cycloaddition Reactions of Heterocumulenes*; Academic Press Inc., 1967; p. 374.
(12) Huisgen, R. *Angew. Chem., Int. Ed.* **1963**, *2*, 565.
(13) Lwowski, W.; de Mauriac, R. A.; Murray, R. A.; Lünow, L. *Tetrahedron Lett.* **1971**, *12*, 425.
(14) Wentrup, C.; Finnerty, J. J.; Koch, R. *Curr. Org. Chem.* **2011**, *15*, 1745.
(15) Cossío, F. P.; Arrieta, A.; Sierra, M. A. *Acc. Chem. Res.* **2008**, *41*, 925.
(16) Domingo, L. R.; Ríos-Gutiérrez, M.; Sáez, J. A. *RSC Adv.* **2015**, *5*, 37119.
(17) Gan, W.; Moon, P. J.; Clavette, C.; Das Neves, N.; Markiewicz, T.; Toderian, A. B.; Beauchemin, A. M. *Org. Lett.* **2013**, *15*, 1890.
(18) Sanderson, R. T. *Chemical bonds and bond energy*; Academic Press, Inc.: University of Michigan, 1971.
(19) Campeau, L.-C.; Chen, Q.; Gauvreau, D.; Girardin, M.; Belyk, K.; Maligres, P.; Zhou, G.; Gu, C.; Zhang, W.; Tan, L.; O'Shea, P. D. *Org. Process Res. Dev.* **2016**, *20*, 1476.
(20) Clavette, C.; Gan, W.; Bongers, A.; Markiewicz, T.; Toderian, A. B.; Gorelsky, S. I.; Beauchemin, A. M. *J. Am. Chem. Soc.* **2012**, *134*, 16111.

Chapter 5. Conclusions and Outlook

A study of the unique 1,3-amphoteric reactivity of imino-isocyanates in [3+2] cycloaddition reactions with alkenes, enol ethers, imines, and other dipolarophiles has been presented. This work demonstrates imino-isocyanates to be effective tools for the synthesis of β-amino carbonyl compounds and heterocycles containing the N-N-CO motif. Information on the fundamental properties of these rare reactive intermediates was obtained, including reactivity trends, geometry, and the first direct detection of imino-isocyanates using in situ IR studies. The study of imino-isocyanate reactivity with alkenes led to the development of a broadly applicable aminocarbonylation reaction, which was established to provide a new route to compounds containing the β-amino carbonyl motif. The cycloaddition of imino-isocyanates with alkenes gives access to complex *N,N'*-cyclic azomethine imines, which are common precursors to pyrazolidinones and β-amino amides.

Following this, an efficient kinetic resolution of the aminocarbonylation products was developed, which makes the overall process a practical route to access the enantioenriched β-amino carbonyl derivatives. This was achieved by enantioselective reduction of the azomethine imine, which was the first example of such reactivity. In addition, activation of the azomethine imine by Brønsted acid catalysis represents a new activation mode, and opens the door to discovering reactivity of these dipoles beyond the typical dipolar cycloadditions. With this reduction method, racemic azomethine imines are used to access both enantiomers of the inherent β-amino amide.

The cycloaddition reactivity of imino-isocyanates was proven to be an effective route to access important 5-membered heterocycles containing the N-N-CO motif. Enol ethers act as alkyne

equivalents in the synthesis of pyrazolones, and cycloaddition reactions of imines provide triazolone cores. Overall, these reactions with imino-isocyanates provide an alternative disconnection and convergent approach to these heterocycles, and there is potential to expand this methodology to new systems.

Computational studies would be an asset in further understanding and exploring the merit of imino-isocyanates in synthesis. Currently, we have only studied simplified imino-isocyanates and blocking groups in reactions with ethylene and norbornene, in vacuum or methanol as solvent. Ideally, the fluorenone-derived reagent **6a** could be studied closer to the reaction conditions. We could calculate the reaction energy profile and transition state for this system, and also explore HOMO/LUMO energies of the imino-isocyanate. Computational studies could give insight into reactivity differences between imino-isocyanate precursors, including imino-iso*thio*cyanates, and substrates such as alkenes, alkynes, and imines. This work could direct our experimental research, allowing the discovery of new imino-isocyanate precursors (e.g. with a traceless blocking group) and expand the cycloaddition reactivity (eg. higher order cycloadditions).

A logical next step in this research is to fully characterize the library of imino-isocyanates and other *N*-isocyanates. This involves systematically studying properties of imino-isocyanate precursors, such as deblocking temperatures with thermogravimetric analysis and mass spectrometry, or with infrared spectroscopy as described herein. The goal of this study would be to match the breadth of literature on *C*-isocyanates, and make isocyanate chemists aware of imino-isocyanates and their properties. For example, there are potential applications for imino-isocyanates as cross-linking components in polymer chemistry, owing to their 1,3-amphoteric properties.

In conclusion, this work shows that cycloaddition reactions of imino-isocyanates are an efficient and a modular way to synthesize molecules containing the β-aminocarbonyl motif, including various heterocycles and β-amino amides. Despite this, there is still more to be understood about the reactivity of imino-isocyanates and other *N*-isocyanates. The reactivity presented herein in the best understood process involving these amphoteric isocyanates, and will guide further studies into their reactivity and their potential in other transformations.

Chapter 6. Experimental Section

6.1. General Information

Materials. All commercially available materials were used without further purification unless otherwise noted. Solvents for reactions were obtained from an LC Technology solvent system or distilled prior to use or dried over 4 Å molecular sieves. Microwave reactions were performed using a Biotage Initiator Eight microwave reactor and Biotage microwave vials. Reactions were monitored by analytical thin layer chromatography (TLC), using glass- or aluminum-backed plates, cut to size. TLC visualization was achieved by UV and stain (such as $KMnO_4$, vanillin, ninhydrin). Flash column chromatography was carried out using 40-63 μm Silicycle silica gel.

Characterization. ^{1}H NMR and ^{13}C NMR spectra were recorded on Bruker AVANCE 300 MHz and 400 MHz spectrometers at ambient temperature, except where noted. Spectral data is reported in ppm using the following solvents as references: ^{1}H NMR: $CDCl_3$ (7.26 ppm), C_6D_6 (7.16 ppm), DMSO-d_6 (2.50 ppm) toluene-d_8 (2.08 ppm); ^{13}C NMR: $CDCl_3$ (77.16 ppm), C_6D_6 (128.06 ppm), DMSO-d_6 (39.52 ppm). ^{1}H data was reported as: multiplicity (s = singlet, d = doublet, t = triplet, q = quartet, m = multiplet, appt = apparent triplet), coupling constants (J) in Hz, and integration. Infrared (IR) spectra were obtained as thin films on a Bruker EQUINOX 55 FTIR or as neat solids on an Agilent Cary 630 FTIR or Thermo Scientific Nicolet 6700 FT-IR (ATR Diamond). High resolution mass spectroscopy (HRMS) was performed at the Ottawa-Carleton Mass Spectroscopy Centre on the Kratos Concept-11A mass spectrometer for Electron Impact (EI) and Waters Micromass Q-TOF I for eletrospray ionization (ESI). The determination of enantiomeric excess was performed by chiral phase HPLC analysis using Agilent 1200 Series instrument and Diacel ChiralPak AD-H column. Optical rotation measured with an Anton Paar MCP 500 Polarimeter.

6.2. Intermolecular Aminocarbonylation of Alkenes

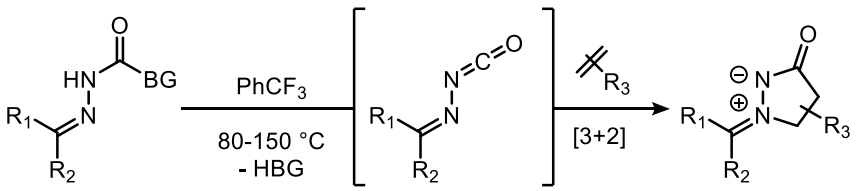

General Procedure 2A: Microwave conditions (100-150 °C and neat reactions)[1]

The acyl hydrazone and the corresponding alkene (1 to 10 equiv) were added to an oven or flame dried microwave vial with a stir bar. The mixture was diluted with α,α,α-trifluorotoluene ($PhCF_3$, 0.5 to 0.05 M), unless noted otherwise (*e.g.* neat conditions or solvent optimization). The vial was sealed with a septum and purged with argon. The mixture was heated at the specified temperature in a microwave reactor for the given time. The reaction solution was cooled to ambient temperature, concentrated under reduced pressure and analyzed by ^1H NMR using 1,4-dimethoxybenzene or 1,3,5-trimethoxybenzene as an internal standard. The azomethine imine product was isolated using silica gel column chromatography.

General procedure 2B: Reflux in trifluorotoluene[1,2]

The hydrazone, the corresponding alkene (1 to 10 equiv) and α,α,α-trifluorotoluene ($PhCF_3$, 0.5 to 0.05 M) were added to an oven or flame dried flask with a stir bar. The flask was equipped with a reflux condenser and purged with argon. The mixture was heated to 100 °C in an oil bath. The mixture was then cooled to ambient temperature, the stir bar removed, and solvent was evaporated to give the crude product. The azomethine imine product was isolated using silica gel column chromatography.

6.2.2. First Generation Aminocarbonylation

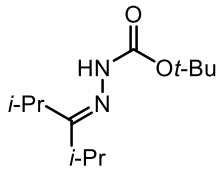

5a. Synthesized following a known procedure.[1] *t*-Bu Carbazate (7.27 g, 55 mmol, 1.1 equiv) and diisopropyl ketone (7.1 mL, 50 mmol, 1 equiv) were combined in a flask and dissolved in MeOH (250 mL). AcOH (3 mL) and one scoop of Na_2SO_4 were added, and the mixture was stirred at reflux for 16 h. The flask was cooled to rt and filtered to remove Na_2SO_4, and the filtrate was concentrated in vacuo to give the crude product as a while solid. The crude product was dissolved in EtOAc and washed with 2 x 20 mL $NaHCO_3$, 1 x 20 mL brine, then dried with Na_2SO_4. Concentration in vacuo provided the purified product as a white solid (9.9 g, 87% yield). ^{1}H NMR (300 MHz, $CDCl_3$) δ 7.64 (br. s., 1 H), 2.92 - 2.72 (m, 1 H), 2.72 - 2.47 (m, 1 H), 1.58 - 1.45 (m, 9 H), 1.23 - 1.01 (m, 12 H).

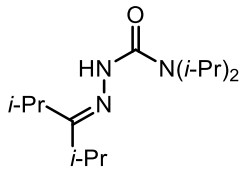

5g. Synthesized following a known procedure with minor modifications.[1] Hydrazone **5a** (1.18 g, 5.17 mmol) and diisopropylamine (10 mL) were combined in a sealed vial and heated by microwave irradiation to 150 °C for 3 minutes. The crude mixture was concentrated in vacuo, and recrystallization in hexane provided the product as a white crystalline solid (0.901 g, 68%). ^{1}H NMR (300 MHz, $CDCl_3$) δ 7.14 (br. s., 1 H), 3.94 (spt, J = 6.8 Hz, 2 H), 2.92 - 2.70 (m, 1 H), 2.70 - 2.44 (m, 1 H), 1.36 - 1.22 (m, 12 H), 1.22 - 1.05 (m, 12 H).

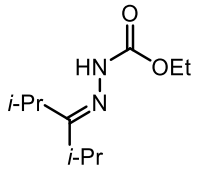

5b. Synthesized following a known procedure with minor modifications.[1] Hydrazone **5a** (1.07 g, 4.69 mmol) and EtOH (10 mL) were combined in a sealed vial and heated by microwave irradiation to 150 °C for 3 minutes. The crude mixture was concentrated in vacuo, to give the product as a white solid (0.85 g, 90%). ^{1}H NMR (300 MHz, $CDCl_3$) δ 7.72 (br. s., 1 H), 4.24 (q, *J* = 7.1 Hz, 2 H), 2.88 - 2.49 (m, 2 H), 1.30 (t, *J* = 7.1 Hz, 3 H), 1.13 (d, *J* = 7.8 Hz, 6 H), 1.16 (d, *J* = 8.0 Hz, 6 H).

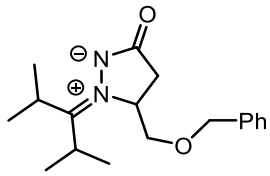

7. Hydrazone **5a** (63.5 mg, 0.249 mmol, 1 equiv) and $PhCF_3$ (5 mL) were combined in a vial, sealed and purged with N_2. Allyl benzyl ether (0.39 mL, 2.5 mmol, 10 equiv) was added and the mixture heated by microwave irradiation to 150 °C for 3 h. The crude mixture was concentrated in vacuo, and ^{1}H NMR with 1,3,5-trimethoxybenzene internal standard showed 12% yield of **7**, and 6% yield of the other regioisomer ***iso*-7**. The product was isolated by column chromatography with 5% MeOH, 95% CH_2Cl_2, to provide the product as an off-white solid (5.2 mg, 7%). TLC R_f = 0.18 (5% MeOH, 95% CH_2Cl_2). ^{1}H (400 MHz) δ 7.40 - 7.26 (m, 5 H), 5.00 - 4.79 (m, 1 H), 4.50 (s, 2 H), 3.65 - 3.45 (m, 2 H), 3.07 (td, *J* = 6.7, 13.5 Hz, 1 H), 2.96 - 2.73 (m, 2 H), 2.44 (dd, *J* = 1.4, 16.1 Hz, 1 H), 1.37 (d, *J* = 8.8 Hz, 3 H), 1.38 (d, *J* = 8.8 Hz, 3 H), 1.13 (d, *J* = 6.9 Hz, 3 H), 1.03 (d, *J* = 6.6 Hz, 3 H). ^{13}C (100 MHz) δ 181.1, 165.4, 136.8, 128.8, 128.4, 128.2, 73.9, 71.3, 65.2, 34.9, 32.9, 30.4, 19.3, 18.9, 17.1, 17.0.

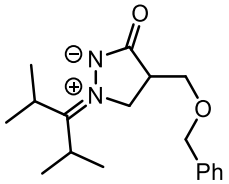

***iso*-7**. Hydrazone **5a** (0.0571 g, 0.224 mmol, 1 equiv) and $PhCF_3$ (5 mL) were combined in a vial, sealed and purged with N_2. Allyl benzyl ether (0.37 mL, 2.4 mmol, 10 equiv) was added and the mixture heated by microwave irradiation to 200 °C for 3 h. The crude mixture was concentrated in vacuo, and ^1H NMR with 1,3,5-trimethoxybenzene internal standard showed 17% yield of ***iso*-7**, and 3% yield of the other regioisomer **7**. The product was isolated by column chromatography with 5% MeOH, 95% CH_2Cl_2, to provide the product as an off-white solid (10.1 mg, 15%). TLC R_f = 0.21 (5% MeOH, 95% CH_2Cl_2). ^1H NMR (400 MHz, $CDCl_3$) δ 7.37 - 7.26 (m, 5 H), 4.56 (d, *J* = 11.8 Hz, 1 H), 4.50 (d, *J* = 11.8 Hz, 1 H), 4.32 (dd, *J* = 9.6, 12.9 Hz, 1 H), 4.18 (dd, *J* = 5.7, 12.9 Hz, 1 H), 3.90 (dd, *J* = 3.9, 9.6 Hz, 1 H), 3.76 (dd, *J* = 7.2, 9.6 Hz, 1 H), 3.22 - 3.05 (m, 1 H), 3.05 - 2.86 (m, 2 H), 1.35 (d, *J* = 7.0 Hz, 3 H), 1.36 (d, *J* = 7.0 Hz, 3 H), 1.17 (d, *J* = 6.8 Hz, 3 H), 1.20 (d, *J* = 6.8 Hz, 3 H). ^{13}C (100 MHz, $CDCl_3$) δ 181.9, 162.3 (br), 138.1, 128.5, 127.9, 127.9, 73.5, 69.8, 57.2, 42.3, 32.2, 30.2, 18.7, 18.6, 17.1.

6.2.3. Second Generation Aminocarbonylation and Derivatization

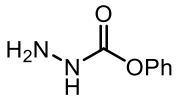

***O*-Phenyl Carbazate**. Synthesized following a known procedure.[3] Hydrazine hydrate (30 mL, 50-60 wt% solution in H_2O, 0.60 mol, 3 equiv) was diluted in CH_2Cl_2 (250 mL). A solution of diphenyl carbonate (43 g, 0.20 mol, 1 equiv) in CH_2Cl_2 (250 mL) was added drop-wise over 2 h while stirring at room temperature. Immediately after the addition was complete, the mixture was concentrated in vacuo. The crude product was isolated by column chromatography (gradient, 50%

EtOAc and 50% hexanes to 100% EtOAc). Fractions contaminated with PhOH were recrystallized in CH_2Cl_2/hexane. The title compound was obtained as a white crystalline solid, 14.6 g (48% isolated yield). ^{1}H NMR spectrum was in agreement with the literature.[1,3]

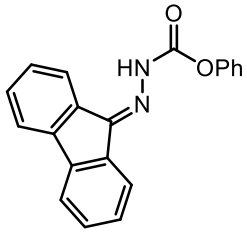

6a. *O*-Phenyl carbazate (2.43 g, 16.0 mmol), fluorenone (2.90 g, 16.0 mmol) and AcOH (0.20 mL) in MeOH (35 mL) were heated to reflux for 6 h. The mixture was cooled to rt, and the product crystallized from crude mixture. The product was obtained as a yellow solid (4.0 g, 80% yield). m.p.: 178-180 °C. TLC R_f = 0.31 in 20% EtOAc/hexanes. ^{1}H NMR (400 MHz, $CDCl_3$) δ 9.18 (s, 1H), 7.91 (d, *J* = 7.48 Hz, 1H), 7.82 (d, *J* = 7.63 Hz, 1H), 7.66 (d, *J* = 7.51 Hz, 1H), 7.56 (d, *J* = 7.43 Hz, 1H), 7.47-7.21 (m, 9H). ^{13}C NMR (100 MHz, $CDCl_3$) δ 152.1(C), 150.6 (C), 142.6 (C), 139.5 (C), 136.8 (C), 131.4 (CH), 130.3 (CH), 129.7 (C), 129.6 (CH), 128.4 (CH), 128.1 (CH), 126.0 (CH), 125.6 (CH), 122.6 (CH), 121.5 (CH), 121.0 (CH), 119.7 (CH).). IR (film) 1716, 1735, 1490, 1471, 1219, 1171, 772 cm^{-1}; HRMS (EI): Exact mass calcd for $C_{20}H_{14}N_2O_2$ $[M]^+$: 314.1050. Found: 314.1056.

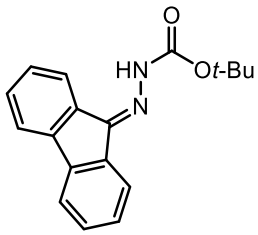

6b. *t*-Butyl Carbazate (6.6 g, 50 mmol), fluorenone (9.0 g, 50 mmol) and AcOH (0.6 mL) in MeOH (250 mL) were heated to reflux for 16 h. The mixture was cooled to rt, and filtered. The filtrate was concentrated in vacuo, and the resulting crude product was diluted in EtOAc/MeOH. The

mixture was filtered again, and the filtrate concentrated in vacuo. The resulting yellow solid (2.7 g) was recrystallized in a minimum volume of MeOH to give the product as a pale yellow crystalline solid (1.3 g, 50% yield). ^{1}H NMR spectrum was in agreement with the literature.[4] ^{1}H NMR (300 MHz, $CDCl_3$) δ 8.85 (s, 1 H), 7.92 (d, *J* = 7.0 Hz, 1 H), 7.76 (d, *J* = 7.6 Hz, 1 H), 7.68 (d, *J* = 7.3 Hz, 1 H), 7.57 (dd, *J* = 0.9, 6.7 Hz, 1 H), 7.49 - 7.27 (m, 4 H), 1.61 (s, 9 H). ^{13}C NMR (76 MHz, $CDCl_3$) δ 152.9, 142.6, 139.3, 137.1, 131.1, 130.0, 129.9, 128.4, 128.0, 125.4, 122.5, 121.0, 119.7, 82.5, 28.4.

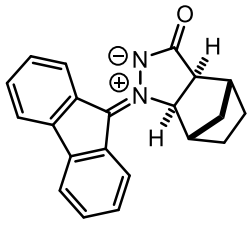

9a. Synthesized according to general procedure 2A using hydrazone **6a** (2.0 g, 6.4 mmol) and norbornene (1.2 g, 13 mmol, 2.0 equiv) in $PhCF_3$ (5 mL). The reaction was heated by microwave irradiation at 150 °C for 10 min. The crude mixture was used directly for column chromatography (1:4 EtOAc/CH_2Cl_2 to remove excess alkene and by-products, then 9:1 EtOAc/MeOH to elute the product). The product was obtained as a yellow solid (1.8 g, 90%). Spectral data is in agreement with the literature.[1]

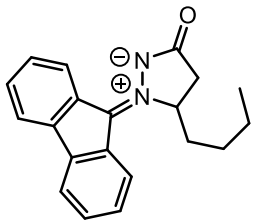

9c. Synthesized according to general procedure 2A using hydrazone **6a** (0.079 g, 0.25 mmol) and 1-hexene (0.31 mL, 2.5 mmol, 10 equiv) in $PhCF_3$ (5 mL). The reaction was heated by microwave irradiation at 150 °C for 3 h. The crude mixture was concentrated in vacuo, and the product isolated

by column chromatography (1:4 EtOAc/CH_2Cl_2 to remove excess alkene and by-products, then 9:1 EtOAc/MeOH to elute the product). The product was obtained as a yellow solid (0.056 g, 73% yield). m.p.: 205-207 °C. TLC R_f = 0.17 in EtOAc. ^{1}H NMR (400 MHz, $CDCl_3$) δ 9.03 - 8.96 (m, 1 H), 7.73 - 7.66 (m, 1 H), 7.63 - 7.58 (m, 1 H), 7.48 (m, 1 H), 7.46 - 7.39 (m, 2 H), 7.38 - 7.29 (m, 2 H), 5.30 - 5.19 (m, 1 H), 3.10 (dd, *J* = 8.4, 16.5 Hz, 1 H), 2.69 (dd, *J* = 1.7, 16.5 Hz, 1 H), 2.16 - 2.04 (m, 1 H), 1.96 - 1.82 (m, 1 H), 1.56 - 1.30 (m, 4 H), 0.94 - 0.85 (m, 3 H). ^{13}C NMR (100 MHz, $CDCl_3$) δ 183.4, 142.0, 139.7, 139.5, 131.9, 131.7, 131.4, 131.0, 129.7, 129.2, 128.2, 125.0, 121.1, 119.6, 68.5, 35.9, 34.5, 27.4, 22.4, 13.8. IR (film); 2957, 2867, 1663, 1606, 1450, 1355, 1278 cm^{-1}. HRMS (EI): Exact mass calcd for $C_{20}H_{20}N_2O$ $[M]^+$: 304.1576. Found: 304.1581.

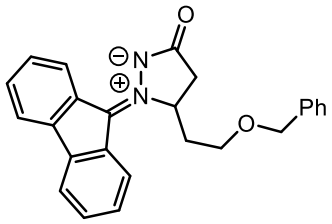

9d. Synthesized according to general procedure 2A using hydrazone **6a** (0.078 g, 0.25 mmol) and homoallyl benzyl ether (0.37 g, 2.5 mmol, 10 equiv) in $PhCF_3$ (5 mL). The reaction was heated in an oil bath at 100 °C for 6 h. The crude mixture was concentrated in vacuo, and the product isolated by column chromatography (1:4 EtOAc/CH_2Cl_2 to remove excess alkene and by-products, then 9:1 EtOAc/MeOH to elute the product). The product was obtained as a yellow solid (0.049 g, 52% yield). m.p.: 158-160 °C. TLC R_f = 0.22 in EtOAc. ^{1}H NMR (400 MHz, $CDCl_3$) δ 8.95 (d, *J* = 7.7 Hz, 1 H), 8.00 (d, *J* = 8.0 Hz, 1 H), 7.59 (d, *J* = 7.3 Hz, 1 H), 7.54 (d, *J* = 7.3 Hz, 1 H), 7.42 - 7.24 (m, 9 H), 7.09 - 7.02 (m, 1 H), 5.50 (m, 1 H), 4.57 (s, 2 H), 3.77 (appt d, *J* = 4.0, 9.4 Hz, 1 H), 3.66 - 3.57 (m, 1 H), 3.03 (dd, *J* = 8.1, 16.4 Hz, 1 H), 2.63 (dd, *J* = 1.3, 16.5 Hz, 1 H), 2.60 - 2.50 (m, 1 H), 1.95 - 1.84 (m, 1 H). ^{13}C NMR (400 MHz, $CDCl_3$) δ 183.2, 141.7, 140.0, 137.8, 131.9, 131.6, 131.4, 131.0, 129.5, 129.0, 128.6 (2C), 128.4, 128.1, 127.7 (2C), 126.7, 120.8, 119.6, 73.6, 66.2,

66.0, 35.6, 35.1. IR (film); 3059, 2854, 1671, 1667, 1603, 1546, 1455, 1360, 1280 cm^{-1}. HRMS (EI): Exact mass calcd for $C_{25}H_{22}N_2O_2$ $[M]^+$: 382.1681. Found: 382.1679.

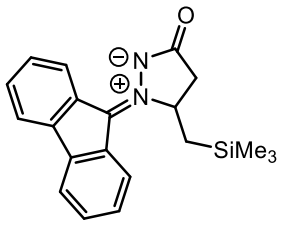

9e. Synthesized according to general procedure 2A using hydrazone **6a** (0.079 g, 0.25 mmol) and allyl trimethylsilane (0.40 mL, 2.5 mmol, 10 equiv) in $PhCF_3$ (5 mL). The reaction was heated by microwave irradiation at 100 °C for 3 h. The crude mixture was concentrated in vacuo, and the product isolated by column chromatography (1:4 EtOAc/CH_2Cl_2 to remove excess alkene and by-products, then 9:1 EtOAc/MeOH to elute the product). The product was obtained as a yellow solid (0.068 g, 81% yield). m.p.: 197-198 °C. TLC R_f = 0.35 in EtOAc. ^{1}H NMR (400 MHz, $CDCl_3$) δ 8.99 (d, *J* = 7.4 Hz, 1 H), 7.70 (d, *J* = 7.3 Hz, 1 H), 7.61 (d, *J* = 7.1 Hz, 1 H), 7.51 (d, *J* = 8.1 Hz, 1 H), 7.46 - 7.38 (m, 2 H), 7.38 - 7.32 (d appt, *J* = 1.2, 7.7 Hz, 1 H), 7.32 - 7.27 (d appt, *J* = 1.1, 7.8 Hz, 1 H), 5.41 - 5.31 (m, 1 H), 3.13 (dd, *J* = 8.4, 16.2 Hz, 1 H), 2.59 (dd, *J* = 1.6, 16.3 Hz, 1 H), 1.57 (dd, *J* = 1.9, 14.4 Hz, 1 H), 1.37 (dd, *J* = 12.8, 14.4 Hz, 1 H), 0.27 - 0.04 (s, 9 H). ^{13}C NMR (400 MHz, $CDCl_3$) δ 183.2, 141.8, 139.6, 138.7, 131.8, 131.7, 131.2, 130.8, 129.6, 129.1, 127.8, 125.3, 121.1, 119.6, 67.2, 37.8, 24.9, -0.7 (3C). IR (film); 3055, 2956, 1668, 1603, 1546, 1447, 1349, 1273, 1254, 1200, 1120, 1094, 1079, 972, 843, 771, 729 cm^{-1}. HRMS (EI): Exact mass calcd for $C_{20}H_{22}N_2OSi$ $[M]^+$: 334.1501. Found: 334.1476.

Gram Scale: Following general procedure 2B. Hydrazone **6a** (0.94 g, 3.0 mmol, 1 equiv), allyl trimethylsilane (2.4 mL, 15 mmol, 5 equiv), and $PhCF_3$ (60 mL) combined in a 100 mL flask, equipped with a reflux condenser, and heated in an oil bath at 100 °C for 6 h. The mixture became

dark purple with some light yellow precipitate. The crude mixture was purified by passing through a silica plug, following the procedure above, to provide a yellow solid (0.82 g, 82%).

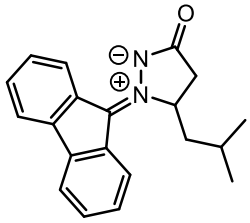

9f. Synthesized according to general procedure 2A using hydrazone **6a** (0.159 g, 0.506 mmol) and 4-methyl-1-pentene (0.32 mL, 2.5 mmol, 5 equiv) in $PhCF_3$ (5 mL). The reaction was heated by microwave irradiation at 150 °C for 3 h. The crude mixture was concentrated in vacuo, and the product isolated by column chromatography (1:3 EtOAc/CH_2Cl_2 to remove excess alkene and by-products, then 9:1 EtOAc/MeOH to elute the product). The product was obtained as a yellow solid (0.069 g, 45% yield). TLC R_f = 0.23 in EtOAc. ^{1}H NMR (400 MHz, $CDCl_3$) δ 9.02 (d, *J* = 7.6 Hz, 1 H), 7.71 (d, *J* = 7.0 Hz, 1 H), 7.62 (d, *J* = 7.5 Hz, 2 H), 7.48 - 7.39 (m, 2 H), 7.39 - 7.30 (m, 2 H), 5.51 - 5.30 (m, 1 H), 3.11 (dd, *J* = 8.2, 16.3 Hz, 1 H), 2.76 (d, *J* = 16.4 Hz, 1 H), 2.05 - 1.88 (m, 2 H), 1.87 - 1.77 (m, 1 H), 1.15 (d, *J* = 6.3 Hz, 3 H), 1.00 (d, *J* = 6.3 Hz, 3 H). ^{13}C NMR (101 MHz, $CDCl_3$) δ 183.4, 142.2, 140.1, 140.0, 132.1, 132.0, 131.7, 131.2, 129.7, 129.4, 128.1, 125.5, 121.3, 119.8, 67.9, 42.8, 35.8, 26.1, 23.7, 21.5. HRMS (EI): Exact mass calcd for $C_{20}H_{20}N_2O$ $[M]^+$: 304.15756. Found: 304.15719. IR (ATR) 3003, 2847, 1699, 1615, 1566, 1326 cm^{-1}.

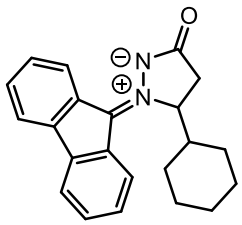

9g. Synthesized according to general procedure 2A using hydrazone **6a** (0.063 g, 0.20 mmol) and vinylcyclohexane (0.14 mL, 1.0 mmol, 5 equiv) in $PhCF_3$ (4 mL). The reaction was heated by

microwave irradiation at 120 °C for 3 h. The crude mixture was concentrated in vacuo, and the product isolated by column chromatography (1:1 EtOAc/hexane, then 20:1 EtOAc/MeOH). The product was obtained as a yellow solid (0.033 g, 50% yield). TLC R_f = 0.33 in EtOAc. ^{1}H NMR (400 MHz, $CDCl_3$) δ 9.06-9.04 (m, 1H), 7.74-7.72 (m, 1H), 7.65 (d, *J* = 7.1, 1H), 7.47-7.43 (m, 3H), 7.36 (dtd, *J* = 1.3, 7.7, 9.0 Hz, 2H), 5.32-5.30 (m, 1H), 2.95 (dd, *J* = 8.9, 16.6 Hz, 1H), 2.73 (dd, *J* = 1.8, 16.6 Hz, 1H), 2.26-2.19 (m, 1H), 1.86 (t, *J* = 10.2, 2H), 1.75-1.66 (m, 2H), 1.55 (d, *J* = 12.6, 1H), 1.31-1.02 (m, 5H). ^{13}C NMR (100 MHz, $CDCl_3$) δ 184.0, 142.3, 139.9, 139.5, 132.09, 132.07, 131.7, 131.1, 130.2, 129.5, 128.6, 125.1, 121.4, 119.9, 72.8, 41.0, 32.4, 29.9, 26.3, 26.1, 25.6, 24.3. IR (film) 2928, 2854, 1659, 1605, 1541, 1448, 1255 cm^{-1}. HRMS (EI): Exact mass calcd for $C_{22}H_{22}N_2O$ $[M]^+$: 330.1732. Found: 330.1734.

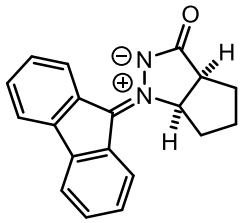

9h. Synthesized according to general procedure 2A using hydrazone **6a** (0.316 g, 1.01 mmol) and cyclopentene (0.92 mL, 10 mmol, 10 equiv) in $PhCF_3$ (20 mL). The reaction was heated by microwave irradiation at 100 °C for 6 h. The crude mixture was concentrated in vacuo, and the product isolated by column chromatography (1:4 EtOAc/CH_2Cl_2 to remove excess alkene and by-products, then 9:1 EtOAc/MeOH to elute the product). The product was obtained as a yellow solid (0.220 g, 76% yield). TLC R_f = 0.10 in EtOAc. ^{1}H NMR (400 MHz, $CDCl_3$) δ 8.92 (d, *J* = 7.8 Hz, 1 H), 7.68 - 7.51 (m, 3 H), 7.39 (ddd, *J* = 1.1, 7.5, 7.5 Hz, 2 H), 7.34 - 7.23 (m, 2 H), 5.59 - 5.36 (m, 1 H), 3.41 (dd, *J* = 7.7, 7.7 Hz, 1 H), 2.46 - 2.51 (m, 1 H), 2.32 - 2.16 (m, 2 H), 1.93 - 1.74 (m, 2 H), 1.64 - 1.45 (m, 1 H). ^{13}C NMR (100 MHz, $CDCl_3$) δ 186.4, 141.6, 139.5, 138.9, 131.7, 131.5, 130.9, 130.8, 129.9, 129.0, 127.9, 124.9, 120.9, 119.5, 73.0, 47.2, 36.0, 30.3, 23.1. IR (film) 3114,

2992, 1696, 1619, 1570, 1315 cm^{-1}; HRMS (EI): Exact mass calcd for $C_{19}H_{16}N_2O$ $[M]^+$: 288.1263. Found: 288.1246.

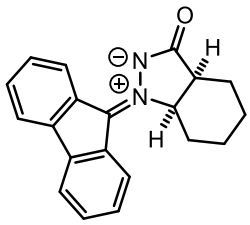

9i. Synthesized according to general procedure 2A using hydrazone **6a** (0.079 g, 0.25 mmol) and a large excess of freshly opened cyclohexene (5.0 mL, 49 mmol) as the solvent. The reaction was heated by microwave irradiation at 150 °C for 3 h. The crude mixture was concentrated in vacuo, and the product isolated by column chromatography (1:4 EtOAc/CH_2Cl_2 to remove excess alkene and by-products, then 9:1 EtOAc/MeOH to elute the product). The product was obtained as a yellow solid (0.037 g, 49% yield). m.p.: 202-205 °C. TLC R_f = 0.26 in EtOAc. ^{1}H NMR (400 MHz, $CDCl_3$) δ 8.97 (d, *J* = 7.7 Hz, 1 H), 7.64 (d, *J* = 7.5 Hz, 1 H), 7.57 (d, *J* = 7.5 Hz, 2 H), 7.38 (app t, J = 7.4 Hz, 2 H), 7.30 (app dt, J = 2.8, 7.5 Hz, 2 H), 5.34 (ddd, J = 7.2, 9.9, 9.9 Hz, 1 H), 3.09 (app t, J = 6.4 Hz, 1 H), 2.55 - 2.42 (m, 2 H), 1.82 - 1.64 (m, 3 H), 1.62 - 1.49 (m, 1 H), 1.46 - 1.27 (m, 2 H). ^{13}C NMR (100 MHz, $CDCl_3$) δ 185.0, 141.9, 139.8, 139.4, 131.8, 131.6, 131.3, 130.8, 129.7, 129.1, 128.3, 125.0, 121.1, 119.6, 67.8, 40.7, 29.0, 21.8, 21.6 (2C). IR (film); 3059, 2938, 2857, 1676, 1607, 1555, 1450, 1372, 1312, 1278, 1249, cm^{-1}. HRMS (EI): Exact mass calcd for $C_{20}H_{18}N_2O$ $[M]^+$: 302.1419. Found: 302.1435.

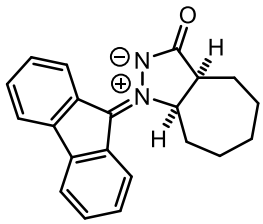

9j. Synthesized according to general procedure 2A using hydrazone **6a** (0.079 g, 0.25 mmol) and cycloheptene (0.29 mL, 2.5 mmol, 10 equiv) in $PhCF_3$ (5 mL). The reaction was heated by microwave irradiation at 100 °C for 6 h. The crude mixture was concentrated in vacuo, and the product isolated by column chromatography (1:4 EtOAc/CH_2Cl_2 to remove excess alkene and by-products, then 9:1 EtOAc/MeOH to elute the product). The product was obtained as a yellow solid (0.032 g, 40%). TLC R_f = 0.27 in EtOAc. ^{1}H NMR (400 MHz, $CDCl_3$) δ 9.00 (d, *J* = 7.5 Hz, 1 H), 7.66 (d, *J* = 7.3 Hz, 1 H), 7.58 (d, *J* = 7.3 Hz, 1 H), 7.48 - 7.36 (m, 3 H), 7.36 - 7.28 (m, 2 H), 5.40 - 5.24 (m, 1 H), 3.33 (ddd, *J* = 5.4, 8.9, 11.1 Hz, 1 H), 2.35 (ddd, *J* = 5.5, 8.7, 14.6 Hz, 1 H), 2.23 - 2.08 (m, 2 H), 2.05 - 1.90 (m, 2 H), 1.90 - 1.75 (m, 2 H), 1.64 - 1.36 (m, 3 H). ^{13}C NMR (100 MHz, $CDCl_3$) δ 185.4, 141.8, 139.4, 139.1, 131.7, 131.6, 131.2, 130.6, 129.6, 129.0, 128.1, 125.1, 121.0, 119.4, 73.5, 45.5, 31.0, 30.6, 26.5, 26.5, 26.4. HRMS (EI): Exact mass calcd for $C_{21}H_{20}N_2O$ $[M]^+$: 316.15756. Found: 316.16049.

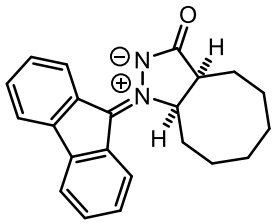

9k. Synthesized according to general procedure 2A using hydrazone **6a** (0.079 g, 0.25 mmol) and cyclooctene (0.30 mL, 2.5 mmol, 10 equiv) in $PhCF_3$ (5 mL). The reaction was heated by microwave irradiation at 100 °C for 6 h. The crude mixture was concentrated in vacuo, and the product isolated by column chromatography (1:4 EtOAc/CH_2Cl_2 to remove excess alkene and by-

products, then 9:1 EtOAc/MeOH to elute the product). The product was obtained as a yellow solid (0.045 g, 54%). TLC R_f = 0.42 in EtOAc. ^{1}H NMR (400 MHz, $CDCl_3$) δ 9.02 (d, *J* = 7.7 Hz, 1 H), 7.66 (d, *J* = 7.5 Hz, 1 H), 7.62 - 7.55 (m, 2 H), 7.43 - 7.37 (m, 2 H), 7.36 - 7.27 (m, 2 H), 5.45 - 5.30 (m, 1 H), 2.86 (ddd, J = 2.0, 8.5, 12.1 Hz, 1 H), 2.55 - 2.42 (m, 1 H), 2.24 - 2.10 (m, 1 H), 2.10 - 1.96 (m, 3 H), 1.94 - 1.54 (m, 5 H), 1.34 - 1.20 (m, 1 H), 1.17 - 1.03 (m, 1 H). ^{13}C NMR (100 MHz, $CDCl_3$) δ 185.0, 141.7, 139.5, 139.3, 132.0, 131.7, 131.4, 130.8, 129.9, 129.2, 128.0, 124.7, 121.0, 119.5, 73.8, 45.6, 31.9, 29.7, 28.1, 26.0, 24.8, 21.8.. HRMS (EI): Exact mass calcd for $C_{22}H_{22}N_2O$ $[M]^+$: 330.1732. Found: 330.1730.

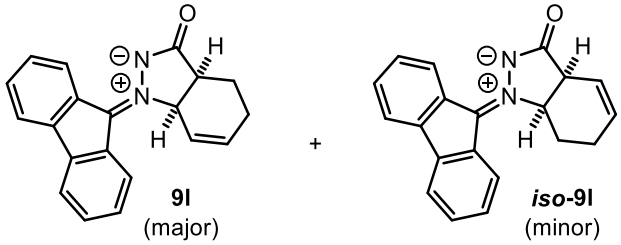

9l (major) + ***iso*-9l** (minor)

9l. Synthesized according to general procedure 2A using hydrazone **6a** (0.076 g, 0.24 mmol) and 1,3-cyclohexadiene (0.24 mL, 2.5 mmol, 10 equiv) in $PhCF_3$ (5 mL). The reaction was heated by microwave irradiation at 100 °C for 3 h. The crude mixture was concentrated in vacuo, and the product isolated by column chromatography (1:3 EtOAc/CH_2Cl_2 to remove excess alkene and by-products, then 9:1 EtOAc/MeOH to elute the product). The product was obtained as a yellow solid (0.039 g, 52% yield, 14:1mixture of alkene regioisomers). m.p.: 205-207 °C. TLC R_f = 0.21 in EtOAc. ^{1}H NMR (400 MHz, $CDCl_3$) δ 8.99 (d, *J* = 7.7 Hz, 1H), 7.65 - 7.73 (m, 2H), 7.62 (d, J = 7.4 Hz, 1H), 7.39 - 7.47 (m, 2H), 7.30 - 7.38 (m, 2H), 6.21 - 6.30 (m, 1H), 5.86 - 6.00 (m, 2H), 3.29 - 3.40 (m, 1H), 2.45 - 2.54 (m, 1H), 2.21 - 2.34 (m, 1H), 2.04 - 2.15 (m, 1H), 1.82 - 1.94 (m, 1H). ^{13}C NMR (100 MHz, $CDCl_3$) δ 184.9, 142.0, 139.8, 139.8, 137.7, 131.9, 131.6, 131.3, 130.9, 129.9, 129.1, 128.3, 125.2, 121.1, 119.6, 119.4, 66.3, 39.7, 20.9, 19.5. IR (film); 3043, 2924, 2852,

1660, 1603, 1549, 1450, 1359, 1302, 1274, 1121, 1073, 963, 777, 725 cm^{-1}. HRMS (EI): Exact mass calcd for $C_{20}H_{16}N_2O$ $[M]^+$: 300.1263. Found: 300.1269.

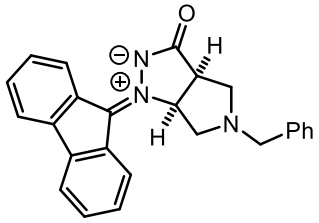

9p. Synthesized according to general procedure 2A using hydrazone **6a** (0.052 g, 0.16 mmol) and 1-benzyl-3-pyrroline (0.30 mL, 1.6 mmol, 10 equiv) in $PhCF_3$ (3.2 mL). The reaction was heated by microwave irradiation at 150 °C for 3 h. ^1H NMR of the crude mixture shows 38% yield of the product with 1,3,5-trimethoxybenzene internal standard, and much of the alkene was observed to oxidize to *N*-benzyl pyrrole. The product isolated by column chromatography (CH_2Cl_2 to remove excess alkene and by-products, then EtOAc/Hexane to elute the product). The product was obtained as a yellow solid with some impurities (0.0095 g, 15% yield). ^1H NMR (400 MHz, $CDCl_3$, contains 9 wt% alkene) δ 9.01 (d, *J* = 7.7 Hz, 1 H), 7.72 - 7.59 (m, 2 H), 7.47 - 7.17 (m, 10 H), 5.59 - 5.53 (m, 1 H), 3.66 - 3.53 (m, 3 H), 3.53 - 3.36 (m, 2 H), 2.87 (dd, *J* = 6.4, 10.8 Hz, 1 H), 2.49 (dd, *J* = 6.6, 9.3 Hz, 1 H).

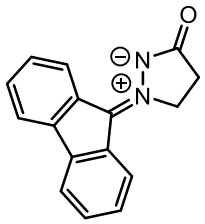

9q. Hydrazone **6a** (0.035 g, 0.11 mmol) was diluted in $PhCF_3$ (2 mL) in a vial, which was sealed and purged with ethylene gas using the freeze-pump-thaw method. The reaction was heated by microwave irradiation at 100 °C for 1 h, and the pressure was observed to stay below 5 bar. ^1H NMR of the crude mixture showed 6% yield of the product and 70% yield of **6a** with 1,3,5-

trimethoxybenzene internal standard. The product isolated by prep-TLC. The product was obtained as a yellow solid (0.001 g, 4% yield). ^{1}H NMR (500 MHz, $CDCl_3$) δ 8.96 (d, *J* = 7.7 Hz, 1 H), 7.72 (d, *J* = 7.0 Hz, 1 H), 7.65 (dd, *J* = 5.0, 7.7 Hz, 2 H), 7.50 - 7.44 (m, 2 H), 7.42 - 7.31 (m, 2 H), 5.00 - 4.81 (m, 2 H), 3.19 - 3.02 (m, 2 H). ^{13}C DEPT-135 NMR (100 MHz, $CDCl_3$) δ 132.1, 131.2, 131.0, 129.3, 128.3, 125.4, 121.4, 120.0, 57.1, 29.7. HRMS (EI): Exact mass calcd for $C_{16}H_{12}N_2O$ $[M]^+$: 248.0950. Found: 248.0927.

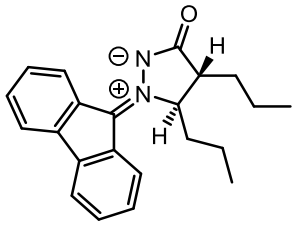

9r. Synthesized according to general procedure 2A using hydrazone **6a** (0.077 g, 0.25 mmol) and trans-4-octene (0.39 mL, 2.5 mmol, 10 equiv) in $PhCF_3$ (5 mL). The reaction was heated by microwave irradiation at 100 °C for 3 h. ^{1}H NMR of the crude mixture shows approximately 3% yield of the product with 1,3,5-trimethoxybenzene internal standard. TLC R_f = 0.24 in EtOAc. The product was not successfully isolated.

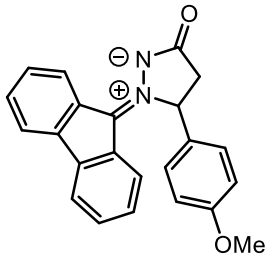

9s. Synthesized according to general procedure 2A using hydrazone **6a** (0.079 g, 0.25 mmol) and 4-methoxystyrene (0.33 mL, 2.5 mmol, 10 equiv) in $PhCF_3$ (5 mL). The reaction was heated at 100 °C for three hours. The crude mixture was concentrated in vacuo, and the product isolated by column chromatography (1:4 EtOAc/CH_2Cl_2 to remove excess alkene and by-products, then 9:1

EtOAc/MeOH to elute the product). The product was obtained as a yellow solid (0.067 g, 74% yield). m.p.: 203-206 °C. TLC R_f = 0.23 in EtOAc. ^{1}H NMR (400 MHz, $CDCl_3$) δ 9.12 (d, *J* = 7.5 Hz, 1 H), 7.58 (dd, *J* = 3.0, 7.2 Hz, 2 H), 7.47 - 7.33 (m, 3 H), 7.29 (m, 1 H), 7.21 - 7.14 (m, 2 H), 7.11 - 7.02 (m, 1 H), 6.88 - 6.81 (m, 2 H), 6.30 (m, 1 H), 3.73 (s, 3 H), 3.46 (dd, *J* = 9.2, 16.3 Hz, 1 H), 2.72 (dd, *J* = 1.8, 16.3 Hz, 1 H). ^{13}C NMR (100 MHz, $CDCl_3$) δ 182.6, 159.7, 141.8, 141.4, 140.3, 132.3, 131.7 (2C), 131.1, 129.9, 129.4, 129.2, 128.0, 126.1, 126.0 (2C), 120.8, 119.7, 115.1 (2C), 71.9, 55.3, 40.9. IR (film): 3063, 2945, 2835, 1664, 1607, 1546, 1508, 1447, 1341, 1299, 1273, 1250, 1177, 1117, 1094, 1078, 1025, 984, 911, 828, 779, 725 cm^{-1}. HRMS (EI): Exact mass calcd for $C_{23}H_{18}N_2O_2$ $[M]^+$: 354.1368. Found: 354.1374.

Gram Scale: Hydrazone **6a** (0.94 g, 3.0 mmol, 1 equiv), 4-methoxystyrene (2.0 mL, 15 mmol, 5.0 equiv), and $PhCF_3$ (60 mL) combined in a 100 mL flask, equipped with a reflux condenser, and heated in an oil bath to 100 °C for 6 h. The mixture became dark brown with some light yellow precipitate. The mixture was cooled to room temperature, the stir bar removed, and $PhCF_3$ evaporated to give a dark oil. This was purified by passing through a silica plug, following the procedure above, to provide a yellow solid (0.749 g, 71% yield).

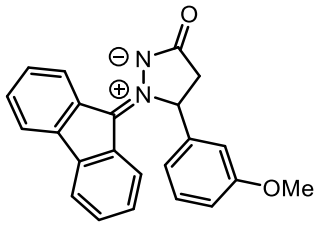

9t. Synthesized according to general procedure 2A using hydrazone **6a** (0.157 g, 0.500 mmol) and 3-methoxystyrene (0.35 mL, 2.5 mmol, 10 equiv) in $PhCF_3$ (10 mL). The reaction was heated at 100 °C for six hours. The crude mixture was concentrated in vacuo, and the product isolated by column chromatography (1:3 EtOAc/CH_2Cl_2 to remove excess alkene and by-products, then 20:1

MeOH/CH_2Cl_2 to elute the product). The product was obtained as a yellow solid (0.051 g, 29% yield). TLC R_f = 0.24 in EtOAc. ^{1}H NMR (300 MHz, $CDCl_3$) δ 9.14 (d, *J* = 7.4 Hz, 1 H), 7.65 - 7.54 (m, 2 H), 7.50 - 7.34 (m, 3 H), 7.33 - 7.24 (m, 3 H), 7.12 - 7.03 (m, 1 H), 6.91 - 6.77 (m, 3 H), 6.30 (dd, *J* = 1.7, 9.4 Hz, 1 H), 3.74 (s, 3 H), 3.47 (dd, *J* = 9.4, 16.2 Hz, 1 H), 2.74 (dd, *J* = 2.0, 16.3 Hz, 1 H). ^{13}C NMR (100 MHz, $CDCl_3$) δ 182.4, 160.6, 141.7, 141.2, 140.2, 139.4, 132.2, 131.7, 131.0, 130.9, 130.9, 129.4, 129.2, 128.0, 125.8, 120.8, 119.7, 116.8, 113.5, 110.8, 72.0, 55.3, 40.7. IR (ATR): 3071, 2982, 2939, 1658, 1605, 1550, 1274 cm^{-1}. HRMS (EI): Exact mass calcd for $C_{23}H_{18}N_2O_2$ $[M]^+$: 354.1368. Found: 354.1396.

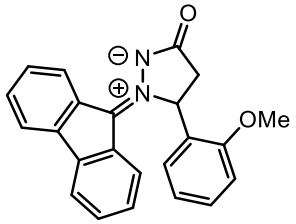

9u. Synthesized according to general procedure 2A using hydrazone **6a** (0.157 g, 0.500 mmol) and 2-methoxystyrene (0.34 mL, 2.5 mmol, 10 equiv) in $PhCF_3$ (10 mL). The reaction was heated at 100 °C for six hours. The crude mixture was concentrated in vacuo, and the product isolated by column chromatography (1:4 EtOAc/CH_2Cl_2 to remove excess alkene and by-products, then 9:1 EtOAc/MeOH to elute the product). The product was obtained as a yellow solid (0.128 g, 72% yield). TLC R_f = 0.31 in EtOAc. ^{1}H NMR (400 MHz, $CDCl_3$) δ 9.12 (d, *J* = 7.3 Hz, 1 H), 7.53 (d, *J* = 7.5 Hz, 1 H), 7.55 (d, *J* = 7.2 Hz, 1 H), 7.45 - 7.32 (m, 2 H), 7.29 - 7.20 (m, 2 H), 7.17 (d, *J* = 8.0 Hz, 1 H), 7.06 - 6.90 (m, 3 H), 6.83 - 6.72 (m, 1 H), 6.49 (dd, *J* = 2.0, 9.2 Hz, 1 H), 4.02 (s, 3 H), 3.43 (dd, *J* = 9.2, 16.6 Hz, 1 H), 2.57 (dd, *J* = 2.3, 16.6 Hz, 1 H). ^{13}C NMR (100 MHz, $CDCl_3$) δ 183.1, 155.0, 141.5, 140.4, 140.1, 132.0, 131.6, 131.4, 130.7, 130.0, 129.5, 129.0, 127.9, 126.0, 125.3, 124.1, 121.8, 120.6, 119.6, 110.5, 67.6, 55.8, 39.4. IR (ATR): 3062, 2930, 2840, 1670, 1544 cm^{-1}. HRMS (EI): Exact mass calcd for $C_{23}H_{18}N_2O_2$ $[M]^+$: 354.1368 Found: 354.1383.

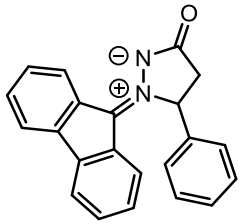

9v. Synthesized according to general procedure 2A using hydrazone **6a** (0.078 g, 0.25 mmol) and styrene (0.30 mL, 2.5 mmol, 10 equiv) in $PhCF_3$ (5 mL). The reaction was heated at 100 °C for six hours. The crude mixture was concentrated in vacuo, and the product isolated by column chromatography (1:4 EtOAc/CH_2Cl_2 to remove excess alkene and by-products, then 9:1 EtOAc/MeOH to elute the product). The product was obtained as a yellow solid (0.052 g, 64% yield). m.p.: 213-214 °C. TLC R_f = 0.27 in EtOAc. ^{1}H NMR (400 MHz, $CDCl_3$) δ 9.13 (d, *J* = 7.5 Hz, 1 H), 7.59 (dd, *J* = 3.9, 7.2 Hz, 2 H), 7.49 - 7.43 (m, 1 H), 7.43 - 7.25 (m, 8 H), 7.05 (m, 1 H), 6.37 (m, 1 H), 3.56 (dd, *J* = 9.6, 16.4 Hz, 1 H), 2.89 - 2.78 (dd, *J* = 1.64, 16.3 Hz, 1 H). ^{13}C NMR (100 MHz, $CDCl_3$) δ 182.4, 141.8, 141.3, 140.3, 137.9, 132.3, 131.7(2), 131.6(8), 131.1, 129.8, 129.3, 129.2, 128.7, 128.0, 125.9, 124.7, 120.8, 119.7, 72.2, 40.7 IR (film); 3067, 3021, 2922, 1668, 1603, 1447, 1345, 1276, 1242, 1124, 1090, 980, 778, 725, 713 cm^{-1} . HRMS (EI): Exact mass calcd for $C_{22}H_{16}N_2O$ $[M]^+$: 324.1263. Found: 324.1272.

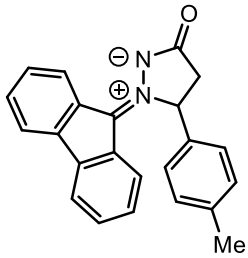

9w. Synthesized according to general procedure 2A using hydrazone **6a** (0.159 g, 0.504 mmol) and 4-methylstyrene (0.66 mL, 5.0 mmol, 10 equiv) in $PhCF_3$ (10 mL). The reaction was heated at 100 °C for three hours. The crude mixture was concentrated in vacuo, and the product isolated by column chromatography (1:1 Et_2O/CH_2Cl_2 then 9:1 Et_2O/MeOH to elute the product). The product was obtained as a yellow solid (0.083 g, 48% yield). TLC R_f = 0.20 in EtOAc. For characterization see Chapter 3.[23]

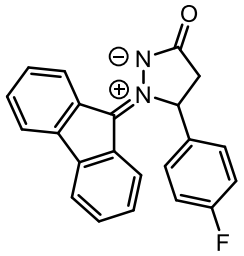

9x. Synthesized according to general procedure 2A using hydrazone **6a** (0.157 g, 0.500 mmol) and 4-fluorostyrene (0.30 mL, 2.5 mmol, 5 equiv) in $PhCF_3$ (10 mL). The reaction was heated at 120 °C for six hours. The crude mixture was concentrated in vacuo, and the product isolated by column chromatography (1:4 EtOAc/CH_2Cl_2 to remove excess alkene and by-products, then 9:1 EtOAc/MeOH to elute the product). The product was obtained as a yellow solid (0.080 g, 47% yield). Spectral data is in agreement with our prior publication.[1]

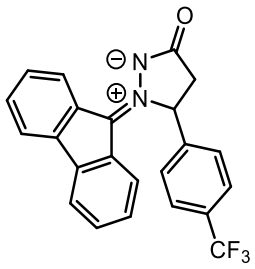

9y. Synthesized according to general procedure 2A using hydrazone **6a** (0.157 g, 0.500 mmol) and 4-(trifluoromethyl)styrene (0.74 mL, 5.0 mmol, 10 equiv) in $PhCF_3$ (10 mL). The reaction was heated at 100 °C for six hours. The crude mixture was concentrated in vacuo, and the product isolated by column chromatography (1:4 EtOAc/CH_2Cl_2 to remove excess alkene and by-products, then 9:1 EtOAc/MeOH to elute the product). The product was obtained as a yellow solid (0.045 g, 23% yield). TLC R_f = 0.17 in EtOAc. ^{1}H NMR (400 MHz, $CDCl_3$) δ 9.24 - 8.96 (m, 1 H), 7.75 - 7.54 (m, 4 H), 7.53 - 7.36 (m, 4 H), 7.36 - 7.28 (m, 1 H), 7.26 (m, 1 H), 7.13 - 7.02 (m, 1 H), 6.46 (d, *J* = 8.4 Hz, 1 H), 3.57 (dd, *J* = 9.5, 16.4 Hz, 1 H), 2.74 (dd, *J* = 2.0, 16.4 Hz, 1 H). ^{13}C NMR (100 MHz, $CDCl_3$) δ 181.8, 141.8, 141.7, 141.4, 140.2, 132.5, 131.6, 131.4, 131.3, 131.0 (q, J_{C-F} = 33.0 Hz), 129.2, 129.0, 128.0, 126.8 (q, J_{C-F} = 3.7 Hz, 2C), 125.5, 125.3 (2C), 123.5 (q, J_{C-F} = 271 Hz), 121.0, 119.8, 71.4, 40.4. ^{19}F NMR (377MHz, $CDCl_3$) δ 62.8. IR (ATR) 3095, 1992, 1733, 1695, 1623, 1577, 1456, 1372 cm^{-1}. HRMS (EI): Exact mass calcd for $C_{23}H_{15}F_3N_2O$ $[M]^+$: 392.1136. Found: 392.1138.

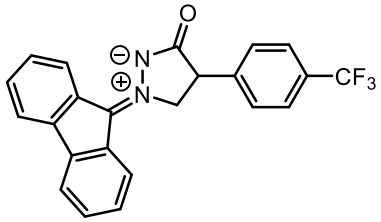

***iso*-9y**. Following same procedure as above for product **9y**, the product ***iso*-9y** was also isolated (9.8 mg, 5% yield). TLC R_f = 0.49 in EtOAc. ^{1}H NMR (400 MHz, $CDCl_3$) δ 9.00 (d, *J* = 7.7 Hz, 1 H), 7.71 (d, *J* = 7.3 Hz, 1 H), 7.69 - 7.58 (m, 4 H), 7.55 - 7.43 (m, 4 H), 7.37 (ddd, *J* = 1.1, 7.7,

7.7 Hz, 1 H), 7.33 - 7.27 (m, 1 H), 5.38 (dd, J = 9.9, 13.5 Hz, 1 H), 4.86 (dd, J = 5.6, 13.5 Hz, 1 H), 4.37 (dd, J = 5.6, 9.9 Hz, 1 H). ^{13}C NMR (100 MHz, $CDCl_3$) δ 183.5, 142.1, 142.0, 141.2, 140.3, 132.6, 131.7, 131.4, 131.2, 130.4, 130.3 (q, J_{C-F} = 32.0 Hz), 129.4, 129.2, 128.5, 128.4, 126.4 (q, J_{C-F} = 4.0 Hz, 2C), 125.7, 124.5, 124.1 (q, J_{C-F} = 270 Hz), 121.5, 120.5, 120.1, 64.5, 47.5. IR (ATR) 3136, 1699, 1634, 1581, 1410, 1395 cm^{-1}. HRMS (EI): Exact mass calcd for $C_{23}H_{15}F_3N_2O$ [M]$^+$: 392.1136. Found: 392.11375.

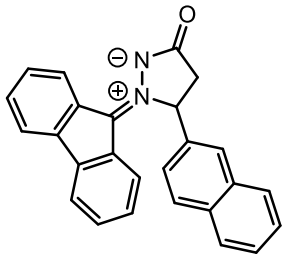

9z. Synthesized according to general procedure 2A using hydrazone **6a** (0.063 g, 0.20 mmol) and 2-vinylnapthalene (0.154 g, 1.0 mmol, 5 equiv) in $PhCF_3$ (4 mL). The reaction was heated at 120 °C for three hours. The crude mixture was concentrated in vacuo, and the product isolated by column chromatography (2:1 EtOAc/hexane, then 9:1 EtOAc/MeOH). The product was obtained as a yellow solid (0.042 g, 56% yield). TLC R_f = 0.21 in EtOAc. ^{1}H NMR (400 MHz, $CDCl_3$) δ 9.22-9.20 (m, 1H), 7.91 (d, J = 8.5, 1H), 7.83-7.80 (m, 1H), 7.76-7.74 (m, 1H), 7.68 (d, J = 1.0 Hz, 1H), 7.62-7.56 (m, 2H), 7.51-7.39 (m, 6H), 7.29-7.25 (m, 1H), 7.01 (td, J = 7.8, 0.9 Hz, 1H), 6.55-6.53 (m, 1H), 3.63 (dd, J = 9.3, 16.4 Hz, 1H), 2.90 (dd, J = 1.9, 16.5 Hz, 1H). ^{13}C NMR (101 MHz, $CDCl_3$) δ 182.7, 142.1, 141.8, 140.7, 135.5, 133.7, 133.3, 132.7, 132.12, 132.06, 131.4, 130.5, 129.66, 129.60, 128.50, 128.38, 128.1, 127.36, 127.20, 126.2, 123.7, 122.8, 121.2, 120.1, 72.7, 41.1. IR (film) 1734, 1663, 1609, 1544, 1506, 1450, 1292 cm^{-1}. HRMS (EI): Exact mass calcd for $C_{26}H_{18}N_2O$ [M]$^+$: 374.1419. Found: 374.1444.

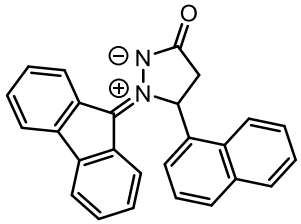

9aa. Synthesized according to general procedure 2A using hydrazone **6a** (0.400 g, 1.27 mmol) and 1-vinylnapthalene (0.98 g, 6.4 mmol, 5 equiv) in $PhCF_3$ (13 mL). The reaction was heated at 120 °C for three hours. The crude mixture was concentrated in vacuo, and the product isolated by column chromatography (2:1 EtOAc/hexane, then 20:1 EtOAc/MeOH). The product was obtained as a yellow solid (0.247 g, 66% yield). TLC R_f = 0.33 in EtOAc. ^{1}H NMR (400 MHz, $CDCl_3$) δ 9.19 (dd, *J* = 0.5, 7.6 Hz 1H), 7.99 (appt, *J* = 9.3 Hz, 2H), 7.82 (d, *J* = 8.2 Hz, 1H), 7.75 (td, *J* = 1.1, 7.7 Hz, 1H), 7.68-7.64 (m, 1H), 7.59 (d, *J* = 7.0 Hz, 1H), 7.55 (d, *J* = 7.4 Hz, 1H), 7.45 (dtd, *J* = 1.2, 7.5, 22.6 Hz, 2H), 7.30 (appt, *J* = 7.8 Hz, 1H), 7.22-7.17 (m, 2H), 6.94 (d, *J* = 7.8 Hz, 1H), 6.88 (d, *J* = 8.1 Hz, 1H), 6.75-6.71 (m, 1H), 3.72 (dd, *J* = 9.3, 16.3 Hz, 1H), 2.80 (dd, *J* = 2.1, 16.3 Hz, 1H). ^{13}C NMR (101 MHz, $CDCl_3$) δ 182.9, 141.9, 141.6, 140.6, 134.4, 133.2, 132.6, 131.97, 131.95, 131.3, 130.1, 129.82, 129.75, 129.58, 129.2, 128.4, 128.0, 126.9, 126.3, 125.6, 121.87, 121.82, 121.1, 120.1, 70.6, 40.3. IR (film) 1663, 1605, 1553, 1450, 1288, 1269, 1232, 1124, 1091, 1018, 802, 773, 711 cm^{-1}. HRMS (EI): Exact mass calcd for $C_{26}H_{18}N_2O$ $[M]^+$: 374.1419. Found: 374.1405.

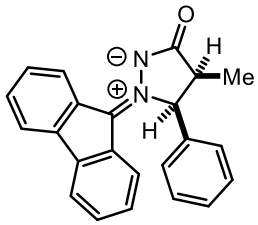

9ab. Synthesized according to general procedure 2A using hydrazone **6a** (0.157 g, 0.499 mmol) and (Z)-prop-1-en-1-ylbenzene (1.3 mL, 10 mmol, 20 equiv) in $PhCF_3$ (0.5 mL). The reaction was

heated at 150 °C for 20 min. The crude mixture was filtered through sand then concentrated in vacuo, and the product isolated by column chromatography (1:1 EtOAc/CH_2Cl_2, then 9:1 EtOAc/MeOH). The product was obtained as a yellow solid (0.066 g, 39% yield). Spectral data is in agreement with the literature.[9,23]

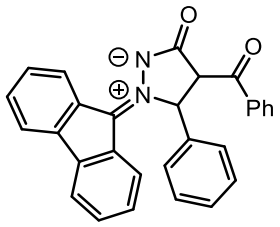

9ac. Synthesized according to general procedure 2A using hydrazone **6a** (0.086 g, 0.27 mmol) and trans-chalcone (0.385 g, 1.37 mmol, 5 equiv) in $PhCF_3$ (5 mL). The reaction was heated by microwave irradiation at 100 °C for 6 h. ^{1}H NMR of the crude mixture shows 14% yield of the product with 1,3,5-trimethoxybenzene internal standard. The product was not isolated.

General Procedure 2C: Synthesis of β-amino amides[1]

Azomethine imine (**9**) was diluted in MeOH. In quick succession, $NaBH_4$ or KBH_4 (6.0-10 equiv) and Raney nickel (0.5 to 1 mL, slurry in MeOH) were added to a screw-top flask which was sealed. Care must be taken in choosing size of the flask to allow a large empty volume of headspace once sealed. The reaction mixture was stirred at 60 ºC for 2-6 hours. The mixture was cooled to rt and filtered through celite to remove Raney nickel. The filtrate was concentrated under reduced pressure and then quenched with saturated NH_4Cl. The crude product was extracted with 3 x CH_2Cl_2 and the combined organic layer was dried over Na_2SO_4, filtered, and concentrated in vacuo to give an oil. Et_2O was then added to precipitate the purified product as a white solid.

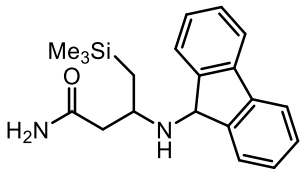

10d. Synthesized according to general procedure 2C (t = 2 h) from **9e** (1.0 mmol, 335 mg), KBH_4 (6.0 mmol, 324 mg) and Ra-Ni slurry in MeOH (0.5 mL). The product was obtained as a white solid (First crop: 199 mg, Second crop: 37 mg, 70% yield). TLC R_f = 0.25 in EtOAc. ^{1}H NMR (400 MHz, $CDCl_3$) δ 8.10 (br. s, 1 H), 7.75 - 7.63 (dd, *J* = 4.1, 7.4 Hz, 2 H), 7.53 (d, *J* = 7.4 Hz, 1 H), 7.57 (d, *J* = 7.4 Hz, 1 H), 7.42 - 7.33 (m, 2 H), 7.33 - 7.25 (m, 2 H), 5.55 (br. s., 1 H), 4.89 (s, 1 H), 3.59 - 3.44 (m, 1 H), 2.58 (dd, *J* = 3.3, 16.0 Hz, 1 H), 2.19 (dd, *J* = 5.1, 15.8 Hz, 1 H), 1.75 (br. s., 1H), 1.01 - 0.91 (dd, *J* = 8.9, 14.5 Hz, 1 H), 0.91 - 0.82 (dd, *J* = 5.0, 14.7 Hz, 1 H), -0.03 (s, 9 H). ^{13}C NMR (400 MHz, $CDCl_3$) δ 174.1, 145.7, 145.6, 140.5, 140.3, 128.5, 128.4, 127.5, 127.4, 125.0, 124.9, 120.2, 120.0, 60.7, 50.0, 41.3, 23.8, -0.9 (3C). IR (film); 3466, 3329, 3192, 3067, 2949, 2895, 2808, 1669, 1444, 1406, 1295, 1245 cm^{-1}. HRMS (EI): Exact mass calcd for $C_{20}H_{26}N_2OSi$ $[M]^+$: 338.18, Not found. Exact mass calcd for $C_7H_{17}N_2OSi$ [M–Fluorenyl]$^+$: 173.1110. Found: 173.1155.

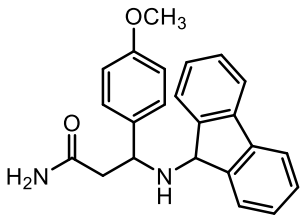

10e. Synthesized according to general procedure 2C (t = 4 h) from **9s** (1.0 mmol, 355 mg), KBH_4 (6.0 mmol, 324 mg) and Ra-Ni slurry in MeOH (0.5 mL). The product (270 mg, 75%) was obtained as a white solid. TLC R_f = 0.31 in EtOAc. ^{1}H NMR (400 MHz, $CDCl_3$) δ 7.62 (dd, *J* = 3.8, 7.4 Hz, 2 H), 7.57 (d, *J* = 7.3 Hz, 1 H), 7.42 (d, *J* = 7.3 Hz, 1 H), 7.36 - 7.18 (m, 6 H), 6.86 (d, *J* = 8.6 Hz, 2 H), 6.45 (br. s., 1 H), 5.35 (br. s., 1 H), 4.69 (s, 1 H), 4.52 (dd, *J* = 4.7, 8.5 Hz, 1 H), 3.78 (s, 3

H), 2.60 (dd, J = 8.5, 15.1 Hz, 1 H), 2.50 (dd, J = 4.7, 15.1 Hz, 1 H), 2.15 (br. s., 1 H). ^{13}C NMR (400 MHz, $CDCl_3$) δ 173.7, 159.1, 146.2, 145.4, 140.4, 140.3, 134.2, 128.4 (2C), 128.3, 128.0, 127.4, 127.3, 125.2, 125.0, 119.9, 119.8, 114.2 (2C), 60.7, 57.6, 55.3, 44.4. IR (film); 3458, 3325, 3192, 3063, 2964, 2907, 2842, 1672, 1607, 1512, 1444, 1398, 1307, 1249 cm^{-1}. HRMS (EI): Exact mass calcd for $C_{23}H_{22}N_2O_2$ $[M]^+$: 358.1681, Not found. Exact mass calcd for $C_{10}H_{13}N_2O_2$ [M–Fluorenyl]$^+$: 193.0977. Found: 193.0999.

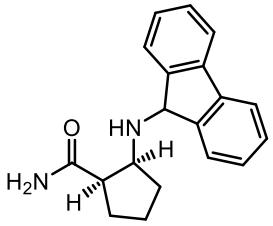

10f. Synthesized according to general procedure 2C (t = 6 h) from **9h** (0.213 mmol, 0.0613 g), $NaBH_4$ (1.7 mmol, 0.064 g) and Ra-Ni slurry in MeOH (1 mL). The product (0.0365 g, 59%) was obtained as a white solid. TLC R_f = 0.25 in EtOAc. ^{1}H NMR (400 MHz, $CDCl_3$) δ 7.68 - 7.72 (m, 3 H), 7.57 (d, J = 7.4 Hz, 1 H), 7.61 (d, J = 7.5 Hz, 1 H), 7.38 (dd, J = 7.4, 7.4 Hz, 2 H), 7.30 (ddt, J = 1.0, 2.9, 7.4 Hz, 2 H), 5.80 (br. s., 1 H), 4.93 (s, 1 H), 3.19 (**M1**, td, J = 6.7, 8.4 Hz, 1 H, NOE with **M2**), 2.47 - 2.40 (**M2**, m, 1 H, NOE with **M1**), 2.33 (br. s, 1 H), 2.13 - 2.01 (m, 1 H), 1.77 - 1.41 (m, 5 H). ^{13}C NMR (400 MHz, $CDCl_3$) δ 177.0, 145.9, 145.2, 140.7, 140.5, 128.3, 128.3, 127.4 (2C), 125.1, 124.8, 120.0, 120.0, 62.5, 58.2, 48.0, 32.1, 27.6, 21.2. IR (ATR): 3487, 3329, 3175, 2840, 1733, 1520 cm^{-1}. HRMS (EI): Exact mass calcd for $C_{19}H_{20}N_2O$ $[M]^+$: 292.1576, Not found. Exact mass calcd for $C_6H_{11}N_2O$ [M–Fluorenyl]$^+$ and $C_{13}H_9$ [Fluorenyl]$^+$: 127.0871 and 165.0704. Found: 127.0865 and 165.071.

General Procedure 2D: Synthesis of β-amino methyl esters[1]

Synthesized according to procedure taken from Zhu *et al*.[5] $SOCl_2$ (3.5 equiv) was added to a vial of methanol at 0 °C, and the mixture was stirred at 0 °C for 10 minutes. This solution was added drop-wise to a vial containing β-amino amide **10** (1 equiv) in MeOH at 0 °C. The vial was sealed and heated to 60 °C for 12 h. The mixture was concentrated under reduced pressure and quenched with aqueous $NaHCO_3$. The crude product was extracted with 3 x CH_2Cl_2 and the combined organic layers were dried over Na_2SO_4, filtered and concentrated in vacuo. The product was purified by column chromatography (EtOAc/Hexane).

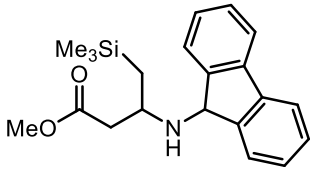

11d. Synthesized according to general procedure 2D from **10d** (0.075 g, 0.22 mmol), $SOCl_2$ (0.060 mL, 0.80 mmol, 3.5 equiv) and methanol (4 mL). The product was obtained as a colourless oil (0.050 g, 64% yield) and 25% of the amide was also recovered. TLC R_f = 0.42 in EtOAc. ^{1}H NMR (400 MHz, $CDCl_3$) δ 7.67 (dd, *J* = 2.7, 7.4 Hz, 2 H), 7.64 - 7.57 (dd, *J* = 1.6, 7.2 Hz, 2 H), 7.35 (appt, *J* = 7.4 Hz, 2 H), 7.31 - 7.28 (m, 2 H), 4.87 (s, 1 H), 3.65 (s, 3 H), 3.54 (qd, *J* = 5.8, 7.9 Hz, 1 H), 2.45 (d, *J* = 5.9 Hz, 2 H), 1.94 (br. s., 1 H), 0.93 - 0.85 (dd, *J* = 5.6, 14.7 Hz, 1 H), 0.85 - 0.76 (dd, *J* = 8.0, 14.8 Hz, 1 H), –0.06 (s, 9 H). ^{13}C NMR (75 MHz, $CDCl_3$) δ 172.8, 146.6, 146.5, 140.4, 140.3, 128.0 (2C), 127.3, 127.2, 125.1 (2C), 119.9, 119.8, 61.4, 51.5, 50.1, 42.2, 24.7, –0.7 (3C). IR (film); 3344, 3066, 3027, 2953, 2894, 1736, 1607, 1450, 1360, 1298, 1247 cm^{-1}. HRMS (EI): Exact mass calcd for $C_{21}H_{27}N_1O_2Si$ $[M]^+$: 353.1811, Not found. Exact mass calcd for $C_8H_{18}NO_2Si$ $[M–Fluorenyl]^+$: 188.1107. Found: 188.1083. Exact mass calcd for $C_{18}H_{22}NSi$ $[M – C_3H_5O_2]^+$: 280.1522. Found: 280.1532.

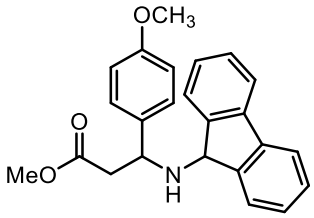

11e. Synthesized according to general procedure 2D from **10e** (0.072 g, 0.20 mmol), $SOCl_2$ (0.050 mL, 0.70 mmol, 3.5 equiv) and methanol (3 mL). The product was obtained as a colourless oily residue (0.045 g, 60% yield). TLC R_f = 0.53 (20% EtOAc in hexanes). ^{1}H NMR (300 MHz, $CDCl_3$) δ 7.65 - 7.57 (m, 3 H), 7.53 (d, *J* = 7.3 Hz, 1 H), 7.38 - 7.25 (m, 5 H), 7.23 - 7.16 (m, 1 H), 6.83 (m, 2 H), 4.70 (s, 1 H), 4.58 (dd, *J* = 5.8, 8.2 Hz, 1 H), 3.77 (s, 3 H), 3.56 (s, 3 H), 2.81 - 2.69 (dd, *J* = 8.3, 15.7 Hz, 1 H), 2.69 - 2.59 (dd, *J* = 5.7, 15.6 Hz, 1 H), 2.13 (br. s., 1 H). ^{13}C NMR (75 MHz, $CDCl_3$) δ 172.0, 159.0, 140.29, 140.26, 128.6 (2C), 128.1, 127.8, 127.3, 127.1, 125.28, 125.25, 119.8, 119.6, 114.0 (2C), 60.9, 57.0, 55.2, 51.6, 43.3. IR (film); 3333, 3066, 2004, 2953, 2832, 1736, 1611, 1505, 1446, 1255 cm^{-1}. HRMS (EI): Exact mass calcd for $C_{24}H_{23}NO_3$ $[M]^+$: 373.1678. Found: 373.1649.

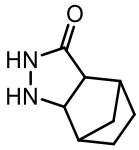

12a. Azomethine imine **9a** (0.298 g, 0.943 mmol) was diluted in MeOH (40 mL), and aqueous NH_2OH (1 mL, 50 wt% in H_2O) was added. The mixture was heated to reflux for 2 h. After cooling to rt, 80 mL H_2O was added and the mixture wascooled in an ice bath to precipitate the fluorenone oxime. The mixture was filtered, rinsing with H_2O. If precipitate appeared in the filtrate, more H_2O was added and the mixture was filtered again. The filtrate was concentrated in vacuo to give the product as a white solid (0.143 g, 99% yield). ^{1}H NMR (400 MHz, DMSO-d_6) δ 8.91 (br. s., 1 H), 5.32 (br. s., 1 H), 2.41 (d, *J* = 8.1 Hz, 1 H), 2.34 (d, *J* = 4.0 Hz, 1 H), 2.13 (d, *J* = 4.4 Hz, 1 H),

1.54 - 1.29 (m, 3 H), 1.22 - 1.12 (m, 1 H), 1.09 (td, J = 1.4, 10.1 Hz, 1 H), 1.07 - 0.97 (m, 1 H). ^{13}C NMR (101 MHz, DMSO-d_6) δ 173.6, 61.4, 50.4, 43.6, 38.6, 32.6, 27.2, 24.5. IR (ATR): 3681, 3389, 2977, 1885, 1395 cm^{-1}. HRMS (EI): Exact mass calcd for $C_8H_{12}N_2O$ $[M]^+$: 152.09496. Found: 152.09580.

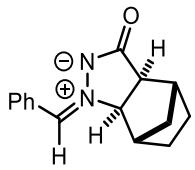

21. Azomethine imine **9a** (0.314 g, 1.00 mmol) was diluted in MeOH (10 mL), and aqueous NH_2OH (0.14 g, 1.0 mmol, 50 wt% in H_2O) was added. The mixture was heated to reflux for 24 h. After cooling to rt, 10 mL H_2O was added and the mixture was cooled in an ice bath to precipitate the fluorenone oxime. The mixture was filtered, rinsing with H_2O. The filtrate was concentrated in vacuo to remove aqueous hydroxylamine. The crude mixture was then diluted in MeOH (10 mL), benzaldehyde (0.108 g, 1.02 mmol) was added, and the mixture stirred at room temperature for 16 h, followed by evaporation under reduced pressure. product was isolated by silica gel chromatography (CH_2Cl_2 then 0-10% MeOH in EtOAc) as a white solid (0.144 g, 60% yield over two steps). Spectral data is in agreement with the literature.[2] See the experimental section of Chapter 3 for the kinetic resolution of **21** and characterization of enantioenriched product.

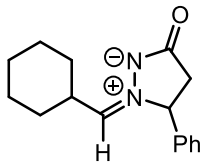

22. Synthesized according to known procedure from Downey *et al.* with minor modifications.[6] Pyrazolidinone **12b** (0.090 g, 0.56 mmol) and cyclohexanecarbaldehyde (0.086 g, 0.77 mmol, 1.4 equiv) were combined in MeOH and stirred at 60 °C for 1 h then room temperature for 16 h, until

consumption of **12b** by TLC (EtOAc, $KMnO_4$ stain). The mixture was concentrated in vacuo and the product isolated by trituration from EtOAc. White solid (1st crop: 0.045 g, 32%). Yield is not optimized. Spectral data is in agreement with the literature.[6] ^{1}H NMR (300 MHz, $CDCl_3$) δ 7.52 - 7.32 (m, 5 H), 6.10 (d, *J* = 7.8 Hz, 1 H), 5.33 (dd, *J* = 5.8, 10.2 Hz, 1 H), 5.01 - 4.77 (m, 1 H), 3.26 (dd, *J* = 10.0, 16.9 Hz, 1 H), 3.21 - 3.08 (m, 1 H), 2.94 - 2.74 (m, 2 H), 1.95 - 1.79 (m, 2 H), 1.74 - 1.58 (m, 2 H), 1.44 - 1.26 (m, 2 H), 1.22 - 1.09 (m, 1 H), 1.09 - 0.96 (m, 1 H). ^{13}C NMR (75 MHz, $CDCl_3$) δ 181.7, 138.4, 129.9, 129.8, 129.1, 128.8, 126.8, 72.5, 62.2, 40.1, 38.3, 38.1, 28.7, 28.2, 25.7, 25.0. IR (ATR) 3122, 2967, 2874, 1686, 1612 cm^{-1}.

General Procedure 2E: Aminocarbyonylation of Enol Ethers[22]

To an oven dried vial was added the hydrazone **6a** (1.0 - 1.5 equiv), $PhCF_3$ (0.1 M), and the enol ether (1.0-2.0 equiv). For some reactions Et_3N (3 mol%) was added. The vial was then sealed and purged with argon for one minute. The reaction mixture was heated for 3 hours at 70-100 °C. All reactions were performed using conventional oil baths, unless otherwise noted. The reaction mixture was cooled to ambient temperature and concentrated under reduced pressure. The crude mixture was purified by column chromatography over silica gel.

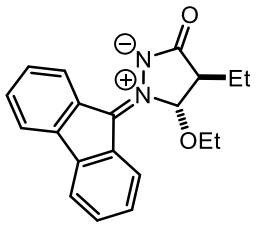

16f. Synthesized according to general procedure 2E from **6a** (0.314 g, 1.00 mmol, 1 equiv) and 2-butenyl methyl ether (0.26 mL, 2.00 mmol, 2 equiv) in $PhCF_3$ (10 mL). The reaction mixture was heated for 2 h at 100 °C. The crude mixture was purified by flash chromatography (1:3 EtOAc/CH_2Cl_2 then 1:9 MeOH/EtOAc). The desired product was obtained as a bright yellow solid

(0.224 g, 70% isolated yield, mixture of 1:16 *syn/anti*). TLC R_f = 0.35 in EtOAc. ^{1}H NMR (*anti* isomer, 400 MHz, $CDCl_3$) δ 9.01 (d, *J* = 7.5 Hz, 1 H), 7.92 (d, *J* = 8.0 Hz, 5 H), 7.64 (d, *J* = 7.4 Hz, 5 H), 7.67 (d, *J* = 7.4 Hz, 5 H), 7.49 - 7.41 (m, 11 H), 7.34 (td, *J* = 7.1, 12.5 Hz, 6 H), 7.35 (td, *J* = 8.2, 12.5 Hz, 6 H), 6.19 (d, *J* = 1.7 Hz, 4 H), 3.81 - 3.66 (m, 5 H), 3.44 (qd, *J* = 7.0, 8.9 Hz, 5 H), 2.87 (ddd, *J* = 1.8, 4.9, 8.6 Hz, 5 H), 2.13 - 1.92 (m, 4 H), 1.87 - 1.61 (m, 5 H), 1.15 (t, *J* = 7.0 Hz, 14 H), 1.09 (t, *J* = 7.4 Hz, 16 H). ^{13}C NMR (*anti* isomer, 100 MHz, $CDCl_3$) δ 184.5, 141.8, 141.5, 140.5, 132.4, 131.6, 131.5, 131.4, 129.8, 129.1, 128.4, 126.8, 120.7, 119.8, 99.1, 59.8, 45.7, 23.6, 14.8, 11.4. IR (film): 2968, 2840, 1670, 1607, 1545, 1450, 1271, 1202 cm^{-1}. HRMS (EI): Exact mass calcd for $C_{20}H_{20}N_2O_2$ $[M]^+$: 320.1525. Found: 320.1501.

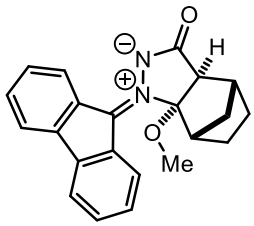

16j. Synthesized according to general procedure 2E from **6a** (0.314 g, 1.00 mmol, 1 equiv) and 2-methoxybicyclo[2.2.1]hept-2-ene (0.248 g, 2.00 mmol, 2 equiv) in $PhCF_3$ (10 mL). The reaction mixture was heated for 1 h at 100 °C. The crude mixture was purified by flash chromatography (1:3 EtOAc/CH_2Cl_2 then 1:9 MeOH/EtOAc). The desired product was obtained as a bright yellow solid (0.336 g, 98% isolated yield). TLC R_f = 0.1 in Et_2O. ^{1}H NMR (400 MHz, $CDCl_3$) δ 9.17 (d, *J* = 7.8 Hz, 1 H), 8.32 (d, *J* = 8.0 Hz, 1 H), 7.70 - 7.51 (m, 2 H), 7.42 (ddd, *J* = 1.1, 7.5, 7.5 Hz, 1 H), 7.38 (ddd, *J* = 0.9, 7.5, 7.5 Hz, 1 H), 7.32 (ddd, *J* = 1.1, 7.5, 7.5 Hz, 1 H), 7.28 - 7.22 (ddd, *J* = 1.1, 7.5, 7.5 Hz, 1 H), 3.35 (s, 3 H), 3.26 (d, *J* = 3.4 Hz, 1 H), 2.82 (d, *J* = 4.0 Hz, 1 H), 2.67 (d, *J* = 2.1 Hz, 1 H), 2.15 - 1.93 (m, 1 H), 1.87 - 1.69 (m, 1 H), 1.68 - 1.42 (m, 3 H), 1.25 (m, 1H). ^{13}C NMR (100 MHz, $CDCl_3$) δ 183.5, 142.2, 140.7, 140.2, 132.5, 132.3, 132.2, 131.1, 129.6, 129.1, 128.8, 128.0, 120.3, 119.4, 115.4, 53.5, 51.3, 43.8, 40.9, 34.4, 27.4, 21.8. IR (film): 2955,

1665, 1647, 1605, 1514, 1448, 1339, 1281, 1242 cm^{-1}. HRMS (EI): Exact mass calcd for $C_{22}H_{20}N_2O_2$ $[M]^+$: 344.1525. Found: 344.1545.

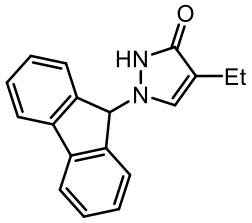

17h. To a mixture of azomethine imine **16f** (0.160 g, 0.500 mmol) in MeOH (0.05 M) was added sodium borohydride (0.080 g, 0.21 mmol). The mixture was stirred at room temperature for 4 hours, then quenched with aq. NH_4Cl and extracted with $CHCl_3$ (3 x 5 mL). The combined organic layers were washed with brine, dried with Na_2SO_4, filtered and concentrated in vacuo. The product was isolated by flash chromatography (10% Et_2O, 90% CH_2Cl_2) to give a white solid (0.110 g, 80%). TLC R_f = 0.3 (10% Et_2O, 90% CH_2Cl_2). ^1H NMR (400 MHz, $CDCl_3$) δ 7.73 (d, *J* = 7.5 Hz, 2 H), 7.65 - 7.51 (m, 2 H), 7.43 (t, *J* = 7.3 Hz, 2 H), 7.37 - 7.26 (m, 2 H), 6.59 (s, 1 H), 6.16 (s, 1 H), 2.28 (q, *J* = 7.6 Hz, 2 H), 1.04 (t, *J* = 7.5 Hz, 3 H). ^{13}C NMR (100 MHz, $CDCl_3$) δ 160.4, 142.0, 140.5, 129.3, 127.9, 126.9, 125.5, 120.2, 108.7, 65.5, 15.7, 14.0. IR (film); 2929, 1724, 1602, 1526, 1448, 1300 cm^{-1}. HRMS (EI): Exact mass calcd for $C_{18}H_{16}N_2O$ $[M]^+$: 276.1263. Found: 276.1253.

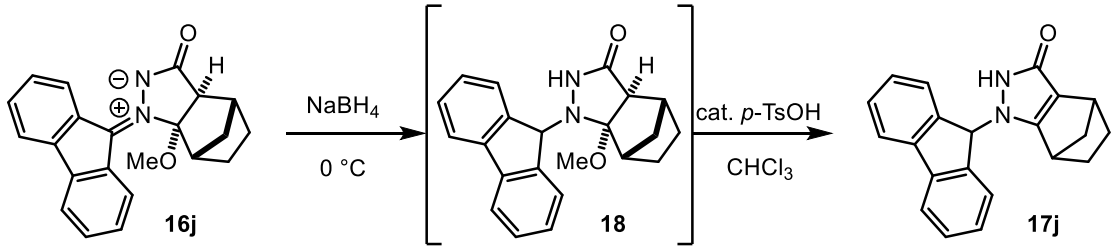

17j. A mixture of the azomethine imine **16f** (0.0758 g, 0.220 mmol) in methanol (0.05 M) was cooled to 0 °C and $NaBH_4$ (0.0120 g, 0.317 mmol, 1.4 equiv) was added. The mixture was stirred at 0 °C for 1 h, then quenched with aq. NH_4Cl and extracted with $CHCl_3$ (3 x 5 mL). Catalytic *p*-

TsOH (0.0040 g, 0.021 mmol) was added to the combined organic layers, and the mixture stirred at 60 °C for 3 h to complete the aromatization. The mixture was cooled to rt and partitioned with water. The organic layer was washed with brine, dried with Na_2SO_4, filtered and concentrated in vacuo. The product was purified by trituration in EtOAc to give a white solid (0.0501 g, 72%). TLC R_f = 0.45 in Et_2O. ^1H NMR (400 MHz, $CDCl_3$) δ 7.76 - 7.71 (m, 2 H), 7.65 (d, *J* = 7.6 Hz, 1 H), 7.57 (d, *J* = 7.4 Hz, 1 H), 7.47 - 7.40 (m, 2 H), 7.35 - 7.26 (m, 2 H), 6.12 (s, 1 H), 3.24 - 3.20 (m, 1 H), 2.03 - 1.98 (m, 1 H), 1.69 - 1.56 (m, 2 H), 1.39 - 1.30 (m, 1 H), 1.22-1.17 (m, 1 H), 1.13 - 1.05 (m, 1 H), 0.56 - 0.47 (m, 1 H). ^{13}C NMR (75 MHz, $CDCl_3$) δ 155.6, 155.4, 142.9, 142.1, 140.7, 140.5, 129.4, 129.3, 128.2, 127.9, 125.7, 125.6, 120.2, 120.2, 114.6, 65.0, 51.6, 40.0, 37.4, 28.1, 26.2. IR (film): 2962, 2635, 1526, 1452, 1284, 1261 cm^{-1}. HRMS (EI): Exact mass calcd for $C_{21}H_{18}N_2O$ $[M]^+$: 314.1419. Found: 314.1422.

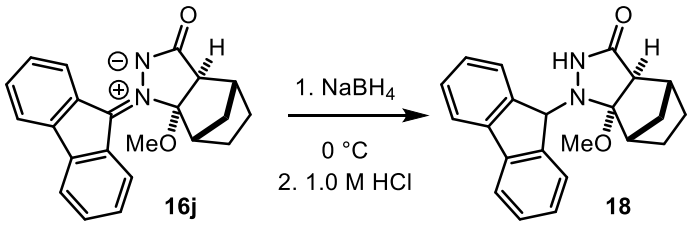

18. A mixture of the azomethine imine **16j** (0.0191 g, 0.0554 mmol) in methanol (1 mL) was cooled to 0 °C and $NaBH_4$ (0.0120 g, 0.317 mmol, 1.4 equiv) was added. The mixture was stirred at 0 °C for 1 h. While stirring at 0 °C, one drop of aq. HCl (1.0 M) was added and the mixture stirred for 5 min, followed by addition of 1 mL H_2O. The product was extracted with CH_2Cl_2 (3 x 5 mL), and concentrated in vacuo to give the product as a white solid containing 5 wt% Et_2O (0.0175 g, 92% corrected yield). This experiment confirmed that the reduced product is an intermediate on the pathway to the pyrazolone. ^1H NMR (400 MHz, benzene-d_6) δ 7.93 - 7.77 (m, 1 H), 7.65 - 7.53 (m, 1 H), 7.51 (dd, *J* = 6.4, 6.5 Hz, 2 H), 7.25 - 7.17 (m, 3 H), 7.15 - 7.08 (m, 1

H), 5.03 (br. s, 1 H), 2.99 (s, 3 H), 2.64 - 2.54 (m, 1 H), 2.47 - 2.19 (m, 2 H), 1.83 (d, *J* = 11.7 Hz, 1 H), 1.77 - 1.56 (m, 1 H), 1.43 - 1.16 (m, 1 H), 1.11 - 0.92 (m, 2 H), 0.86 (d, *J* = 10.1 Hz, 1 H).

Table 6.1. Attempts toward alkyne aminocarbonylation.[a]

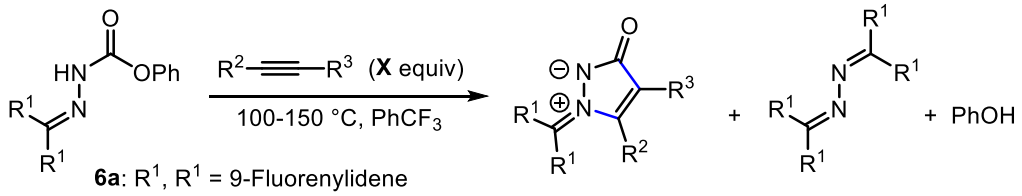

Entry	R^1	R^2	R^3	X (equiv)	T (°C)	t (h)	Yield (%)[b]		
							24	**AZ**	PhOH
1	**1a**	C_4H_9	H	10	100	3	-	35	<1%
2	**1a**	C_4H_9	H	40	120	0.5	-	6	54
3	**1a**	C_4H_9	H	40	150	0.5	(4)[c]	17	64
4	**1a**	C_6H_{13}	H	10	150	3	-	14	quant
5	**1a**	Ph	H	10	150	3	-	18	quant
6	**1a**	C_6H_{13}	Cu(I)	10	100	3	-	nd	nd
7	**1b**	C_4H_9	H	10	150	1	-	nd	61
8	**1b**	Ph	H	10	150	1	-	nd	74

a) Conditions: Hydrazone **1a** or **1b** (0.10-0.25 mmol, 1 equiv) and alkyne (10-40 equiv), and $PhCF_3$ (1-2 mL) were combined in a vial and purged with nitrogen. The reaction was heated by microwave irradiation. b) NMR yields are reported, determined using 1,3,5-trimethoxybenzene internal standard. nd = not determined. c) Possible product indicated by doublet at 8.92 ppm, isolation was unsuccessful.

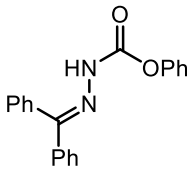

4b. Synthesized according to a known procedure, spectral data are in agreement with the literature.[1]

6.2.4. Mechanistic Investigations

Equilibration Study:

Measurement of K_{eq}: Hydrazone **1c** was taken up in a known volume of toluene-d_8 (0.023 M), with 1,3,5-trimethoxybenzene internal standard to measure in situ concentration of components. Slight variations in overall concentration are observed. Consistent concentrations of hydrazone and PhOH were observed between 27.5 and 35 min, the average of concentration of each component over this time is used as the equilibrium concentration.

Table 6.2. Concentrations of components from UDEFT NMR experiment[a]

Spectrum	t (min)	**1c** (M)	PhOH (M)	**19** (M)	Sum (M)
0	0	0.0198	0	0	0.0198
1	0.5	0.0186	0.0013	0.0006	0.0205
3	5	0.0144	0.0055	0.0055	0.0254
5	10	0.0117	0.0079	0.0037	0.0233
6	12.5	0.0113	0.0087	0.0027	0.0227
8	17.5	0.0122	0.0095	0.0038	0.0255
10	22.5	0.0098	0.0103	0.0023	0.0224
12	27.5	0.0090	0.0105	0.0019	0.0214
14	32.5	0.0093	0.0103	0.0022	0.0218
15	35	0.0090	0.0110	0.0019	0.0219
				Average:	0.0228

a) U-DEFT experiment on Bruker Avance II 300 MHz spectrometer. Spectrum 0 (t=0) at 50 °C, Spectra 1-15 at 90 °C.

Amount of by-product formed = [**19**] = 0.020 M = x

For **1c**:
Initial concentration $[\mathbf{1c}]_1$ = 0.0198 M
Concentration after loss to by-product **19** = $[\mathbf{1c}]_2$ = 0.0198 M – 2x = 0.016 M

Equilibrium [**1c**] = 0.009 M (average value from 27.5 min - 35 min)

For PhOH:
Initial concentration $[PhOH]_1$ = 0 M
Concentration after formation of by-product **19** = $[PhOH]_2$ = + 2x = 0.040 M

Equilibrium [PhOH] = 0.011 M (average value from 27.5 min - 35 min)

Table 6.3. Determination of K_{eq}[a]

t (min)	**1c** (M)	PhOH (M)	Isocyanate (M)
[Initial]$_2$	0.016	0.004	0
[Change]	– 0.007	+ 0.007	+ 0.007
[Equilibrium]	0.009	0.011	0.007

Equilibrium [Isocyanate] = 0.007 M

a[**1c**] ⇆ b[PhOH] + c[Isocyanate]

a = 1
b = 1.2
c = 0.8

$K_{eq} = [PhOH]^b[Isocyanate]^c/[\mathbf{1c}]^a$
$K_{eq} = [0.011]^{1.2}[0.007]^{0.8}/[0.009] = 0.009 = 9 \times 10^{-3}$

IR Study:

Bruker ALPHA-T Liquid Measurement FTIR-spectrometer with Flow Cell (100 um, ZnSe).

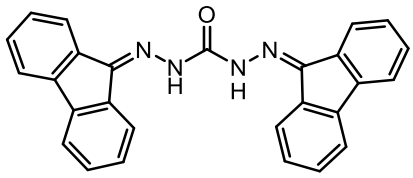

19. Isolated as a precipitate from an aminocarbonylation reaction of **6a** (0.500 g, 1.59 mmol) and vinyl cyclohexane (1.09 mL, 7.95 mmol, 5 equiv). Pale yellow solid (0.053 g, 8% yield) with low solubility in common organic solvents. ^{1}H NMR (400 MHz, DMSO-d_6) δ 11.08 (br. s, 2 H), 8.35 (d, J = 7.9 Hz, 2 H), 7.98 (d, J = 7.3 Hz, 2 H), 7.89 (dd, J = 2.6, 7.1 Hz, 4 H), 7.59 (appt, J = 7.6 Hz, 2 H), 7.56 - 7.28 (m, 6 H). ^{13}C NMR (400 MHz, DEPT-135, DMSO-d_6) δ 135.4 (CH), 129.5 (CH), 124.0 (CH), 121.2 (CH). IR (ATR) 3414, 3376, 3334, 1791, 1746, 1539, 1227 cm^{-1}. HRMS (ESI): Exact mass calcd for $C_{27}H_{18}N_4O$ $[M+Na]^+$: 437.1378. Found: 437.1402.

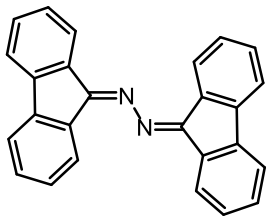

1,2-Di(9H-fluoren-9-ylidene)hydrazine. Isolated as a product when heating **6a** in $PhCF_3$ at 100 °C for 1 h. Also observed in crude mixtures after attempted alkyne aminocarbonylation reactions. Dark red crystalline solid. Spectral data is in agreement with the literature.[7] ^{1}H NMR (300 MHz, $CDCl_3$) δ 8.14 (d, J = 7.6 Hz, 2 H), 8.06 (d, J = 6.7 Hz, 2 H), 7.66 (d, J = 7.5 Hz, 4 H), 7.54 - 7.36 (m, 6 H), 7.25 - 7.19 (m, 2 H). ^{13}C NMR (101 MHz, $CDCl_3$) δ 157.4, 155.0, 142.4, 141.4, 136.7, 131.5, 131.1, 130.0, 128.4, 128.4, 123.1, 120.3, 120.2.

6.2.5. Carbonyl Catalysis

Background Reactions (Scheme 2.20): *O*-Ph Carbazate (0.5 mmol, 1 equiv) and alkene (norbornene or styrene, 0.5 mmol, 1 equiv) were combined with $PhCF_3$ (2 mL) in a microwave vial, purged with Argon, and heated by microwave irradiation to 100 or 150 °C for 80 minutes. Mixture concentrated in vacuo and evaluated by ^{1}H NMR (DMSO-*d6*) with 1,3,5-trimethoxybenzene internal standard. The aminocarbonylation product was not observed.

Turn-over step 3 test (Scheme 2.22): Azomethine imine (**21** or **22**, 0.2 equiv) and *O*-Ph carbazate (1 equiv) were combined with $PhCF_3$ (2 mL) in a microwave vial, purged with Argon, and heated by microwave irradiation to 100 °C for 80 min (**22**) or 120 °C for 60 min (**21**). Mixture concentrated in vacuo and evaluated by ^{1}H NMR (DMSO-d_6) with 1,3,5-trimethoxybenzene internal standard. **22**: No product was observed. **21**: ^{1}H NMR of the crude mixture shows 100% yield of **12b**, 39% yield of **20b**, 42% yield PhOH, and 4 equivalents of remaining *O*-Ph carbazate. In a reaction without added *O*-Ph carbazate, product **12b** was not observed.

Catalytic reaction attempts (Scheme 2.23a): *O*-Ph Carbazate (0.75 mmol, 1.5 equiv) and norbornene (0.5 mmol, 1 equiv) and hydrazone catalyst (**6a** or **20f-g**, 0.1 mmol, 0.2 equiv) were combined with $PhCF_3$ (2 mL) in a microwave vial, purged with Argon, and heated by microwave irradiation to 100 or 150 °C for 80 minutes. Mixture concentrated in vacuo and evaluated by ^{1}H NMR (DMSO-d_6) with 1,3,5-trimethoxybenzene internal standard. The aminocarbonylation product was not observed.

Test for aminocarbonylation reactivity (Scheme 2.23b): 12b (0.0241 g, 0.0980 mmol, 1 equiv) was combined with norbornene (0.045 g, 0.48 mmol, 5 equiv) in a vial with $PhCF_3$, heated at 100 °C for 80 minutes. Mixture concentrated in vacuo and evaluated by ^{1}H NMR (DMSO-*d6*) with

1,3,5-trimethoxybenzene internal standard. The aminocarbonylation product (**23**) was not observed. The reaction was repeated at 120 °C and also showed no product.

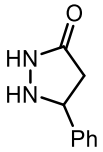

12b. Synthesized following a known procedure, spectral data was in agreement with the literature.[8] ^{1}H NMR (400 MHz, $CDCl_3$) δ 7.49 - 7.31 (m, 5 H), 4.99 - 4.74 (m, 1 H), 2.93 - 2.64 (m, 2 H).

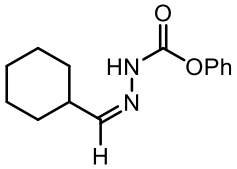

20b. Diphenyl carbonate (2.20 g, 10 mmol, 1 equiv) was diluted in MeOH (20 mL) and cooled in an ice bath. Hydrazine hydrate (50-60 wt% in H_2O, 0.5 mL, 10 mmol, 1 equiv) was added slowly, and the mixture stirred at around 0 °C for 30 min until all carbonate was consumed, as judged by TLC. The cyclohexanecarbaldehyde (1.20 g, 11 mmol, 1.1 equiv) was then added and the mixture warmed to rt, then heated at reflux for 16 h. The mixture was concentrated in vacuo, and the product isolated by recrystallization of the crude residue from hexane/Et_2O. The product was obtained as a white solid (1.22 g, 49%). The yield was not optimized. Spectral data is in agreement with that which was previously reported in a patent.[9] TLC R_f= 0.25 in 1:1 Hexane/Et_2O. ^{1}H NMR (400 MHz, $CDCl_3$) δ 7.95 (br. s, 1 H), 7.54 - 7.29 (m, 2 H), 7.25 - 7.06 (m, 3 H), 2.48 - 2.30 (m, 1 H), 1.93 - 1.73 (m, 4 H), 1.69 (d, *J* = 12.4 Hz, 1 H), 1.40 - 1.13 (m, 5 H). ^{13}C NMR (75 MHz, $CDCl_3$) δ 154.2, 150.8, 143.2, 129.5, 125.7, 121.7 40.8, 30.3, 25.9, 25.5. ^{13}C NMR (100 MHz, DMSO-*d6*) δ 153.3, 150.5, 142.9, 129.4, 125.3, 121.8, 29.7, 25.4, 25.0.

6.2.6. X-ray Crystallographic Information

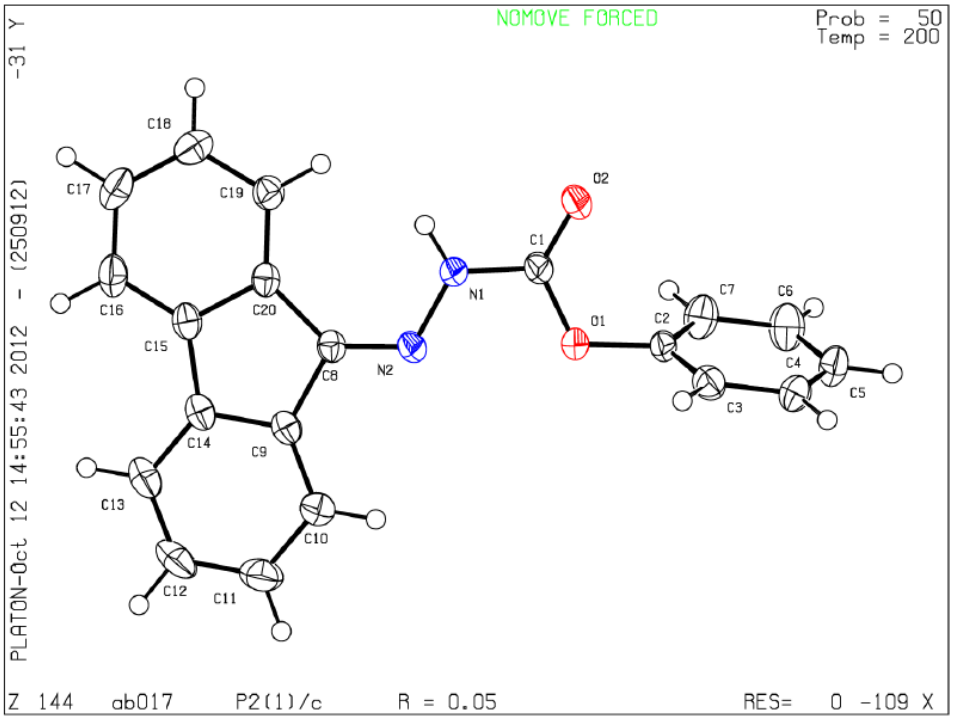

Datablock: ab017

Bond precision: C-C = 0.0020 A Wavelength=0.71073

Cell: a=9.2930(2) b=17.2480(5) c=9.7290(2)
alpha=90 beta=94.173(1) gamma=90
Temperature: 200 K

	Calculated	Reported
Volume	1555.29(6)	1555.29(6)
Space group	P 21/c	P2(1)/c
Hall group	-P 2ybc	?
Moiety formula	C20 H14 N2 O2	?
Sum formula	C20 H14 N2 O2	C20 H14 N2 O2
Mr	314.33	314.33
Dx,g cm-3	1.342	1.342
Z	4	4
Mu (mm-1)	0.088	0.088
F000	656.0	656.0
F000'	656.28	
h,k,lmax	12,23,12	12,23,12
Nref	3878	3821
Tmin,Tmax	0.983,0.988	0.983,0.988
Tmin'	0.983	

Correction method= MULTI-SCAN

Data completeness= 0.985 Theta(max)= 28.330

R(reflections)= 0.0499(2780) wR2(reflections)= 0.1261(3821)

S = 1.056 Npar= 217

Figure 6.1. Single crystal X-ray ellipsoid plot and acquisition information for ***6a****.*

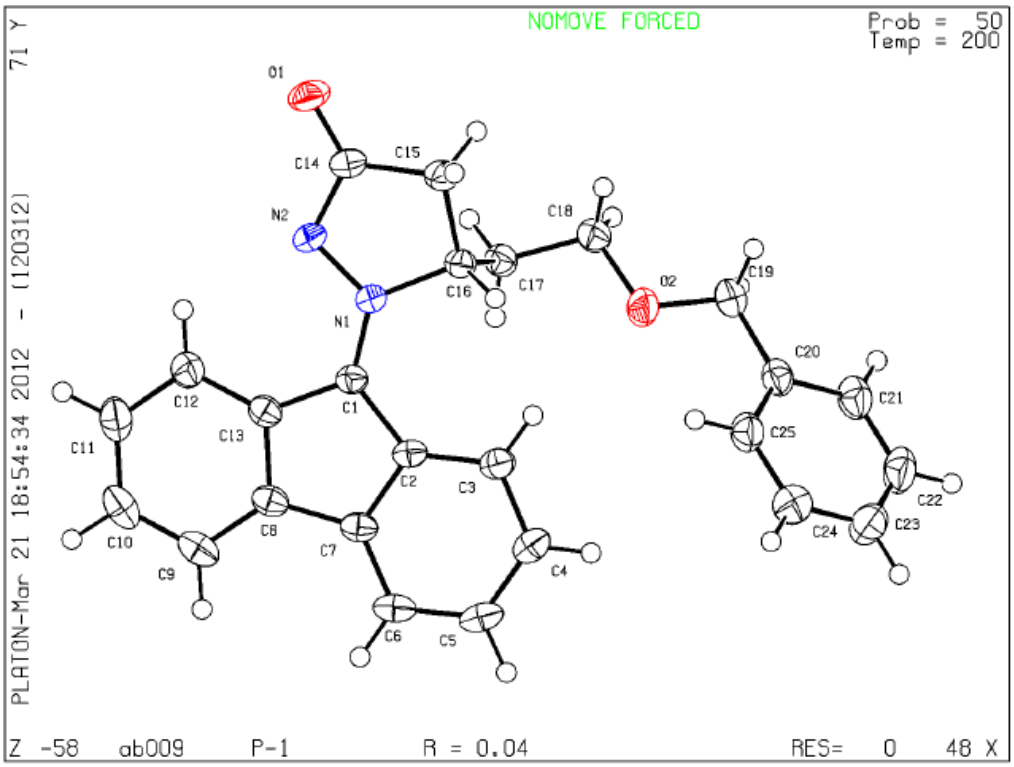

Datablock: ab009

```
Bond precision:  C-C = 0.0016 A          Wavelength=0.71073

Cell:          a=7.8494(2)        b=11.1800(3)     c=12.5458(3)
               alpha=106.824(1)   beta=98.571(1)   gamma=109.145(1)
Temperature:   200 K

                 Calculated                Reported
Volume           958.65(4)                 958.65(4)
Space group      P -1                      P-1
Hall group       -P 1                      ?
Moiety formula   C25 H22 N2 O2             ?
Sum formula      C25 H22 N2 O2             C25 H22 N2 O2
Mr               382.45                    382.45
Dx,g cm-3        1.325                     1.325
Z                2                         2
Mu (mm-1)        0.085                     0.085
F000             404.0                     404.0
F000'            404.17
h,k,lmax         10,14,16                  10,14,16
Nref             4771                      4631
Tmin,Tmax        0.988,0.990               0.988,0.990
Tmin'            0.988

Correction method= MULTI-SCAN

Data completeness= 0.971          Theta(max)= 28.300

R(reflections)= 0.0379( 3841)     wR2(reflections)= 0.1047( 4631)

S = 1.045                 Npar= 262
```

Figure 6.2. Single crystal X-ray ellipsoid plot and acquisition information for ***9d****.*

6.3. Kinetic Resolution of Azomethine Imines by Reduction

The following section is an abridged version of the supporting information for the article presented in Chapter 3,[23] including compound characterization and optimization tables. Additional unpublished optimization data (Table 6.7) and reactions of acyclic azomethine imines (Table 6.8 & Table 6.9) are also included. The supplementary HPLC chromatograms are provided in Appendix II.

Synthesis of Racemic Pyrazolidinones (2a-n)

Racemic pyrazolidinones for HPLC analysis were synthesized by reduction of azomethine imines following a known procedure.[2] The azomethine imines were dissolved in methanol, followed by the addition of excess $NaBH_4$ at room temperature. After 10 minutes, the reaction was quenched with aqueous ammonium chloride and extracted with CH_2Cl_2. The combined organic layers were washed many times with water, then brine, then dried with Na_2SO_4. Concentration in vacuo gave the unpurified product, used directly for HPLC analysis.

General Procedure 3A: for the Kinetic Resolution of Azomethine Imines[23]

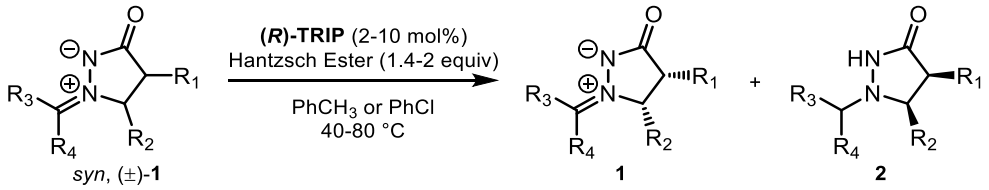

Azomethine imine and Hantzsch ester[10] (1.4-2.0 equiv) and (*R*)-TRIP phosphoric acid[11] (2-10 mol%) were combined in a flask. The flask was purged with argon, then solvent ($PhCH_3$ or PhCl, 0.01 to 0.04 M) was added. The mixture was heated at 40-80°C for 6-72 hours. The reaction was cooled to room temperature and the solvent evaporated under reduced pressure. The crude mixture was then passed through a plug of basic alumina (activated Brockmann I), eluting with 10% *i*-

PrOH/ 90% CH_2Cl_2. The crude mixture was then purified by silica gel chromatography or prep TLC. The enantiomeric excess of the recovered azomethine imine **1** and pyrazolidinone product **2** was determined by chiral HPLC (ChiralPak AD-H). The HPLC data of each enantioenriched compound was compared to the corresponding racemate. Conversion (*C*) was determined by analysis of the ^{1}H NMR spectrum of the crude mixture. Selectivity factor ($s = k_{fast}/k_{slow}$) was determined by the Equation 6.1.[12] The specific rotation $[\alpha]_D^{20}$ was calculated using Equation 6.2 with the following parameters: α = optical rotation, c = g/100 mL, l = 0.1 dm

$$s = \frac{ln[(1-C)(1-ee(azo)\,)]}{ln\big[(1-C)\big(1+ee(azo)\big)\big]} \tag{6.1}$$

$$[\alpha]_D^{20} = \frac{\alpha \times 100}{l \times c} \tag{6.2}$$

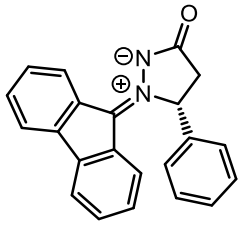

Following general procedure 3A, using azomethine imine (±)-**1a** (32.2 mg, 0.0993 mmol), Hantzsch ester (35.2 mg, 0.139 mmol, 1.4 equiv), and (*R*)-TRIP (3.8 mg, 5 mol%) in toluene (4 mL). The reaction mixture heated was at 60°C for 6 hours. The ^{1}H NMR of the crude mixture showed 54% conversion.

Recovered **1a**: 14.4 mg (45% yield) yellow solid, 96% ee. TLC R_f = 0.27 (EtOAc).

$[\alpha]^{20}_{D}$ +586° (*c* 0.43, CH_2Cl_2). Chiral HPLC: ChiralPak AD-H, *i*-PrOH/hexane = 10/90, 1.0 mL/min, 254 nm, t_{major} = 39.5 min, t_{minor} = 45.7 min.

^{1}H NMR (400 MHz, $CDCl_3$) δ 9.15 (d, *J* = 7.8 Hz, 1 H), 7.60 (dd, *J* = 3.4, 7.3 Hz, 2 H), 7.55 - 7.44 (m, 1 H), 7.44 - 7.27 (m, 8 H), 7.15 - 6.97 (m, 1 H), 6.39 (dd, *J* = 1.2, 9.3 Hz, 1 H), 3.56 (dd, *J* = 9.4, 16.4 Hz, 1 H), 2.81 (dd, *J* = 1.9, 16.4 Hz, 1 H). ^{13}C NMR (100 MHz, $CDCl_3$) δ 182.5, 142.3, 142.1, 140.6, 137.9, 132.7, 132.0, 131.8, 131.5, 130.0, 129.5, 129.4, 128.9, 128.2, 126.2, 124.8, 121.0, 119.9, 72.3, 40.9.

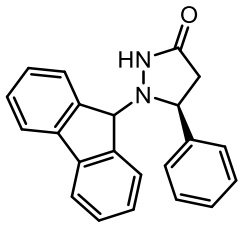

Pyrazolidinone **2a**: 13.2 mg (41% yield) white solid, 73% ee. TLC R_f = 0.38 (Et_2O).

$[\alpha]^{20}_{D}$ -76° (*c* 0.35, CH_2Cl_2). Chiral HPLC: ChiralPak AD-H, *i*-PrOH/hexane = 10/90, 1.0 mL/min, 210 nm, t_{major} = 11.1 min, t_{minor} = 17.2 min.

^{1}H NMR (400 MHz, $CDCl_3$) δ 8.37 (br. s, 1 H), 7.86 (d, *J* = 7.4 Hz, 1 H), 7.82 - 7.67 (m, 2 H), 7.56 - 7.43 (m, 2 H), 7.43 - 7.30 (m, 2 H), 7.26 - 7.14 (m, 4 H), 7.13 - 7.03 (m, 2 H), 5.14 (s, 1 H), 3.84 (dd, *J* = 3.9, 9.6 Hz, 1 H), 2.69 (dd, *J* = 9.7, 17.1 Hz, 1 H), 2.27 (dd, *J* = 3.9, 17.1 Hz, 1 H). ^{13}C NMR (100 MHz, $CDCl_3$) δ 174.7, 142.3, 142.0, 141.8, 141.3, 140.9, 129.4, 129.3, 128.6, 128.1, 127.7, 127.6, 126.7, 126.6, 126.4, 120.4, 120.0, 69.9, 60.3, 39.4. IR (neat); 3180, 3064, 2931, 2854, 1686, 1605, 1495, 1450, 1419, 1308 cm^{-1}. HRMS (EI): Exact mass calcd for $C_{22}H_{18}N_2O$ $[M]^+$: 326.14191 Found: 326.14079.

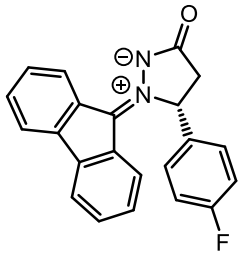

Following general procedure 3A, using azomethine imine (±)-**1b** (34.2 mg, 0.0999 mmol), Hantzsch ester (35.6 mg, 0.141 mmol, 1.4 equiv), and (*R*)-TRIP (3.9 mg, 5 mol%) in toluene (4 mL). The reaction mixture was heated at 60°C for 6 hours. The ^{1}H NMR of the crude mixture showed 58% conversion.

Recovered **1b**: 10.7 mg (32% yield) yellow solid, 96% ee. TLC R_f = 0.25 (EtOAc).

$[\alpha]^{20}_D$ +622° (*c* 0.24, $CHCl_3$). Azomethine imine was reduced to pyrazolidinone with sodium borohydride before analysis by chiral HPLC: ChiralPak AD-H, *i*-PrOH/hexane = 10/90, 1.0 mL/min, 254 nm, t_{minor} = 10.3 min, t_{major} = 12.3 min.

^{1}H NMR (400 MHz, $CDCl_3$) δ 9.10 (d, *J* = 7.6 Hz, 1 H), 7.57 (d, *J* = 7.3 Hz, 2 H), 7.51 - 7.34 (m, 2 H), 7.34 - 7.20 (m, 4 H), 7.13 - 6.96 (m, 3 H), 6.35 (d, *J* = 8.5 Hz, 1 H), 3.49 (dd, *J* = 9.3, 16.3 Hz, 1 H), 2.70 (dd, *J* = 1.7, 16.2 Hz, 1 H). ^{13}C NMR (75 MHz, $CDCl_3$) δ 182.4, 162.6 (d, J_{C-F} =

248.1 Hz), 141.8, 141.2, 140.3, 133.9 (d, $J_{C\text{-}F}$ = 3.3 Hz), 132.4, 131.6 (2C), 131.2, 129.2 (2C), 128.0, 126.7 (d, $J_{C\text{-}F}$ = 8.3 Hz, 2C), 125.9, 120.9, 119.8, 116.9 (d, $J_{C\text{-}F}$ = 22.0 Hz, 2C), 71.6, 40.8.

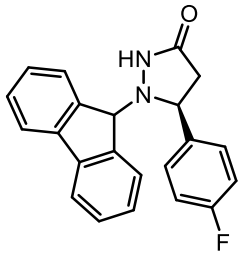

Pyrazolidinone **2b**: 10.9 mg (32% yield) white solid, 76% ee. TLC R_f = 0.29 (Et_2O).

$[\alpha]^{20}_D$ -87.9° (*c* 0.36, CH_2Cl_2). Chiral HPLC: ChiralPak AD-H, *i*-PrOH/hexane = 10/90, 1.0 mL/min, 254 nm, t_{major} = 10.3 min, t_{minor} = 12.3 min.

^{1}H NMR (400 MHz, $CDCl_3$) δ 8.06 (br. s., 1 H), 7.83 (d, *J* = 7.5 Hz, 1 H), 7.76 (d, *J* = 7.5 Hz, 1 H), 7.69 (d, *J* = 7.6 Hz, 1 H), 7.52 - 7.40 (m, 2 H), 7.40 - 7.30 (m, 2 H), 7.20 - 7.12 (m, 1 H), 7.07 - 6.97 (m, 2 H), 6.95 - 6.81 (m, 2 H), 5.11 (s, 1 H), 3.77 (dd, *J* = 3.9, 9.6 Hz, 1 H), 2.66 (dd, *J* = 9.6, 17.1 Hz, 1 H), 2.18 (dd, *J* = 3.9, 17.1 Hz, 1 H). ^{13}C NMR (100 MHz, $CDCl_3$) δ 174.4, 162.1 (d, $J_{C\text{-}F}$ = 246.5 Hz), 141.8, 141.2, 140.9, 138.2 (d, $J_{C\text{-}F}$ = 2.9 Hz), 129.4, 128.1, 128.0, 127.9, 127.7, 126.5, 126.5, 120.3 (d, $J_{C\text{-}F}$ = 36.0 Hz), 115.4 (d, $J_{C\text{-}F}$ = 21.6 Hz), 70.0, 59.6, 39.4. IR (neat); 3167, 3061, 2855, 1681, 1604, 1560, 1508, 1478, 1450, 1346, 1296, 1220 cm^{-1}. HRMS (EI): Exact mass calcd for $C_{22}H_{17}FN_2O$ $[M]^+$: 344.13249. Found: 344.13120.

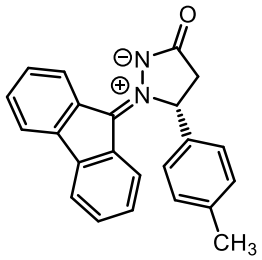

Following general procedure 3A, using azomethine imine (±)-**1c** (58.0 mg, 0.171 mmol), Hantzsch ester (60.8 mg, 0.239 mmol, 1.4 equiv), and (*R*)-TRIP (6.4 mg, 5 mol%) in toluene (4 mL). The

reaction mixture was heated at 60°C for 16 hours. The ^{1}H NMR of the crude mixture showed 57% conversion.

Recovered **1c**: 24.4 mg (42% yield) yellow solid, 95% ee. TLC R_f = 0.20 (EtOAc).

$[\alpha]^{20}_{D}$ +614° (*c* 0.84, CH_2Cl_2). Chiral HPLC: ChiralPak AD-H, *i*-PrOH/hexane = 10/90, 1.0 mL/min, 254 nm, t_{major} = 33.8 min, t_{minor} = 40.8 min.

^{1}H NMR (400 MHz, $CDCl_3$) δ 9.16 (d, *J* = 7.5 Hz, 1 H), 7.61 (dd, *J* = 4.1, 7.2 Hz, 2 H), 7.51 - 7.35 (m, 3 H), 7.34 - 7.28 (m, 1 H), 7.16 (s, 4 H), 7.12 - 7.03 (m, 1 H), 6.33 (dd, *J* = 1.5, 9.2 Hz, 1 H), 3.50 (dd, *J* = 9.3, 16.3 Hz, 1 H), 2.77 (dd, *J* = 1.8, 16.3 Hz, 1 H), 2.30 (s, 3 H). ^{13}C NMR (100 MHz, $CDCl_3$) δ 182.7, 141.9, 141.5, 140.4, 138.8, 135.1, 132.4, 131.9, 131.8, 131.2, 130.5, 129.5, 129.4, 128.1, 126.2, 124.7, 120.9, 119.8, 72.2, 41.0, 21.2. IR (neat); 2922, 2862, 1655, 1605, 1544, 1509, 1474, 1449, 1343, 1266, 1246, 1193, 1118, 1091, 980, 963, 870, 816, 776, 741, 723, 708 cm^{-1}.

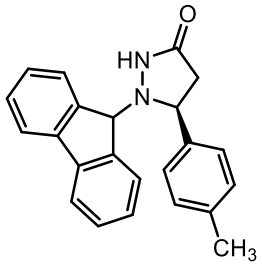

Pyrazolidinone **2c**: 28.0 mg (48% yield) white solid, 74% ee. TLC R_f = 0.28 (Et_2O).

$[\alpha]^{20}_{D}$ -287° (*c* 0.21, CH_2Cl_2). Chiral HPLC: ChiralPak AD-H, *i*-PrOH/hexane = 10/90, 1.0 mL/min, 210 nm, t_{major} = 10.5 min, t_{minor} = 14.7 min.

^{1}H NMR (400 MHz ,$CDCl_3$) δ 7.87 (d, *J* = 7.5 Hz, 1 H), 7.77 (d, *J* = 7.5 Hz, 1 H), 7.71 (d, *J* = 7.5 Hz, 1 H), 7.60 - 7.56 (m, 1 H), 7.53 - 7.44 (m, 1 H), 7.44 - 7.31 (m, 2 H), 7.21 - 7.15 (m, 1 H), 7.06 - 6.85 (m, 4 H), 5.20 (br. s, 1 H), 3.84 (dd, *J* = 4.3, 9.5 Hz, 1 H), 2.65 (dd, *J* = 9.5, 17.2 Hz, 1

H), 2.25 (s, 3 H). ^{13}C NMR (100 MHz, $CDCl_3$) δ 174.9, 142.1, 141.9, 141.3, 141.1, 139.4, 137.3, 129.4, 129.3, 129.2, 128.0, 127.7, 126.7, 126.5, 126.3, 120.4, 120.0, 69.9, 60.1, 39.3, 21.1. HRMS (EI): Exact mass calcd for $C_{23}H_{20}N_2O$ $[M]^+$: 340.15756 Found: 340.15640. IR (neat); 3248, 3054, 2920, 2856, 1674, 1606, 1549, 1505, 1446, 1299, 1281 cm^{-1}

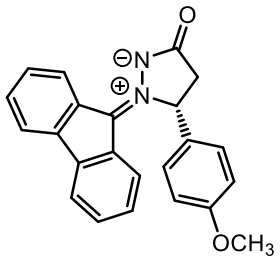

Following general procedure 3A, using azomethine imine (±)-**1d** (34.6 mg, 0.0977 mmol), Hantzsch ester (34.7 mg, 0.137 mmol, 1.4 equiv), and (*R*)-TRIP (3.8 mg, 5 mol%) in toluene (5 mL). The reaction mixture was heated at 60 °C for 16 hours. The ^{1}H NMR of the crude mixture showed 55% conversion.

Recovered **1d**: 16.4 mg (43% yield) yellow solid, 95% ee. TLC R_f = 0.23 in EtOAc.

$[\alpha]^{20}_D$ +395° (*c* 0.53, $CHCl_3$). Chiral HPLC: ChiralPak AD-H, *i*-PrOH/hexane = 10/90, 1.0 mL/min, 254 nm, t_{major} = 50.1 min, t_{minor} = 61.4 min.

^{1}H NMR (400 MHz, $CDCl_3$) δ 9.15 (d, *J* = 7.6 Hz, 1 H), 7.60 (dd, *J* = 3.1, 7.3 Hz, 2 H), 7.46 (dt, *J* = 1.1, 7.4 Hz, 1 H), 7.43 - 7.34 (m, 2 H), 7.30 (t, *J* = 7.4 Hz, 1 H), 7.24 - 7.15 (m, 2 H), 7.12 - 7.03 (m, 1 H), 6.94 - 6.78 (m, 2 H), 6.31 (d, *J* = 7.8 Hz, 1 H), 3.75 (s, 3 H), 3.46 (dd, *J* = 9.2, 16.2 Hz, 1 H), 2.71 (dd, *J* = 1.9, 16.2 Hz, 1 H). ^{13}C NMR (100 MHz, $CDCl_3$) δ 182.8, 159.8, 141.9, 141.1, 140.4, 132.3, 131.9, 131.8, 131.1, 130.1, 129.5, 129.3, 128.1, 126.2, 120.9, 119.8, 115.2, 72.0, 55.4, 41.0.

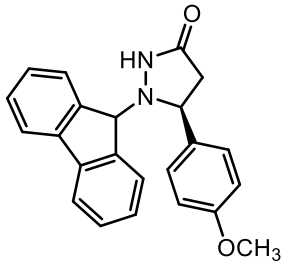

Pyrazolidinone **2d**: 13.2 mg (43% yield) white solid, 77% ee. TLC R_f = 0.29 in Et_2O.

$[\alpha]^{20}_D$ -75.7° (*c* 0.54, $CHCl_3$). Chiral HPLC: ChiralPak AD-H, *i*-PrOH/hexane = 10/90, 1.0 mL/min, 210 nm, t_{major} = 14.9 min, t_{minor} = 19.5 min.

^{1}H NMR (400 MHz, $CDCl_3$) δ 7.84 (d, *J* = 7.4 Hz, 1 H), 7.80 - 7.63 (m, 2 H), 7.54 (d, *J* = 7.4 Hz, 1 H), 7.48 (dd, *J* = 7.4, 7.4 Hz, 1 H), 7.43 - 7.30 (m, 2 H), 7.25 - 7.12 (m, 1 H), 7.12 - 6.88 (m, 2 H), 6.86 - 6.66 (m, 2 H), 5.13 (s, 1 H), 3.85 (dd, *J* = 4.3, 9.5 Hz, 1 H), 3.75 (s, 3 H), 2.65 (dd, *J* = 9.4, 17.1 Hz, 1 H), 2.26 (dd, *J* = 4.3, 17.1 Hz, 1 H). ^{13}C NMR (75 MHz, $CDCl_3$) δ 174.8, 159.0, 141.9, 141.9, 141.2, 141.0, 134.5, 129.4, 129.2, 128.0, 127.6, 127.6, 126.7, 126.5, 120.4, 120.0, 114.0, 69.8, 59.7, 55.3, 39.3. IR (neat); 3067, 2962, 2836, 1685, 1610, 1513, 1452, 1348, 1303, 1249, 1180, 1109, 1034, 951, 829, 746 cm^{-1}. HRMS (EI): Exact mass calcd for $C_{23}H_{20}N_2O_2$ $[M]^+$: 356.15248. Found:356.15257.

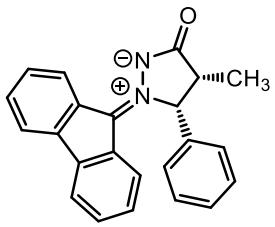

Following general procedure 3A, using azomethine imine (±)-**1e** (48.6 mg, 0.144 mmol), Hantzsch ester (51.1 mg, 0.202 mmol, 1.4 equiv), and (*R*)-TRIP (10.8 mg, 10 mol%) in chlorobenzene (7.2 mL). The reaction mixture was heated at 80°C for 24 hours. The ^{1}H NMR of the crude mixture showed 54% conversion.

Recovered **1e**: 20.8 mg (43% yield) yellow solid, 93% ee. TLC R_f = 0.24 (1/1 : CH_2Cl_2/EtOAc). $[\alpha]^{20}_D$ +617° (*c* 0.69, $CHCl_3$). Azomethine imine was reduced to pyrazolidinone with sodium borohydride before analysis by chiral HPLC: ChiralPak AD-H, *i*-PrOH/hexane = 10/90, 1.0 mL/min, 254 nm, t_{minor} = 10.8 min, t_{major} = 13.4 min.

^{1}H NMR (400 MHz, $CDCl_3$) δ 9.27 - 9.15 (m, 1 H), 7.59 (dd, *J* = 3.3, 7.2 Hz, 2 H), 7.47 - 7.24 (m, 10 H), 7.14 - 6.99 (m, 1 H), 6.36 (d, *J* = 9.0 Hz, 1 H), 3.57 - 3.29 (m, 1 H), 0.90 (d, *J* = 7.3 Hz, 3 H). ^{13}C NMR (100 MHz, $CDCl_3$) δ 185.4, 141.8, 140.8, 140.3, 134.0, 132.2, 131.9, 131.7, 130.9, 129.6, 129.5, 129.3, 129.0, 128.0, 126.6, 126.0, 120.9, 119.8, 76.6, 41.5, 11.5. IR (neat); 3062, 2976, 1652, 1606, 1544, 1453, 1267 cm^{-1}.

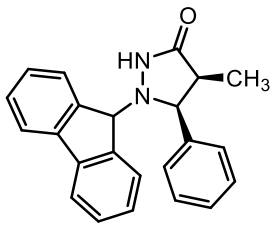

Pyrazolidinone **2e**: 25.4 mg (52% yield) white solid, 79% ee. TLC R_f = 0.58 (1/1 : CH_2Cl_2/EtOAc). $[\alpha]^{20}_D$ -102° (*c* 0.47, CH_2Cl_2). Chiral HPLC: ChiralPak AD-H, *i*-PrOH/hexane = 10/90, 1.0 mL/min, 230 nm, t_{major} = 10.8 min, t_{minor} = 13.4 min.

^{1}H NMR (400 MHz ,$CDCl_3$) δ 7.87 (d, J = 7.3 Hz, 1 H), 7.83 - 7.69 (m, 2 H), 7.51 - 7.31 (m, 4 H), 7.25 - 7.19 (m, 3 H), 7.19 - 7.11 (m, 1 H), 7.11 - 6.97 (m, 2 H), 5.16 (s, 1 H), 4.02 (d, J = 9.7 Hz, 1 H), 2.71 (m, 1 H), 0.62 (d, J = 7.4 Hz, 3 H). ^{13}C NMR (100 MHz, $CDCl_3$) δ 177.3, 142.5, 141.8, 141.3, 141.3, 138.9, 129.3, 129.1, 128.3, 128.1, 127.6, 127.5, 127.4, 126.5, 126.3, 120.4, 120.0, 69.4, 65.2, 40.2, 11.4. IR (neat); 3154, 3061, 2982, 2934, 2878, 1684, 1450, 1379, 1105, 1064, 777, 742, 724, 703, 673 cm^{-1}. HRMS (EI): Exact mass calcd for $C_{23}H_{20}N_2O$ $[M]^+$: 340.15756 Found: 340.15839.

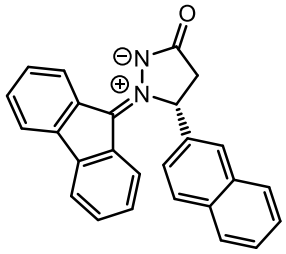

Following general procedure 3A, using azomethine imine (±)-**1f** (37.4 mg, 0.100 mmol), Hantzsch ester (35.5 mg, 0.140 mmol, 1.4 equiv), and (*R*)-TRIP (7.5 mg, 10 mol%) in chlorobenzene (10 mL). The reaction mixture was heated at 80 °C for 24 hours. The ^{1}H NMR of the crude mixture showed 53% conversion.

Recovered **1f**: 16.8 mg (45% yield) yellow solid, 95% ee. TLC R_f = 0.21 (EtOAc).

$[\alpha]^{20}_{D}$ +545° (*c* 0.56, CH_2Cl_2). Chiral HPLC: ChiralPak AD-H, *i*-PrOH/hexane = 10/90, 1.0 mL/min, 254 nm, t_{major} = 45.1 min, t_{minor} = 53.0 min.

^{1}H NMR (400 MHz, $CDCl_3$) δ 9.21 (d, *J* = 7.5 Hz, 1 H), 7.90 (d, *J* = 8.5 Hz, 1 H), 7.84 - 7.70 (m, 2 H), 7.68 (s, 1 H), 7.58 (dd, *J* = 7.5, 15.7 Hz, 2 H), 7.51 - 7.34 (m, 6 H), 7.28 - 7.19 (m, 1 H), 7.00 (t, *J* = 7.7 Hz, 1 H), 6.50 (d, *J* = 7.9 Hz, 1 H), 3.57 (dd, *J* = 9.4, 16.3 Hz, 1 H), 2.81 (dd, *J* = 1.8, 16.3 Hz, 1 H). ^{13}C NMR (100 MHz ,$CDCl_3$) δ□182.5, 141.9, 141.6, 140.5, 135.3, 133.5, 133.2, 132.5, 131.9, 131.9, 131.2, 130.3, 129.5, 129.4, 128.3, 128.2, 127.9, 127.2, 127.0, 126.0, 123.5, 122.6, 121.0, 119.9, 72.5, 40.9. IR (neat) 1734, 1663, 1609, 1544, 1506, 1450, 1292, 1271, 1244, 1126, 1111, 970, 818, 731 cm^{-1}.

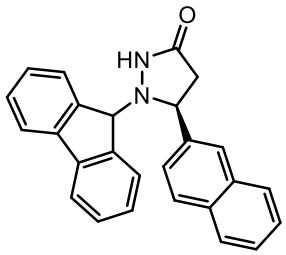

Pyrazolidinone **2f**: 17.1 mg (45% yield) white solid, 74% ee. TLC R_f = 0.38 (Et_2O).

$[\alpha]^{20}_D$ -84.2° (*c* 0.57, CH_2Cl_2). Chiral HPLC: ChiralPak AD-H, *i*-PrOH/hexane = 5/95, 1.0 mL/min, 230 nm, t_{major} = 28.2 min, t_{minor} = 41.1 min.

^{1}H NMR (mixture of rotamers, 400 MHz, $CDCl_3$) δ 8.37 (br. s, 1 H), 7.98 - 7.84 (m, 1 H), 7.80 (d, *J* = 7.5 Hz, 1 H), 7.77 - 7.65 (m, 4 H), 7.59 - 7.47 (m, 3 H), 7.47 - 7.31 (m, 4 H), 7.23 - 7.15 (m, 1 H), 7.11 (t, *J* = 7.4 Hz, 1 H), 5.20 (s, 1 H), 4.00 (dd, *J* = 3.9, 9.6 Hz, 1 H), 2.75 (dd, *J* = 9.7, 17.2 Hz, 1 H), 2.38 (dd, *J* = 4.0, 17.2 Hz, 1 H). ^{13}C NMR (100 MHz, $CDCl_3$) δ 174.6, 142.1, 141.6, 141.3, 140.8, 139.4, 133.3, 132.9, 129.5, 129.3, 128.6, 128.1, 128.1, 127.7, 126.7, 126.6, 126.3, 126.1, 125.2, 124.5, 120.4, 120.0, 70.0, 60.4, 39.2. IR (neat) 2366, 1684, 1558, 1554, 1452 cm^{-1}. HRMS (EI): Exact mass calcd for $C_{26}H_{20}N_2O$ $[M]^+$: 376.1576. Found: 376.1553.

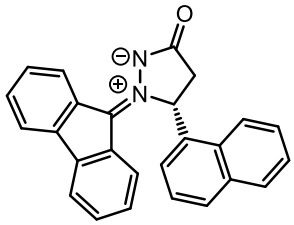

Following general procedure 3A, using azomethine imine (±)-**1g** (37.4 mg, 0.100 mmol), Hantzsch ester (35.5 mg, 0.140 mmol, 1.4 equiv), and (*R*)-TRIP (7.5 mg, 10 mol%) in chlorobenzene (10 mL). The reaction mixture was heated at 80°C for 24 hours. The ^{1}H NMR of the crude mixture showed 50% conversion.

Recovered **1g**: 17.8 mg (48% yield) yellow solid, 82% ee. TLC R_f = 0.33 (EtOAc).

$[\alpha]^{20}_D$ +269° (*c* 0.19, CH_2Cl_2). Chiral HPLC: ChiralPak AD-H, *i*-PrOH/hexane = 15/85, 1.0 mL/min, 230 nm, t_{major} = 27.1 min, t_{minor} = 42.5 min.

^{1}H NMR (400 MHz, $CDCl_3$) δ 9.23 (d, *J* = 7.3 Hz, 1 H), 7.99 (dd, *J* = 3.5, 8.1 Hz, 2 H), 7.86 - 7.71 (m, 2 H), 7.71 - 7.61 (m, 2 H), 7.70 - 7.56 (m, 3 H), 7.54 - 7.40 (m, 2 H), 7.36 - 7.29 (m, 1 H), 7.25 - 7.17 (m, 2 H), 6.91 (dd, *J* = 7.8, 16.7 Hz, 2 H), 6.81 - 6.67 (m, 1 H), 3.66 (dd, *J* = 9.4, 16.2 Hz,

1 H), 2.77 (dd, J = 2.1, 16.1 Hz, 1 H). ^{13}C NMR (100 MHz, $CDCl_3$) δ 182.7, 142.2, 141.9, 140.5, 134.8, 134.2, 132.9, 132.6, 131.9, 131.7, 131.3, 129.9, 129.7, 129.5, 129.4, 129.2, 129.0, 128.3, 127.9, 126.8, 126.0, 125.6, 124.4, 121.7, 121.6, 120.9, 120.4, 119.9, 70.4, 40.1. IR (neat) 1663, 1605, 1553, 1450, 1288, 1269, 1232, 1124 cm^{-1}.

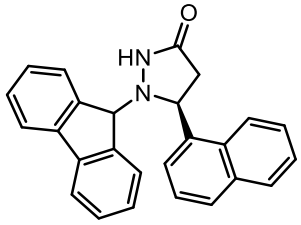

Pyrazolidinone **2g**: 17.1 mg (45% yield) white solid, 81% ee. TLC R_f = 0.55 (Et_2O).

$[\alpha]^{20}_D$ -204° (c 0.31, CH_2Cl_2). Chiral HPLC: ChiralPak AD-H, i-PrOH/hexane = 5/95, 1.0 mL/min, 254 nm, t_{major} = 28.7 min, t_{minor} = 39.9 min.

^{1}H NMR (400 MHz, $CDCl_3$) δ 8.01 - 7.85 (m, 2 H), 7.81 (dd, J = 3.8, 7.8 Hz, 2 H), 7.77 - 7.63 (m, 2 H), 7.56 - 7.27 (m, 8 H), 7.06 (t, J = 7.4 Hz, 1 H), 5.23 (s, 1 H), 4.63 (dd, J = 3.8, 9.7 Hz, 1 H), 2.99 (dd, J = 9.7, 17.0 Hz, 1 H), 2.26 (dd, J = 3.9, 17.0 Hz, 1 H). ^{13}C NMR (75 MHz, $CDCl_3$) δ 174.6, 142.2, 142.0, 141.1, 141.0, 137.6, 134.0, 129.6, 129.4, 129.2, 129.1, 128.1, 128.0, 127.8, 126.5, 126.3, 126.1, 125.7, 125.5, 123.8, 122.8, 120.5, 120.1, 70.2, 57.7, 40.1. IR (neat) 3296, 1713, 1701, 1539, 1452, 1202, 741 cm^{-1}. HRMS (EI): Exact mass calcd for $C_{26}H_{20}N_2O$ $[M]^+$: 376.1576. Found: 376.1618.

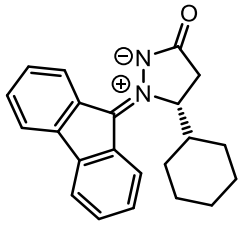

Following general procedure 3A, using azomethine imine (±)-**1h** (45.0 mg, 0.136 mmol), Hantzsch ester (69.0 mg, 0.272 mmol, 2.0 equiv), and (*R*)-TRIP (10.2 mg, 10 mol%) in chlorobenzene (9 mL). The reaction mixture was heated at 80°C for 24 hours. The ^{1}H NMR of the crude mixture showed 46% conversion.

Recovered **1h**: 21.3 mg (47% yield) yellow solid, 72% ee. TLC R_f = 0.33 (EtOAc).

$[\alpha]^{20}_{D}$ +363° (*c* 0.70, CH_2Cl_2). Chiral HPLC: ChiralPak AD-H, *i*-PrOH/hexane = 10/90, 1.0 mL/min, 230 nm, t_{major} = 26.2 min, t_{minor} = 20.9 min.

^{1}H NMR (400 MHz, $CDCl_3$) δ 9.01 (d, *J* = 7.7 Hz, 1 H), 7.70 (d, *J* = 7.3 Hz, 1 H), 7.62 (d, *J* = 7.4 Hz, 1 H), 7.53 - 7.39 (m, 3 H), 7.39 - 7.27 (m, 2 H), 5.30 (s, 1 H), 2.97 (dd, *J* = 8.9, 16.7 Hz, 1 H), 2.73 (dd, *J* = 1.7, 16.7 Hz, 1 H), 2.32 - 2.07 (m, 1 H), 1.94 - 1.76 (m, 2 H), 1.76 - 1.60 (m, 2 H), 1.58 - 1.44 (m, 1 H), 1.30 - 1.00 (m, 5 H). ^{13}C NMR (100 MHz, $CDCl_3$) δ 183.8, 142.1, 139.7, 139.3, 131.9, 131.9, 131.5, 130.9, 130.0, 129.3, 128.4, 124.9, 121.3, 119.7, 72.6, 40.8, 32.2, 29.7, 26.1, 25.9, 25.4, 24.1. IR (neat) 2928, 2854, 1659, 1605, 1541, 1448, 1255, 1232 cm^{-1}.

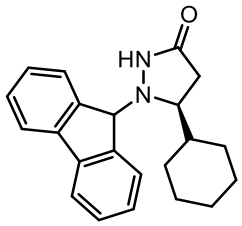

Pyrazolidinone **2h**: 17.4 mg (38% yield) white solid, 83% ee. TLC R_f = 0.52 (Et_2O).

$[\alpha]^{20}_D$ -28.9° (*c* 0.38, CH_2Cl_2). Chiral HPLC: ChiralPak AD-H, *i*-PrOH/hexane = 5/95, 1.0 mL/min, 230 nm, t_{major} = 14.1 min, t_{minor} = 32.5 min.

^{1}H NMR (400 MHz, $CDCl_3$) δ 7.83 (s, 1 H), 7.81 - 7.75 (m, 1 H), 7.75 - 7.61 (m, 3 H), 7.47 - 7.37 (m, 2 H), 7.36 - 7.26 (m, 2 H), 5.01 (s, 1 H), 2.61 (ddd, *J* = 1.9, 5.8, 9.3 Hz, 1 H), 2.30 (ddd, *J* = 3.2, 9.4, 17.2 Hz, 1 H), 1.93 (dd, *J* = 2.1, 17.2 Hz, 1 H), 1.78 - 1.52 (m, 4 H), 1.48 - 1.38 (m, 1 H), 1.21 - 0.97 (m, 4 H), 0.97 - 0.67 (m, 2 H). ^{13}C NMR (100 MHz, $CDCl_3$) δ 176.3, 142.5, 141.8, 141.4, 141.4, 129.1, 127.9, 127.4, 126.8, 126.4, 120.2, 119.9, 71.0, 61.9, 43.5, 34.2, 28.5, 28.4, 26.5, 26.2. IR (neat) 2918, 2368, 1684, 1555, 1452, 860, 746, 623 cm^{-1}. HRMS (EI): Exact mass calcd for $C_{22}H_{24}N_2O$ $[M]^+$: 332.1889. Found: 332.1882.

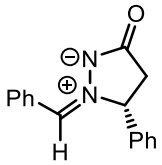

The racemic azomethine imine (±)-**1i** was synthesized according to a known procedure;[6,13] spectral data is in agreement with the literature. Kinetic Resolution following general procedure II, using azomethine imine (±)-**1i** (25.0 mg, 0.0999 mmol), Hantzsch ester (34.6 mg, 0.137 mmol, 1.4 equiv), and (*R*)-TRIP (1.9 mg, 2.5 mol%) in toluene (4 mL). The reaction mixture was heated at 40°C for 6 hours. The ^{1}H NMR of the crude mixture showed 57% conversion.

Recovered **1i**: 10.3 mg (41% yield) white solid, 95% ee.

$[\alpha]^{20}_D$ +28° (*c* 0.42, MeOH). Chiral HPLC: ChiralPak AD-H, *i*-PrOH/hexane = 10/90, 1.0 mL/min, 254 nm, t_{major} = 53.6 min, t_{minor} = 62.5 min.

Spectral data is in agreement with the literature.[6,13]

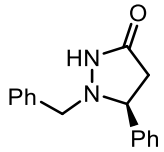

Pyrazolidinone **2i**: 10.8 mg (43% yield) viscous oil, 86% ee.

$[\alpha]^{20}_{D}$ -189° (*c* 0.45, CH_2Cl_2). Literature: 93%ee, $[\alpha]^{19}_{D}$ -79.3° (*c* 0.90, CH_2Cl_2);[13] 99% ee, $[\alpha]^{20}_{D}$ -163° (*c* 0.90, CH_2Cl_2).[6] Chiral HPLC: ChiralPak AD-H, *i*-PrOH/hexane = 10/90, 1.0 mL/min, 254 nm, t_{major} = 11.7 min, t_{minor} = 13.8 min.

Spectral data is in agreement with the literature.[6,13]

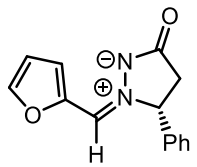

Racemic azomethine imine (±)-**1j** synthesized by adapting a known procedure.[6] Freshly distilled furfural (96.1 mg, 1.00 mmol) was added to 5-phenyl pyrazolidinone[8] (162 mg, 1.00 mmol) in MeOH (2 mL), stirred at 65 °C for 4 h. After cooling to room temperature, the solvent was evaporated under reduced pressure to give the crude product, which was isolated by trituration in 10% MeOH, 90% EtOAc. The product was obtained as a white solid (108 mg, 45%, yield not optimized). Kinetic Resolution following general procedure 3A, using azomethine imine (±)-**1j** (24.7 mg, 0.103 mmol), Hantzsch ester (35.0 mg, 0.138 mmol, 1.4 equiv), and (*R*)-TRIP (1.9 mg, 2.5 mol%) in toluene (4 mL). Reaction mixture heated at 60°C for 6 hours. ^{1}H NMR of crude mixture showed 56% conversion.

Recovered **1j**: 11.1 mg (45% yield) white solid, 94% ee. TLC R_f = 0.20 (10% MeOH, 90% EtOAc).

$[\alpha]^{20}_{D}$ +46.7° (*c* 0.21, CH_2Cl_2). Chiral HPLC: ChiralPak AD-H, *i*-PrOH/hexane = 10/90, 1.0 mL/min, 254 nm, t_{major} = 46.0 min, t_{minor} = 52.9 min.

^{1}H NMR (400 MHz, $CDCl_3$) δ 8.00 (d, *J* = 3.6 Hz, 1 H), 7.56 (d, *J* = 1.5 Hz, 1 H), 7.50 - 7.39 (m, 3 H), 7.39 - 7.29 (m, 2 H), 6.93 (s, 1 H), 6.71 - 6.59 (m, 1 H), 5.51 (dd, *J* = 5.9, 9.6 Hz, 1 H), 3.34 (dd, *J* = 9.8, 17.0 Hz, 1 H), 2.93 (dd, *J* = 6.0, 17.0 Hz, 1 H). ^{13}C NMR (100 MHz, $CDCl_3$) δ 182.6, 146.5, 145.9, 137.6, 129.8, 129.8, 127.0, 122.0, 121.8, 113.8, 72.5, 39.6. IR (neat); 3140, 3060, 2963, 1655, 1591, 1555, 1497, 1466, 1406, 1375, 1299 cm^{-1}. HRMS (EI): Exact mass calcd for $C_{14}H_{12}N_2O_2$ $[M]^+$: 240.0899. Found: 240.0892.

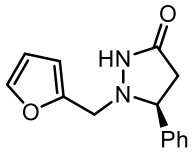

Pyrazolidinone **2j**: 13.4 mg (54%) colourless oil, 75% ee. TLC R_f = 0.30 in Et_2O.

$[\alpha]^{20}_D$ -136° (*c* 0.44, CH_2Cl_2). Chiral HPLC: ChiralPak AD-H, *i*-PrOH/hexane = 10/90, 1.0 mL/min, 254 nm, t_{major} = 13.8 min, t_{minor} = 16.5 min.

^{1}H NMR (400 MHz, $CDCl_3$) δ 7.46 - 7.28 (m, 6 H), 7.22 (br. s., 1 H), 6.40 - 6.31 (m, 1 H), 6.30 - 6.25 (m, 1 H), 4.25 (dd, *J* = 8.5, 9.0 Hz, 1 H), 3.95 (d, *J* = 14.1 Hz, 1 H), 3.71 (d, *J* = 14.0 Hz, 1 H), 2.86 (dd, *J* = 8.3, 16.8 Hz, 1 H), 2.54 (dd, *J* = 9.0, 16.8 Hz, 1 H). ^{13}C NMR (100 MHz, $CDCl_3$) 172.9, 150.0, 143.1, 139.3, 129.0, 128.3, 127.2, 110.7, 109.9, 67.0, 54.1, 39.2. IR (neat); 3165, 3060, 2831, 1682, 1603, 1560, 1497, 1420, 1341, 1289, 1066, 1046, 1012, 919, 737, 697 cm^{-1}. HRMS (EI): Exact mass calcd for $C_{14}H_{14}N_2O_2$ $[M]^+$: 242.10553. Found: 242.10522.

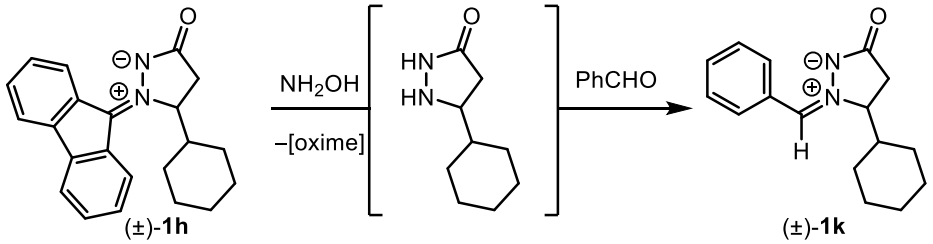

Racemic azomethine imine (±)-**1k** was prepared using a one pot, two step procedure from (±)-**1h**. Hydroxylamine (50% in H_2O, 49.0 mg, 0.742 mmol, 1.5 equiv) was added to (±)-**1h** (0.169 g, 0.510 mmol) in methanol (5 mL). The reaction was heated to reflux for 16 hours. After cooling to room temperature, an equal volume of water was added. The resulting precipitate was separated, and the filtrate evaporated to dryness under reduced pressure. The crude mixture was diluted in methanol (5 mL) and benzaldehyde (59.5 mg, 0.507 mmol, 1.1 equiv) was added. The mixture was stirred at room temperature for 16 h, followed by evaporation under reduced pressure. The product was isolated by silica gel chromatography (5-10% MeOH in EtOAc) as a white solid (0.104 g, 79% yield over two steps).

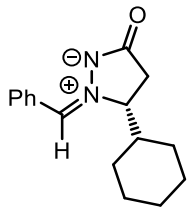

Recovered azomethine imine **1k**: 8.8 mg (35% yield) white solid, 93% ee. TLC R_f = 0.10 in EtOAc $[\alpha]^{20}_D$ +38° (*c* 0.1, CH_2Cl_2). Chiral HPLC: ChiralPak AD-H, *i*-PrOH/hexane = 10/90, 1.0 mL/min, 254 nm, t_{major} = 32.9 min, t_{minor} = 59.0 min.

^{1}H NMR (400 MHz, CD_3OD) δ 8.38 - 8.25 (m, 9 H), 7.75 (s, 5 H), 7.61 - 7.36 (m, 13 H), 4.79 - 4.68 (m, 5 H), 2.82 (dd, *J* = 9.5, 16.9 Hz, 5 H), 2.53 (dd, *J* = 3.3, 16.9 Hz, 5 H), 2.10 - 1.96 (m, 5 H), 1.86 - 1.58 (m, 23 H), 1.41 - 1.27 (m, 10 H), 1.25 - 1.02 (m, 21 H). ^{13}C NMR (100 MHz, CD_3OD) δ 187.4, 138.2, 133.6, 133.4, 130.7, 129.9, 75.9, 44.2, 32.9, 30.0, 27.1, 27.1, 26.6, 25.8.

IR (neat); 2956, 2917, 2849, 1706, 1463, 1376, 1161, 1129, 1107, 952, 816, 720 cm^{-1}. HRMS (EI): Exact mass calcd for $C_{16}H_{20}N_2O$ $[M]^+$: 256.15756. Found: 256.15667.

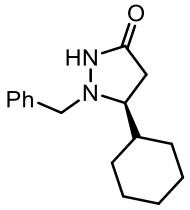

Pyrazolidinone **2k**: 10.4 mg (41% yield) colourless oil, 76% ee. TLC R_f = 0.25 in Et_2O

$[\alpha]^{20}_D$ -91° (*c* 0.1, CH_2Cl_2). Chiral HPLC: ChiralPak AD-H, *i*-PrOH/hexane = 5/95, 1.0 mL/min, 230 nm, t_{major} = 15.2 min, t_{minor} = 25.0 min.

^1H NMR (400 MHz, $CDCl_3$) δ 7.43 - 7.25 (m, 5 H), 6.89 (br. s., 1H), 3.93 (d, *J* = 12.3 Hz, 1 H), 3.77 (d, *J* = 12.4 Hz, 1 H), 3.06 (ddd, *J* = 3.7, 6.9, 8.8 Hz, 1 H), 2.74 (dd, *J* = 8.9, 17.1 Hz, 1 H), 2.20 (dd, *J* = 3.8, 17.0 Hz, 1 H), 1.93 - 1.85 (m, 1 H), 1.78 - 1.60 (m, 4 H), 1.54 - 1.35 (m, 1 H), 1.30 - 0.83 (m, 5 H). ^{13}C NMR (100 MHz, $CDCl_3$) δ 174.4, 136.0, 129.7, 128.7, 128.2, 67.4, 64.3, 41.7, 32.2, 29.2, 28.9, 26.5, 26.12, 26.10. IR (neat); 2957, 2916, 2849, 1464, 1377, 953, 729, 721 cm^{-1}. HRMS (EI): Exact mass calcd for $C_{16}H_{22}N_2O$ $[M]^+$: 258.17321. Found: 258.17273.

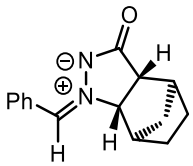

Kinetic Resolution following general procedure 3A, using azomethine imine (±)-**1l** (49.0 mg, 0.204 mmol), Hantzsch ester (71.1 mg, 0.281 mmol, 1.4 equiv), and (*R*)-TRIP (3.4 mg, 2.5 mol%) in toluene (8 mL). The reaction mixture heated at 60°C for 6 hours. The ^1H NMR of the crude mixture showed 63% conversion.

Recovered **1l**: 15.7 mg (32% yield) white solid, 99% ee. TLC R_f = 0.10 in EtOAc.

$[\alpha]^{20}_D$ -45.2° (*c* 0.53, CH_2Cl_2). Chiral HPLC: ChiralPak AD-H, *i*-PrOH/hexane = 10/90, 1.0 mL/min, 254 nm, t_{major} = 40.8 min, t_{minor} = 60.1 min.

^{1}H NMR (400 MHz, $CDCl_3$) δ 8.51 - 8.07 (m, 2 H), 7.56 - 7.37 (m, 3 H), 7.13 (s, 1 H), 4.45 (d, *J* = 7.1 Hz, 1 H), 2.85 - 2.60 (m, 3 H), 1.82 - 1.55 (m, 2 H), 1.52 - 1.19 (m, 4 H). ^{13}C NMR (75 MHz, $CDCl_3$) δ 186.2, 132.4, 131.7, 131.6, 129.5, 128.8, 76.8, 50.0, 44.3, 39.2, 32.4, 27.5, 24.9.

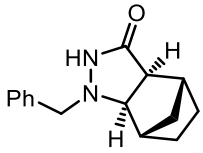

Pyrazolidinone **2l**: 25.7 mg (52% yield) white solid, 66% ee. TLC R_f = 0.29 in EtOAc.

$[\alpha]^{20}_D$ -54.0° (*c* 0.37, CH_2Cl_2). Chiral HPLC: ChiralPak AD-H, *i*-PrOH/hexane = 10/90, 1.0 mL/min, 254 nm, t_{major} = 9.8 min, t_{minor} = 12.2 min.

^{1}H NMR (400 MHz, $CDCl_3$) δ 7.50 - 7.26 (m, 5 H), 3.94 - 3.68 (m, 2 H), 3.12 (d, *J* = 8.0 Hz, 1 H), 2.69 (d, *J* = 8.1 Hz, 1 H), 2.59 (d, *J* = 3.9 Hz, 1 H), 2.24 (d, *J* = 4.4 Hz, 1 H), 1.67 - 1.50 (m, 2 H), 1.50 - 1.33 (m, 1 H), 1.28 - 1.11 (m, 2 H), 1.09 - 0.86 (m, 1 H). ^{13}C NMR (100 MHz, $CDCl_3$) δ 173.9, 136.2, 129.5, 128.7, 128.0, 70.3, 65.9, 50.4, 43.7, 39.5, 33.6, 27.9, 25.0. IR (neat); 3148, 3029, 2957, 2872, 1677, 1658, 1453, 1374, 1294, 1104, 1066, 989, 911, 867, 748, 723, 698 cm^{-1}. HRMS (EI): Exact mass calcd for $C_{15}H_{18}N_2O$ $[M]^+$: 242.14191. Found: 242.14044.

Large Scale Kinetic Resolution: Following general procedure 3A, using azomethine imine (±)-**1l** (0.240 g, 1.00 mmol), Hantzsch ester (0.354 g, 1.40 mmol, 1.4 equiv), and (*R*)-TRIP (19.1 mg, 2.5 mol%) in chlorobenzene (20 mL). The reaction mixture was heated at 60°C for 4 hours. The ^{1}H NMR of the crude mixture showed 61% conversion. The product was isolated by silica gel chromatography, the crude mixture was loaded in dichloromethane, followed by elution with 0-10% MeOH in EtOAc.

Recovered **1l**: 0.0926 g (39% yield) white solid, 99% ee. $[\alpha]^{20}_D$ -44.6° (*c* 1.85, CH_2Cl_2)

^{1}H NMR (400 MHz, $CDCl_3$) δ 8.37 - 8.22 (m, 2 H), 7.56 - 7.32 (m, 3 H), 7.12 (s, 1 H), 4.52 - 4.36 (m, 1 H), 2.81 - 2.76 (m, 1 H), 2.76 - 2.61 (m, 2 H), 1.77 - 1.54 (m, 2 H), 1.47 - 1.17 (m, 4 H). ^{13}C NMR (75 MHz, $CDCl_3$) δ 186.2, 131.9, 131.8, 131.6, 129.6, 128.9, 77.0, 50.1, 44.4, 39.3, 32.6, 27.6, 25.0.

Pyrazolidinone **2l**: 0.121 g (50% yield) white solid, 67% ee. Recrystallization from *i*-PrOH/ hexanes gave an almost racemic precipitate (6% ee). The solvent was evaporated from the mother liquor solution (filtrate) to give 70.5 mg (29% yield) of a white, crystalline solid (98% ee).

$[\alpha]^{20}_D$ -51.3° (*c* 2.42, CH_2Cl_2) for 98% ee.

^{1}H NMR (400 MHz, $CDCl_3$) δ 7.76 (br. s., 1 H), 7.39 - 7.16 (m, 5 H), 3.89 - 3.62 (m, 2 H), 3.10 (d, J = 8.1 Hz, 1 H), 2.68 (d, J = 8.1 Hz, 1 H), 2.59 (d, J = 3.9 Hz, 1 H), 2.20 (d, J = 4.4 Hz, 1 H), 1.66 - 1.48 (m, 2 H), 1.48 - 1.30 (m, 1 H), 1.27 - 1.08 (m, 2 H), 1.08 - 0.88 (m, 1 H). ^{13}C NMR (100 MHz, $CDCl_3$) δ 173.9, 136.1, 129.5, 128.7, 128.0, 70.1, 65.8, 50.5, 43.7, 39.5, 33.6, 27.9, 25.0.

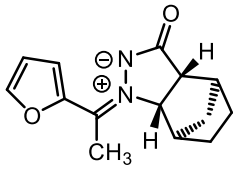

Following general procedure II, using azomethine imine (±)-**1m** (52.3 mg, 0.214 mmol), Hantzsch ester (76.0 mg, 0.300 mmol, 1.4 equiv), and (*R*)-TRIP (8.0 mg, 5.0 mol%) in chlorobenzene (4 mL). The reaction mixture was heated at 80°C for 24 hours. The ^{1}H NMR of the crude mixture showed 56% conversion.

Recovered **1m**: 19.1 mg (37% yield) white solid, 85% ee. TLC R_f = 0.1 (EtOAc)

$[\alpha]^{20}_{D}$ +78° (*c* 0.27, *i*-PrOH). Azomethine imine was reduced to pyrazolidinone with sodium borohydride before analysis by chiral HPLC. This gave a mixture of two diastereomers (d.r. = 76:24), each being 85% ee: ChiralPak AD-H, *i*-PrOH/hexane = 5/95, 1.0 mL/min, 230 nm. Major Diastereomer: t_{minor} = 19.4 min, t_{major} = 31.4 min. Minor Diastereomer: t_{minor} = 16.2 min, t_{major} = 33.2 min.

^{1}H NMR (400 MHz, C_6D_6) δ 8.50 (d, *J* = 3.5 Hz, 1 H), 6.93 (d, *J* = 1.1 Hz, 1 H), 6.14 (dd, *J* = 1.7, 3.6 Hz, 1 H), 3.20 (d, *J* = 7.1 Hz, 1 H), 2.82 (d, *J* = 3.3 Hz, 1 H), 2.41 (d, *J* = 7.3 Hz, 1 H), 1.82 (d, *J* = 4.8 Hz, 1 H), 1.73 (s, 3 H), 1.34 (m, 1 H), 1.18 (dddd, *J* = 4.3, 4.3, 11.9, 12.0 Hz, 1 H), 0.98 (dddd, *J* = 4.5, 4.3, 12.1, 12.2 Hz, 1 H), 0.91 - 0.81 (m, 1 H), 0.65 (m, 1 H), 0.60 - 0.44 (m, 1 H)
^{13}C NMR (100 MHz, C_6D_6) δ 183.5, 148.5, 144.2, 128.4, 121.9, 113.8, 72.2, 51.3, 42.0, 39.6, 32.3, 27.1, 25.3, 14.8.

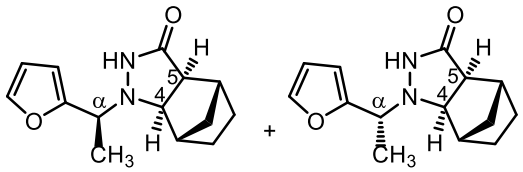

(α-*S*,4-*S*,5-*S*) major 78% ee (α-*R*,4-*S*,5-*S*) minor 58% ee

Pyrazolidinone **2m**: 27.0 mg (51%) white solid, diastereomeric mixture, d.r. = 67:33, major = 78% ee, minor = 58% ee. The ^{1}H and ^{13}C NMR spectra of the major diastereomer are in agreement with the literature, identifying the major diastereomer as (α-*S*, 4-*S*, 5-*S*).[2] TLC R_f = 0.33 in EtOAc (major isomer)

$[\alpha]^{20}_{D}$ -33° (*c* 0.90, *i*-PrOH). Chiral HPLC: ChiralPak AD-H, *i*-PrOH/hexane = 5/95, 1.0 mL/min, 230 nm. Major Diastereomer: t_{major} = 19.6 min, t_{minor} = 31.6 min. Minor Diastereomer: t_{major} = 16.3 min, t_{minor} = 33.5 min.

^{1}H NMR (400 MHz, C_6D_6, mixture of diastereomers d.r. = 67:33) δ 10.01 (br. s., 1 H), 7.13 - 6.99 (m, 1 H), 6.26 - 5.97 (m, 2 H), 3.87 - 3.68 (m, 1 H), 3.21 - 3.05 (m, 1 H), 2.71 - 2.46 (m, 1 H), 2.39 - 2.20 (m, 1 H), 2.15 (m, 1 H), 1.71 (m, 1 H), 1.43 (d, *J* = 7.1 Hz, 2 H), 1.39 - 1.29 (m, 1 H), 1.29 - 0.99 (m, 2 H), 0.99 - 0.56 (m, 3 H). ^{13}C NMR (100 MHz, C_6D_6, d.r. = 67:33) Major Diastereomer = δ 175.3, 154.9, 142.0, 110.7, 108.6, 68.2, 60.4, 51.0, 44.0, 39.6, 33.6, 27.8, 25.4, 17.6. Minor Diastereomer = δ 174.7, 155.0, 142.1, 110.6, 108.4, 66.6, 60.5, 50.9, 44.4, 39.7, 33.6, 27.9, 25.1, 16.7. IR (neat); 3351, 3169, 2962, 2874, 1672, 1376, 1153, 1010, 732 cm^{-1}. HRMS (EI): Exact mass calcd for $C_{14}H_{18}N_2O_2$ $[M]^+$: 246.13683. Found: 246.13748.

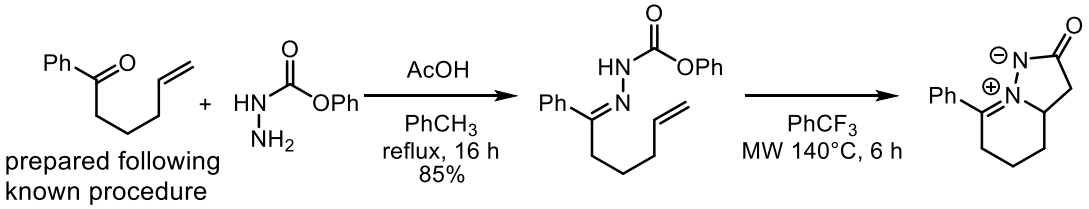

Racemic azomethine imine (±)-**1n** was synthesized as shown above. The hydrazone was first synthesized following a known procedure for a similar compound.[2] The hydrazone (0.157 g, 0.200 mmol) and $PhCF_3$ (10 mL) were combined in a vial and purged with Argon. The mixture was heated at 140°C for 6 hours. The ^{1}H NMR of the crude mixture ($CDCl_3$) showed 50% yield of product using 1,3,5-trimethoxybenzene as internal standard. The product was isolated by column chromatography and obtained as a white solid (36.7 mg, 34% isolated yield, not optimized).

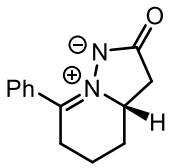

Following general procedure **II**, using azomethine imine (±)-**1n** (23.5 mg, 0.110 mmol), Hantzsch ester (35.0 mg, 0.138 mmol, 1.4 equiv), and (*R*)-TRIP (10.0 mg, 12 mol%) in chlorobenzene (2

mL). The reaction mixture was heated at 80°C for 24 hours. The ^{1}H NMR of the crude mixture showed 40% conversion.

Recovered **1n**: 10.7 mg (45% yield) white solid, 51% ee. TLC R_f = 0.1 (5% MeOH, 95% CH_2Cl_2). $[\alpha]^{20}_D$ −163° (*c* 3.6, $CHCl_3$). Azomethine imine was reduced to pyrazolidinone with sodium borohydride before analysis by chiral HPLC. This gave a single diastereomer. $[\alpha]^{20}_D$ +107° (*c* 2.6, $CHCl_3$) for this pyrazolidinone. ChiralPak AD-H, *i*-PrOH/hexane = 5/95, 1.0 mL/min, 230 nm, t_{major} = 18.4 min, t_{minor} = 33.4 min.

^{1}H NMR (400 MHz, $CDCl_3$) δ 8.09 - 7.79 (m, 2 H), 7.58 - 7.32 (m, 3 H), 4.44 - 4.32 (m, 1 H), 3.16 - 2.91 (m, 2 H), 2.86 (dd, J = 8.5, 16.0 Hz, 1 H), 2.58 (dd, J = 9.3, 16.0 Hz, 1 H), 2.48 - 2.25 (m, 1 H), 2.11 - 1.91 (m, 2 H), 1.89 - 1.76 (m, 1 H). ^{13}C NMR (100 MHz, $CDCl_3$) δ 181.9, 144.7, 132.6, 131.0, 129.4, 128.3, 66.0, 36.8, 28.7, 27.5, 18.4. IR (neat); 3000, 2936, 1651, 1558, 1301 cm^{-1}. HRMS (EI): Exact mass calcd for $C_{13}H_{14}N_2O$ $[M]^+$: 214.11061. Found: 214.11062.

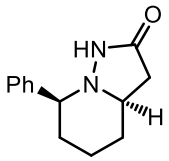

Pyrazolidinone **2n**: 9.0 mg (38%) white solid, 86% ee, single diastereomer. TLC R_f = 0.3 in EtOAc. $[\alpha]^{20}_D$ −162° (*c* 3.0, $CHCl_3$). Chiral HPLC: ChiralPak AD-H, *i*-PrOH/hexane = 5/95, 1.0 mL/min, 254 nm, t_{minor} = 18.8 min, t_{major} = 33.5 min.

^{1}H NMR (400 MHz, $CHCl_3$) δ 7.53 - 7.27 (m, 5 H), 6.23 (br. s., 1 H), 3.53 - 3.36 (m, 1 H), 2.98 (br. s., 1 H), 2.56 - 2.27 (m, 2 H), 1.99 - 1.71 (m, 5 H), 1.71 - 1.49 (m, 1 H). IR (neat); 3133 (br), 3032, 2939, 2846, 1677 cm^{-1}. HRMS (EI): Exact mass calcd for $C_{13}H_{16}N_2O$ $[M]^+$: 216.12626. Found: 246.12568.

6.3.2. Synthesis of β-Amino Amides (+)-3l and (–)-3l

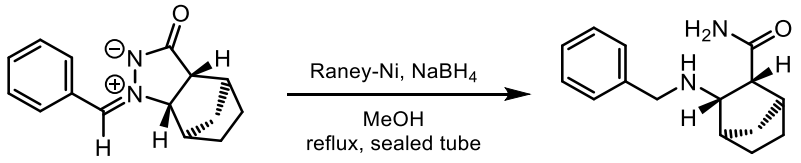

(–)-**1l**, 99% ee (+)-**3l**, 98% ee

Reduction and Ring Opening of Azomethine Imine: Following procedure adapted from our communication on alkene aminocarbonylation.[1] To the azomethine imine (–)-**1l** (91.6 mg, 0.381 mmol, 1.0 equiv) and Raney-nickel in methanol (8 mL) at room temperature was added sodium borohydride (0.143 g, 3.79 mmol, 10 equiv). The flask was quickly sealed and the mixture stirred at 60°C for 6 h. The crude mixture was filtered through celite, rinsing well with methanol. Solvent was evaporated to give the crude product, which was diluted with CH_2Cl_2 and saturated $NaHCO_3$. The organic phase was washed 1x satd. $NaHCO_3$, 2x brine, then dried with sodium sulphate, then concentrated in vacuo to give the product (no further purification was required).

β-Amino Amide (+)-**3l**. White crystalline solid, 54.0 mg (59% yield, not optimized), 98% ee

TLC R_f = 0.1 (EtOAc). ^{1}H NMR (400 MHz, $CDCl_3$) δ 7.39 - 7.17 (m, 5 H), 6.63 (br. s., 1 H), 5.61 (br. s., 1 H), 3.82 (d, *J* = 13.3 Hz, 1 H), 3.70 (d, *J* = 13.4 Hz, 1 H), 2.92 (dd, *J* = 1.4, 8.0 Hz, 1 H), 2.55 - 2.33 (m, 2 H), 2.30 - 2.26 (m, 1 H), 1.91 - 1.85 (m, 1 H), 1.73 (br. s., 1 H), 1.65 - 1.45 (m, 2 H), 1.28 - 0.98 (m, 3 H). ^{13}C NMR (100 MHz, $CDCl_3$) δ 176.1, 140.3, 128.5, 128.1, 127.0, 64.1, 53.7, 52.6, 40.9, 40.7, 34.6, 29.4, 26.9. IR (neat); 3462, 3327, 3189, 2954, 2873, 1664, 1618, 1599, 1449, 1420, 1380, 1349, 1302, 1266, 1231, 1136, 964, 775, 728, 696 cm^{-1}. HRMS (EI): Exact mass calcd for $C_{15}H_{20}N_2O$ $[M]^+$: 244.15756. Found: 244.15643.

$[\alpha]^{20}_D$ +14.3° (*c* 1.8, $CHCl_3$). The product was derivatized for HPLC analysis: The amide (31.9 mg, 0.131 mmol, 1.0 equiv) was combined with triethylamine (20 μL, 0.14 mmol, 1.1 equiv) in

CH_2Cl_2 (1.2 mL) and the mixture cooled in an ice bath. Benzoyl chloride (15 μL, 0.13 mmol, 1.0 equiv) was added and the mixture was stirred until TLC showed complete consumption of starting materials. The mixture was diluted with CH_2Cl_2 and washed with saturated ammonium chloride and water. The organic phase was dried with sodium sulphate. Solvent evaporated to give the crude product as a white solid, this was used for HPLC analysis (98% ee). ChiralPak AD-H, *i*-PrOH/hexane = 15/85, 0.8 mL/min, 230 nm, t_{minor} = 36.4 min, t_{major} = 52.5 min.

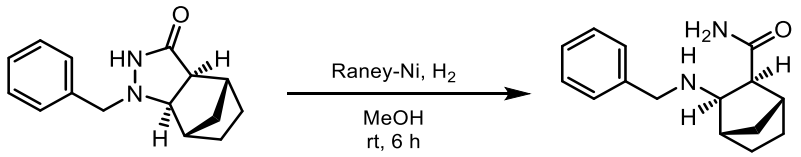

(–)-**2l**, 98% ee (–)-**3l**, 97% ee

Reduction and Ring Opening of Pyrazolidinone: The pyrazolidinone (–)-**2l** (70.5 mg, 0.291 mmol, 1.0 equiv) and Raney-nickel were stirred in methanol (6 mL) at room temperature under a balloon of hydrogen for 6 hours. The crude mixture was filtered through celite, rinsing well with methanol. The solvent was evaporated to give the product, no further purification was required.

β-Amino Amide (-)-**3l**. White solid, 62.1 mg (87% yield). 97% ee (benzoylated product) TLC R_f= 0.1 (EtOAc). Spectral data the same as enantiomer (+)-**3l**.

$[\alpha]^{20}_D$ –13.2° (*c* 2.1, $CHCl_3$). The product was benzoylated according to the preceding method for HPLC analysis. ChiralPak AD-H, *i*-PrOH/hexane = 15/85, 0.8 mL/min, 230 nm, t_{major} = 35.1 min, t_{major} = 52.5 min.

6.3.3. Optimization Tables

Table 6.4. Optimization of conditions for azomethine imine **1d**[a]

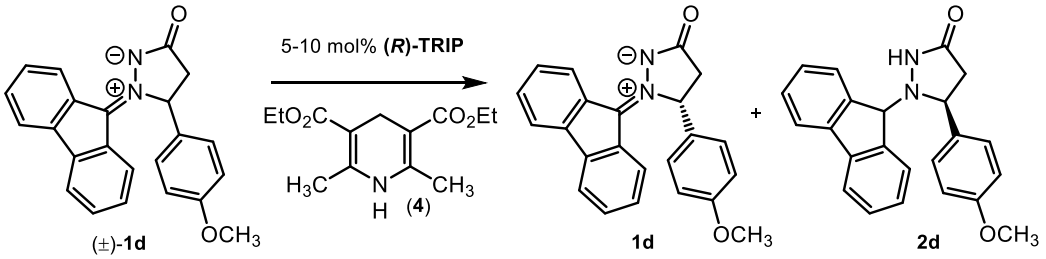

Entry	Equiv **4**	mol% (*R*)-TRIP	T(°C)	solvent	[**1d**] M	t (h)	% Conversion[b]	**1d**[c] %ee	**2d**[c] %ee
1	1.4	5	rt	CH_2Cl_2	0.10	48	16	nd	82
2	1.4	5	rt	CH_2Cl_2	0.05	48	13	nd	89
3	1.4	5	rt	CH_2Cl_2	0.02	50	9	nd	88
4	1.4	5	35	CH_2Cl_2	0.02	50	15	nd	89
5	1.4	10	60	$PhCH_3$	0.04	17	60	99	66
6	1.4	5	60	$PhCH_3$	0.02	5	49	82	85
7	1.4	5	60	$PhCH_3$	0.02	16	55	95	77
8	0	10	60	$PhCH_3$	0.04	16	0	0	nd

a) Conditions: azomethine imine (±)-1d (1 equiv), 4 (1.4 or 0 equiv), and (R)-TRIP (5-10 mol%) in solvent (0.02 -0.10 M) stirred under Argon. b) Conversion (%) determined by 1H NMR of crude mixture c) Enantiomeric excess determined by HPLC Chiral-Pak ADH column, compared to corresponding racemate, nd = not determined.

Table 6.5. Optimization of conditions for azomethine imine **1f**[a]

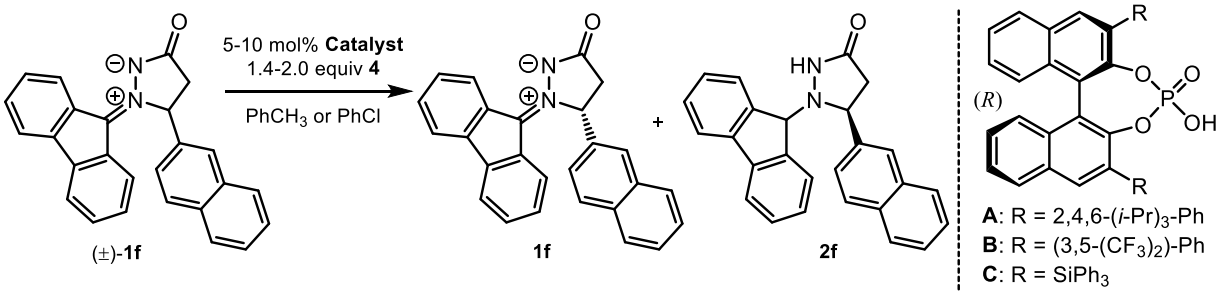

Entry	Catalyst	mol% Catalyst	Equiv **4**	T (°C)	solvent	[**1f**] M	t (h)	% Conversion[b]	**1f**[c] %ee	**2f**[c] %ee
1	A	10	1.4	60	$PhCH_3$	0.02	21	17	nd	nd
2	A	5	1.4	60	$PhCH_3$	0.02	70	26	nd	nd
3	B	5	1.4	60	$PhCH_3$	0.04	73	17	nd	nd
4	C	5	1.4	80	$PhCH_3$	0.04	73	21	nd	nd
5	A	10	1.4	60	PhCl	0.01	20	52	85	82
6	A	10	1.4	80	PhCl	0.01	24	53	94	74
7	A	10	2.0	80	PhCl	0.01	73	59	98	67

a) Conditions: azomethine imine (±)-**1f** (1 equiv), **4** (1.4 or 2 equiv), and (*R*)-TRIP (5-10 mol%) in solvent (0.01-0.04 M) stirred under Argon. b) Conversion (%) determined by ^{1}H NMR of crude mixture c) Enantiomeric excess determined by HPLC Chiral-Pak ADH column, compared to corresponding racemate, nd = not determined.

Table 6.6. Optimization of conditions for azomethine imine **1h**[a]

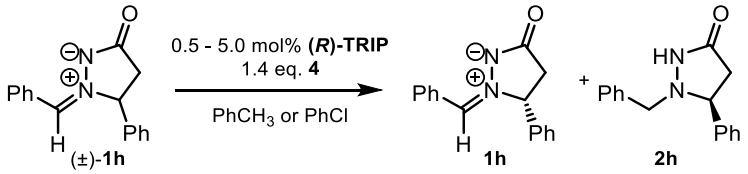

Entry	mol% (*R*)-TRIP	T (°C)	solvent	t (h)	% Conversion[b]	**1h**[c] %ee	**2h**[c] %ee
1	0.5	60	$PhCH_3$	5	52	73	75
2	0.5	60	$PhCH_3$	21	68	99	70
3	0.5	60	$PhCH_3$	16	41	47	92-98
4	1.0	50	PhCl	16	51	77	81
5	1.0	50	PhCl	40	61	91	80
6	5.0	50	$PhCH_3$	16	71	nd	nd
7	2.5	40	$PhCH_3$	6	57	94	86
8	5.0	40	PhCl	16	68	>99	67
9	5.0	40	$PhCH_3$	16	67	>99	63

a) Conditions: azomethine imine (±)-**1h** (1 equiv), **4** (1.4 equiv), and (*R*)-TRIP (0.5-5 mol%) in solvent (0.025 M in $PhCH_3$ or 0.05 M in PhCl) stirred under Argon. b) Conversion (%) determined by ^{1}H NMR of crude mixture c) Enantiomeric excess determined by HPLC Chiral-Pak ADH column, compared to corresponding racemate, nd = not determined.

Table 6.7. Optimization of conditions for azomethine imine **1o**[a]

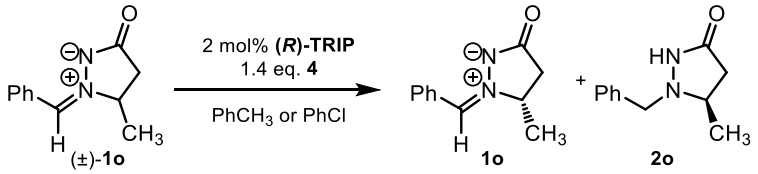

Entry	T(°C)	solvent	t (h)	% Conversion[b]	**1o**[c] %ee	**2o**[c] %ee
1	40	$PhCH_3$	6	<5%	nd	nd
2	60	PhCl	16	54	45	55

a) Conditions: azomethine imine (±)-**1o** (1 equiv), **4** (1.4 equiv), and (*R*)-TRIP (2 mol%) in solvent ($PhCH_3$ or PhC, 0.05 Ml) stirred under Argon. b) Conversion (%) determined by ^{1}H NMR of crude mixture. c) Enantiomeric excess determined by HPLC Chiral-Pak ADH column, compared to corresponding racemate, nd = not determined.

6.3.4. Additional kinetic resolution attempts for ketone-derived azomethine imines

Complex ketone-derived azomethine imines are difficult to synthesize with available methods.[2,14–16] Condensation gave very low yields, and both condensation and aminocarbonylation can give an inseparable mixture of E/Z diastereomers. Also, aliphatic azomethine imines are unstable towards hydrolysis and difficult to isolate. Attempts at the synthesis of ketone-derived azomethine imines (various methods and conditions were used), and an unsuccessful kinetic resolution, are given below.

Attempted syntheses of azomethine imines

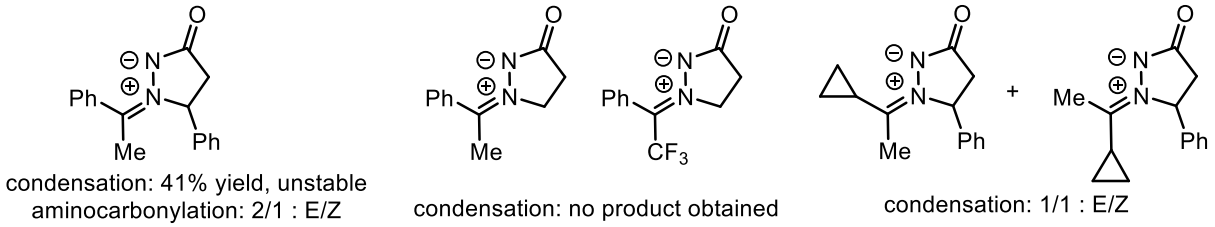

Unsuccessful kinetic resolution

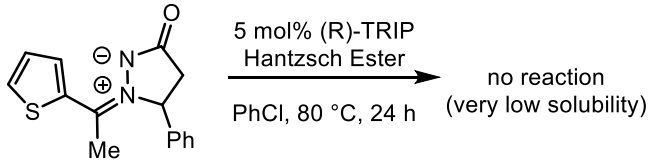

Scheme 6.1 Attempted kinetic resolution of a complex ketone-derived azomethine imines.

6.3.5. Additional kinetic resolution attempts for acyclic azomethine imines

This work was not presented in the article or its published supporting information.

Table 6.8. Exploration into reduction of acyclic azomethine imines from hydrazones.[a]

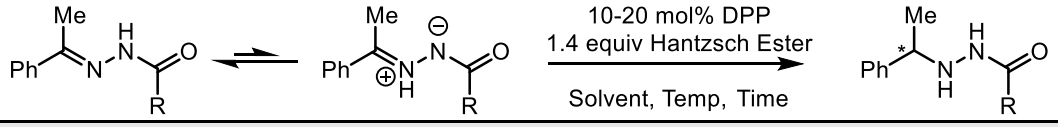

Entry	R	mol% DPP	T (°C)	solvent	t (h)	Result[b]
1	O*t*-Bu	10	rt	$PhCH_3$	16	no reaction
2	O*t*-Bu	10	110	$PhCH_3$	1	trace product
3	Ph	20	110	$PhCH_3$	2	mixture

a) Conditions: Hydrazone (1 equiv), Hantzsch Ester (1.4 equiv), and DPP (10-20 mol%) in solvent (0.025-0.05 M in $PhCH_3$) stirred under Argon at the given temperature and time, and monitored by TLC. b) Determined by analysis of the ^{1}H NMR of the crude mixture

Table 6.9. Exploration into reduction of acyclic azomethine imines from 1,2-disubstituted hydrazines.[a]

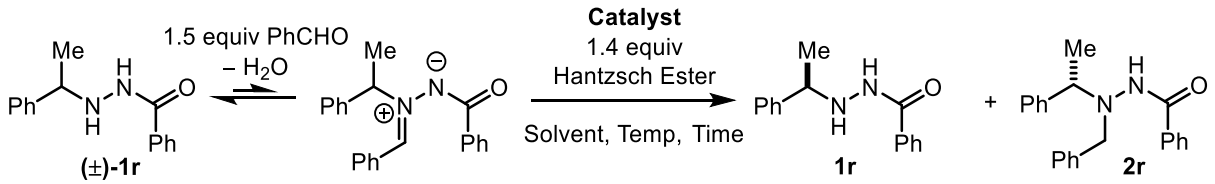

Entry	Additive	Catalyst	T(°C)	solvent	t (h)	**1r**[b] (e.r.)[c]	**2r**[b] (e.r.)[c]
1	4 Å MS	20 mol% DPP	100	$PhCH_3$	16	nd	trace
2	-	20 mol% DPP	100	$PhCH_3$	16	nd	trace
3	4 Å MS	20 mol% DPP	50	$PhCF_3$	24	nd	<5%
4	4 Å MS	20 mol% DPP	41	CH_2Cl_2	24	83%	17%
5	4 Å MS	2 mol% (*R*)-TRIP	41	CH_2Cl_2	24	16% [52:48]	12% (55:45)

a) Conditions: **(±)-1r** (1 equiv), Hantzsch Ester (1.4 equiv), benzaldehyde (1.5 equiv), and catalyst (2-20 mol%) in solvent (0.025-0.05 M) stirred under Argon at the given temperature and time, and monitored by TLC. b) NMR yield determined by analysis of the ^{1}H NMR of the crude mixture with 1,2,5-trimethoxybenzene internal standard, nd = not determined. c) Enantiomeric excess determined by HPLC Chiral-Pak ADH column, compared to corresponding racemate. d) isolated yield obtained by prep TLC, **1r** was difficult to isolate while product **2r** was easily isolated.

6.4. Intermolecular Aminocarbonylation of Imines

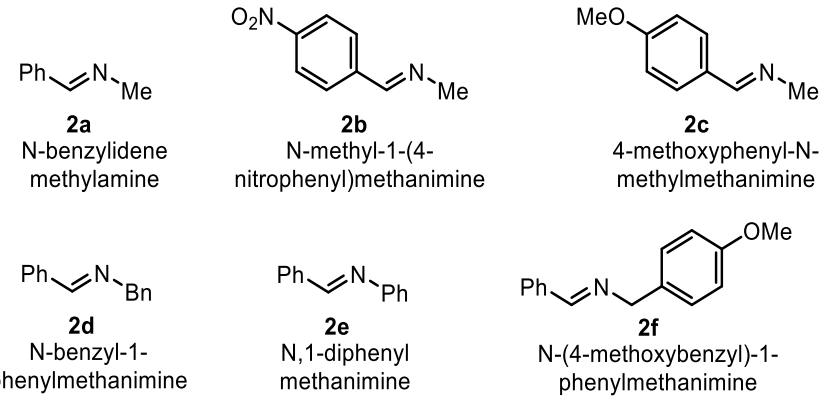

Imines **2a**,[17] **b**,[18] **c**,[17] **d-f**,[19] and hydrazones **1a**,**d**,**g** [2] were prepared by known methods following literature procedures.

General Procedure 4A: Synthesis of Aldehyde-derived Hydrazones[24]

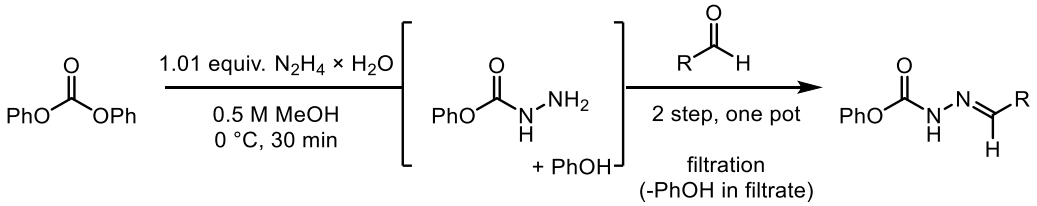

Hydrazones **1b**,**c**,**e** were synthesized by the following one-pot method, which is a modification of the known two-step procedure.[2] Diphenyl carbonate (1.0 equiv) in MeOH (0.5 M) in a round bottom flask was cooled in an ice bath with stirring. Hydrazine hydrate (50-60 wt%, 1.01 equiv) was added and the mixture stirred for 30 minutes in the ice bath until TLC analysis in 1/1:Et_2O/Hexane showed complete consumption of diphenyl carbonate. Aldehyde (1.05 equiv) was added and the mixture was allowed to warm to room temperature. The hydrazone precipitates from the mixture and was isolated by filtration, rinsing the precipitate with diethyl ether.

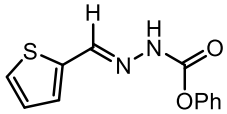

1b. Synthesized according to general procedure 4A from diphenyl carbonate (2.12 g, 9.9 mmol) and 2-thiophene carboxaldehyde (0.94 mL, 10 mmol). White solid (1.96 g, 80% isolated yield). Spectral data is in agreement with the literature.[2,20]

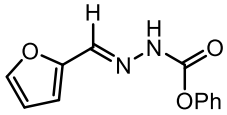

1c. Synthesized according to general procedure 4A from diphenyl carbonate (14.8 g, 69.0 mmol) and freshly distilled furfural (6.0 mL, 72 mmol). White solid (11.2 g, 71% isolated yield). Spectral data is in agreement with the literature.[2,20]

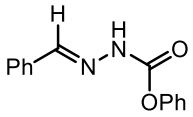

1e. Synthesized according to general procedure 4A from diphenyl carbonate (2.12 g, 9.9 mmol) and benzaldehyde (1.02 mL, 10.0 mmol). White solid (1.78 g, 75% isolated yield). Spectral data is in agreement with the literature.[2,20]

General Procedure 4B: Aminocarbonylation of Imines with Imino-isocyanates[24]

Hydrazone **1** (1.0 equiv), imine **2** (1.5-2.0 equiv), and $PhCF_3$ (0.05-0.10 M) were combined in a dry vial, which was sealed and purged with Argon. The mixture was heated (by microwave irradiation or conventional heating) to 120-130 °C for 1-3 hours. The reaction mixture was cooled to ambient temperature and concentrated under reduced pressure. The crude mixture was purified by silica gel column chromatography or by trituration in Et_2O, isolated yields are provided.

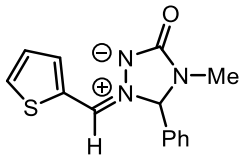

3b. Synthesized according to general procedure 4B, from **1b** (0.044 g, 0.18 mmol, 1 equiv), **2a** (0.043 g, 0.36 mmol, 2 equiv), and $PhCF_3$ (3.6 mL) were combined in a microwave vial. The reaction time was 2 h at 130 °C. Crude ^1H NMR with 1,3,5-trimethoxybenzene internal standard showed 78% yield of the dipole. The crude mixture was purified by chromatography using EtOAc/CH_2Cl_2 (80:20). The fractions containing the product were combined and concentrated in vacuo, providing a light yellow fine powder (0.034 g, 69% yield). TLC R_f = 0.15 (8/2 : EtOAc /CH_2Cl_2). ^1H NMR (400 MHz, DMSO-d_6) δ 7.94 (d, *J* = 5.00 Hz, 1H), 7.66 (d, *J* = 1.96 Hz, 1H), 7.63 (d, *J* = 3.82 Hz, 1H), 7.44 - 7.56 (m, 5H), 7.20 (dd, *J* = 3.87, 5.05 Hz, 1H), 6.61 (d, *J* = 1.86 Hz, 1H), 2.63 (s, 3H). ^{13}C NMR (101 MHz, DMSO-d_6) δ 164.8, 135.5, 133.6, 132.4, 132.1, 130.6, 129.5, 127.7, 127.7, 121.6, 84.4, 27.1. IR (ATR diamond): 3053, 1681, 1586, 1368, 1351, 1233, 1193, 1096, 1043, 780, 722 cm^{-1}. HRMS (EI): Exact mass calculated for $C_{14}H_{13}N_3OS$ $[M]^+$: 271.07793. Found: 271.07952.

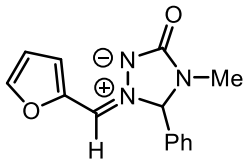

3c. Synthesized according to general procedure 4B, from **1c** (0.463 g, 2.01 mmol, 1 equiv) and **2a** (0.358 g, 3.00 mmol, 1.5 equiv) in 20 mL (0.10 M) $PhCF_3$. The reaction time was 3 hours at 120 °C. The product was isolated by trituration in Et_2O followed by filtration, and obtained as a yellow solid (0.296 g, 58%). TLC R_f = 0.13 (EtOAc). ^1H NMR (400 MHz, DMSO-d_6) δ 7.90 (s, 1 H), 7.57 (d, *J* = 3.3 Hz, 1 H), 7.55 - 7.50 (m, 3 H), 7.50 - 7.41 (m, 2 H), 7.24 (d, *J* = 1.9 Hz, 1 H), 6.77 (dd, *J* = 1.5, 3.2 Hz, 1 H), 6.58 (s, 1 H), 2.64 (s, 3 H). ^{13}C NMR (76 MHz, DMSO-d_6) δ 165.2,

146.2, 146.1, 135.5, 130.6, 129.5, 127.6, 117.8, 115.0, 113.4, 84.9, 27.0. IR (ATR diamond) 3115, 3090, 1726, 1684, 1591, 1353 cm^{-1}. HRMS (EI): Exact mass calculated for $C_{14}N_{13}N_3O_2$ $[M]^+$: 255.10078. Found: 255.10023.

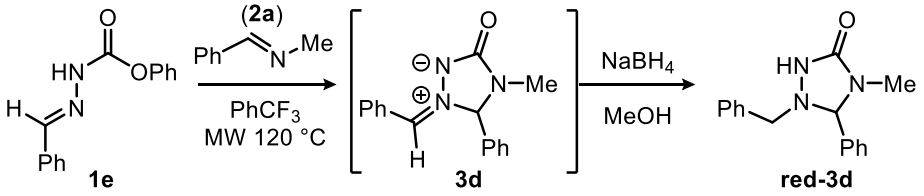

3d. Hydrazone (**1e**, 0.117 g, 0.487 mmol, 1 equiv), **2a** (0.120 g, 1.01 mmol, 2 equiv), and $PhCF_3$ (10 mL) were combined in a microwave vial. The vial was sealed and purged with Argon, then heated by microwave irradiation at 120 °C for one hour. The mixture was concentrated in vacuo to remove solvent (rotavap) and excess imine (60 °C, 2 mmHg). Crude ^1H NMR with 1,3,5-trimethoxybenzene internal standard showed 50% yield of **3d**. Product **3d** was unstable towards hydrolysis in $CDCl_3$ and on silica gel.

The crude mixture was diluted in MeOH (10 mL) and treated with excess sodium borohydride (~30 mg). The reaction was stirred at room temperature until completion as judged by TLC (5/95:MeOH/CH_2Cl_2, CAM stain). The reaction was quenched with aqueous NH_4Cl, extracted with 3x10 mL CH_2Cl_2, and the organic phase washed with brine then dried with Na_2SO_4. The product was isolated by column chromatography, providing ***red*-3d** as a crystalline white solid (0.0491 g, 39% yield over two steps). TLC R_f = 0.3 (1/1 : EtOAc/Hexane). ^1H NMR (400 MHz, $CDCl_3$) δ 7.54 - 7.34 (m, 5 H), 7.34 - 7.05 (m, 5 H), 5.62 (s, 1 H), 4.87 (s, 1 H), 3.91 (d, J = 12.5 Hz, 1 H), 3.71 (d, J = 12.5 Hz, 1 H), 2.59 (s, 3 H). ^{13}C NMR (100 MHz, $CDCl_3$) δ 160.7, 136.4, 136.3, 129.9, 129.4, 129.0, 128.7, 128.3, 128.0, 84.6, 61.5, 28.0. IR (ATR diamond) 3179, 3047, 2963, 2909, 2852, 2807, 1708, 1437, 1357 cm^{-1}. HRMS (EI): Exact mass calculated for $C_{16}N_{17}N_3O$ $[M]^+$: 267.13716. Found: 267.13922.

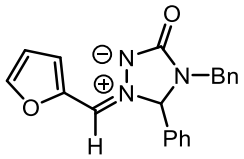

3e. Synthesized according to general procedure 4B, from **1c** (0.231 g, 1.00 mmol, 1 equiv) and **2d** (0.391 g, 2.01 mmol, 2 equiv) in 10 mL (0.10 M) $PhCF_3$. The reaction time was 3 hours at 120 °C. Product isolated by trituration in Et_2O followed by filtration. Pale yellow solid (0.211 g, 64%). TLC R_f = 0.38 (EtOAc). ^{1}H NMR (300 MHz, DMSO-d_6) δ 7.97 - 7.85 (m, 1 H), 7.61 (d, J = 3.5 Hz, 1 H), 7.56 - 7.34 (m, 5 H), 7.34 - 7.20 (m, 3 H), 7.20 - 7.08 (m, 3 H), 6.78 (dd, J = 1.7, 3.5 Hz, 1 H), 6.46 (d, J = 1.5 Hz, 1 H), 4.79 (d, J = 15.5 Hz, 1 H), 3.77 (d, J = 15.5 Hz, 1 H). ^{13}C NMR (76 MHz, DMSO-d_6) δ 164.9, 146.4, 145.9, 136.9, 135.4, 130.6, 129.5, 128.6, 127.8, 127.6, 127.4, 118.2, 115.9, 113.4, 83.0, 43.8. IR (ATR diamond) 3113, 3058, 1665, 1595, 1551, 1467 cm^{-1}. HRMS (EI): Exact mass calculated for $C_{20}N_{17}N_3O_2$ $[M]^+$: 331.13208. Found: 331.13087.

One-pot reaction (3e): Benzaldehyde (0.021 g, 0.20 mmol) was weighed into a clean, dry flask and diluted with $PhCF_3$ (2 mL) with 4 Å molecular sieves (0.033 g). Benzylamine (21 µL, 0.20 mmol) was added, followed by **1c** (0.023 g, 0.10 mmol, 1.0 equiv) The mixture was heated at 120 °C for 3 hours. The ^{1}H NMR of the crude mixture showed 40% yield of the desired product using 1,3,5-trimethoxybenzene internal standard (13.6 mg).

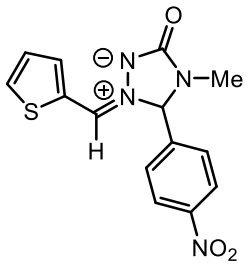

3f. Synthesized according to general procedure 4B from **1b** (0.223 g, 0.905 mmol, 1 equiv), **2b** (0.254 g, 1.55 mmol, 2 equiv), and $PhCF_3$ (18 mL). The reaction time was 2 hours at 120 °C.

Analysis of the crude mixture by ^{1}H NMR with 1,3,5-trimethoxybenzene internal standard showed 73% yield of the dipole. The crude mixture was diluted in $PhCF_3$ (6 mL) and stirred in an ice bath for 15 min. Product isolated by trituration in Et_2O (6 mL) followed by filtration, providing an orange-yellow powder (0.116 g, 41% yield). TLC R_f = 0.15 (2/8 CH_2Cl_2/EtOAc). ^{1}H NMR (400 MHz, DMSO-d_6) δ 8.33 - 8.43 (m, 2H), 7.97 (d, J = 5.09 Hz, 1H), 7.71 - 7.85 (m, 3H), 7.63 (d, J = 3.72 Hz, 1H), 7.22 (dd, J = 3.92, 5.09 Hz, 1H), 6.77 - 6.84 (m, 1H), 2.65 (s, 3H). ^{13}C NMR (101 MHz, DMSO-d_6) δ 164.7, 148.8, 142.1, 134.1, 132.9, 132.0, 129.4, 127.8, 124.7, 122.5, 83.1, 27.2. IR (ATR diamond) 3113, 3058, 1595, 1552, 1467, 1454, 1426, 1411, 1380, 1349, 1322, 1275, 1235, 1197 cm^{-1}. HRMS (ESI): Exact mass calculated for $C_{14}H_{12}N_4O_2SNa$ $[M+Na]^+$: 339.0528. Found: 339.0550.

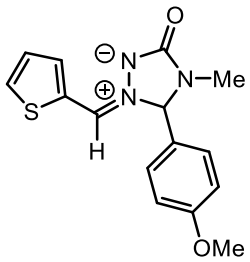

3g. Synthesized according to general procedure 4B from **1b** (0.222 g, 0.900 mmol, 1 equiv), **2c** (0.269 g, 1.80 mmol, 2 equiv), and $PhCF_3$ (18 mL) The reaction time was 1 h at 120 °C. Analysis of the crude mixture by ^{1}H NMR with 1,3,5-trimethoxybenzene internal standard showed 84% yield of the dipole. The crude mixture was diluted in $PhCF_3$ (6 mL) and stirred in an ice bath for 15 min. The precipitate was filtered and triturated in Et_2O (6 mL) for 30 min. The solid was filtered, rinsed with Et_2O and dried, providing a light yellow fine powder (0.186 g, 69% yield). TLC R_f = 0.13 (2/8 CH_2Cl_2/EtOAc). ^{1}H NMR (400 MHz, DMSO-d_6) δ 7.92 (d, J = 5.00 Hz, 1H), 7.56 - 7.67 (m, 2H), 7.40 (d, J = 8.62 Hz, 2H), 7.18 - 7.25 (m, 1H), 7.07 (d, J = 8.62 Hz, 2H), 6.54 (d, J = 1.47 Hz, 1H), 3.79 (s, 3H), 2.62 (s, 3H). ^{13}C NMR (101 MHz, DMSO-d_6) δ 164.7, 160.8, 133.4, 132.3,

132.2, 129.3, 127.6, 127.2, 121.3, 114.8, 84.2, 55.3, 27.1. IR (ATR diamond): 3070, 2954, 2838, 1684, 1666, 1584, 1509, 1417, 1368, 1306, 1233, 1195 cm^{-1}. HRMS (EI): Exact mass calculated for $C_{15}H_{15}N_3O_2S$ $[M]^+$: 301.08850. Found: 301.08807.

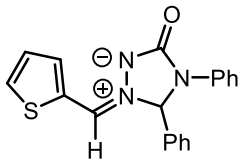

3h. Synthesized according to general procedure 4B, from **1b** (0.045 g, 0.18 mmol, 1 equiv), **2e** (0.065 g, 0.36 mmol, 2 equiv), and $PhCF_3$ (3.6 mL) were combined in a microwave vial. The reaction time was 1 h at 120 °C. The crude mixture was purified by chromatography using EtOAc/CH_2Cl_2/Hexanes/Et_3N (50:30:20:0.1). The fractions containing the product were combined and concentrated in vacuo, providing a light yellow fine powder (0.024 g, 39% yield). TLC R_f = 0.39 (3/7/0.1 Hexanes/EtOAc/Et_3N). ^1H NMR (400 MHz, DMSO-d_6) δ 8.02 (d, J = 5.00 Hz, 1H), 7.90 (s, 1H), 7.75 (d, J = 3.82 Hz, 1H), 7.58 - 7.65 (m, 2H), 7.39 - 7.54 (m, 6H), 7.19 - 7.30 (m, 3H), 6.96 (app t, J = 7.35 Hz, 1H). ^{13}C NMR (101 MHz, DMSO-d_6) δ 161.6, 137.0, 136.0, 134.7, 133.7, 131.7, 130.5, 129.6, 128.6, 127.8, 127.4, 122.9, 122.7, 119.4, 82.0. IR (ATR diamond): 3062, 2918, 1674, 1538, 1497, 1328, 1240, 1208 cm^{-1}. HRMS (EI): Exact mass calculated for $C_{19}N_{15}N_3OS$ $[M]^+$: 333.09358. Found: 333.09459.

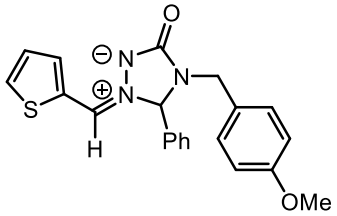

3i. Synthesized according to general procedure 4B, from **1b** (0.045 g, 0.183 mmol, 1 equiv), **2g** (0.082 g, 0.365 mmol, 2 equiv), and $PhCF_3$ (3.6 mL) The reaction time was 42 min at 130 °C. Analysis of the crude mixture by ^1H NMR with 1,3,5-trimethoxybenzene internal standard showed

80% yield of the dipole. The crude mixture was diluted in $PhCF_3$ (1.8 mL) and stirred in an ice bath for 15 min. The precipitate was filtered and triturated in Et_2O (3 mL) for 30 min. The solid was filtered, rinsed with Et_2O and dried, providing a light yellow fine powder (0.042 g, 62% yield). TLC R_f = 0.43 (1/1 CH_2Cl_2/EtOAc). ^{1}H NMR (300 MHz, DMSO-d_6) δ 7.92 - 8.00 (m, 1H), 7.59 - 7.67 (m, 1H), 7.56 (d, *J* = 2.0 Hz, 1H), 7.45 - 7.54 (m, 3H), 7.35 - 7.44 (m, 2H), 7.20 (dd, *J* = 3.9, 5.2 Hz, 1H), 7.05 (d, *J* = 8.7 Hz, 2H), 6.85 (d, *J* = 8.7 Hz, 2H), 6.44 (d, *J* = 1.9 Hz, 1H), 4.72 (d, *J* = 15.3 Hz, 1H), 3.72 (s, 3H), 3.67 (d, *J* = 15.1 Hz, 1H). ^{13}C NMR (101 MHz, DMSO-d_6) δ 164.4, 158.5, 135.4, 133.9, 132.7, 132.0, 130.5, 129.4, 129.2, 128.7, 127.8, 127.7, 122.3, 113.9, 82.4, 55.0, 43.3. IR (ATR diamond): 3043, 2832, 1719, 1676, 1580, 1458, 1232 cm^{-1}. HRMS (EI): Exact mass calculated for $C_{21}H_{19}N_3O_2S$ $[M]^+$: 377.11980. Found: 377.12486.

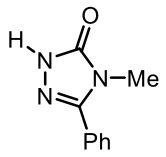

6. Azomethine imine **3c** (0.122 g, 0.478 mmol, 1 equiv) was combined with hydroxylamine (50 wt% in H_2O, 70.6 mg, 1.07 mmol, 2 equiv) in MeOH (10 mL). The mixture was heated to reflux for 5 hours. The mixture was concentrated in vacuo, and the product isolated by column chromatography with EtOAc eluent and obtained as a white, crystalline solid (0.062 g, 74% isolated yield from dipole). Spectral data in agreement with the literature.[21] ^{1}H NMR (300 MHz, $CDCl_3$) δ 11.10 (br. s, 1 H), 7.67 - 7.55 (m, 2 H), 7.55 - 7.31 (m, 3 H), 3.38 (s, 3 H). ^{13}C NMR (75 MHz, $CDCl_3$) δ 156.6, 147.8, 130.5, 129.1, 128.1, 127.1, 29.1. IR (ATR diamond) 3166, 3056, 2836, 1690, 1508, 1452 cm^{-1}.

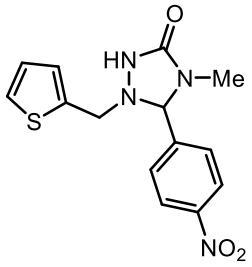

7. Azomethine imine **3f** (0.0270 g, 0.0854 mmol, 1 equiv) in MeOH (2 mL) was cooled to 0 °C, then $NaBH_4$ (8 mg, 0.2 mmol, ~2 equiv) was added. The mixture was stirred for 30 min at 0 °C. The mixture was quenched with aqueous NH_4Cl and extracted with EtOAc. The combined organic layers were dried with Na_2SO_4, filtered, then concentrated in vacuo to give the product as an off-white, crystalline solid (0.0242 g, 89%). TLC R_f = 0.14 (50% EtOAc, 50% Hexane). ^{1}H NMR (400 MHz, $CDCl_3$) δ 8.32 - 8.15 (m, 2 H), 7.58 - 7.39 (m, 2 H), 7.28 - 7.24 (m, 1 H), 7.05 - 6.98 (m, 1 H), 6.95 (dd, *J* = 3.5, 5.1 Hz, 1 H), 6.17 (br. s., 1 H), 5.07 (s, 1 H), 4.21 - 4.00 (m, 2 H), 2.63 (s, 3 H). ^{13}C NMR (101 MHz, $CDCl_3$) δ 160.1, 148.8, 143.8, 137.6, 128.8, 127.8, 126.9, 126.7, 124.2, 82.5, 57.0, 28.1. IR (ATR diamond) 3189, 3081, 2954, 2851, 1705, 1657, 1516, 1347 cm^{-1}. LRMS (ESI): Exact mass calculated for $C_{14}H_{13}N_4O_3S$ $[M–H]^{\bullet+}$: 317.07138. Found: 317.0792.

Competition experiment

Hydrazones **1b** and **1c** (1 equiv each) were combined in a vial with imine **2a** (1 equiv) and $PhCF_3$ and heated by microwave irradiation at 130 °C for 10 min. ^{1}H NMR of the crude mixture (DMSO-d_6) cleanly showed 98% conversion of the imine to products **3c** (62% conversion of **1c**) and **3b** (33% conversion of **1b**), and production of approximately 1 equiv PhOH. *Assuming equal ability to generate the imino-isocyanate at this temperature*, this result shows the increased reactivity of the furyl imino-isocyanate at short reaction times, and supports our argument that the lower yield of **3c** vs. **3b** after a reaction time of 2 hours (Table 4.2) is due to differences in product stability.

Cycloreversion Experiment

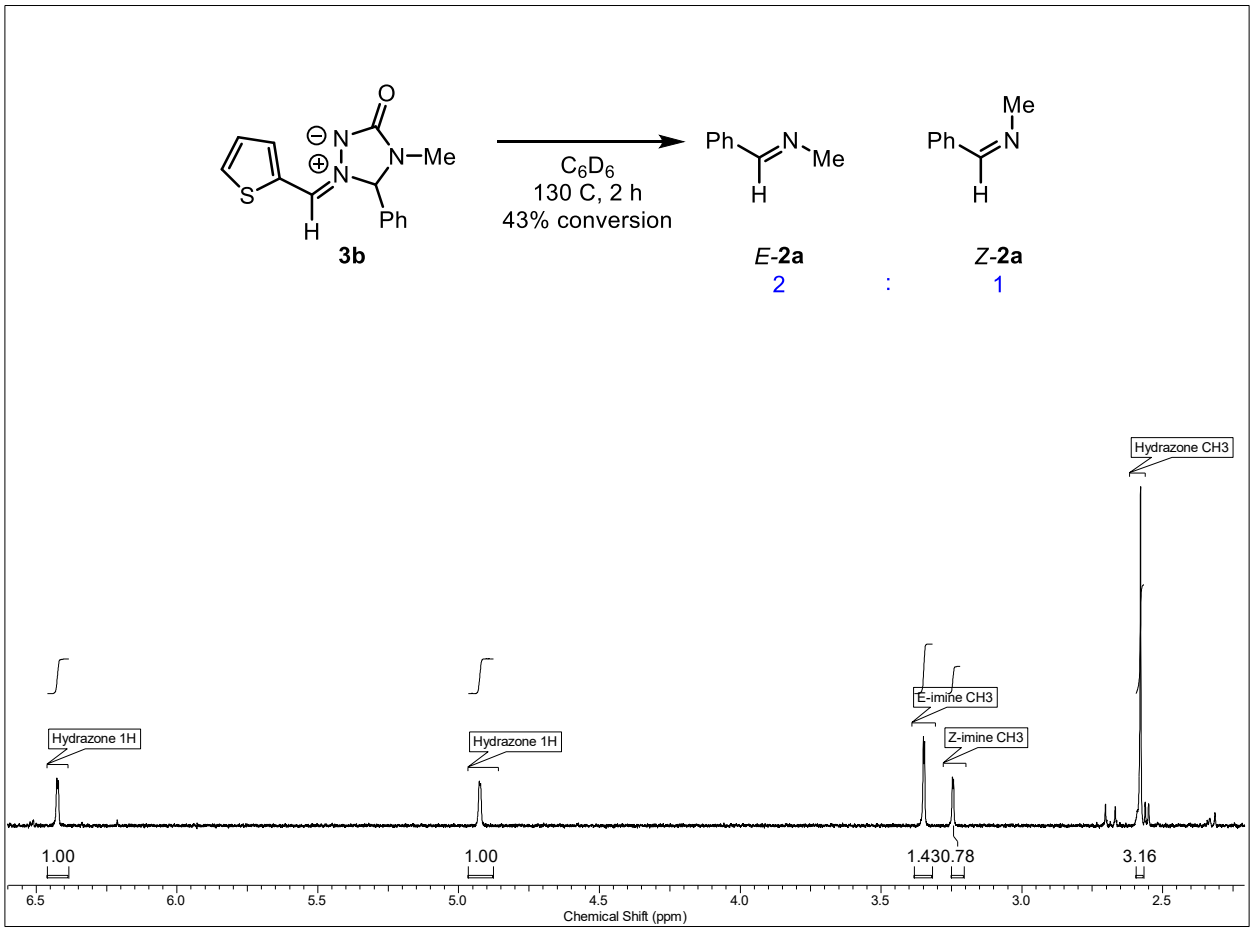

*Figure 6.3 Spectrum showing cycloreversion products from **3b**, the E-**2a** and Z-**2a**. The dipole **3b** was heated for 2 hours in benzene-d_6 at 130 ℃. Direct analysis of the reaction mixture showed 43% conversion to a 2:1 mixture of E-**2a**:Z-**2a**. Isocyanate degradation producucts were observed in the aromatic region.*

6.4.2. X-ray Crystallographic Information

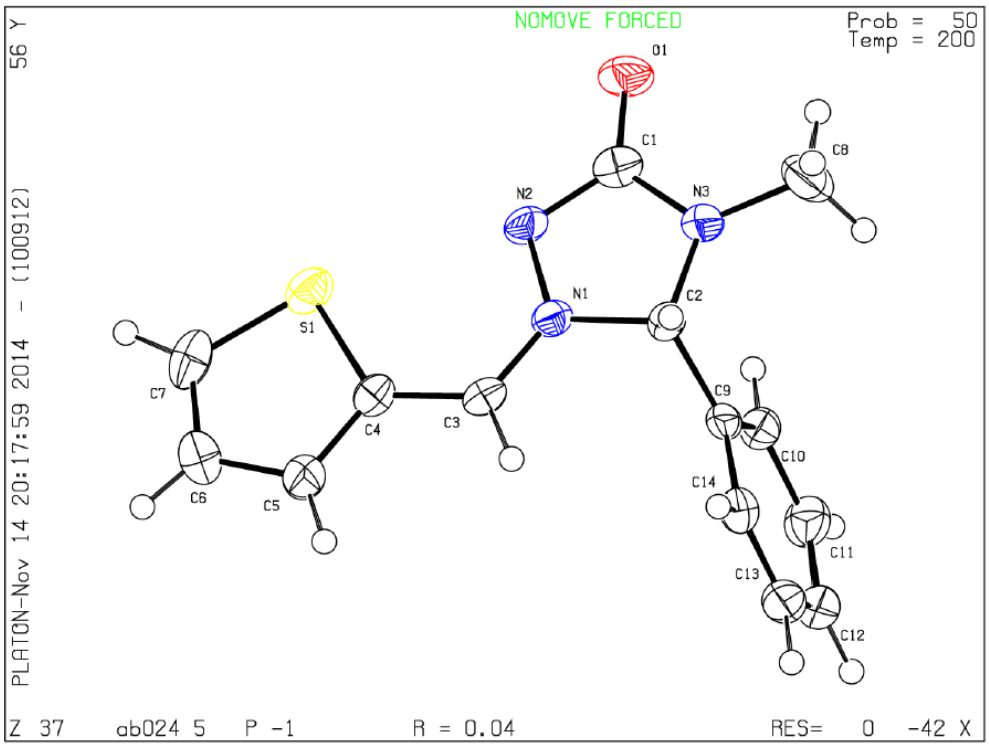

Datablock: ab024_5

Bond precision: C-C = 0.0054 A Wavelength=0.71073

Cell: a=5.6316(4) b=8.8731(6) c=13.3605(7)
alpha=76.690(3) beta=87.767(3) gamma=85.418(3)
Temperature: 200 K

	Calculated	Reported
Volume	647.47(7)	647.47(7)
Space group	P -1	P -1
Hall group	-P 1	-P 1
Moiety formula	C14 H13 N3 O S	?
Sum formula	C14 H13 N3 O S	C14 H13 N3 O S
Mr	271.33	271.33
Dx,g cm-3	1.392	1.392
Z	2	2
Mu (mm-1)	0.245	0.245
F000	284.0	284.0
F000'	284.34	
h,k,lmax	6,10,15	6,10,15
Nref	2223	2138
Tmin,Tmax	0.983,0.998	0.644,0.745
Tmin'	0.964	

Correction method= MULTI-SCAN

Data completeness= 0.962 Theta(max)= 24.746

R(reflections)= 0.0415(1723) wR2(reflections)= 0.1199(2138)

S = 1.055 Npar= 173

*Figure 6.4. Single crystal X-ray ellipsoid plot and acquisition information for **3b**.*

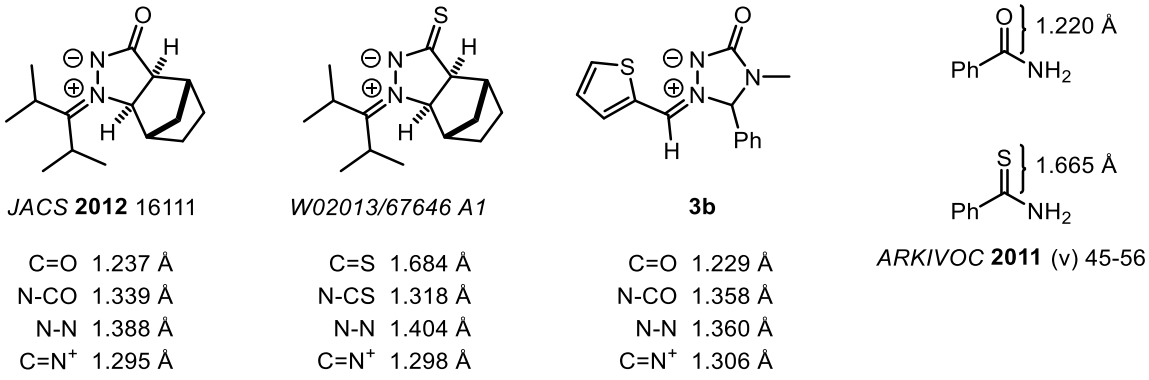

*Figure 6.5. Comparison of selected bond lengths from X-ray crystal structures: Compound **3b**, a previously reported azomethine imine,[1] the thioxo-analog,[2] and (thio)benzamides.[25]*

6.5. Supporting Information References

(1) Clavette, C.; Gan, W.; Bongers, A.; Markiewicz, T.; Toderian, A. B.; Gorelsky, S. I.; Beauchemin, A. M. *J. Am. Chem. Soc.* **2012**, *134*, 16111.
(2) Gan, W.; Moon, P. J.; Clavette, C.; Das Neves, N.; Markiewicz, T.; Toderian, A. B.; Beauchemin, A. M. *Org. Lett.* **2013**, *15*, 1890.
(3) Lu, X.; Reid, D. L.; Warkentin, J. *Can. J. Chem.* **2001**, *79*, 319.
(4) Garcia-Ramos, Y.; Proulx, C.; Lubell, W. D. *Can. J. Chem.* **2012**, *90*, 985.
(5) Li, L.-C.; Ren, J.; Liao, T.-G.; Jiang, J.-X.; Zhu, H.-J. *European J. Org. Chem.* **2007**, 1026.
(6) Suárez, A.; Downey, C. W.; Fu, G. C. *J. Am. Chem. Soc.* **2005**, *127*, 11244.
(7) Geraghty, N. W. A.; McArdle, P.; Mullen, L. M. A. *Tetrahedron* **2011**, *67*, 3546.
(8) Shintani, R.; Soh, Y.-T.; Hayashi, T. *Org. Lett.* **2010**, *12*, 4106.
(9) Beauchemin, A. M.; Clavette, C.; Gan, W.; Markiewicz, T.; Toderian, A. B. Process for the Synthesis of Beta-Amino Carbonyls. W02013/67646 A1.
(10) Wang, G.-W.; Xia, J.-J.; Miao, C.-B.; Wu, X.-L. *Bull. Chem. Soc. Jpn.* **2006**, *79*, 454.
(11) Klussmann, M.; Ratjen, L.; Hoffmann, S.; Wakchaure, V.; Goddard, R.; List, B. *Synlett* **2010**, *2010*, 2189.
(12) Keith, J. M.; Larrow, J. F.; Jacobsen, E. N. *Adv. Synth. Catal.* **2001**, *343*, 5.
(13) Wang, M.; Huang, Z.; Xu, J.; Chi, Y. R. *J. Am. Chem. Soc.* **2014**, *136*, 1214.
(14) Shintani, R.; Fu, G. C. *J. Am. Chem. Soc.* **2003**, *125*, 10778.
(15) Dorn, H.; Otto, A. *Angew. Chemie Int. Ed.* **1968**, *7*, 214.
(16) Shantl, J. G. Pawda, A.; Bellus, D., Eds.; Thieme, 2004; Vol. 27, pp. 731–824.
(17) Zhang, Y.; Ji, J.; Zhang, X.; Lin, S.; Pan, Q.; Jia, L. *Org. Lett.* **2014**, *16*, 2130.
(18) Tanaka, S.; Tagashira, N.; Chiba, K.; Yasuda, M.; Baba, A. *Angew. Chemie Int. Ed.* **2008**, *47*, 6620.
(19) Derdau, V.; Snieckus, V. *J. Org. Chem.* **2001**, *66*, 1992.
(20) Berger, R.; Duff, K.; Leighton, J. L. *J. Am. Chem. Soc.* **2004**, *126*, 5686.
(21) Kane, J. M. *Synthesis* **1987**, *1987*, 912.
(22) K. Lavergne, A. Bongers, L. Betit, A. M. Beauchemin, *Org. Lett*. **2015**, *17*, 3612.
(23) Bongers, A.; Moon, P. J.; Beauchemin, A. M. *Angew. Chemie Int. Ed.* **2015**, *54*, 15516.
(24) Bongers, A.; Ranasinghe, I.; Lemire, P.; Perozzo, A.; Vincent-Rocan, J.-F.; Beauchemin, A. M. *Org. Lett.* **2016**, *18*, 3778
(25) Wiberg, K. B.; Wang, Y. *ARKIVOC*, **2011**, *(V)*, 45-56.

Appendix I

i. Claims to Original Research

1. Development of intermolecular aminocarbonylation of imino-isocyanates with alkenes and enol ethers, including exploration into limits of this reactivity.
2. Development of conditions for pyrazolone synthesis from bicyclic enol ether cycloadducts.
3. Discovery of conditions for the kinetic resolution of *N,N'*-cyclic azomethine imines and access to enantioenriched β-amino amides.
4. Direct detection of imino-isocyanates under reaction conditions using in situ IR spectroscopy.
5. Exploration into carbonyl catalysis of intermolecular alkene aminocarbonylation.
6. Discovery of intermolecular aminocarbonylation of imino-isocyanates with imines, including development of a multi-component reaction.
7. Exploration into reaction mechanisms with imino-isocyanates, including isolation of by-products from isocyanate degradation, and the discovery of degradation pathways with imine cycloadducts.

ii. Publications from this Work

1. "Synthesis of Cyclic Azomethine Imines by Cycloaddition Reactions of N-Isocyanates and N-Isothiocyanates." **A. Bongers**, I. Ranasinghe, P. Lemire, A. Perozzo, J. F. Vincent-Rocan, A. M. Beauchemin. *Org. Lett.* **2016**, 3778-3781.
2. "Kinetic Resolution of Azomethine Imines by Brønsted Acid Catalyzed Enantioselective Reduction." **A. Bongers**, P. J. Moon, A. M. Beauchemin. *Angew. Chem., Int. Ed.* **2015**, *54* 15516-15519.
3. "Modular Synthesis of Pyrazolones Using an Alkene Aminocarbonylation Reaction." K. Lavergne, **A. Bongers**, L. Betit, A. Beauchemin. *Org. Lett.* **2014**, 3612-3515.
4. "A Tunable Route for the Synthesis of Azomethine Imines and β-Aminocarbonyl Compounds from Alkenes." C. Clavette, W. Gan, **A. Bongers**, T. Markiewicz, A. B. Toderian, S. Gorelsky, A. M. Beauchemin. *J. Am. Chem. Soc.* **2012**, 16111-16114.

5. "Intermolecular Aminocarbonylation of Alkenes using Concerted Cycloadditions of Imino-isocyanates." **A. Bongers**, C. Clavette, W. Gan, T. Markiewicz, P. Moon, L. Betit, K. Lavergne, N. Das Neves, A. Toderian, S. Gorelsky, A. M. Beauchemin. *Journal of Organic Chemistry*. [Online early access]. DOI: 10.1021/acs.joc.6b02713. Published online: December 22, 2016.

iii. Presentations of this Work

1. "Conversion of Alkenes into Enantioenriched β-Aminocarbonyl Compounds" *Synthesis Day, Ottawa.* **2016**. [Poster, awarded 3rd place prize]
2. "Conversion of Alkenes into Enantioenriched β-Aminocarbonyl Compounds" *ISACS 19: Challenges in Organic Chemistry, Irvine, CA.* **2016**. [Poster]
3. "Intermolecular Aminocarbonylation of C=C and C=N Bonds" *Canadian Society for Chemistry Conference, Ottawa.* **2015** [Oral Presentation]
4. "Brønsted Acid Catalyzed Kinetic Resolution of Azomethine Imines" *Quebec Ontario Mini-Symposium on Synthetic and Bio-organic Chemistry.* **2014** [selected as Best Oral Presentation]
5. "Kinetic Resolution of Azomethine Imines to Access Enantioenriched β-Aminocarbonyls" *International Symposium on Homogeneous Catalysis.* **2014** [Poster]
6. "Enantioenriched β-Aminocarbonyl Compounds from Azomethine Imines" *Quebec Ontario Mini-Symposium on Synthetic and Bio-organic Chemistry.* **2013** [Poster]
7. "Accessing β-Aminocarbonyl Compounds from Azomethine Imines" *Canadian Society for Chemistry Conference, Quebec City.* **2013** [Poster]
8. "Accessing β-Aminocarbonyl Compounds from Azomethine Imines" *Ottawa Carleton Chemistry Institute Day.* **2011** [selected as Best Poster Presentation]

iv. License to Republish Article

JOHN WILEY AND SONS LICENSE TERMS AND CONDITIONS

Aug 19, 2016

This Agreement between Amanda L Bongers ("You") and John Wiley and Sons ("John Wiley and Sons") consists of your license details and the terms and conditions provided by John Wiley and Sons and Copyright Clearance Center.

License Number	3932560663700
License date	Aug 19, 2016
Licensed Content Publisher	John Wiley and Sons
Licensed Content Publication	Angewandte Chemie International Edition
Licensed Content Title	Kinetic Resolution of Azomethine Imines by Brønsted Acid Catalyzed Enantioselective Reduction
Licensed Content Author	Amanda Bongers,Patrick J. Moon,André M. Beauchemin
Licensed Content Date	Nov 11, 2015
Licensed Content Pages	4
Type of use	Dissertation/Thesis
Requestor type	Author of this Wiley article
Format	Print and electronic
Portion	Full article
Will you be translating?	No
Title of your thesis / dissertation	Intermolecular [3+2] Cycloadditions of Imino-isocyanates to Access β-Amino Carbonyl Compounds
Expected completion date	Sep 2016
Expected size (number of pages)	250

Appendix II

Spectra: Chapter 2

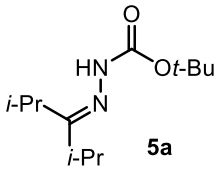

5a

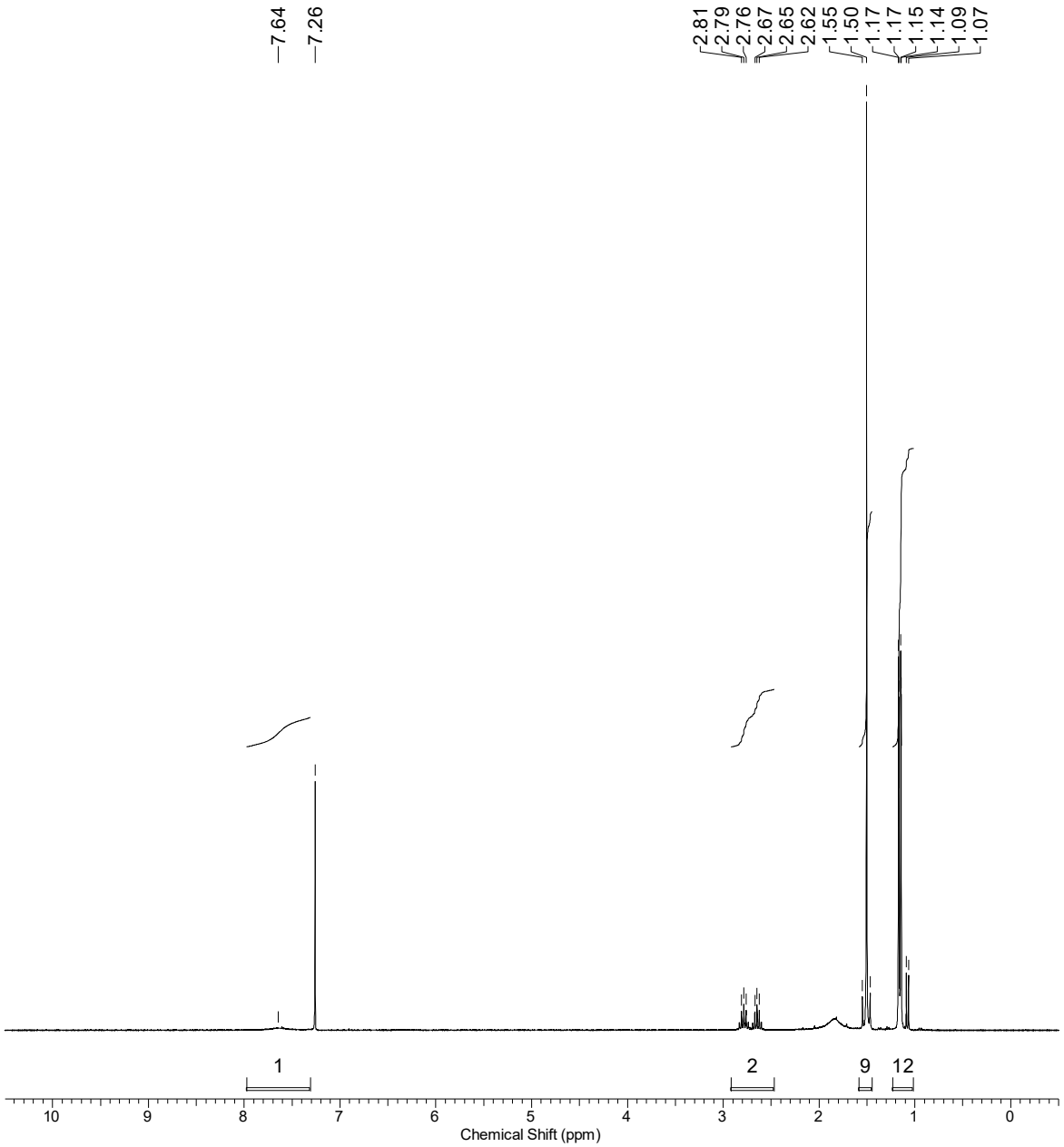

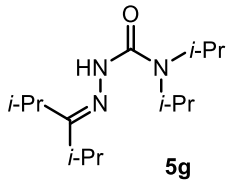
O
HN
N
i-Pr
i-Pr
N
i-Pr
i-Pr

5g

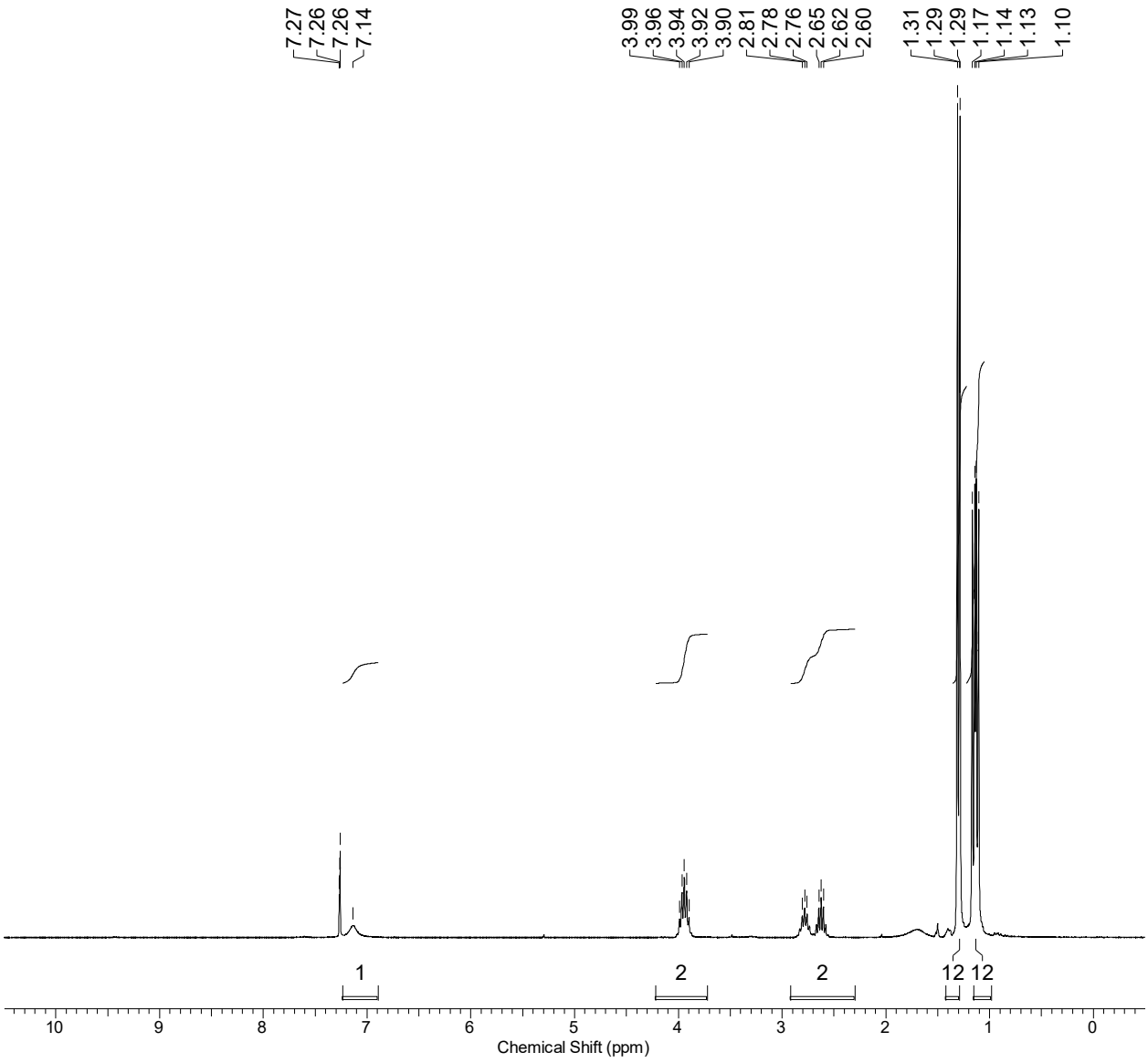
7.27
7.26
7.26
7.14
3.99
3.96
3.94
3.92
3.90
2.81
2.78
2.76
2.65
2.62
2.60
1.31
1.29
1.29
1.17
1.14
1.13
1.10
1
2
2
12
12
10
9
8
7
6
5
4
3
2
1
0
Chemical Shift (ppm)

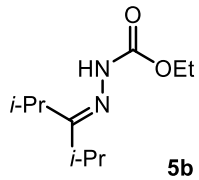
O
HN
OEt
i-Pr
N
i-Pr

5b

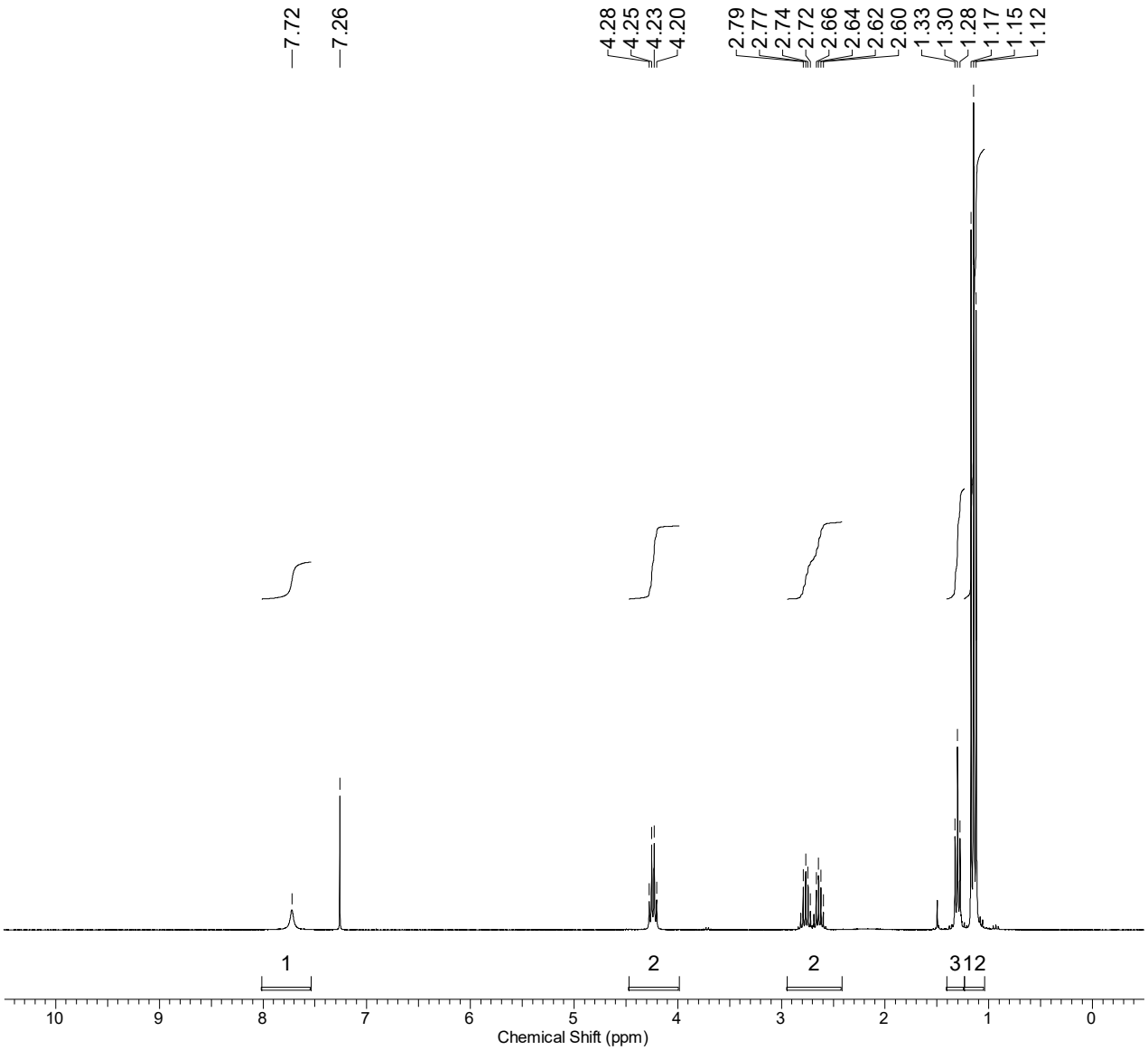
7.72
7.26
4.28
4.25
4.23
4.20
2.79
2.77
2.74
2.72
2.66
2.64
2.62
2.60
1.33
1.30
1.28
1.17
1.15
1.12
1
2
2
312
10
9
8
7
6
5
4
3
2
1
0
Chemical Shift (ppm)

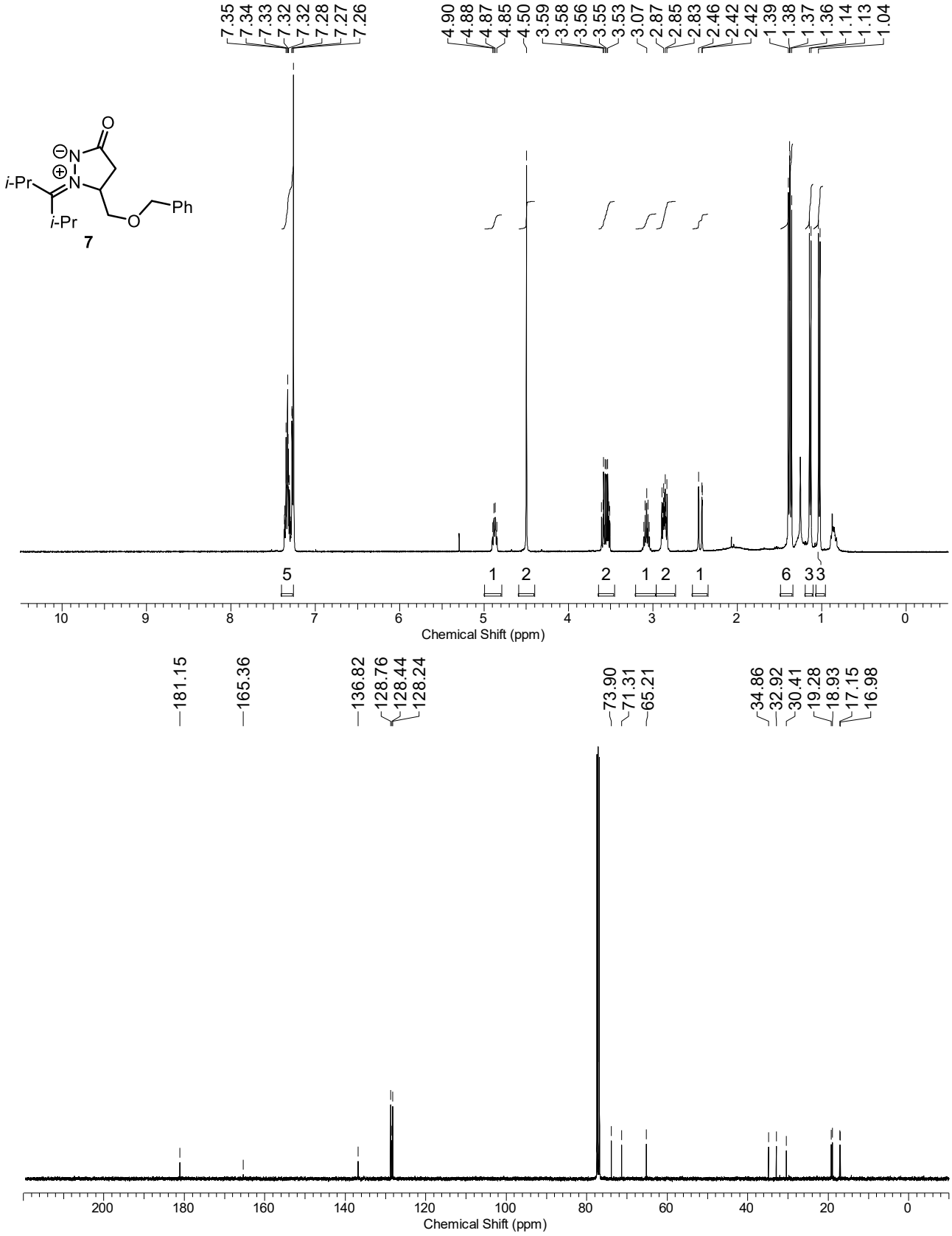
7.35
7.34
7.33
7.32
7.32
7.28
7.27
7.26
4.90
4.88
4.87
4.85
4.50
3.59
3.58
3.56
3.55
3.53
3.07
2.87
2.85
2.83
2.46
2.42
2.42
1.39
1.38
1.37
1.36
1.14
1.13
1.04
i-Pr
i-Pr
Ph
7
5
1
2
2
1
2
1
6
3
3
Chemical Shift (ppm)
181.15
165.36
136.82
128.76
128.44
128.24
73.90
71.31
65.21
34.86
32.92
30.41
19.28
18.93
17.15
16.98
Chemical Shift (ppm)

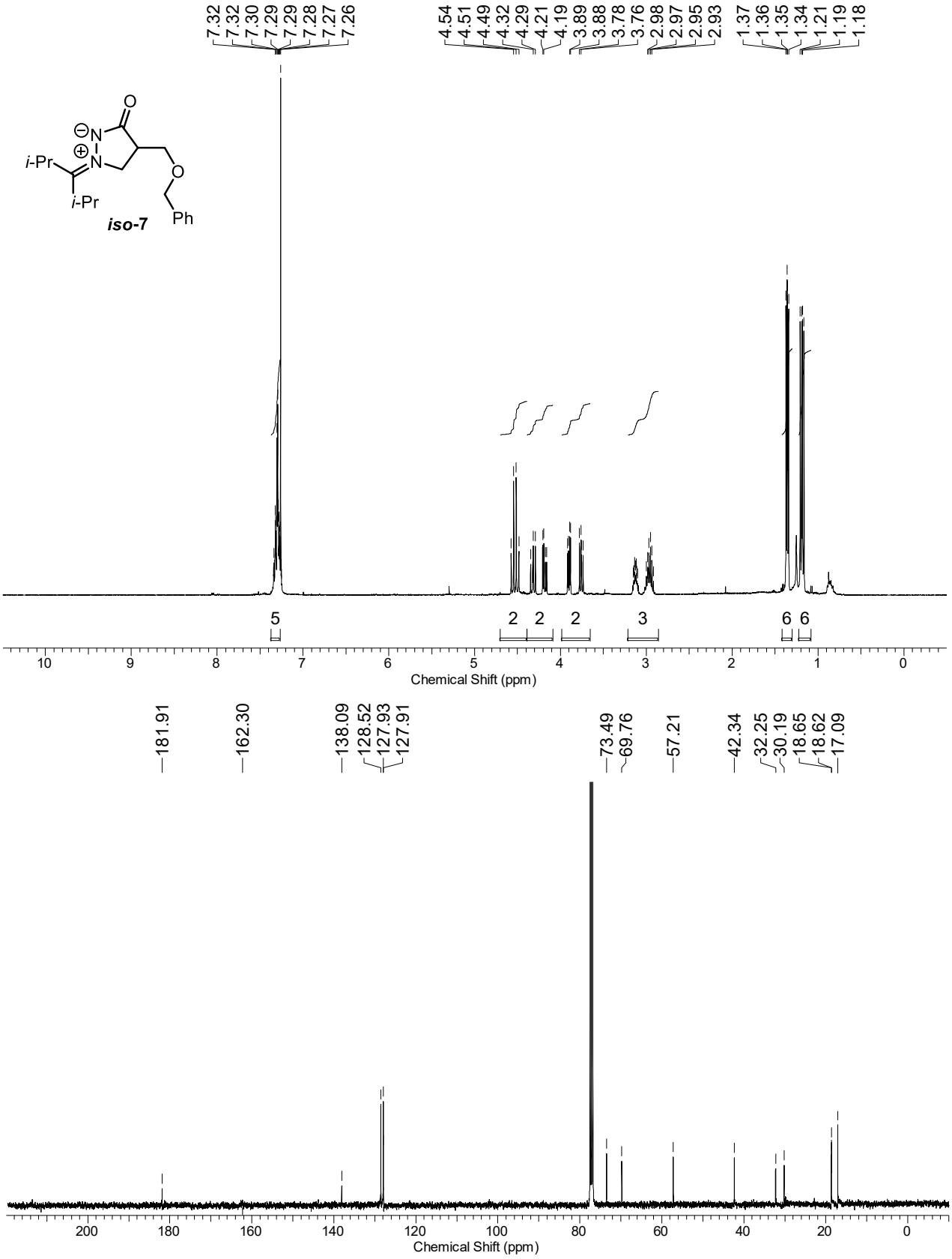
7.32
7.32
7.30
7.29
7.29
7.28
7.27
7.26
4.54
4.51
4.49
4.32
4.29
4.21
4.19
3.89
3.88
3.78
3.76
2.98
2.97
2.95
2.93
1.37
1.36
1.35
1.34
1.21
1.19
1.18
i-Pr
i-Pr
Ph
iso-7
5
2
2
2
3
6
6
Chemical Shift (ppm)
181.91
162.30
138.09
128.52
127.93
127.91
73.49
69.76
57.21
42.34
32.25
30.19
18.65
18.62
17.09
Chemical Shift (ppm)

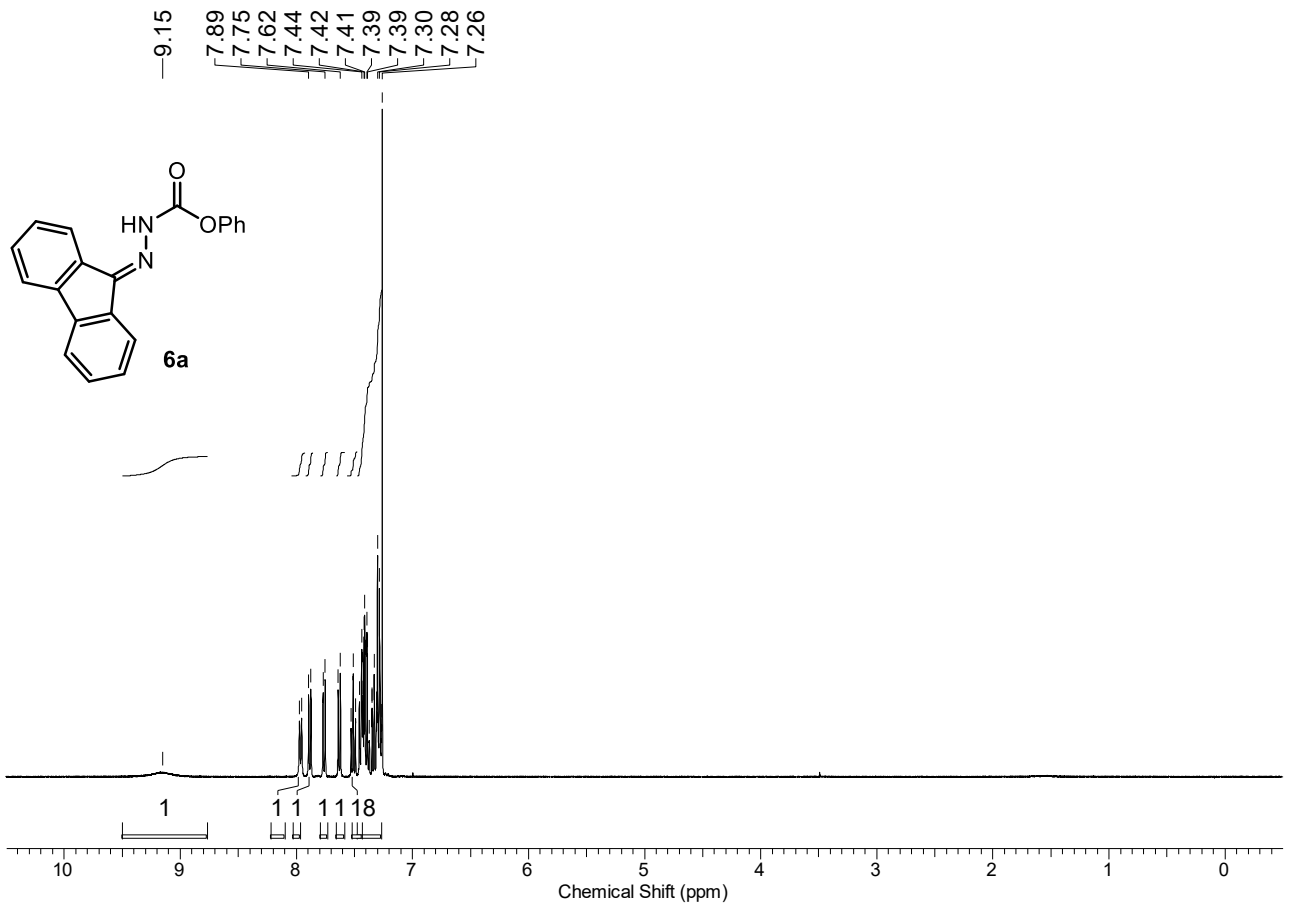
9.15
7.89
7.75
7.62
7.44
7.42
7.41
7.39
7.39
7.30
7.28
7.26
O
HN
OPh
N
6a
1
1 1
1 1
8
10
9
8
7
6
5
4
3
2
1
0
Chemical Shift (ppm)

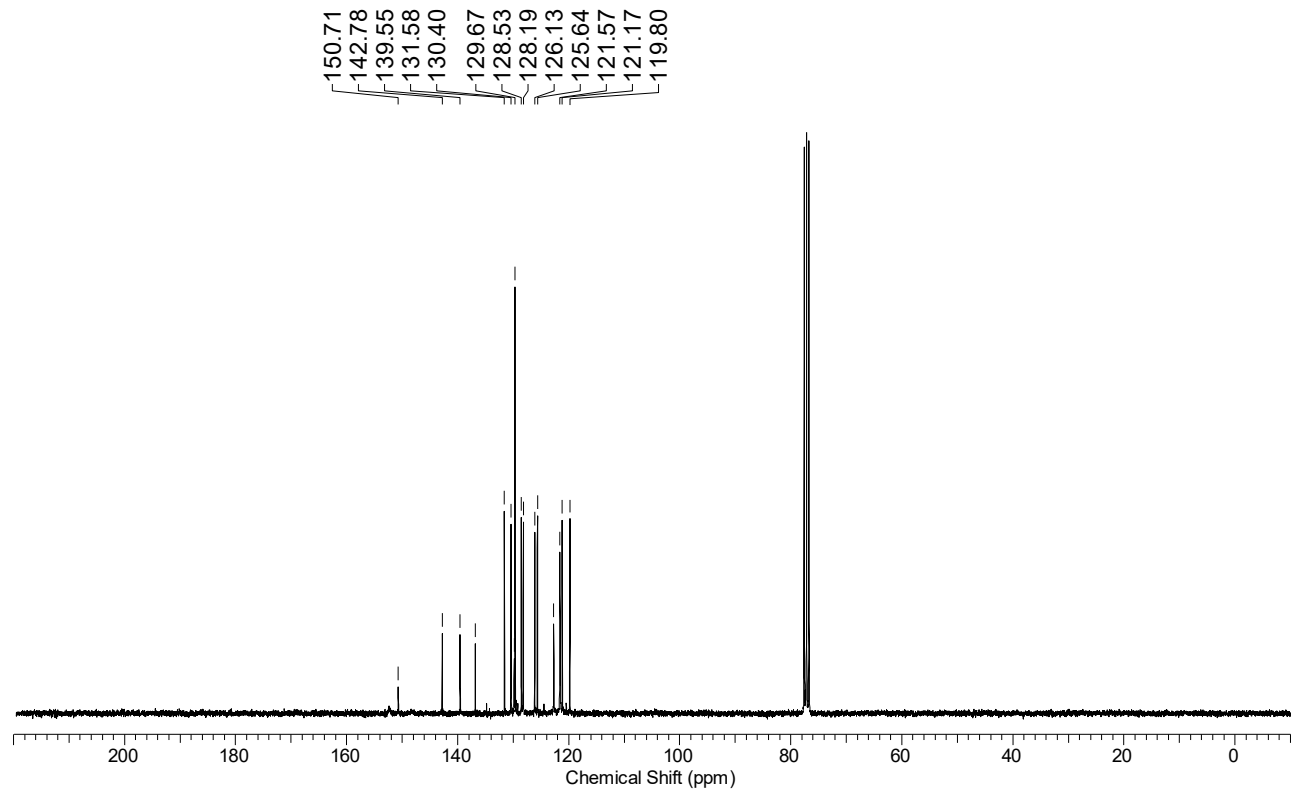
150.71
142.78
139.55
131.58
130.40
129.67
128.53
128.19
126.13
125.64
121.57
121.17
119.80
200
180
160
140
120
100
80
60
40
20
0
Chemical Shift (ppm)

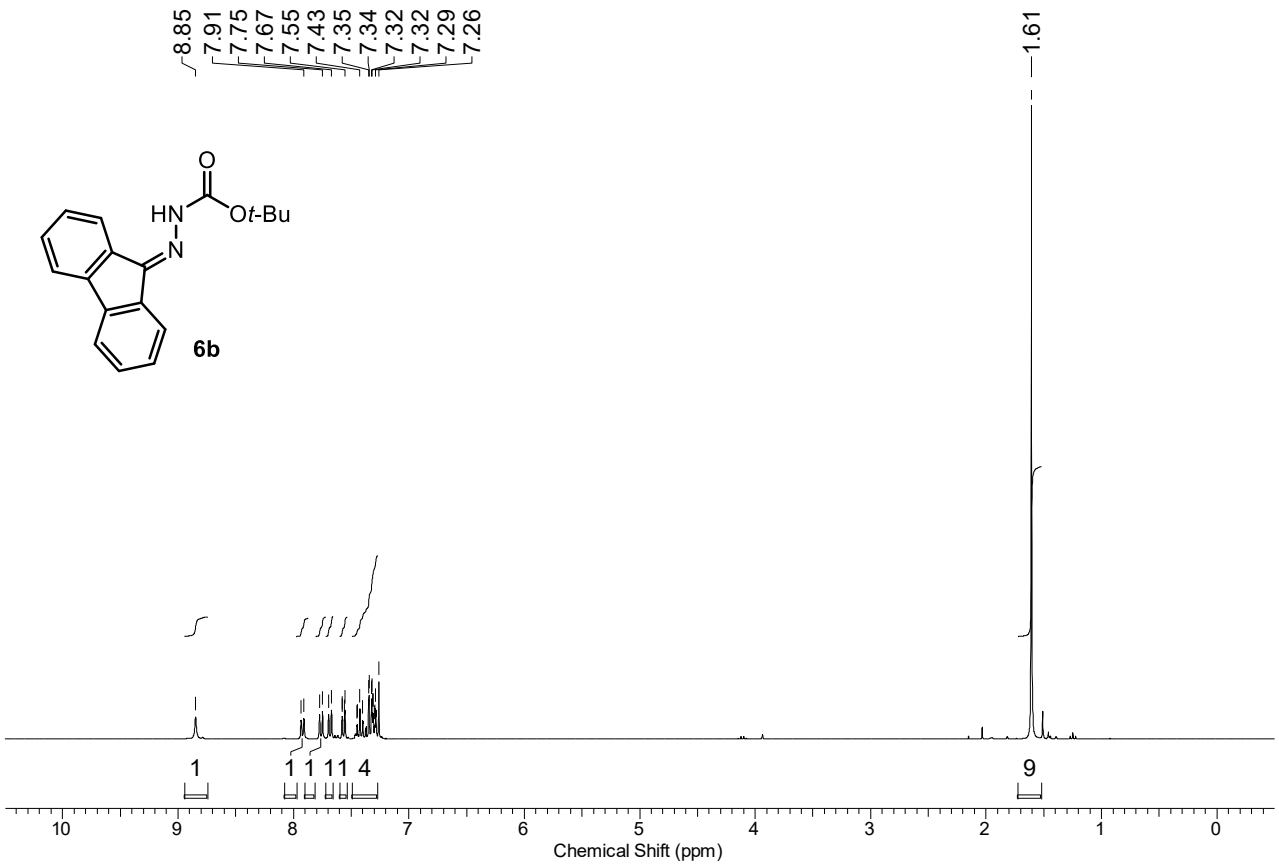
8.85
7.91
7.75
7.67
7.55
7.43
7.35
7.34
7.32
7.32
7.29
7.26
1.61
HN
N
O
Ot-Bu
6b
1
1 1 1 1 4
9
10
9
8
7
6
5
4
3
2
1
0
Chemical Shift (ppm)

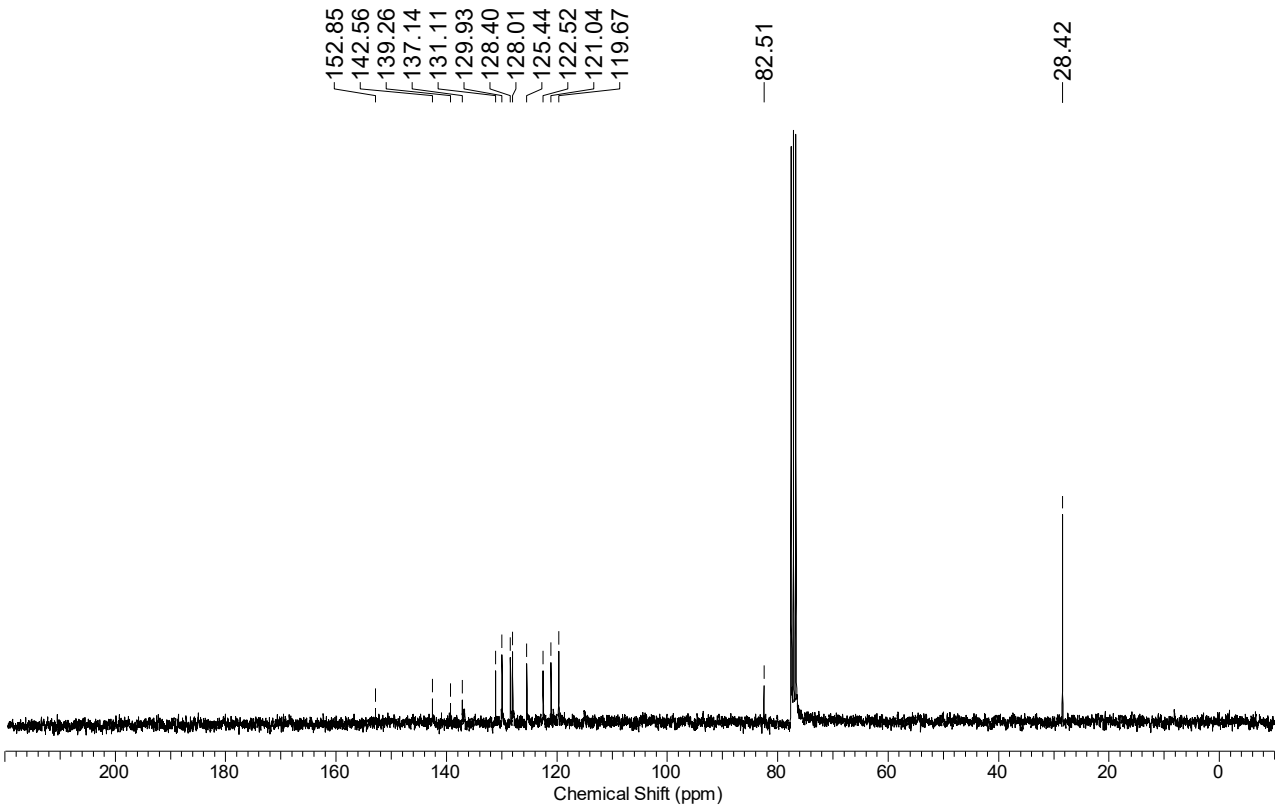
152.85
142.56
139.26
137.14
131.11
129.93
128.40
128.01
125.44
122.52
121.04
119.67
82.51
28.42
200
180
160
140
120
100
80
60
40
20
0
Chemical Shift (ppm)

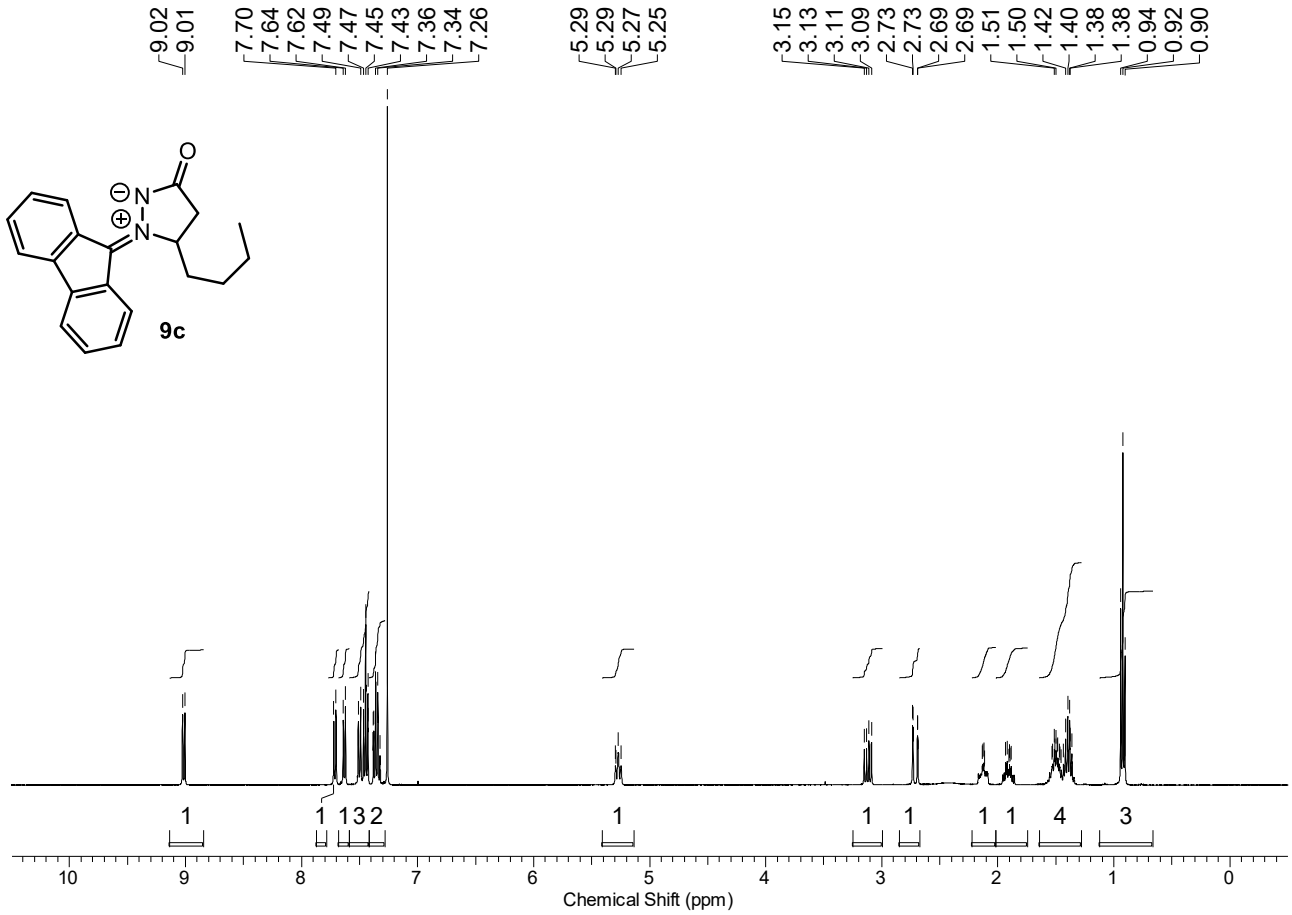
9.02
9.01
7.70
7.64
7.62
7.49
7.47
7.45
7.43
7.36
7.34
7.26
5.29
5.29
5.27
5.25
3.15
3.13
3.11
3.09
2.73
2.73
2.69
2.69
1.51
1.50
1.42
1.40
1.38
1.38
0.94
0.92
0.90
O
N
N
9c
1
1
1
3
2
1
1
1
1
1
4
3
10
9
8
7
6
5
4
3
2
1
0
Chemical Shift (ppm)

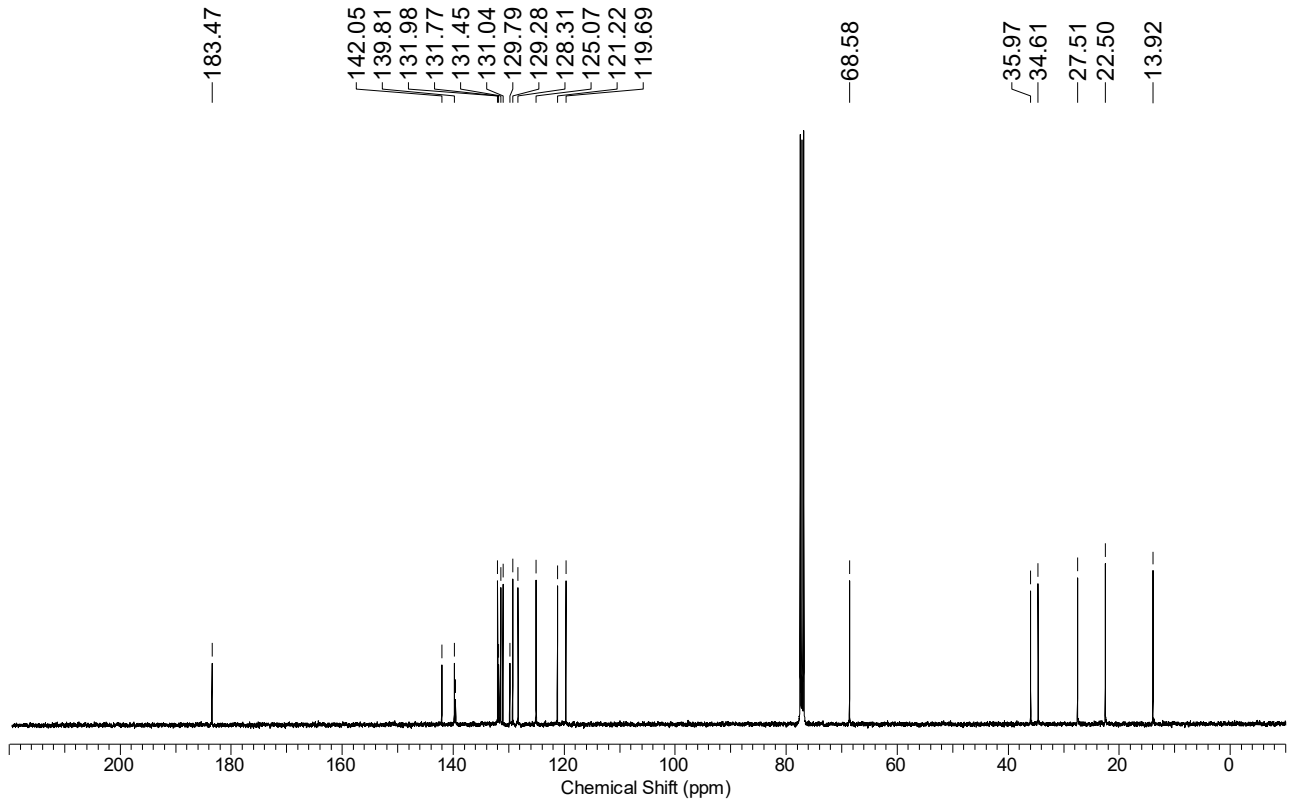
183.47
142.05
139.81
131.98
131.77
131.45
131.04
129.79
129.28
128.31
125.07
121.22
119.69
68.58
35.97
34.61
27.51
22.50
13.92
200
180
160
140
120
100
80
60
40
20
0
Chemical Shift (ppm)

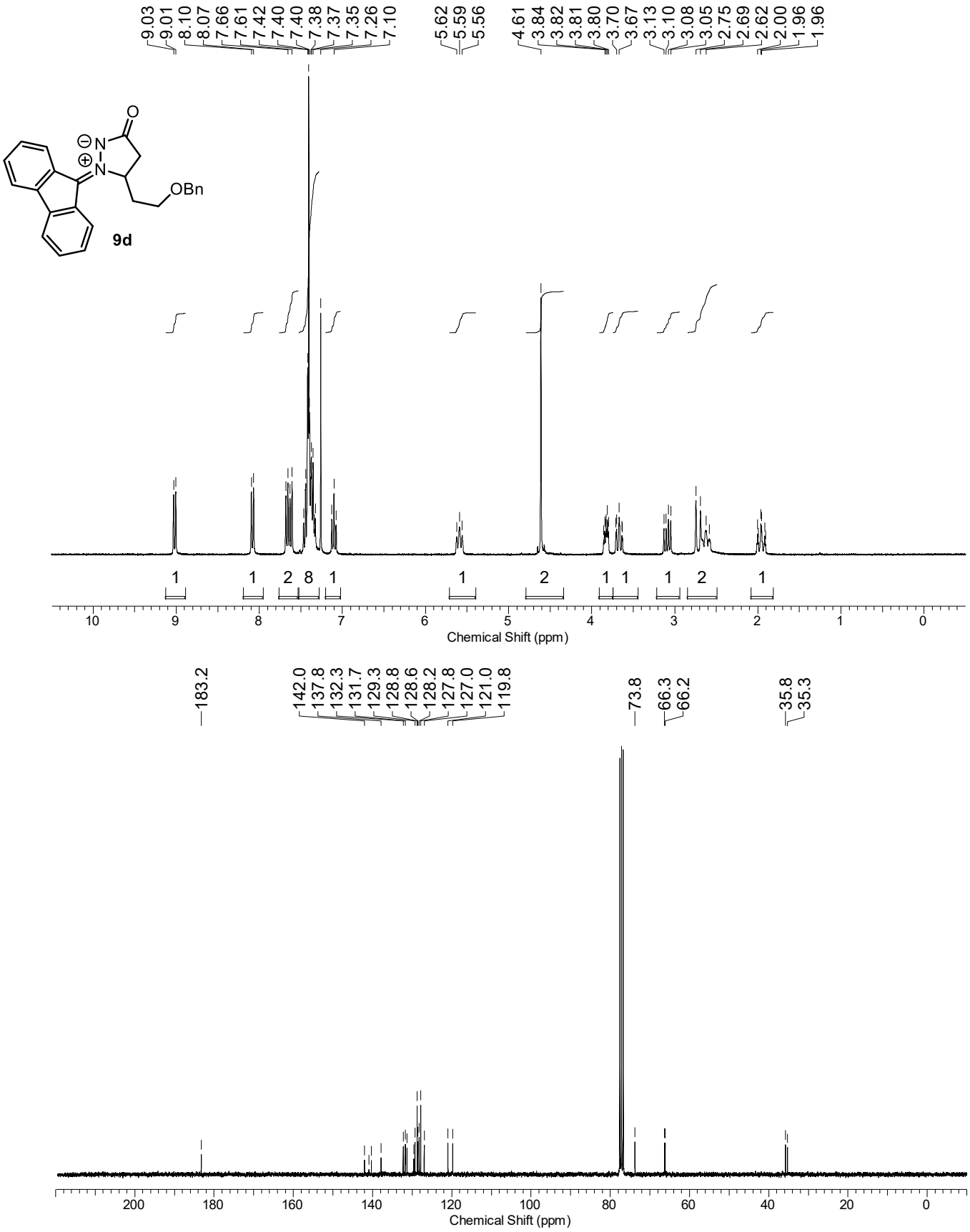
9.03
9.01
8.10
8.07
7.66
7.61
7.42
7.40
7.40
7.38
7.37
7.35
7.26
7.10
5.62
5.59
5.56
4.61
3.84
3.82
3.81
3.80
3.70
3.67
3.13
3.10
3.08
3.05
2.75
2.69
2.62
2.00
1.96
1.96
O
N
N
OBn
9d
1 1 2 8 1 1 2 1 1 1 2 1
Chemical Shift (ppm)
183.2
142.0
137.8
132.3
131.7
129.3
128.8
128.6
128.2
127.8
127.0
121.0
119.8
73.8
66.3
66.2
35.8
35.3
Chemical Shift (ppm)

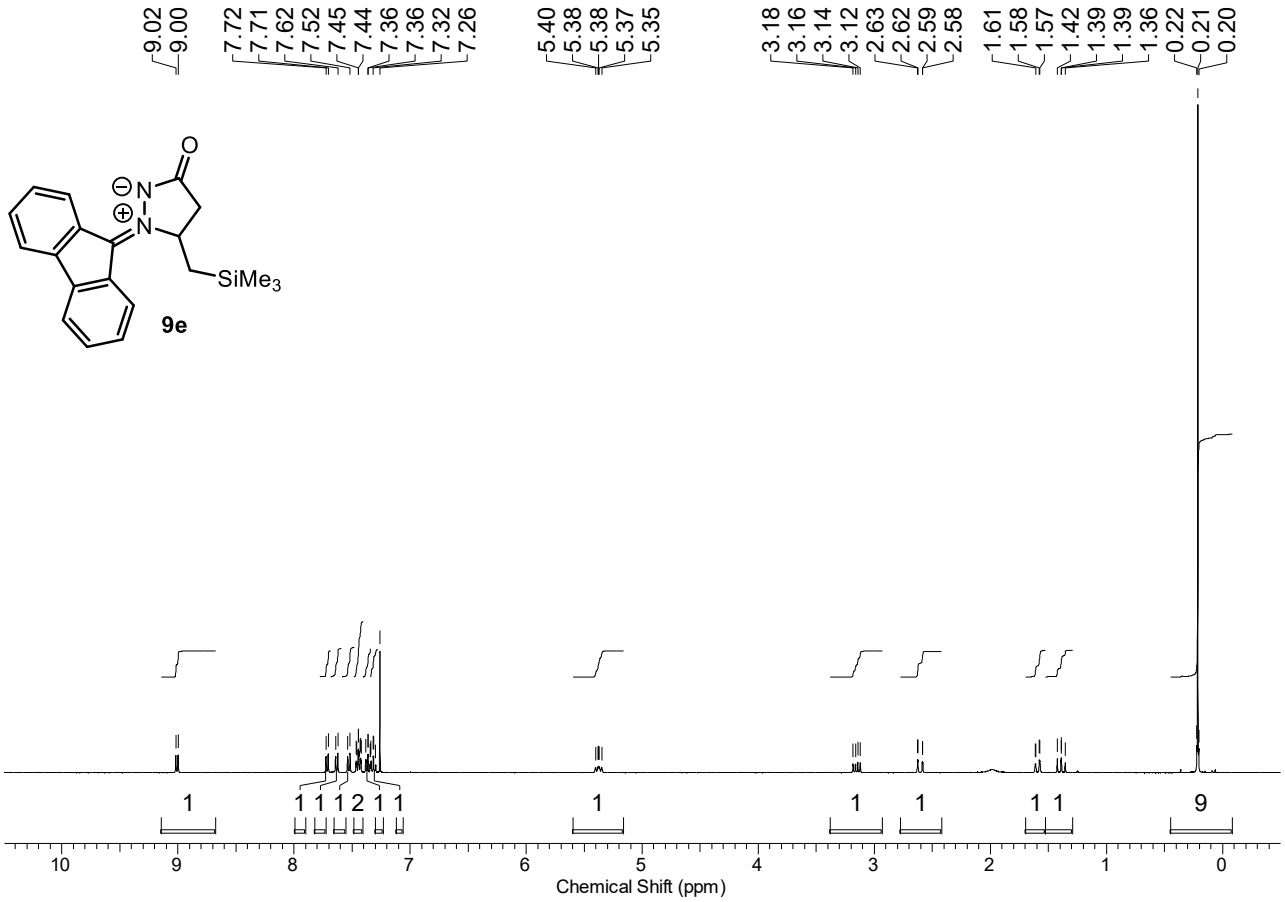
9.02
9.00
7.72
7.71
7.62
7.52
7.45
7.44
7.36
7.36
7.32
7.26
5.40
5.38
5.38
5.37
5.35
3.18
3.16
3.14
3.12
2.63
2.62
2.59
2.58
1.61
1.58
1.57
1.42
1.39
1.39
1.36
0.22
0.21
0.20
O
N
N
SiMe3
9e
1
1 1 1 2 1 1
1
1
1
1 1
9
10
9
8
7
6
5
4
3
2
1
0
Chemical Shift (ppm)

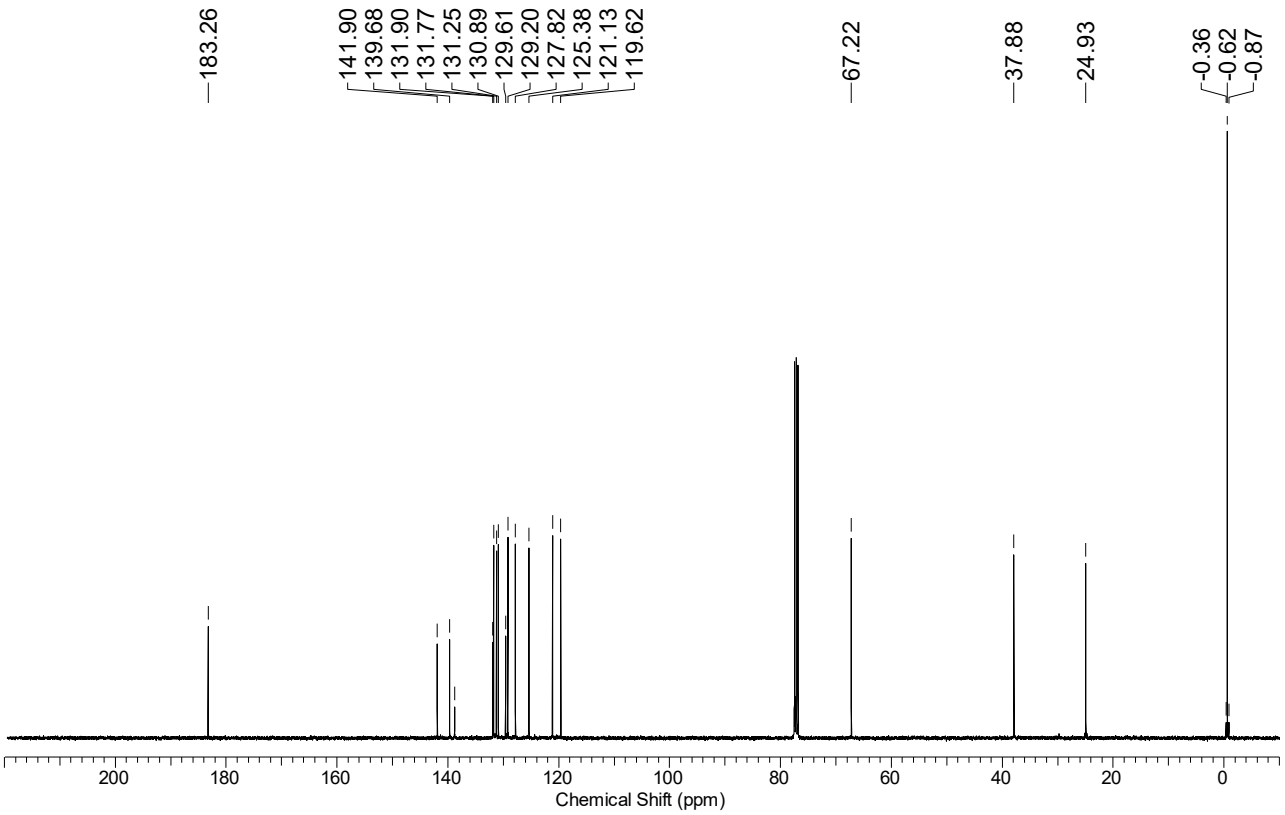
183.26
141.90
139.68
131.90
131.77
131.25
130.89
129.61
129.20
127.82
125.38
121.13
119.62
67.22
37.88
24.93
-0.36
-0.62
-0.87
200
180
160
140
120
100
80
60
40
20
0
Chemical Shift (ppm)

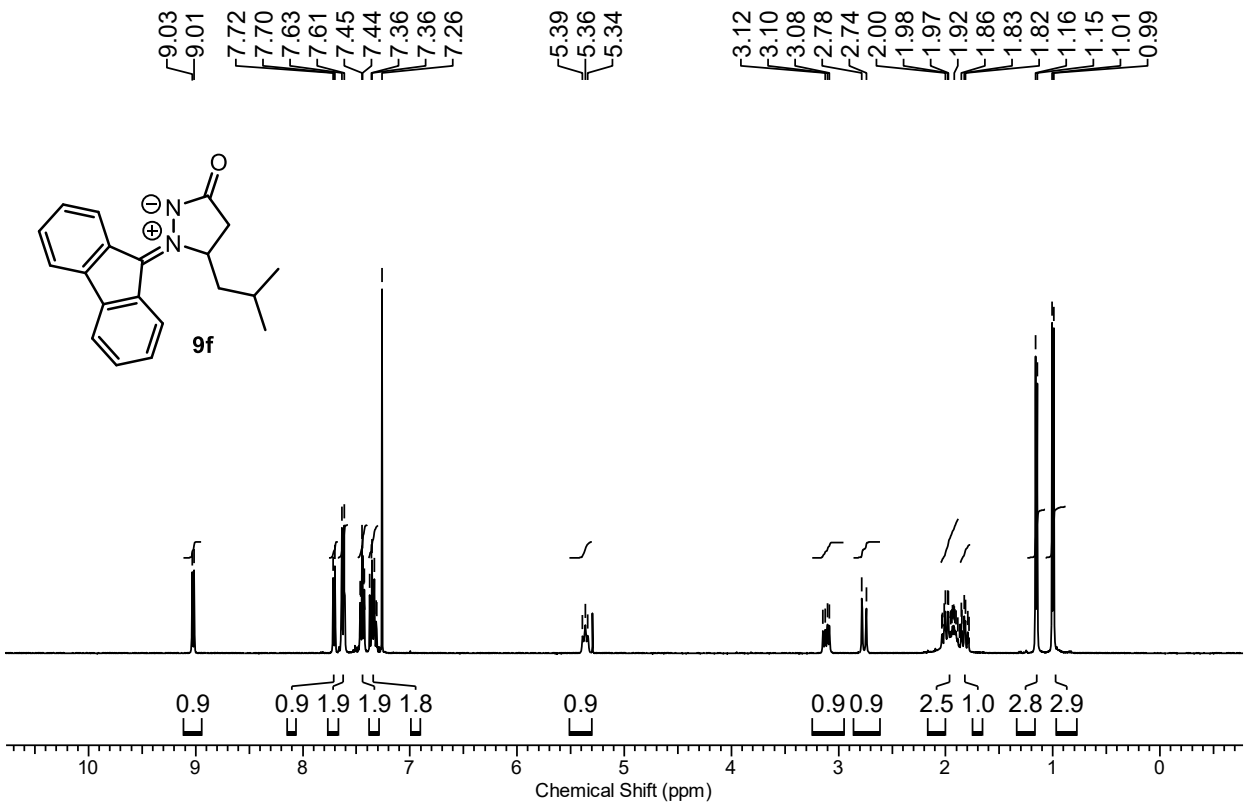
9.03
9.01
7.72
7.70
7.63
7.61
7.45
7.44
7.36
7.36
7.26
5.39
5.36
5.34
3.12
3.10
3.08
2.78
2.74
2.00
1.98
1.97
1.92
1.86
1.83
1.82
1.16
1.15
1.01
0.99
O
N
N
9f
0.9
0.9
1.9
1.9
1.8
0.9
0.9
0.9
2.5
1.0
2.8
2.9
Chemical Shift (ppm)

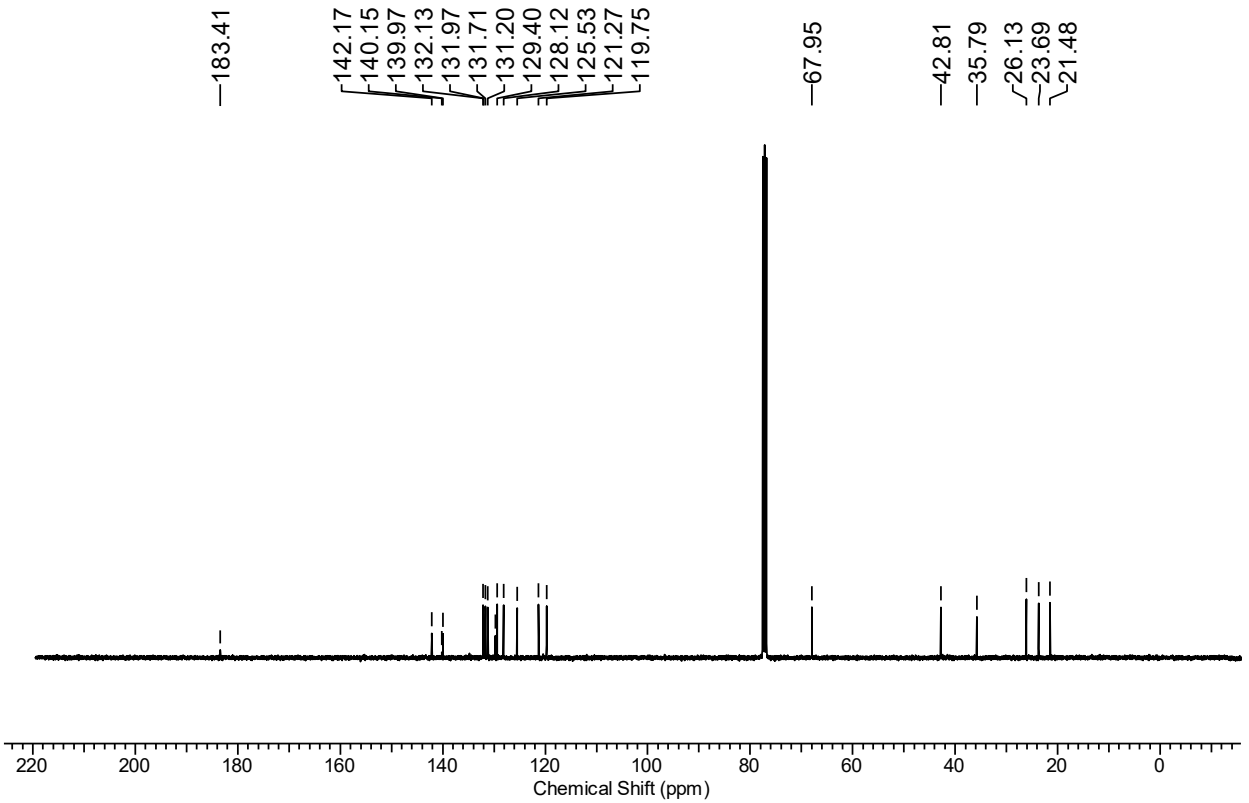
183.41
142.17
140.15
139.97
132.13
131.97
131.71
131.20
129.40
128.12
125.53
121.27
119.75
67.95
42.81
35.79
26.13
23.69
21.48
Chemical Shift (ppm)

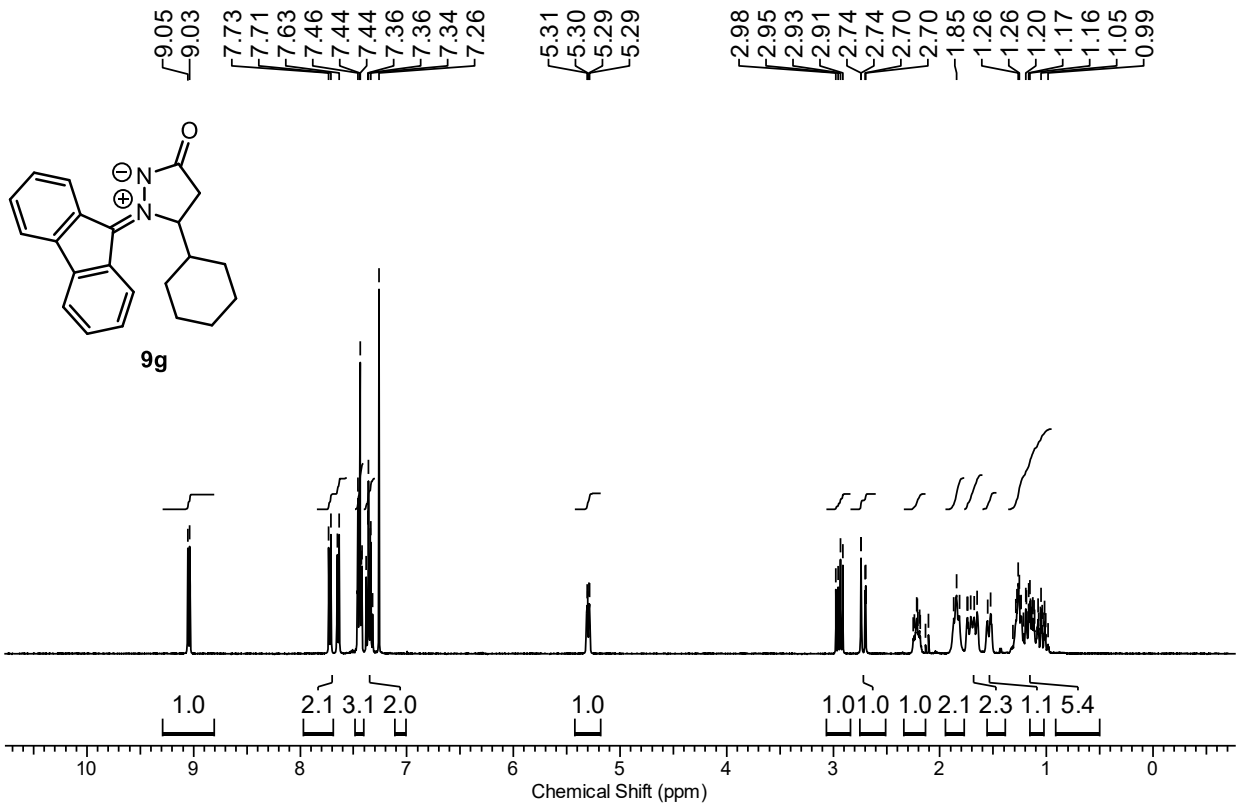
9.05
9.03
7.73
7.71
7.63
7.46
7.44
7.44
7.36
7.36
7.34
7.26
5.31
5.30
5.29
5.29
2.98
2.95
2.93
2.91
2.74
2.74
2.70
2.70
1.85
1.26
1.26
1.20
1.17
1.16
1.05
0.99
O
N
N
9g
1.0
2.1
3.1
2.0
1.0
1.0
1.0
1.0
2.1
2.3
1.1
5.4
10
9
8
7
6
5
4
3
2
1
0
Chemical Shift (ppm)

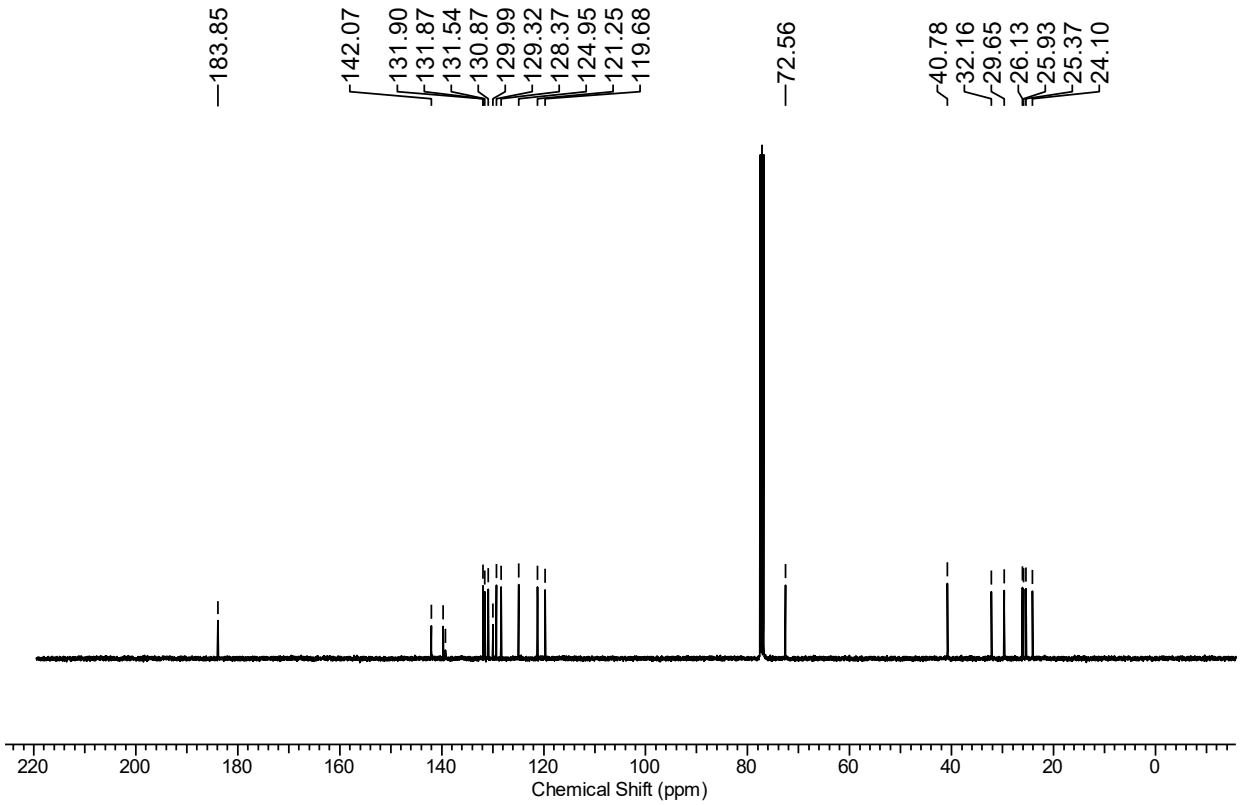
183.85
142.07
131.90
131.87
131.54
130.87
129.99
129.32
128.37
124.95
121.25
119.68
72.56
40.78
32.16
29.65
26.13
25.93
25.37
24.10
220
200
180
160
140
120
100
80
60
40
20
0
Chemical Shift (ppm)

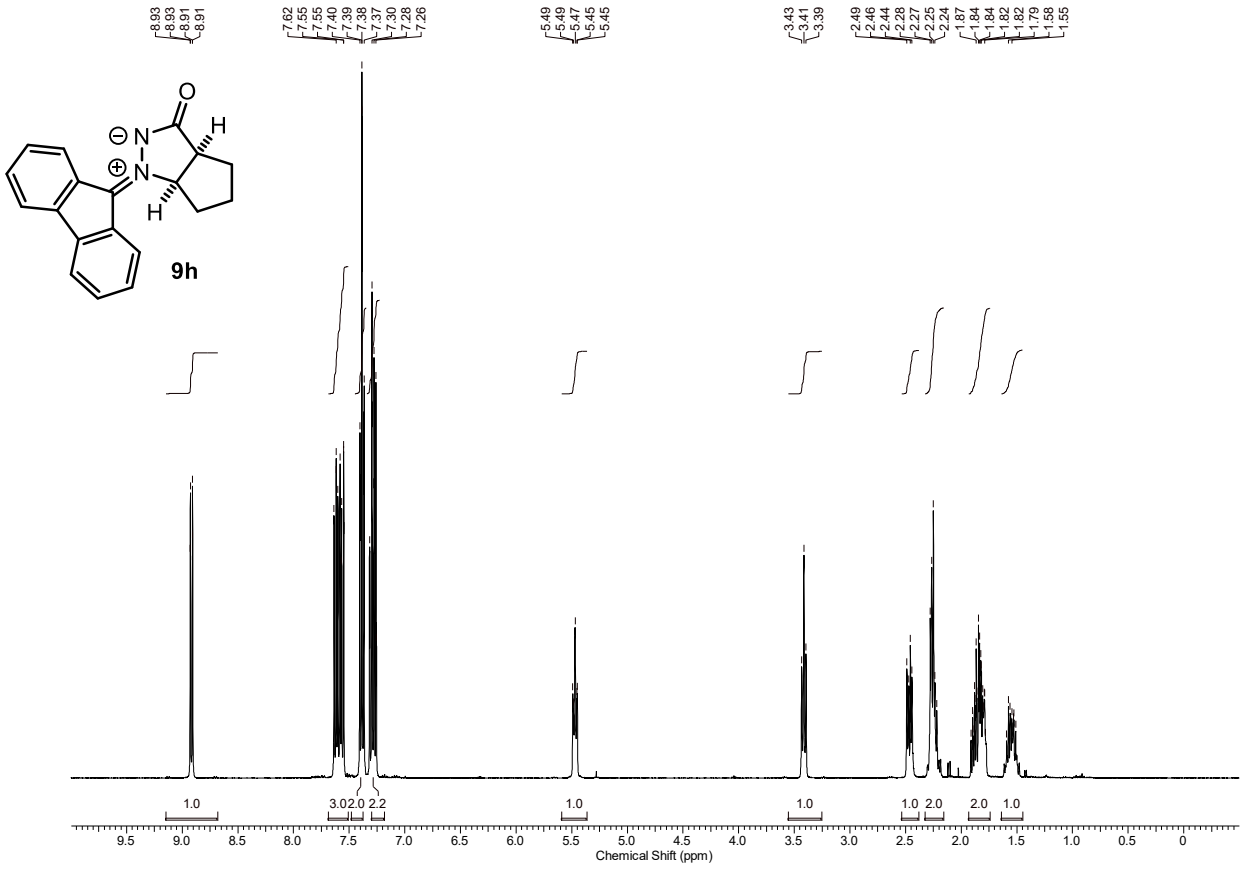
8.93
8.93
8.91
8.91
7.62
7.55
7.55
7.40
7.39
7.38
7.37
7.30
7.28
7.26
5.49
5.49
5.47
5.45
5.45
3.43
3.41
3.39
2.49
2.46
2.44
2.28
2.27
2.25
2.24
1.87
1.84
1.84
1.82
1.82
1.79
1.58
1.55
O
H
N
N
H
9h
1.0
3.02
0
2.2
1.0
1.0
1.0
2.0
2.0
1.0
Chemical Shift (ppm)

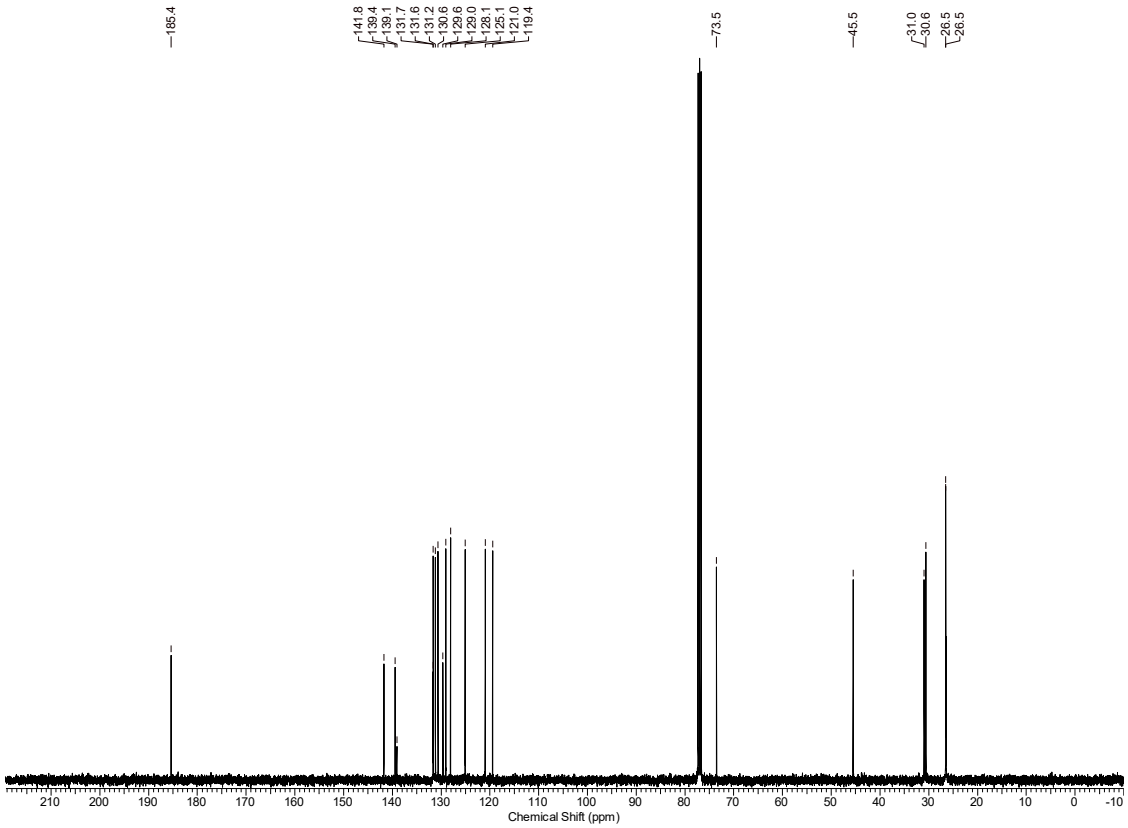
185.4
141.8
139.4
139.1
131.7
131.6
131.2
130.6
129.6
129.0
128.1
125.1
121.0
119.4
73.5
45.5
31.0
30.6
26.5
26.5
Chemical Shift (ppm)

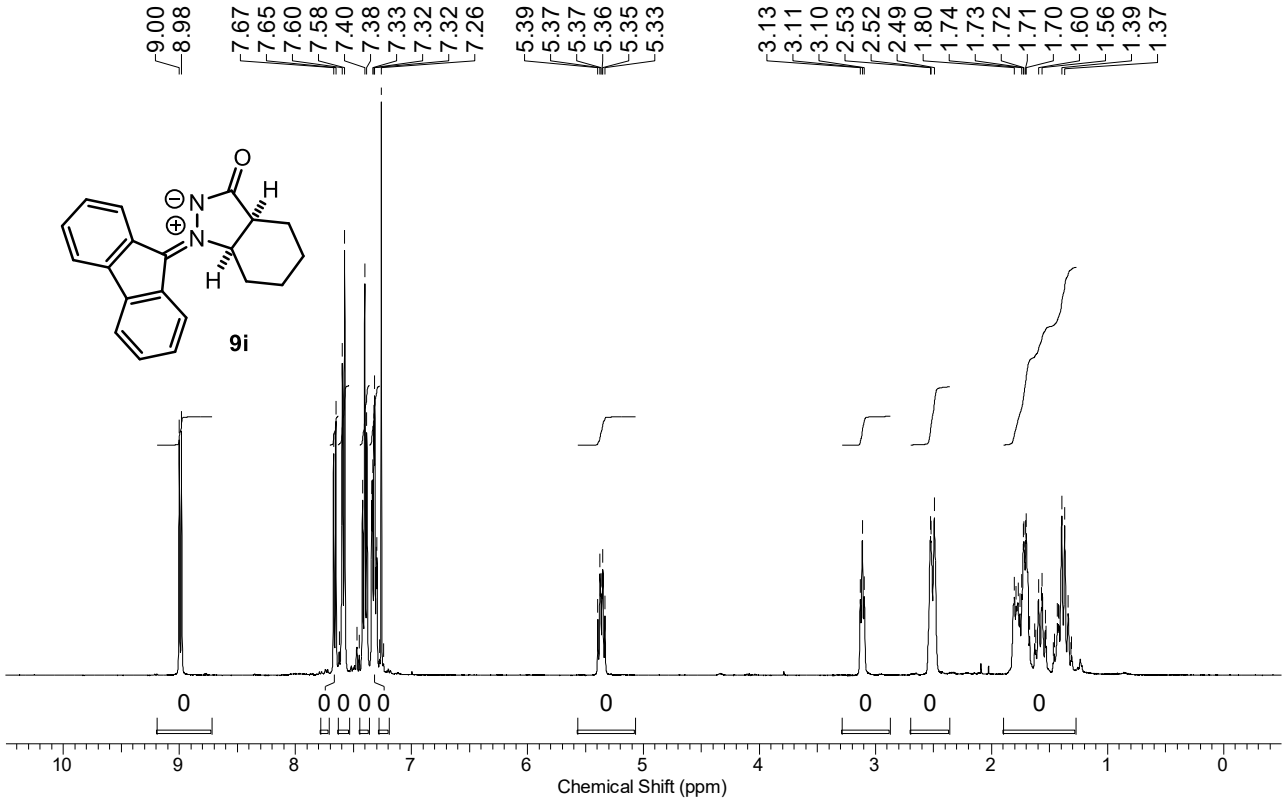
9.00
8.98
7.67
7.65
7.60
7.58
7.40
7.38
7.33
7.32
7.32
7.26
5.39
5.37
5.37
5.36
5.35
5.33
3.13
3.11
3.10
2.53
2.52
2.49
1.80
1.74
1.73
1.72
1.71
1.70
1.60
1.56
1.39
1.37
9i
Chemical Shift (ppm)

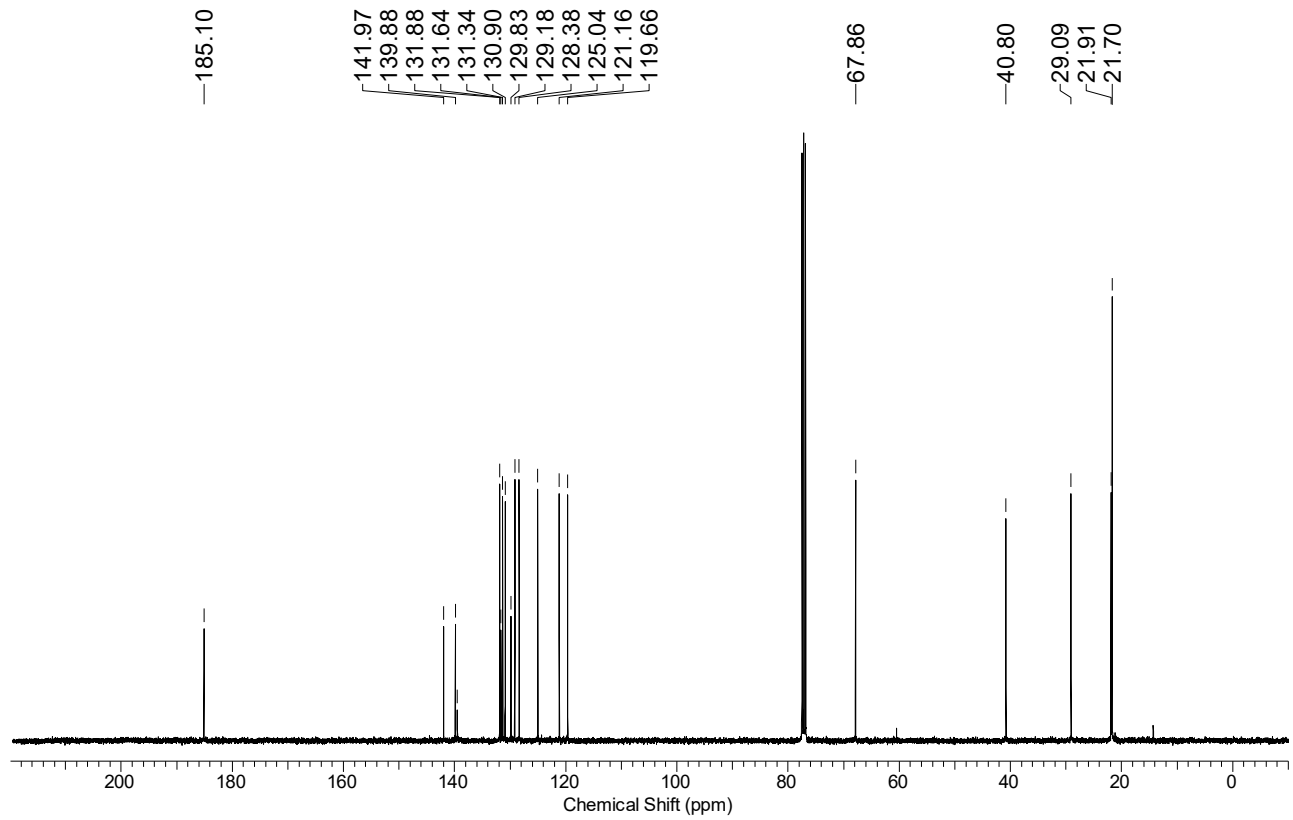
185.10
141.97
139.88
131.88
131.64
131.34
130.90
129.83
129.18
128.38
125.04
121.16
119.66
67.86
40.80
29.09
21.91
21.70
Chemical Shift (ppm)

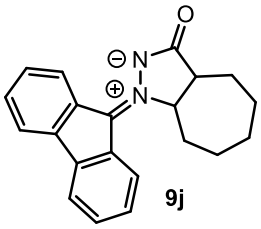

9j

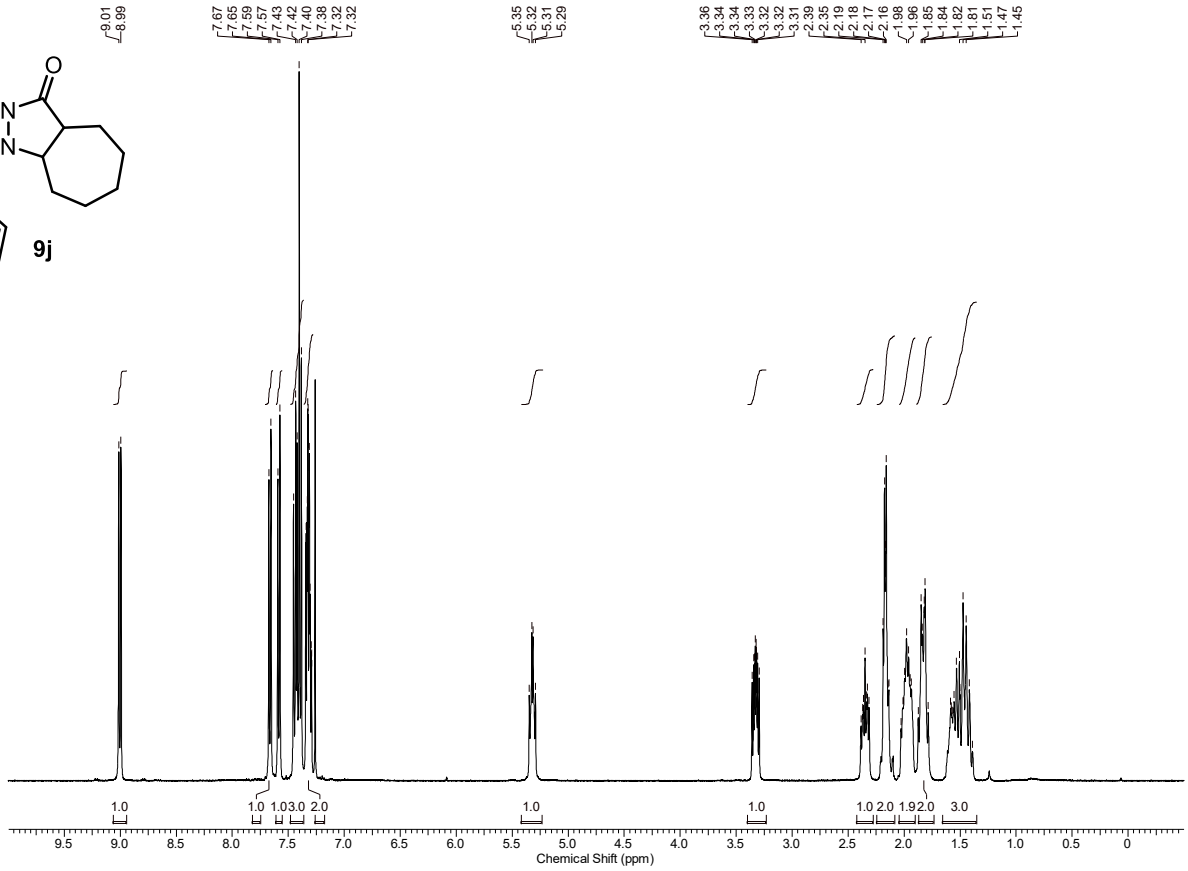
9.01
8.99
7.67
7.65
7.59
7.57
7.43
7.42
7.40
7.38
7.32
7.32
5.35
5.32
5.31
5.29
3.36
3.34
3.34
3.33
3.32
3.32
3.31
2.39
2.35
2.19
2.18
2.17
2.16
1.98
1.96
1.85
1.84
1.82
1.81
1.51
1.47
1.45
1.0
1.0
1.0
3.0
2.0
1.0
1.0
1.0
2.0
1.9
2.0
3.0
Chemical Shift (ppm)

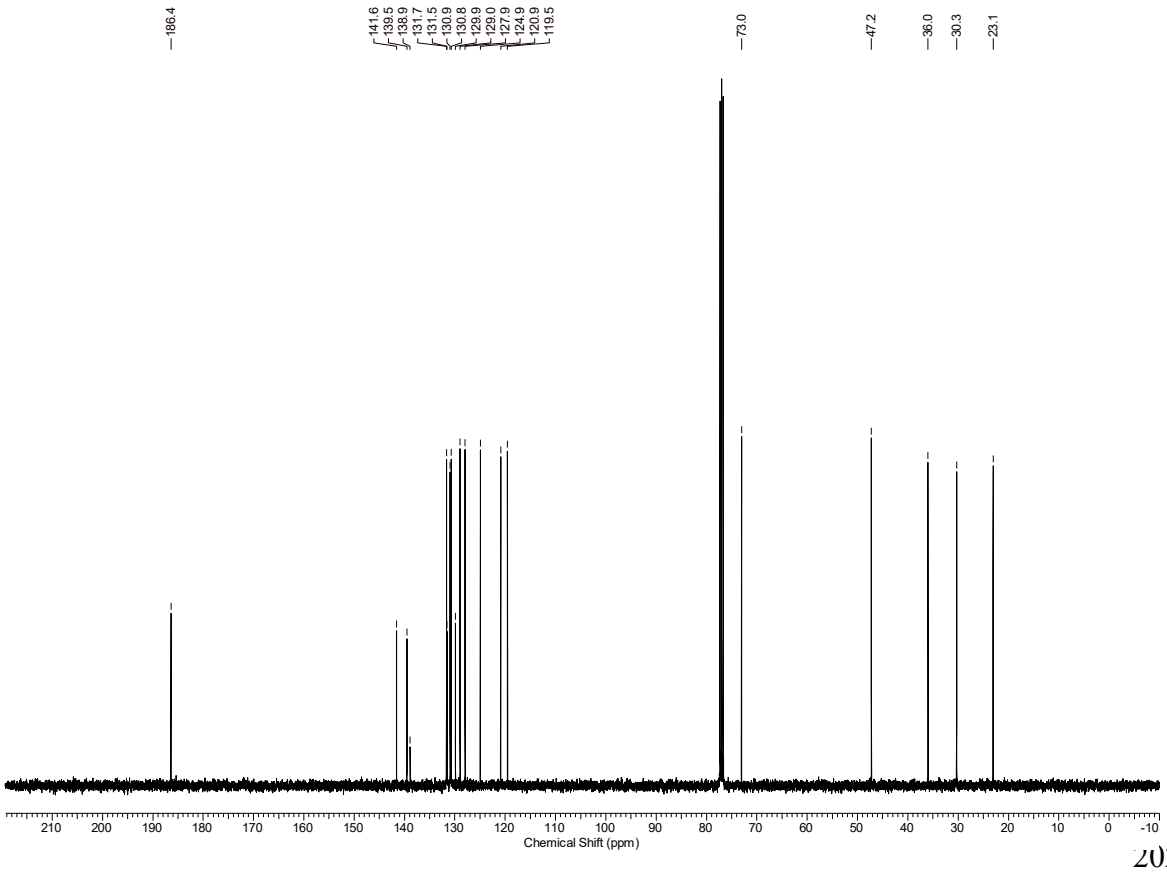
186.4
141.6
139.5
138.9
131.7
131.5
130.9
130.8
129.9
129.0
127.9
124.9
120.9
119.5
73.0
47.2
36.0
30.3
23.1
Chemical Shift (ppm)

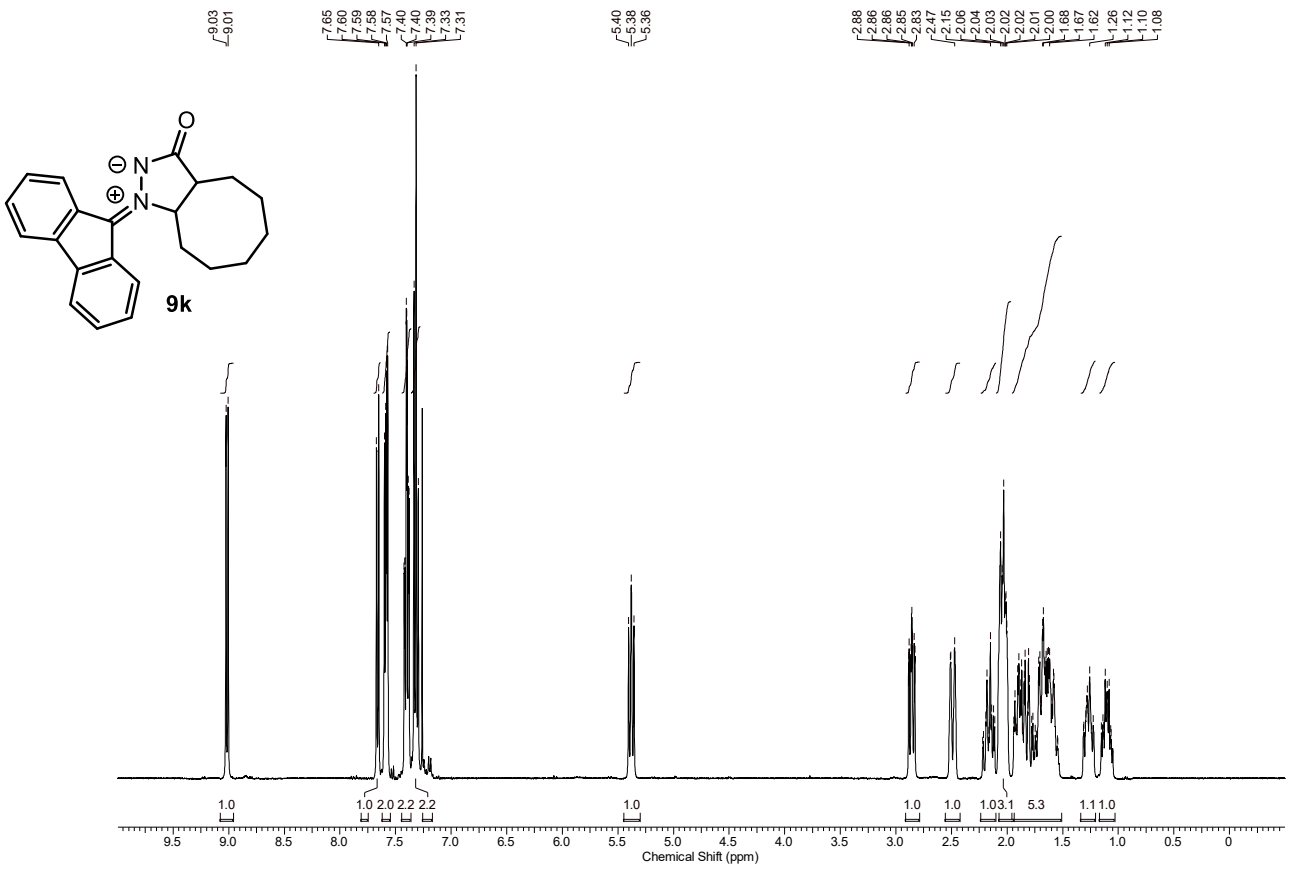
9.03
9.01
7.65
7.60
7.59
7.58
7.57
7.40
7.40
7.39
7.33
7.31
5.40
5.38
5.36
2.88
2.86
2.86
2.85
2.83
2.47
2.15
2.06
2.04
2.03
2.02
2.02
2.01
2.00
1.68
1.67
1.62
1.26
1.12
1.10
1.08
O
N
N
9k
1.0
1.0
2.0
2.2
2.2
1.0
1.0
1.0
1.0
3.1
5.3
1.1
1.0
Chemical Shift (ppm)

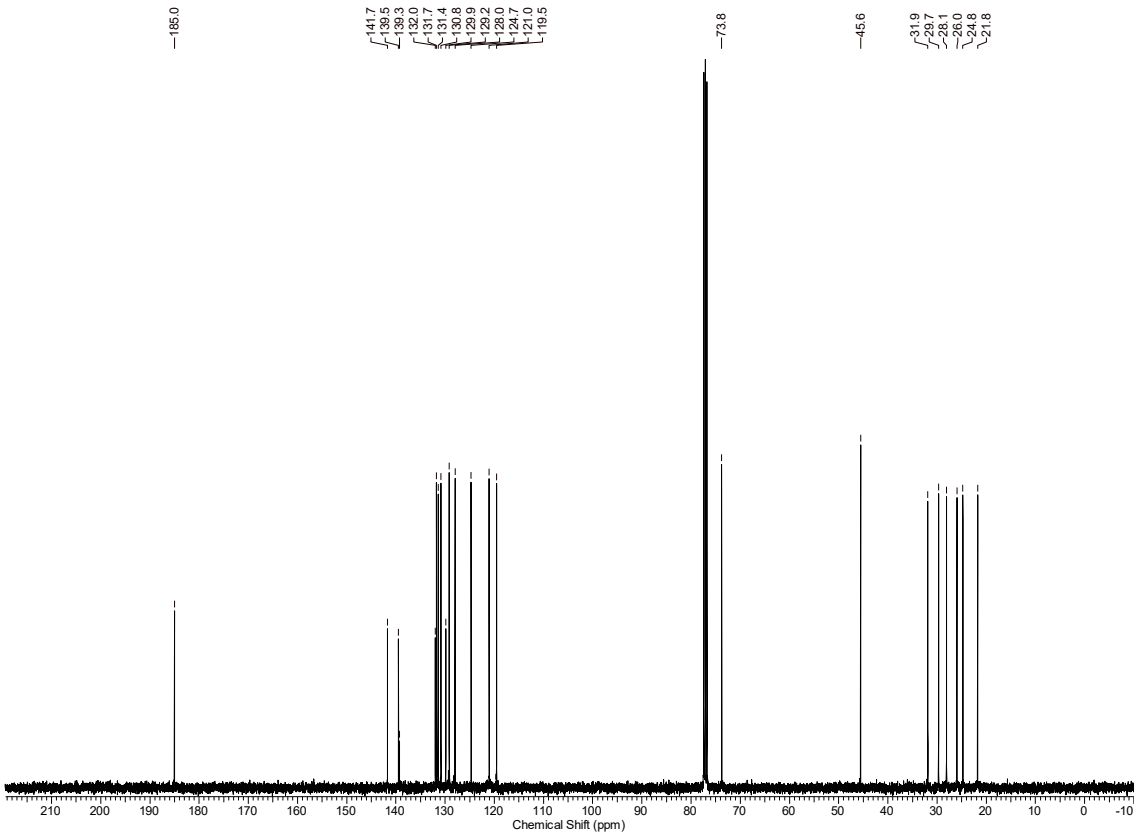
185.0
141.7
139.5
139.3
132.0
131.7
131.4
130.8
129.9
129.2
128.0
124.7
121.0
119.5
73.8
45.6
31.9
29.7
28.1
26.0
24.8
21.8
Chemical Shift (ppm)

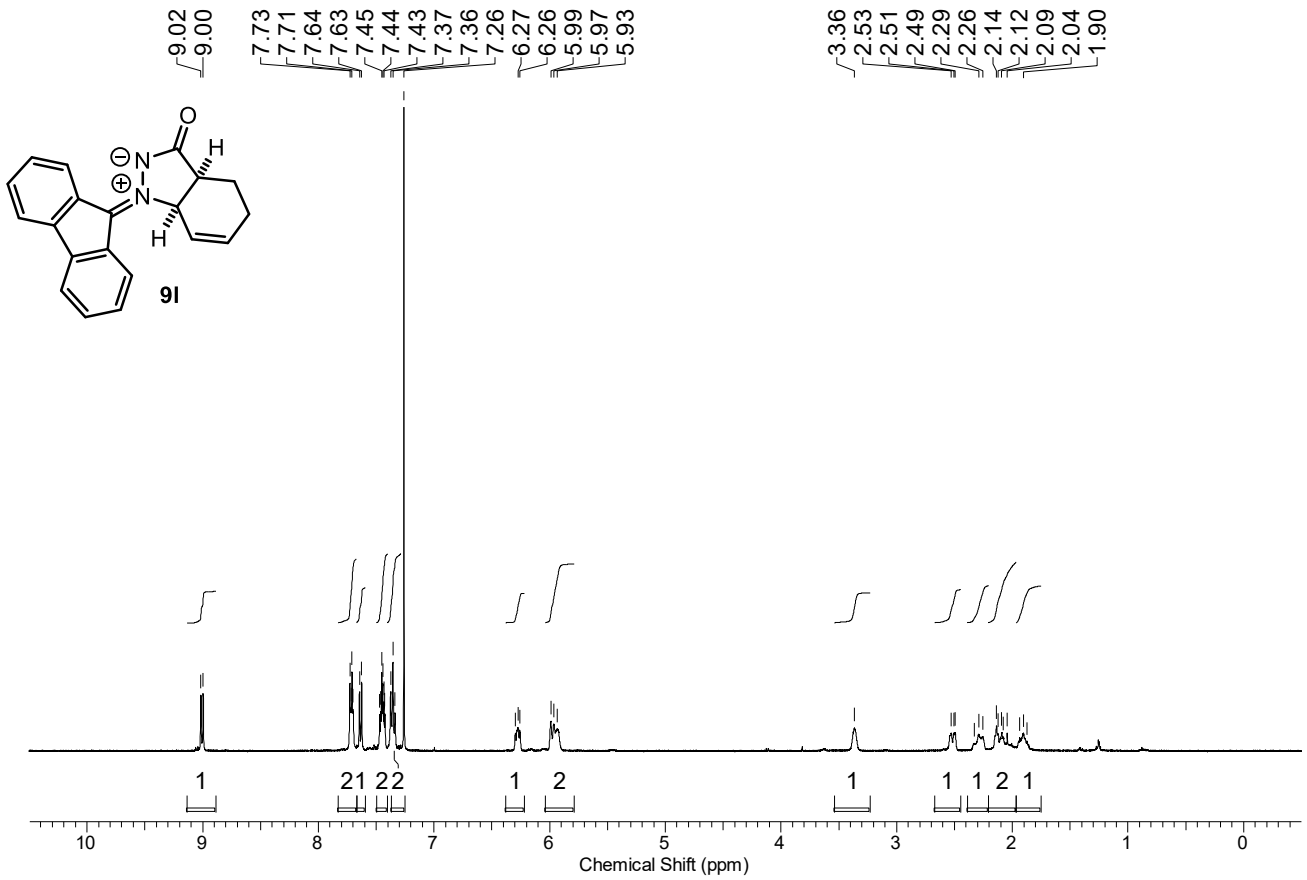
9.02
9.00
7.73
7.71
7.64
7.63
7.45
7.44
7.43
7.37
7.36
7.26
6.27
6.26
5.99
5.97
5.93
3.36
2.53
2.51
2.49
2.29
2.26
2.14
2.12
2.09
2.04
1.90
O
H
N
N
H
9l
1
2 1 2 2
1
2
1
1 1 2 1
Chemical Shift (ppm)

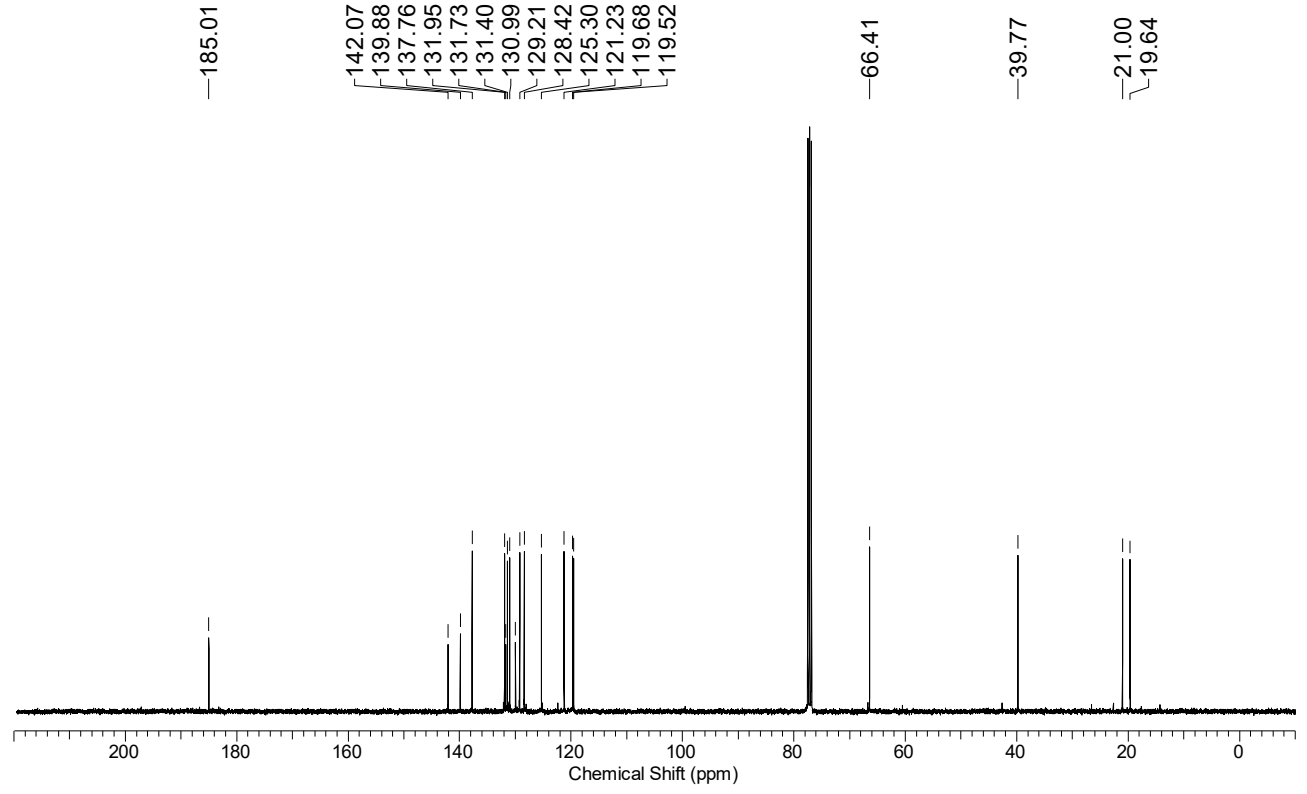
185.01
142.07
139.88
137.76
131.95
131.73
131.40
130.99
129.21
128.42
125.30
121.23
119.68
119.52
66.41
39.77
21.00
19.64
Chemical Shift (ppm)

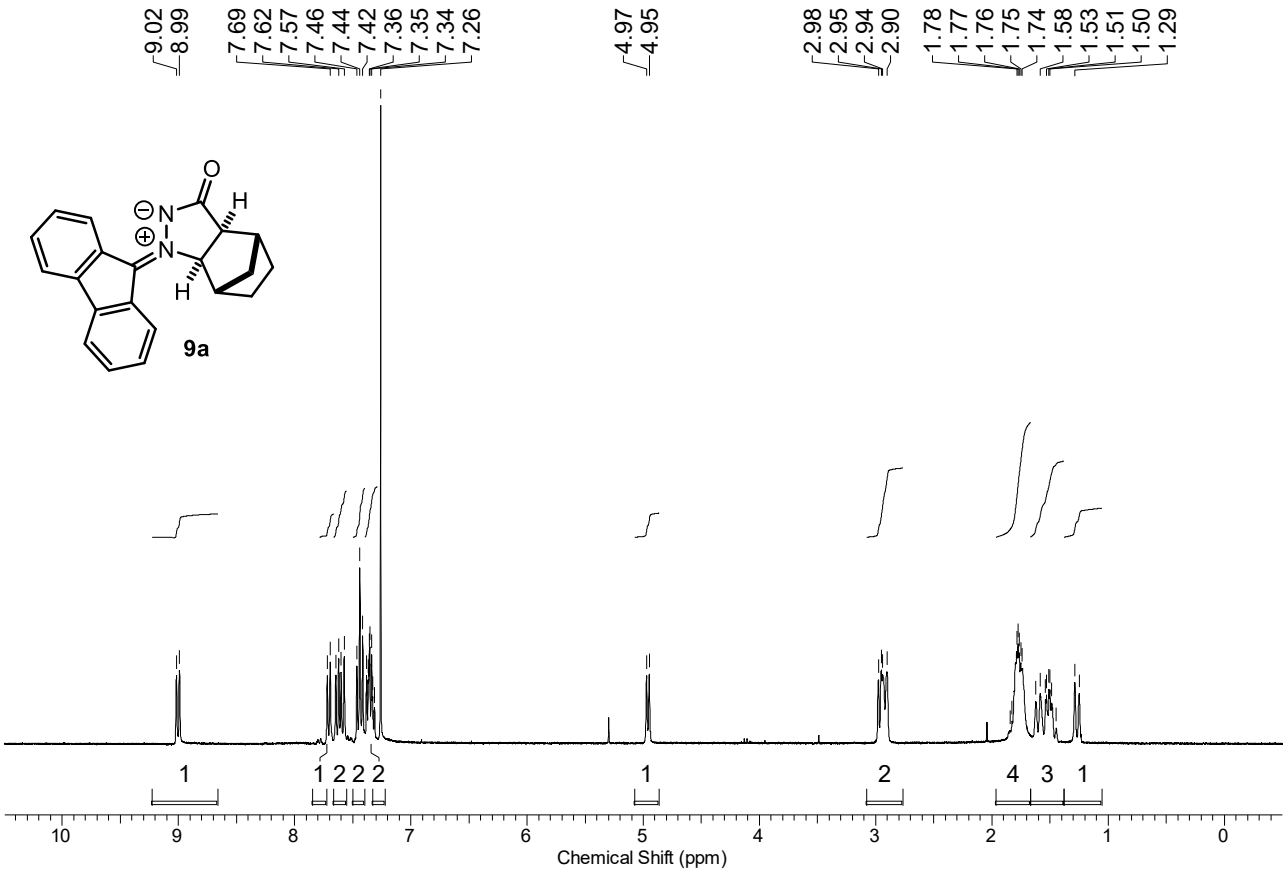
9.02
8.99
7.69
7.62
7.57
7.46
7.44
7.42
7.36
7.35
7.34
7.26
4.97
4.95
2.98
2.95
2.94
2.90
1.78
1.77
1.76
1.75
1.74
1.58
1.53
1.51
1.50
1.29
O
H
N
N
H
9a
1
1 2 2 2
1
2
4 3 1
10
9
8
7
6
5
4
3
2
1
0
Chemical Shift (ppm)

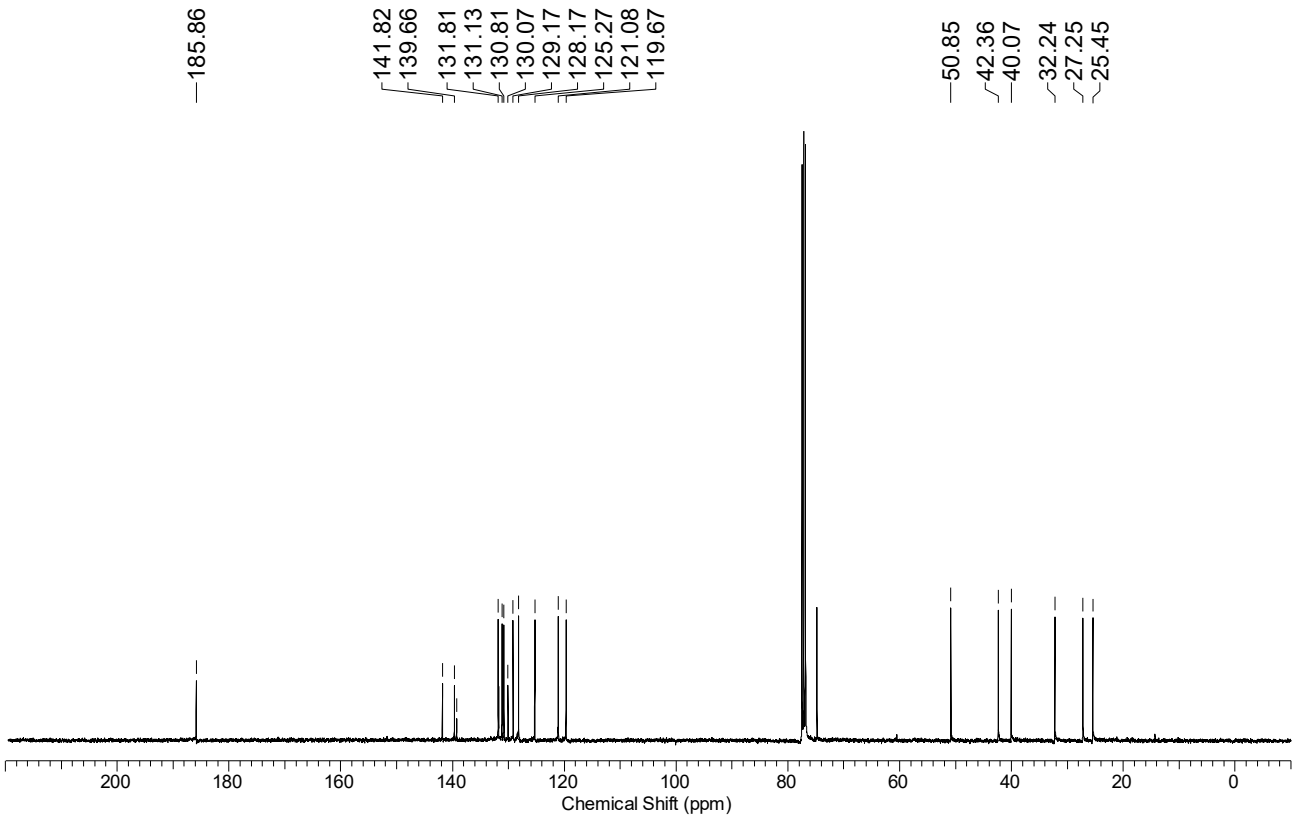
185.86
141.82
139.66
131.81
131.13
130.81
130.07
129.17
128.17
125.27
121.08
119.67
50.85
42.36
40.07
32.24
27.25
25.45
200
180
160
140
120
100
80
60
40
20
0
Chemical Shift (ppm)

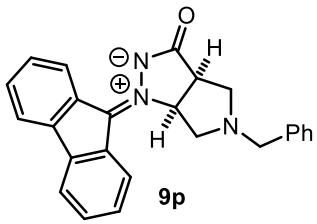
O
H
N
N
H
N
Ph

9p

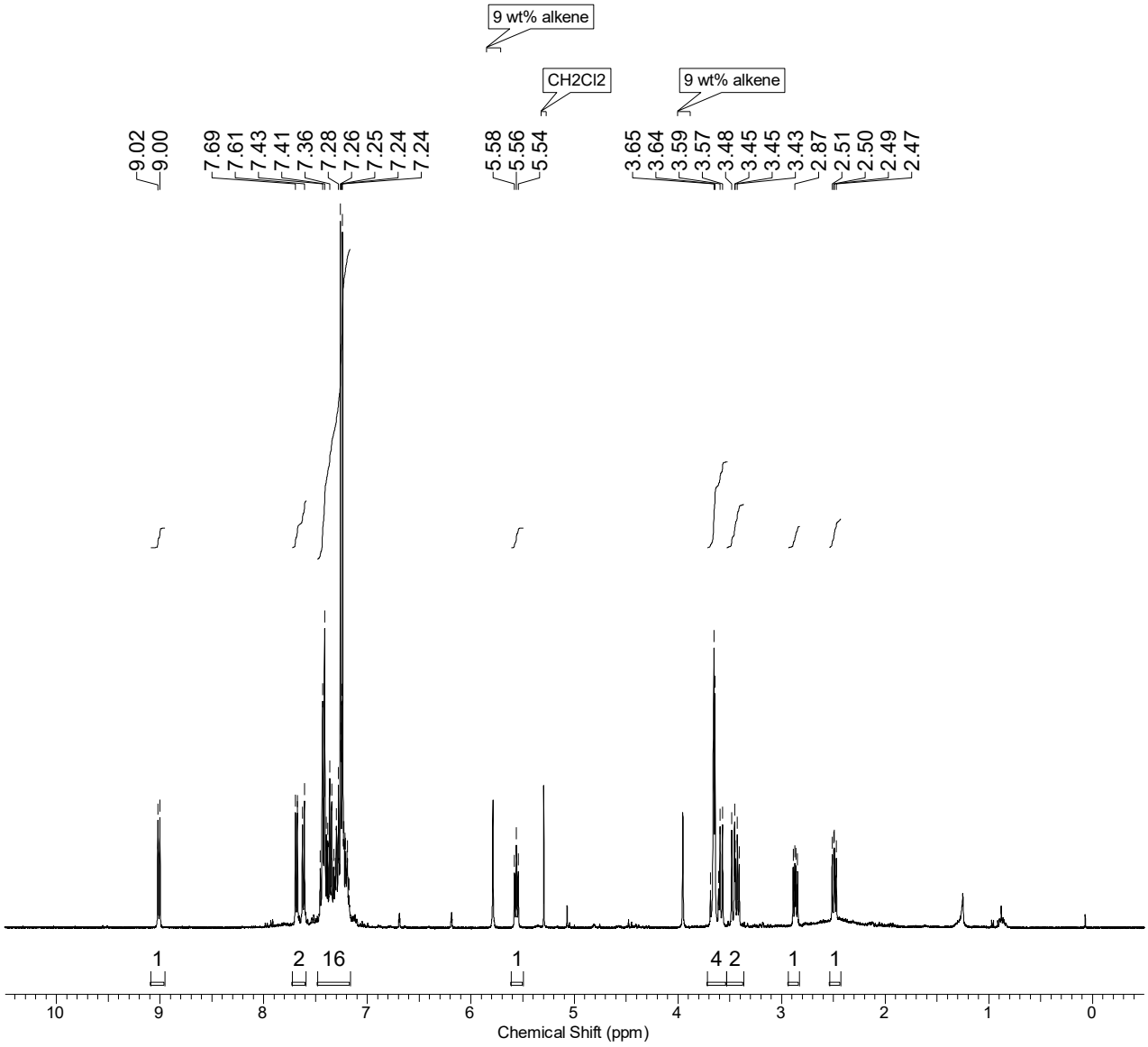
9 wt% alkene
CH2Cl2
9 wt% alkene
9.02
9.00
7.69
7.61
7.43
7.41
7.36
7.28
7.26
7.25
7.24
7.24
5.58
5.56
5.54
3.65
3.64
3.59
3.57
3.48
3.45
3.45
3.43
2.87
2.51
2.50
2.49
2.47
1
2
16
1
4
2
1
1
10
9
8
7
6
5
4
3
2
1
0
Chemical Shift (ppm)

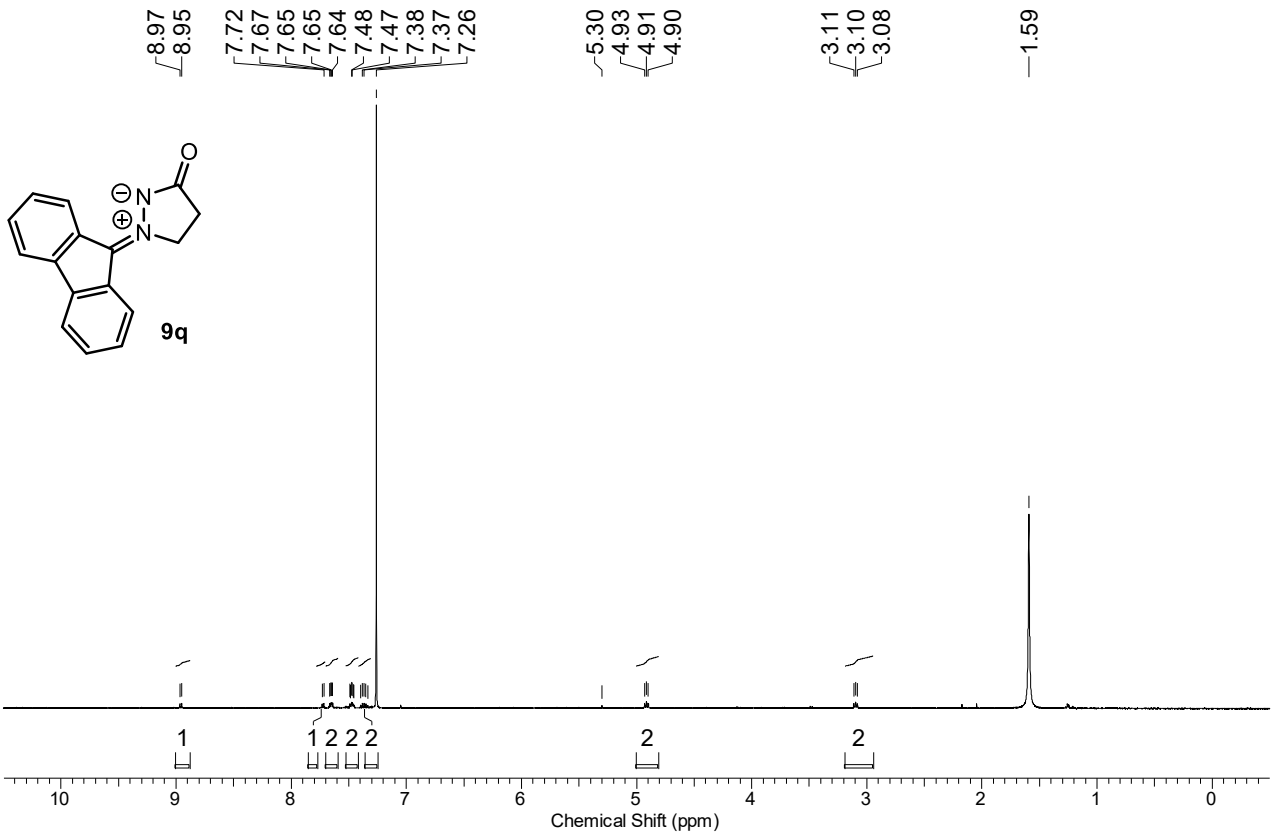
8.97
8.95
7.72
7.67
7.65
7.65
7.64
7.48
7.47
7.38
7.37
7.26
5.30
4.93
4.91
4.90
3.11
3.10
3.08
1.59
O
N
N
9q
1
1 2 2 2
2
2
10
9
8
7
6
5
4
3
2
1
0
Chemical Shift (ppm)

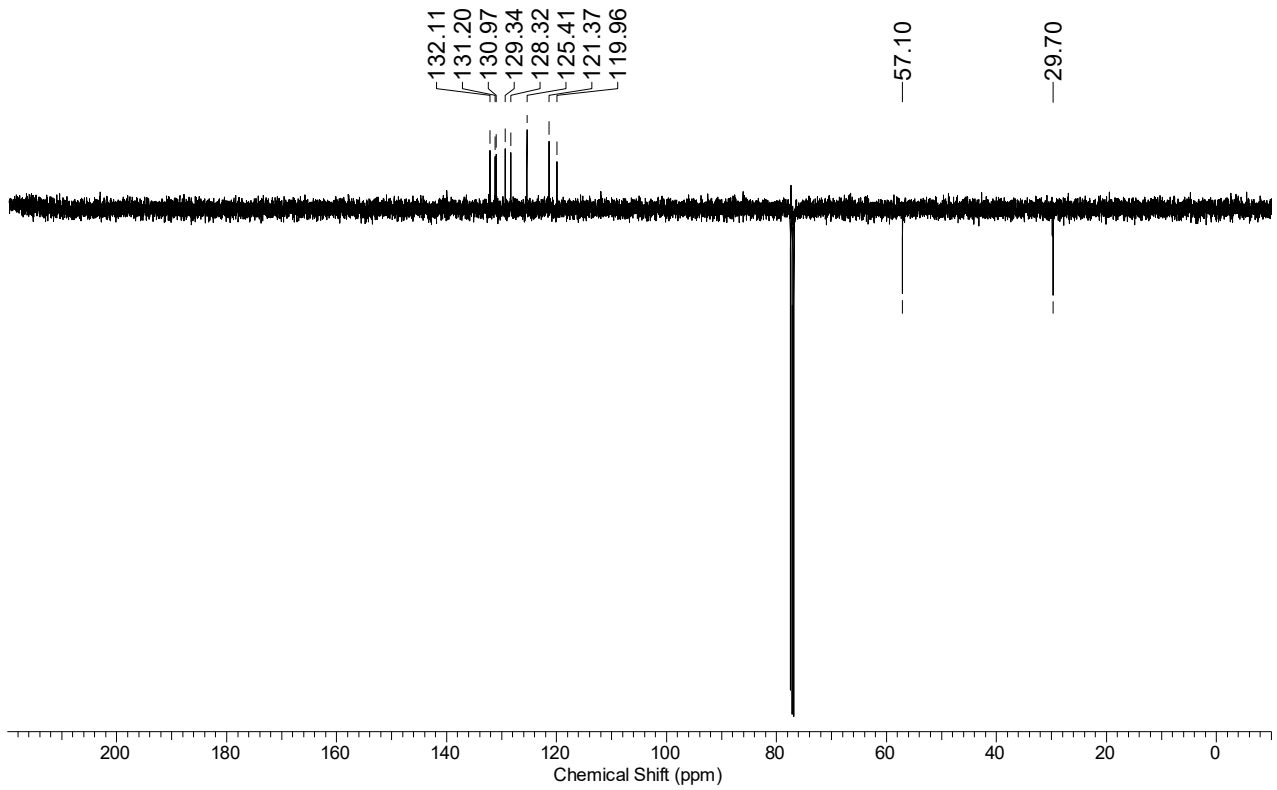
132.11
131.20
130.97
129.34
128.32
125.41
121.37
119.96
57.10
29.70
200
180
160
140
120
100
80
60
40
20
0
Chemical Shift (ppm)

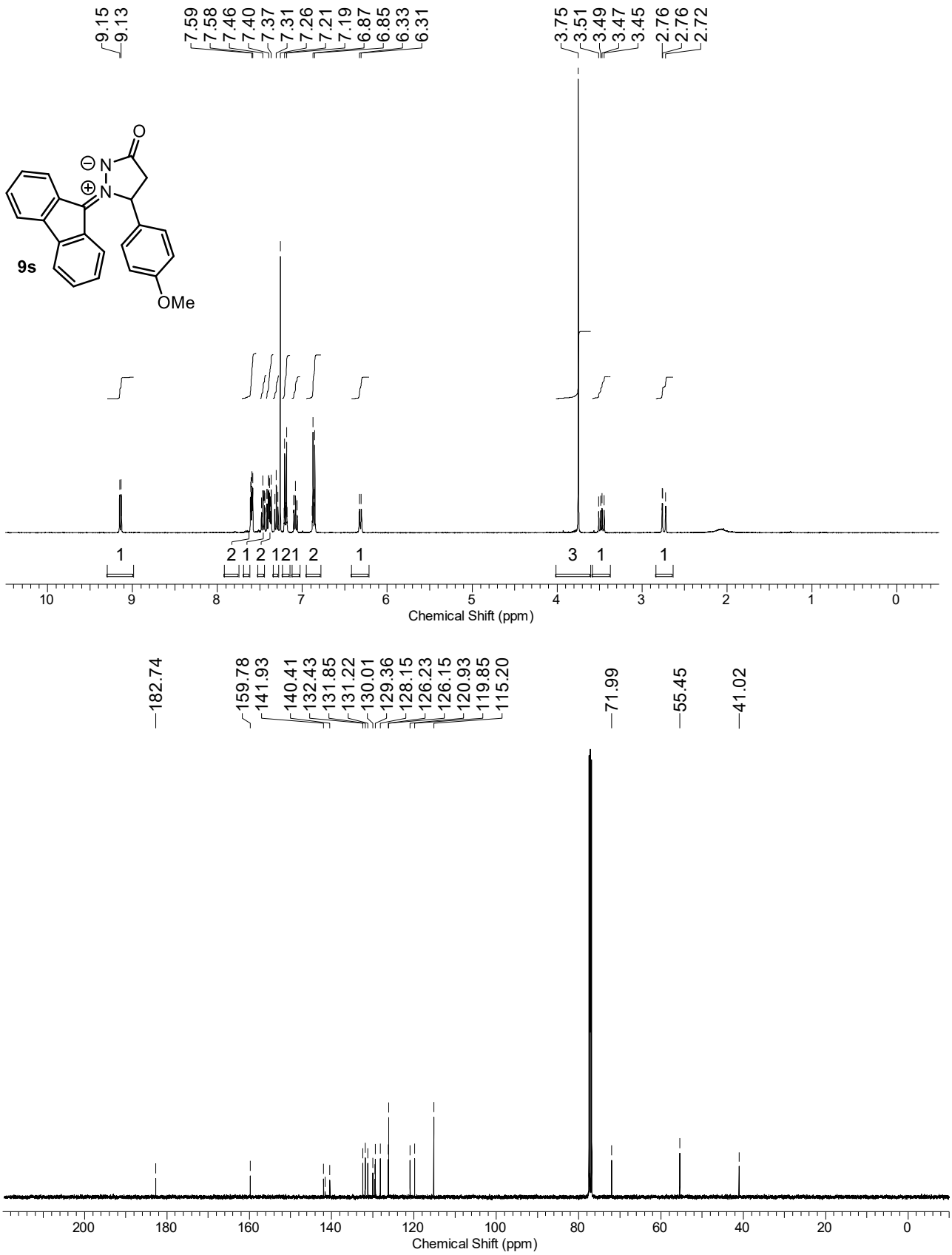
9.15
9.13
7.59
7.58
7.46
7.40
7.37
7.31
7.26
7.21
7.19
6.87
6.85
6.33
6.31
3.75
3.51
3.49
3.47
3.45
2.76
2.76
2.72
O
N
N
9s
OMe
1
2 1 2 1 2 1 2
1
3 1
1
Chemical Shift (ppm)
182.74
159.78
141.93
140.41
132.43
131.85
131.22
130.01
129.36
128.15
126.23
126.15
120.93
119.85
115.20
71.99
55.45
41.02
Chemical Shift (ppm)

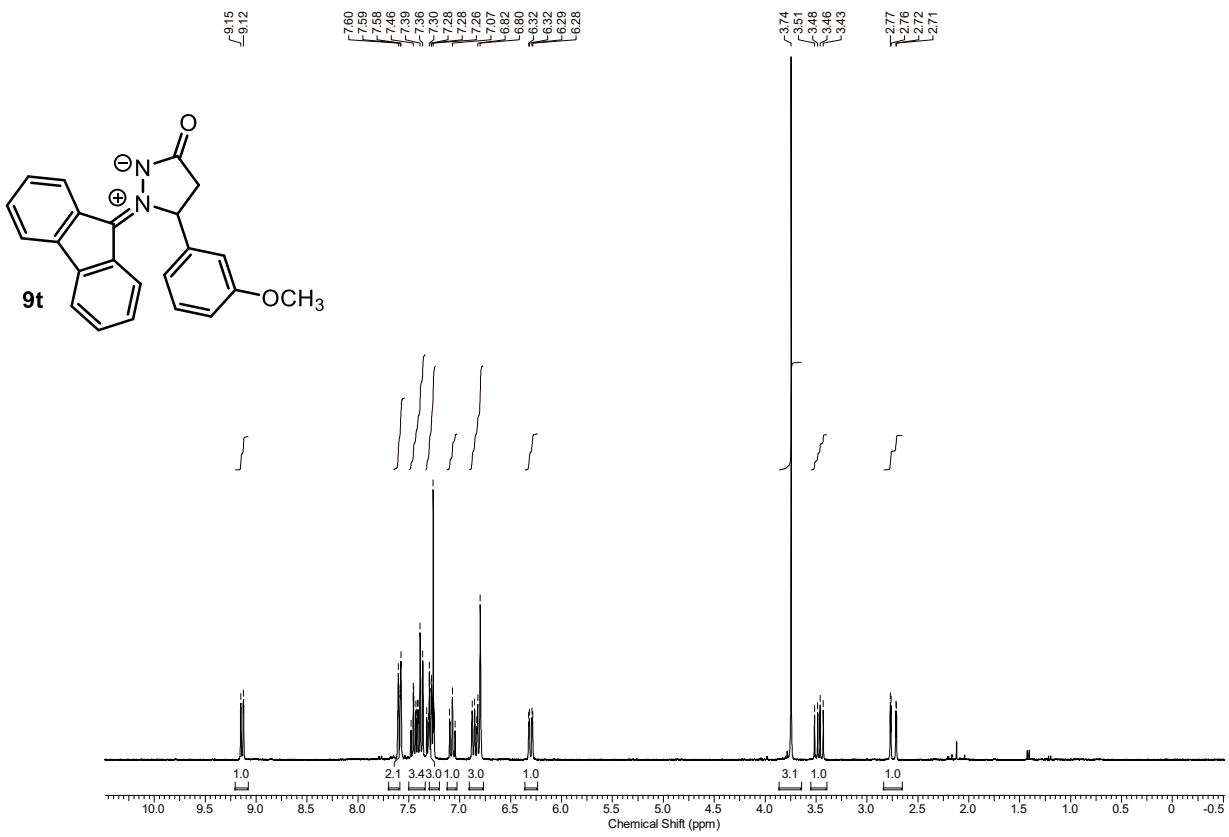
9.15
9.12
7.60
7.59
7.58
7.46
7.39
7.36
7.30
7.28
7.28
7.26
7.07
6.82
6.80
6.32
6.32
6.29
6.28
3.74
3.51
3.48
3.46
3.43
2.77
2.76
2.72
2.71
O
N
N
OCH3
9t
1.0
2.1
3.4
3.0
1.0
3.0
1.0
3.1
1.0
1.0
Chemical Shift (ppm)

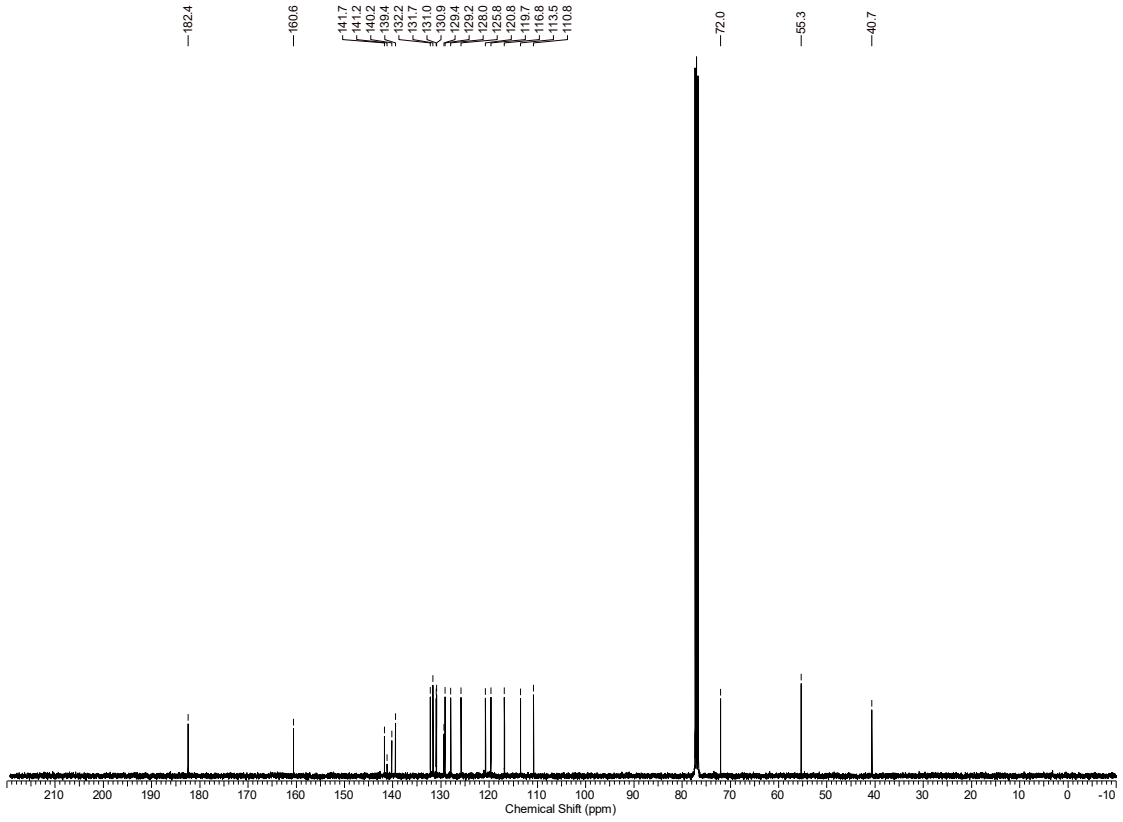
182.4
160.6
141.7
141.2
140.2
139.4
132.2
131.7
131.0
130.9
129.4
129.2
128.0
125.8
120.8
119.7
116.8
113.5
110.8
72.0
55.3
40.7
Chemical Shift (ppm)

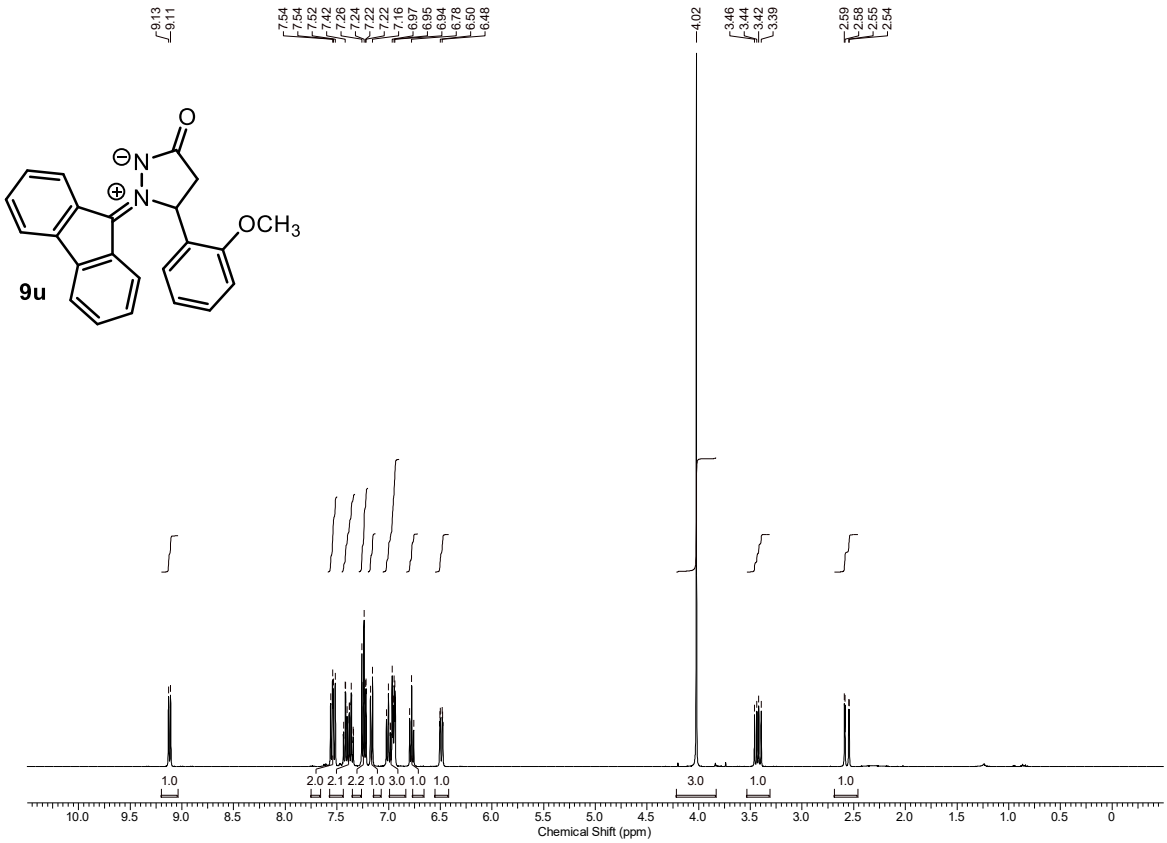
9.13
9.11
7.54
7.54
7.52
7.42
7.26
7.24
7.22
7.22
7.16
6.97
6.95
6.94
6.78
6.50
6.48
4.02
3.46
3.44
3.42
3.39
2.59
2.58
2.55
2.54
O
N
N
OCH3
9u
1.0
2.0
2.1
2.2
1.0
3.0
1.0
1.0
3.0
1.0
1.0
Chemical Shift (ppm)

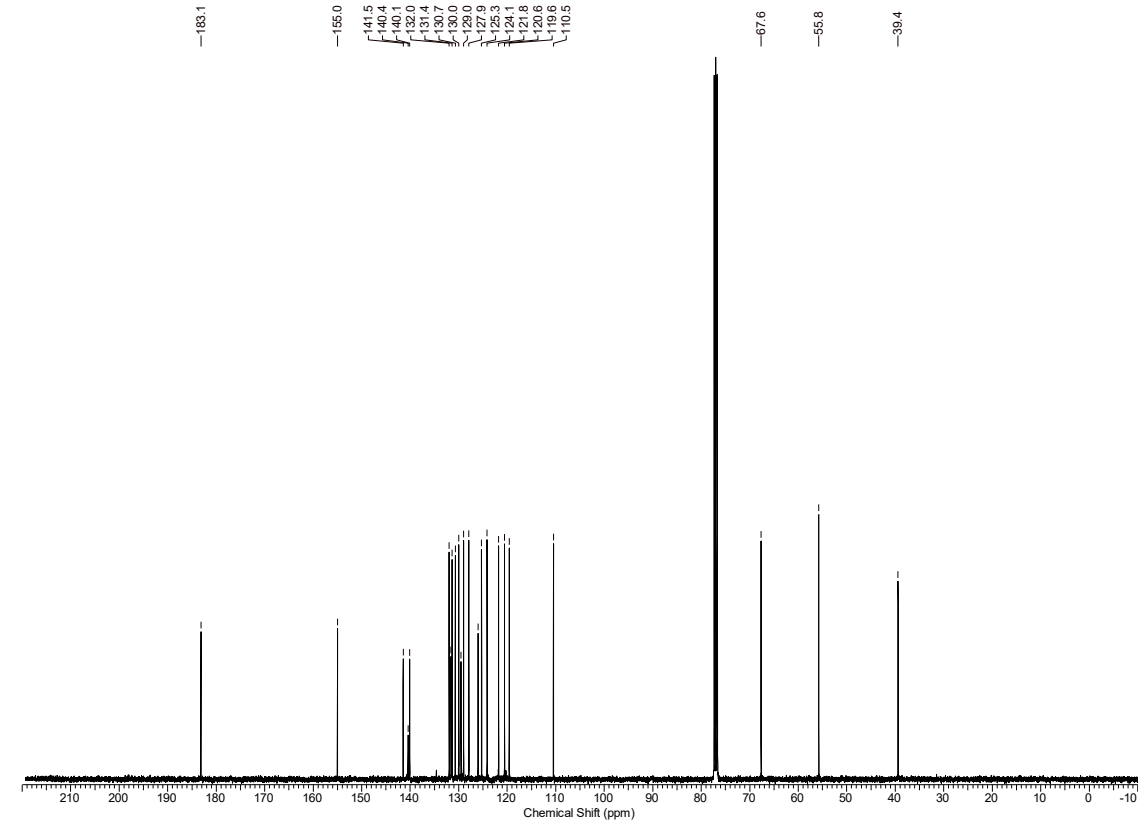
183.1
155.0
141.5
140.4
140.1
132.0
131.4
130.7
130.0
129.0
127.9
125.3
124.1
121.8
120.6
119.6
110.5
67.6
55.8
39.4
Chemical Shift (ppm)

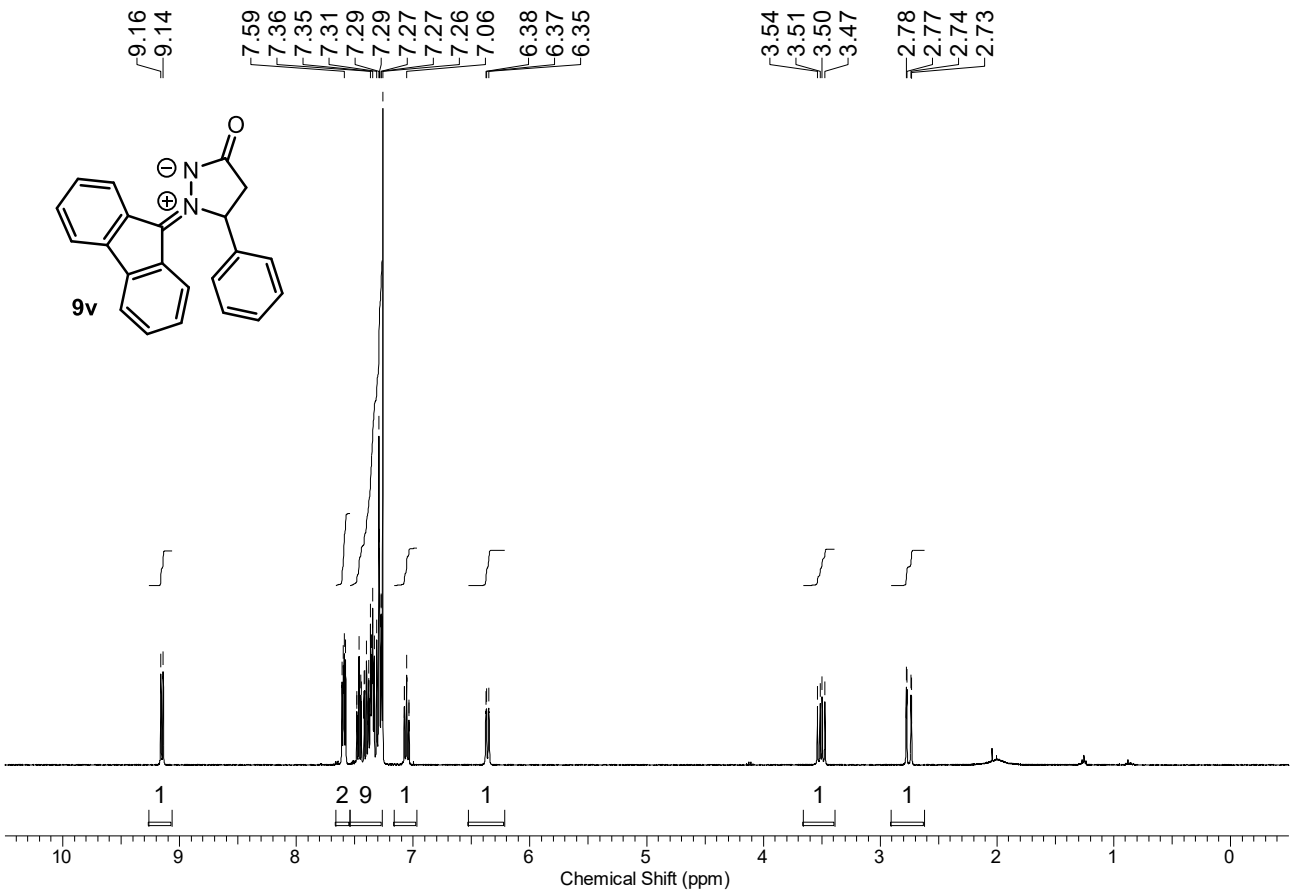
9.16
9.14
7.59
7.36
7.35
7.31
7.29
7.29
7.27
7.27
7.26
7.06
6.38
6.37
6.35
3.54
3.51
3.50
3.47
2.78
2.77
2.74
2.73
9v
1
2 9
1
1
1
1
Chemical Shift (ppm)

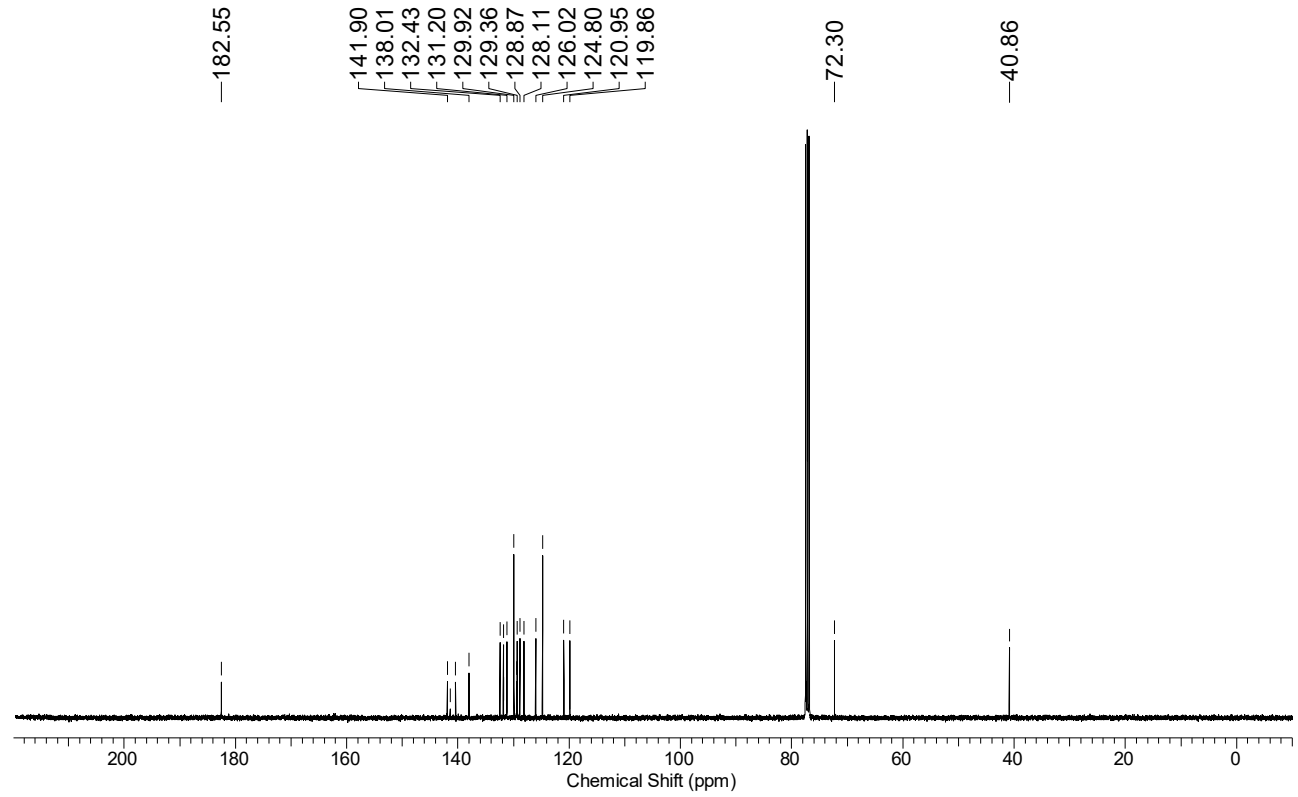
182.55
141.90
138.01
132.43
131.20
129.92
129.36
128.87
128.11
126.02
124.80
120.95
119.86
72.30
40.86
Chemical Shift (ppm)

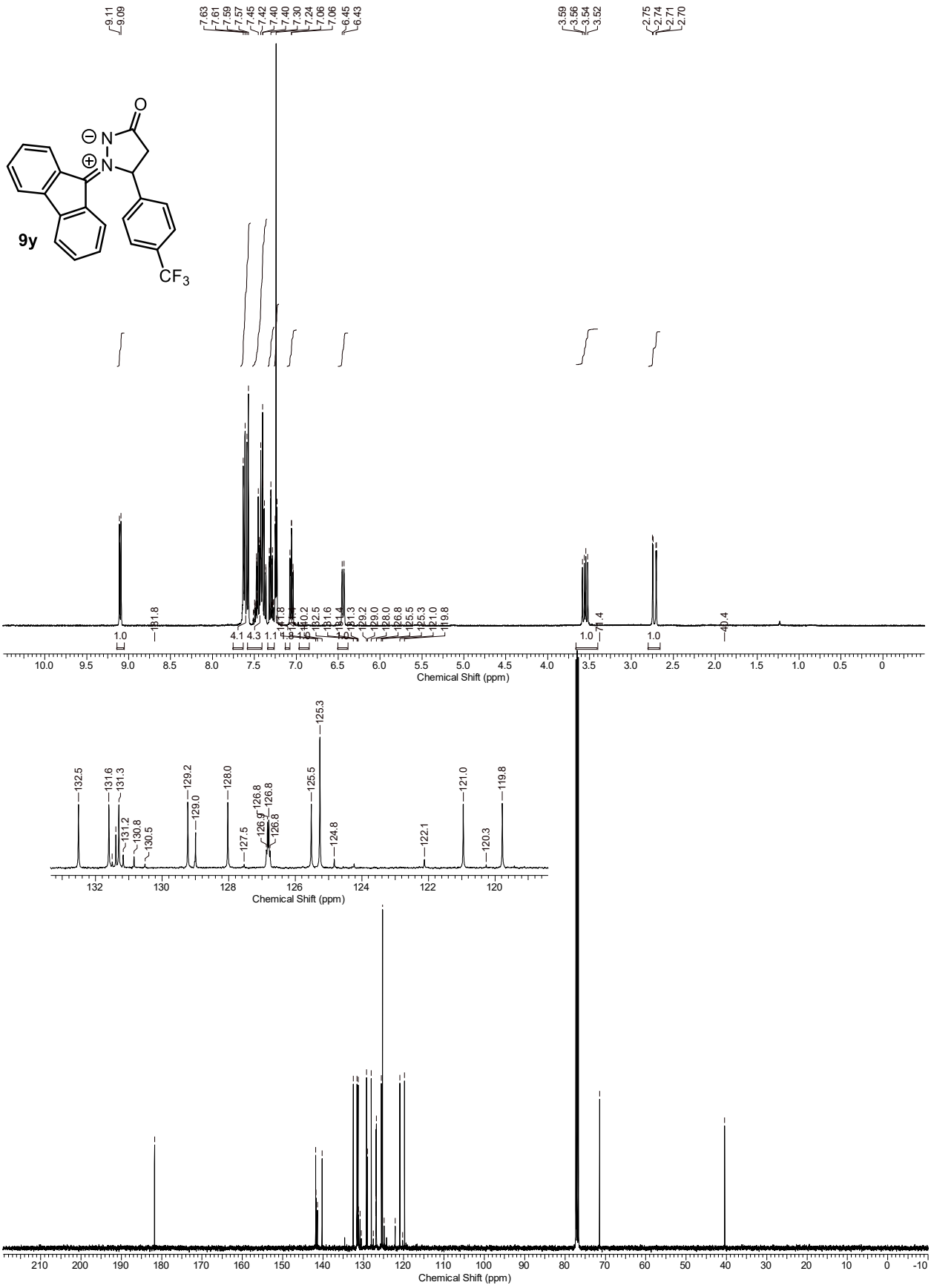
9y
Chemical Shift (ppm)
Chemical Shift (ppm)
Chemical Shift (ppm)

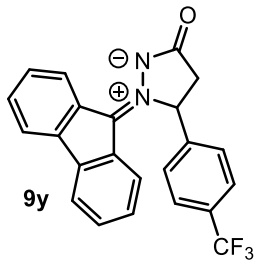
O
N
N
9y
CF3

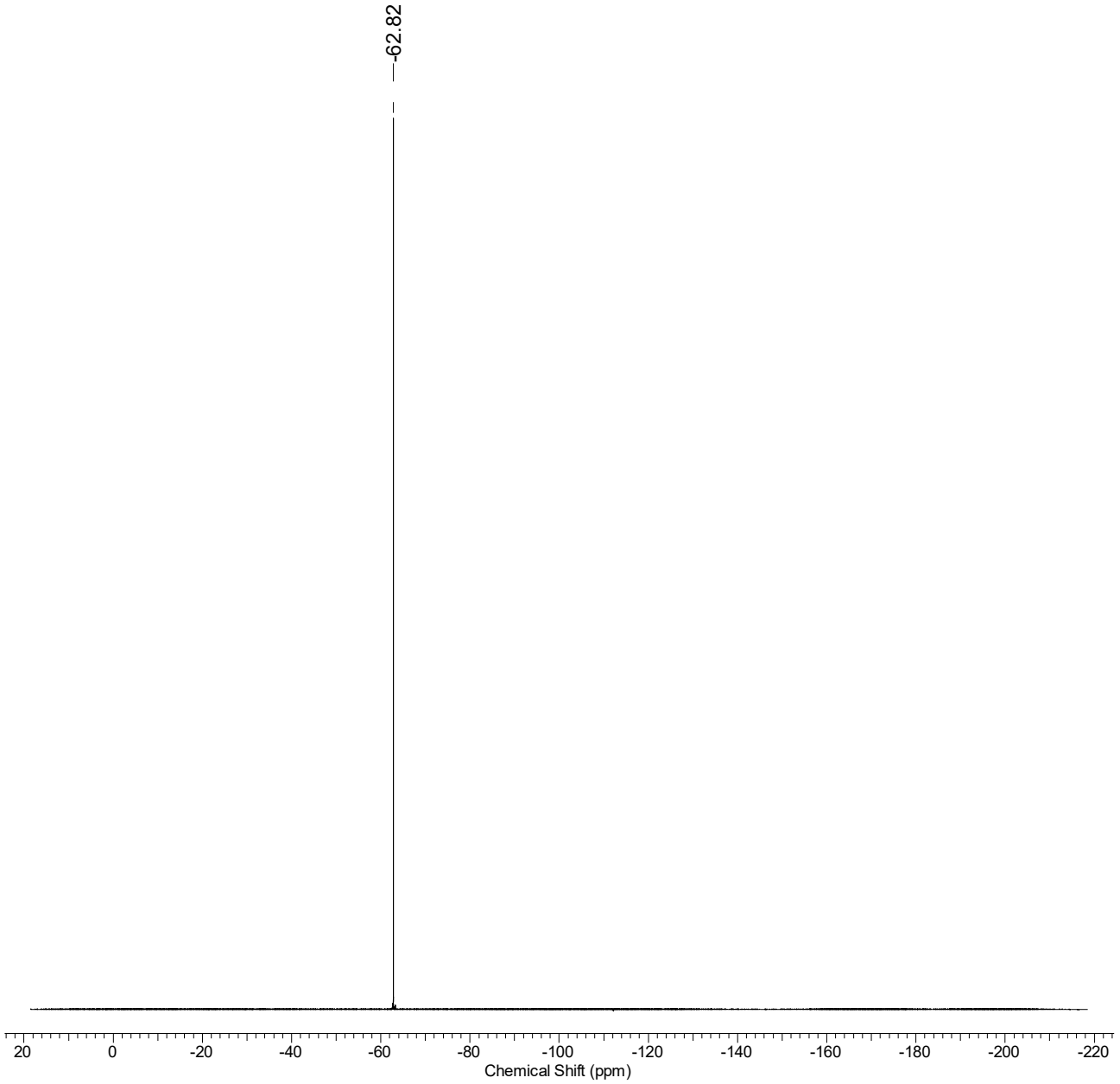
-62.82
20
0
-20
-40
-60
-80
-100
-120
-140
-160
-180
-200
-220
Chemical Shift (ppm)

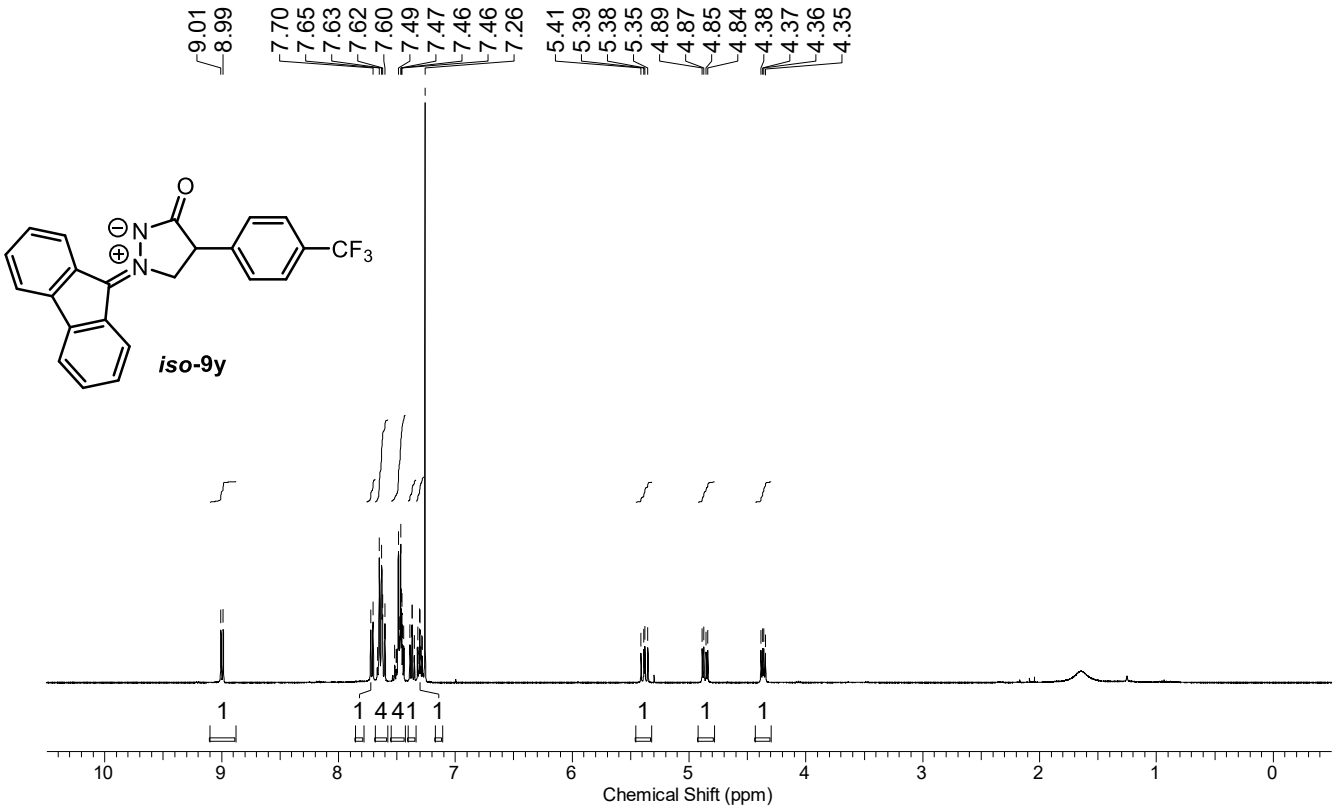
9.01
8.99
7.70
7.65
7.63
7.62
7.60
7.49
7.47
7.46
7.46
7.26
5.41
5.39
5.38
5.35
4.89
4.87
4.85
4.84
4.38
4.37
4.36
4.35
O
N
N
CF3
iso-9y
1
1 4 4 1 1
1
1
1
10
9
8
7
6
5
4
3
2
1
0
Chemical Shift (ppm)

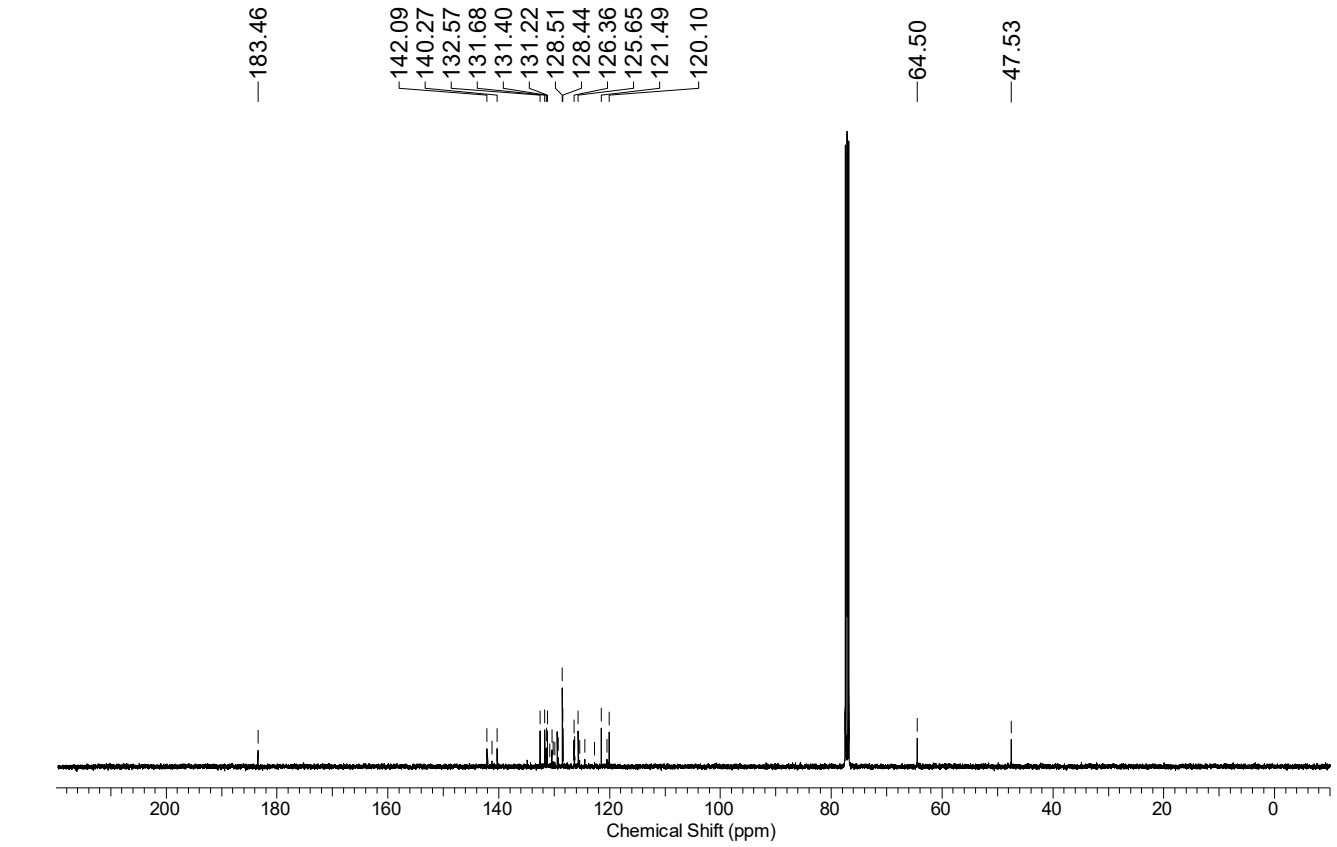
183.46
142.09
140.27
132.57
131.68
131.40
131.22
128.51
128.44
126.36
125.65
121.49
120.10
64.50
47.53
200
180
160
140
120
100
80
60
40
20
0
Chemical Shift (ppm)

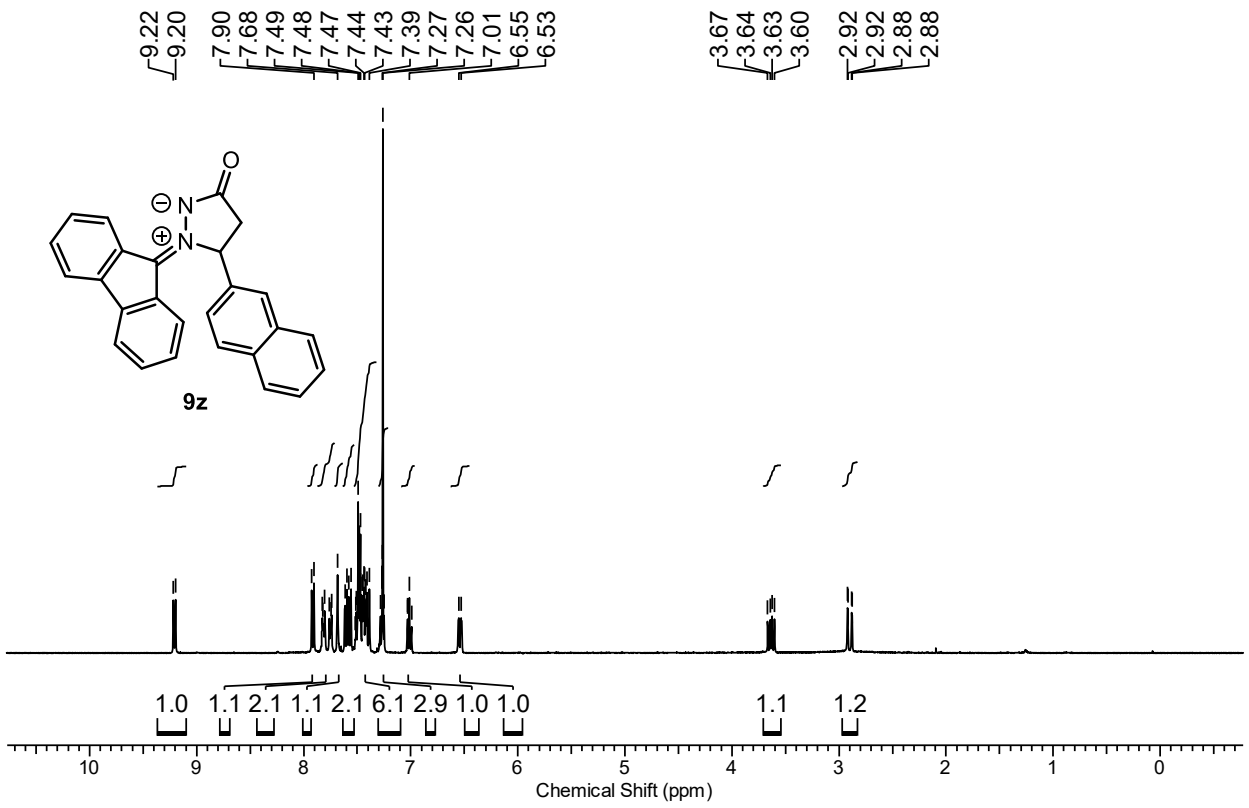
9.22
9.20
7.90
7.68
7.49
7.48
7.47
7.44
7.43
7.39
7.27
7.26
7.01
6.55
6.53
3.67
3.64
3.63
3.60
2.92
2.92
2.88
2.88
9z
1.0
1.1
2.1
1.1
2.1
6.1
2.9
1.0
1.0
1.1
1.2
Chemical Shift (ppm)

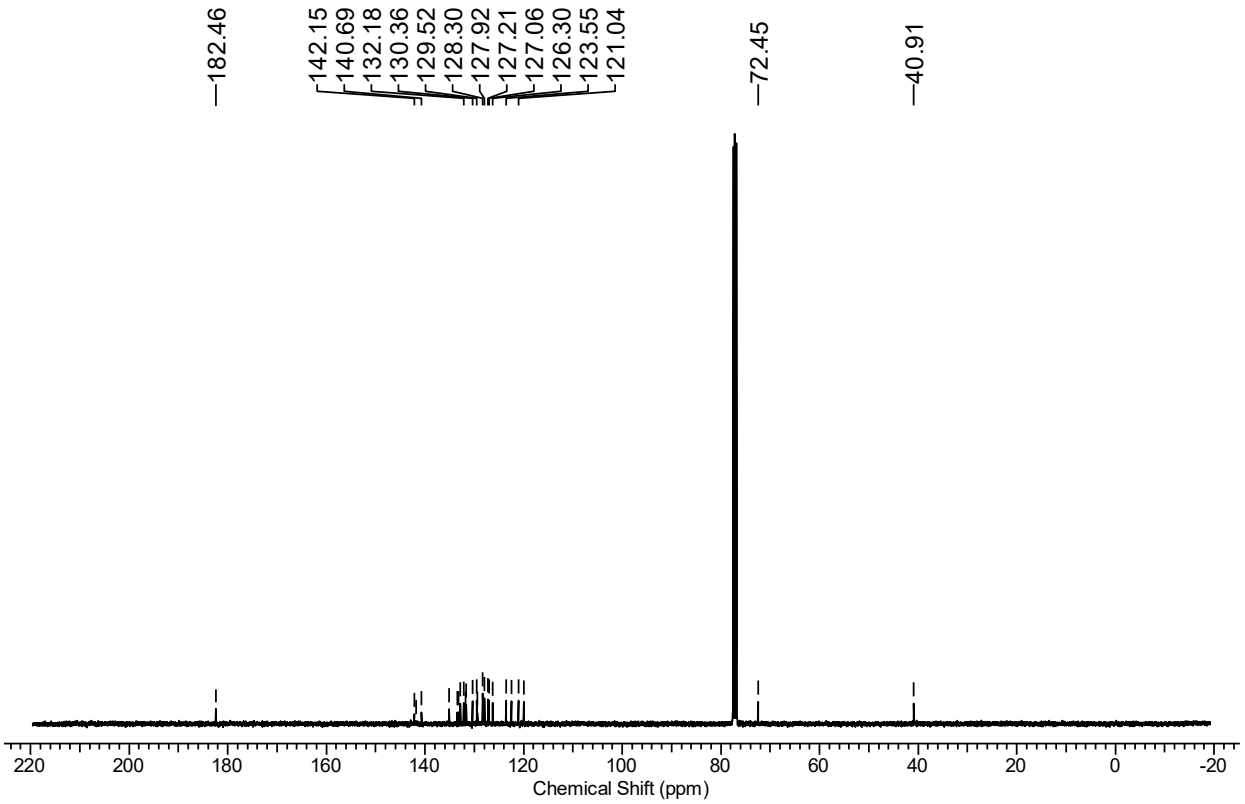
182.46
142.15
140.69
132.18
130.36
129.52
128.30
127.92
127.21
127.06
126.30
123.55
121.04
72.45
40.91
Chemical Shift (ppm)

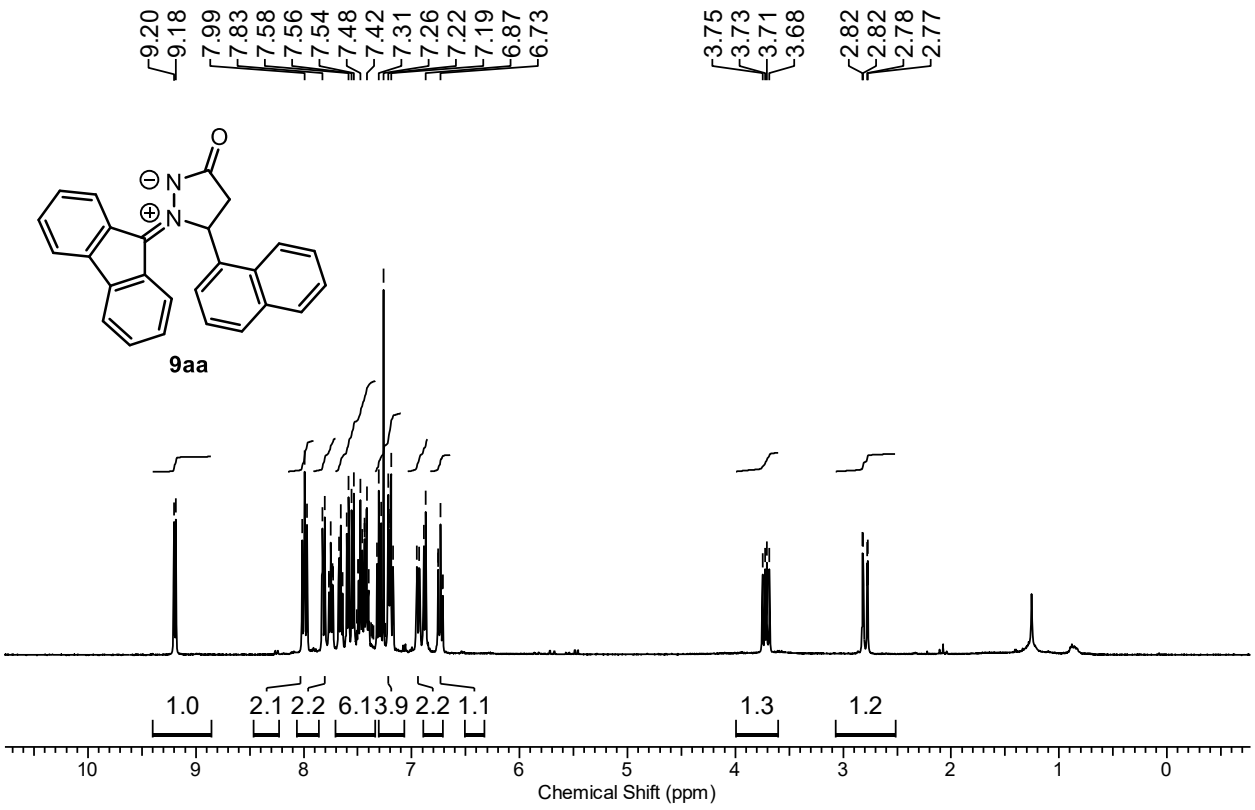
9.20
9.18
7.99
7.83
7.58
7.56
7.54
7.48
7.42
7.31
7.26
7.22
7.19
6.87
6.73
3.75
3.73
3.71
3.68
2.82
2.82
2.78
2.77
O
N
N
9aa
1.0
2.1
2.2
6.1
3.9
2.2
1.1
1.3
1.2
10
9
8
7
6
5
4
3
2
1
0
Chemical Shift (ppm)

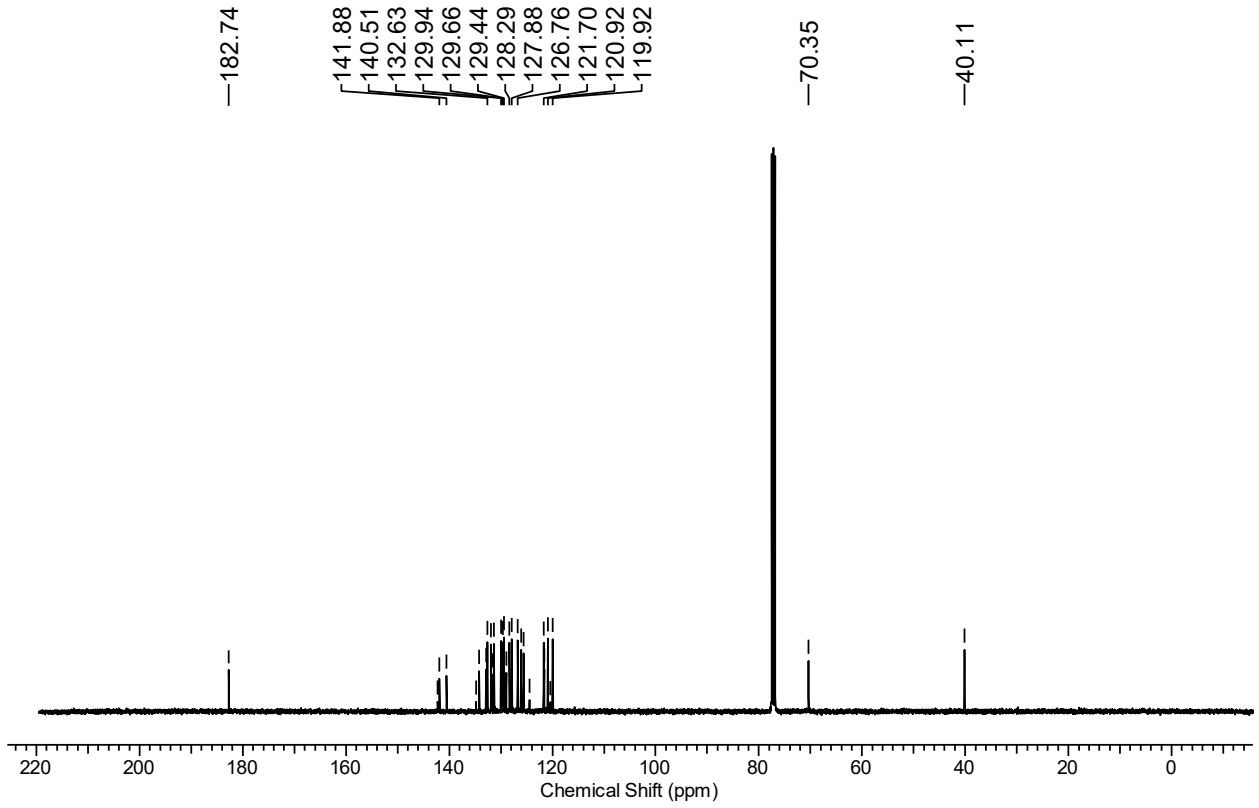
182.74
141.88
140.51
132.63
129.94
129.66
129.44
128.29
127.88
126.76
121.70
120.92
119.92
70.35
40.11
220
200
180
160
140
120
100
80
60
40
20
0
Chemical Shift (ppm)

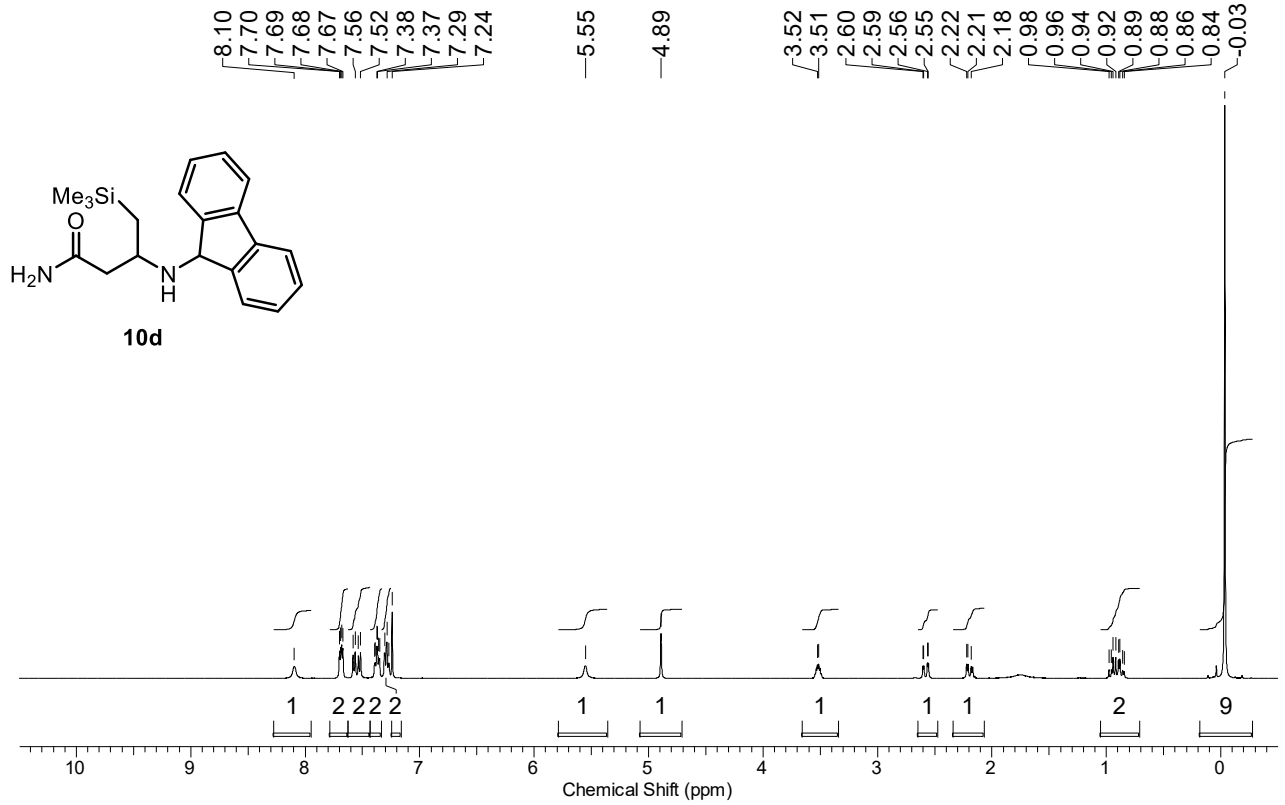
8.10
7.70
7.69
7.68
7.67
7.56
7.52
7.38
7.37
7.29
7.24
5.55
4.89
3.52
3.51
2.60
2.59
2.56
2.55
2.22
2.21
2.18
0.98
0.96
0.94
0.92
0.89
0.88
0.86
0.84
-0.03
Me3Si
O
H2N
N
H
10d
1 2 2 2 2 1 1 1 1 1 2 9
Chemical Shift (ppm)

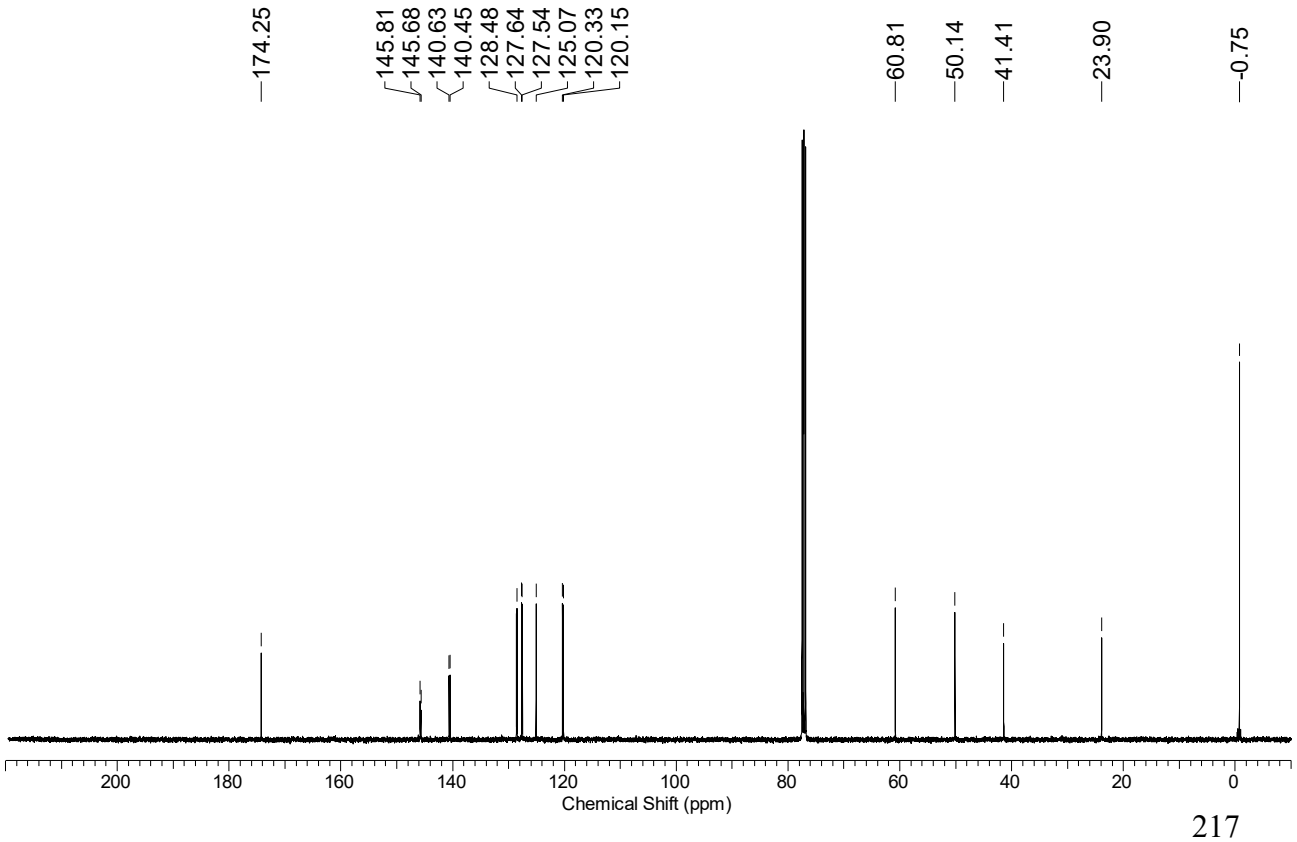
174.25
145.81
145.68
140.63
140.45
128.48
127.64
127.54
125.07
120.33
120.15
60.81
50.14
41.41
23.90
-0.75
Chemical Shift (ppm)

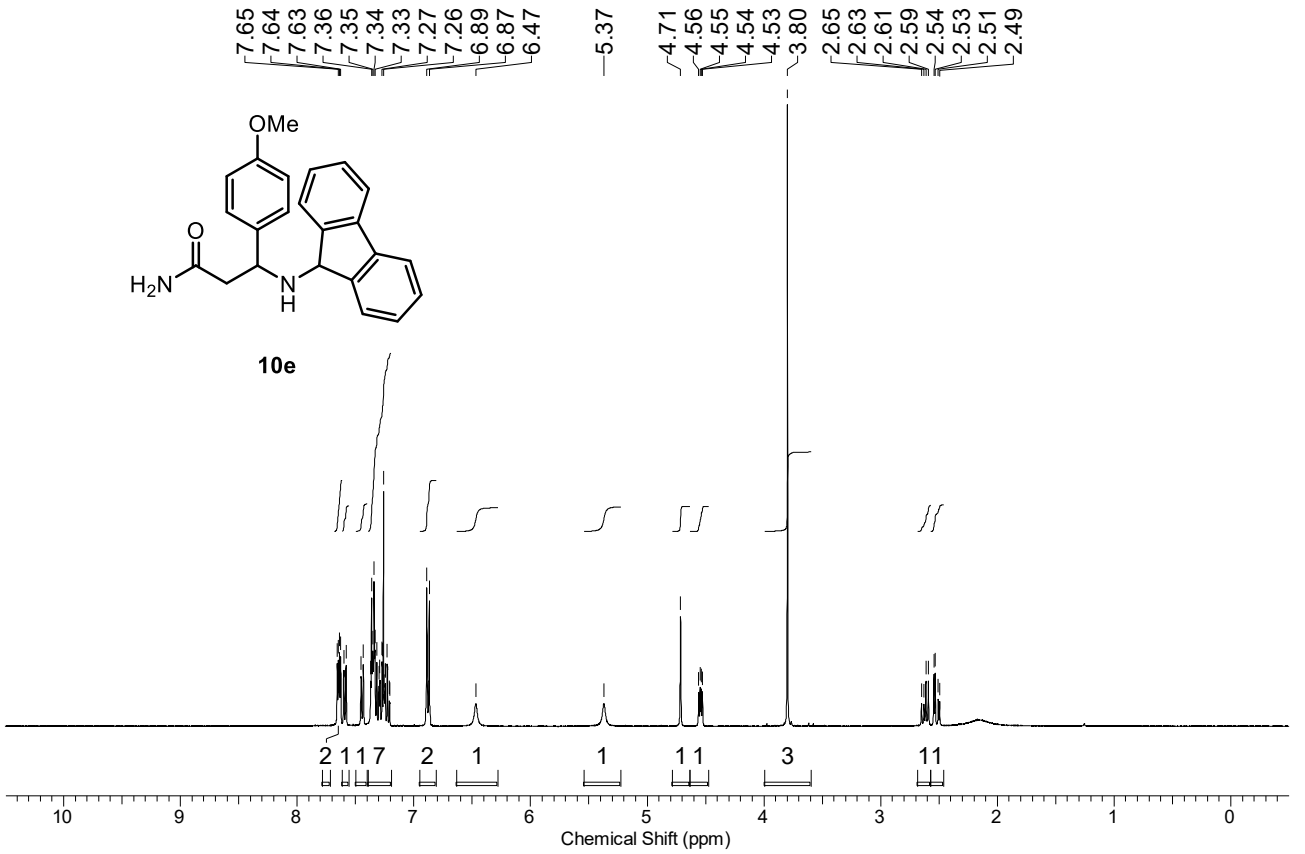
7.65
7.64
7.63
7.36
7.35
7.34
7.33
7.27
7.26
6.89
6.87
6.47
5.37
4.71
4.56
4.55
4.54
4.53
3.80
2.65
2.63
2.61
2.59
2.54
2.53
2.51
2.49
OMe
O
H2N
N
H
10e
2 1 1 7 2 1 1 1 1 3 1 1
Chemical Shift (ppm)

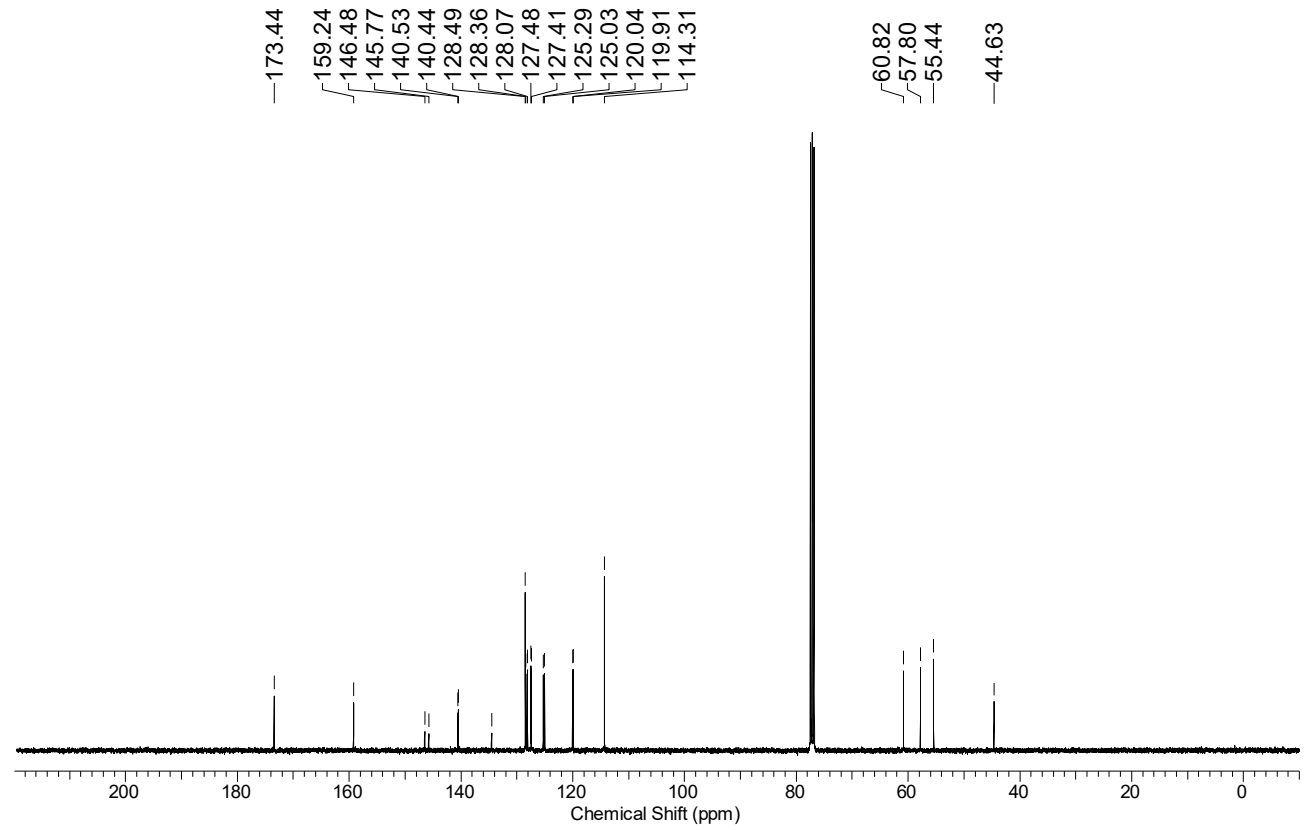
173.44
159.24
146.48
145.77
140.53
140.44
128.49
128.36
128.07
127.48
127.41
125.29
125.03
120.04
119.91
114.31
60.82
57.80
55.44
44.63
Chemical Shift (ppm)

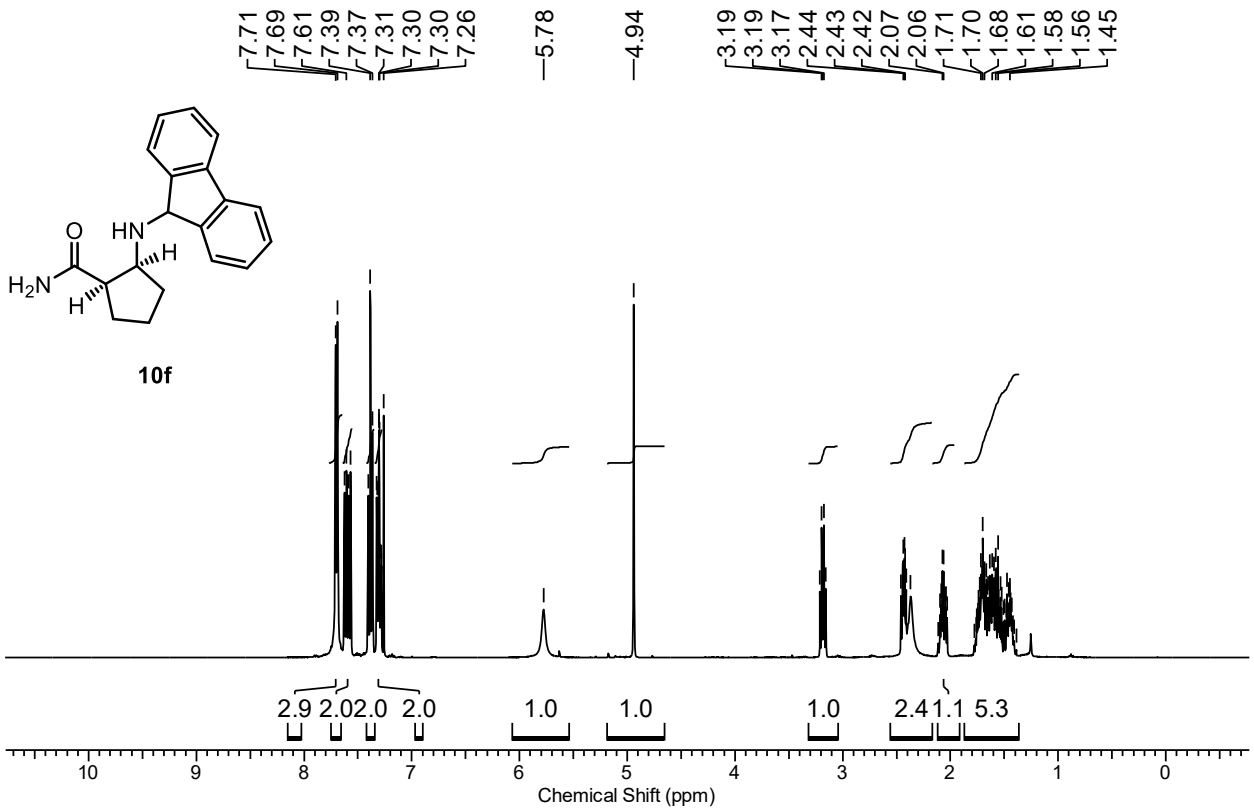
7.71
7.69
7.61
7.39
7.37
7.31
7.30
7.30
7.26
5.78
4.94
3.19
3.19
3.17
2.44
2.43
2.42
2.07
2.06
1.71
1.70
1.68
1.61
1.58
1.56
1.45
O
HN
H
H2N
H
10f
2.9 2.0 2.0 2.0
1.0
1.0
1.0
2.4 1.1 5.3
Chemical Shift (ppm)

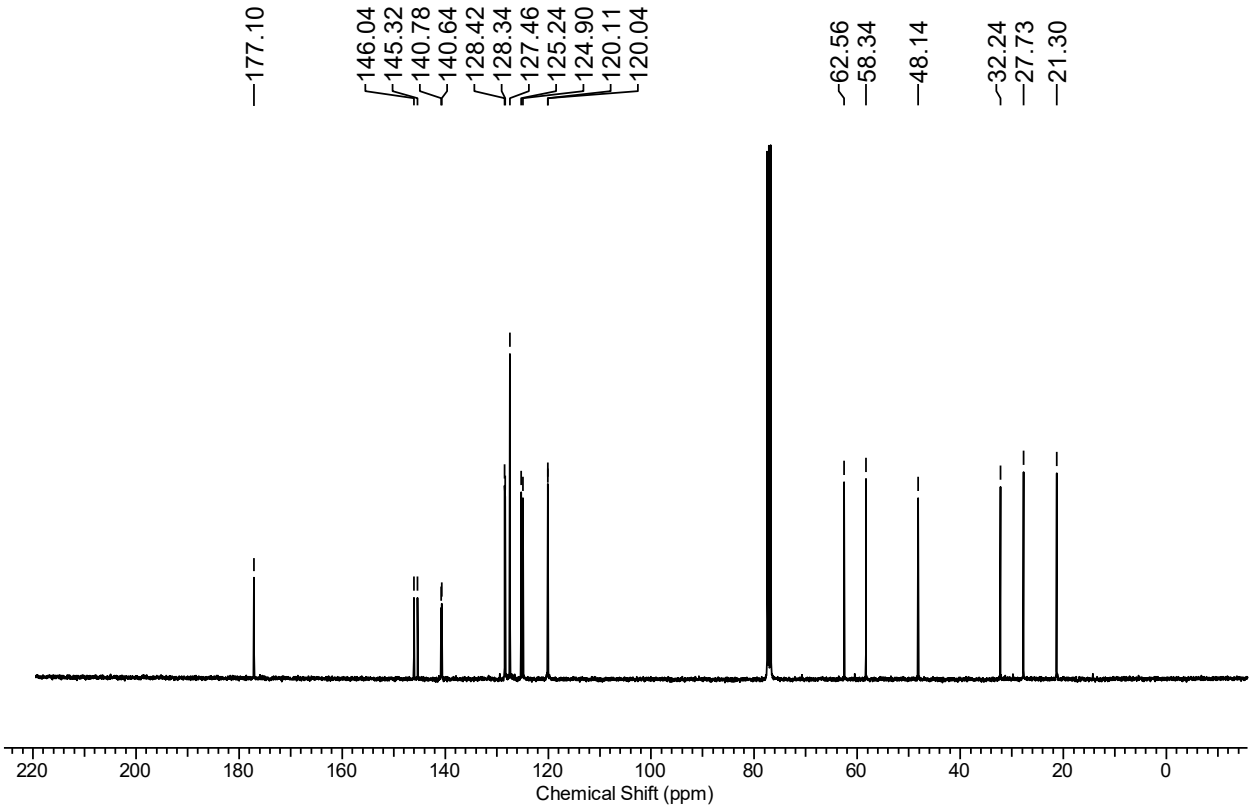
177.10
146.04
145.32
140.78
140.64
128.42
128.34
127.46
125.24
124.90
120.11
120.04
62.56
58.34
48.14
32.24
27.73
21.30
Chemical Shift (ppm)

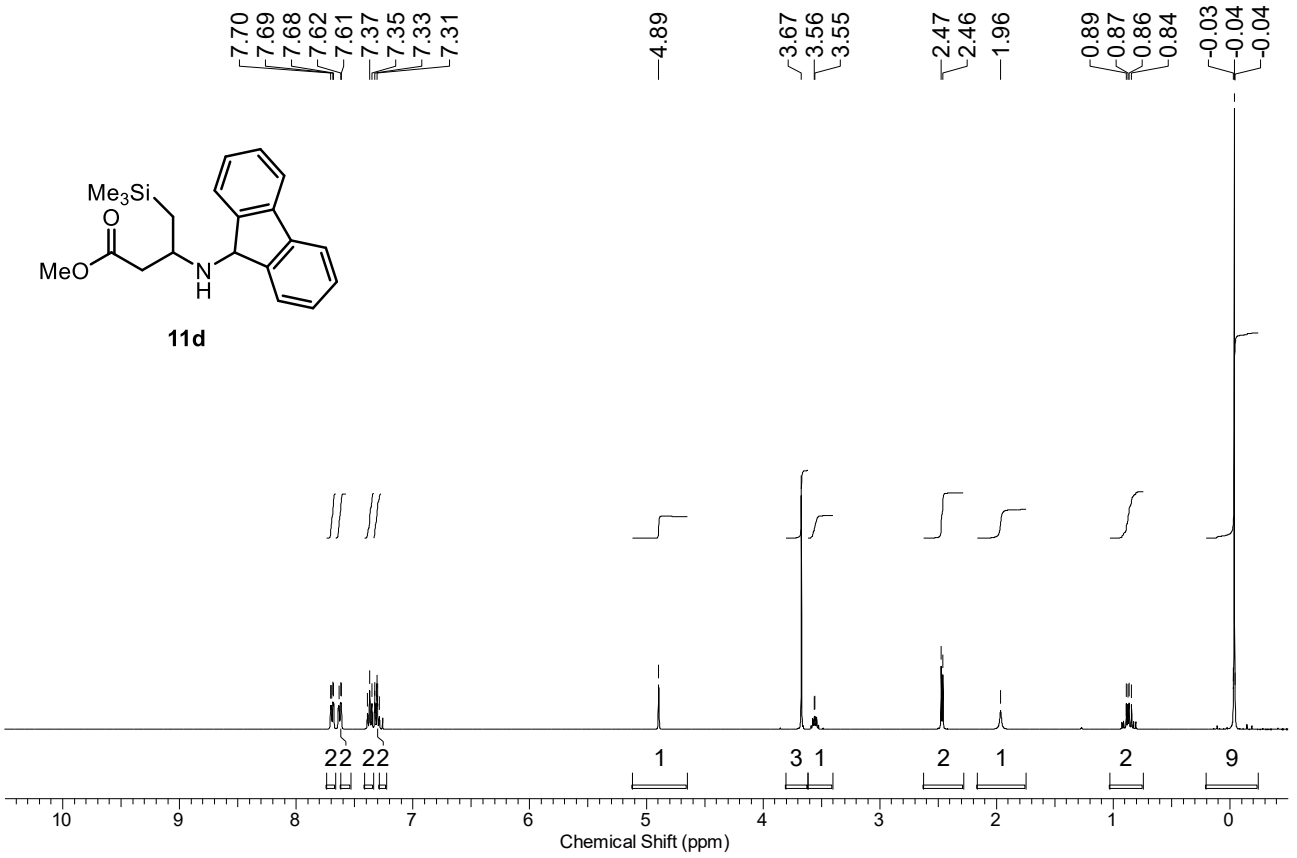
7.70
7.69
7.68
7.62
7.61
7.37
7.35
7.33
7.31
4.89
3.67
3.56
3.55
2.47
2.46
1.96
0.89
0.87
0.86
0.84
-0.03
-0.04
-0.04
Me3Si
O
MeO
N
H
11d
22 22
1
3 1
2
1
2
9
Chemical Shift (ppm)

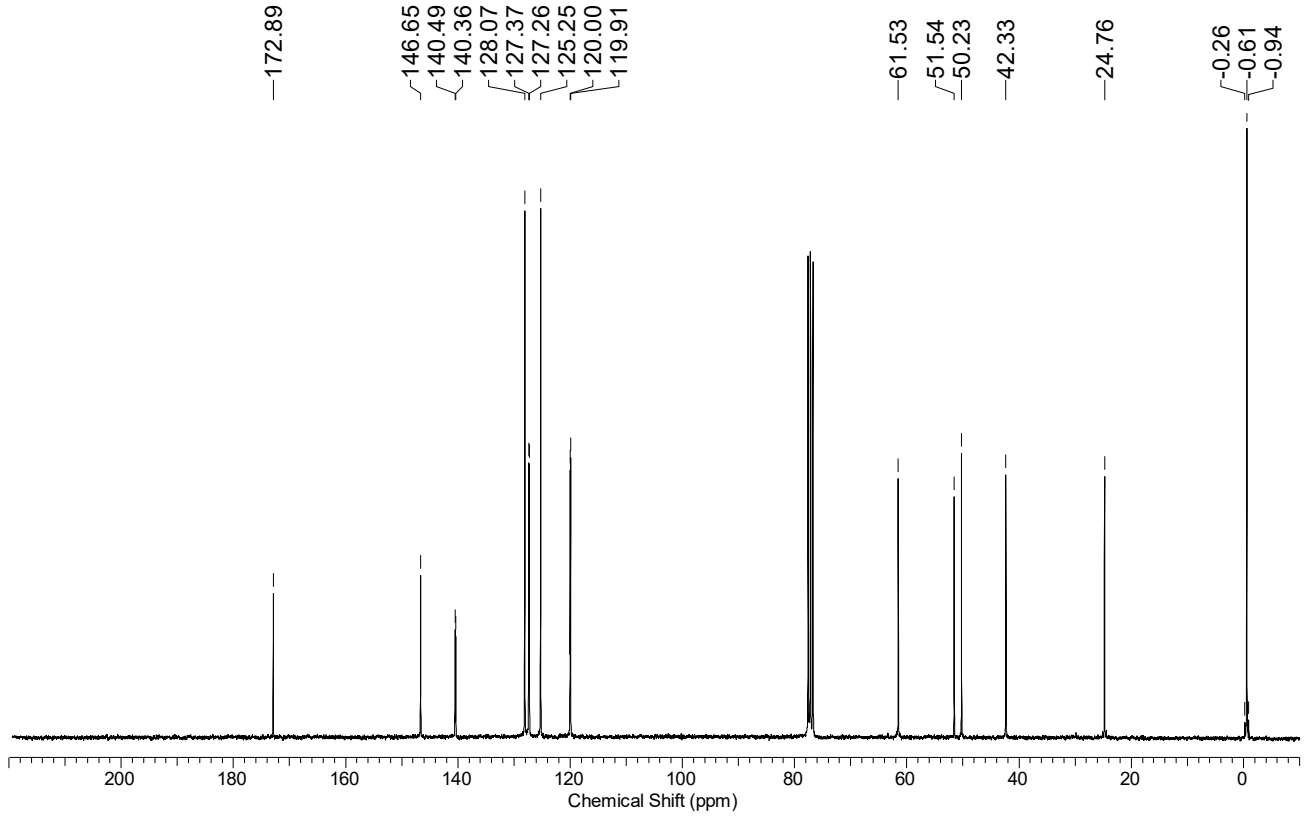
172.89
146.65
140.49
140.36
128.07
127.37
127.26
125.25
120.00
119.91
61.53
51.54
50.23
42.33
24.76
-0.26
-0.61
-0.94
Chemical Shift (ppm)

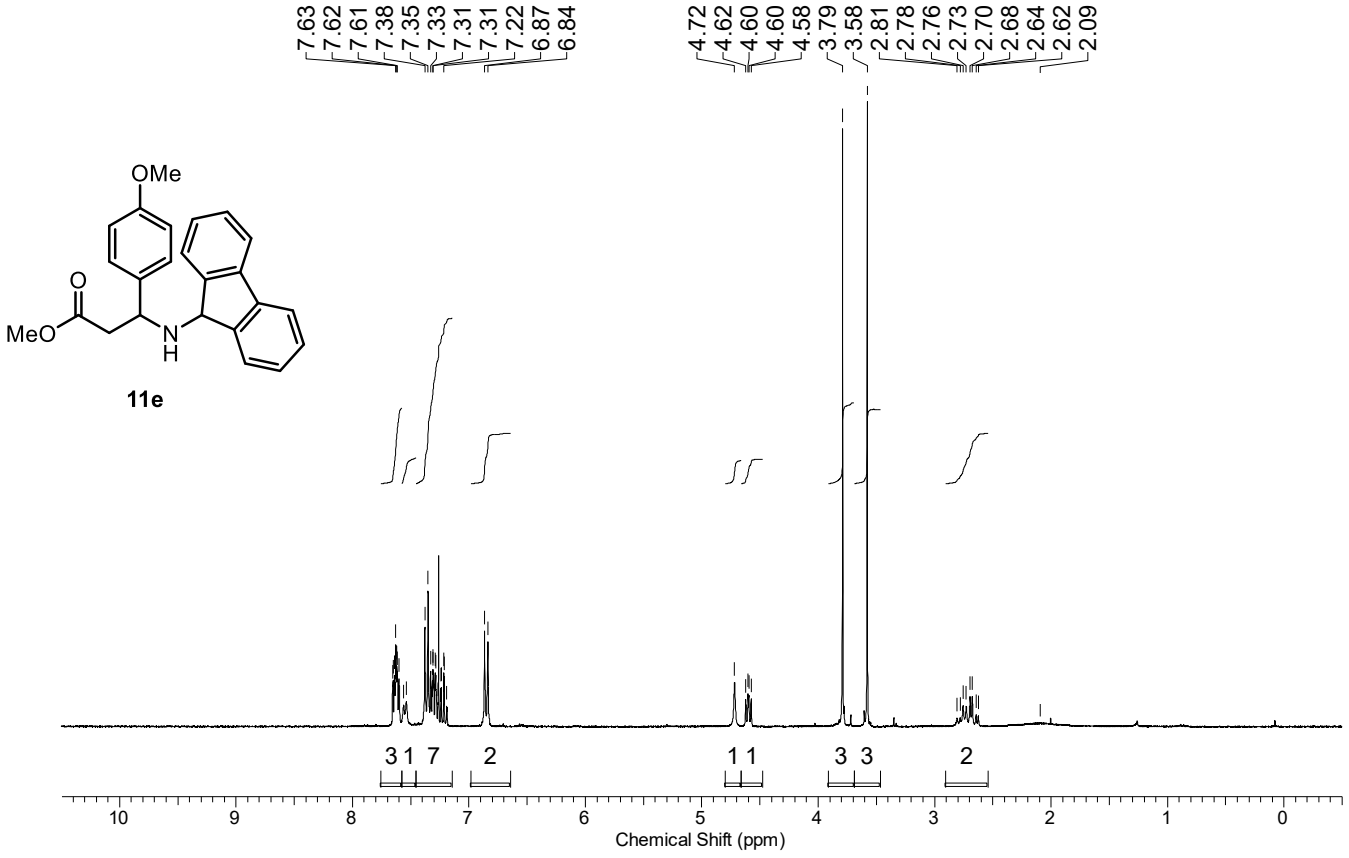
7.63
7.62
7.61
7.38
7.35
7.33
7.31
7.31
7.22
6.87
6.84
4.72
4.62
4.60
4.60
4.58
3.79
3.58
2.81
2.78
2.76
2.73
2.70
2.68
2.64
2.62
2.09
OMe
O
MeO
N
H
11e
3 1 7 2 1 1 3 3 2
Chemical Shift (ppm)

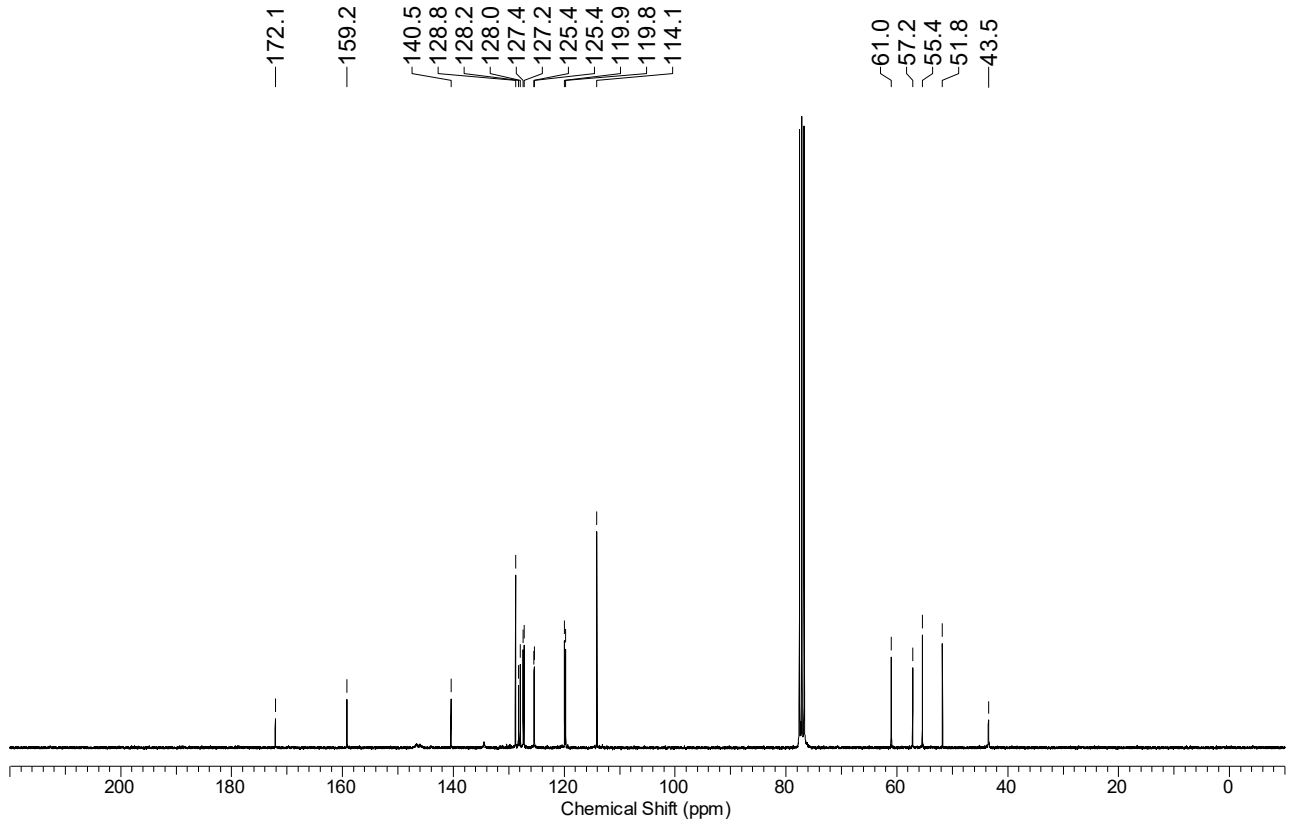
172.1
159.2
140.5
128.8
128.2
128.0
127.4
127.2
125.4
125.4
119.9
119.8
114.1
61.0
57.2
55.4
51.8
43.5
Chemical Shift (ppm)

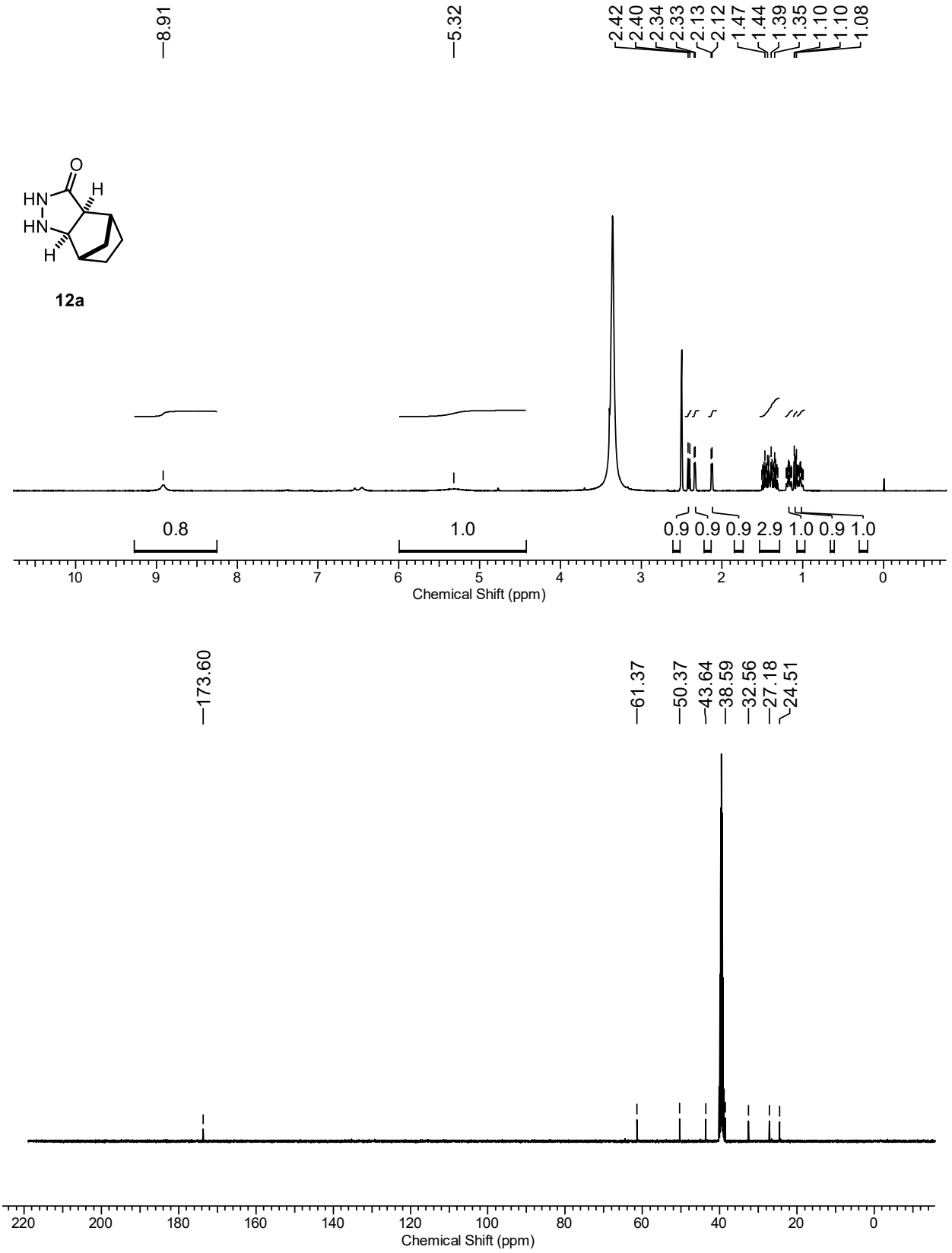
8.91
5.32
2.42
2.40
2.34
2.33
2.13
2.12
1.47
1.44
1.39
1.35
1.10
1.10
1.08
O
H
HN
HN
H
12a
0.8
1.0
0.9 0.9 0.9 2.9 1.0 0.9 1.0
Chemical Shift (ppm)
173.60
61.37
50.37
43.64
38.59
32.56
27.18
24.51
Chemical Shift (ppm)

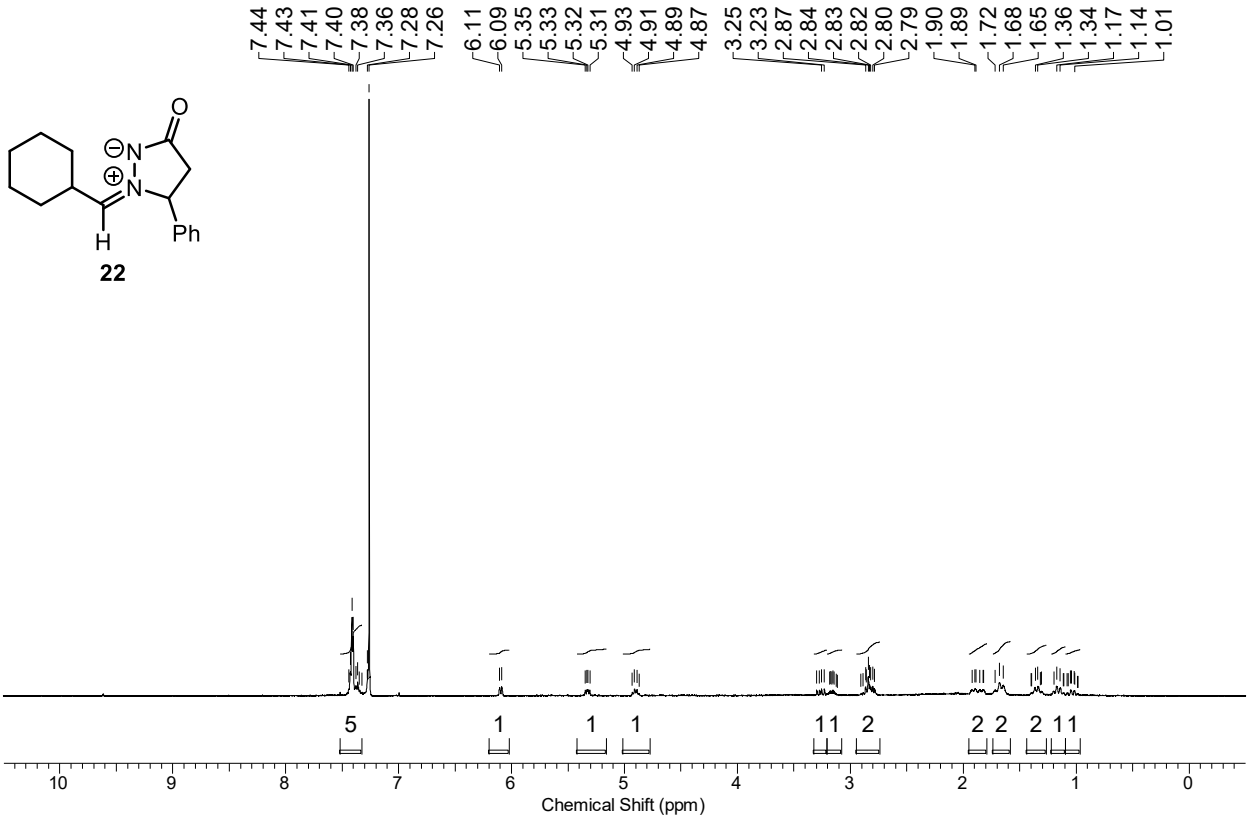
7.44
7.43
7.41
7.40
7.38
7.36
7.28
7.26
6.11
6.09
5.35
5.33
5.32
5.31
4.93
4.91
4.89
4.87
3.25
3.23
2.87
2.84
2.83
2.82
2.80
2.79
1.90
1.89
1.72
1.68
1.65
1.36
1.34
1.17
1.14
1.01
O
N
N
H
Ph
22
5
1
1
1
1 1
2
2 2
2 1 1
10
9
8
7
6
5
4
3
2
1
0
Chemical Shift (ppm)

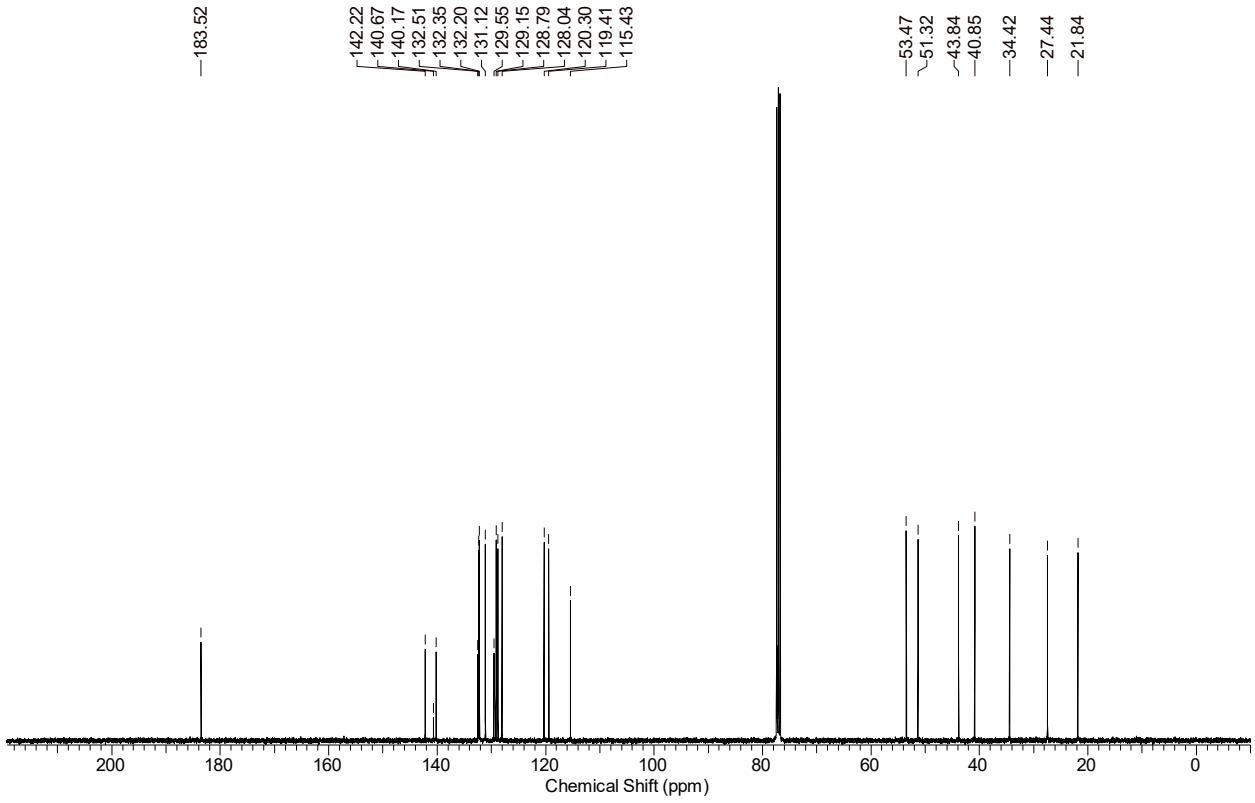
183.52
142.22
140.67
140.17
132.51
132.35
132.20
131.12
129.55
129.15
128.79
128.04
120.30
119.41
115.43
53.47
51.32
43.84
40.85
34.42
27.44
21.84
200
180
160
140
120
100
80
60
40
20
0
Chemical Shift (ppm)

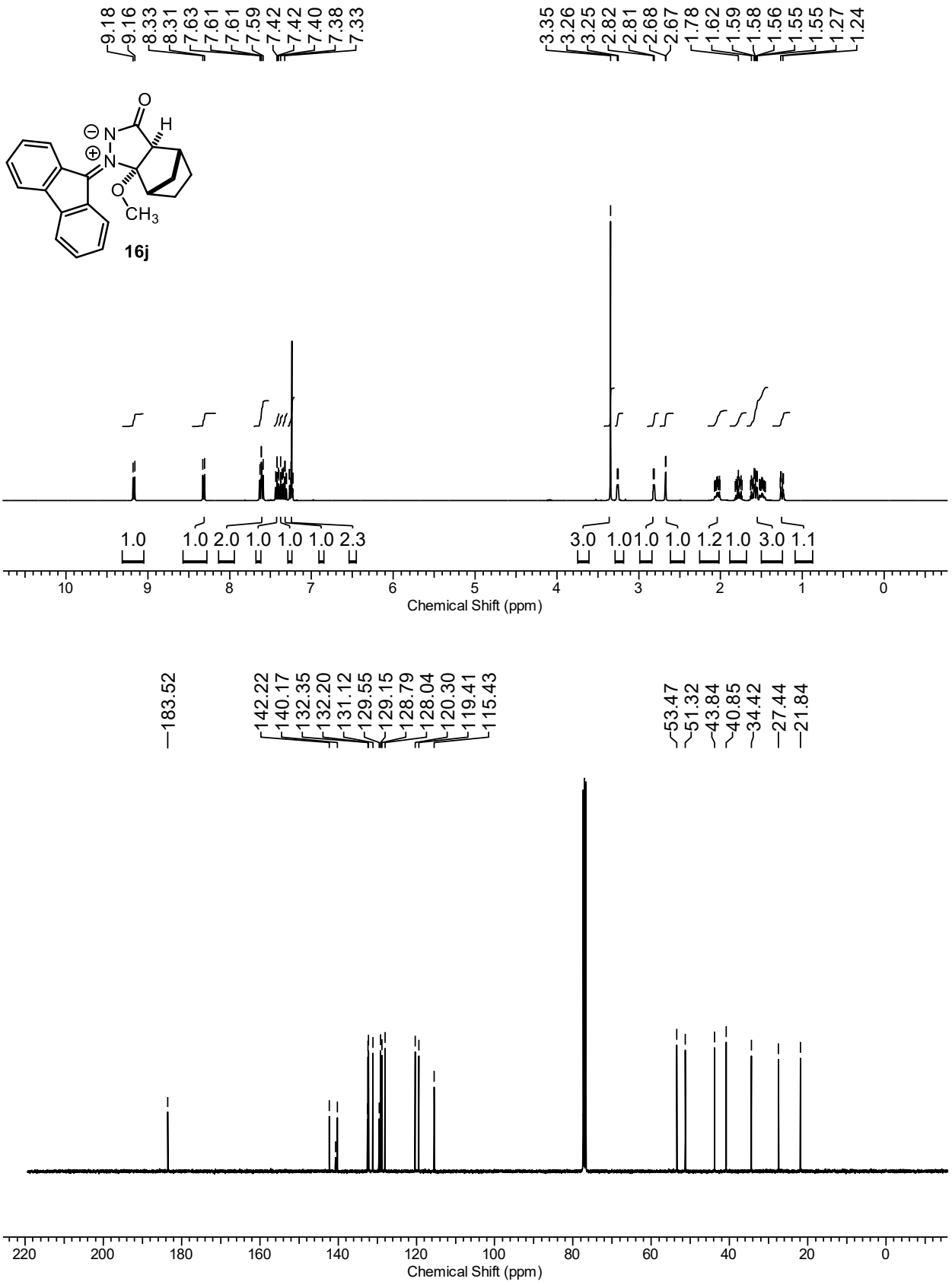
9.18
9.16
8.33
8.31
7.63
7.61
7.61
7.59
7.42
7.42
7.40
7.38
7.33
3.35
3.26
3.25
2.82
2.81
2.68
2.67
1.78
1.62
1.59
1.58
1.56
1.55
1.55
1.27
1.24
16j
1.0 1.0 2.0 1.0 1.0 1.0 2.3
3.0 1.0 1.0 1.0 1.2 1.0 3.0 1.1
Chemical Shift (ppm)
183.52
142.22
140.17
132.35
132.20
131.12
129.55
129.15
128.79
128.04
120.30
119.41
115.43
53.47
51.32
43.84
40.85
34.42
27.44
21.84
Chemical Shift (ppm)

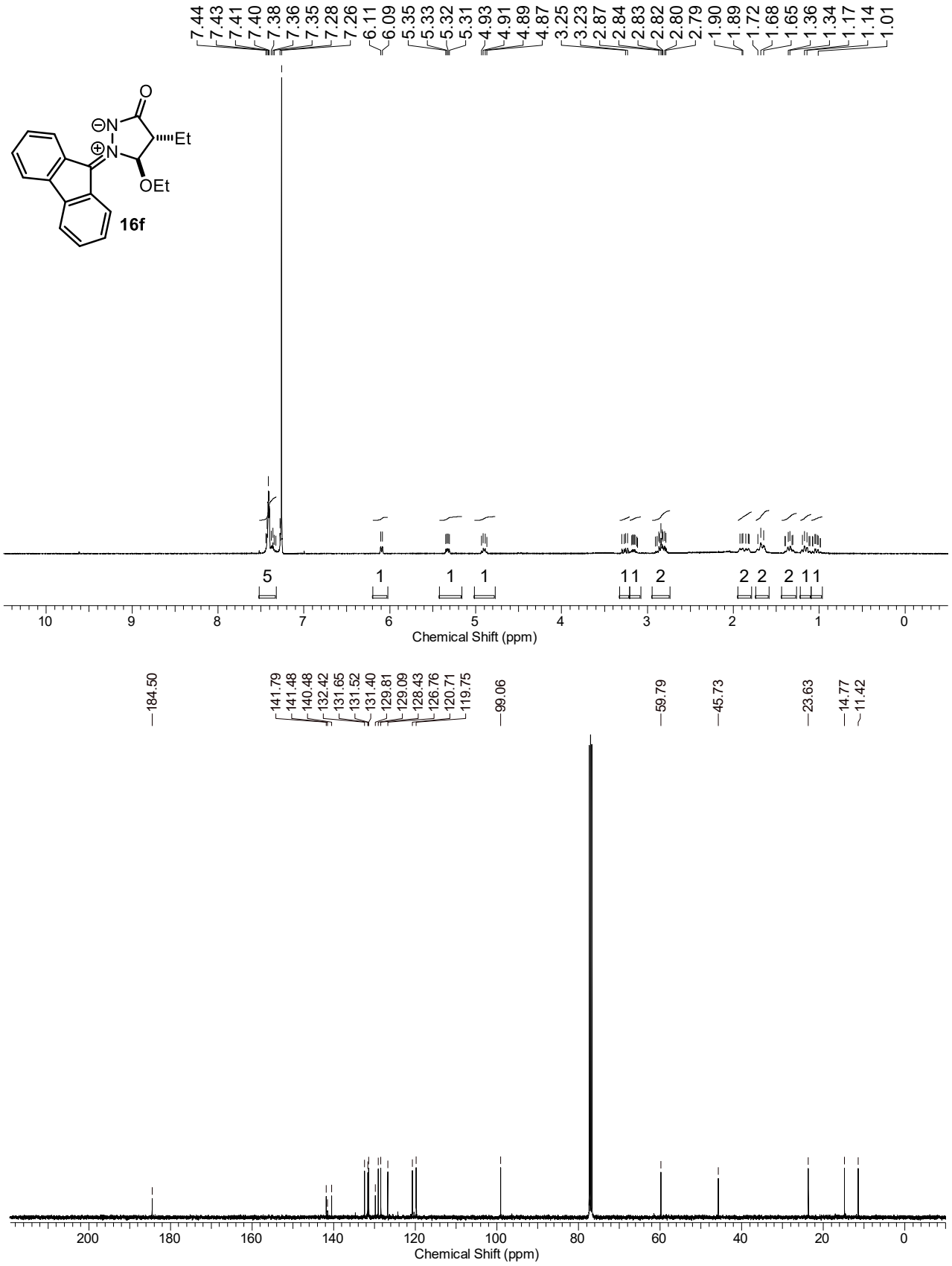
7.44
7.43
7.41
7.40
7.38
7.36
7.35
7.28
7.26
6.11
6.09
5.35
5.33
5.32
5.31
4.93
4.91
4.89
4.87
3.25
3.23
2.87
2.84
2.83
2.82
2.80
2.79
1.90
1.89
1.72
1.68
1.65
1.36
1.34
1.17
1.14
1.01
O
N
N
Et
OEt
16f
5
1
1
1
1 1
2
2 2
2
1 1
Chemical Shift (ppm)
184.50
141.79
141.48
140.48
132.42
131.65
131.52
131.40
129.81
129.09
128.43
126.76
120.71
119.75
99.06
59.79
45.73
23.63
14.77
11.42
Chemical Shift (ppm)

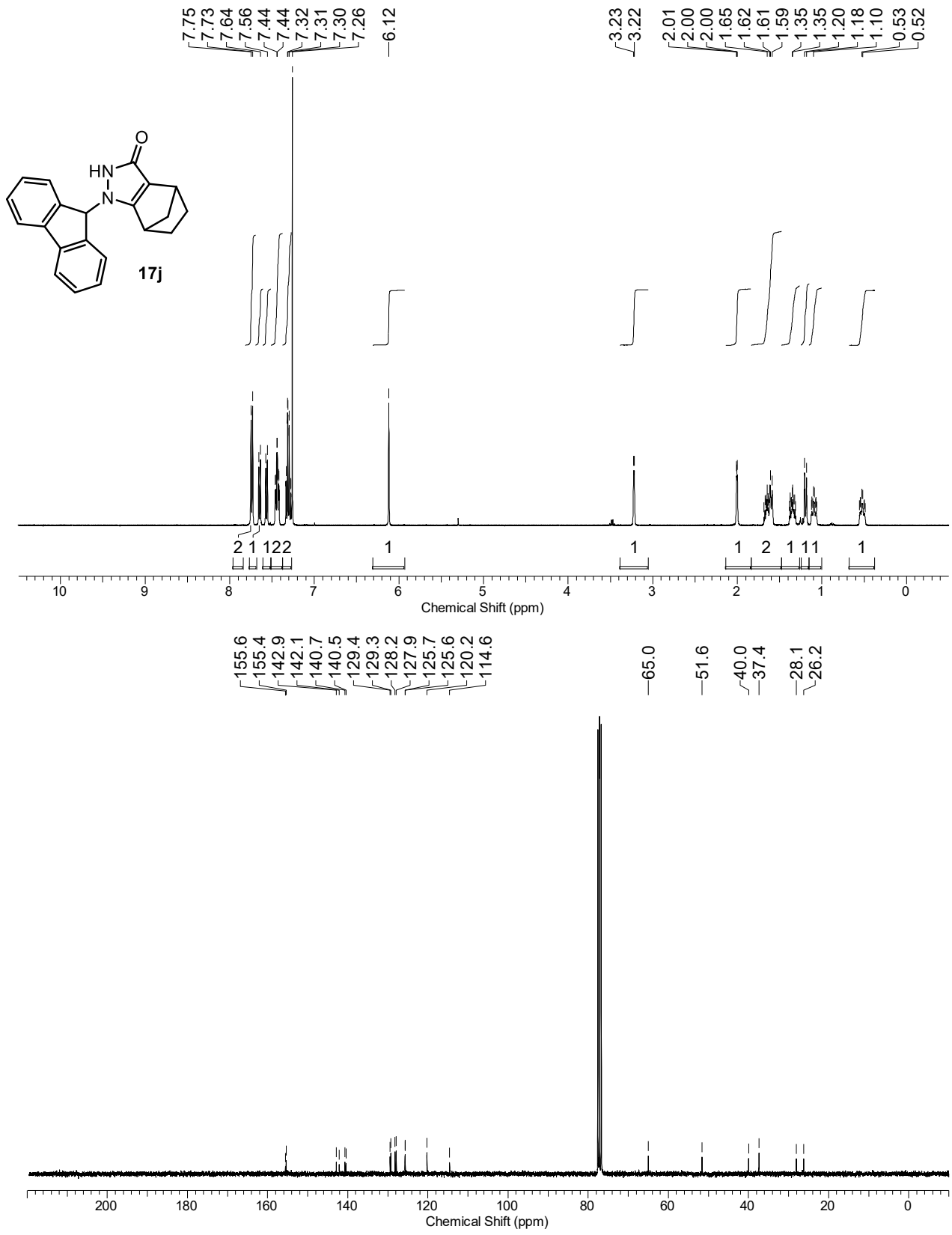
7.75
7.73
7.64
7.56
7.44
7.44
7.32
7.31
7.30
7.26
6.12
3.23
3.22
2.01
2.00
2.00
1.65
1.62
1.61
1.59
1.35
1.35
1.20
1.18
1.10
0.53
0.52
O
HN
N
17j
2 1 1 2 2
1
1
1 2 1 1 1
Chemical Shift (ppm)
155.6
155.4
142.9
142.1
140.7
140.5
129.4
129.3
128.2
127.9
125.7
125.6
120.2
114.6
65.0
51.6
40.0
37.4
28.1
26.2
Chemical Shift (ppm)

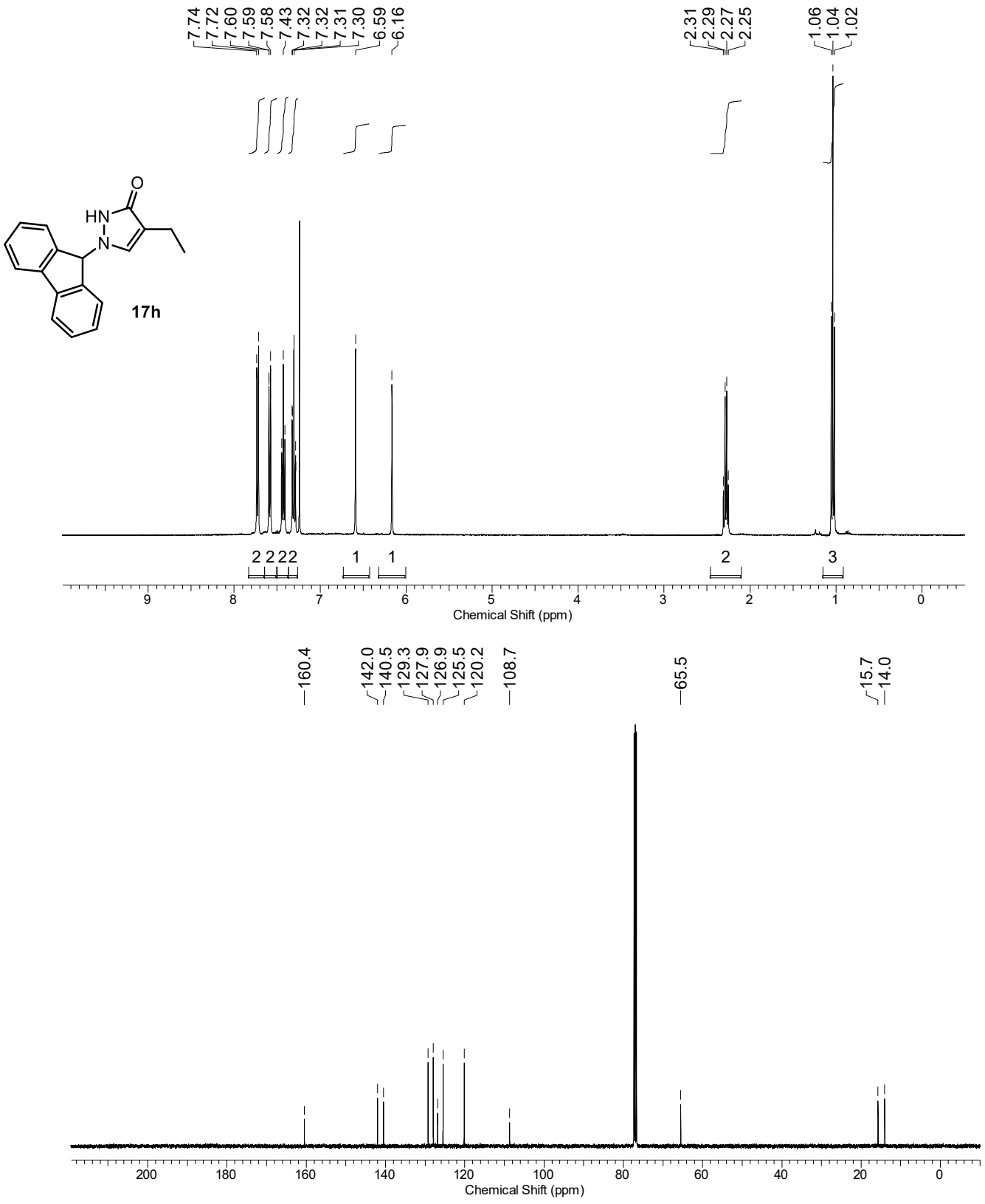
7.74
7.72
7.60
7.59
7.58
7.43
7.32
7.32
7.31
7.30
6.59
6.16
2.31
2.29
2.27
2.25
1.06
1.04
1.02
O
HN
N
17h
2 2 2 2
1
1
2
3
Chemical Shift (ppm)
160.4
142.0
140.5
129.3
127.9
126.9
125.5
120.2
108.7
65.5
15.7
14.0
Chemical Shift (ppm)

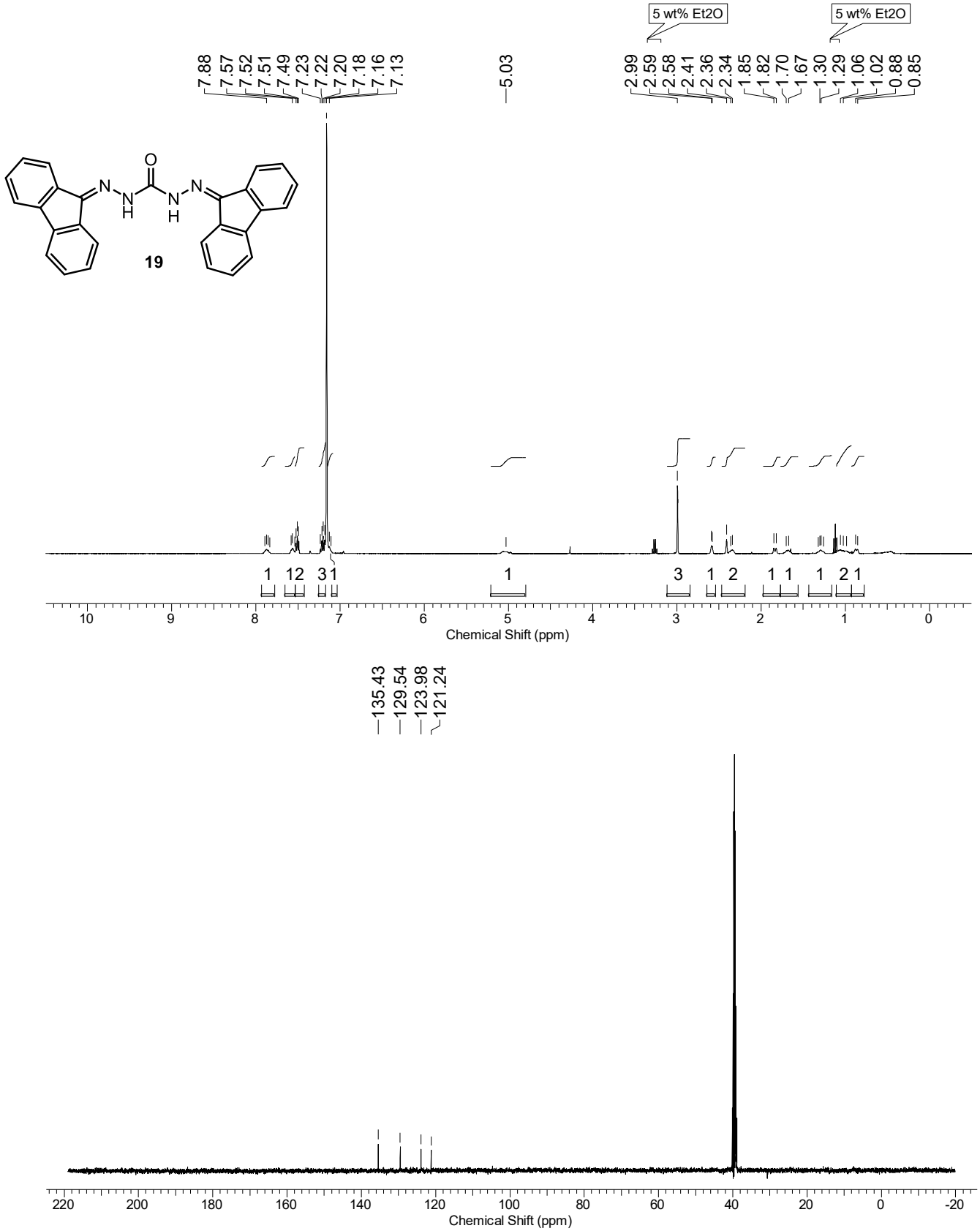
5 wt% Et2O
5 wt% Et2O
7.88
7.57
7.52
7.51
7.49
7.23
7.22
7.20
7.18
7.16
7.13
5.03
2.99
2.59
2.58
2.41
2.36
2.34
1.85
1.82
1.70
1.67
1.30
1.29
1.06
1.02
0.88
0.85
19
1 12 3 1 1 3 1 2 1 1 1 2 1
Chemical Shift (ppm)
135.43
129.54
123.98
121.24
Chemical Shift (ppm)

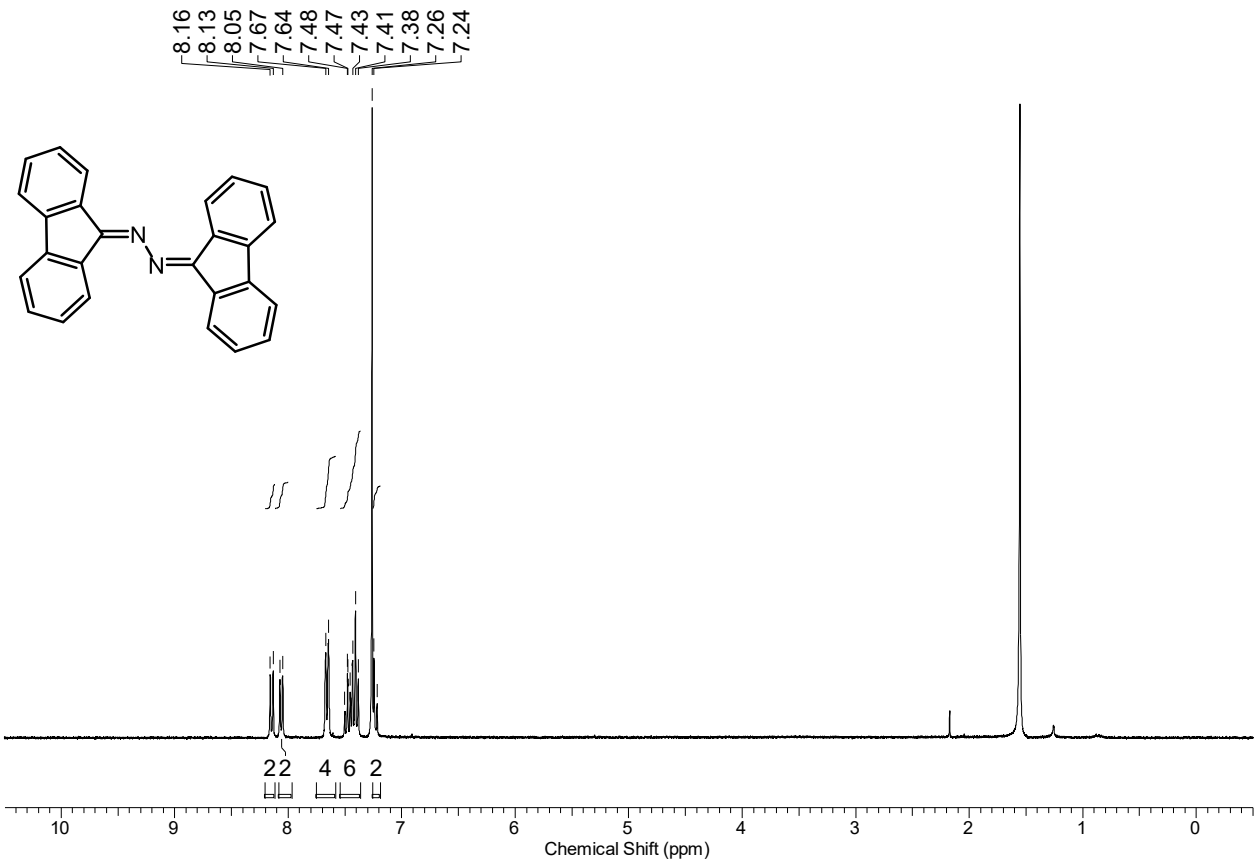
8.16
8.13
8.05
7.67
7.64
7.48
7.47
7.43
7.41
7.38
7.26
7.24
2 2 4 6 2
Chemical Shift (ppm)

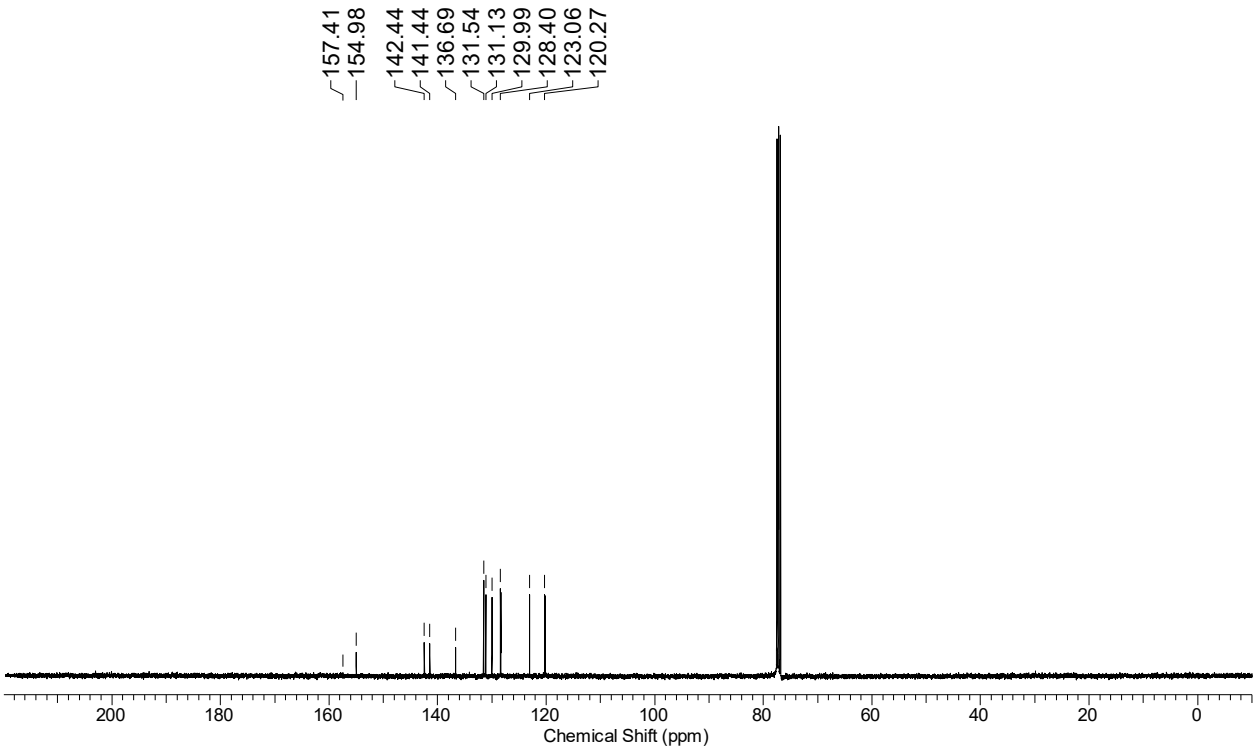
157.41
154.98
142.44
141.44
136.69
131.54
131.13
129.99
128.40
123.06
120.27
Chemical Shift (ppm)

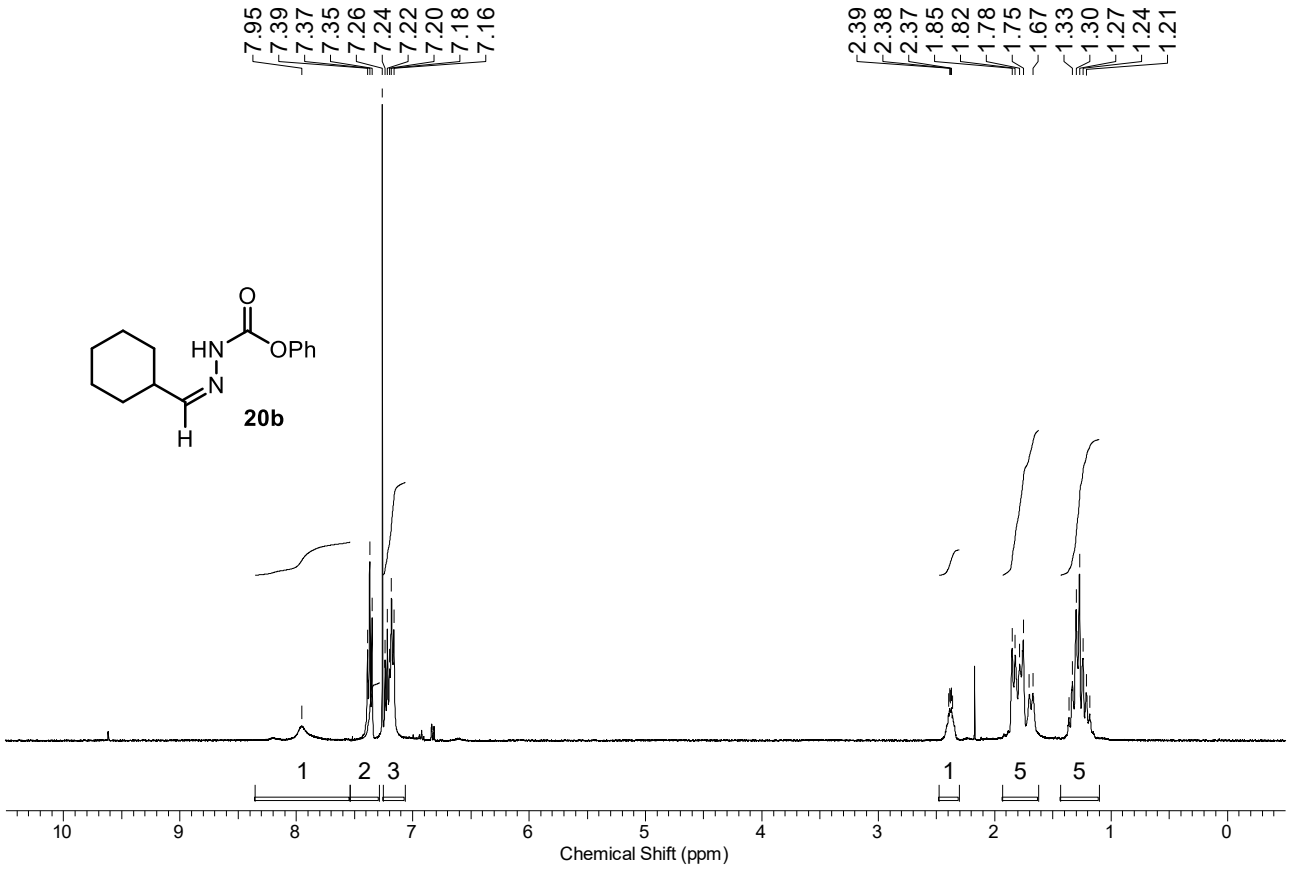
7.95
7.39
7.37
7.35
7.26
7.24
7.22
7.20
7.18
7.16
2.39
2.38
2.37
1.85
1.82
1.78
1.75
1.67
1.33
1.30
1.27
1.24
1.21
O
HN
OPh
N
H
20b
1
2
3
1
5
5
10
9
8
7
6
5
4
3
2
1
0
Chemical Shift (ppm)

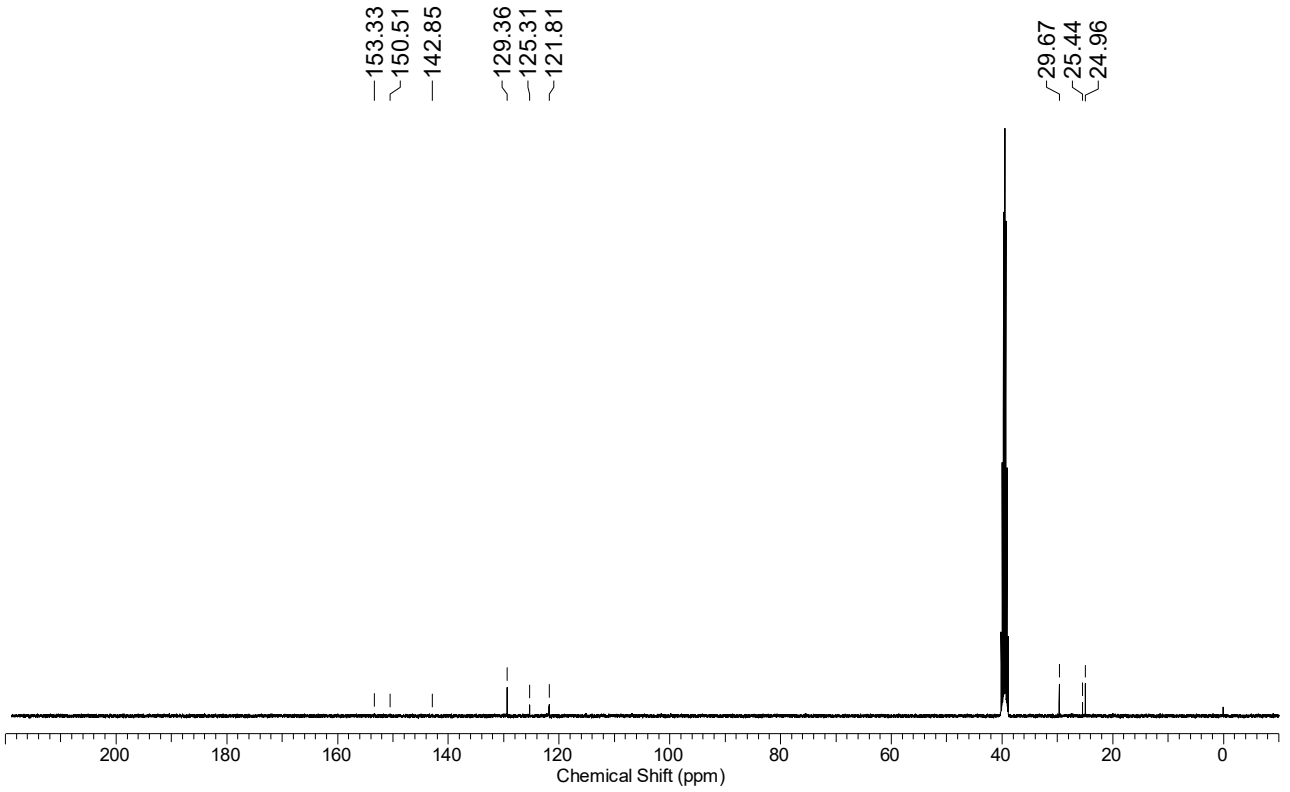
153.33
150.51
142.85
129.36
125.31
121.81
29.67
25.44
24.96
200
180
160
140
120
100
80
60
40
20
0
Chemical Shift (ppm)

Spectra: Chapter 3

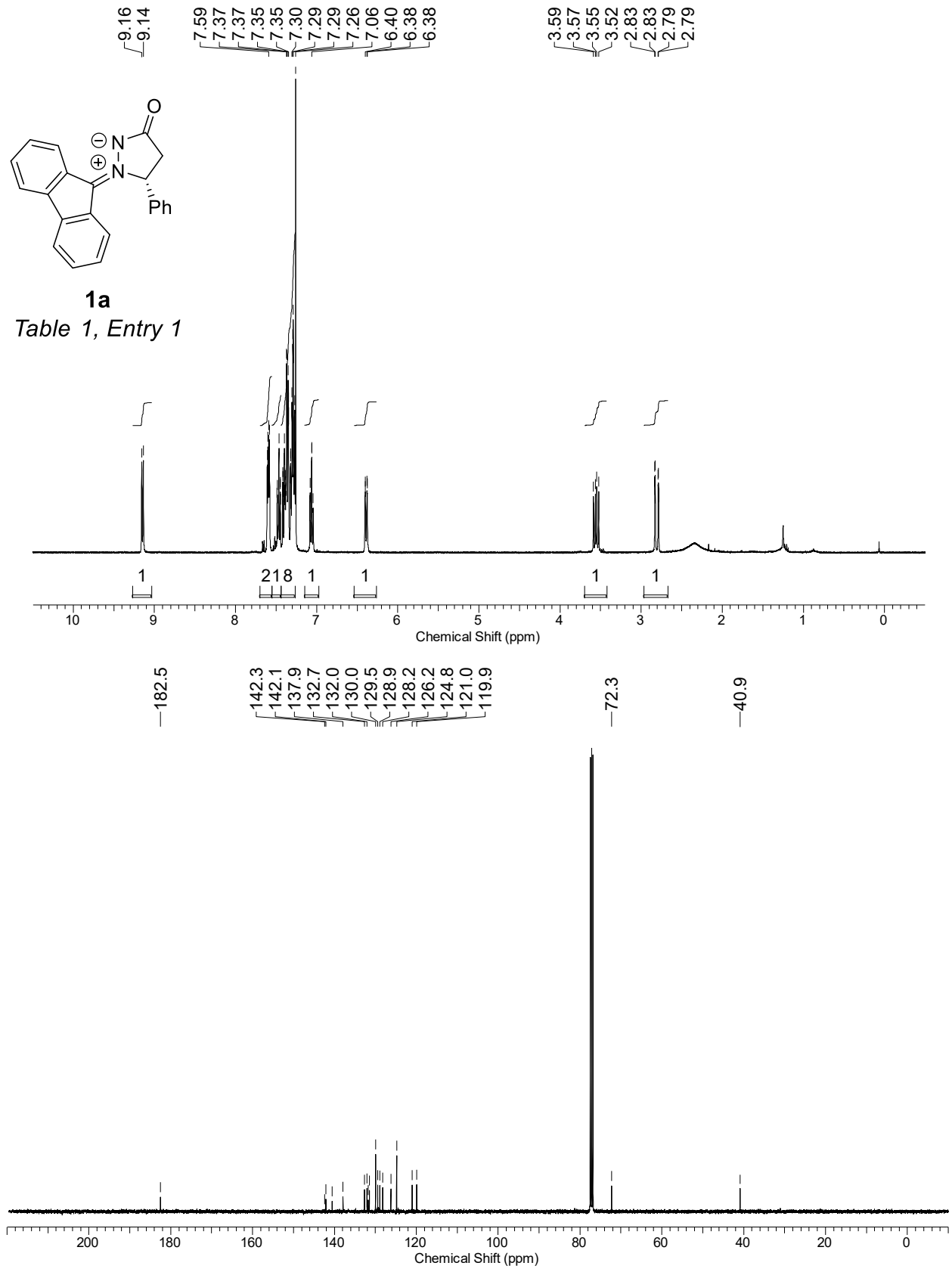

1a

Table 1, Entry 1

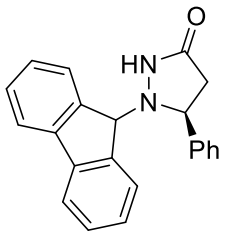

2a

Table 1, Entry 1

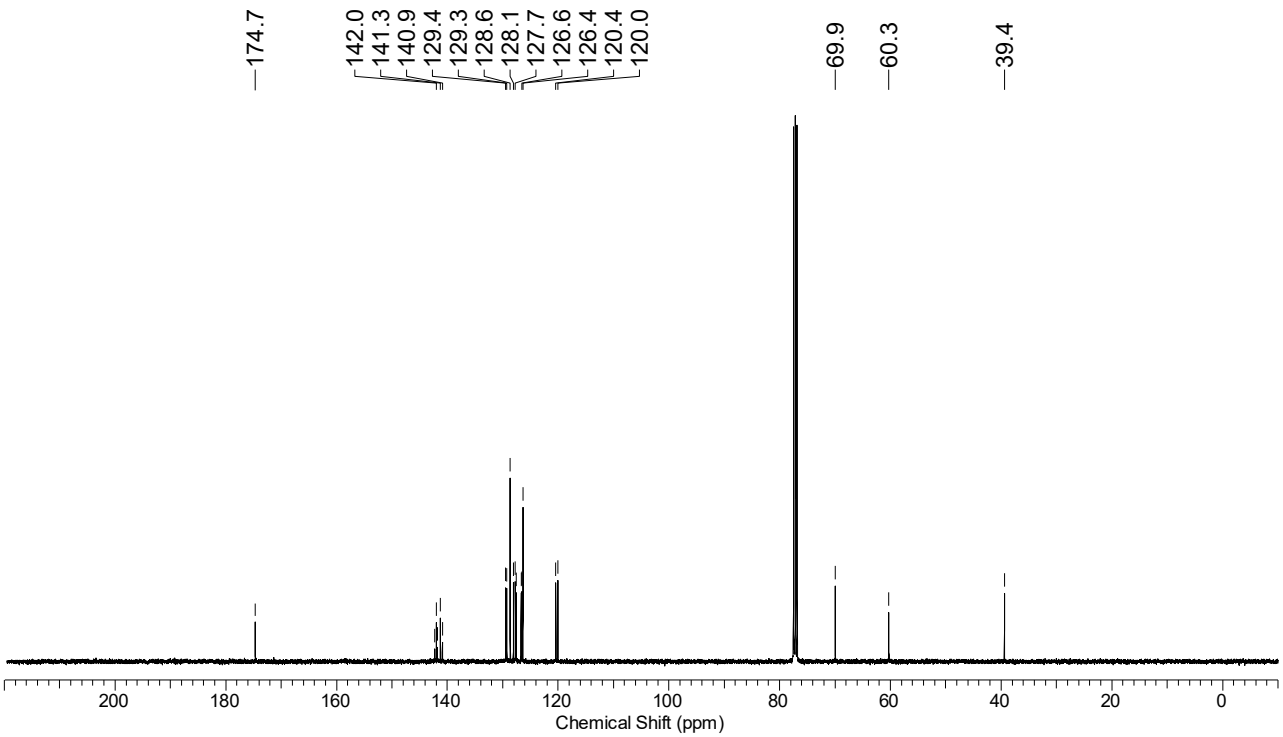

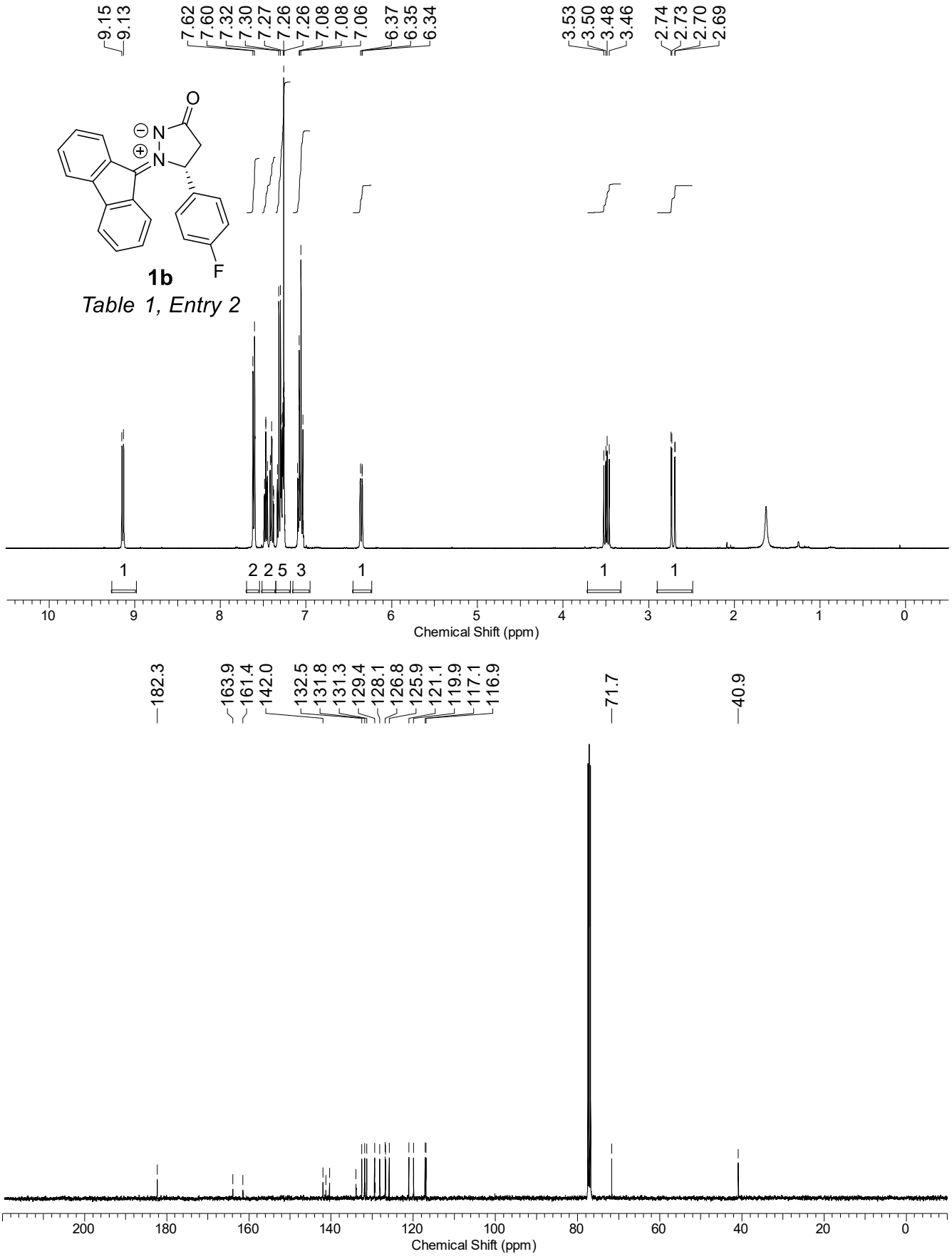
9.15
9.13
7.62
7.60
7.32
7.30
7.27
7.26
7.26
7.08
7.08
7.06
6.37
6.35
6.34
3.53
3.50
3.48
3.46
2.74
2.73
2.70
2.69
O
N
N
F
1b
Table 1, Entry 2
1
2 2 5 3
1
1
1
Chemical Shift (ppm)
182.3
163.9
161.4
142.0
132.5
131.8
131.3
129.4
128.1
126.8
125.9
121.1
119.9
117.1
116.9
71.7
40.9
Chemical Shift (ppm)

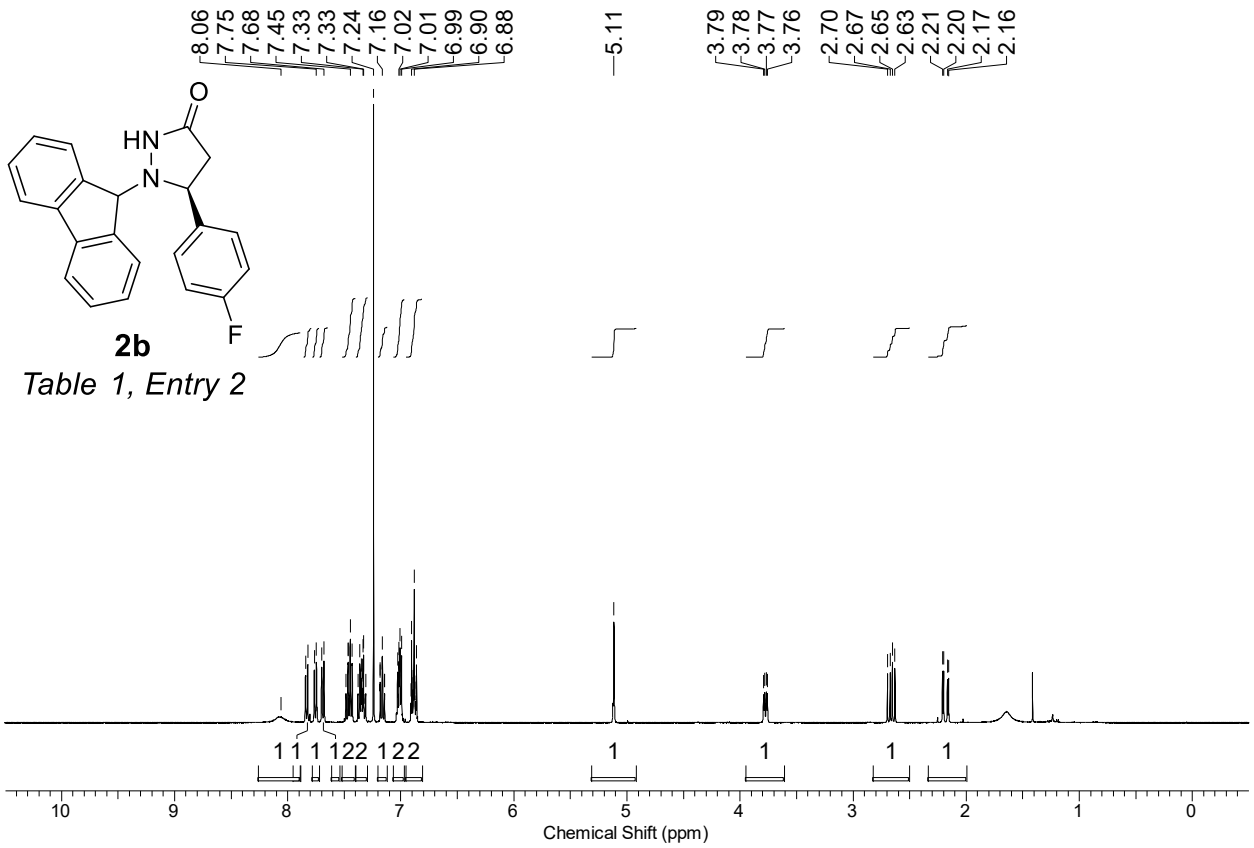

2b

Table 1, Entry 2

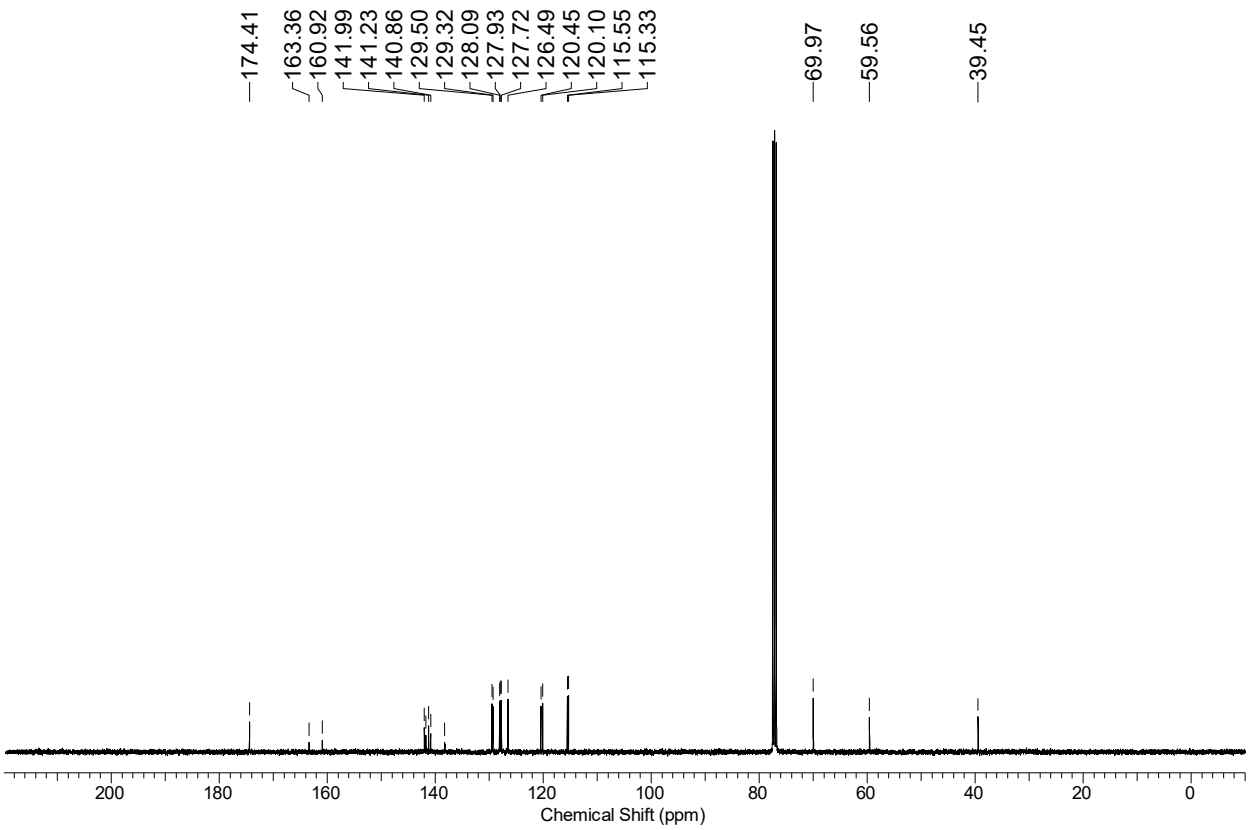

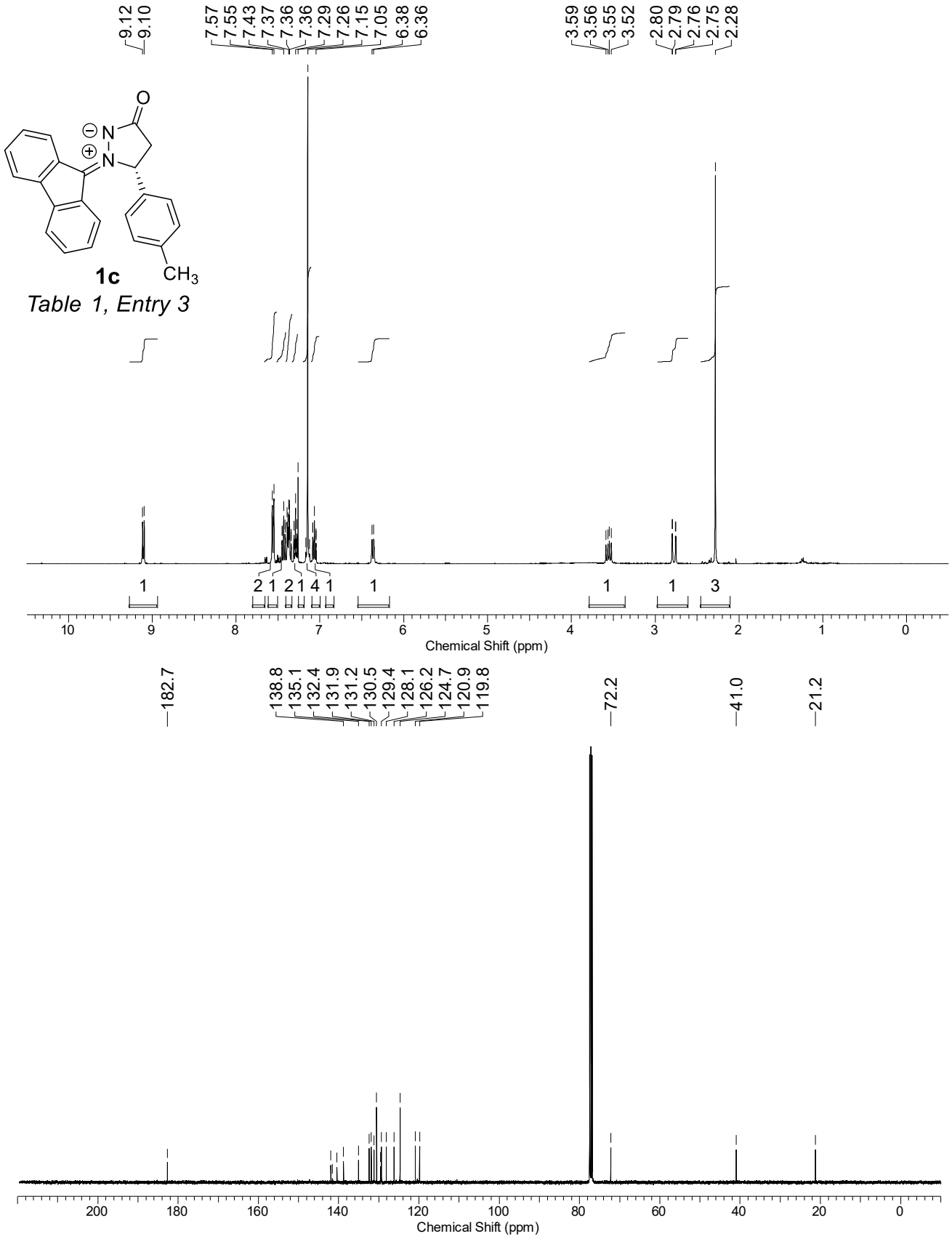
9.12
9.10
7.57
7.55
7.43
7.37
7.36
7.36
7.29
7.26
7.15
7.05
6.38
6.36
3.59
3.56
3.55
3.52
2.80
2.79
2.76
2.75
2.28
O
N
N
CH3
1c
Table 1, Entry 3
1
2 1 2 1 4 1
1
1
1
3
Chemical Shift (ppm)
182.7
138.8
135.1
132.4
131.9
131.2
130.5
129.4
128.1
126.2
124.7
120.9
119.8
72.2
41.0
21.2
Chemical Shift (ppm)

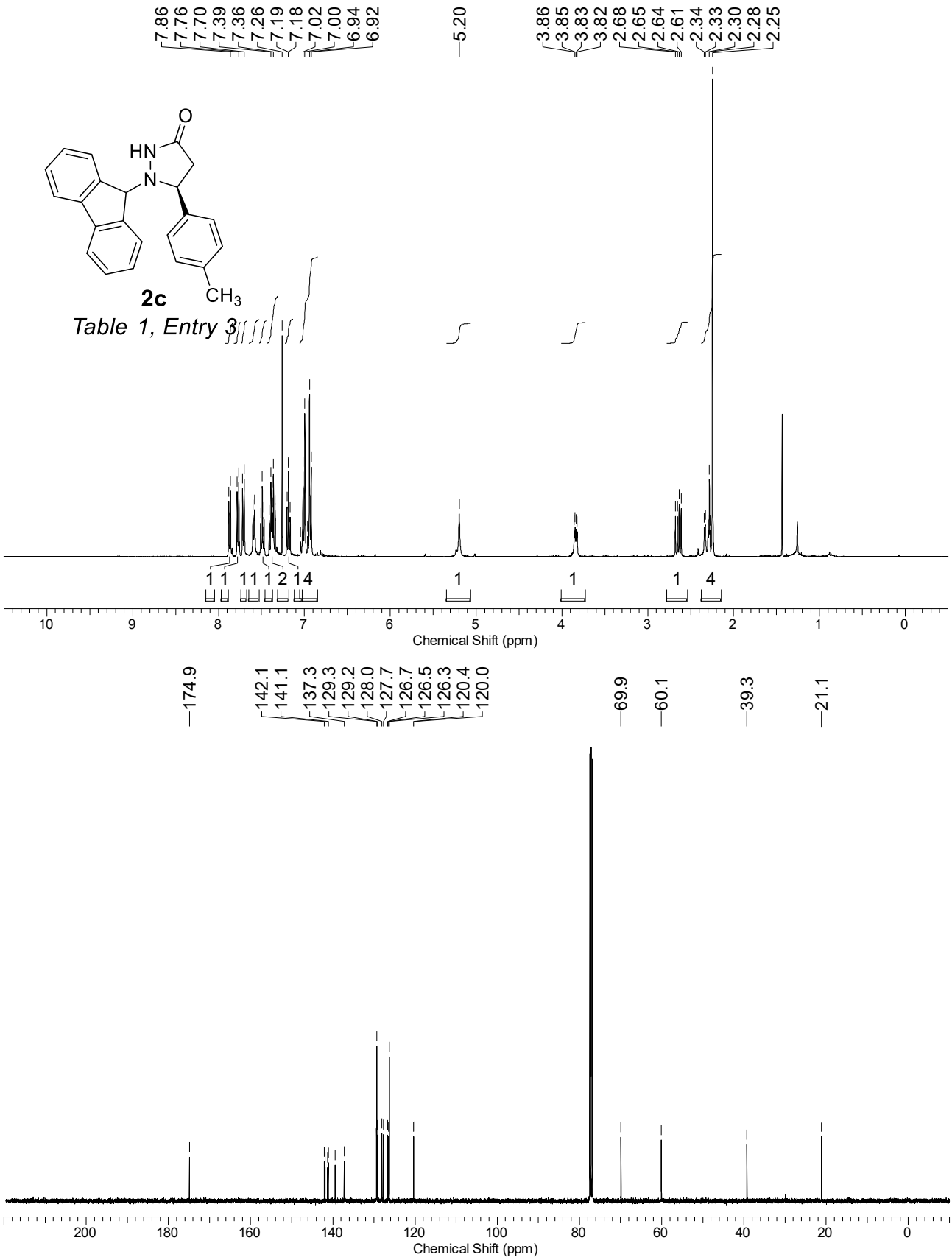
7.86
7.76
7.70
7.39
7.36
7.26
7.19
7.18
7.02
7.00
6.94
6.92
5.20
3.86
3.85
3.83
3.82
2.68
2.65
2.64
2.61
2.34
2.33
2.30
2.28
2.25
O
HN
N
CH3
2c
Table 1, Entry 3
1 1 1 1 1 2 1 4
1
1
1 4
Chemical Shift (ppm)
174.9
142.1
141.1
137.3
129.3
129.2
128.0
127.7
126.7
126.5
126.3
120.4
120.0
69.9
60.1
39.3
21.1
Chemical Shift (ppm)

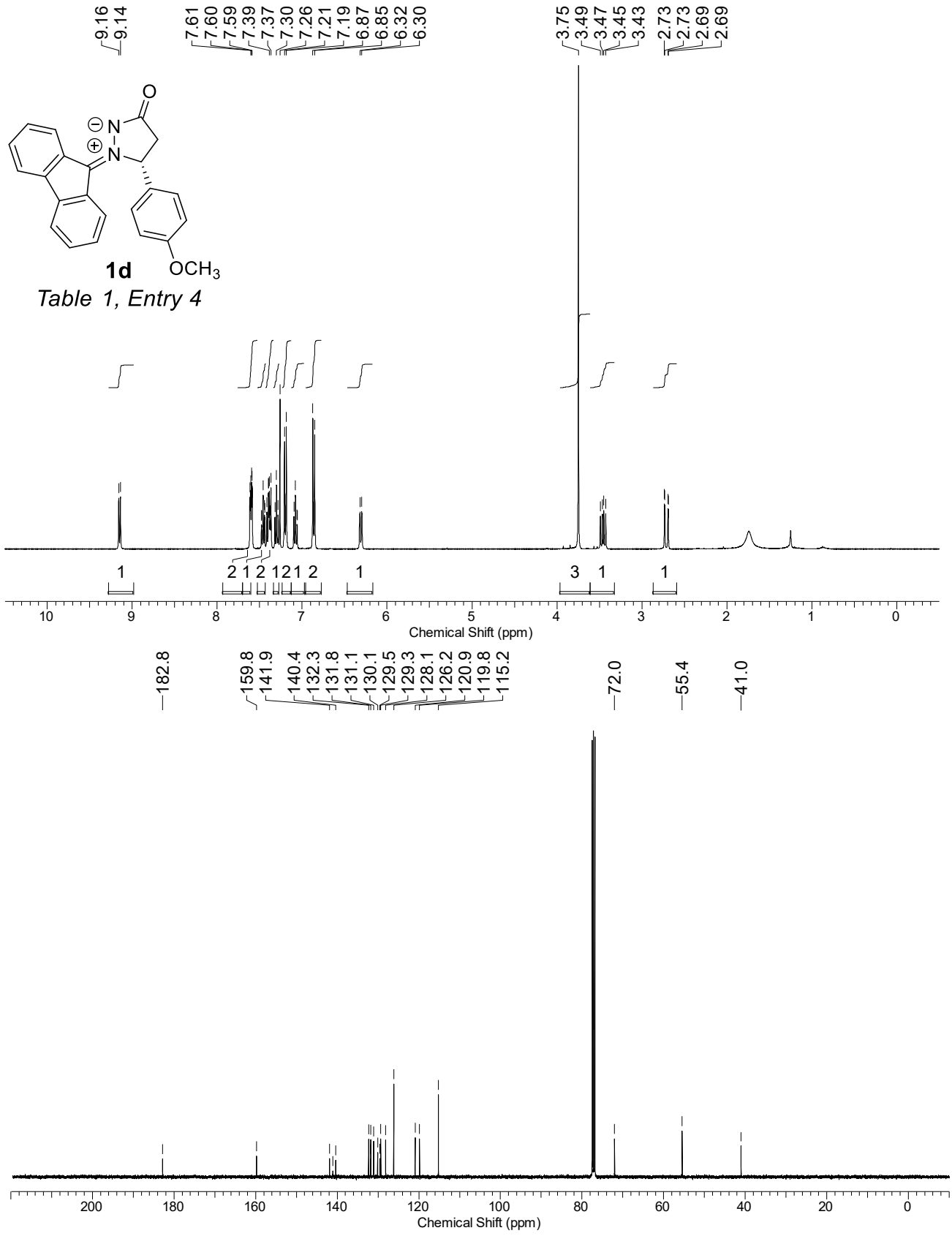
9.16
9.14
7.61
7.60
7.59
7.39
7.37
7.30
7.26
7.21
7.19
6.87
6.85
6.32
6.30
3.75
3.49
3.47
3.45
3.43
2.73
2.73
2.69
2.69
O
N
N
1d
OCH3
Table 1, Entry 4
1
2 1 2 1 2 1 2
1
3 1
1
Chemical Shift (ppm)
182.8
159.8
141.9
140.4
132.3
131.8
131.1
130.1
129.5
129.3
128.1
126.2
120.9
119.8
115.2
72.0
55.4
41.0
Chemical Shift (ppm)

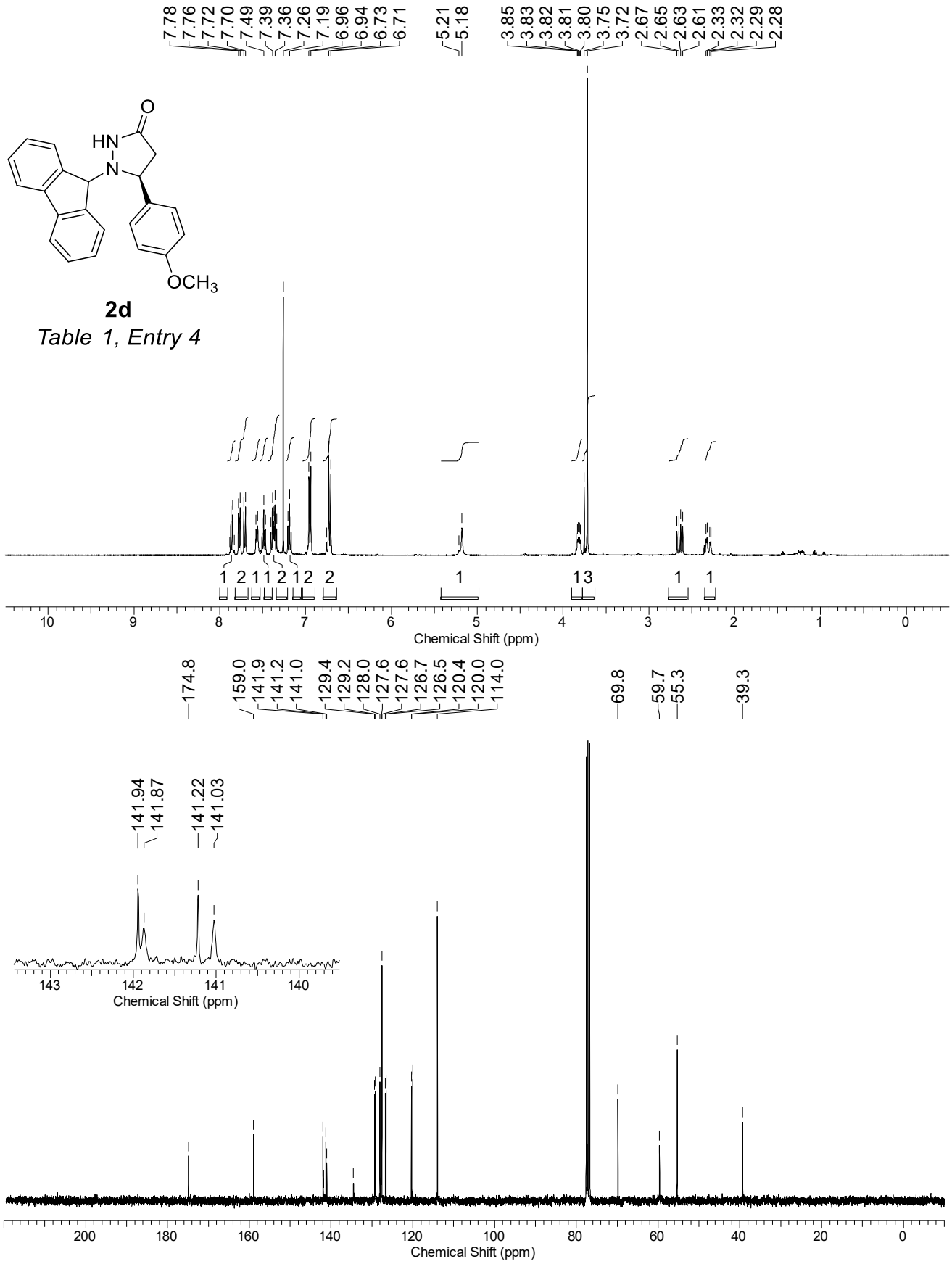
7.78
7.76
7.72
7.70
7.49
7.39
7.36
7.26
7.19
6.96
6.94
6.73
6.71
5.21
5.18
3.85
3.83
3.82
3.81
3.80
3.75
3.72
2.67
2.65
2.63
2.61
2.33
2.32
2.29
2.28
O
HN
N
OCH3
2d
Table 1, Entry 4
1 2 1 1 2 1 2 2
1
1 3
1 1
Chemical Shift (ppm)
174.8
159.0
141.9
141.2
141.0
129.4
129.2
128.0
127.6
127.6
126.7
126.5
120.4
120.0
114.0
69.8
59.7
55.3
39.3
141.94
141.87
141.22
141.03
Chemical Shift (ppm)
Chemical Shift (ppm)

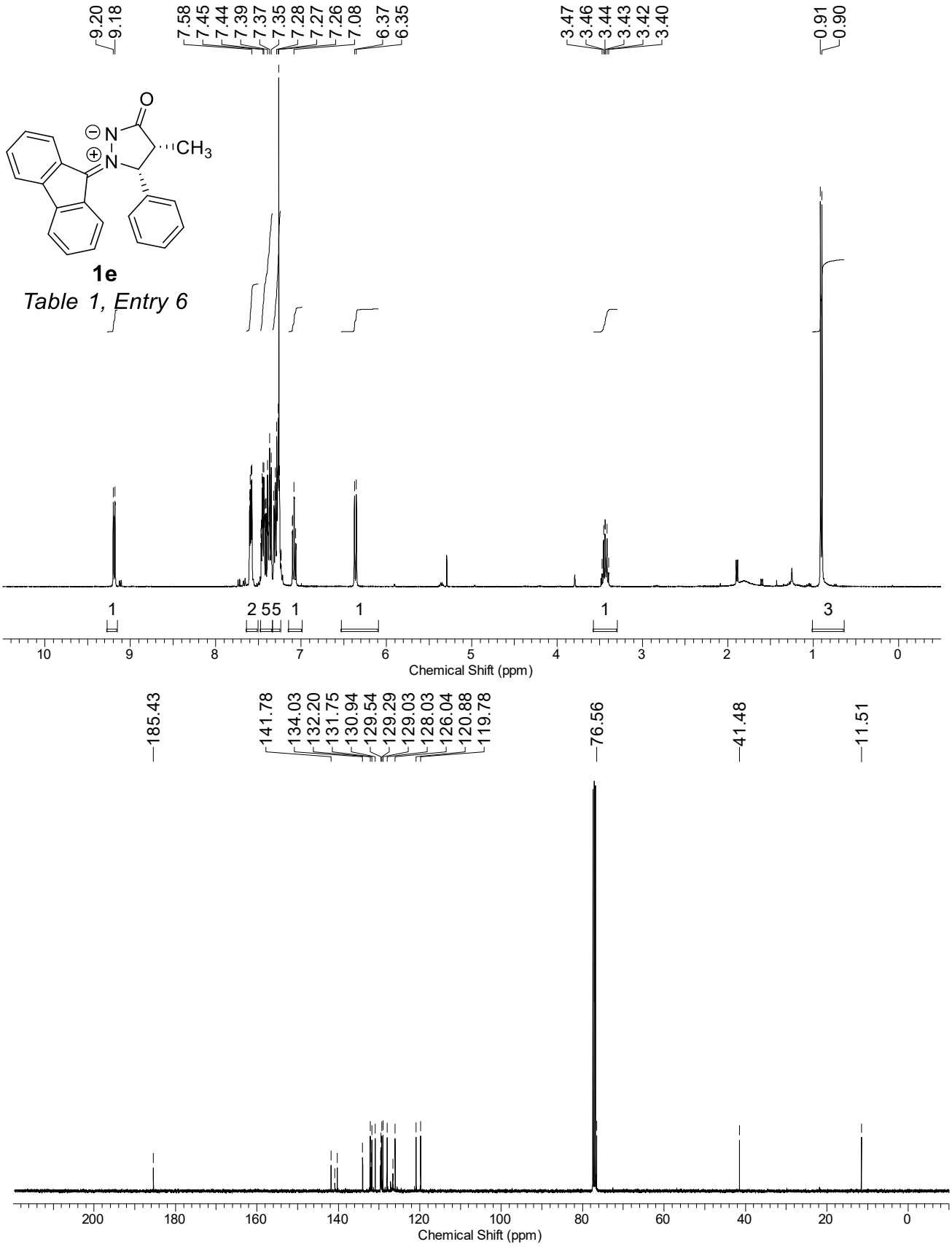
9.20
9.18
7.58
7.45
7.44
7.39
7.37
7.35
7.28
7.27
7.26
7.08
6.37
6.35
3.47
3.46
3.44
3.43
3.42
3.40
0.91
0.90
O
N
N
CH3
1e
Table 1, Entry 6
1
2 55 1
1
1
3
Chemical Shift (ppm)
185.43
141.78
134.03
132.20
131.75
130.94
129.54
129.29
129.03
128.03
126.04
120.88
119.78
76.56
41.48
11.51
Chemical Shift (ppm)

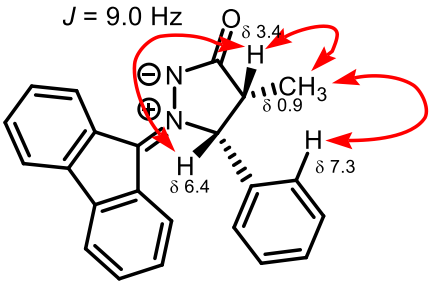

AB4-52 Azo 2.002.001.2rr.esp

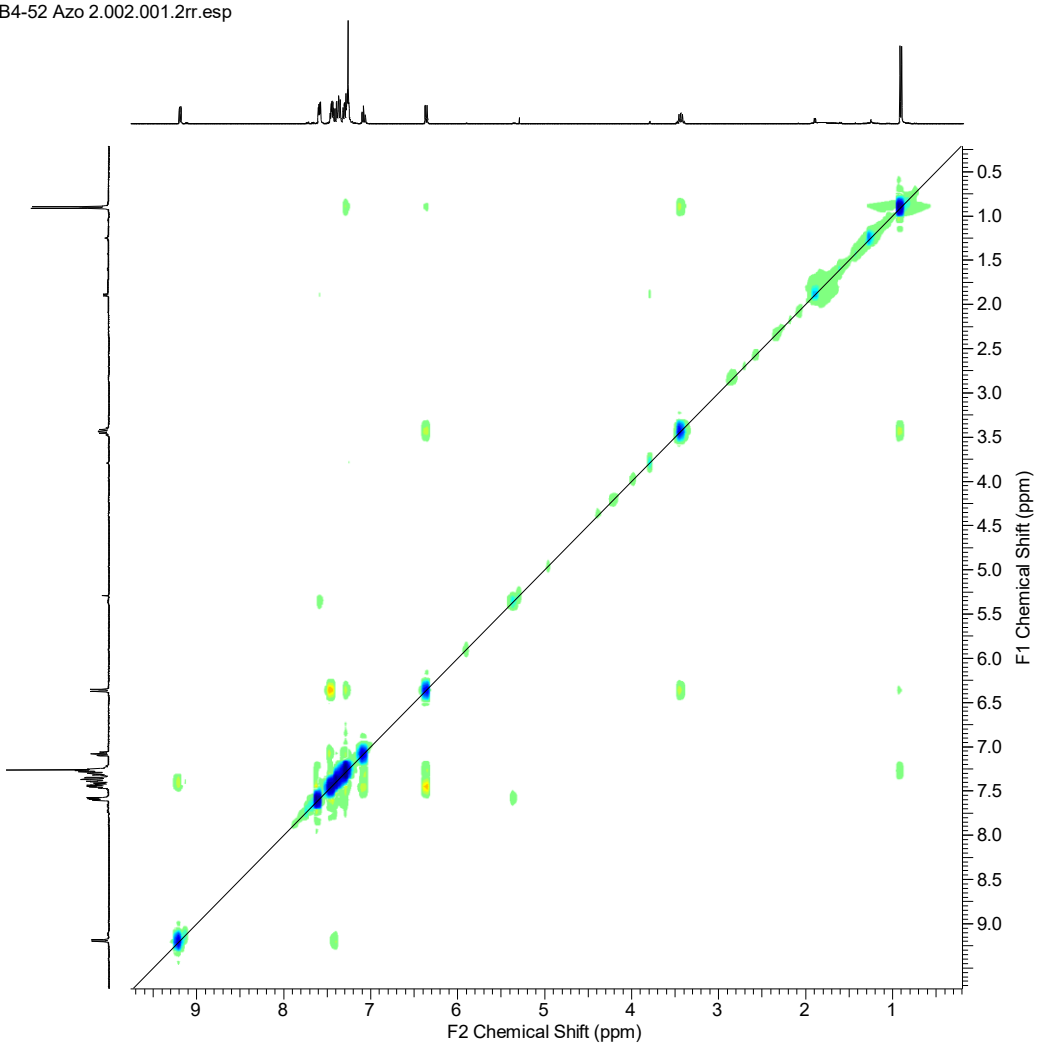

Acquisition Time (sec)	(0.0882, 0.0441)	***Comment***	5 mm PABBO BB-1H/D Z-GRD Z104450/0026
Date	01 Apr 2015 11:06:24	***File Name***	
Frequency (MHz)	(400.32, 400.32)	***Nucleus***	(1H, 1H)
Origin	spect	***Original Points Count***	(512, 256)
Points Count	(512, 512)	***Pulse Sequence***	noesygpph
Spectrum Type	NOESY	***Sweep Width (Hz)***	(5793.62, 5792.50)
Title	2d_NOESY_wide_1hour CDCl3 D:\\ Beau 19		

Number of Transients	8
Owner	bloch
Solvent	CDCl3
Temperature (degree C)	24.260

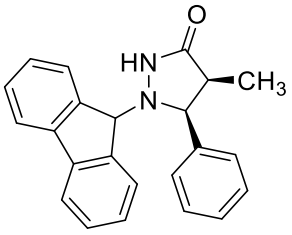

2e

Table 1, Entry 6

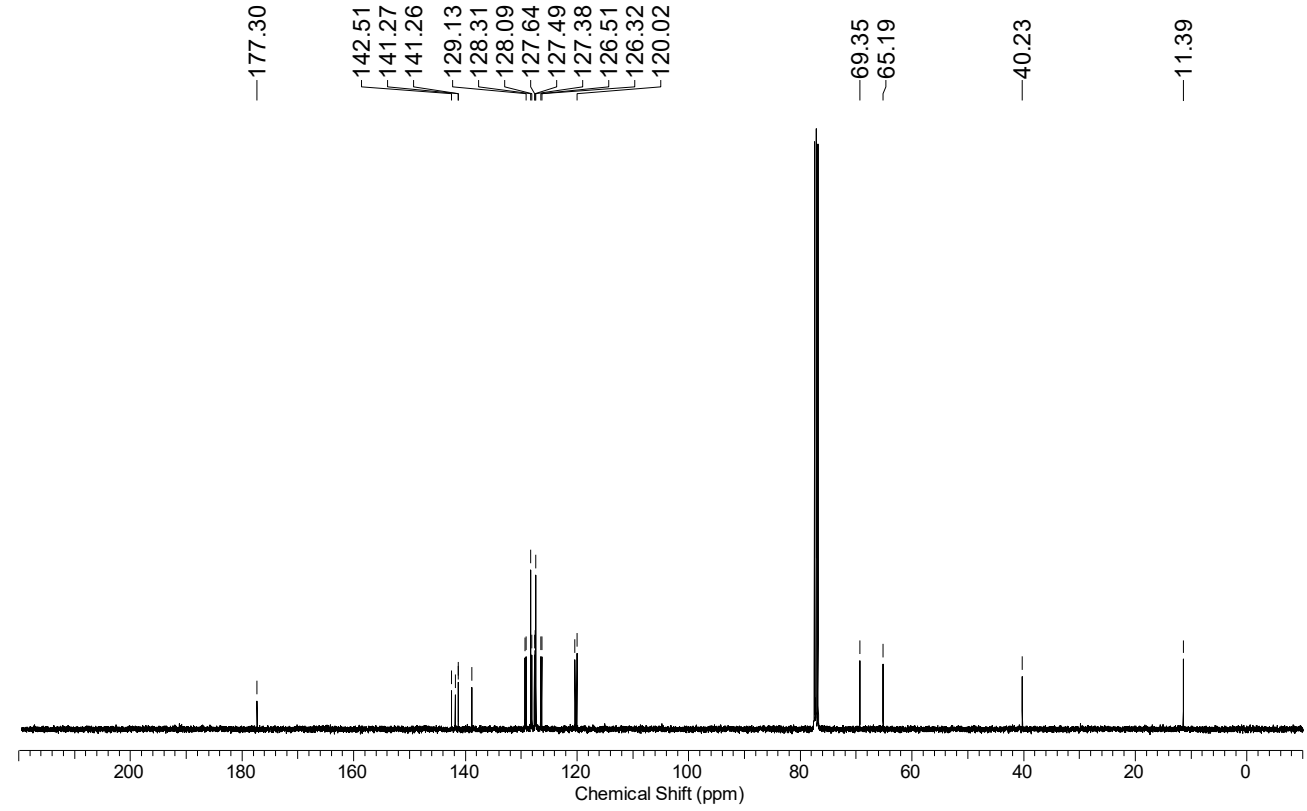

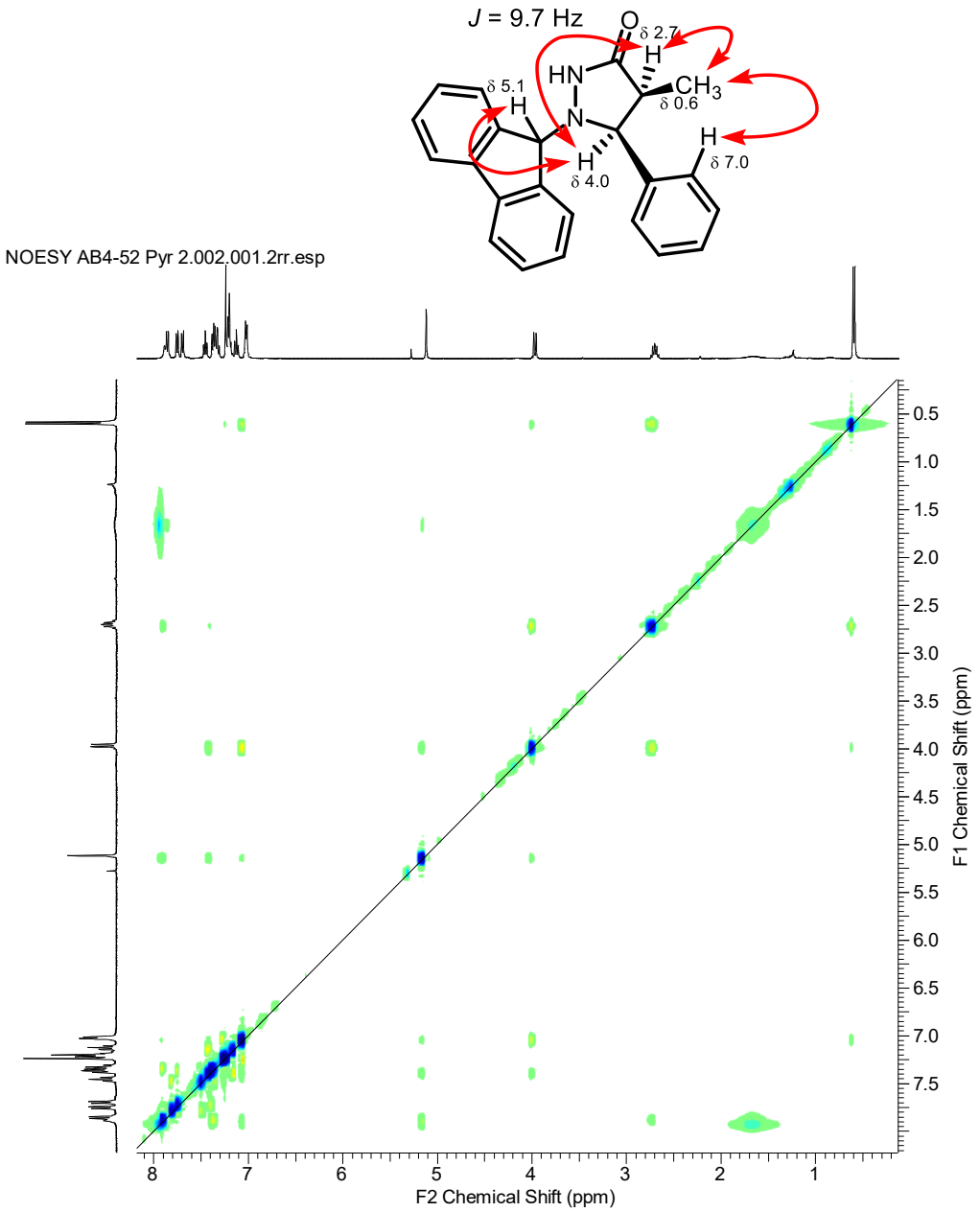

Acquisition Time (sec)	(0.1219, 0.0609)	***Comment***	5 mm PABBO BB-1H/D Z-GRD Z104450/0026
Date	01 Apr 2015 11:06:12	***File Name***	
Frequency (MHz)	(400.32, 400.32)	***Nucleus***	(1H, 1H)
Origin	spect	***Original Points Count***	(512, 256)
Points Count	(512, 512)	***Pulse Sequence***	noesygpph
Spectrum Type	NOESY	***Sweep Width (Hz)***	(4193.47, 4195.24)
Title	2d_NOESY_1_hour CDCl3 D:\\ Beau 20		

Number of Transients	8

Owner	bloch
Solvent	CDCl3
Temperature (degree C)	24.260

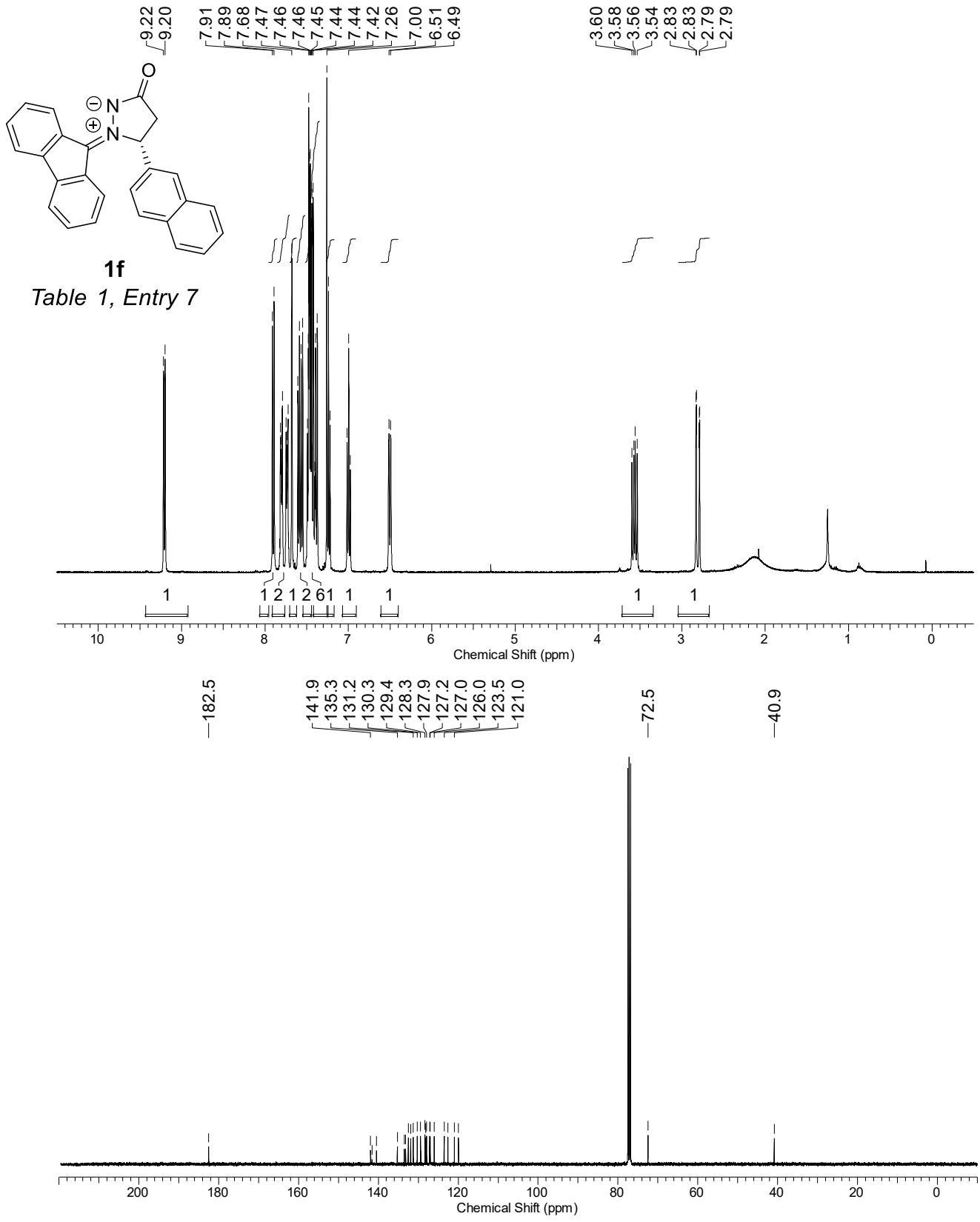
9.22
9.20
7.91
7.89
7.68
7.47
7.46
7.46
7.45
7.44
7.44
7.42
7.26
7.00
6.51
6.49
3.60
3.58
3.56
3.54
2.83
2.83
2.79
2.79
O
N
N
1f
Table 1, Entry 7
1
1 2 1 2 6 1 1
1
1
1
Chemical Shift (ppm)
182.5
141.9
135.3
131.2
130.3
129.4
128.3
127.9
127.2
127.0
126.0
123.5
121.0
72.5
40.9
Chemical Shift (ppm)

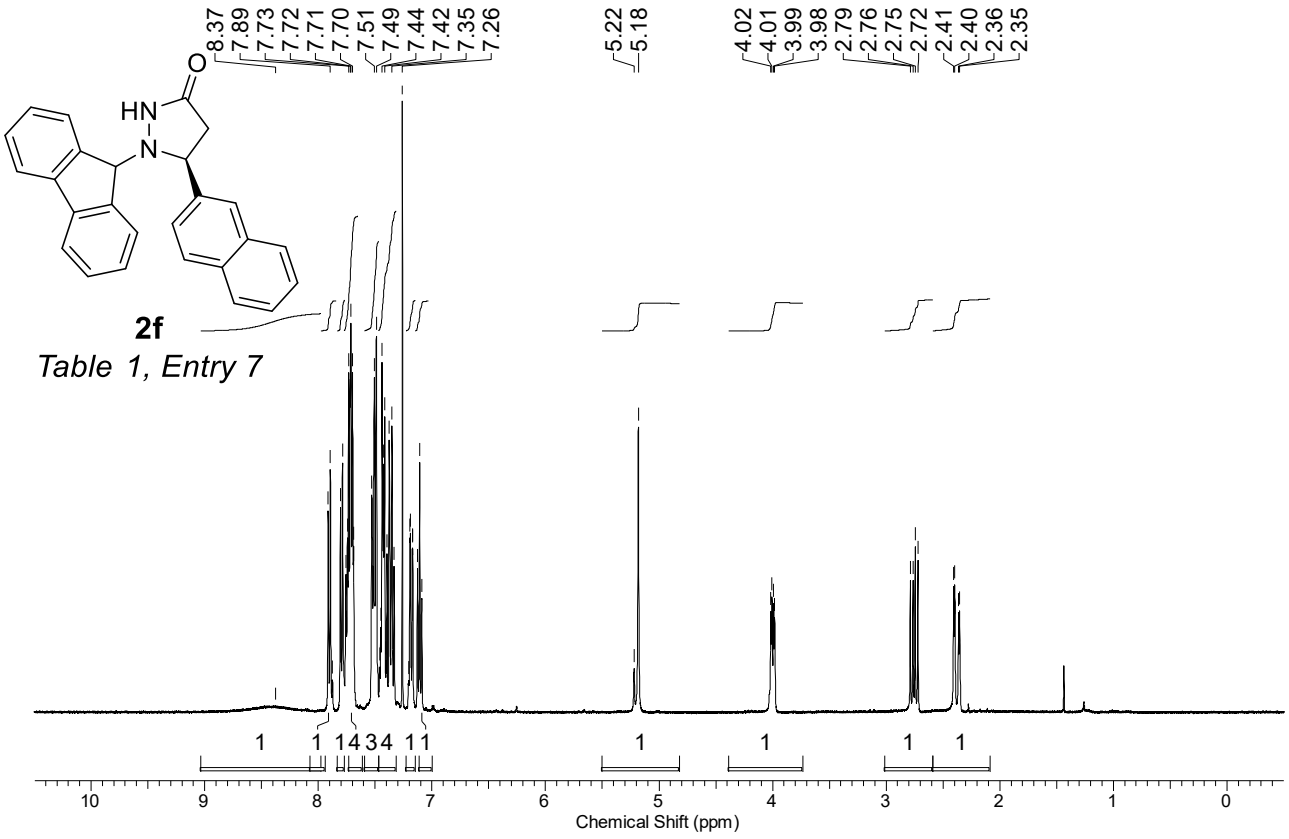

2f

Table 1, Entry 7

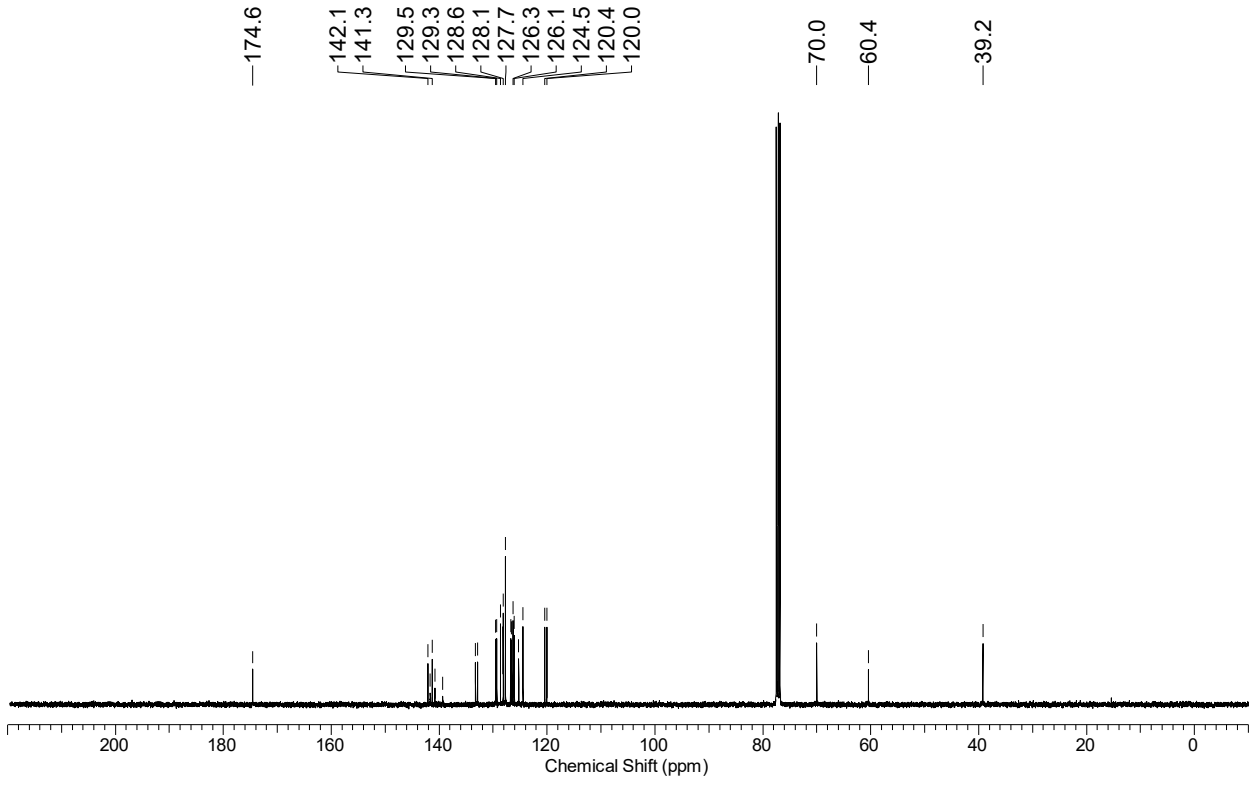

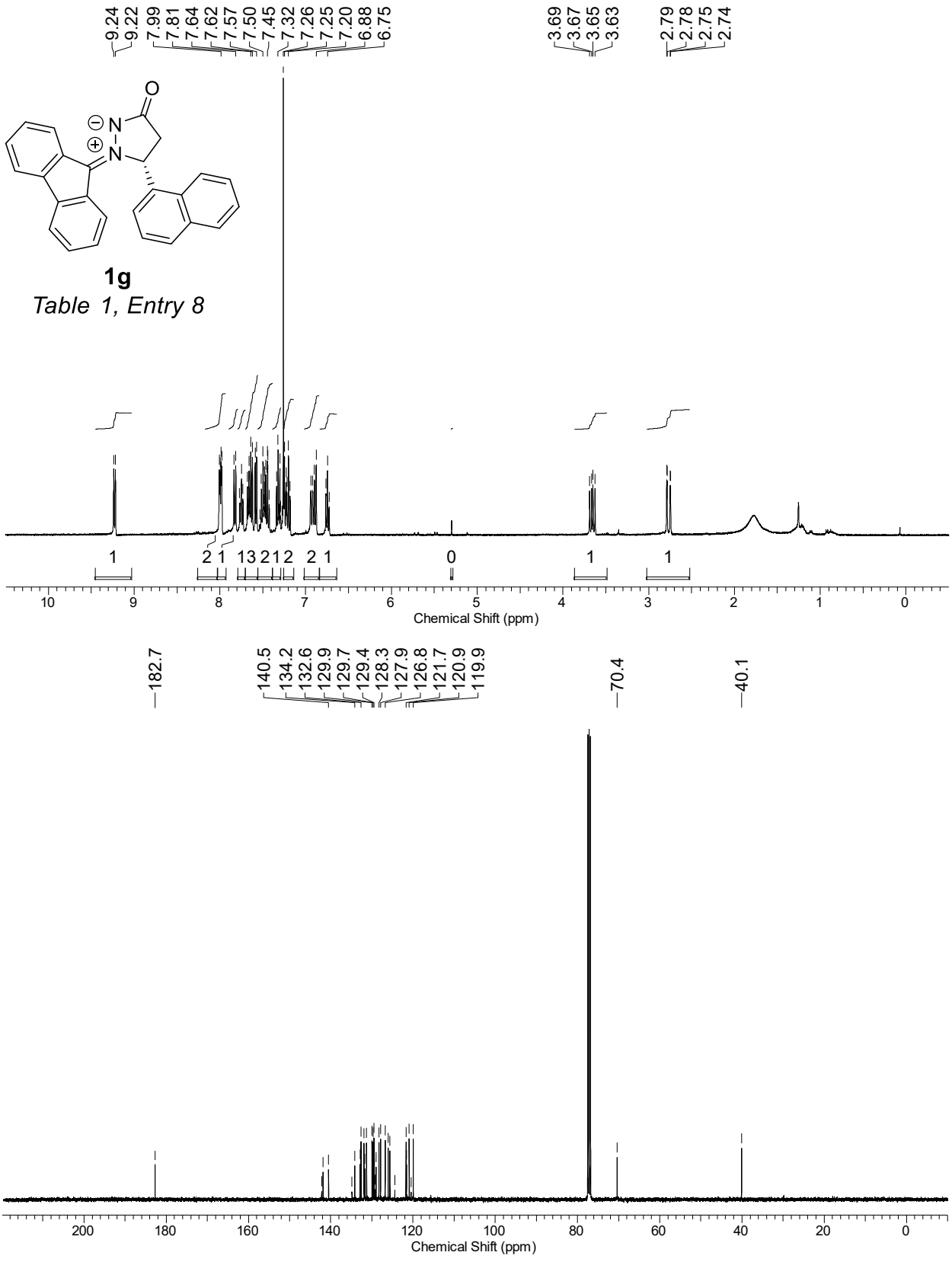

1g

Table 1, Entry 8

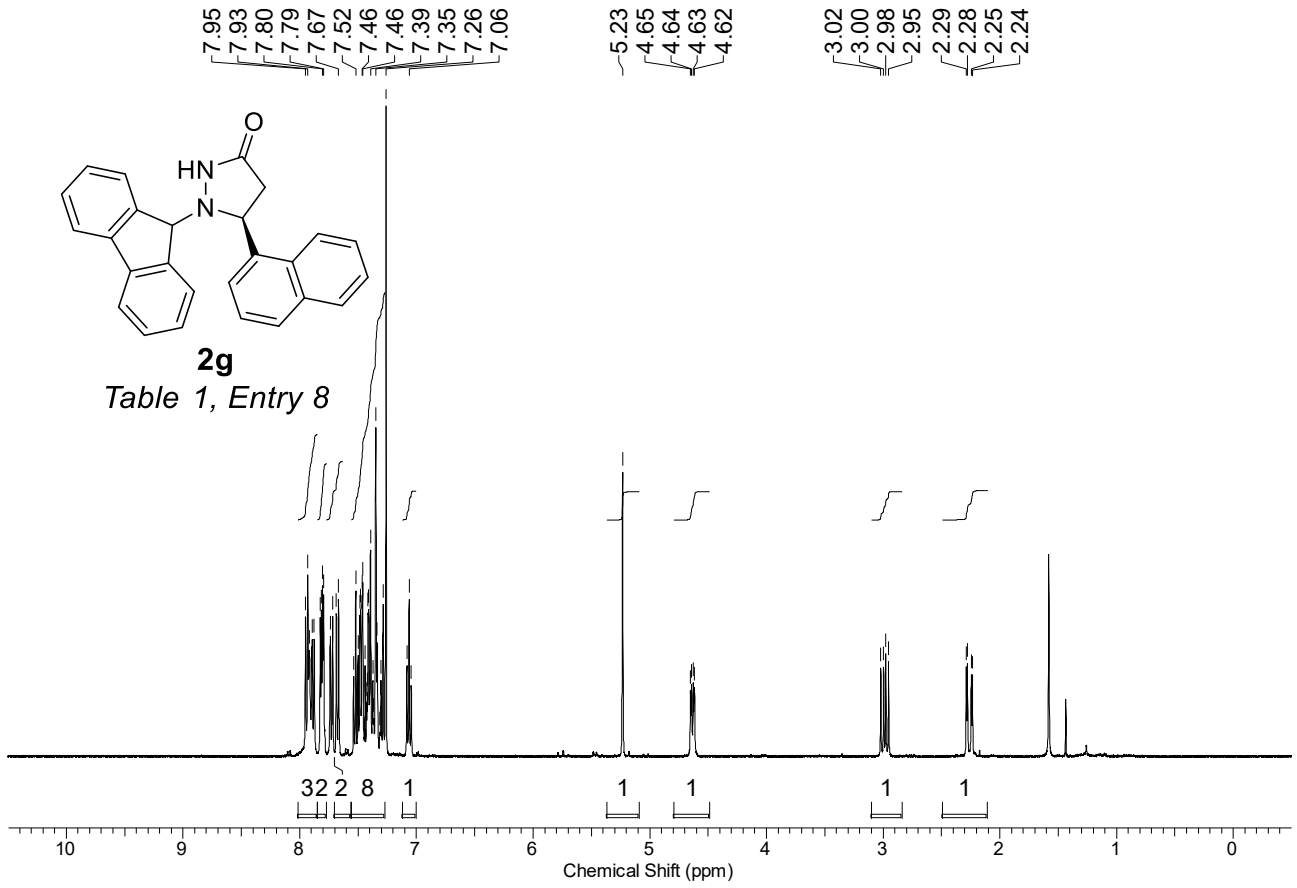

2g

Table 1, Entry 8

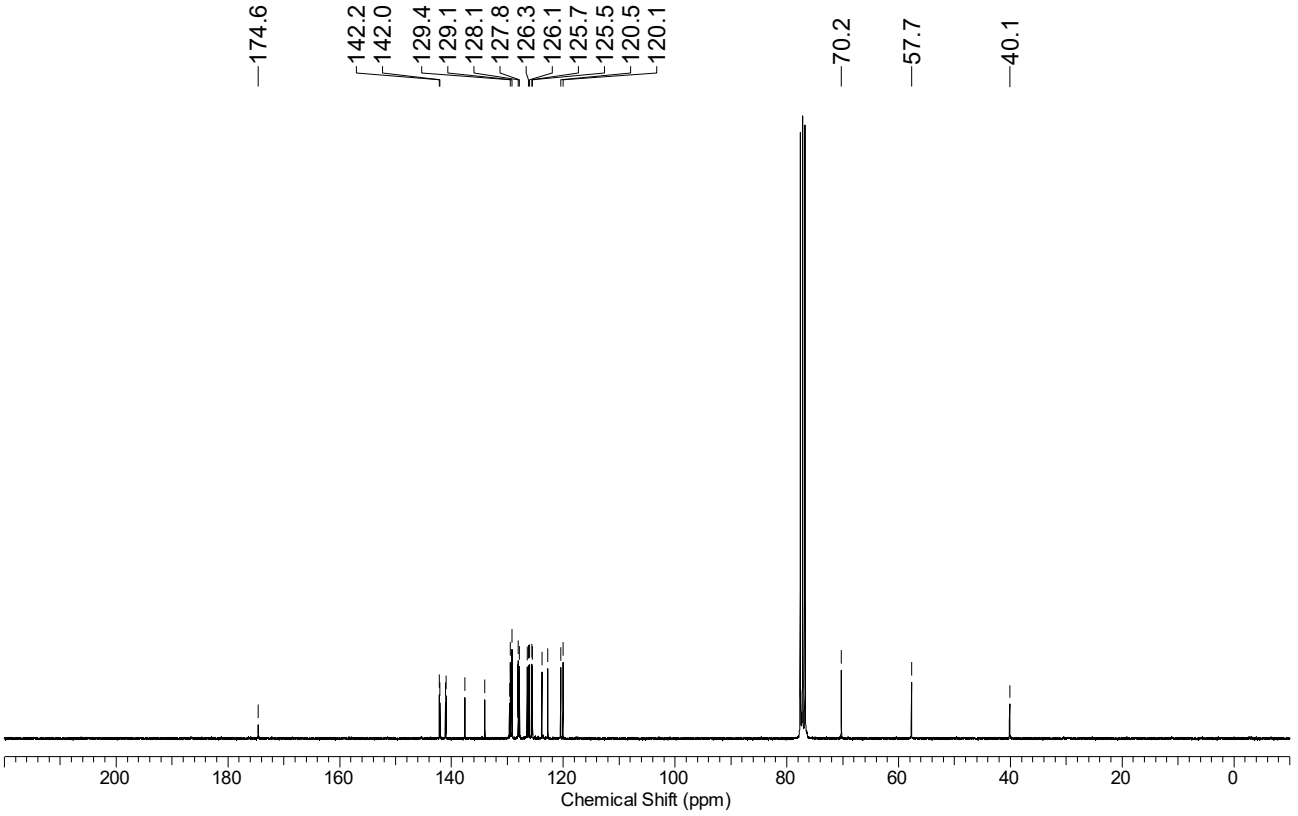

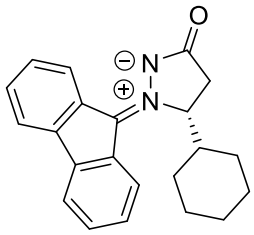

1h

Table 1, Entry 9

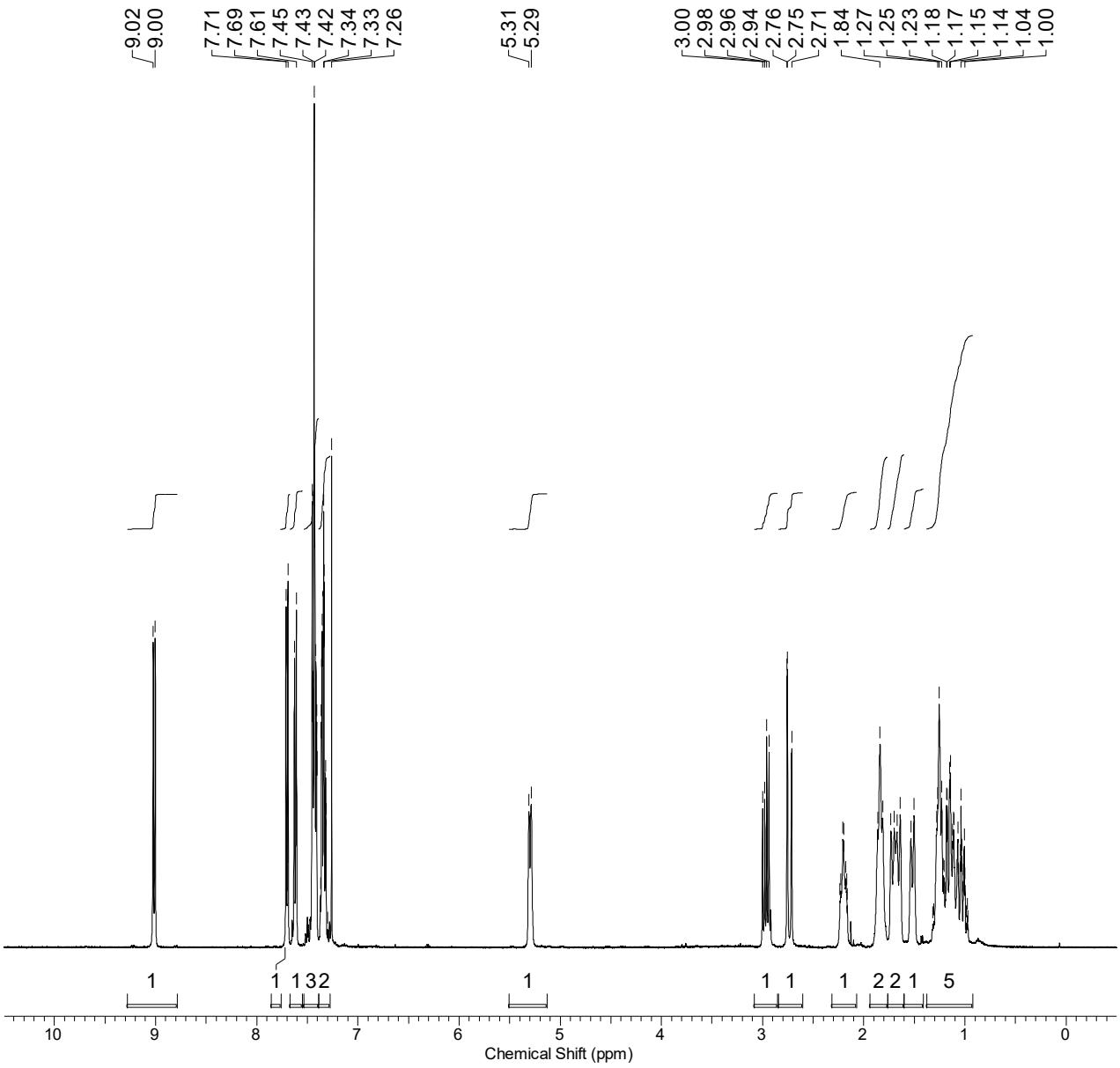

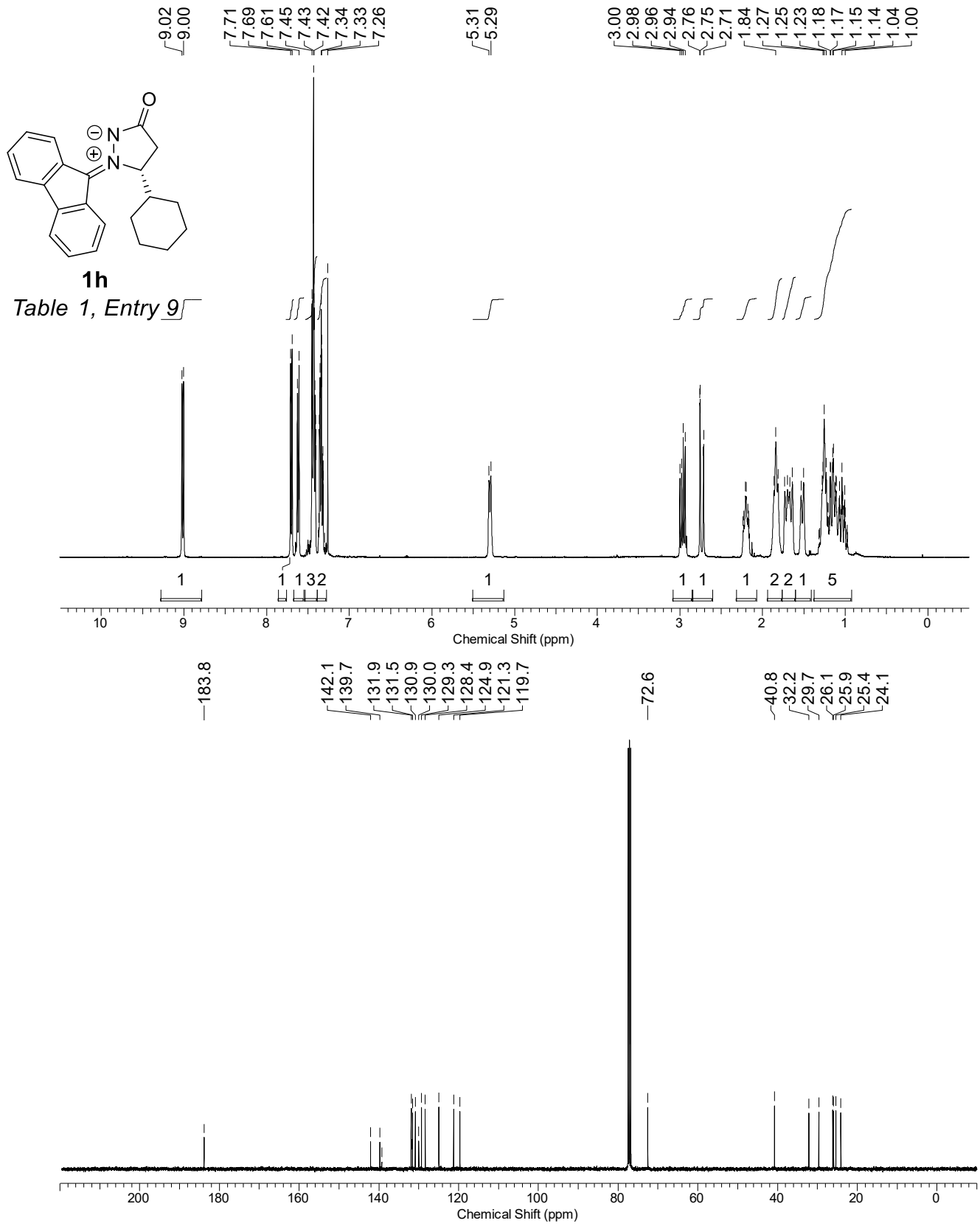
9.02
9.00
7.71
7.69
7.61
7.45
7.43
7.42
7.34
7.33
7.26
5.31
5.29
3.00
2.98
2.96
2.94
2.76
2.75
2.71
1.84
1.27
1.25
1.23
1.18
1.17
1.15
1.14
1.04
1.00
O
N
N
1h
Table 1, Entry 9
1
1 1 3 2
1
1 1
1
2 2 1
5
Chemical Shift (ppm)
183.8
142.1
139.7
131.9
131.5
130.9
130.0
129.3
128.4
124.9
121.3
119.7
72.6
40.8
32.2
29.7
26.1
25.9
25.4
24.1
Chemical Shift (ppm)

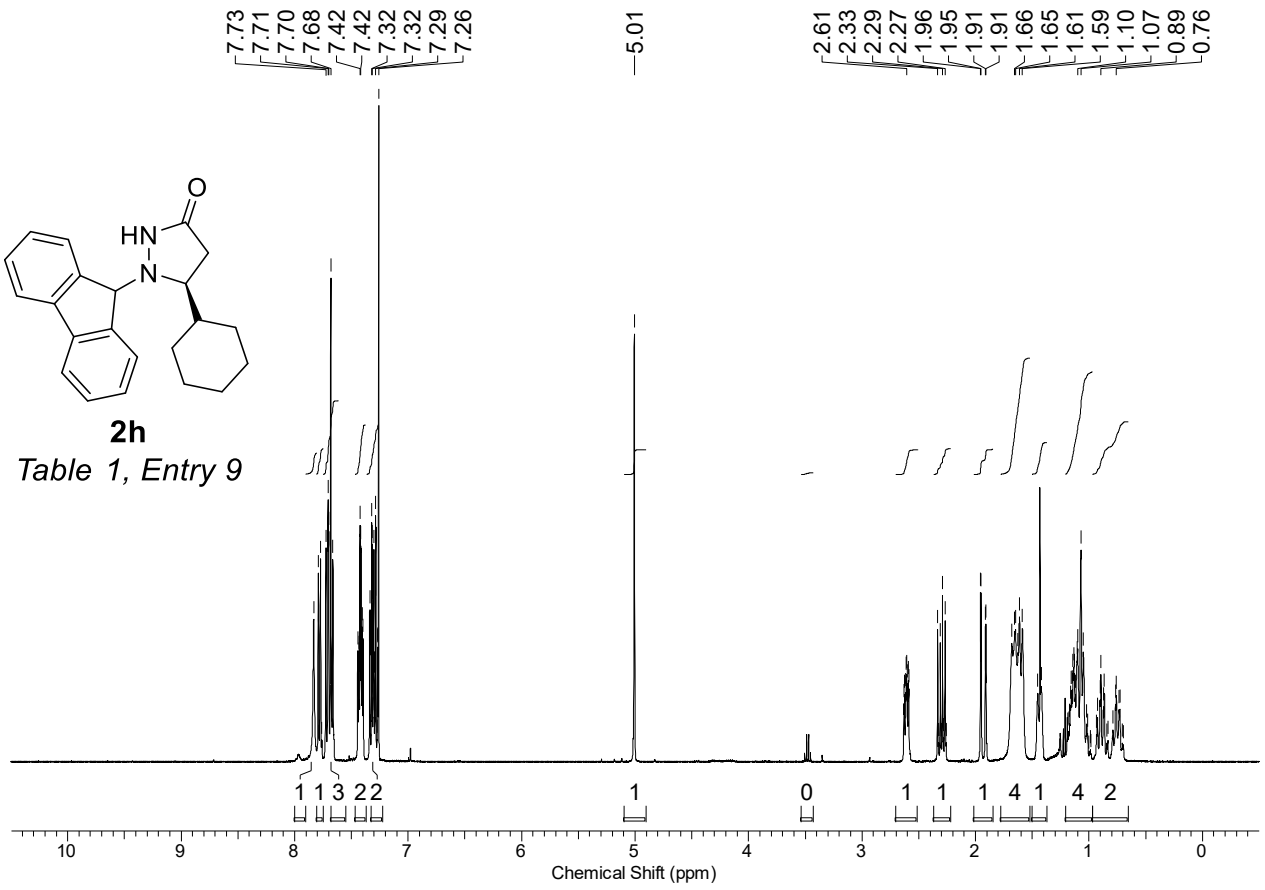

2h

Table 1, Entry 9

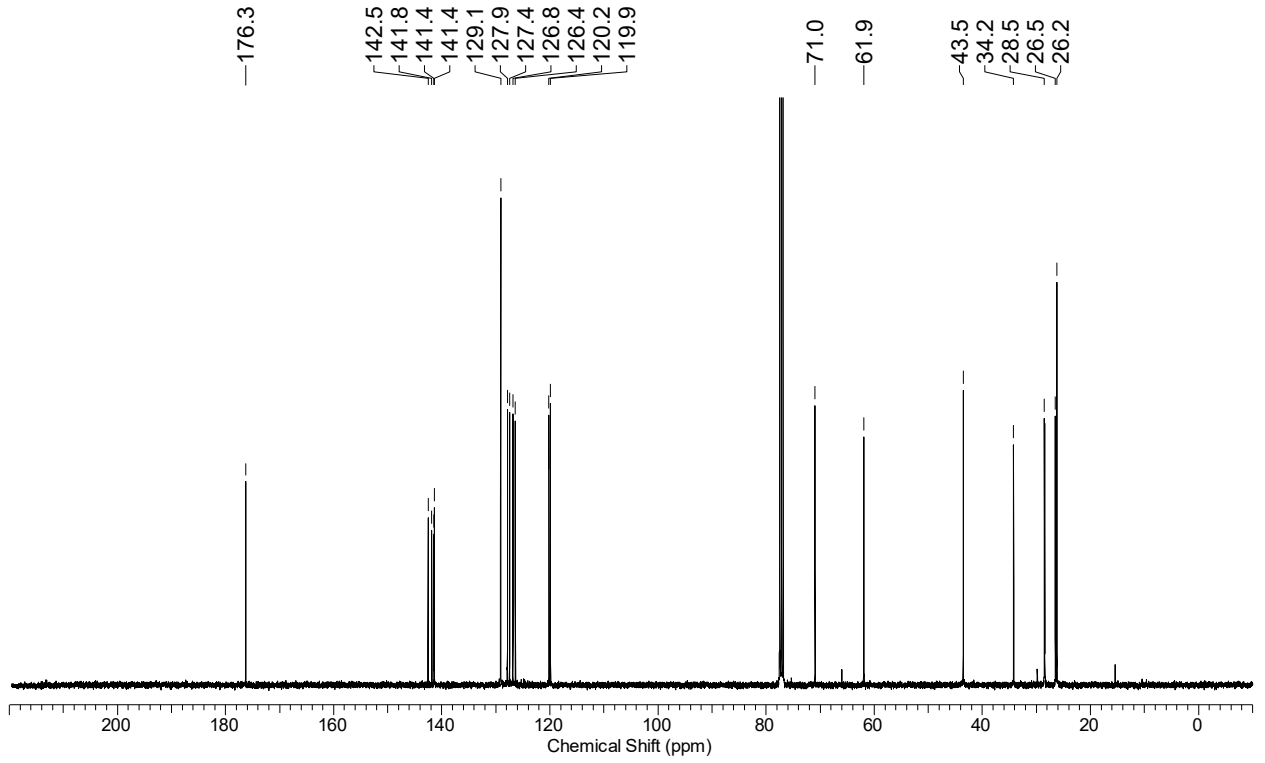

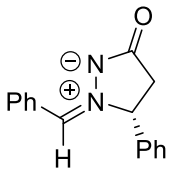

1i

Table 2, Entry 1

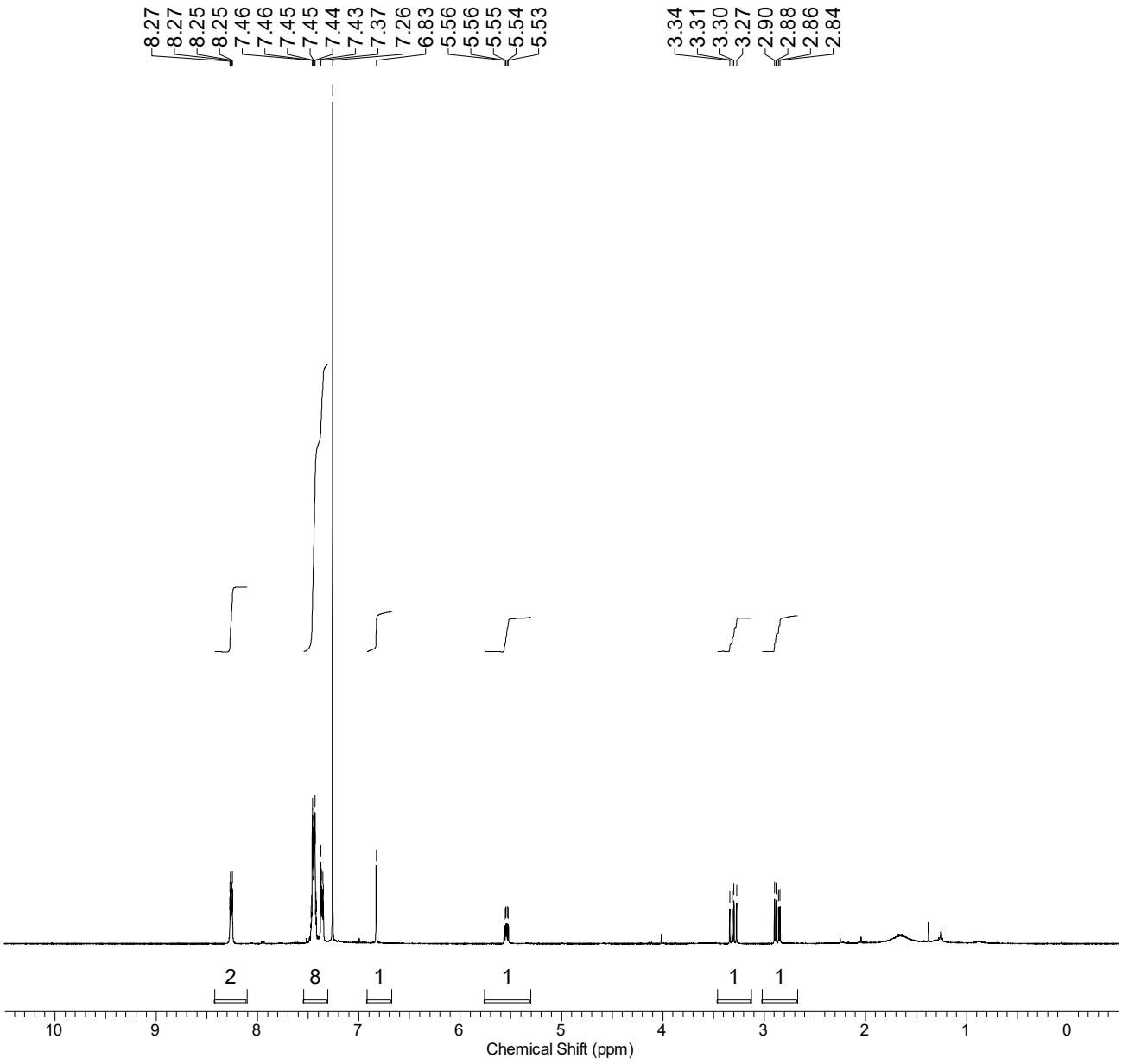

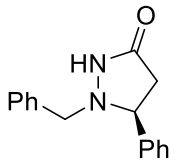

2i

Table 2, Entry 1

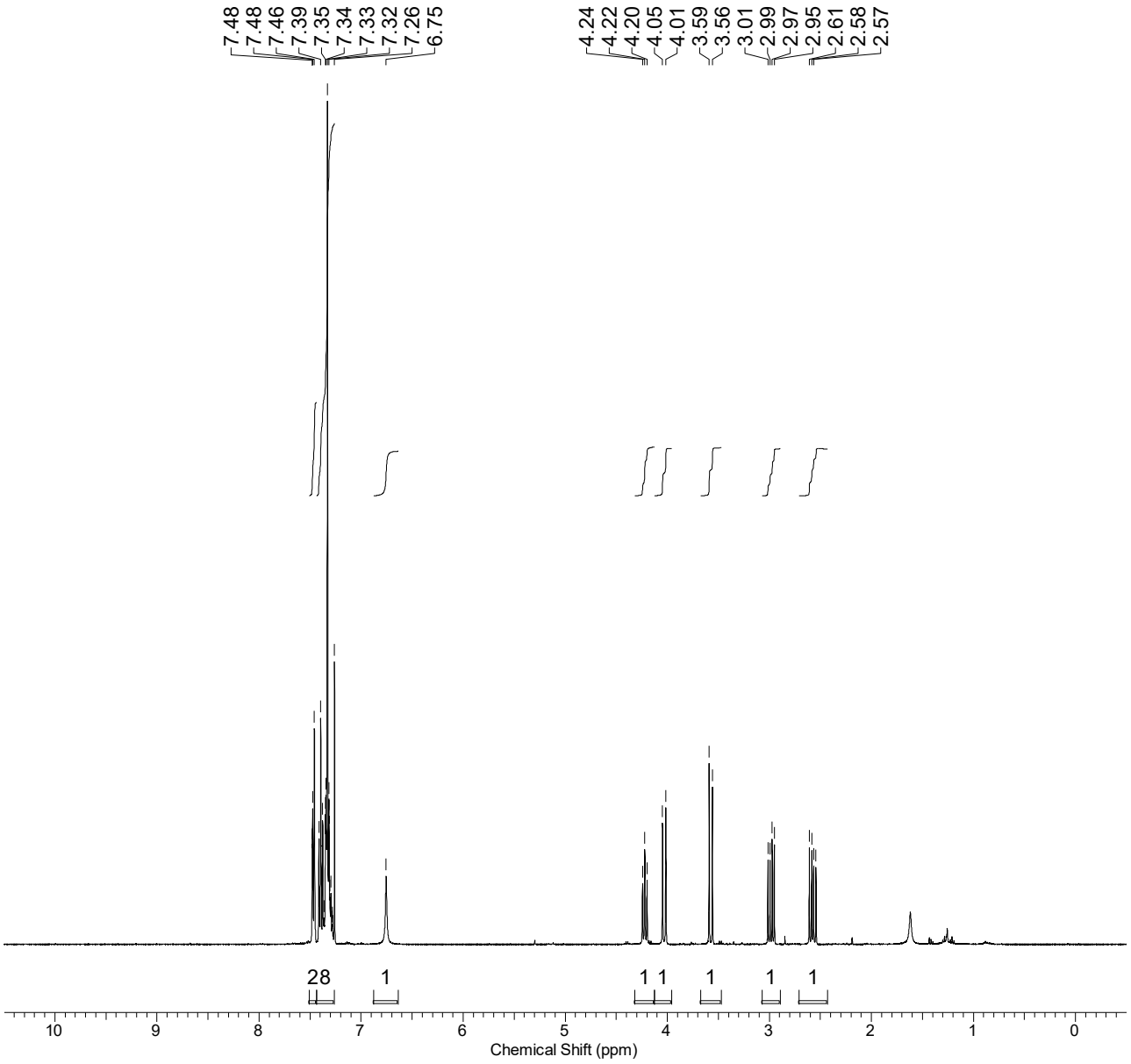

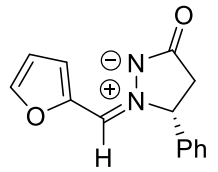

1j

Table 2, Entry 2

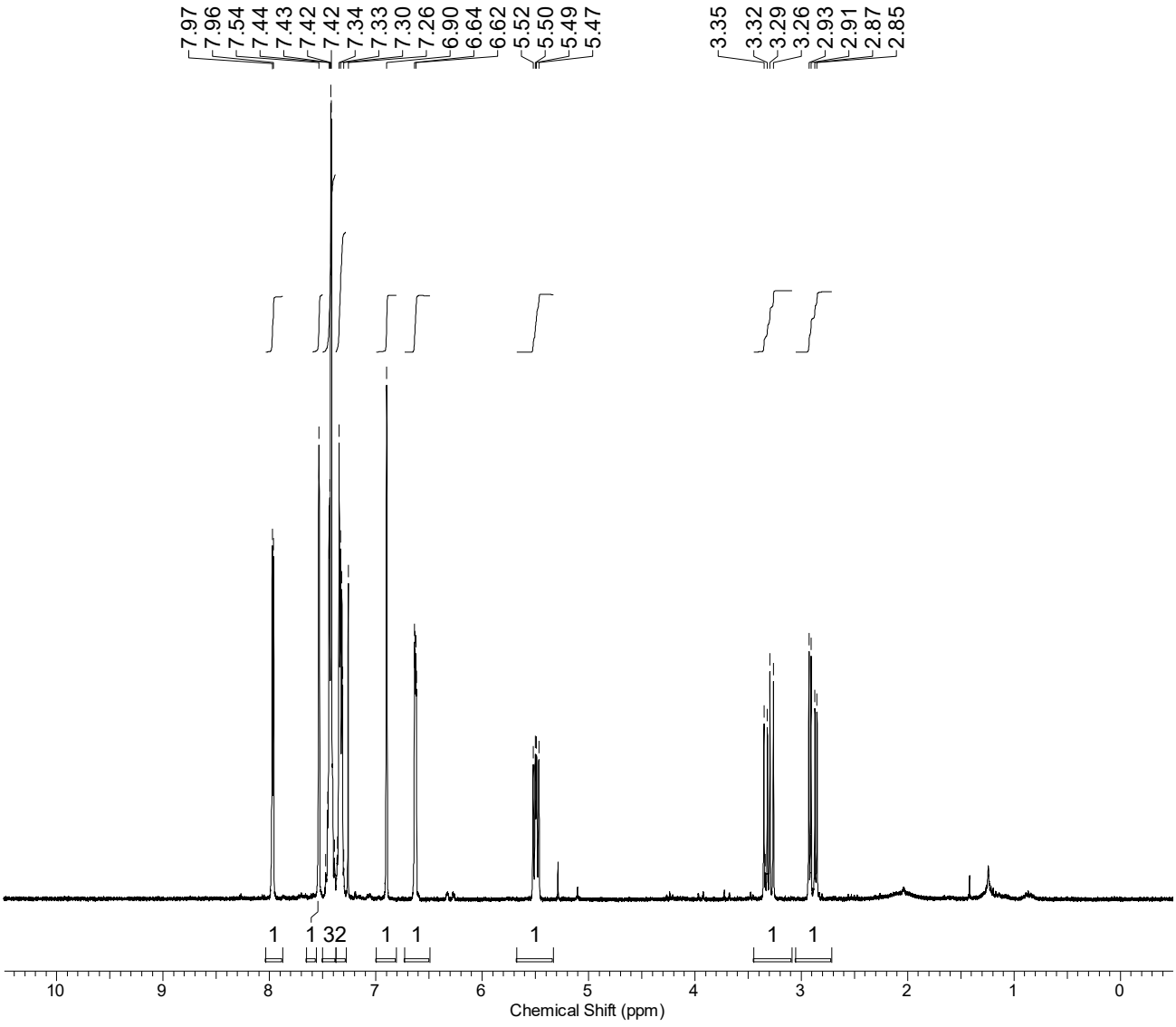

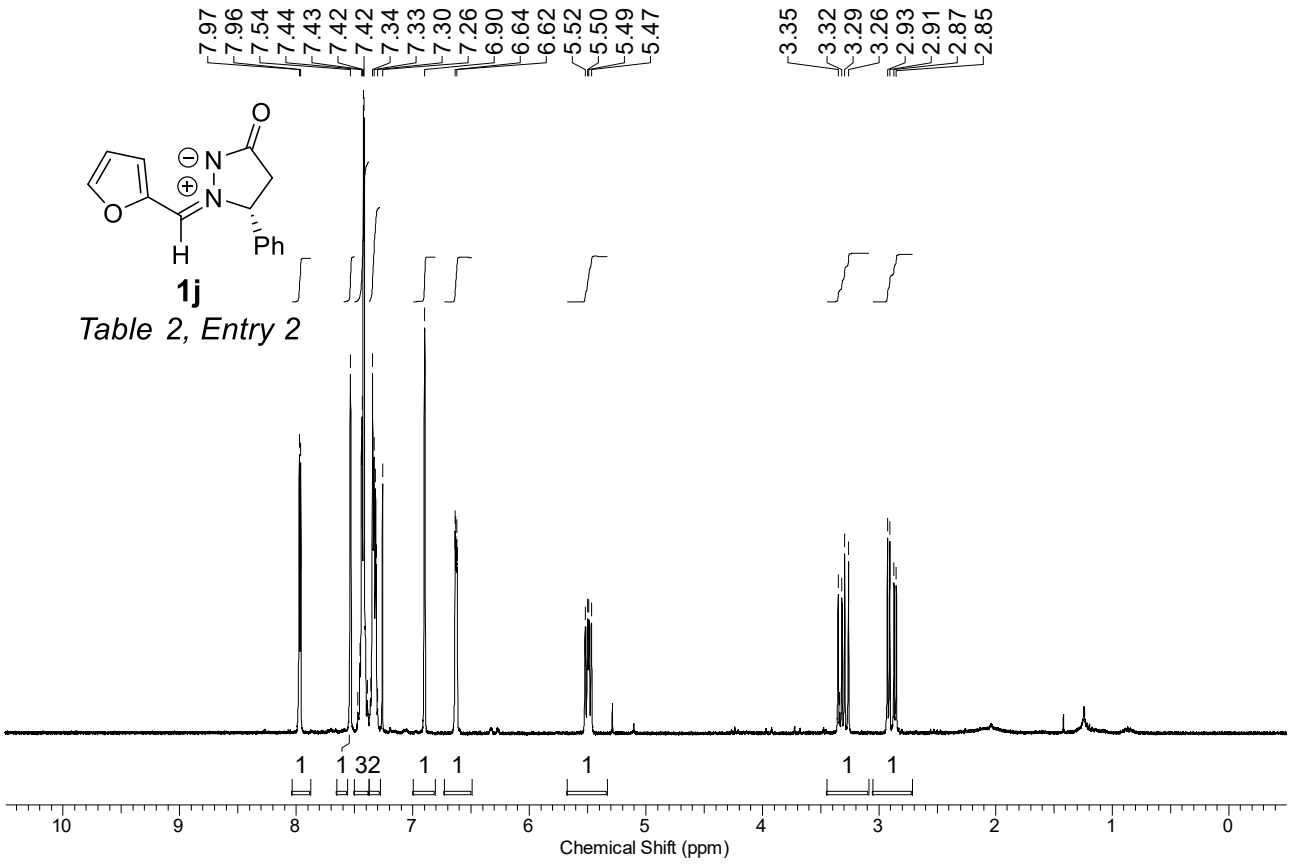
7.97
7.96
7.54
7.44
7.43
7.42
7.42
7.34
7.33
7.30
7.26
6.90
6.64
6.62
5.52
5.50
5.49
5.47
3.35
3.32
3.29
3.26
2.93
2.91
2.87
2.85
O
N
N
O
H
Ph
1j
Table 2, Entry 2
1 1 3 2 1 1 1 1 1
10 9 8 7 6 5 4 3 2 1 0
Chemical Shift (ppm)

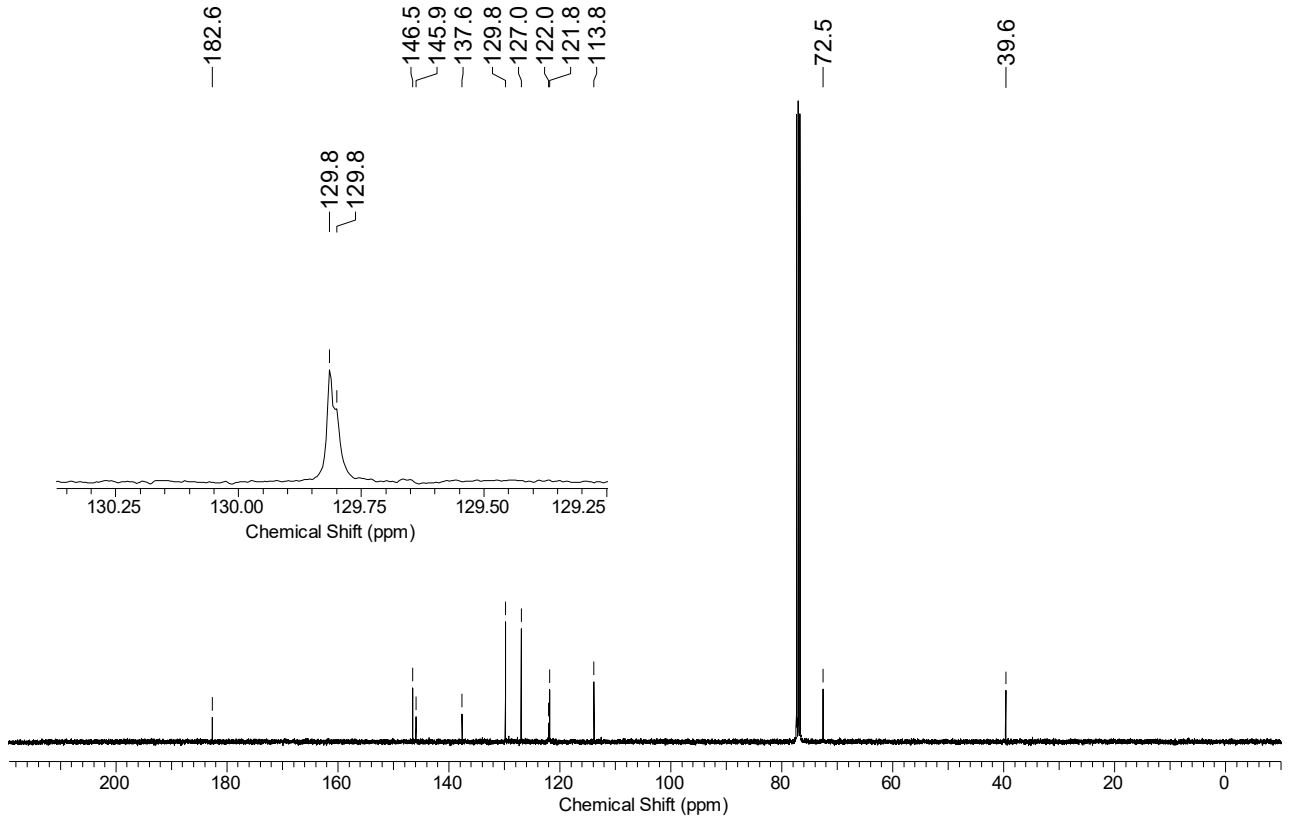
182.6
146.5
145.9
137.6
129.8
127.0
122.0
121.8
113.8
72.5
39.6
129.8
129.8
130.25 130.00 129.75 129.50 129.25
Chemical Shift (ppm)
200 180 160 140 120 100 80 60 40 20 0
Chemical Shift (ppm)

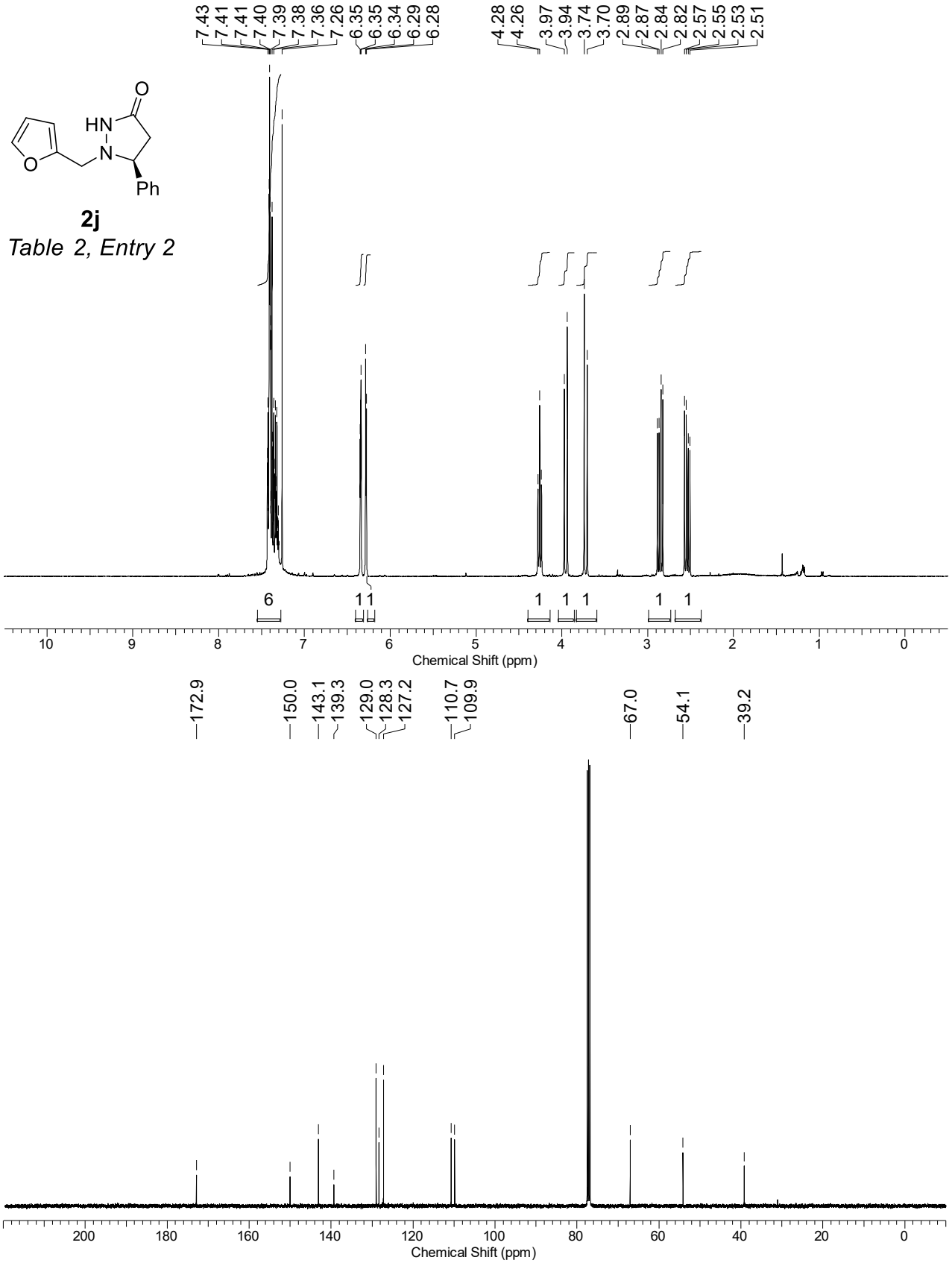
7.43
7.41
7.41
7.40
7.39
7.38
7.36
7.26
6.35
6.35
6.34
6.29
6.28
4.28
4.26
3.97
3.94
3.74
3.70
2.89
2.87
2.84
2.82
2.57
2.55
2.53
2.51
O
HN
N
O
Ph
2j
Table 2, Entry 2
6
1
1
1
1
1
1
1
10
9
8
7
6
5
4
3
2
1
0
Chemical Shift (ppm)
172.9
150.0
143.1
139.3
129.0
128.3
127.2
110.7
109.9
67.0
54.1
39.2
200
180
160
140
120
100
80
60
40
20
0
Chemical Shift (ppm)

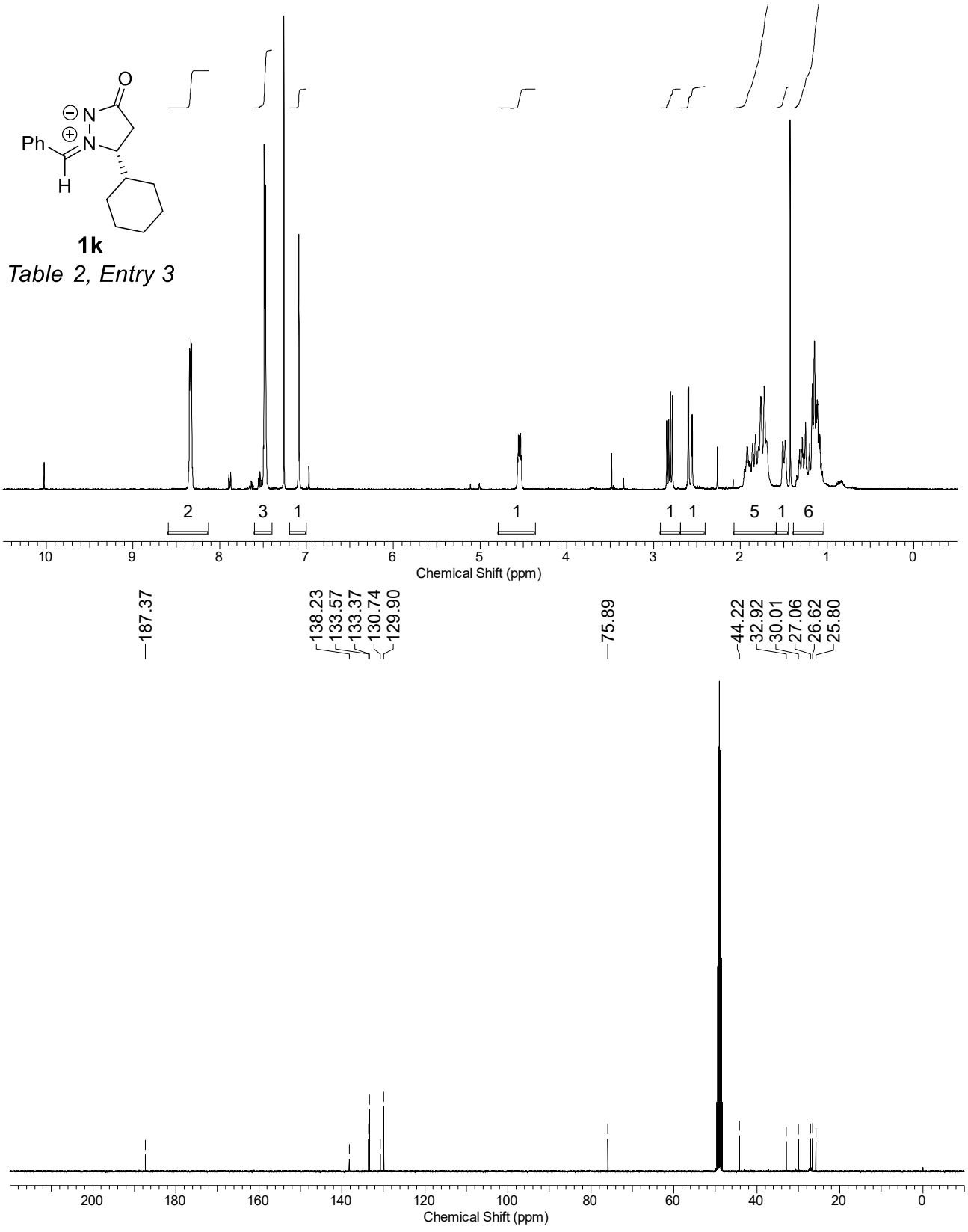
O
N
Ph
N
H
1k
Table 2, Entry 3
2
3
1
1
1
1
5
1
6
10
9
8
7
6
5
4
3
2
1
0
Chemical Shift (ppm)
187.37
138.23
133.57
133.37
130.74
129.90
75.89
44.22
32.92
30.01
27.06
26.62
25.80
200
180
160
140
120
100
80
60
40
20
0
Chemical Shift (ppm)

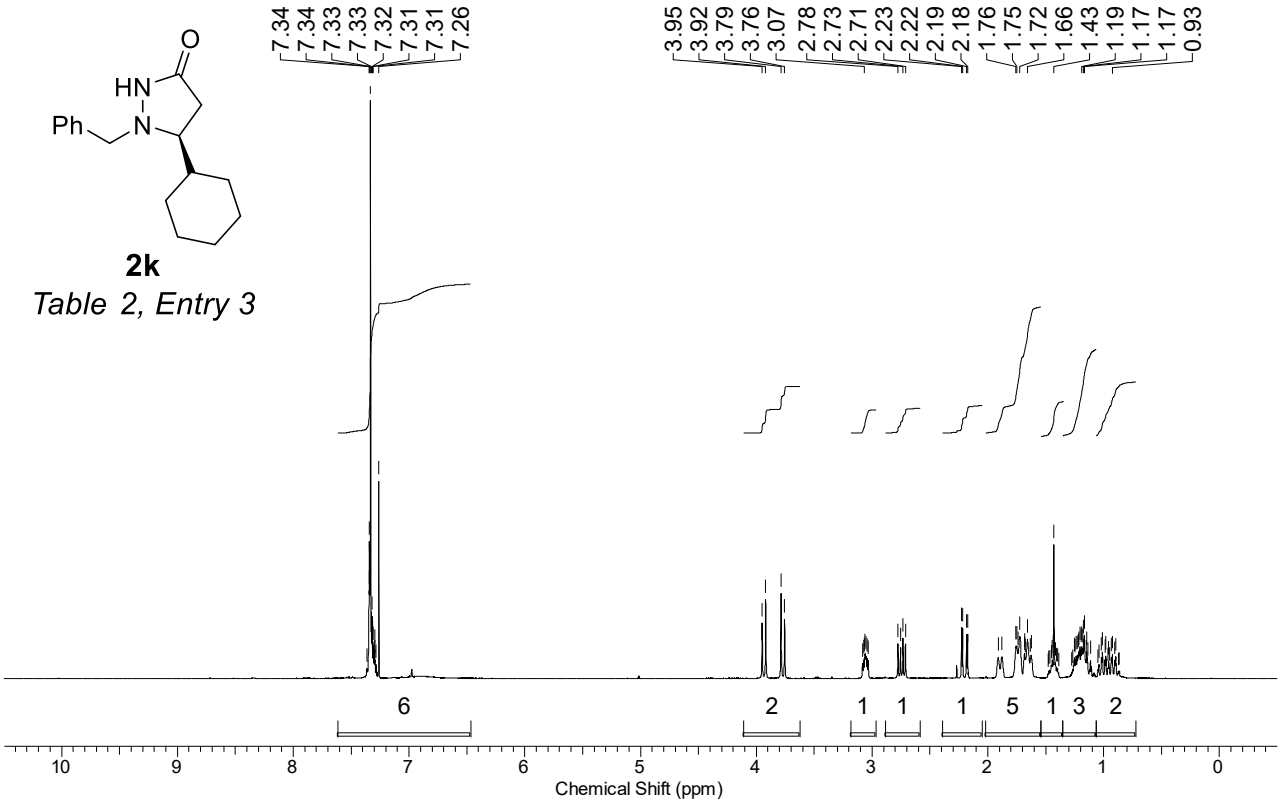

2k

Table 2, Entry 3

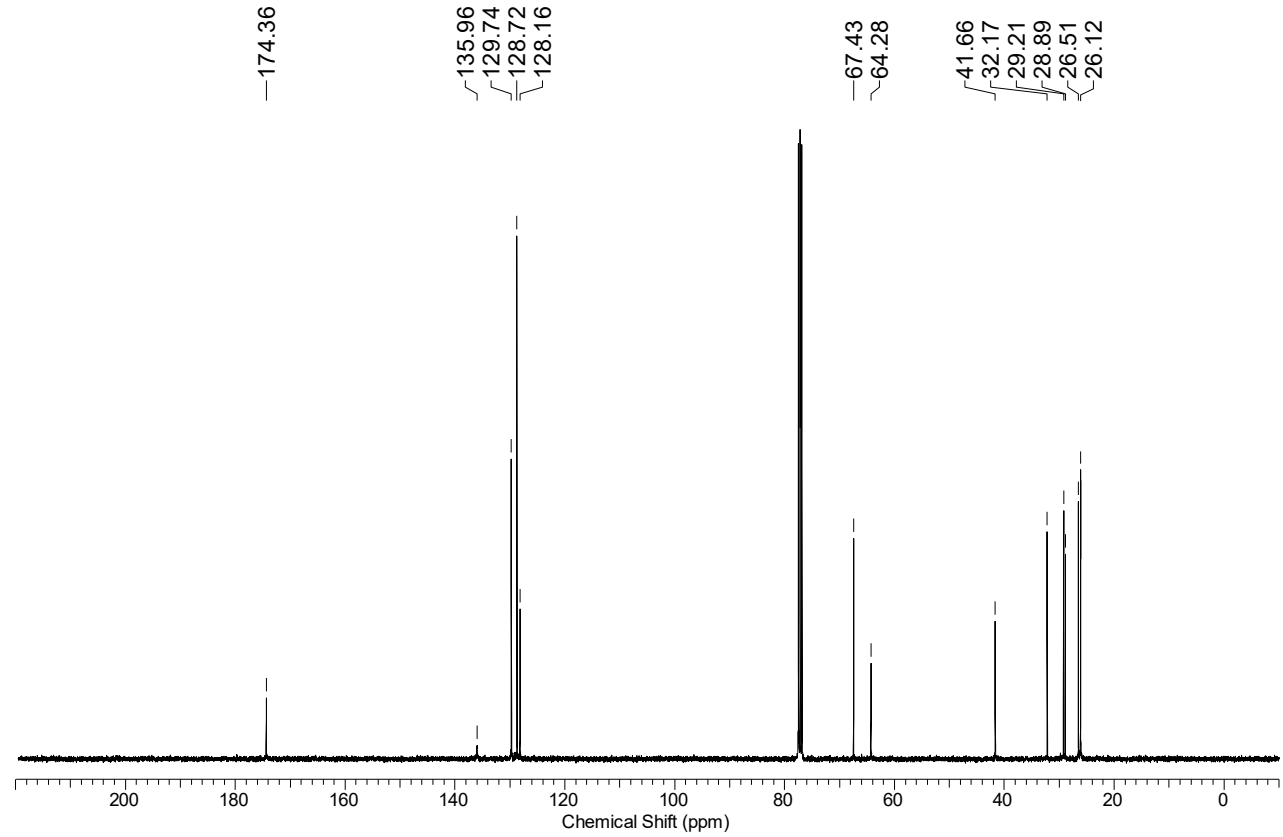

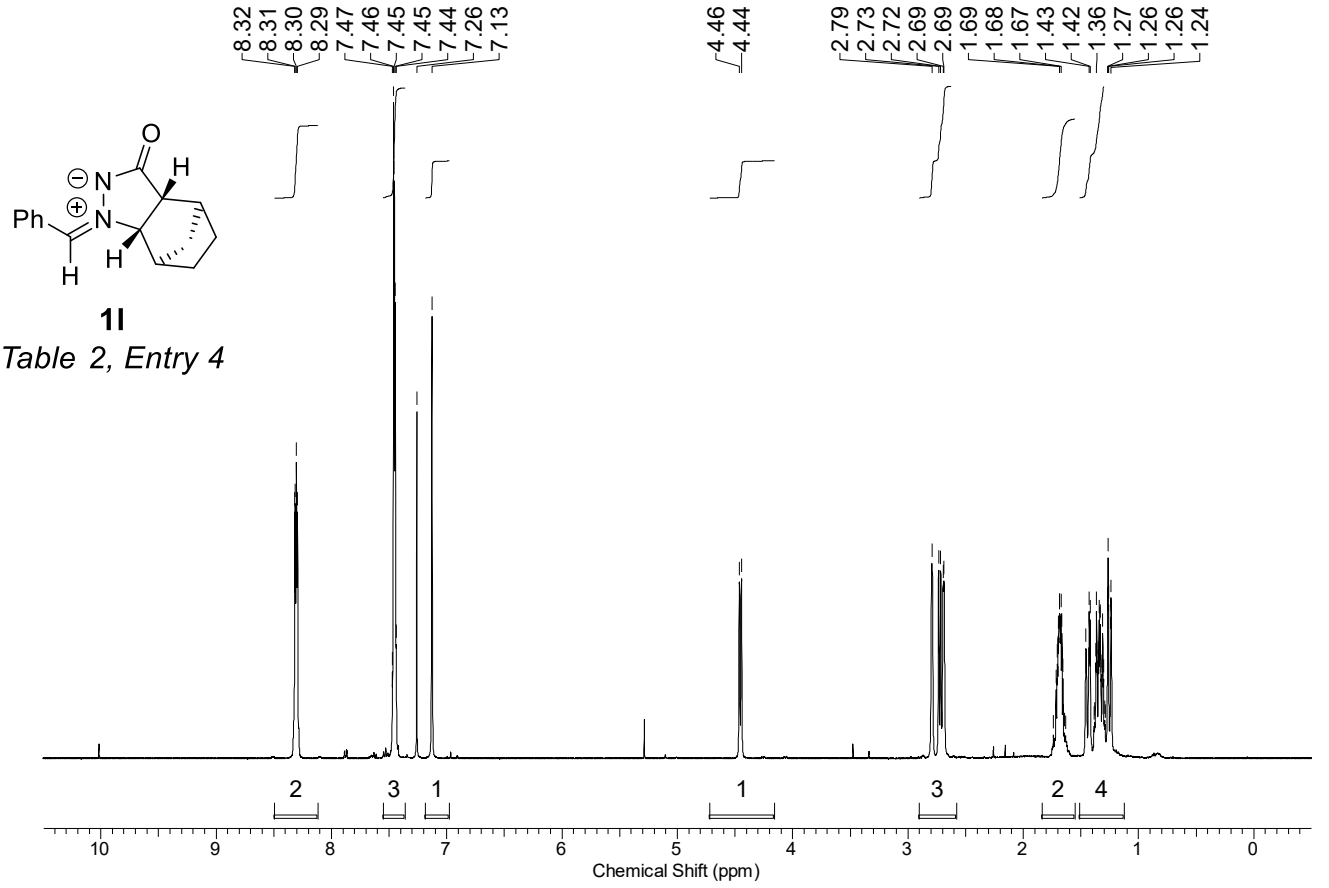

1l

Table 2, Entry 4

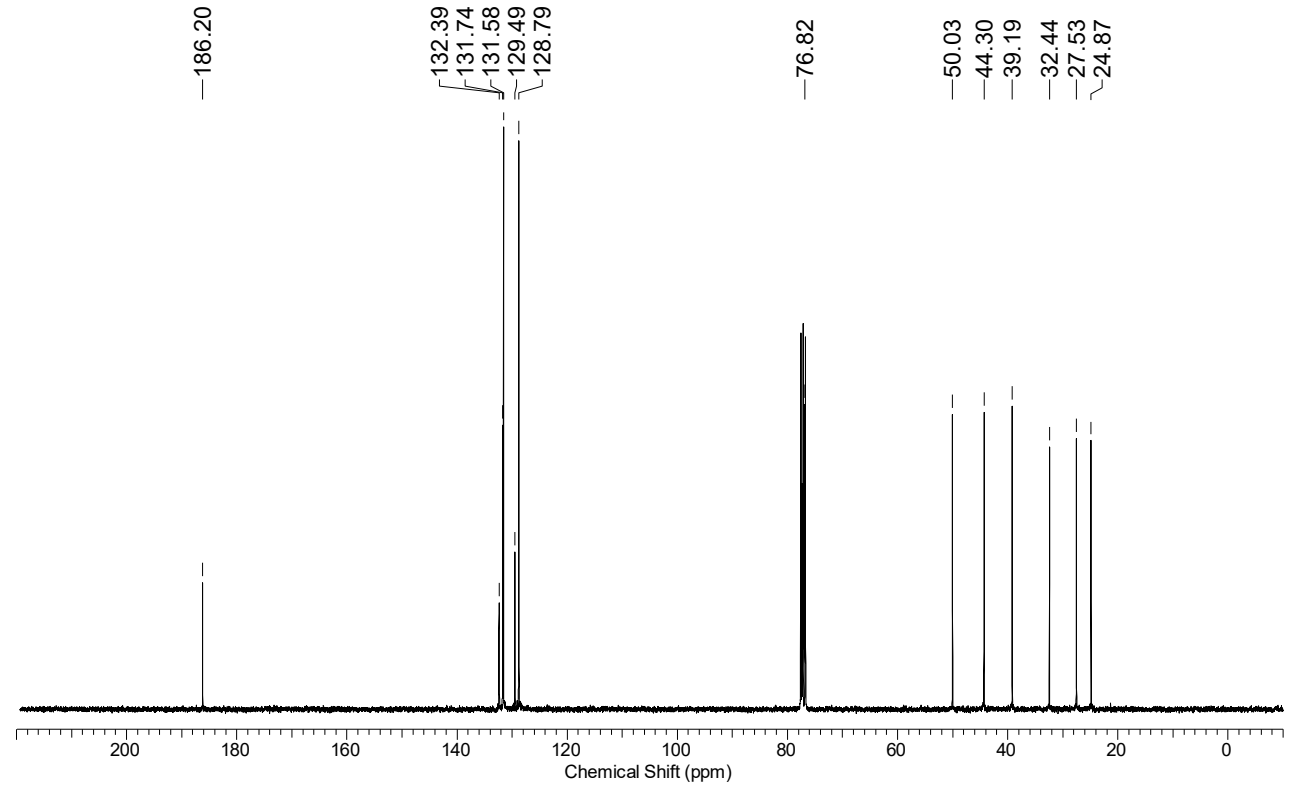

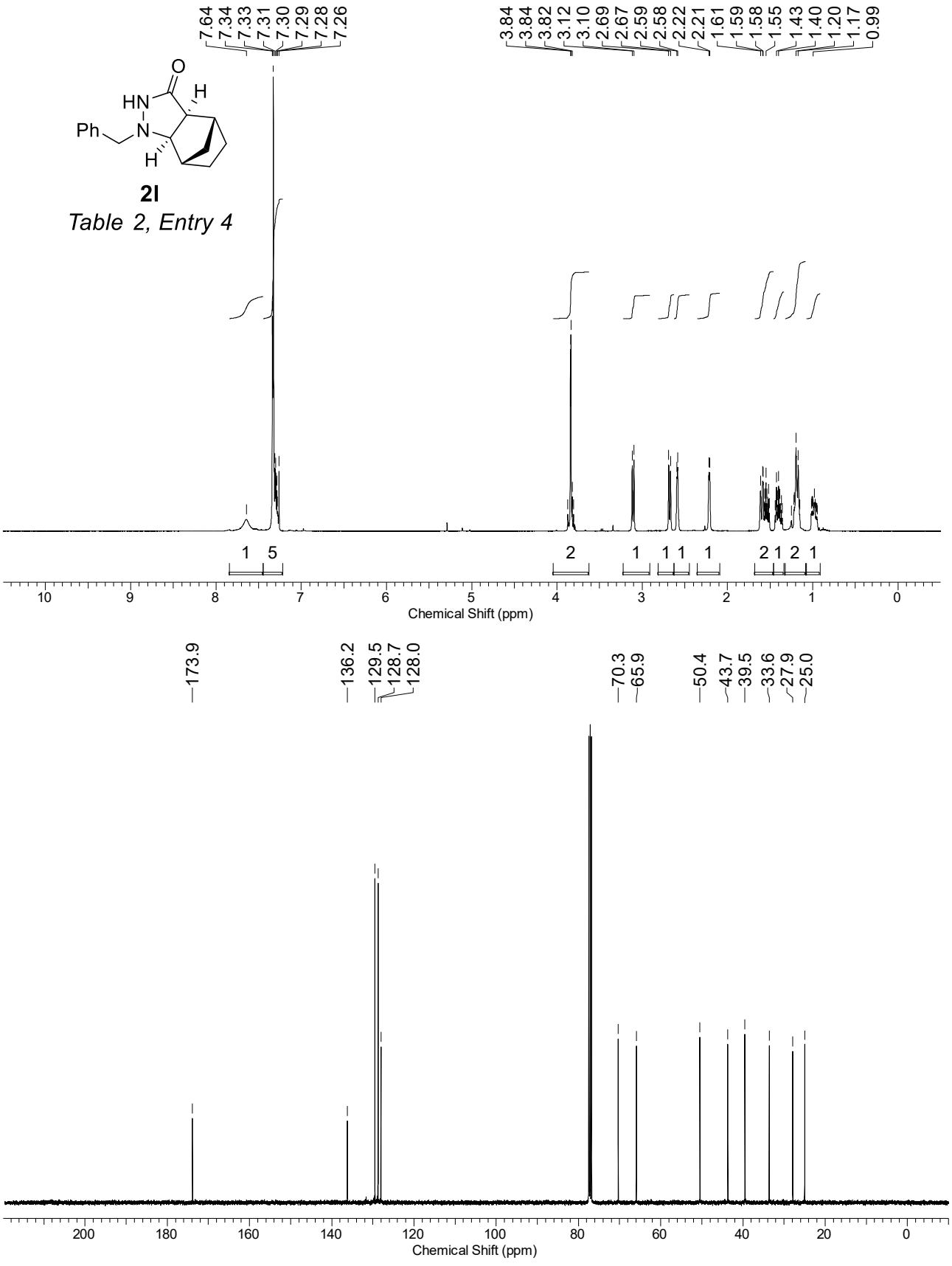
7.64
7.34
7.33
7.31
7.30
7.29
7.28
7.26
3.84
3.84
3.82
3.12
3.10
2.69
2.67
2.59
2.58
2.22
2.21
1.61
1.59
1.58
1.55
1.43
1.40
1.20
1.17
0.99
O
HN
H
Ph
N
H
2l
Table 2, Entry 4
1 5
2
1
1 1
1
2 1 2 1
Chemical Shift (ppm)
173.9
136.2
129.5
128.7
128.0
70.3
65.9
50.4
43.7
39.5
33.6
27.9
25.0
Chemical Shift (ppm)

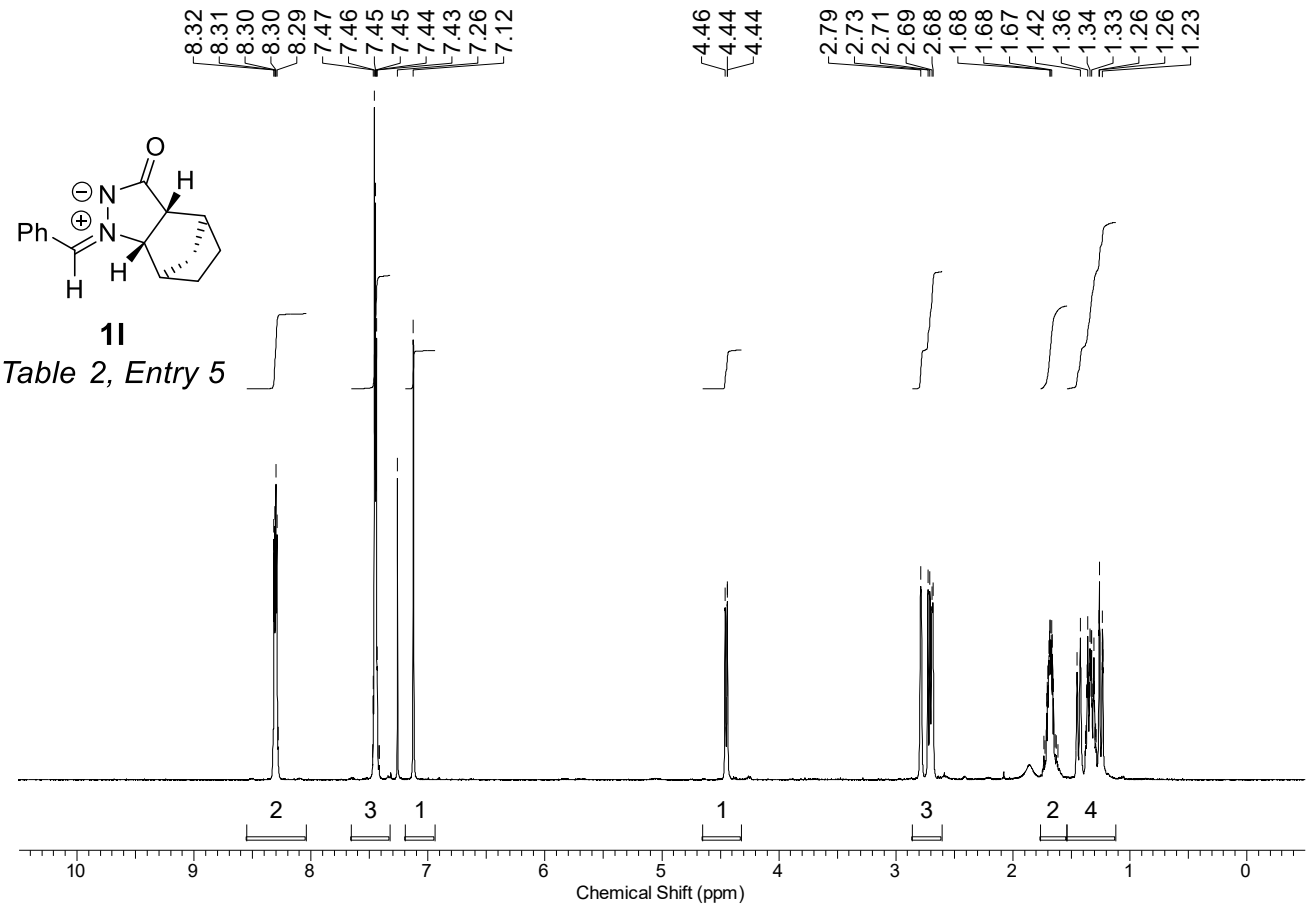

1l

Table 2, Entry 5

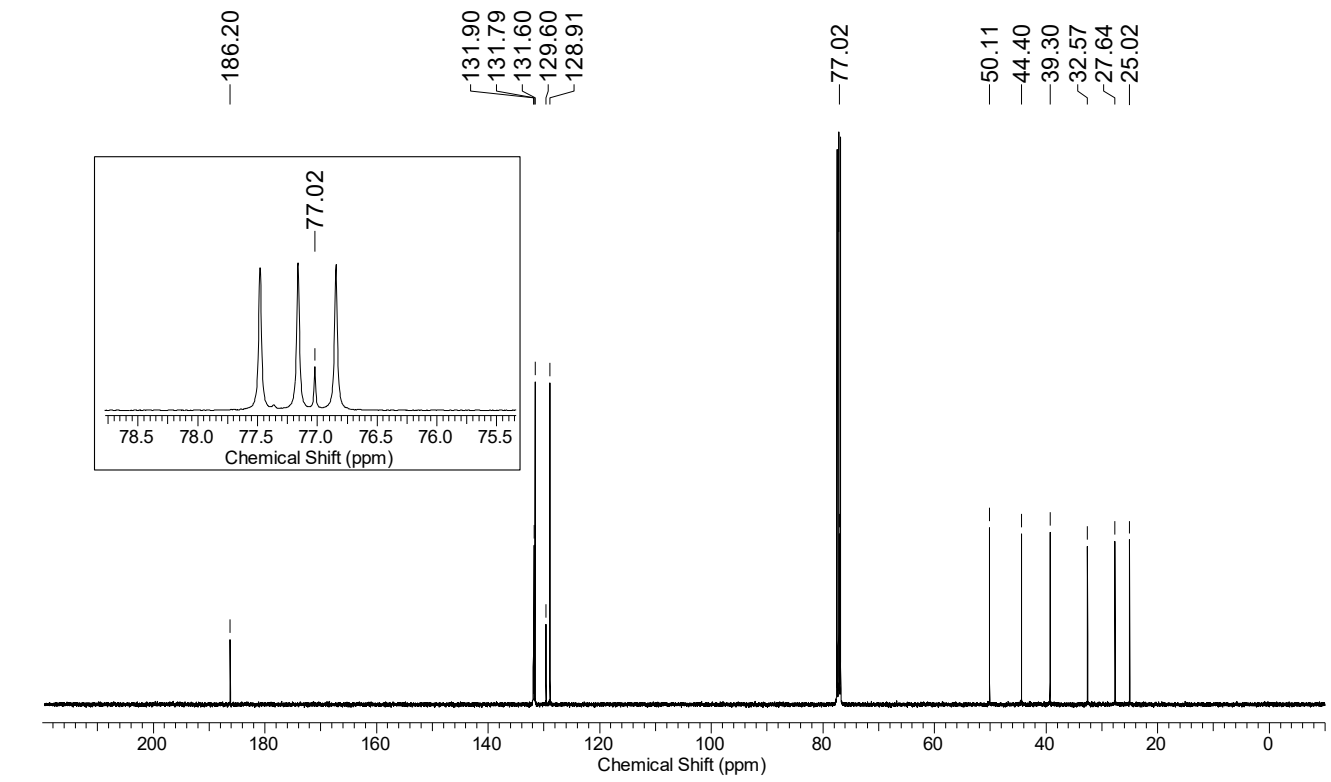

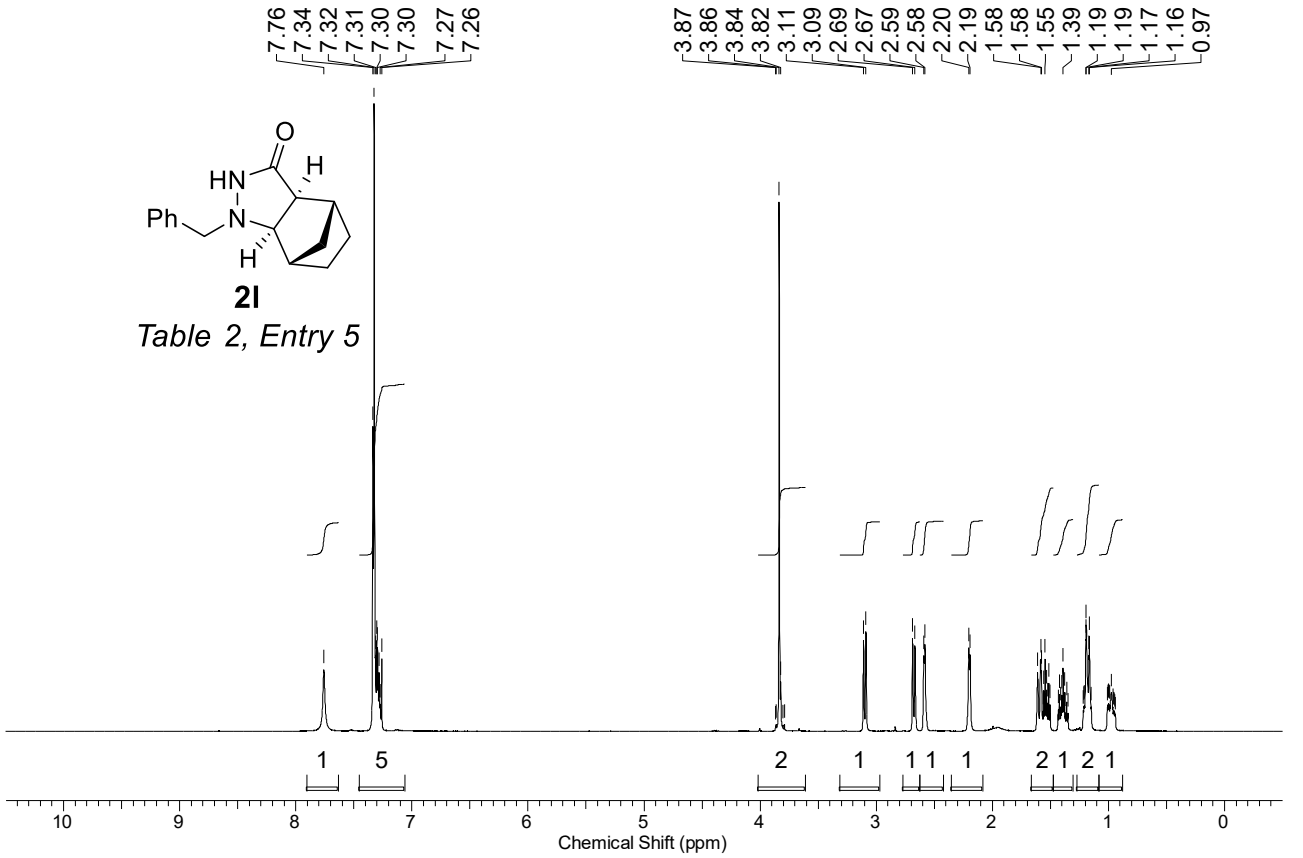
7.76
7.34
7.32
7.31
7.30
7.30
7.27
7.26
3.87
3.86
3.84
3.82
3.11
3.09
2.69
2.67
2.59
2.58
2.20
2.19
1.58
1.58
1.55
1.39
1.19
1.19
1.17
1.16
0.97
O
HN
H
Ph
N
H
2l
Table 2, Entry 5
1
5
2
1
1
1
1
2
1
2
1
Chemical Shift (ppm)

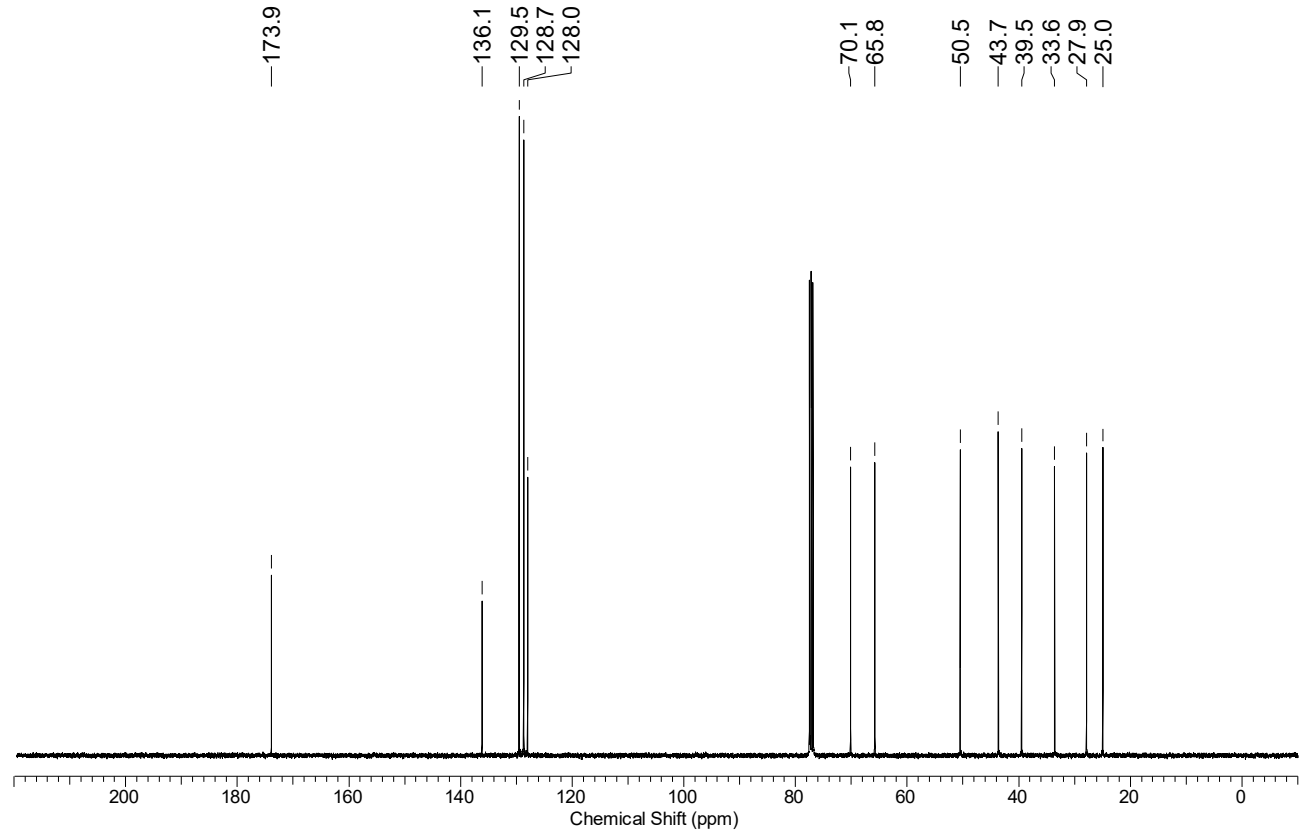
173.9
136.1
129.5
128.7
128.0
70.1
65.8
50.5
43.7
39.5
33.6
27.9
25.0
Chemical Shift (ppm)

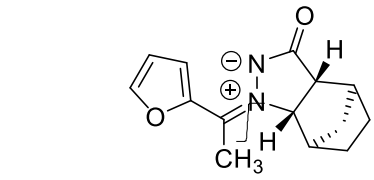

1m

Table 2, Entry 6

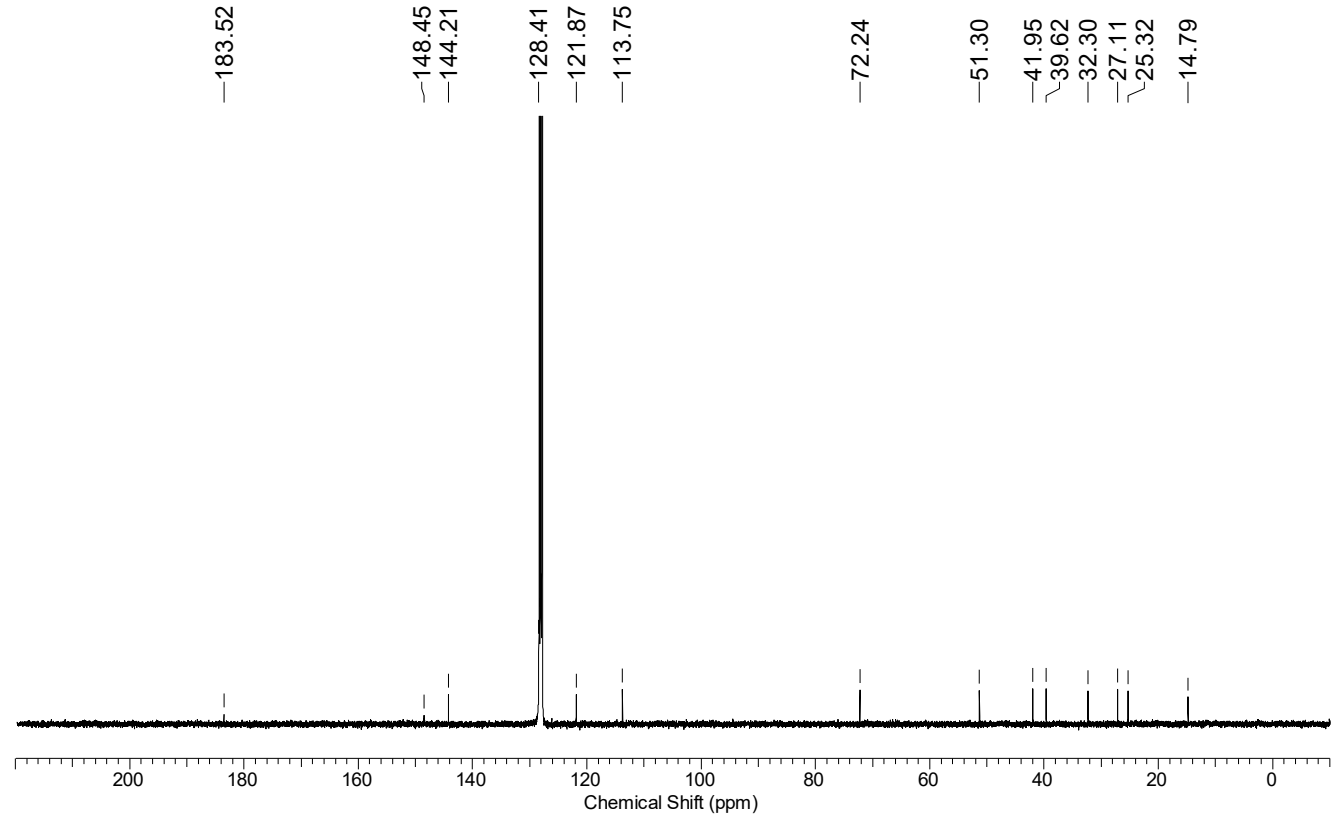

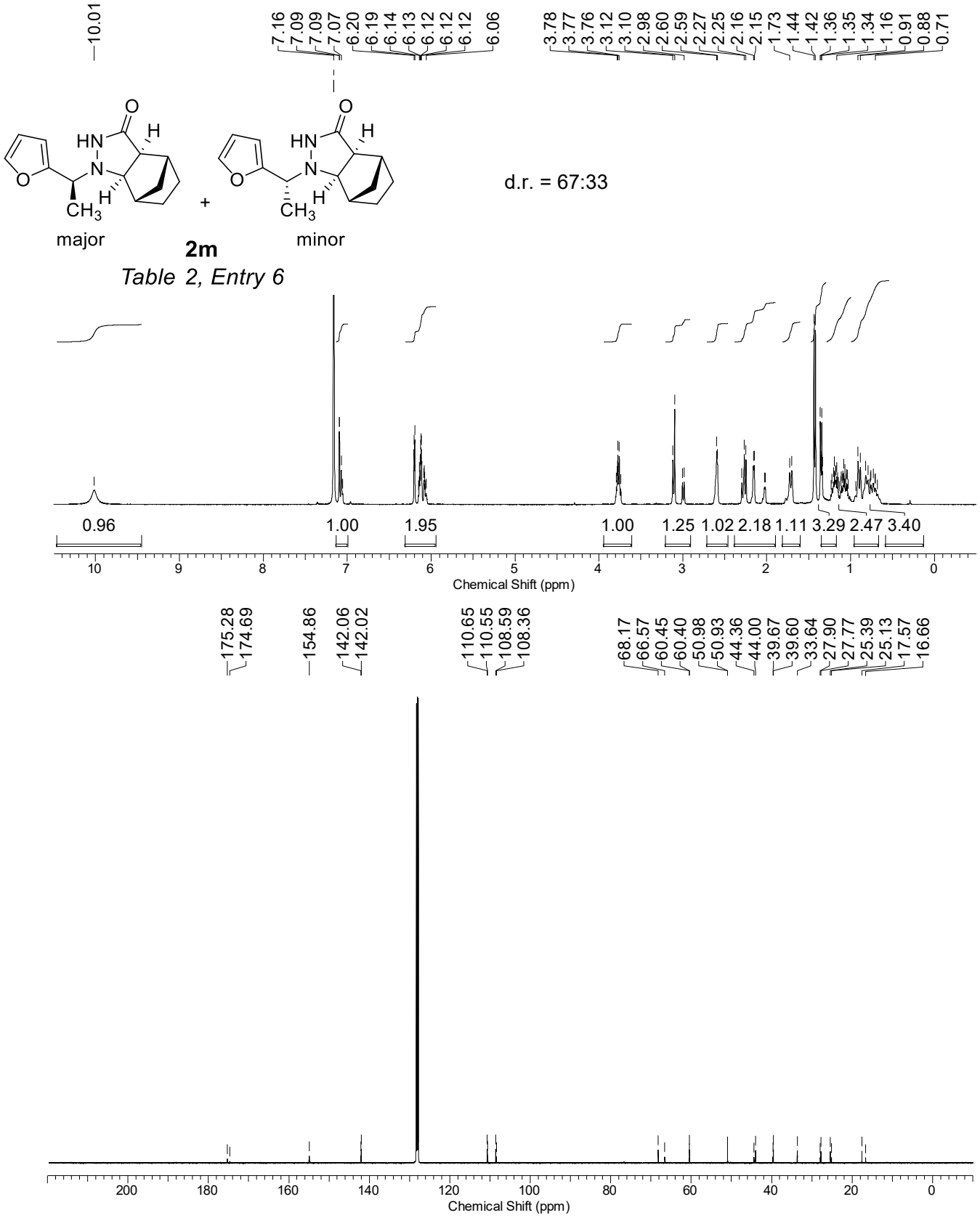
10.01
7.16
7.09
7.09
7.07
6.20
6.19
6.14
6.13
6.12
6.12
6.12
6.06
3.78
3.77
3.76
3.12
3.10
2.98
2.60
2.59
2.27
2.25
2.16
2.15
1.73
1.44
1.42
1.36
1.35
1.34
1.16
0.91
0.88
0.71
HN
N
O
H
CH3
major
+
minor
d.r. = 67:33
2m
Table 2, Entry 6
0.96
1.00
1.95
1.00
1.25
1.02
2.18
1.11
3.29
2.47
3.40
Chemical Shift (ppm)
175.28
174.69
154.86
142.06
142.02
110.65
110.55
108.59
108.36
68.17
66.57
60.45
60.40
50.98
50.93
44.36
44.00
39.67
39.60
33.64
27.90
27.77
25.39
25.13
17.57
16.66
Chemical Shift (ppm)

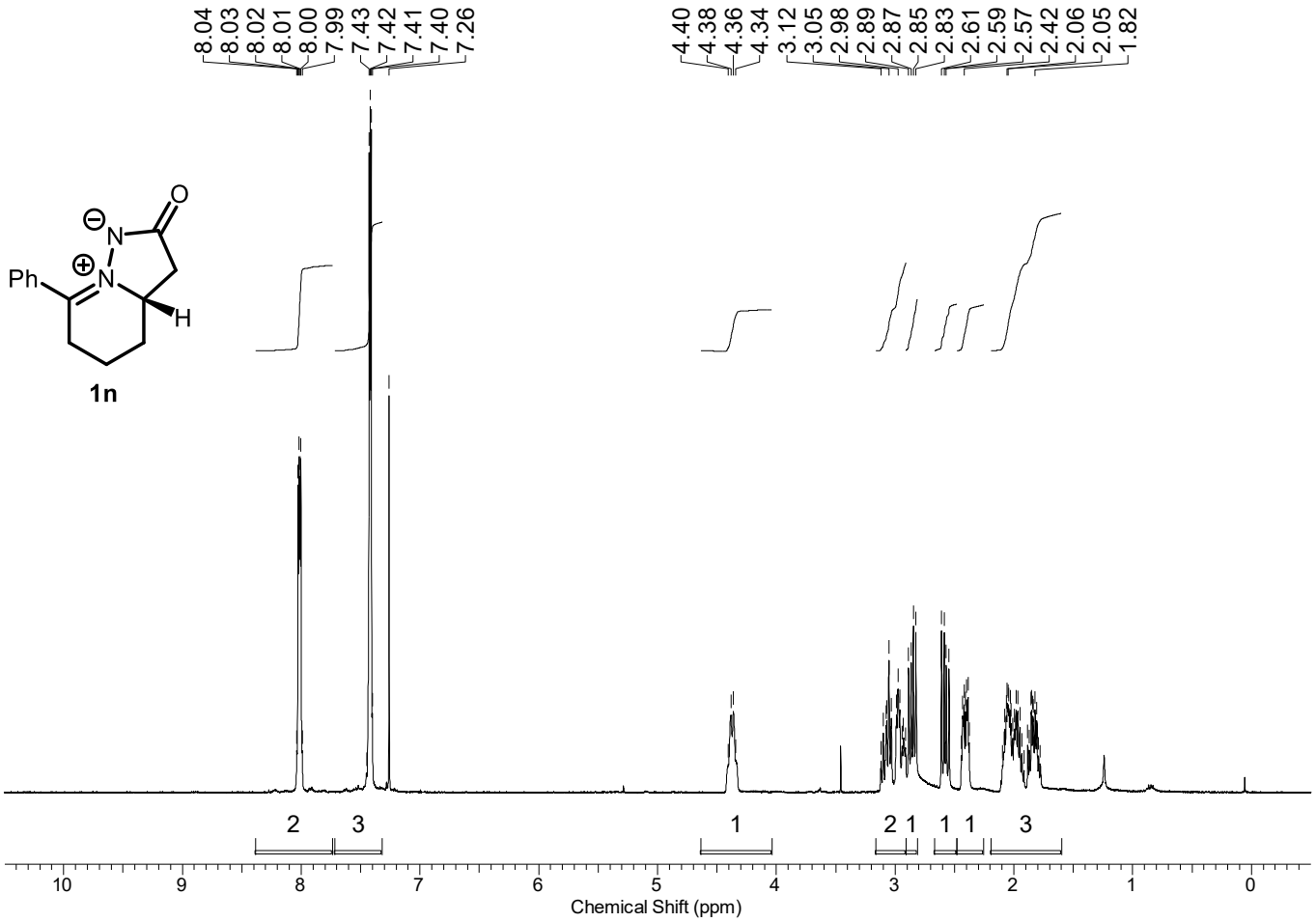
8.04
8.03
8.02
8.01
8.00
7.99
7.43
7.42
7.41
7.40
7.26
4.40
4.38
4.36
4.34
3.12
3.05
2.98
2.89
2.87
2.85
2.83
2.61
2.59
2.57
2.42
2.06
2.05
1.82
Ph
H
O
1n
2 3 1 2 1 1 1 3
Chemical Shift (ppm)

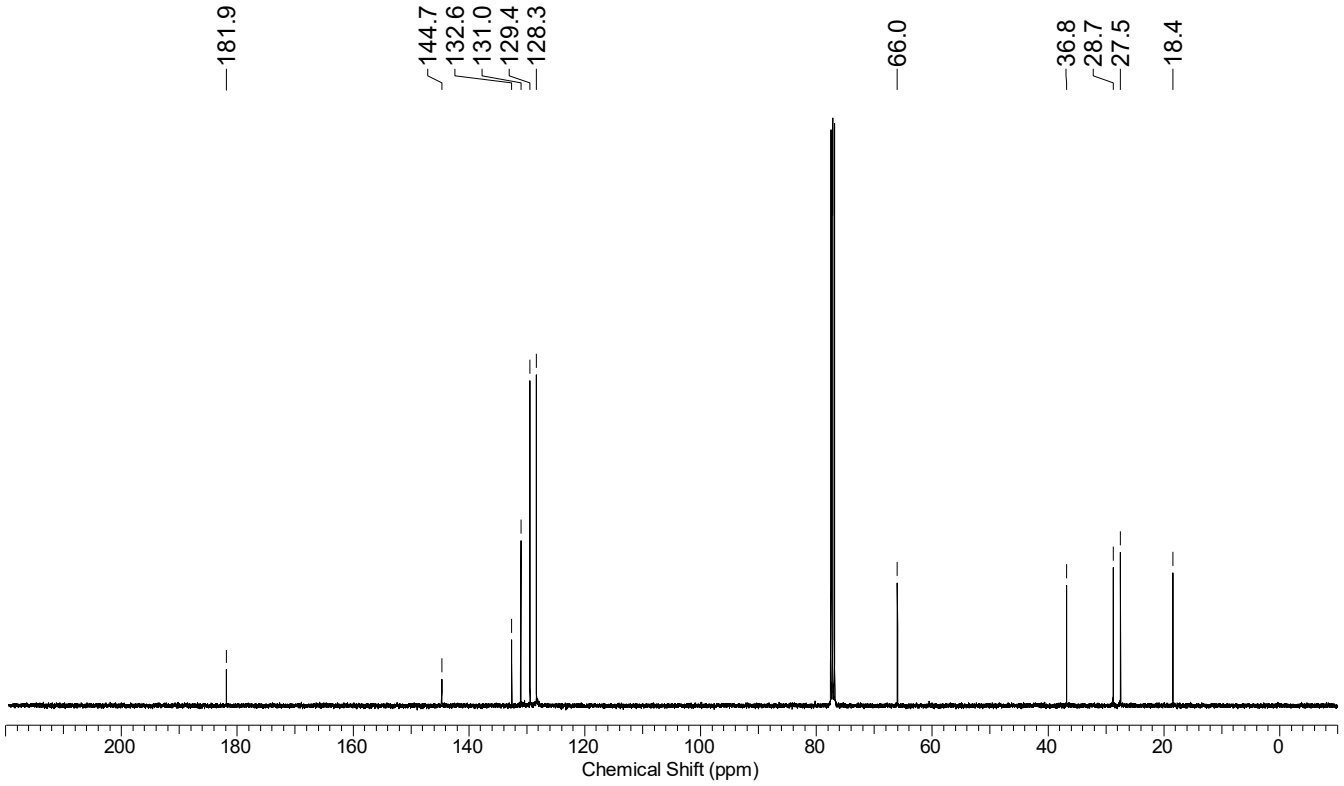
181.9
144.7
132.6
131.0
129.4
128.3
66.0
36.8
28.7
27.5
18.4
Chemical Shift (ppm)

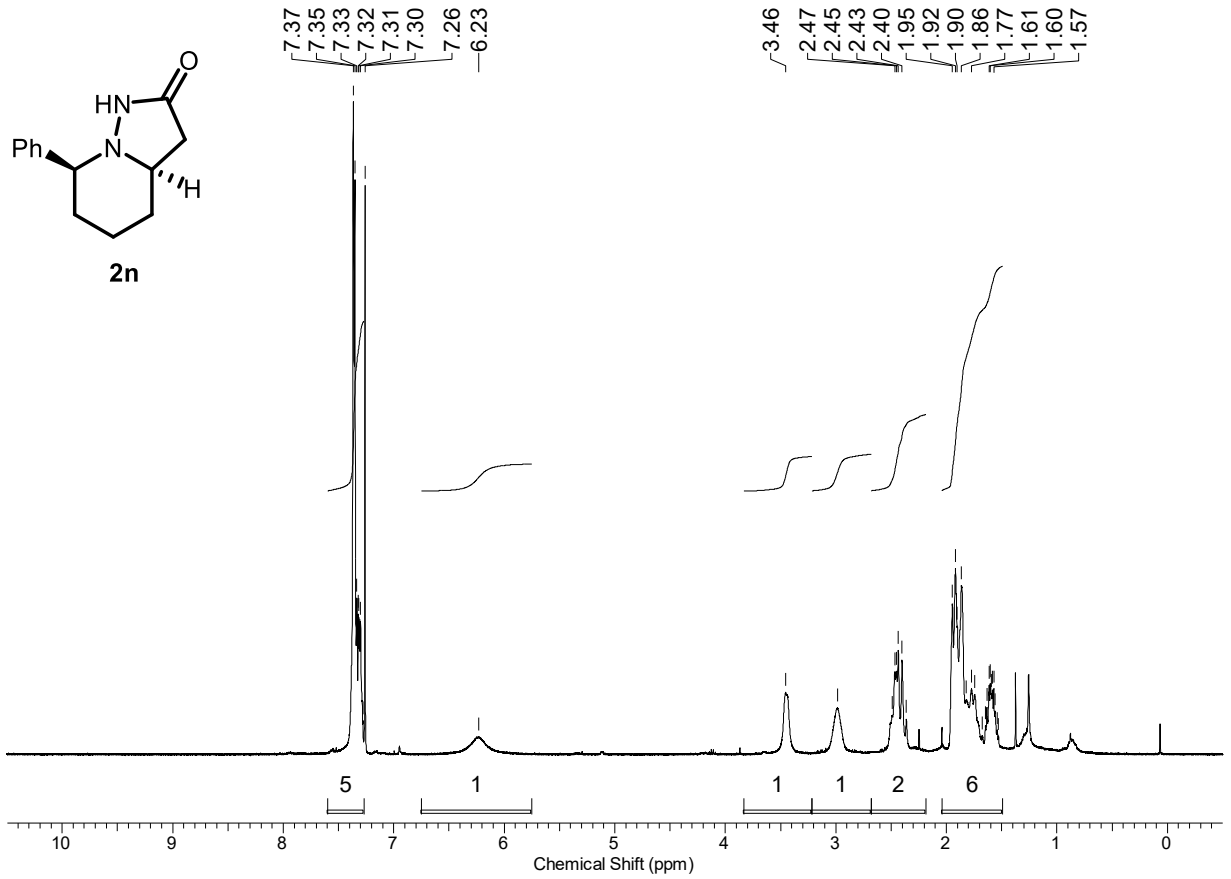
7.37
7.35
7.33
7.32
7.31
7.30
7.26
6.23
3.46
2.47
2.45
2.43
2.40
1.95
1.92
1.90
1.86
1.77
1.61
1.60
1.57
O
HN
N
Ph
H
2n
5
1
1
1
2
6
Chemical Shift (ppm)

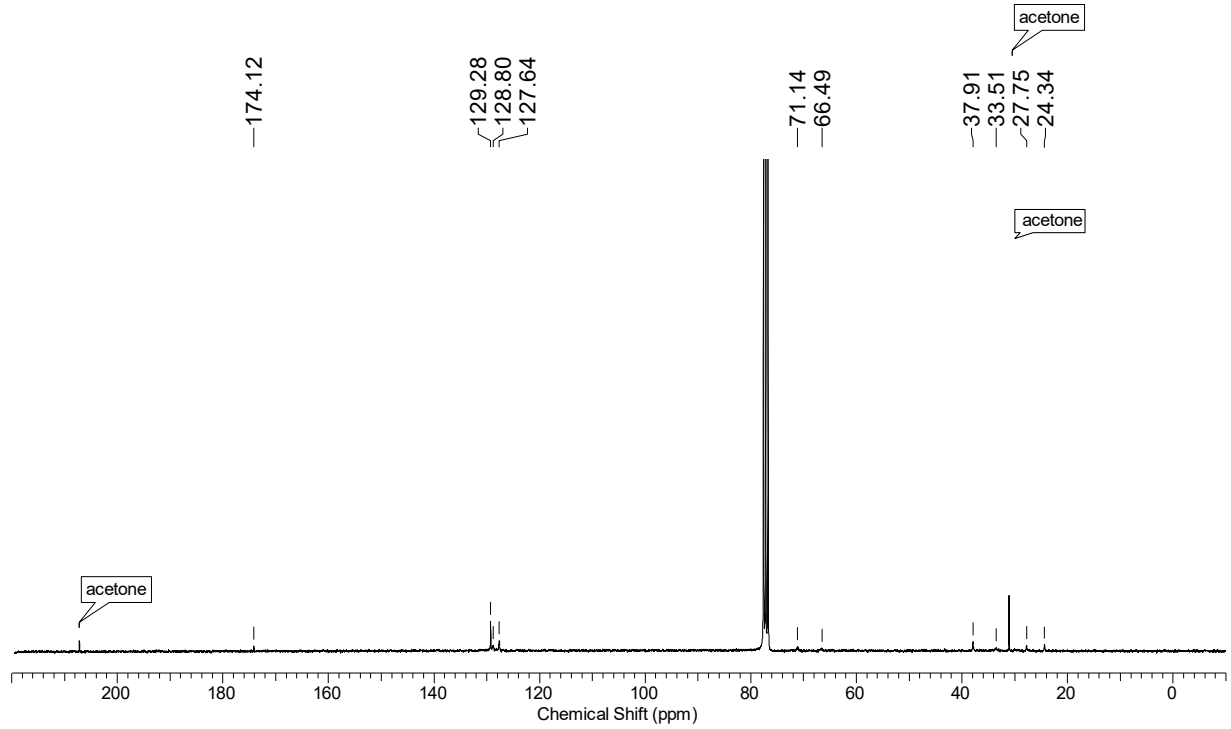
acetone
174.12
129.28
128.80
127.64
71.14
66.49
37.91
33.51
27.75
24.34
acetone
acetone
Chemical Shift (ppm)

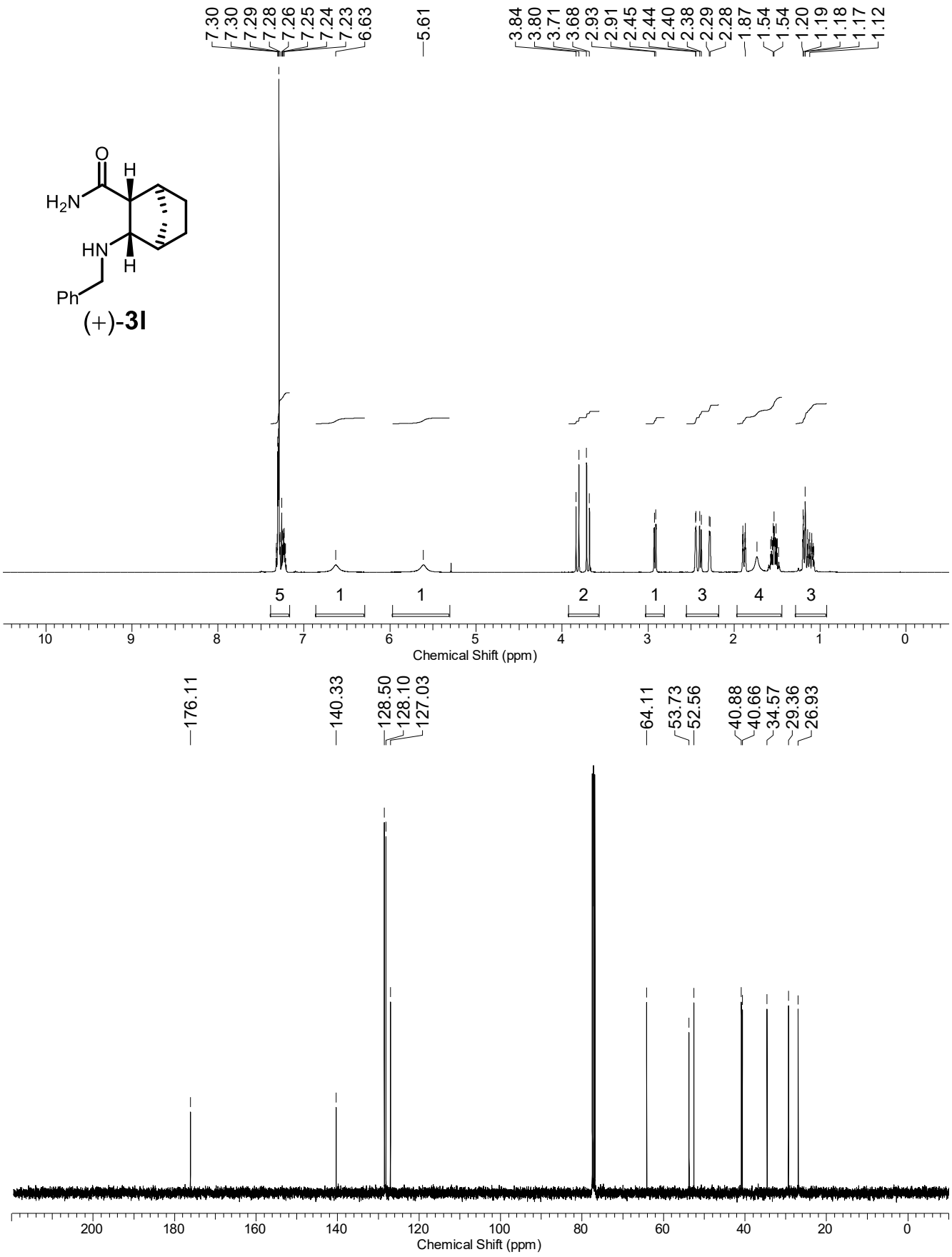
7.30
7.30
7.29
7.28
7.26
7.25
7.24
7.23
6.63
5.61
3.84
3.80
3.71
3.68
2.93
2.91
2.45
2.44
2.40
2.38
2.29
2.28
1.87
1.54
1.54
1.20
1.19
1.18
1.17
1.12
O
H
H2N
HN
H
Ph
(+)-3l
5
1
1
2
1
3
4
3
Chemical Shift (ppm)
176.11
140.33
128.50
128.10
127.03
64.11
53.73
52.56
40.88
40.66
34.57
29.36
26.93
Chemical Shift (ppm)

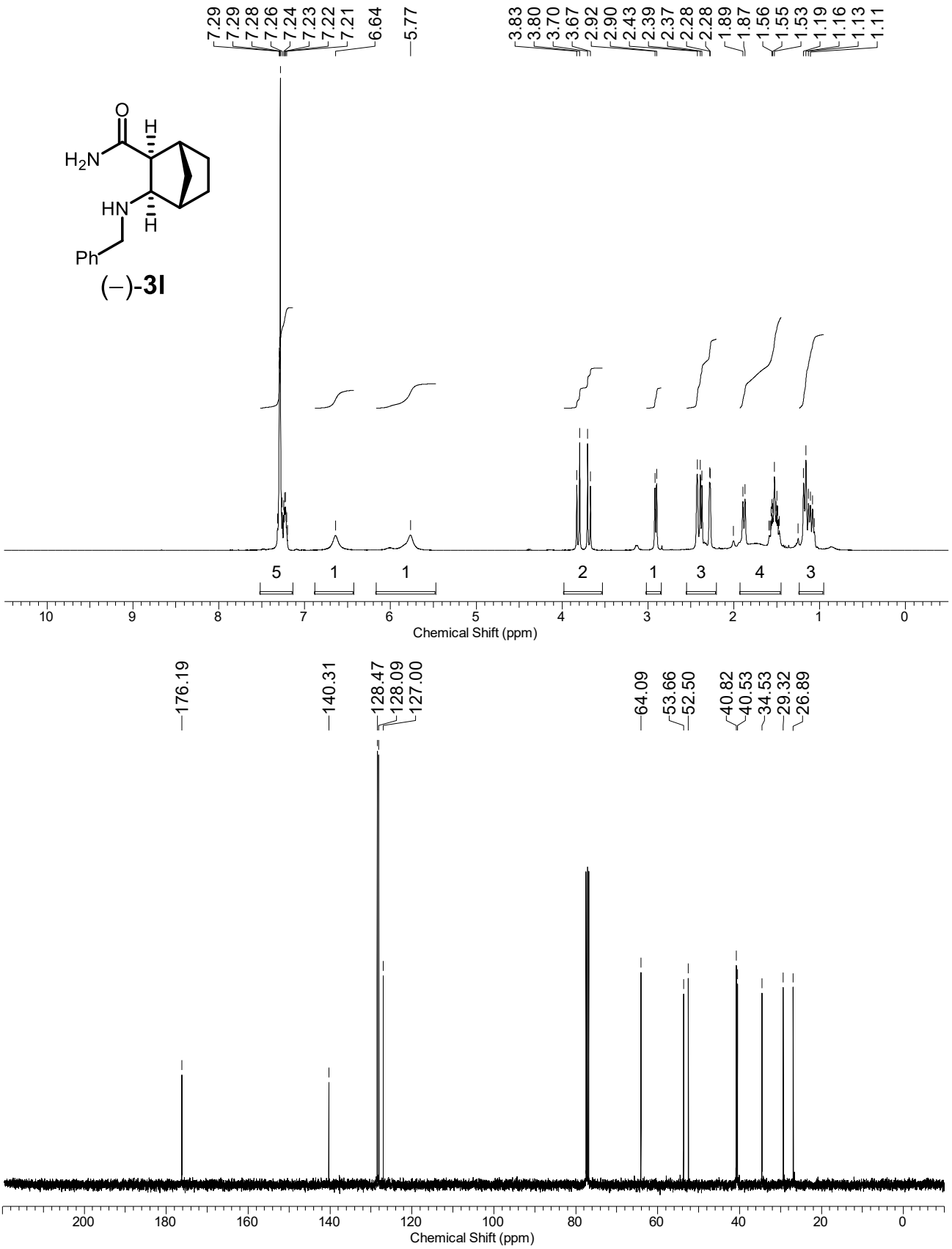
7.29
7.29
7.28
7.26
7.24
7.23
7.22
7.21
6.64
5.77
3.83
3.80
3.70
3.67
2.92
2.90
2.43
2.39
2.37
2.28
2.28
1.89
1.87
1.56
1.55
1.53
1.19
1.16
1.13
1.11
O
H
H2N
HN
H
Ph
(−)-3l
5
1
1
2
1
3
4
3
Chemical Shift (ppm)
176.19
140.31
128.47
128.09
127.00
64.09
53.66
52.50
40.82
40.53
34.53
29.32
26.89
Chemical Shift (ppm)

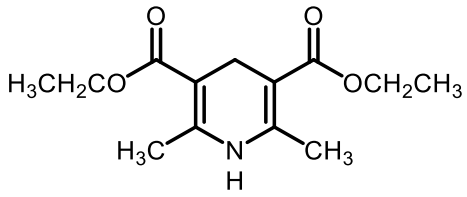

4 Hantzsch Ester

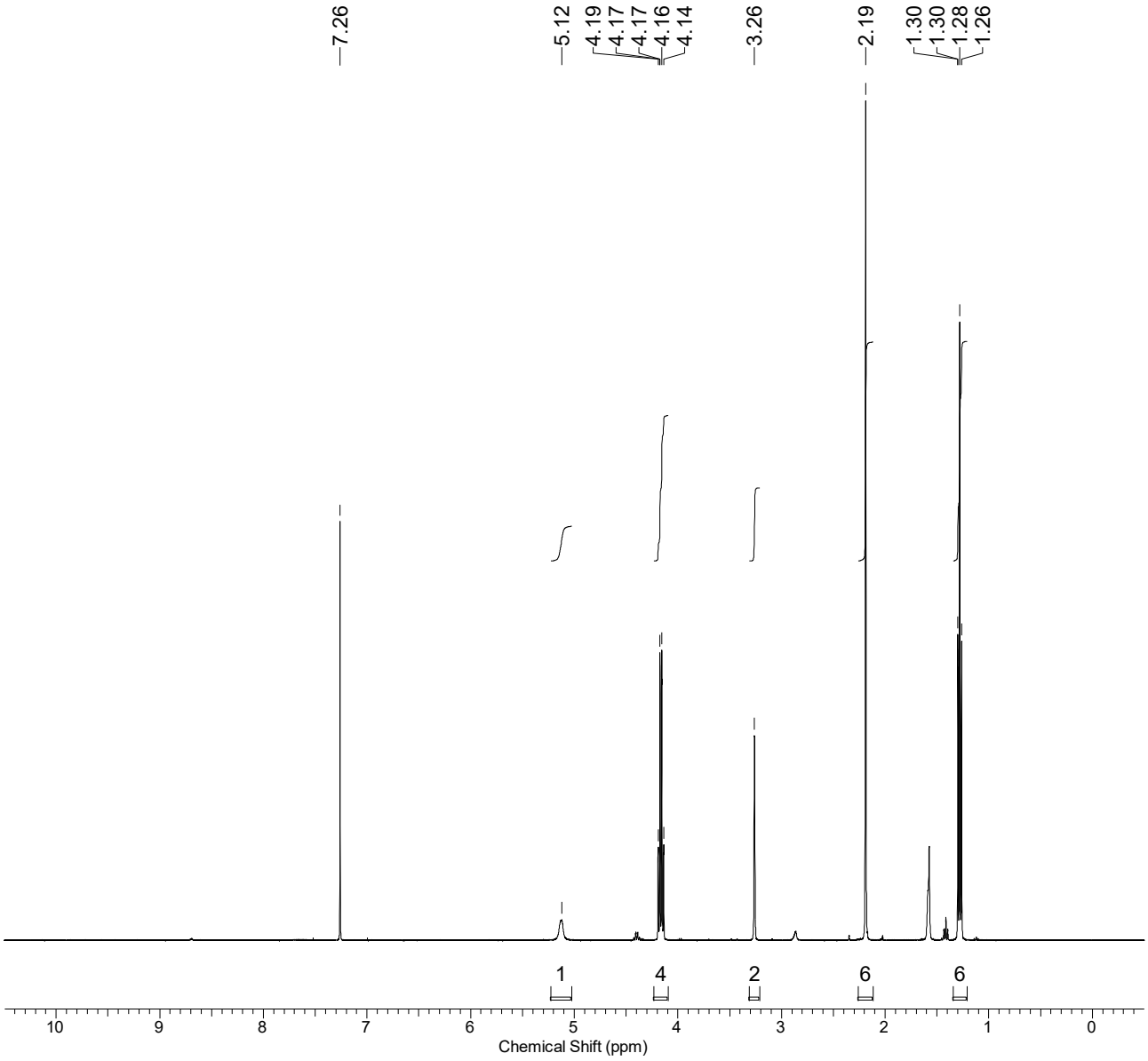

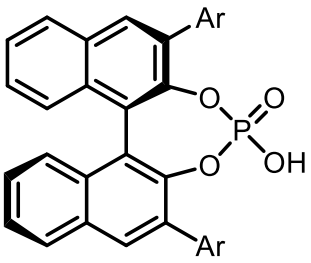

(*R*)-TRIP

Ar = 2,4,6-(*i*-Pr)$_3$-Ph

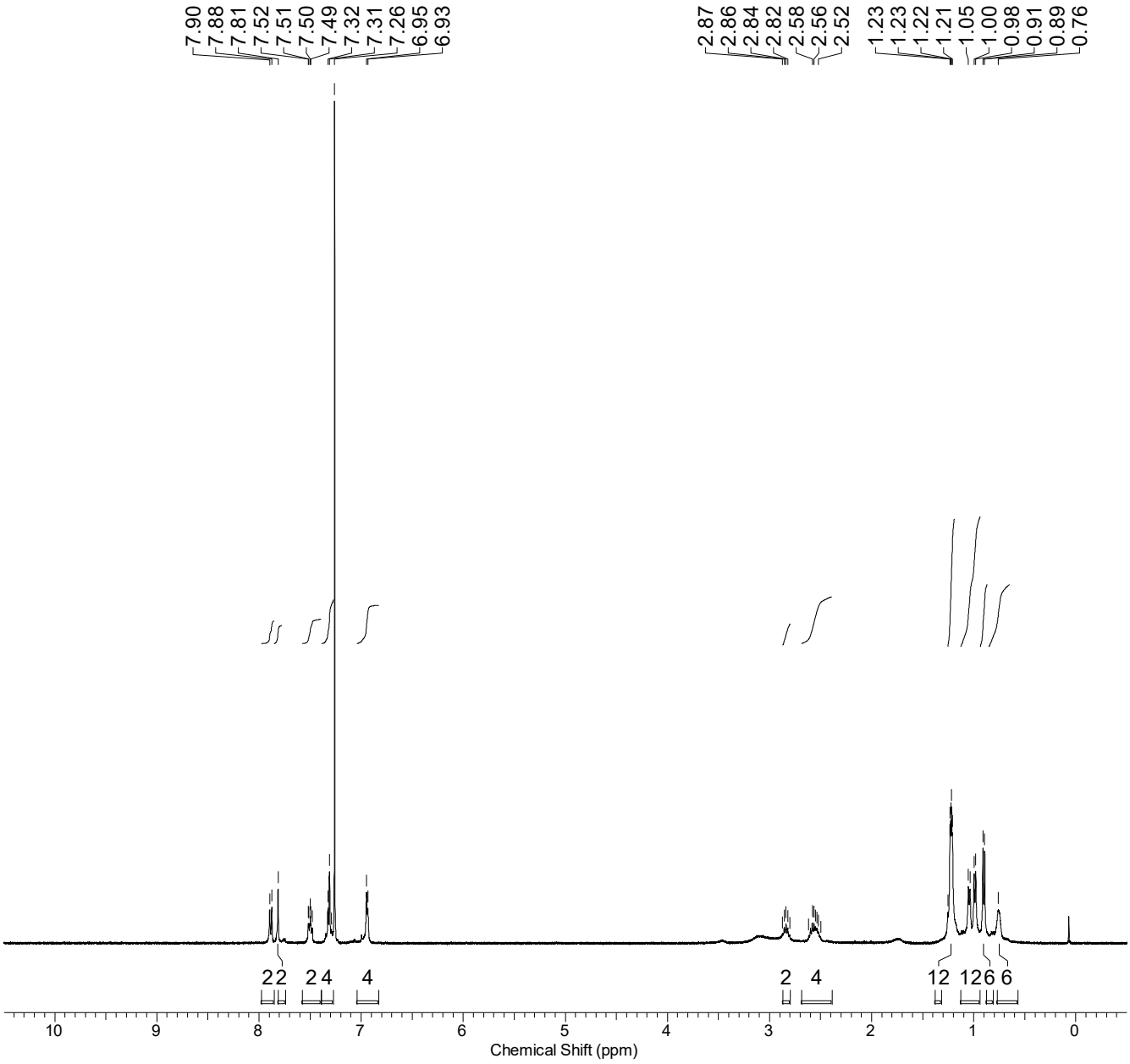

Spectra: Chapter 4

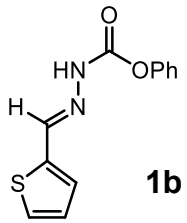

1b

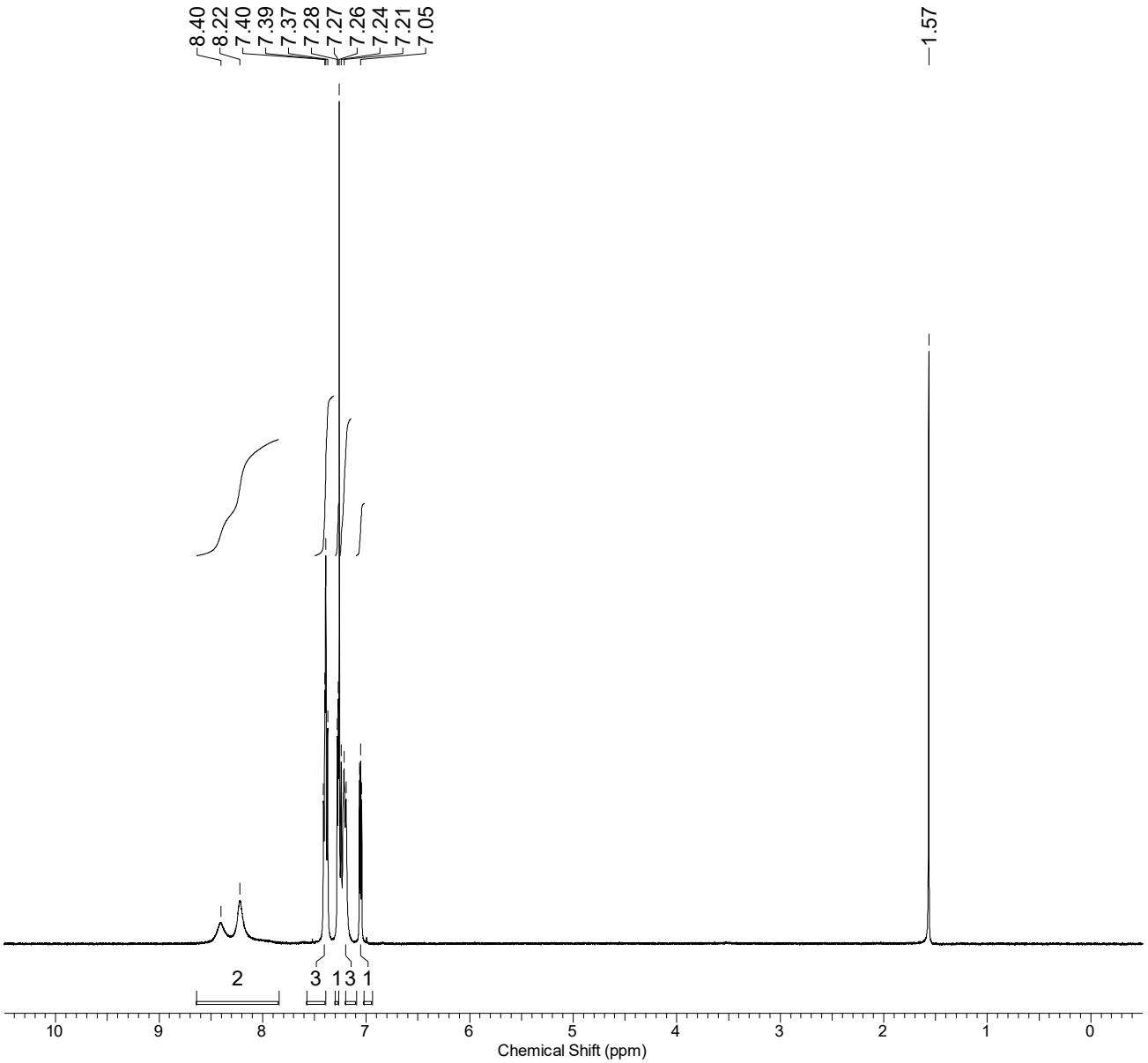

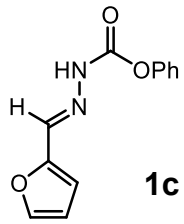
O
HN
OPh
H
N
O

1c

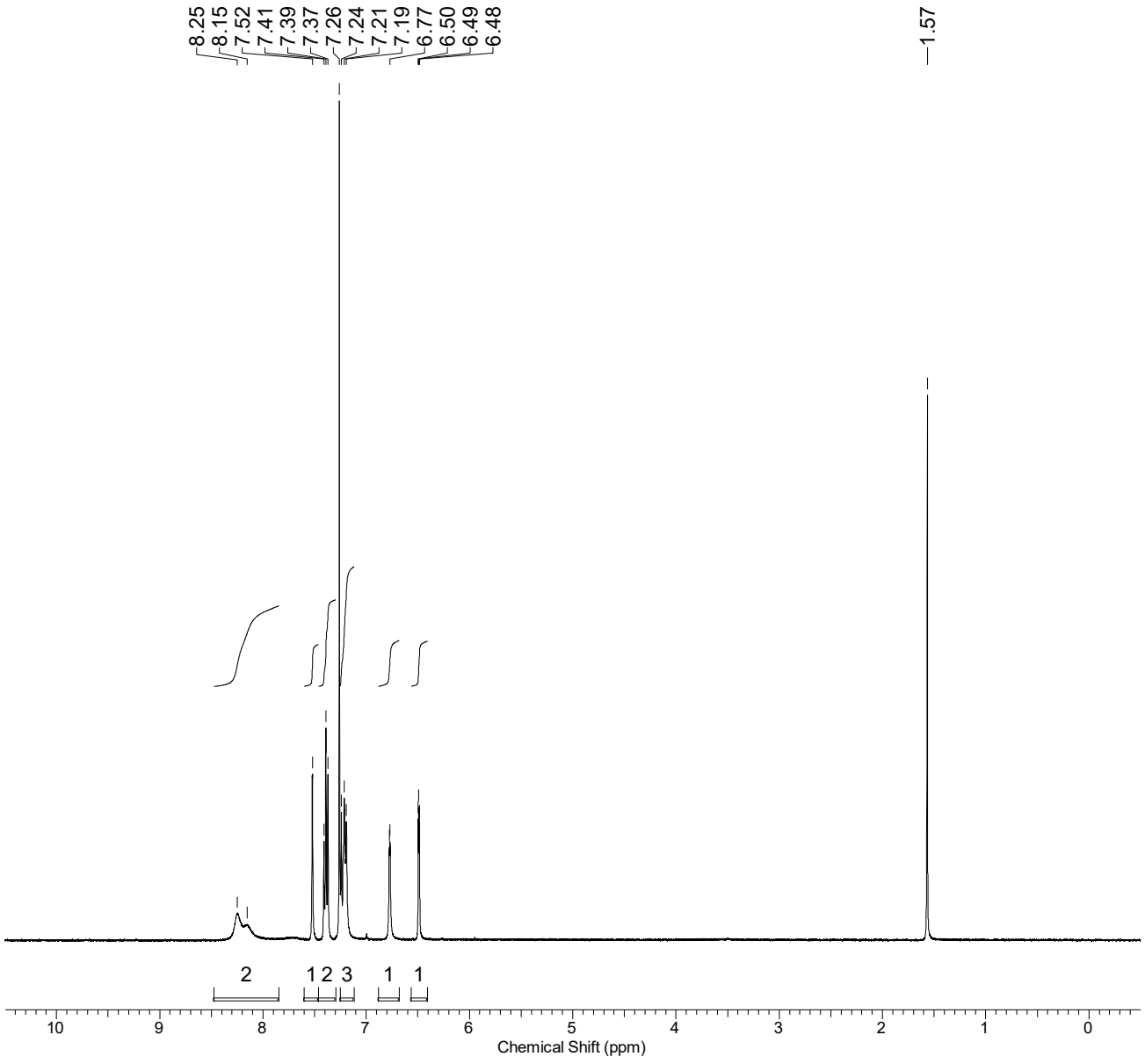
8.25
8.15
7.52
7.41
7.39
7.37
7.26
7.24
7.21
7.19
6.77
6.50
6.49
6.48
1.57
2
1 2 3
1
1
10
9
8
7
6
5
4
3
2
1
0
Chemical Shift (ppm)

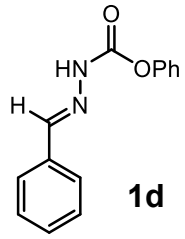
O
HN
OPh
H
N

1d

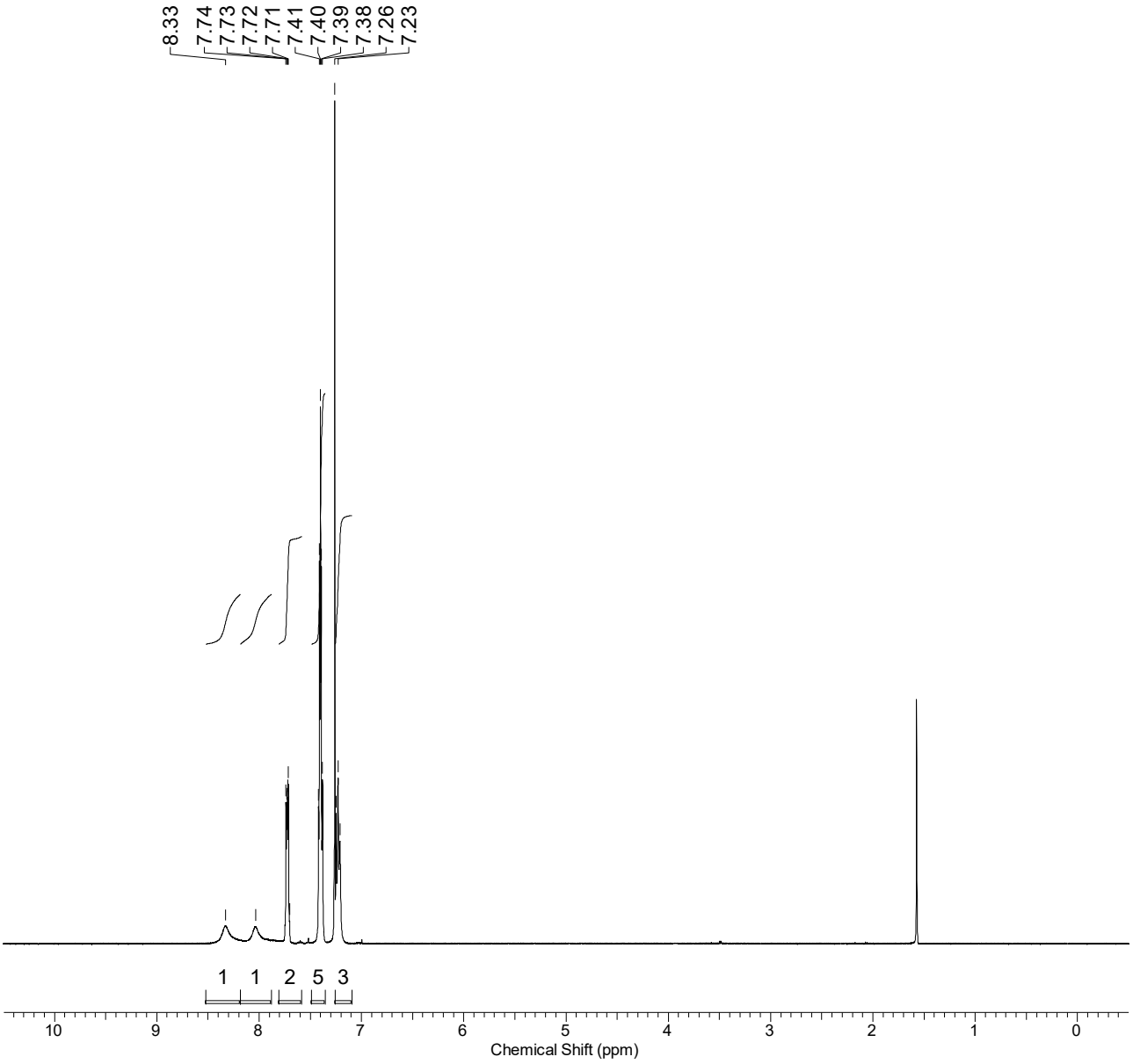
8.33
7.74
7.73
7.72
7.71
7.41
7.40
7.39
7.38
7.26
7.23
1 1 2 5 3
10 9 8 7 6 5 4 3 2 1 0
Chemical Shift (ppm)

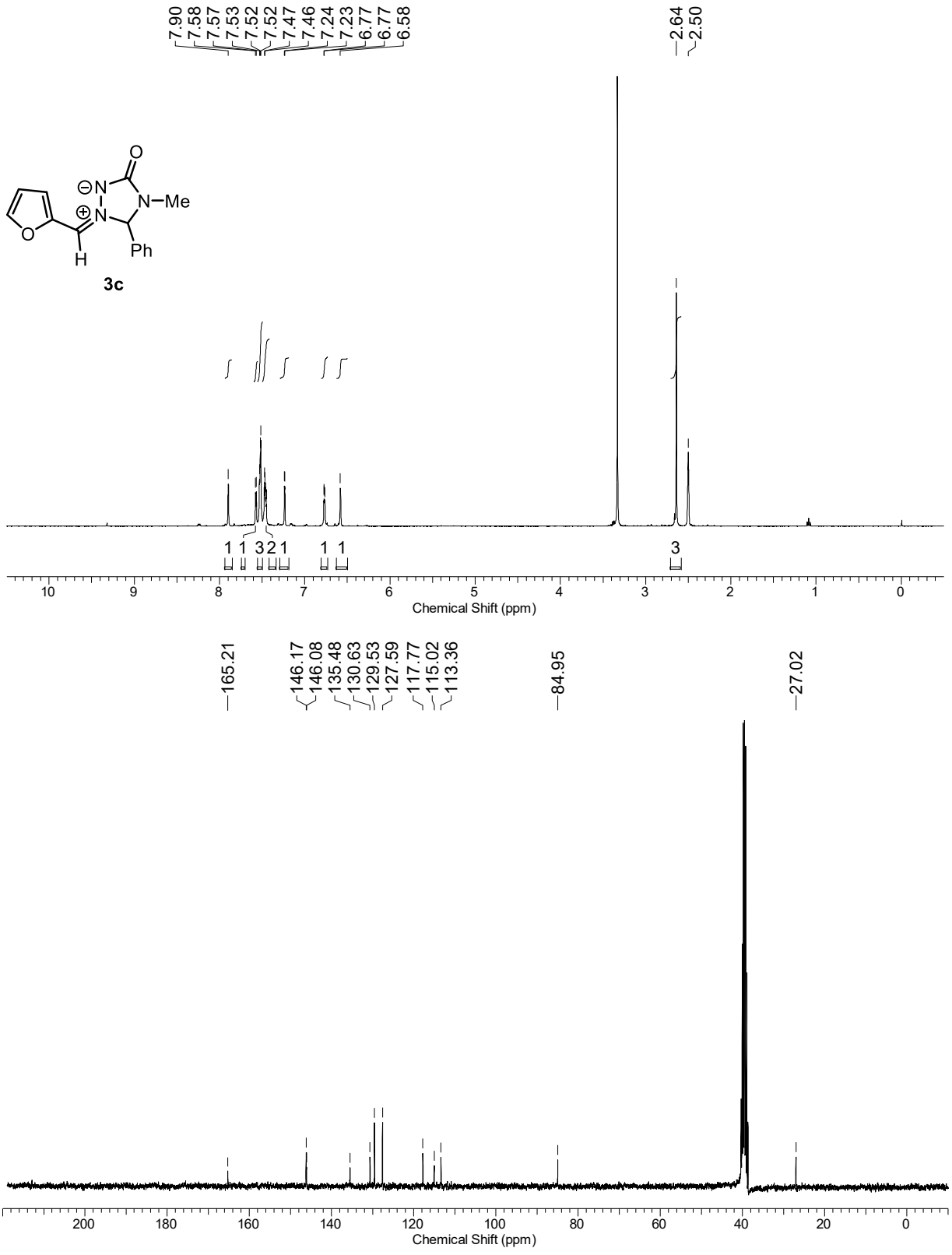
7.90
7.58
7.57
7.53
7.52
7.52
7.47
7.46
7.24
7.23
6.77
6.77
6.58
2.64
2.50
O
⊖N
⊕N
N–Me
O
H
Ph
3c
1 1 3 2 1 1 1 3
10 9 8 7 6 5 4 3 2 1 0
Chemical Shift (ppm)
165.21
146.17
146.08
135.48
130.63
129.53
127.59
117.77
115.02
113.36
84.95
27.02
200 180 160 140 120 100 80 60 40 20 0
Chemical Shift (ppm)

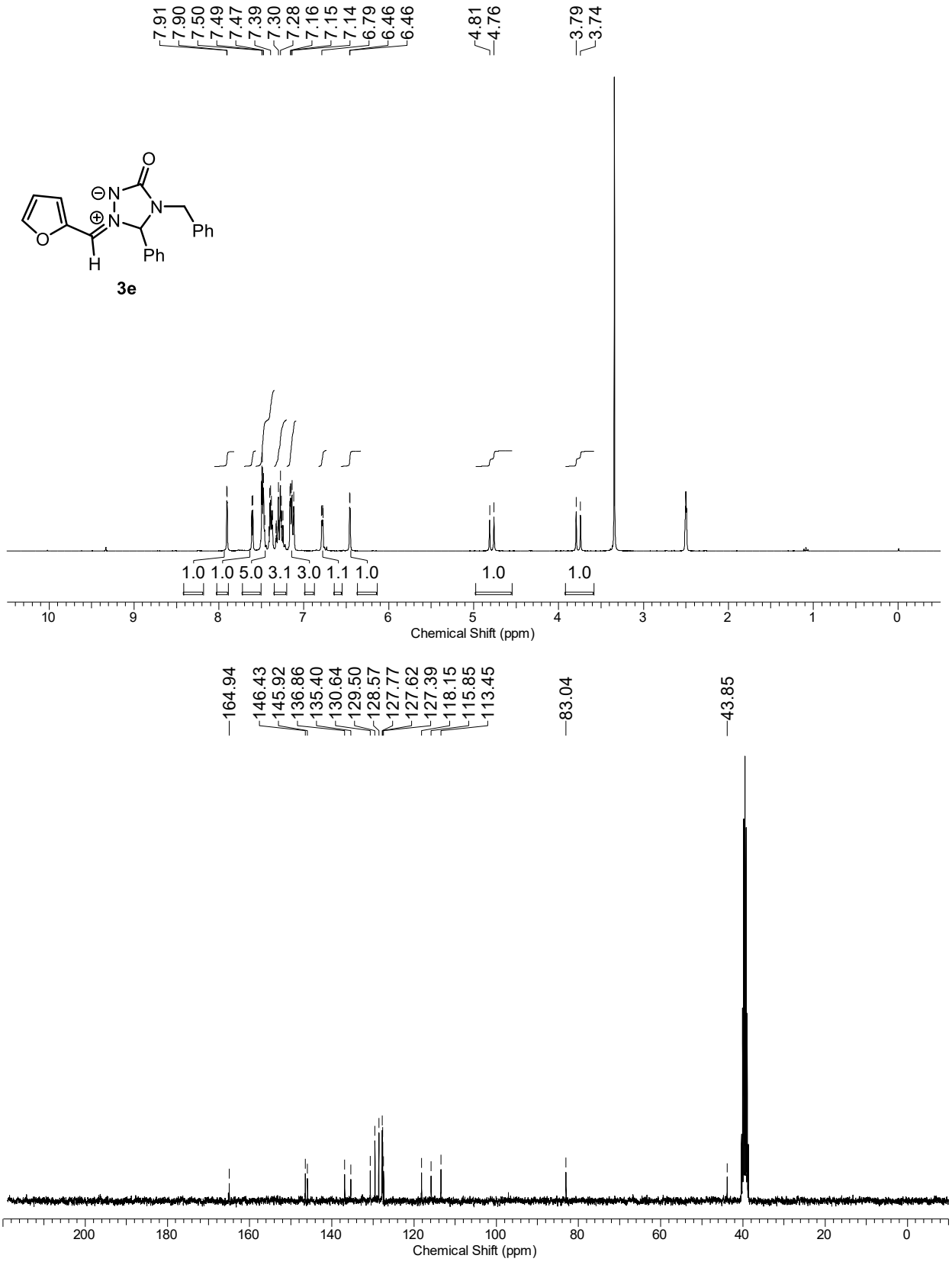
7.91
7.90
7.50
7.49
7.47
7.39
7.30
7.28
7.16
7.15
7.14
6.79
6.46
6.46
4.81
4.76
3.79
3.74
O
N
N
N
Ph
Ph
H
O
3e
1.0 1.0 5.0 3.1 3.0 1.1 1.0
1.0
1.0
10 9 8 7 6 5 4 3 2 1 0
Chemical Shift (ppm)
164.94
146.43
145.92
136.86
135.40
130.64
129.50
128.57
127.77
127.62
127.39
118.15
115.85
113.45
83.04
43.85
200 180 160 140 120 100 80 60 40 20 0
Chemical Shift (ppm)

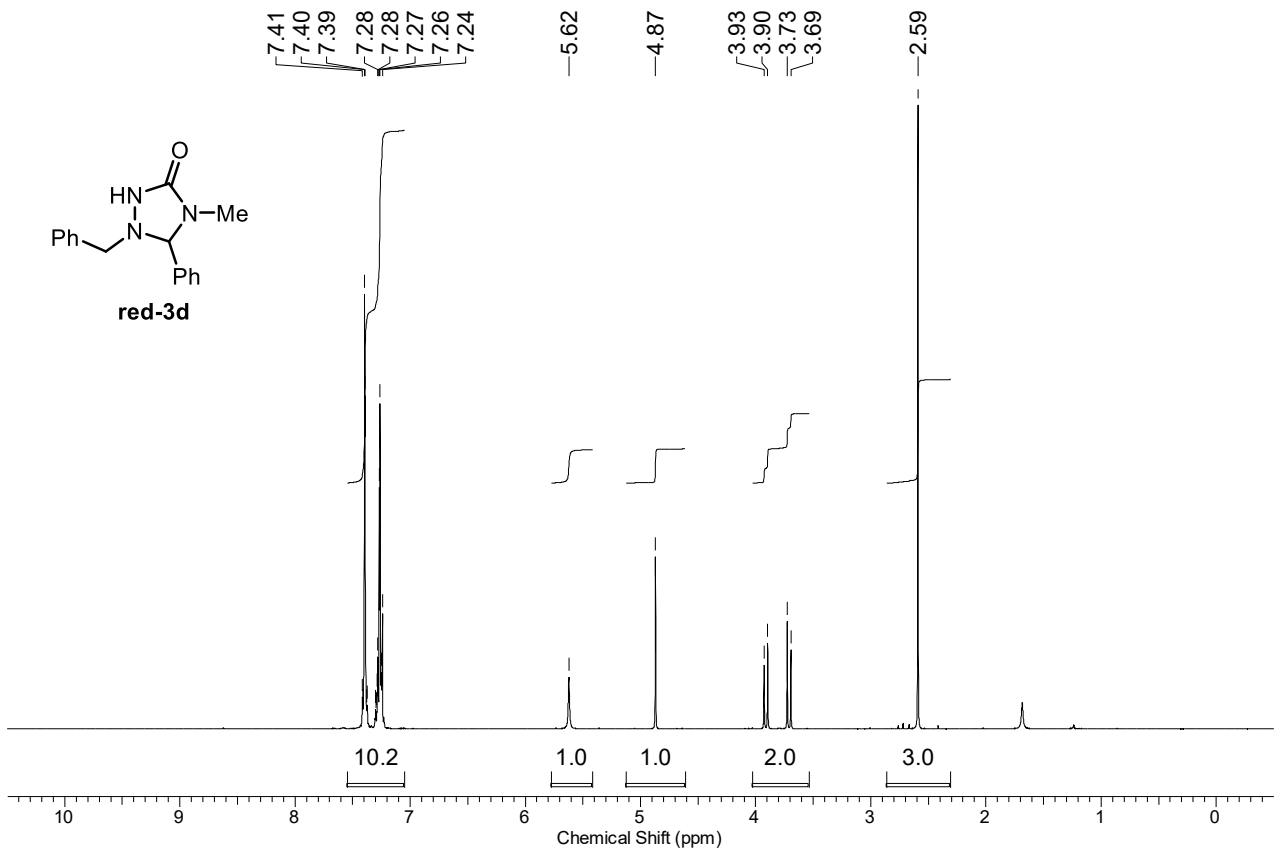
7.41
7.40
7.39
7.28
7.28
7.27
7.26
7.24
5.62
4.87
3.93
3.90
3.73
3.69
2.59
O
HN
N
N–Me
Ph
Ph
red-3d
10.2
1.0
1.0
2.0
3.0
Chemical Shift (ppm)

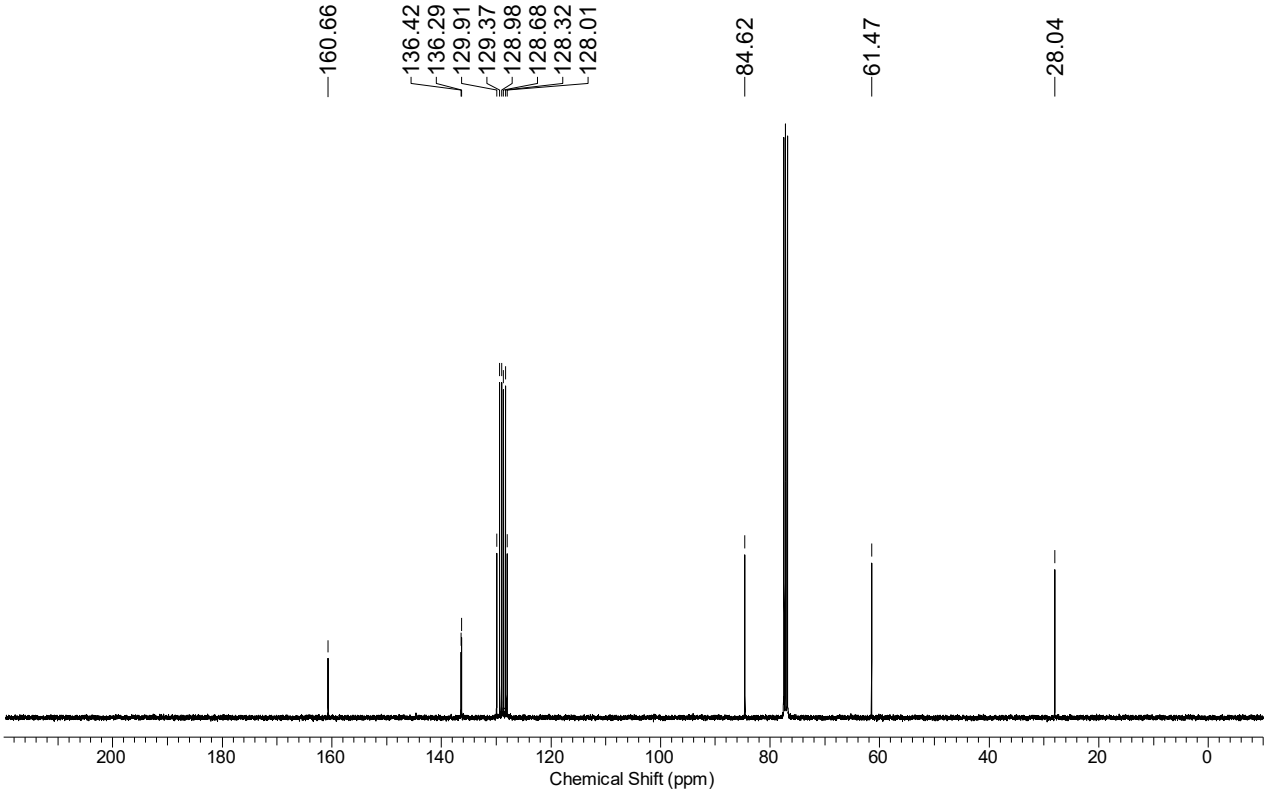
160.66
136.42
136.29
129.91
129.37
128.98
128.68
128.32
128.01
84.62
61.47
28.04
Chemical Shift (ppm)

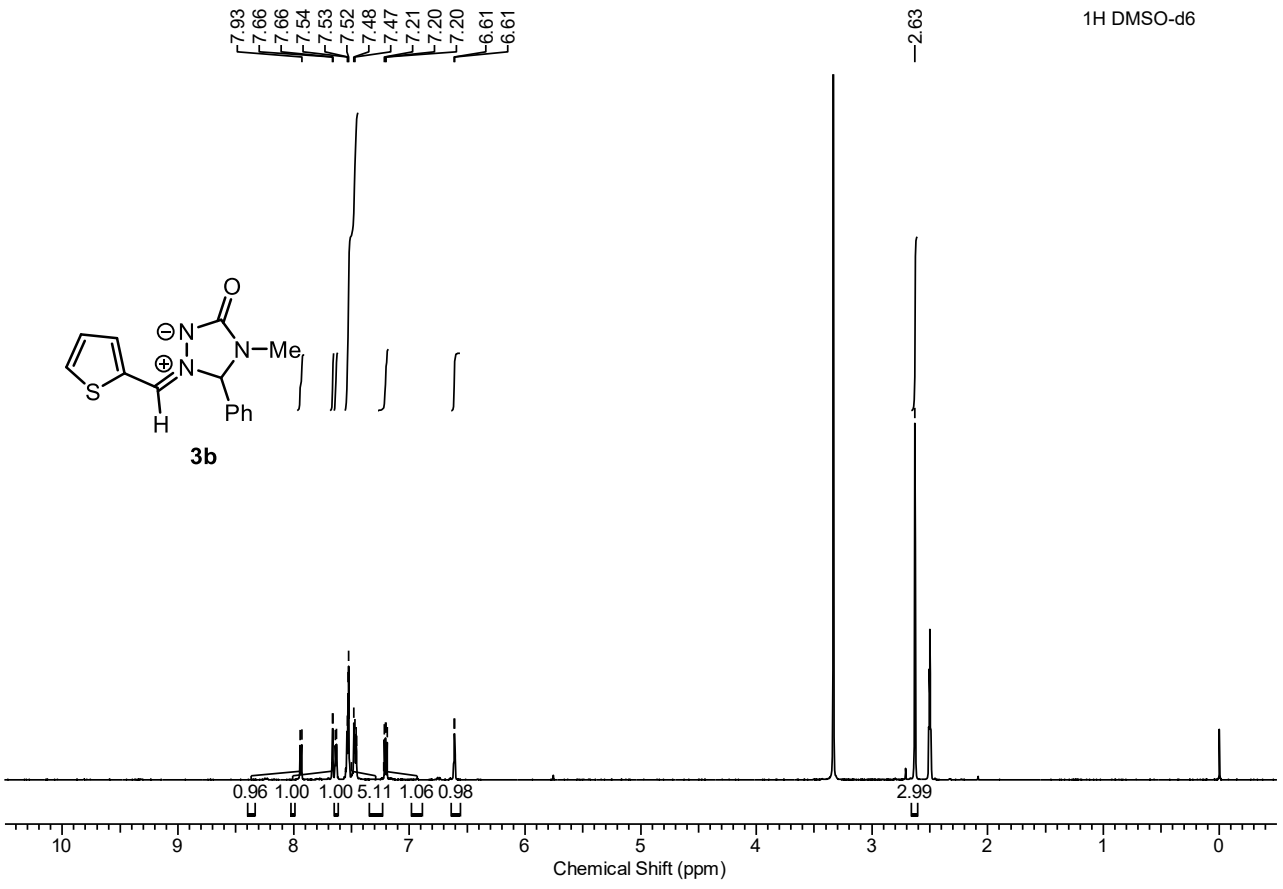
1H DMSO-d6
7.93
7.66
7.66
7.54
7.53
7.52
7.48
7.47
7.21
7.20
7.20
6.61
6.61
2.63
O
N
N
N–Me
S
Ph
H
3b
0.96 1.00 1.00 5.11 1.06 0.98
2.99
10 9 8 7 6 5 4 3 2 1 0
Chemical Shift (ppm)

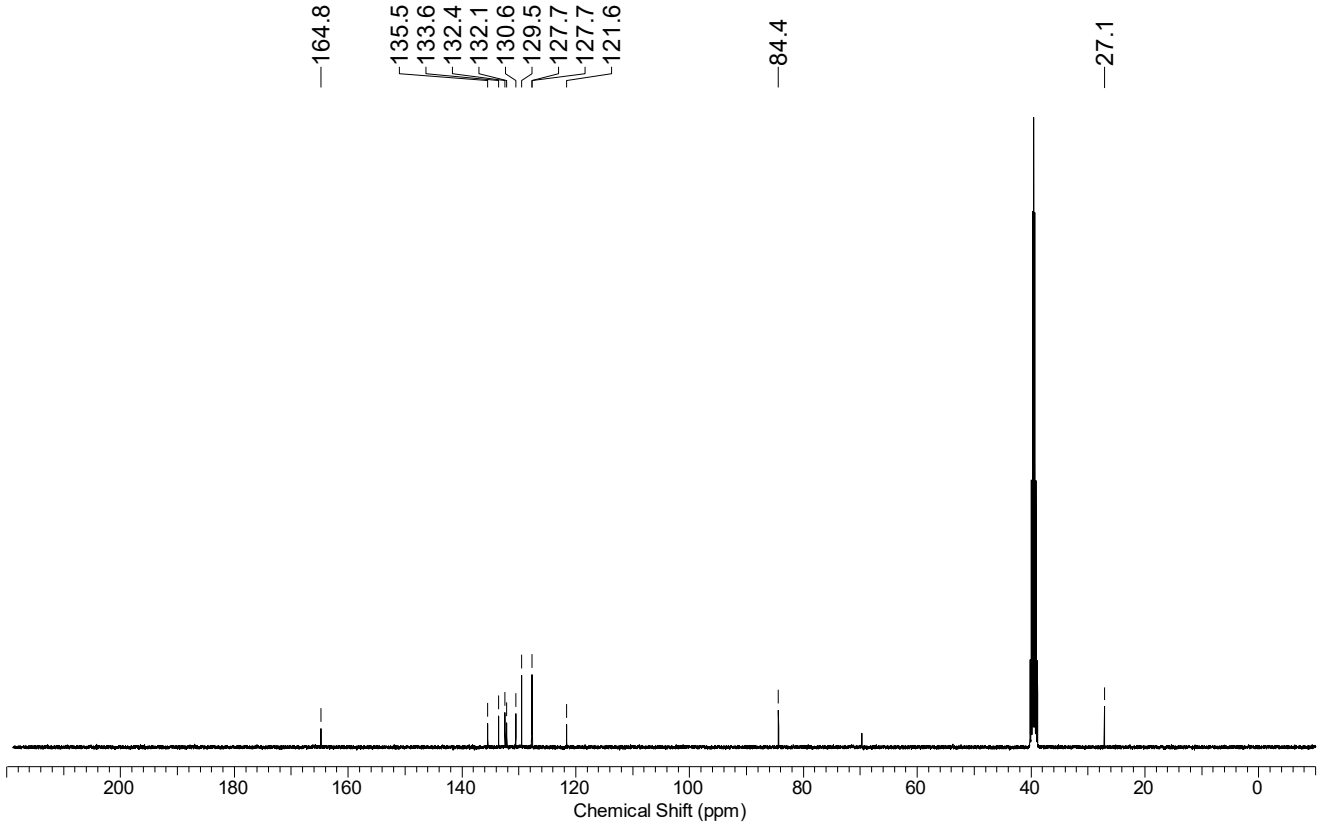
164.8
135.5
133.6
132.4
132.1
130.6
129.5
127.7
127.7
121.6
84.4
27.1
200 180 160 140 120 100 80 60 40 20 0
Chemical Shift (ppm)

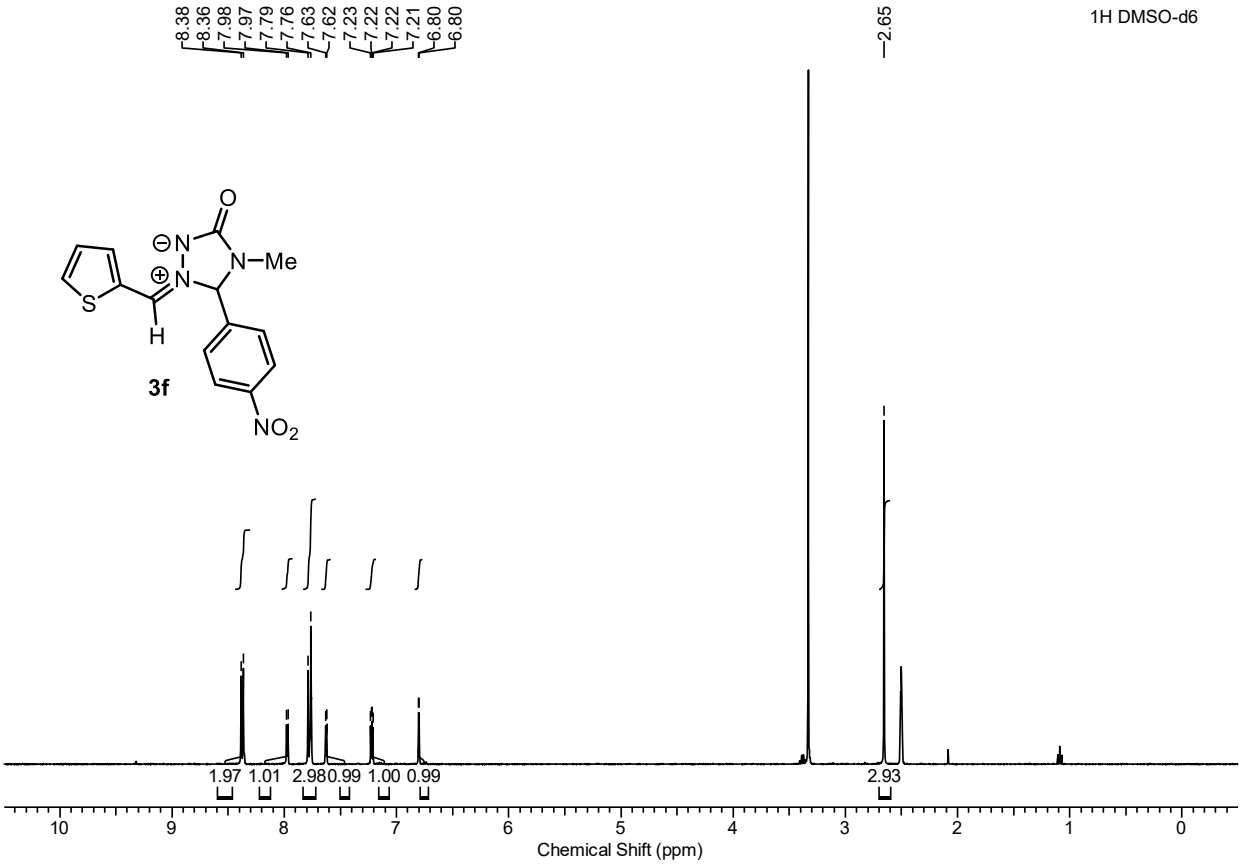
8.38
8.36
7.98
7.97
7.79
7.76
7.63
7.62
7.23
7.22
7.22
7.21
6.80
6.80
2.65
1H DMSO-d6
O
N
N
N–Me
S
H
3f
NO2
1.97 1.01 2.98 0.99 1.00 0.99
2.93
10 9 8 7 6 5 4 3 2 1 0
Chemical Shift (ppm)

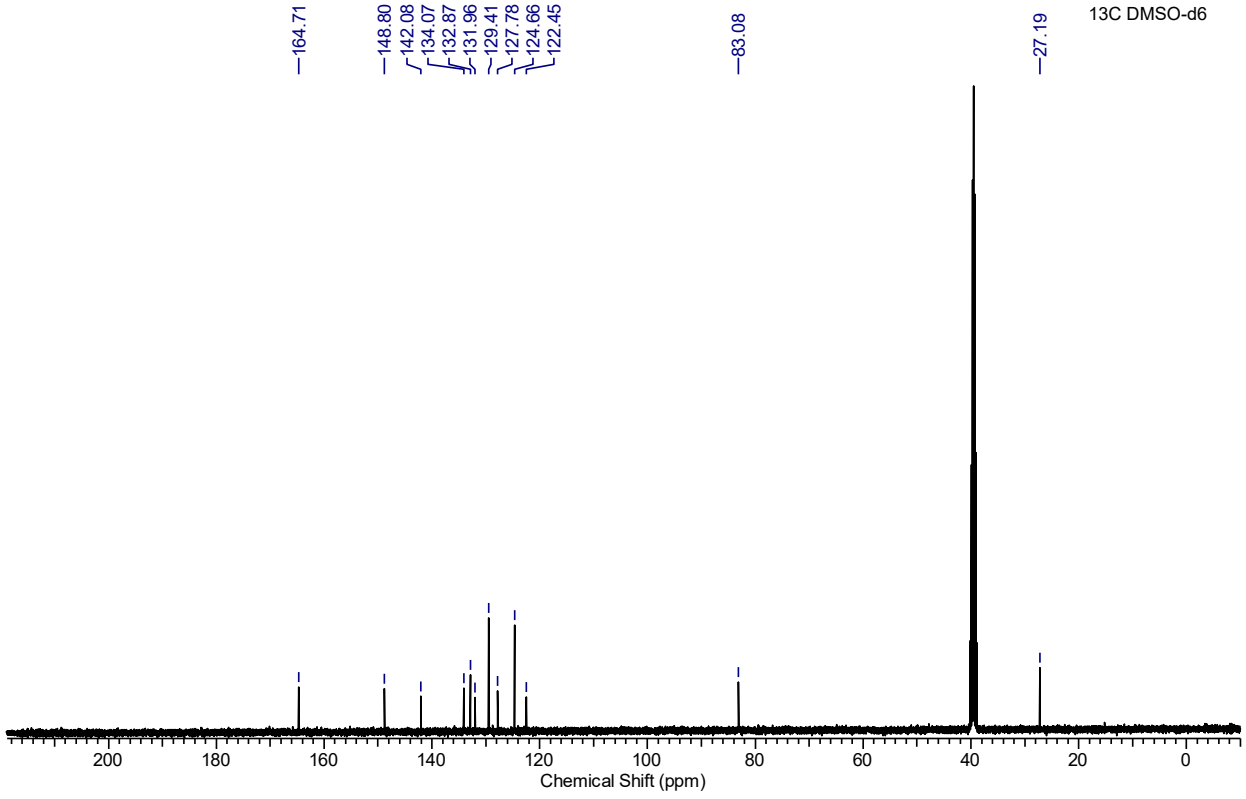
164.71
148.80
142.08
134.07
132.87
131.96
129.41
127.78
124.66
122.45
83.08
27.19
13C DMSO-d6
200 180 160 140 120 100 80 60 40 20 0
Chemical Shift (ppm)

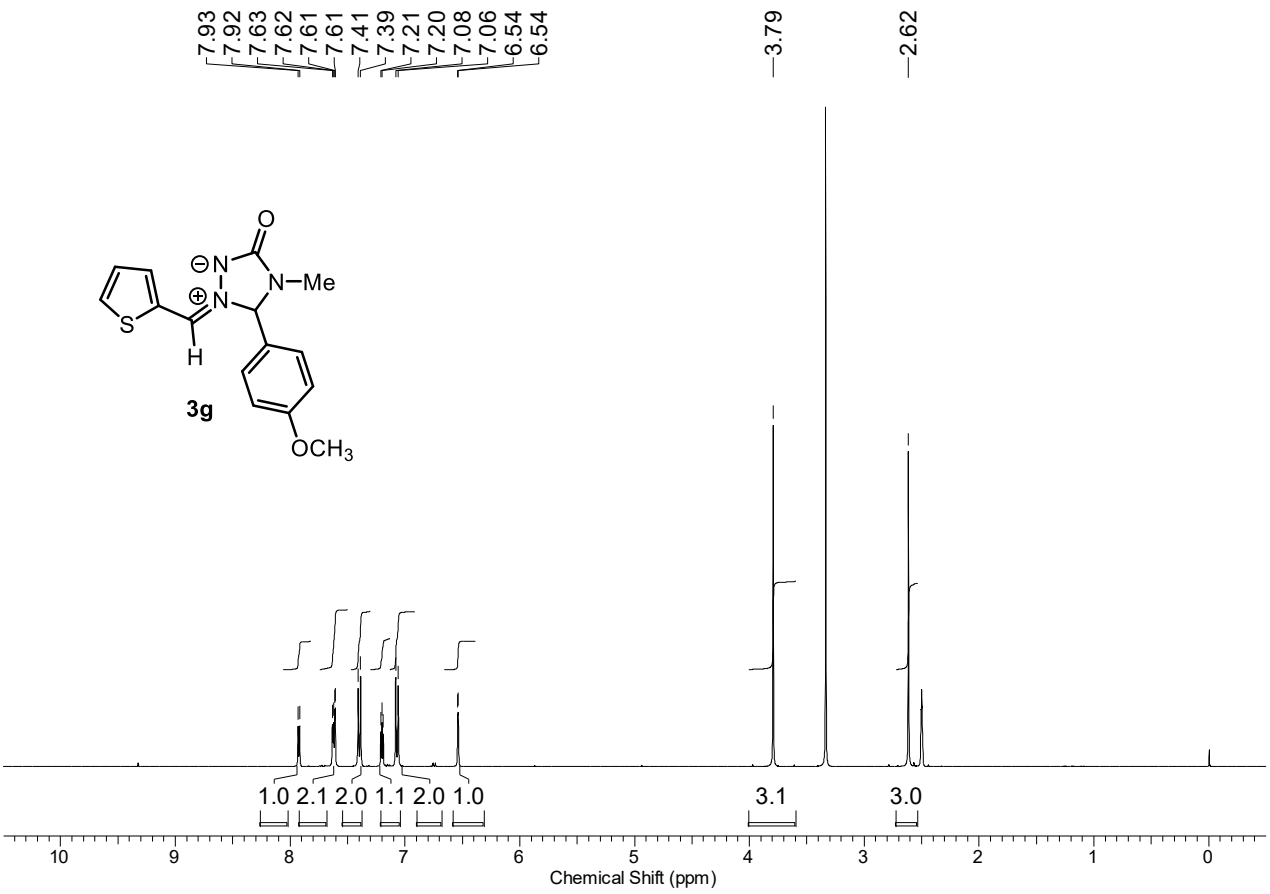
7.93
7.92
7.63
7.62
7.61
7.61
7.41
7.39
7.21
7.20
7.08
7.06
6.54
6.54
3.79
2.62
O
N
N
N–Me
S
H
3g
OCH3
1.0 2.1 2.0 1.1 2.0 1.0
3.1
3.0
Chemical Shift (ppm)

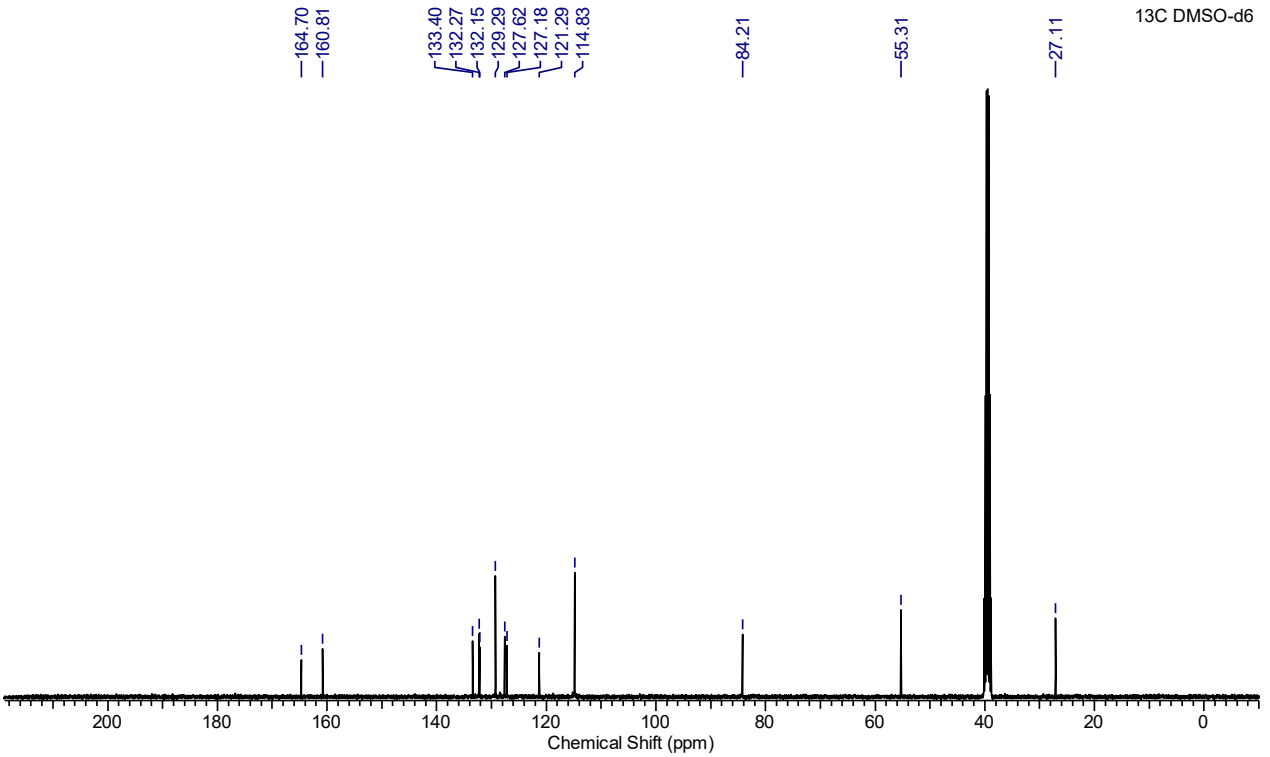
13C DMSO-d6
164.70
160.81
133.40
132.27
132.15
129.29
127.62
127.18
121.29
114.83
84.21
55.31
27.11
Chemical Shift (ppm)

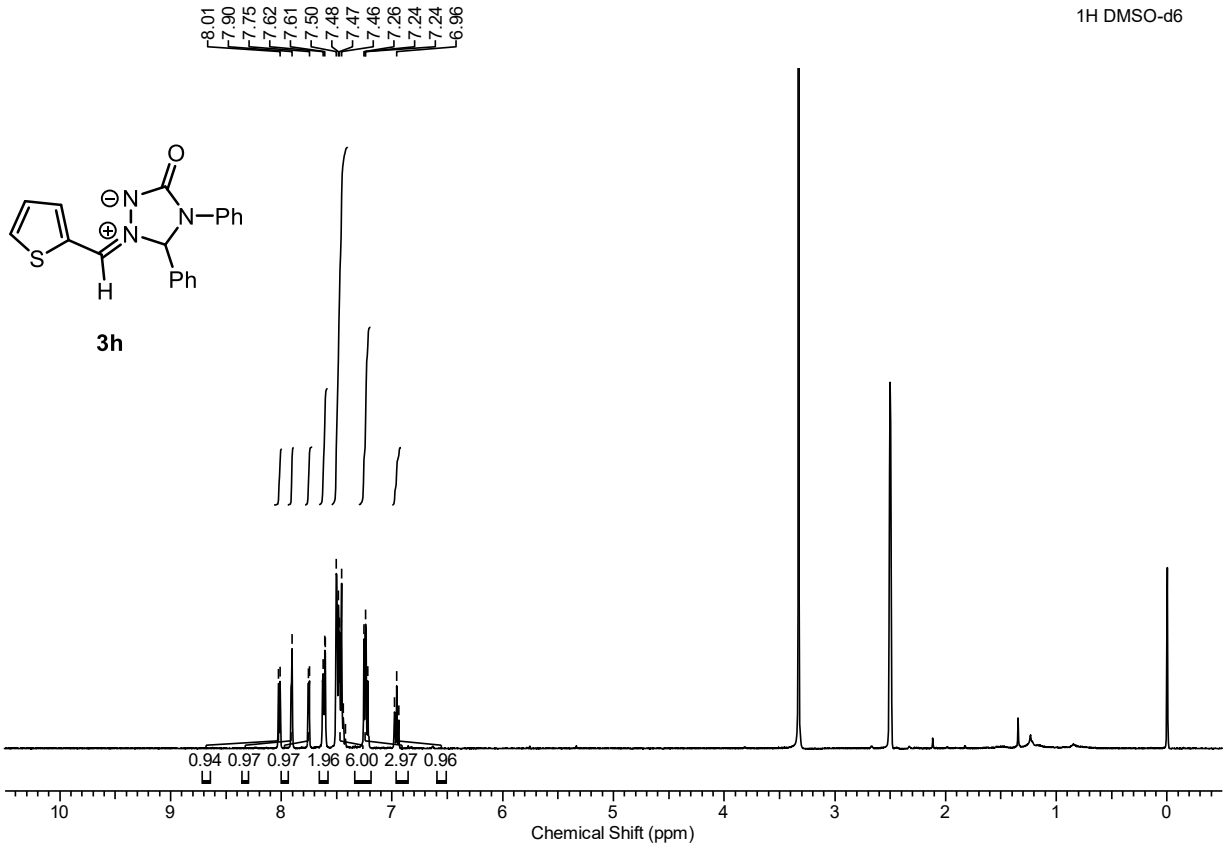
1H DMSO-d6
8.01
7.90
7.75
7.62
7.61
7.50
7.48
7.47
7.46
7.26
7.24
7.24
6.96
O
N
N
N—Ph
S
Ph
H
3h
0.94 0.97 0.97 1.96 6.00 2.97 0.96
10 9 8 7 6 5 4 3 2 1 0
Chemical Shift (ppm)

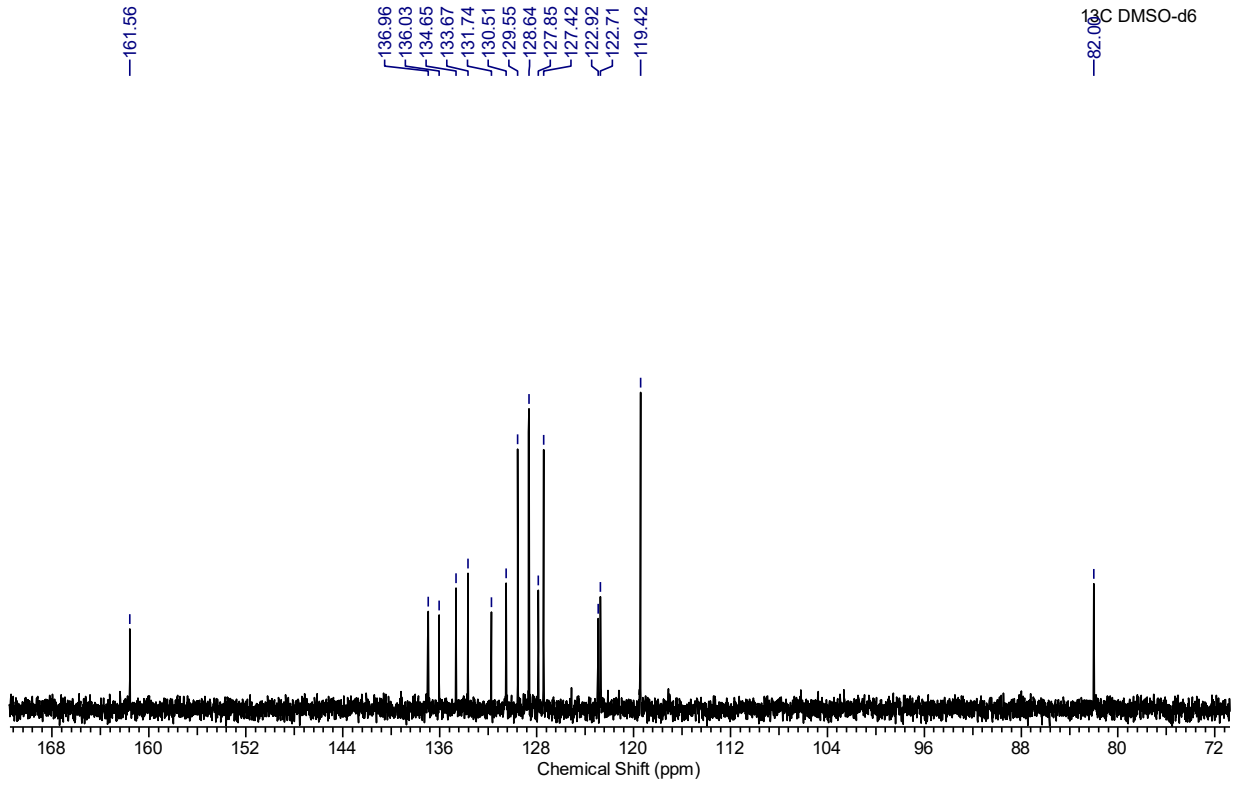
13C DMSO-d6
161.56
136.96
136.03
134.65
133.67
131.74
130.51
129.55
128.64
127.85
127.42
122.92
122.71
119.42
82.06
168 160 152 144 136 128 120 112 104 96 88 80 72
Chemical Shift (ppm)

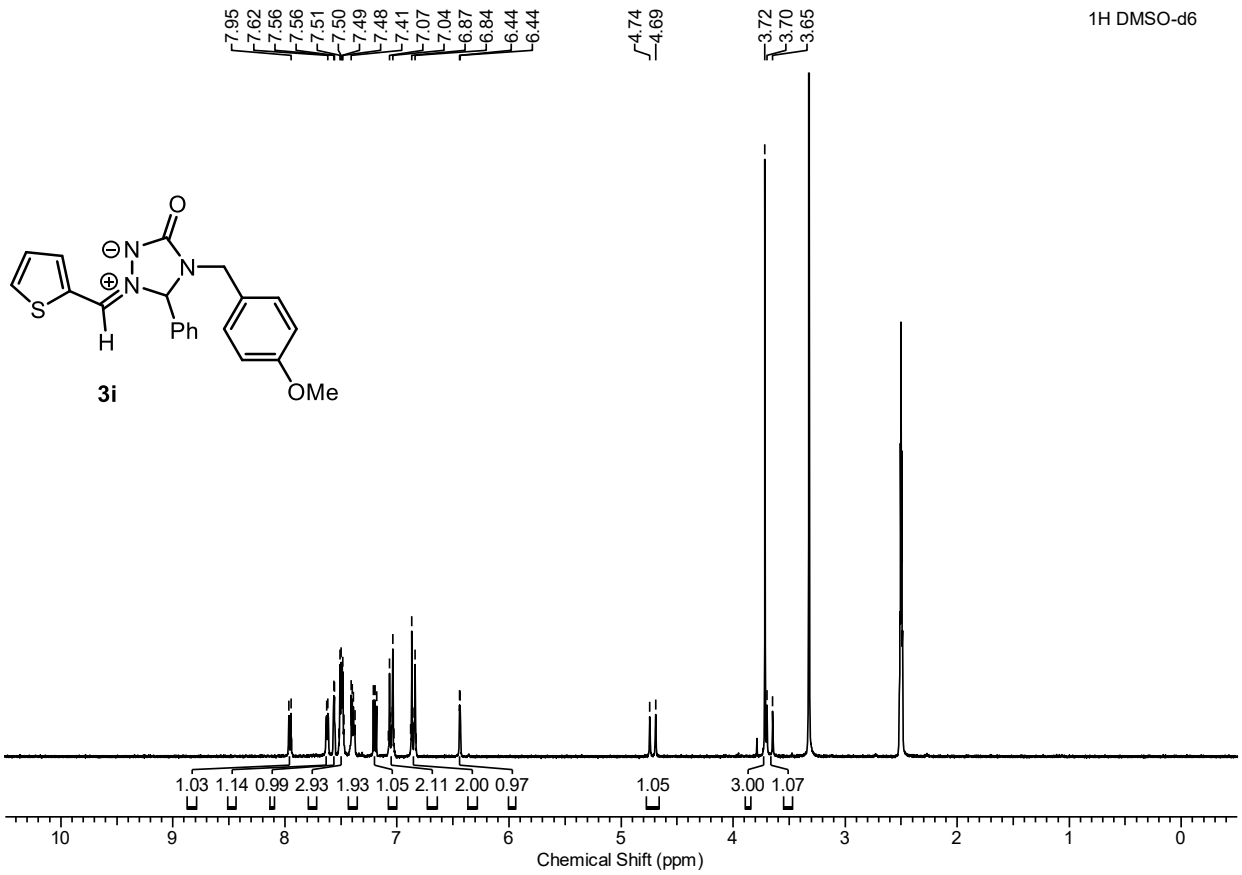
1H DMSO-d6
7.95
7.62
7.56
7.56
7.51
7.50
7.49
7.48
7.41
7.07
7.04
6.87
6.84
6.44
6.44
4.74
4.69
3.72
3.70
3.65
1.03 1.14 0.99 2.93 1.93 1.05 2.11 2.00 0.97
1.05
3.00 1.07
Chemical Shift (ppm)

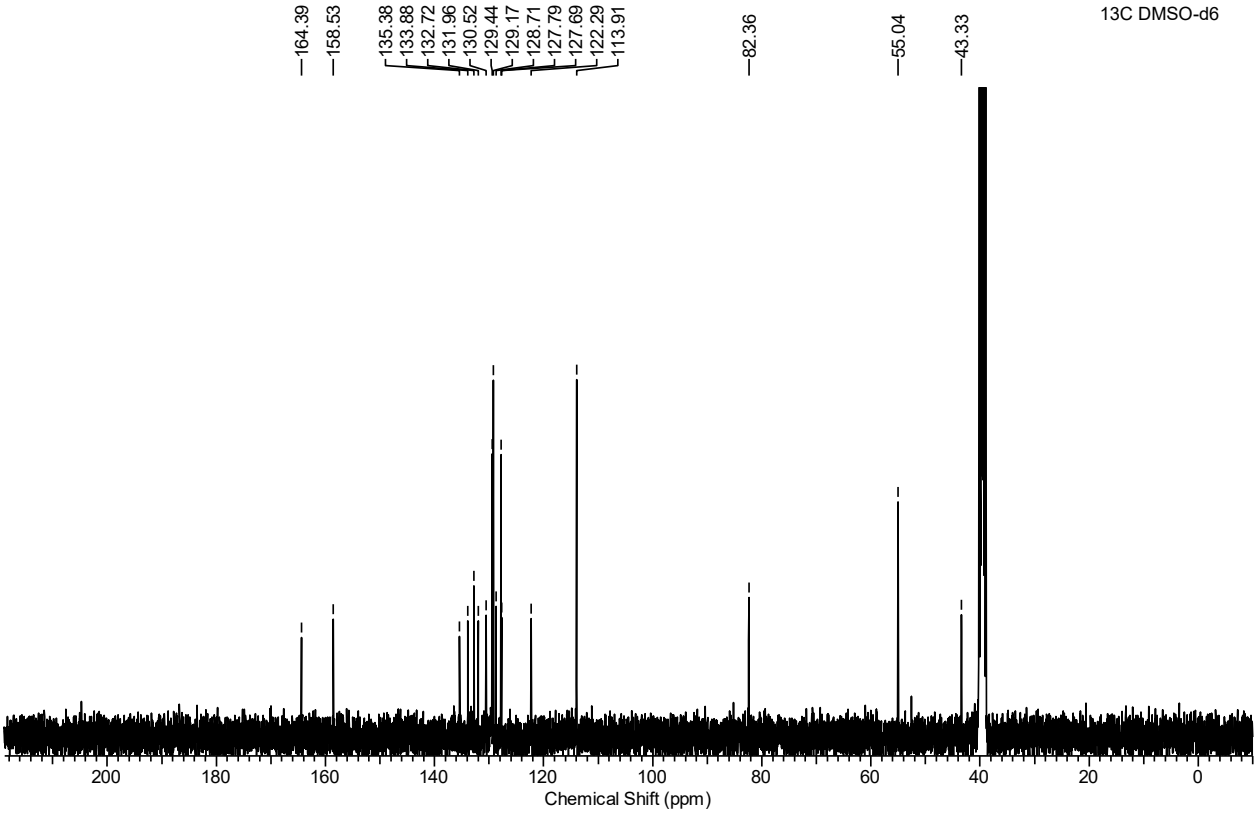
13C DMSO-d6
164.39
158.53
135.38
133.88
132.72
131.96
130.52
129.44
129.17
128.71
127.79
127.69
122.29
113.91
82.36
55.04
43.33
Chemical Shift (ppm)

3i

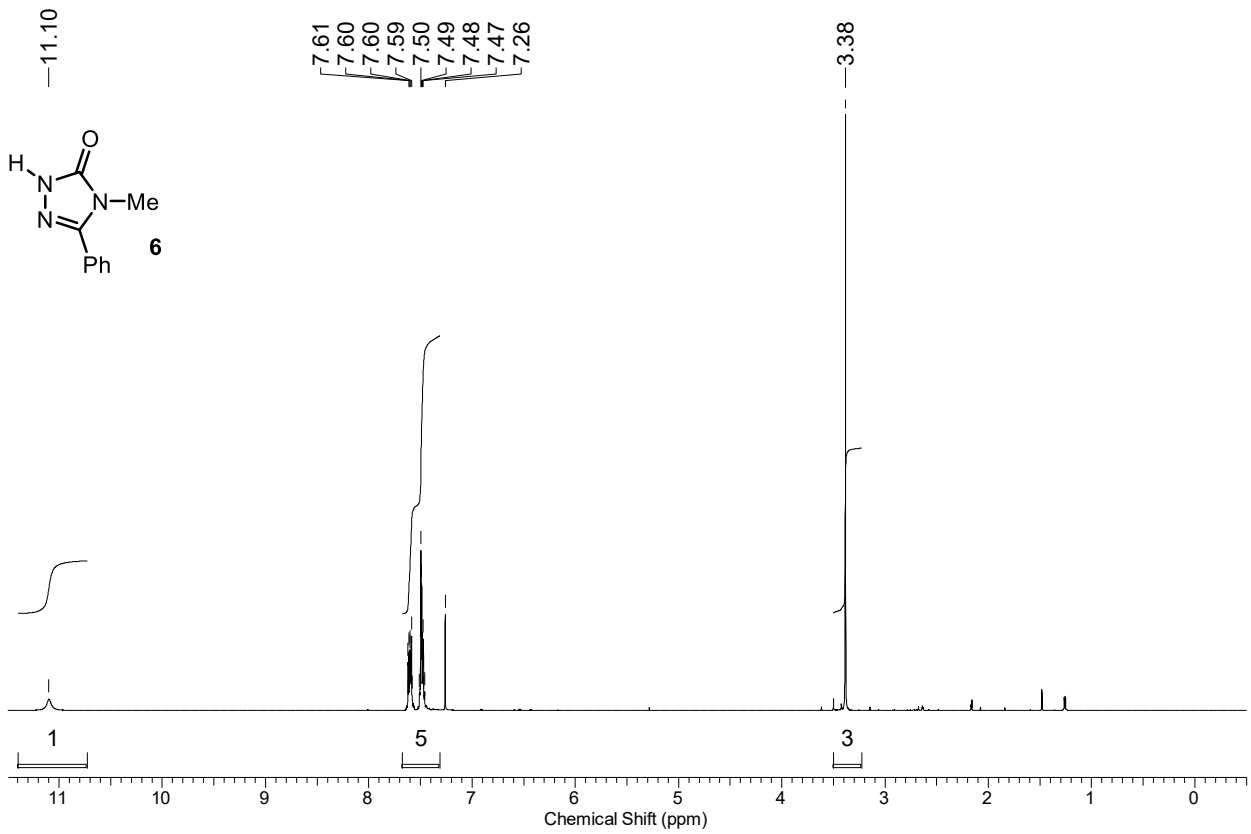
11.10
7.61
7.60
7.60
7.59
7.50
7.49
7.48
7.47
7.26
3.38
H
N
N
O
N–Me
Ph
6
1
5
3
11
10
9
8
7
6
5
4
3
2
1
0
Chemical Shift (ppm)

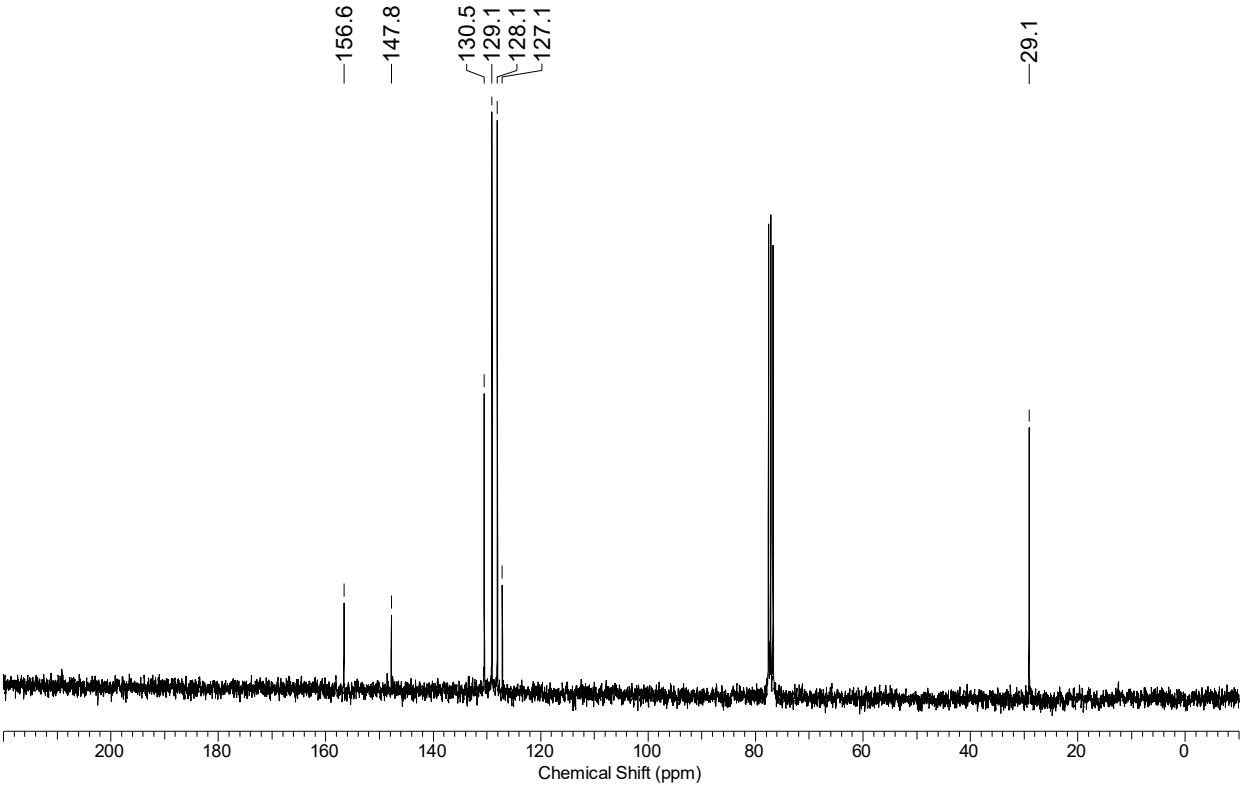
156.6
147.8
130.5
129.1
128.1
127.1
29.1
200
180
160
140
120
100
80
60
40
20
0
Chemical Shift (ppm)

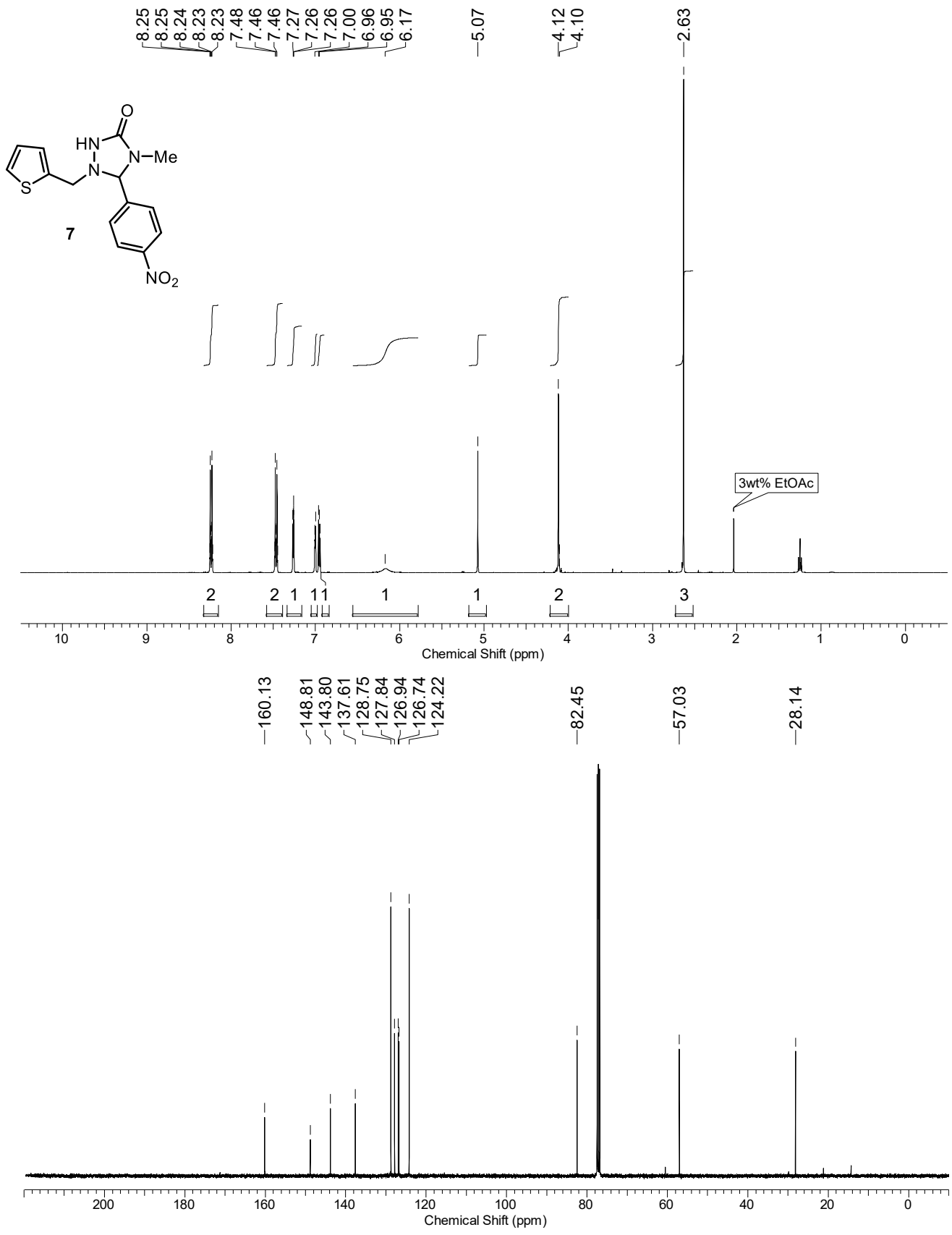
8.25
8.25
8.24
8.23
8.23
7.48
7.46
7.46
7.27
7.26
7.26
7.00
6.96
6.95
6.17
5.07
4.12
4.10
2.63
O
HN
N
N–Me
S
7
NO2
3wt% EtOAc
2 2 1 1 1 1 2 3
10 9 8 7 6 5 4 3 2 1 0
Chemical Shift (ppm)
160.13
148.81
143.80
137.61
128.75
127.84
126.94
126.74
124.22
82.45
57.03
28.14
200 180 160 140 120 100 80 60 40 20 0
Chemical Shift (ppm)

HPLC Chromatograms

(±)-**1a** Azomethine Imine, Racemic

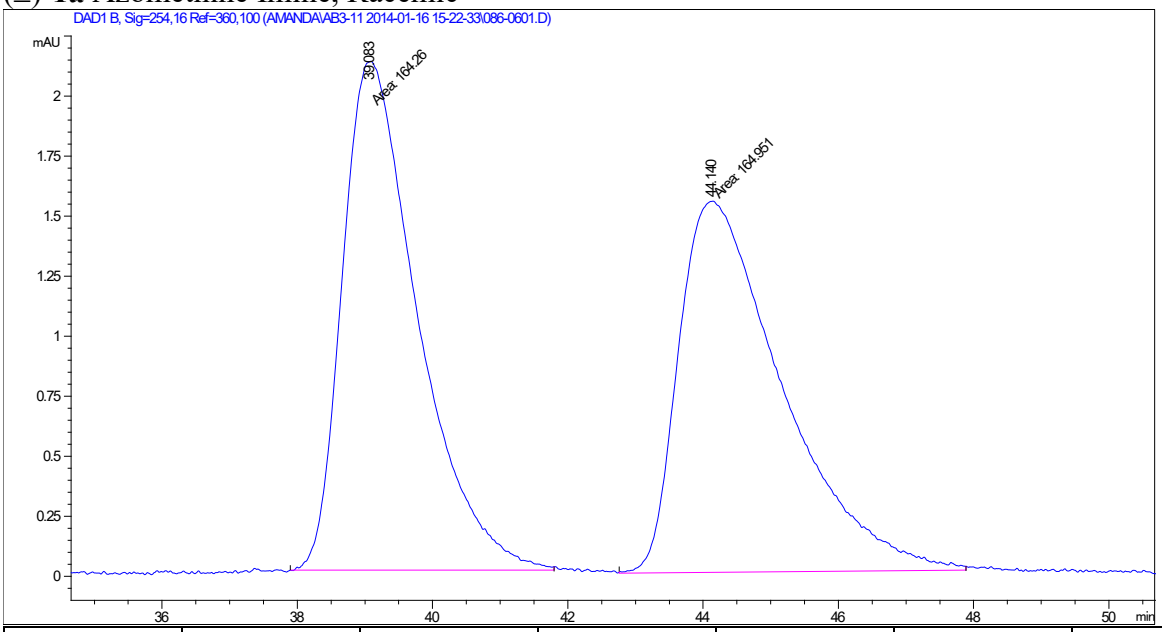

#	Time	Area	Height	Width	Area%	Symmetry
1	39.083	164.3	2.1	1.291	49.895	0.587
2	44.14	165	1.5	1.7764	50.105	0.477

1a Azomethine Imine, Recovered

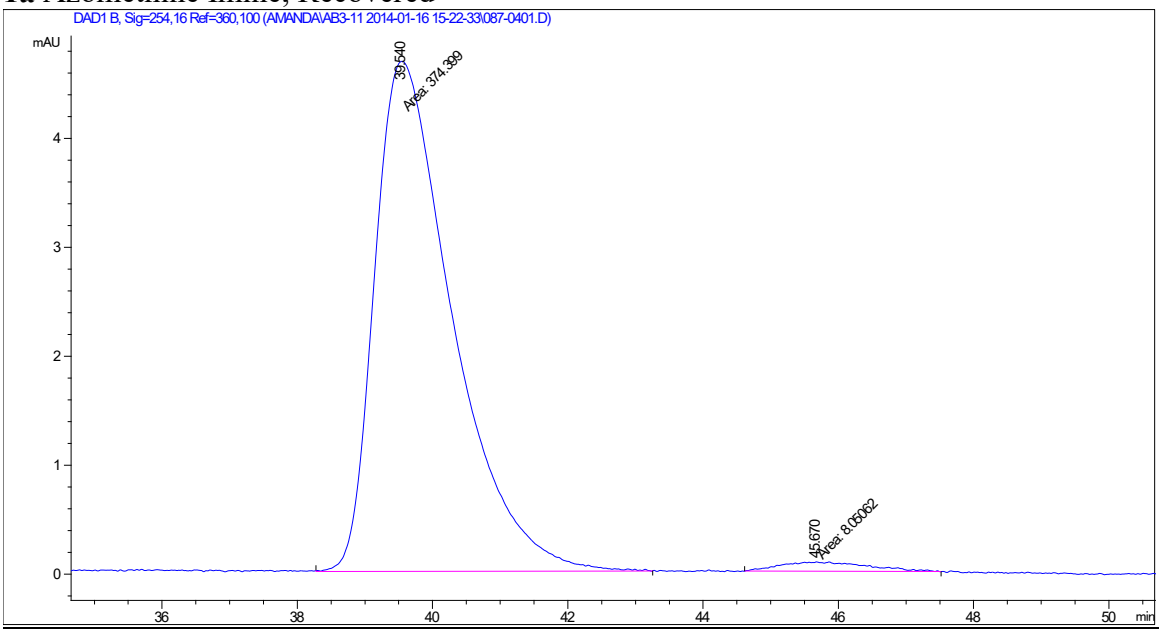

#	Time	Area	Height	Width	Area%	Symmetry
1	39.54	374.4	4.7	1.3327	97.895	0.519
2	45.67	8.1	8.8E-2	1.5256	2.105	1.63E-2

(±)-**2a** Pyrazolidinone, Racemic

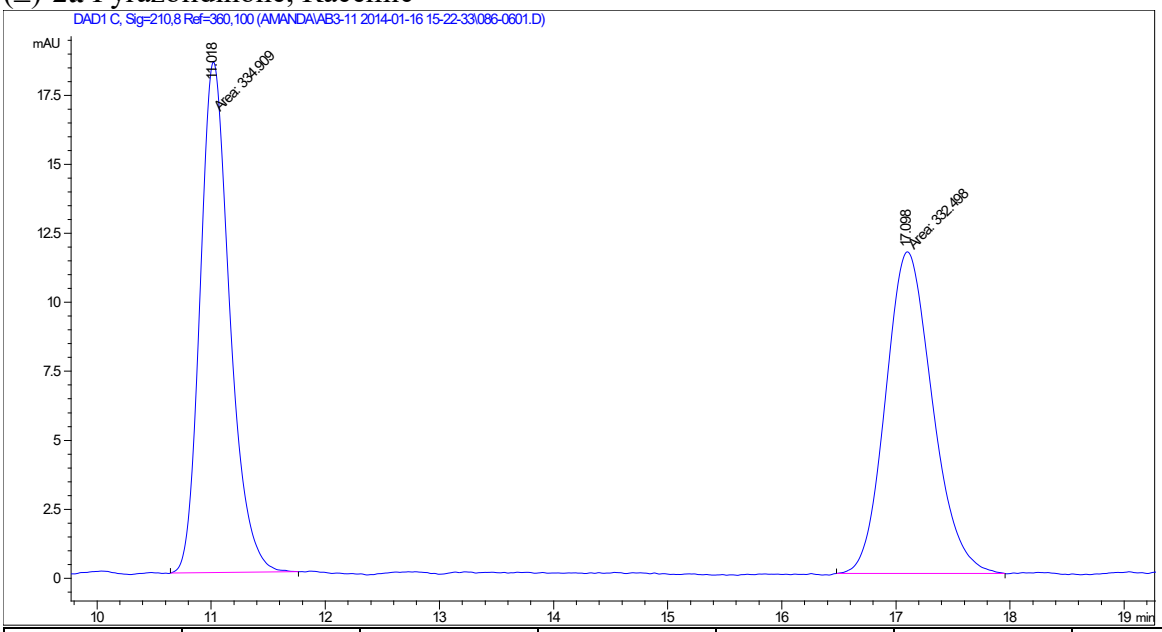

#	Time	Area	Height	Width	Area%	Symmetry
1	11.018	334.9	18.5	0.3013	50.181	0.78
2	17.098	332.5	11.7	0.4752	49.819	0.843

2a Pyrazolidinone

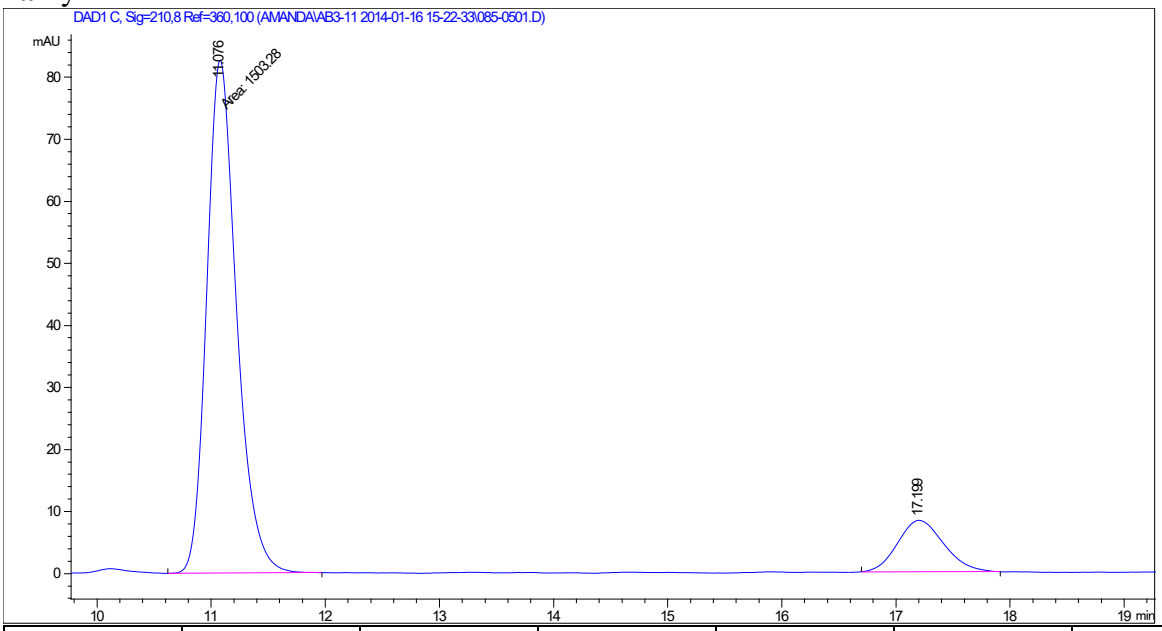

#	Time	Area	Height	Width	Area%	Symmetry
1	11.076	1503.3	82.7	0.3029	86.502	0.777
2	17.199	234.6	8.3	0.4246	13.498	0.828

(±)-**2b** Pyrazolidinone, Racemic

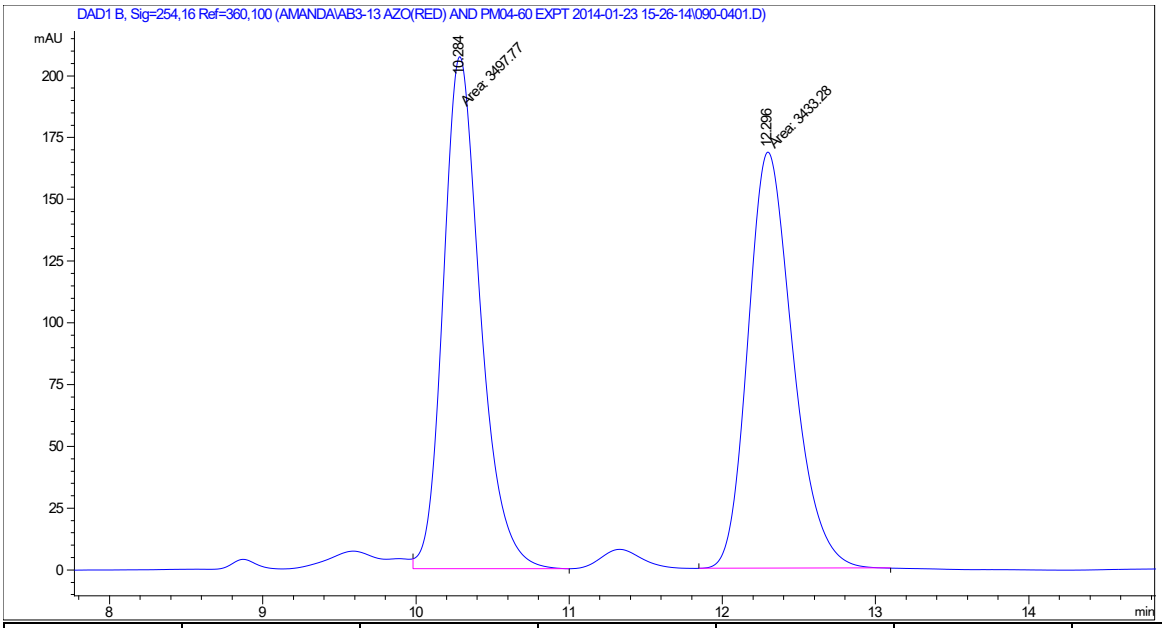

#	Time	Area	Height	Width	Area%	Symmetry
1	10.284	3497.8	207.4	0.2811	50.465	0.771
2	12.296	3433.3	168.5	0.3395	49.535	0.775

1b Azomethine Imine, Recovered and reduced to a pyrazolidinone

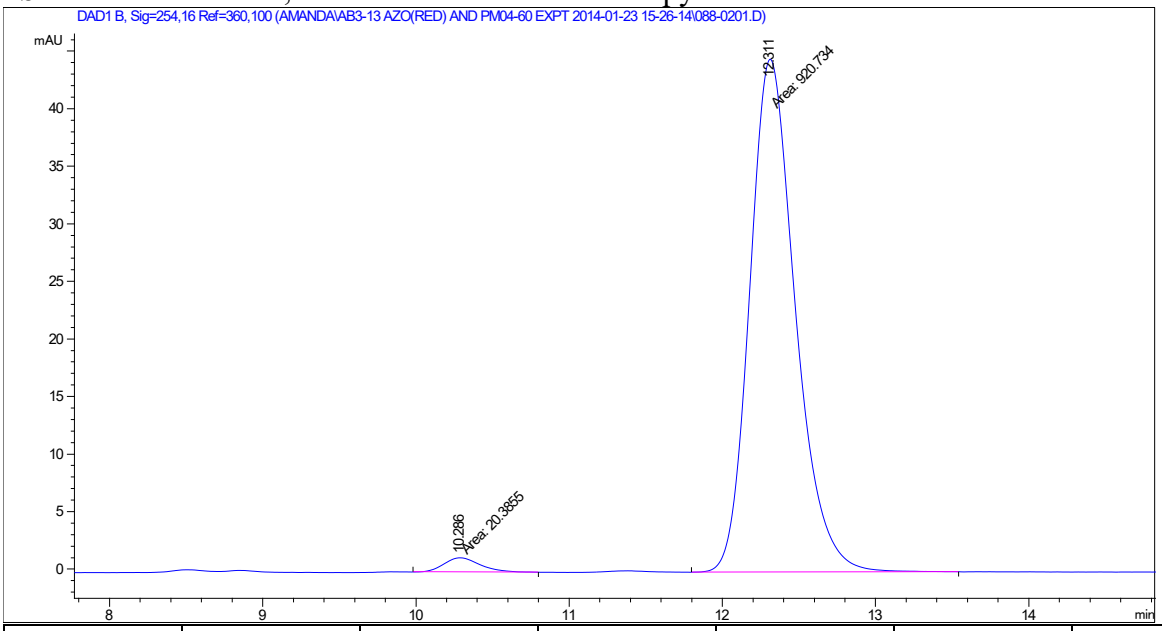

#	Time	Area	Height	Width	Area%	Symmetry
1	10.286	20.4	1.2	0.2749	2.166	0.776
2	12.311	920.7	44.6	0.3444	97.834	0.784

2b Pyrazolidinone

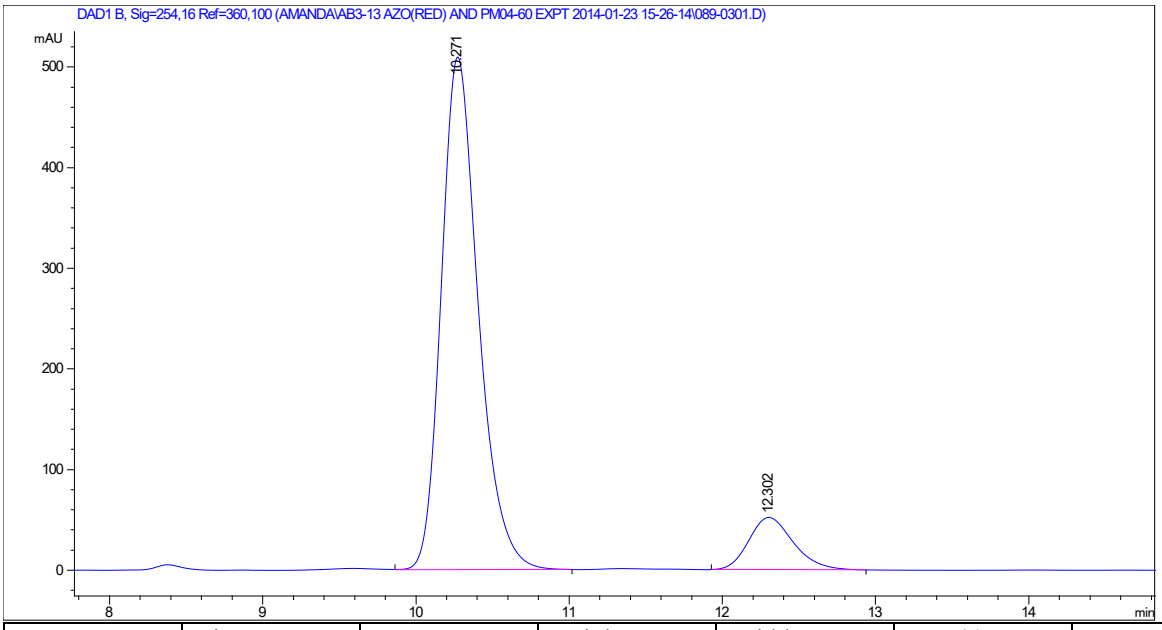

#	Time	Area	Height	Width	Area%	Symmetry
1	10.271	8560.9	509.6	0.256	89.046	0.748
2	12.302	1053.1	52	0.3105	10.954	0.772

(±)-**1c** Azomethine Imine, Racemic

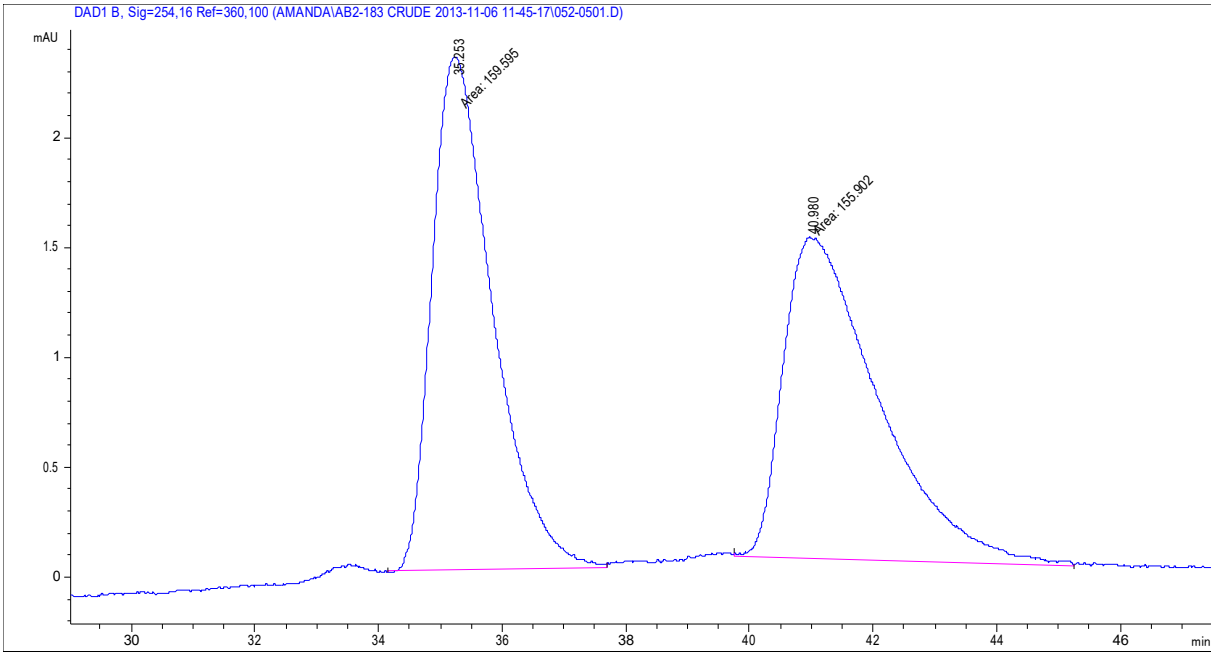

	Time	Area	Height	Width	Area%	Symmetry
1	34.407	278	4	1.1665	50.404	0.524
2	40.069	273.5	2.5	1.8311	49.596	0.433

1c Azomethine Imine, Recovered

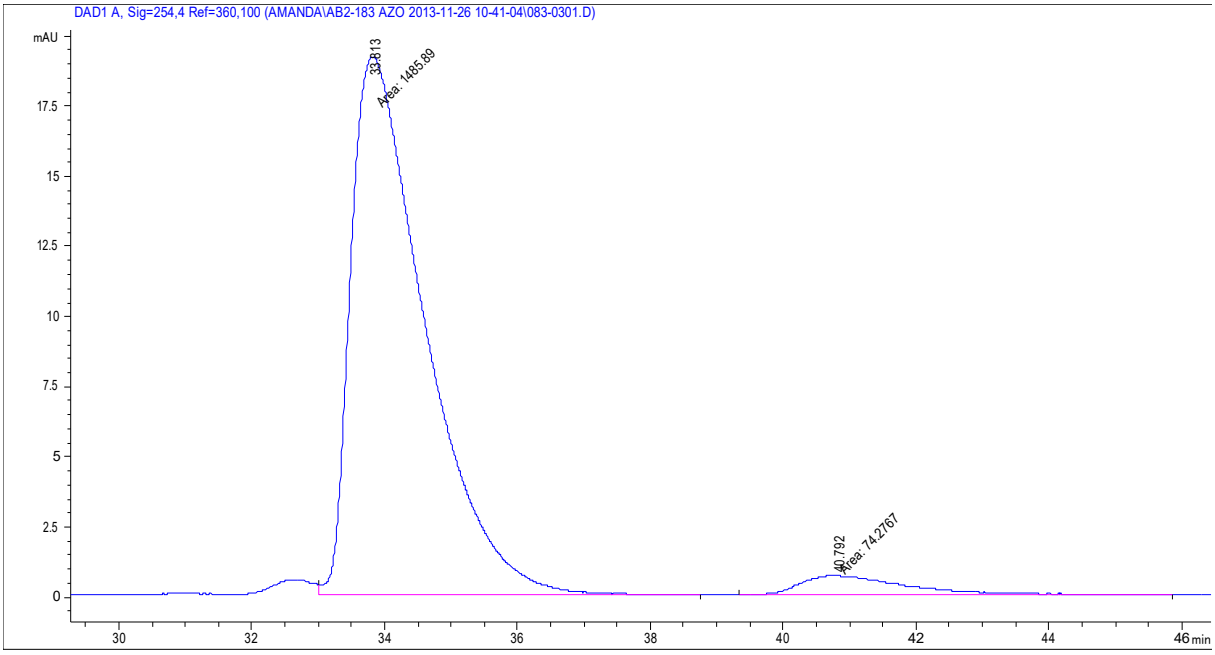

	Time	Area	Height	Width	Area%	Symmetry
1	33.812	1485.9	19.2	1.293	95.239	0
2	40.792	74.3	6.7E-1	1.8473	4.761	3.25E-5

(±)-**2c** Pyrazolidinone, Racemic

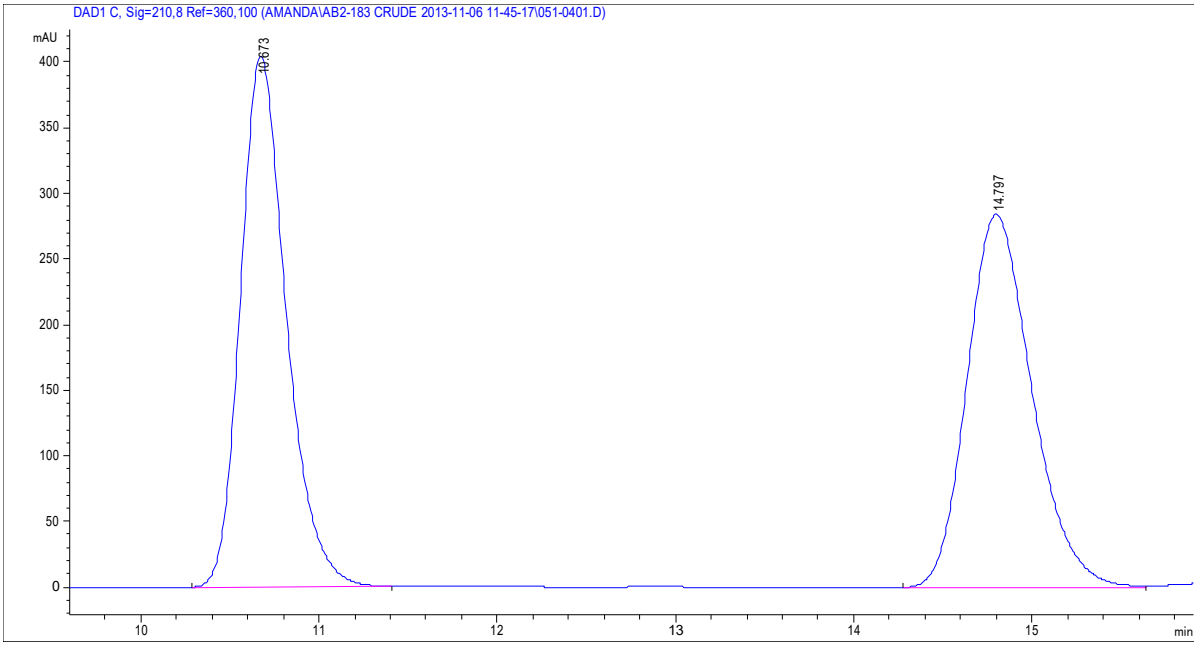

	Time	Area	Height	Width	Area%	Symmetry
1	10.673	7228.3	404.7	0.2724	50.022	0.75
2	14.797	7222	284.8	0.3899	49.978	0.765

2c Pyrazolidinone

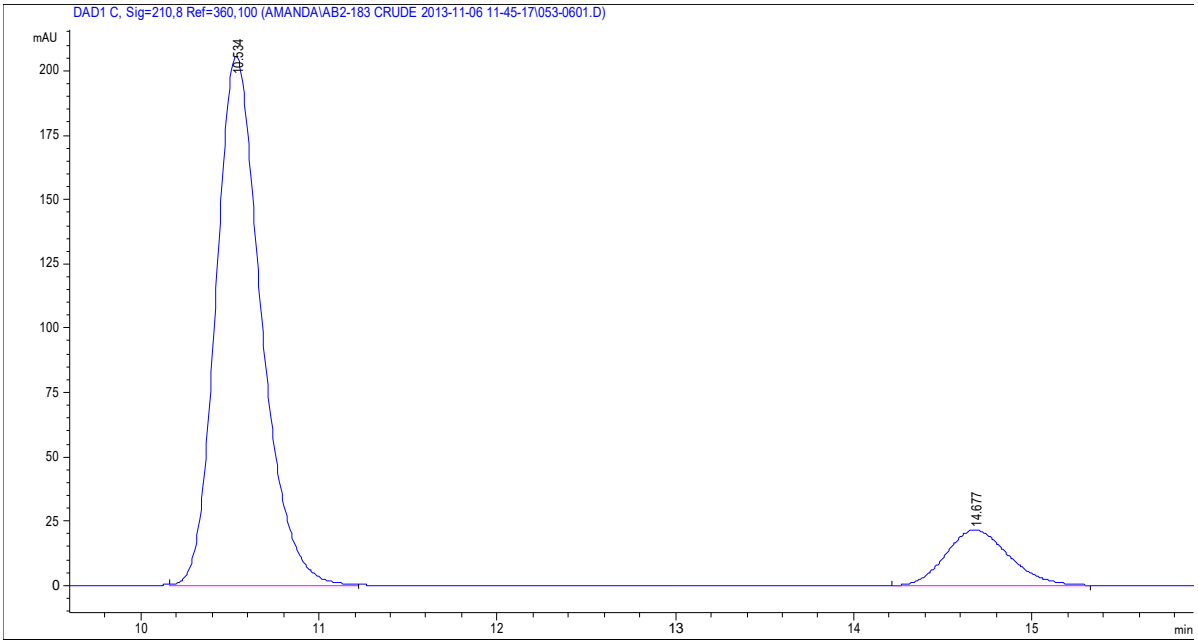

	Time	Area	Height	Width	Area%	Symmetry
1	10.534	3615.7	205.6	0.2692	87.009	0.754
2	14.677	539.8	21.6	0.383	12.991	0.812

(±)-**1d** Azomethine Imine, Racemic

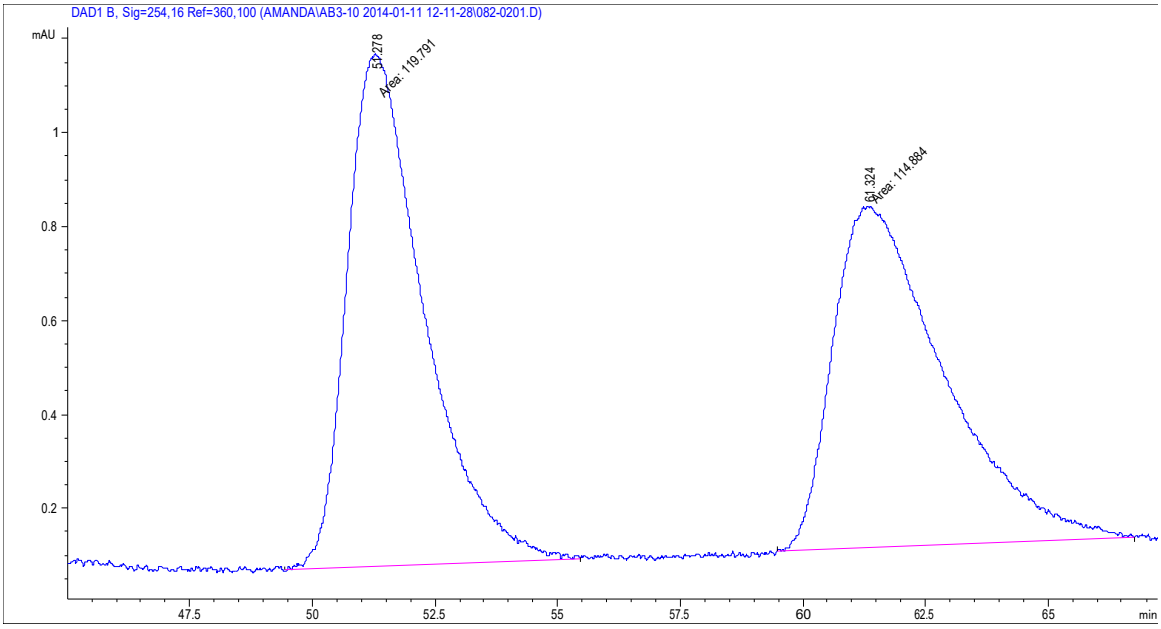

	Time	Area	Height	Width	Area%	Symmetry
1	51.278	119.7	1.1	1.8248	50.242	1.14E-4
2	61.324	118.6	7.4E-1	2.6811	49.758	3.88E-5

1d Azomethine Imine, Recovered (entry 4)

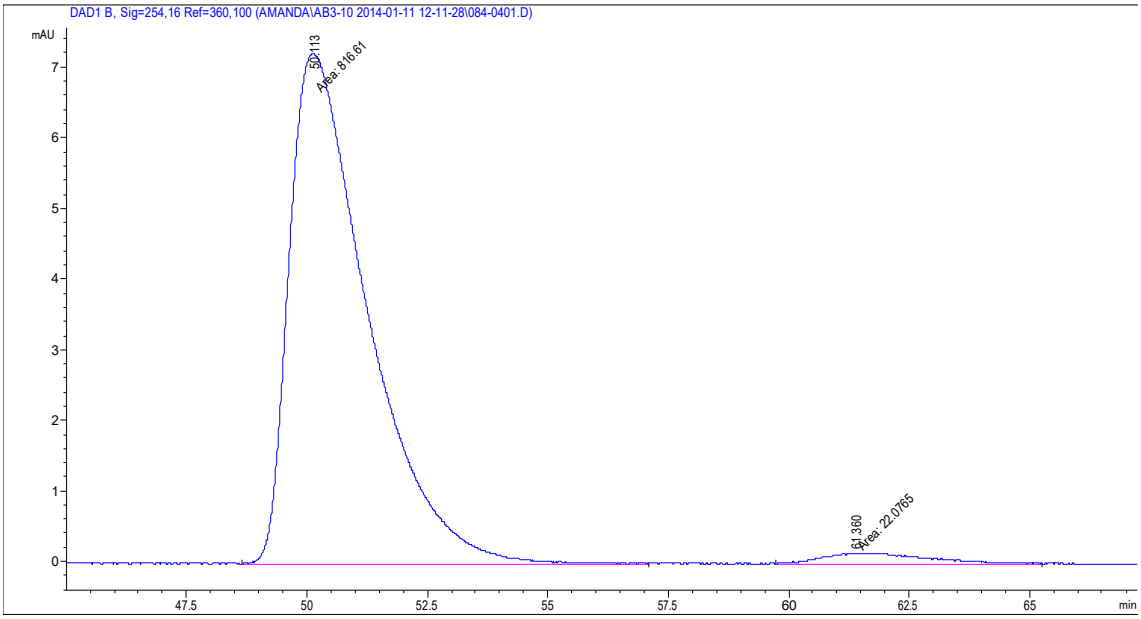

	Time	Area	Height	Width	Area%	Symmetry
1	50.113	816.6	7.2	1.8833	97.368	4.42E-5
2	61.36	22.1	1.5E-1	2.4338	2.632	6.81E-4

(±)-**2d** Pyrazolidinone, Racemic

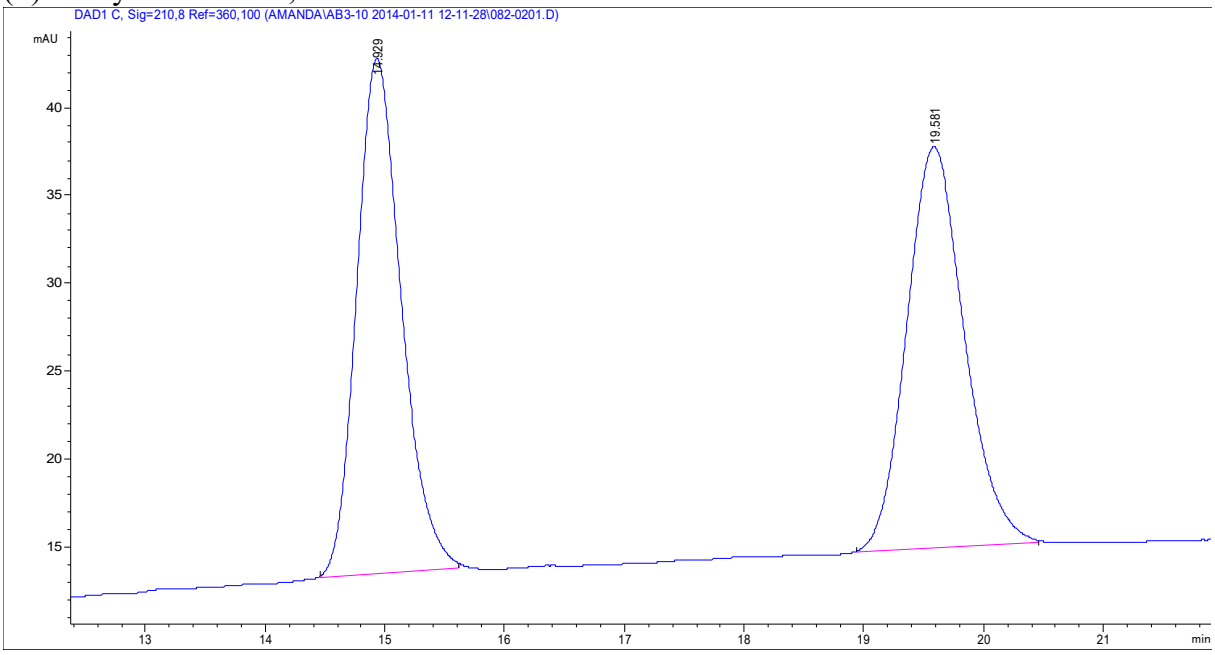

	Time	Area	Height	Width	Area%	Symmetry
1	14.929	760.2	29.4	0.3962	49.732	0.772
2	19.581	768.4	22.8	0.5127	50.268	0.841

2d Pyrazolidinone (entry 4)

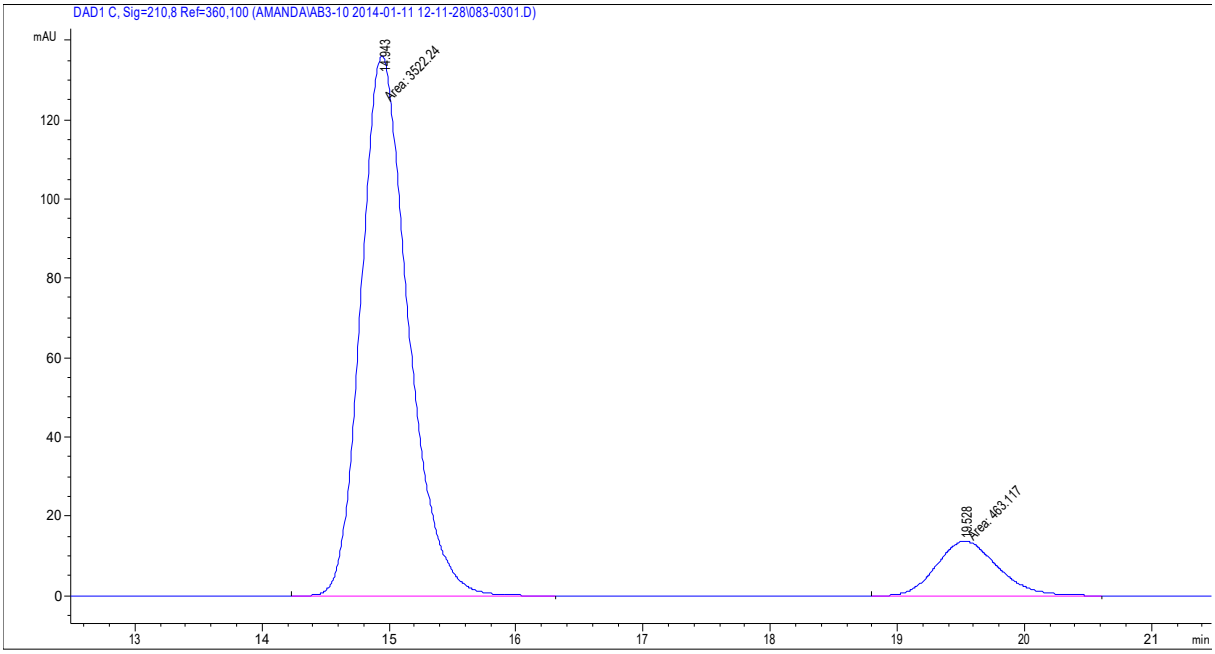

	Time	Area	Height	Width	Area%	Symmetry
1	14.943	3520.2	136.2	0.4307	88.373	0.769

2	19.528	463.2	13.8	0.5599	11.627	0.835

1d Azomethine Imine, Recovered (entry 5)

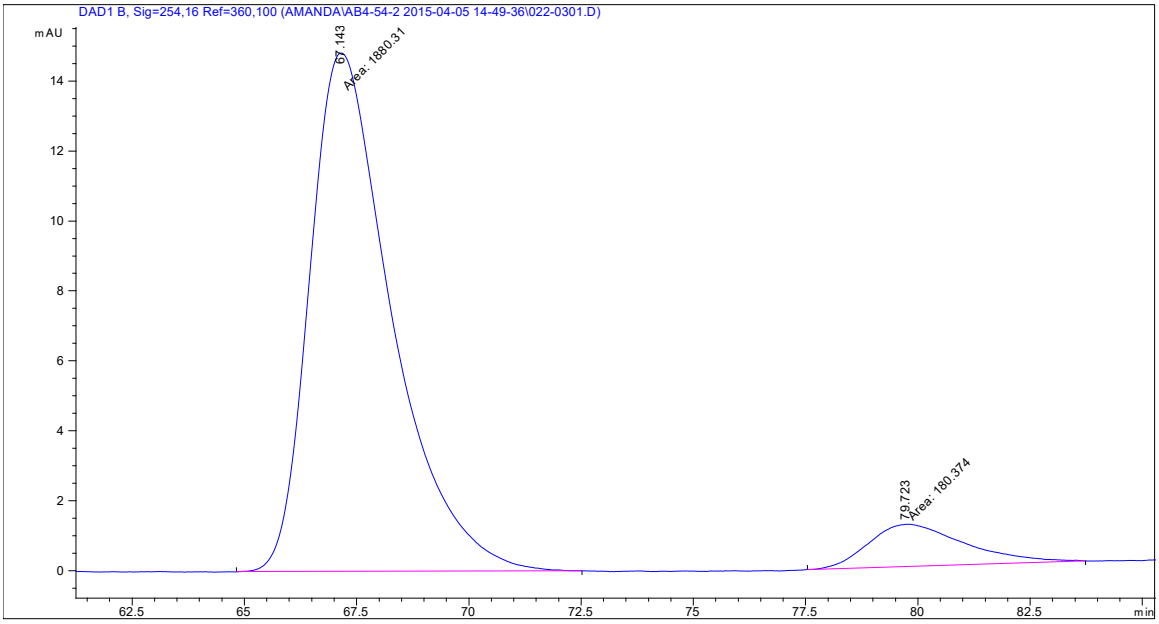

#	Time	Area	Height	Width	Area%	Symmetry
1	67.143	1880.3	14.8	2.1134	91.247	3.51E-6
2	79.723	180.4	1.2	2.4757	8.753	8.91E-5

2d Pyrazolidinone (entry 5)

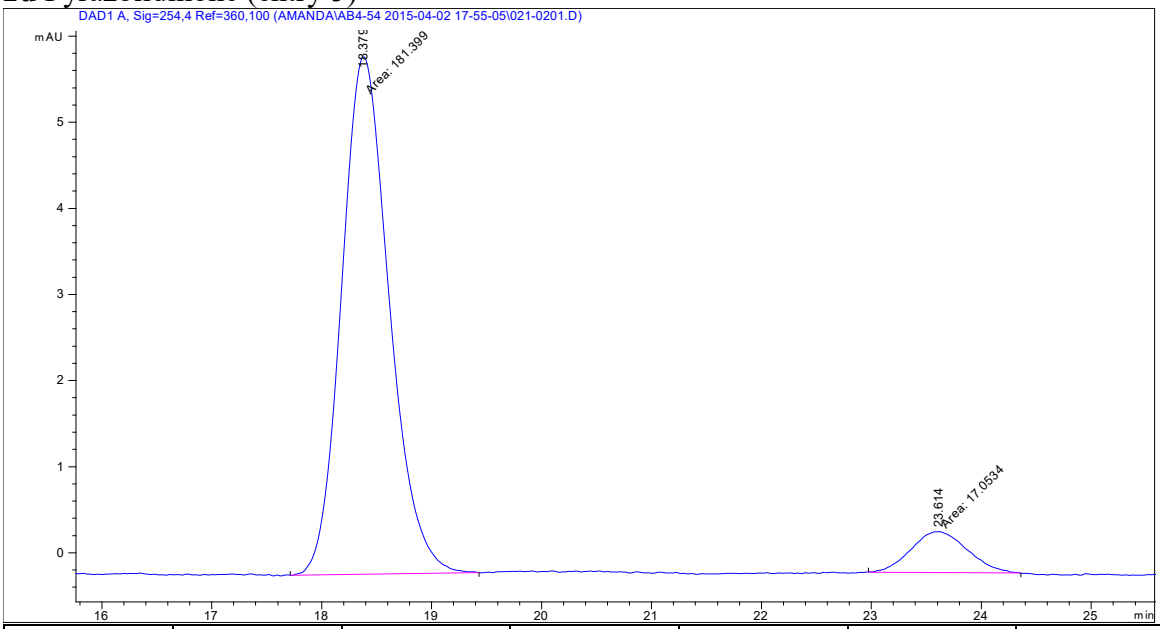

#	Time	Area	Height	Width	Area%	Symmetry
1	18.379	181.4	6	0.5029	91.407	0.823
2	23.614	17.1	4.8E-1	0.5949	8.593	0.957

(±)-**2e** Pyrazolidinone, Racemic

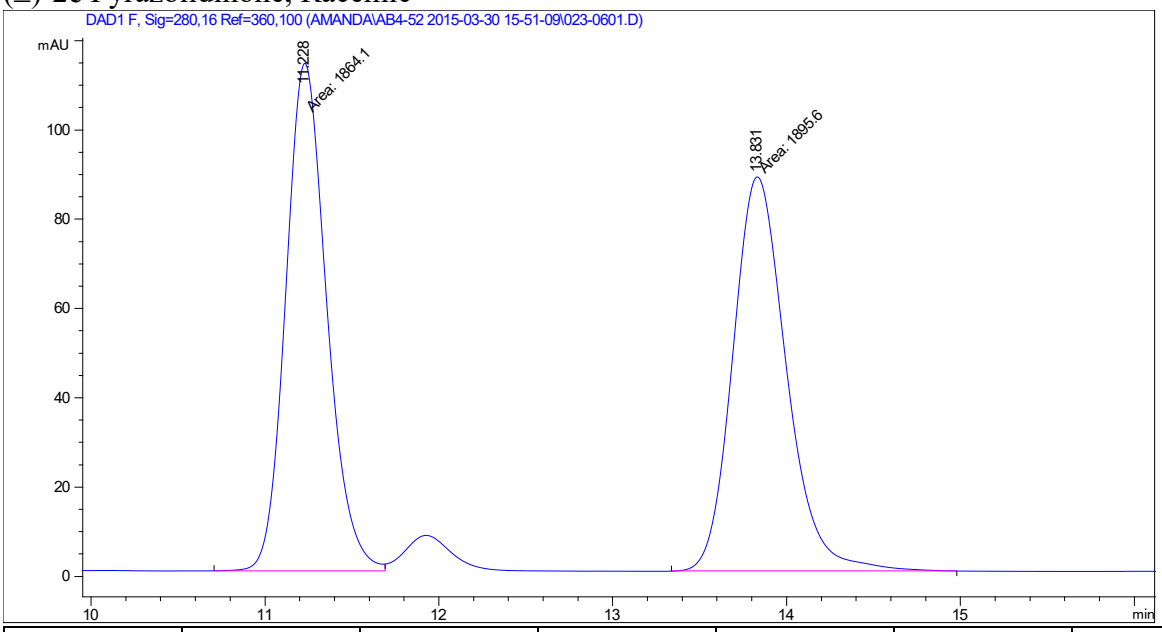

#	Time	Area	Height	Width	Area%	Symmetry
1	11.228	1864.1	113.8	0.2731	49.581	0.84
2	13.831	1895.6	88.3	0.3577	50.419	0.807

1e Azomethine Imine, reduced to the pyrazolidinone

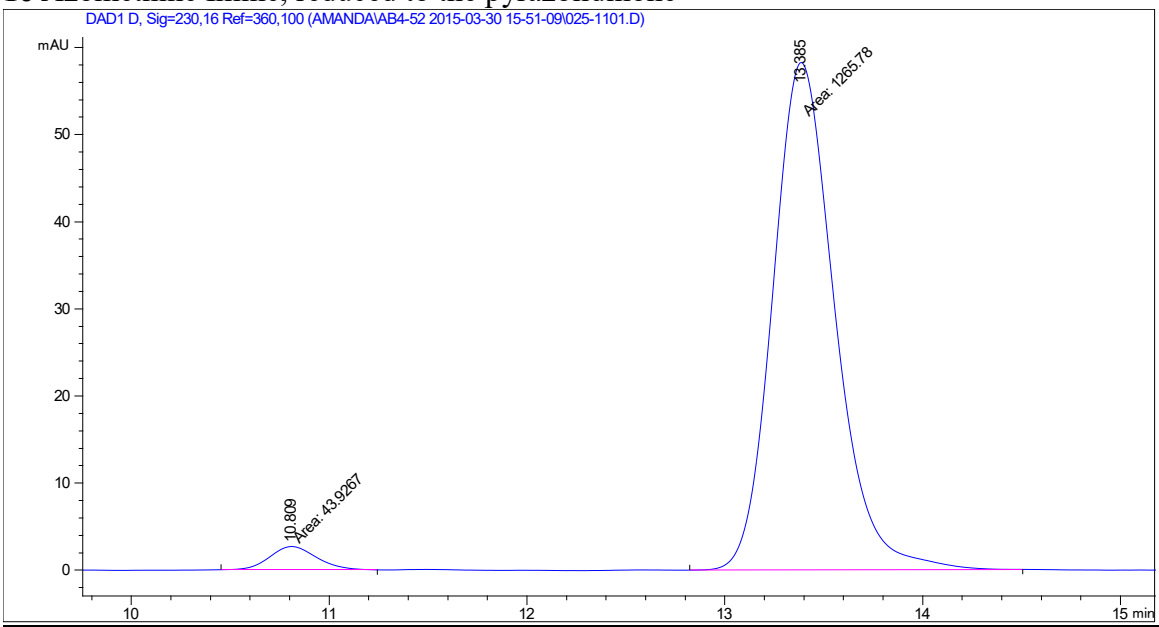

#	Time	Area	Height	Width	Area%	Symmetry
1	10.809	43.9	2.7	0.2741	3.354	0.864
2	13.385	1265.8	58.2	0.3622	96.646	0.815

2e Pyrazolidinone

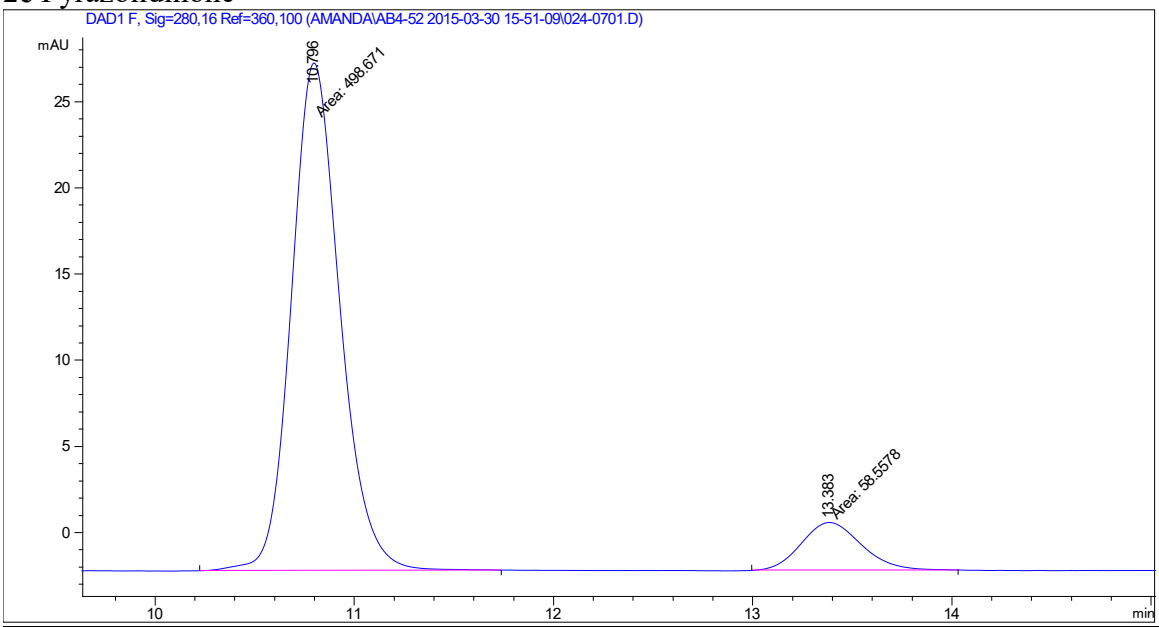

#	Time	Area	Height	Width	Area%	Symmetry
1	10.796	498.7	29.5	0.2822	89.491	0.842
2	13.383	58.6	2.8	0.3516	10.509	0.84

(±)-**1f** Azomethine Imine, Racemic

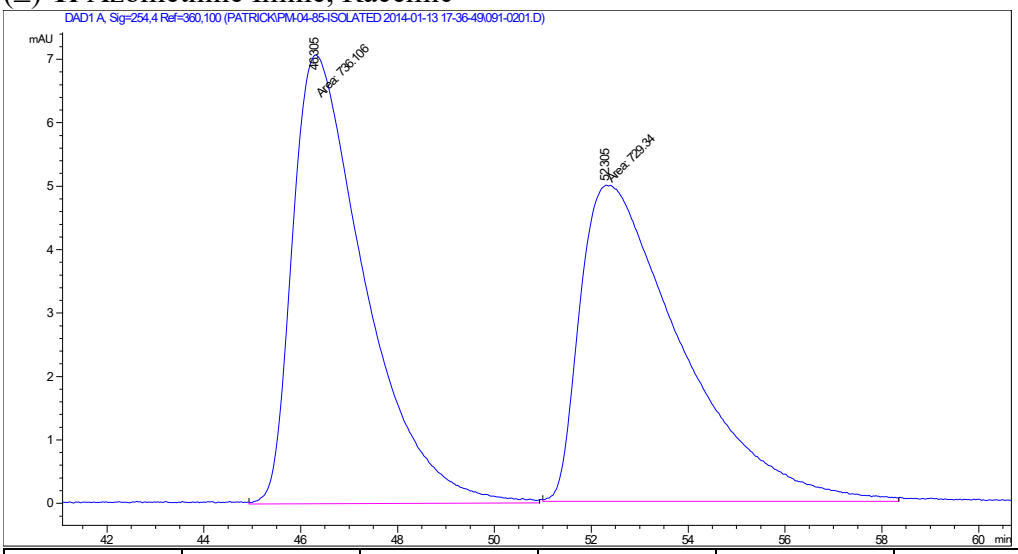

#	Time	Area	Height	Width	Area%	Symmetry
1	46.305	736.1	7.1	1.7332	50.231	0
2	52.305	729.3	5	2.4355	49.769	0

1f Azomethine Imine, Recovered

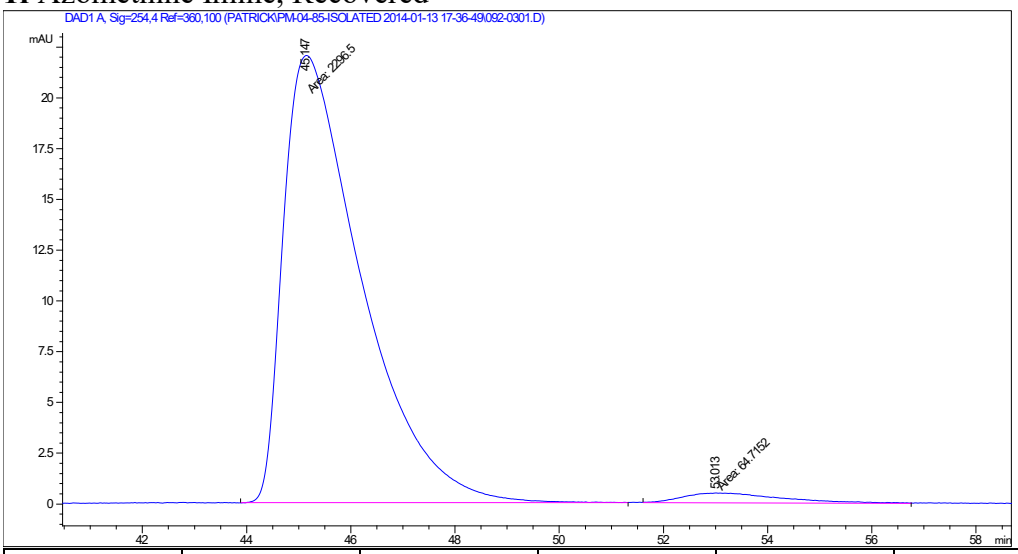

#	Time	Area	Height	Width	Area%	Symmetry
1	45.147	2296.5	22	1.7382	97.259	7.36E-6
2	53.013	64.7	0.49	2.2038	2.741	2.74E-3

(±)-**2f** Pyrazolidinone, Racemic

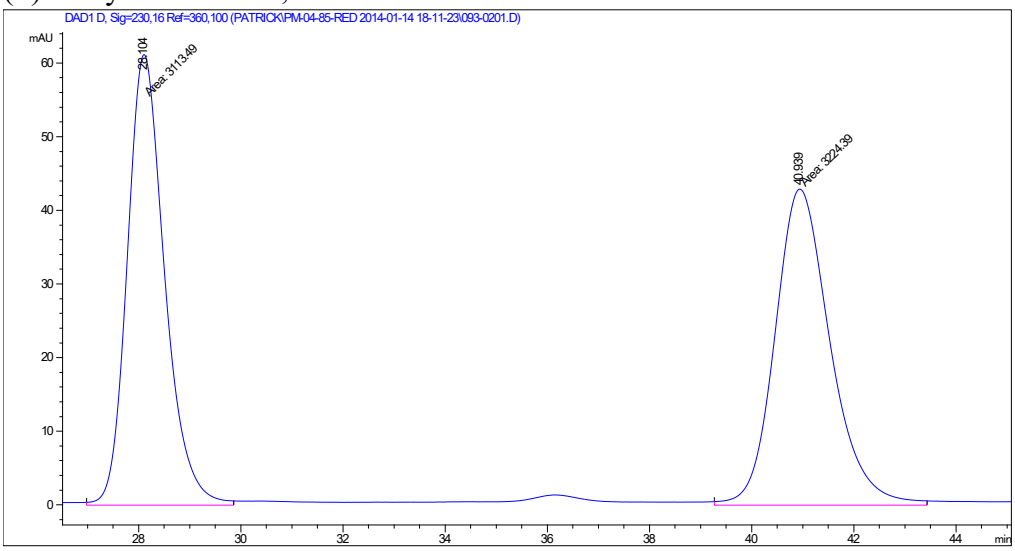

#	Time	Area	Height	Width	Area%	Symmetry
1	28.104	3113.5	61.2	0.8481	49.125	0.789
2	40.939	3224.4	42.9	1.2522	50.875	0.789

2f Pyrazolidinone

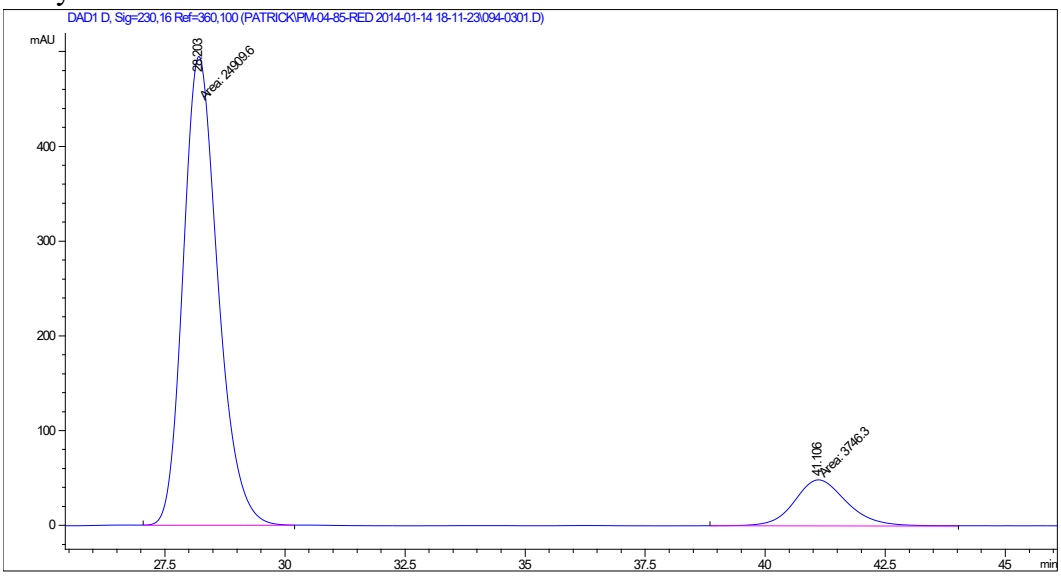

#	Time	Area	Height	Width	Area%	Symmetry
1	28.203	24909.6	494.9	0.8389	86.927	0.787
2	41.106	3746.3	48.7	1.2817	13.073	0.829

(±)-**1g** Azomethine Imine, Racemic

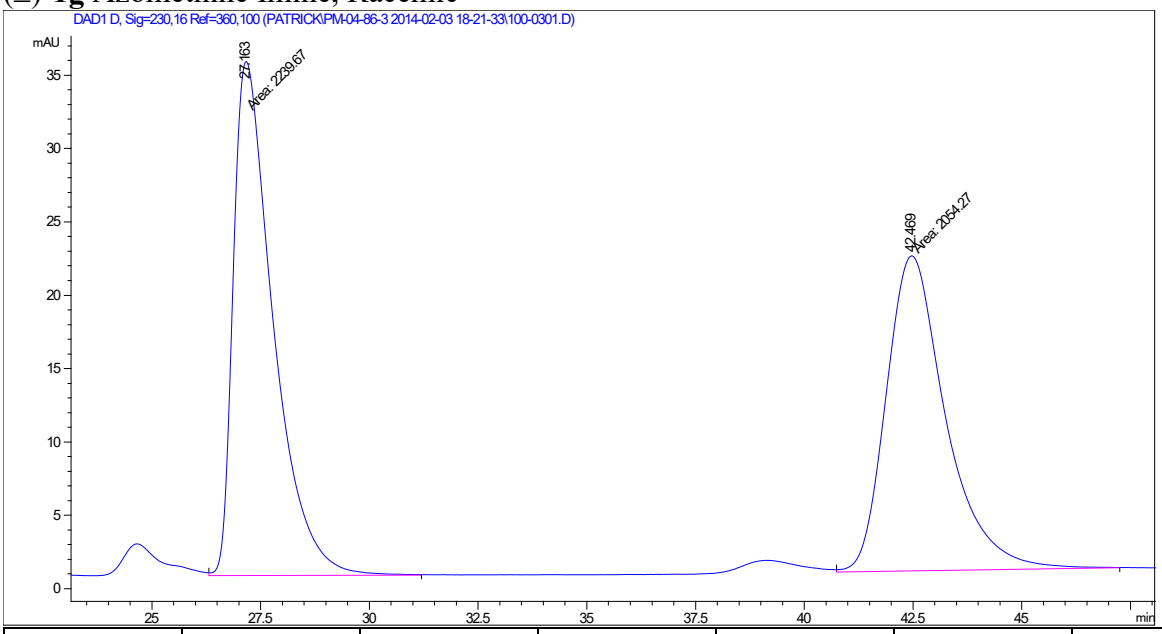

#	Time	Area	Height	Width	Area%	Symmetry
1	27.163	2239.7	35.1	1.0646	52.159	0
2	42.469	2054.3	21.5	1.7465	47.841	1.13E-2

1g Azomethine Imine, Recovered

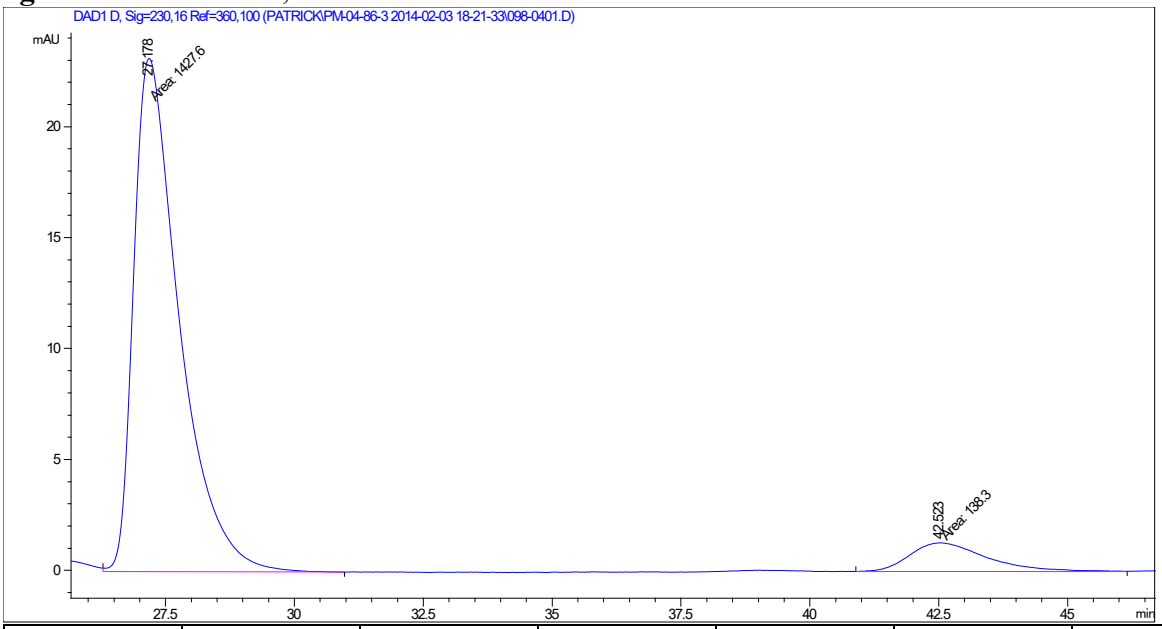

#	Time	Area	Height	Width	Area%	Symmetry
1	27.178	1427.6	23.2	1.0277	91.168	0.49
2	42.523	138.3	1.3	1.7617	8.832	1.05E-3

(±)-**2g** Pyrazolidinone, Racemic

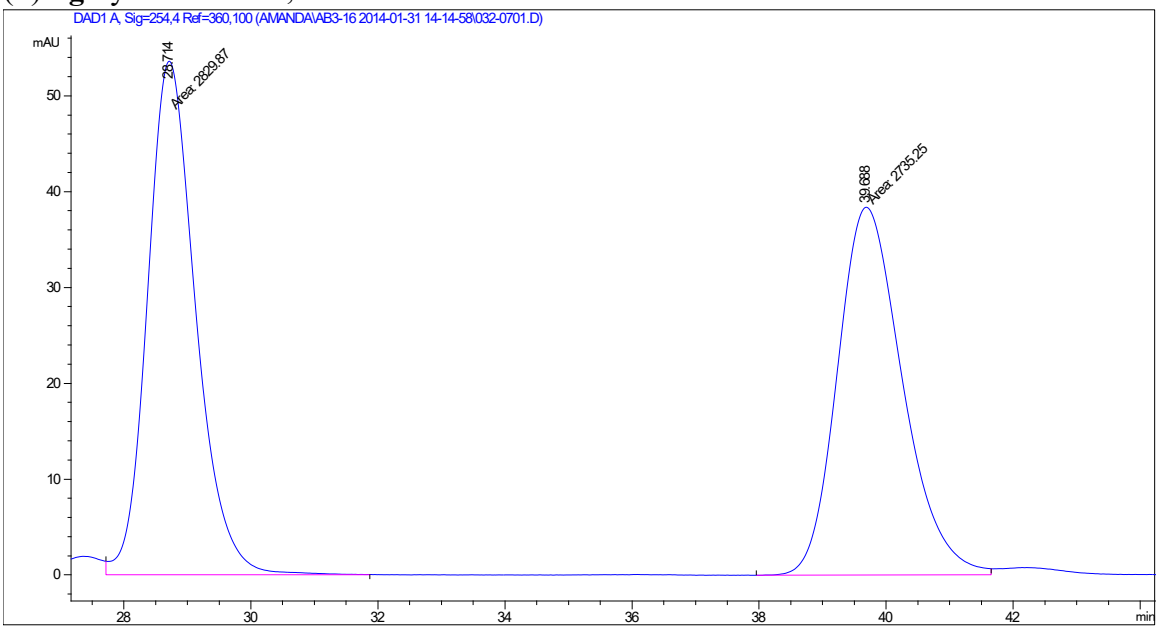

#	Time	Area	Height	Width	Area%	Symmetry
1	28.714	2829.9	53.6	0.8799	50.850	0
2	39.687	2735.3	38.4	1.1869	49.150	0

2g Pyrazolidinone

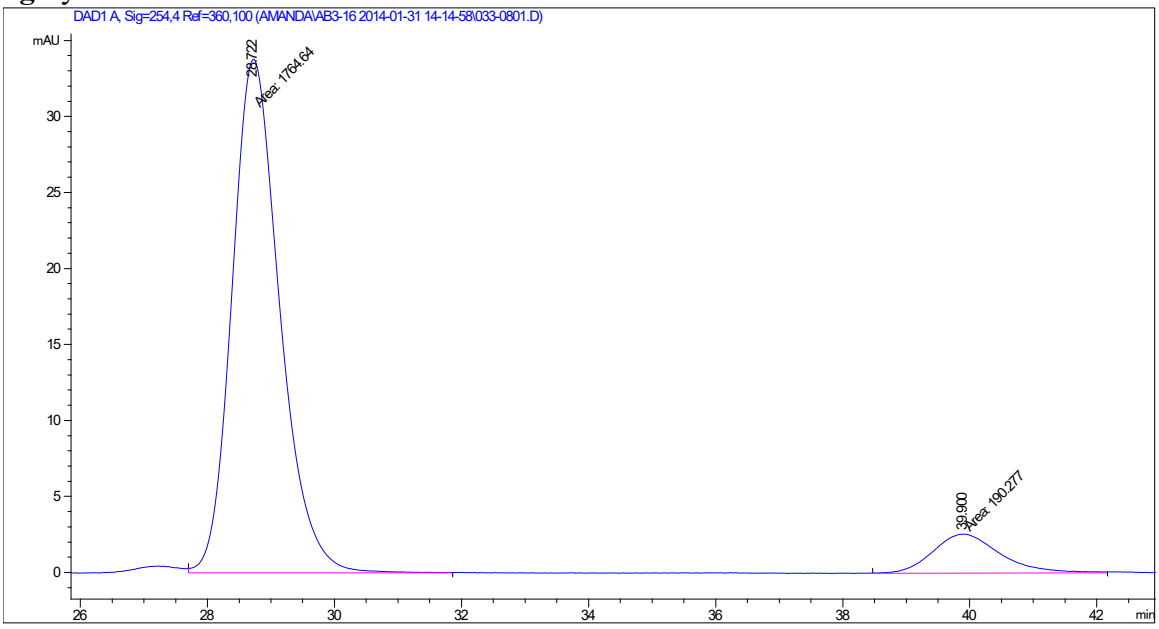

#	Time	Area	Height	Width	Area%	Symmetry
1	28.722	1764.6	33.8	0.8703	90.267	0.788
2	39.9	190.3	2.6	1.2343	9.733	1.51E-4

(±)-**1h** Azomethine Imine, Racemic

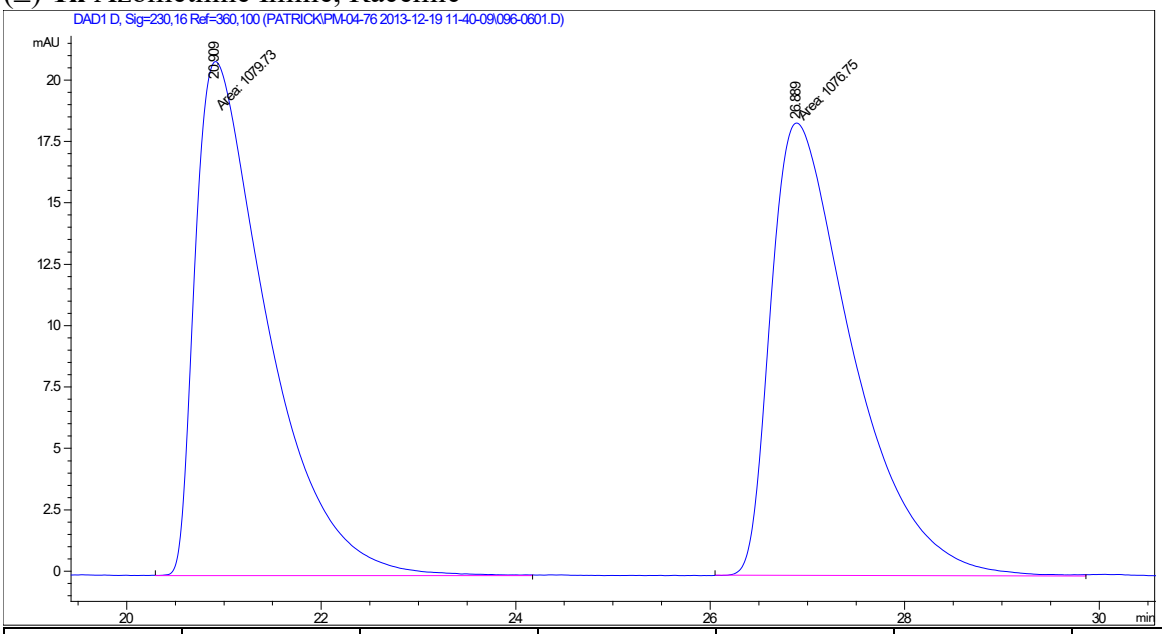

#	Time	Area	Height	Width	Area%	Symmetry
1	20.909	1079.7	20.9	0.8657	50.069	0
2	26.889	1076.7	18.4	0.9741	49.931	3.39E-6

1h Azomethine Imine, Recovered

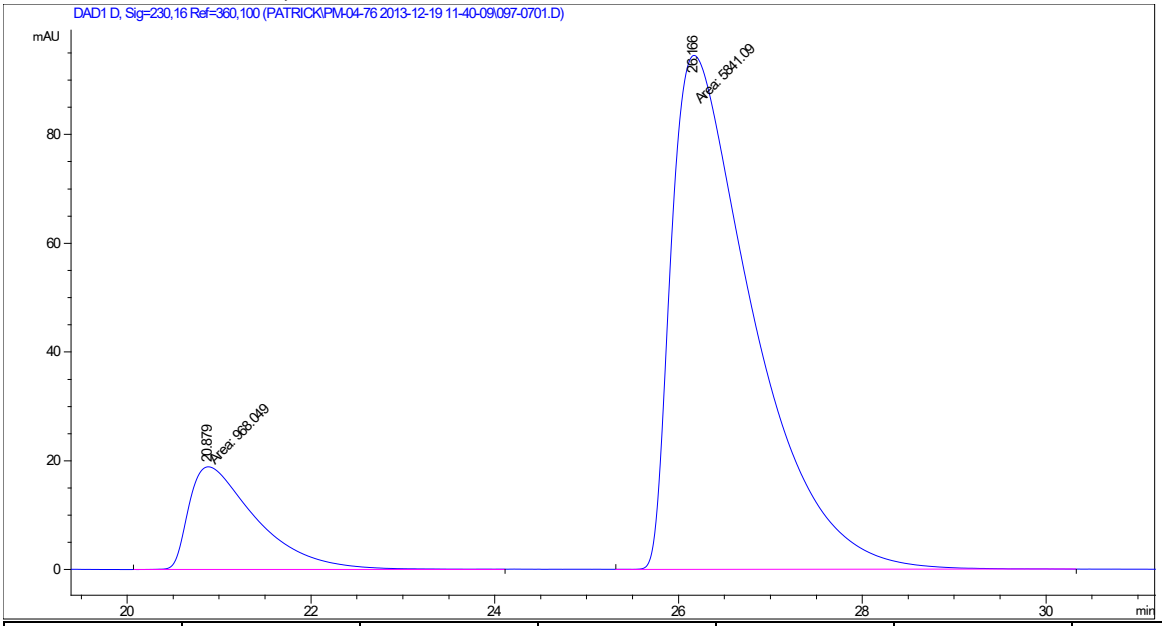

#	Time	Area	Height	Width	Area%	Symmetry
1	20.879	968	18.9	0.8539	14.217	0
2	26.166	5841.1	94.5	1.0301	85.783	0

(±)-**2h** Pyrazolidinone, Racemic

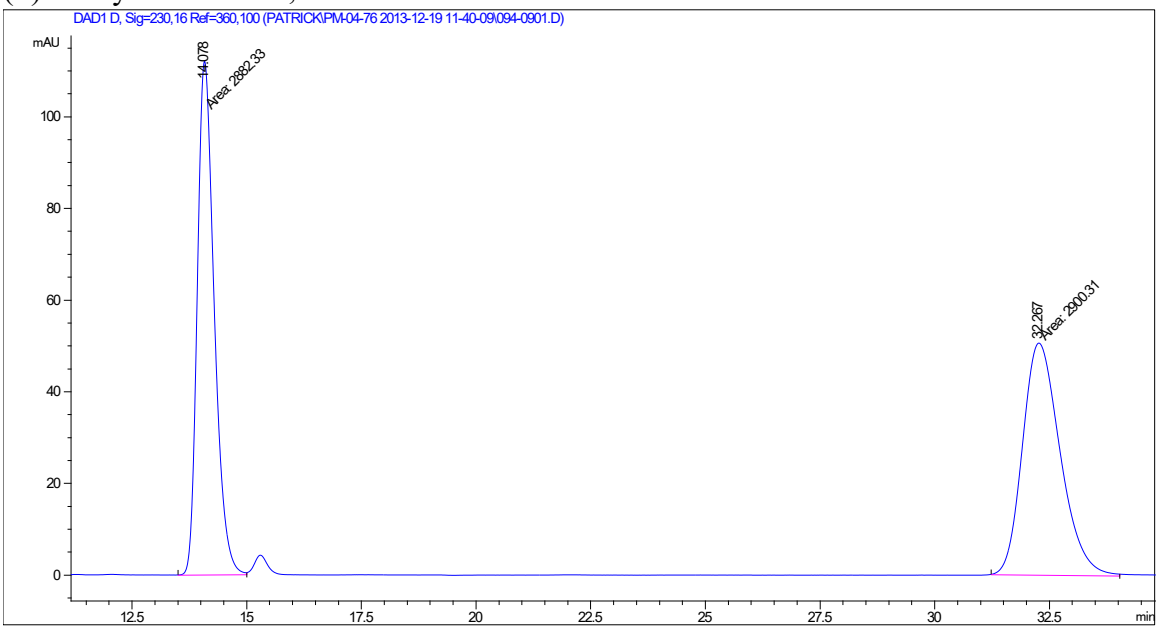

#	Time	Area	Height	Width	Area%	Symmetry
1	14.078	2882.3	112.2	0.4281	49.845	0.714
2	32.267	2900.3	50.7	0.9532	50.155	0.744

2h Pyrazolidinone

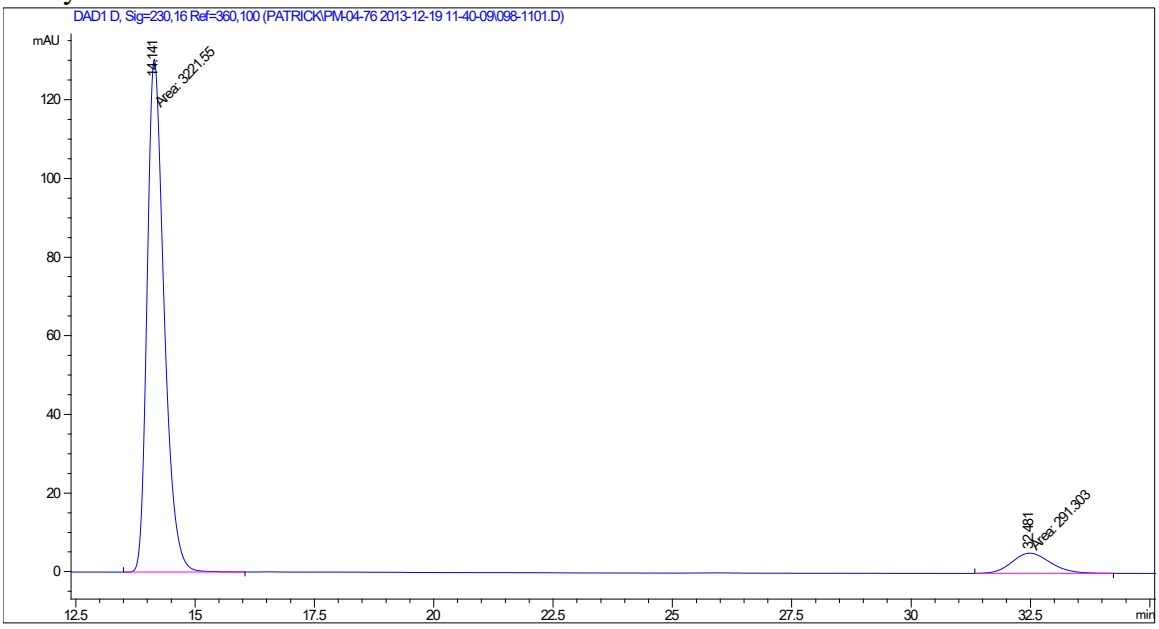

#	Time	Area	Height	Width	Area%	Symmetry
1	14.141	3221.6	130.4	0.4118	91.708	0.694
2	32.481	291.3	5.1	0.9432	8.292	0.844

(±)-**1i** Azomethine Imine, Racemic

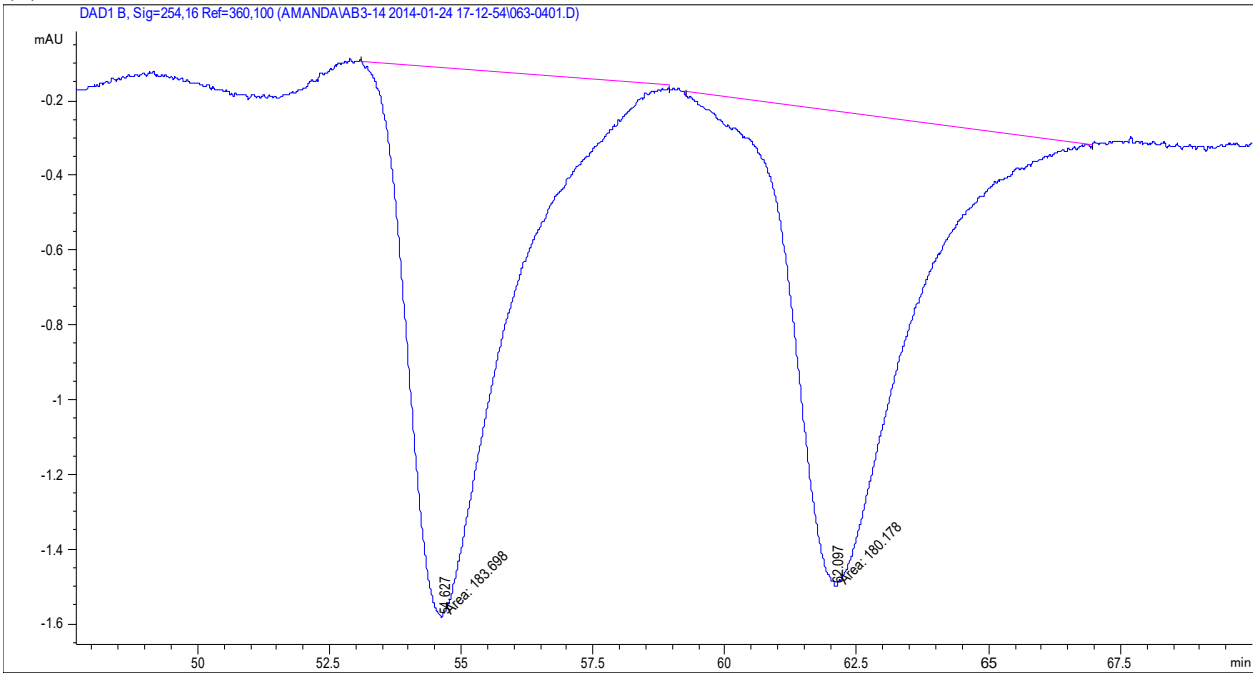

#	Time	Area	Height	Width	Area%	Symmetry
1	54.627	183.7	1.5	2.084	50.484	0
2	62.097	180.2	1.3	2.3641	49.516	0

1i Azomethine Imine, Recovered

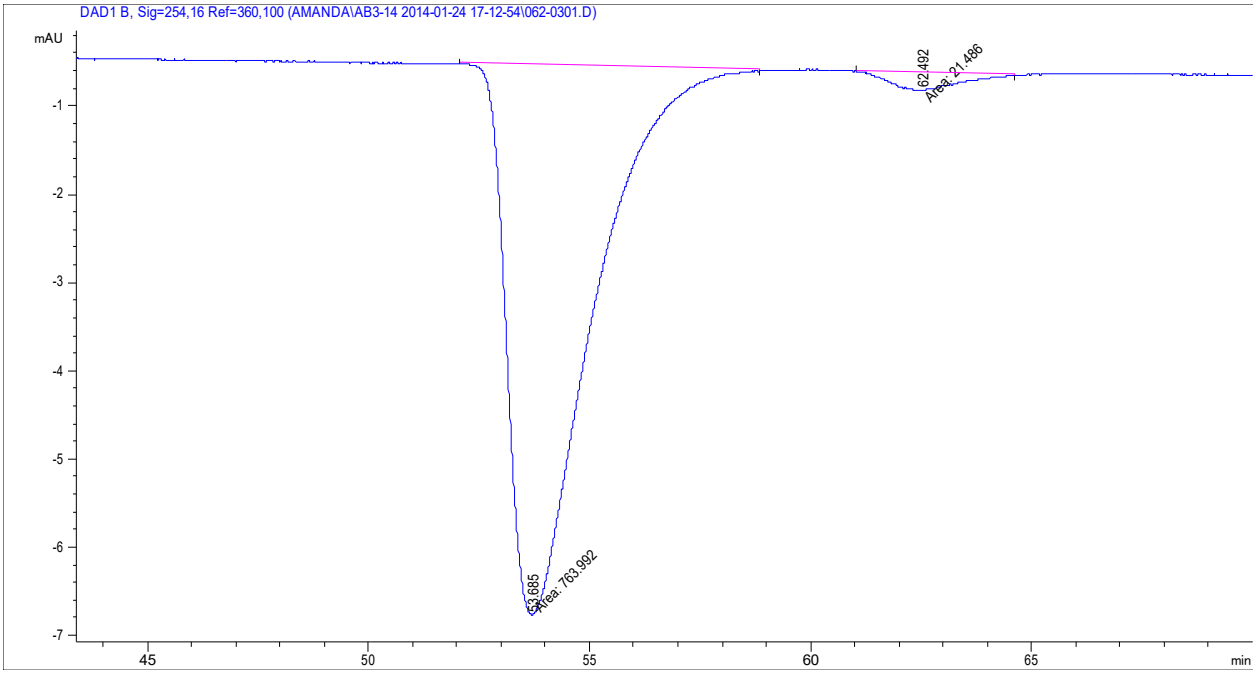

#	Time	Area	Height	Width	Area%	Symmetry
1	53.685	764	6.2	2.0429	97.265	0
2	62.492	21.5	2E-1	1.7577	2.735	0

(±)-**2i** Pyrazolidinone, Racemic

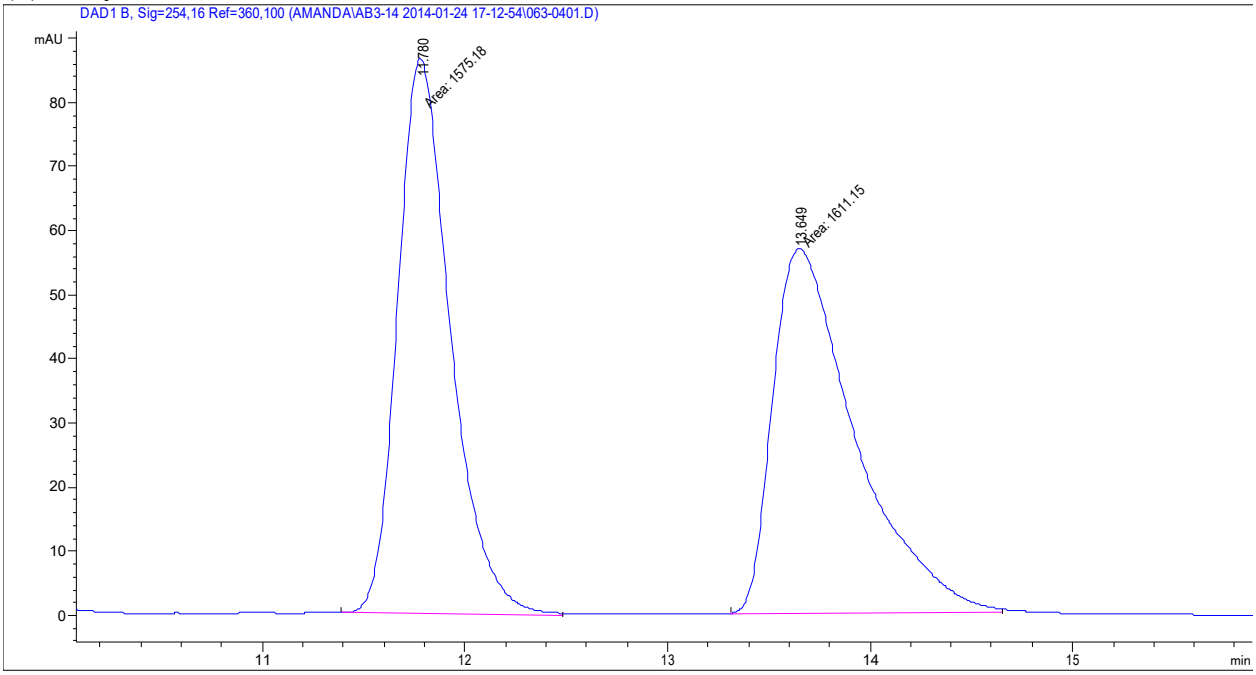

#	Time	Area	Height	Width	Area%	Symmetry
1	11.78	1575.2	86.6	0.3032	49.436	0.725
2	13.649	1611.2	56.9	0.4722	50.564	0.459

2i Pyrazolidinone

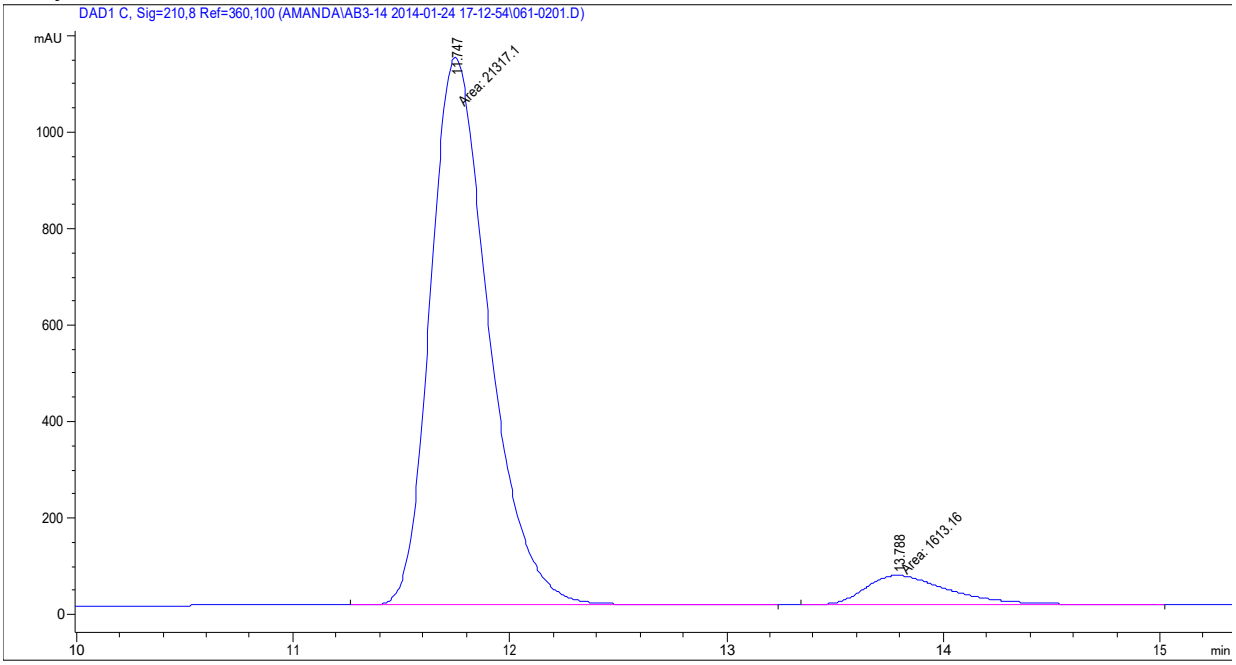

#	Time	Area	Height	Width	Area%	Symmetry
1	11.747	21317.1	1134.9	0.313	92.965	0.712
2	13.788	1613.2	60.1	0.447	7.035	0.593

(±)-**1i** Azomethine Imine, Racemic

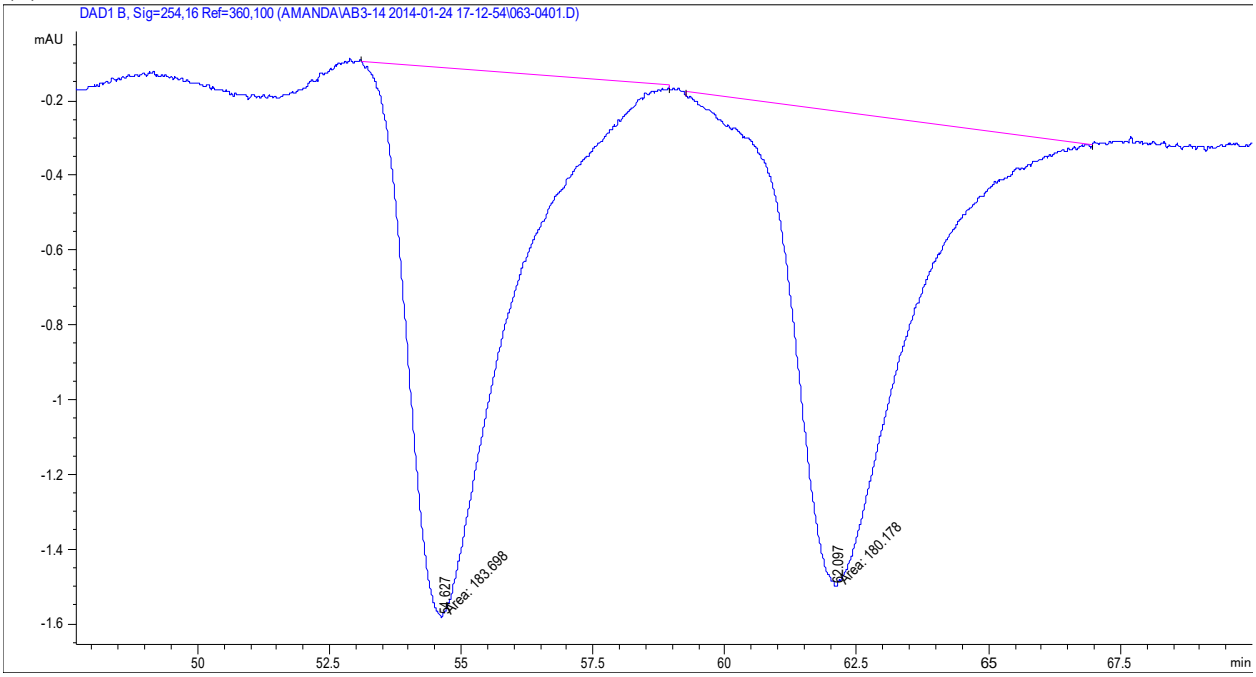

#	Time	Area	Height	Width	Area%	Symmetry
1	54.627	183.7	1.5	2.084	50.484	0
2	62.097	180.2	1.3	2.3641	49.516	0

1j Azomethine Imine, Recovered

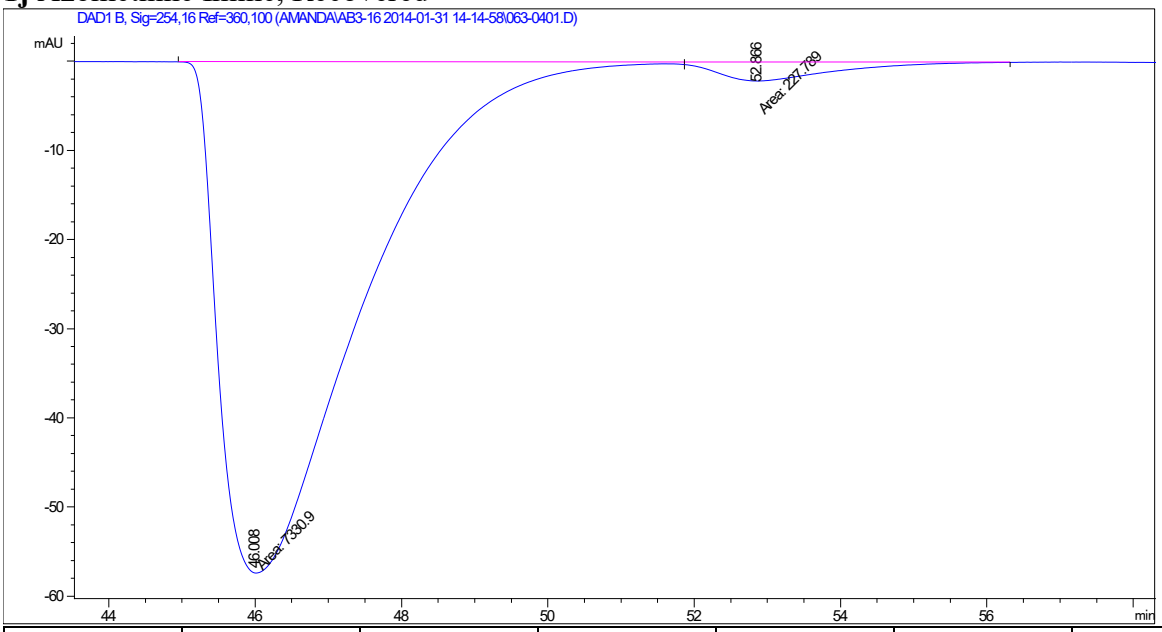

#	Time	Area	Height	Width	Area%	Symmetry
1	46.008	7330.9	57.3	2.1308	96.986	0
2	52.866	227.8	2.1	1.7854	3.014	0

(±)-**2j** Pyrazolidinone, Racemic

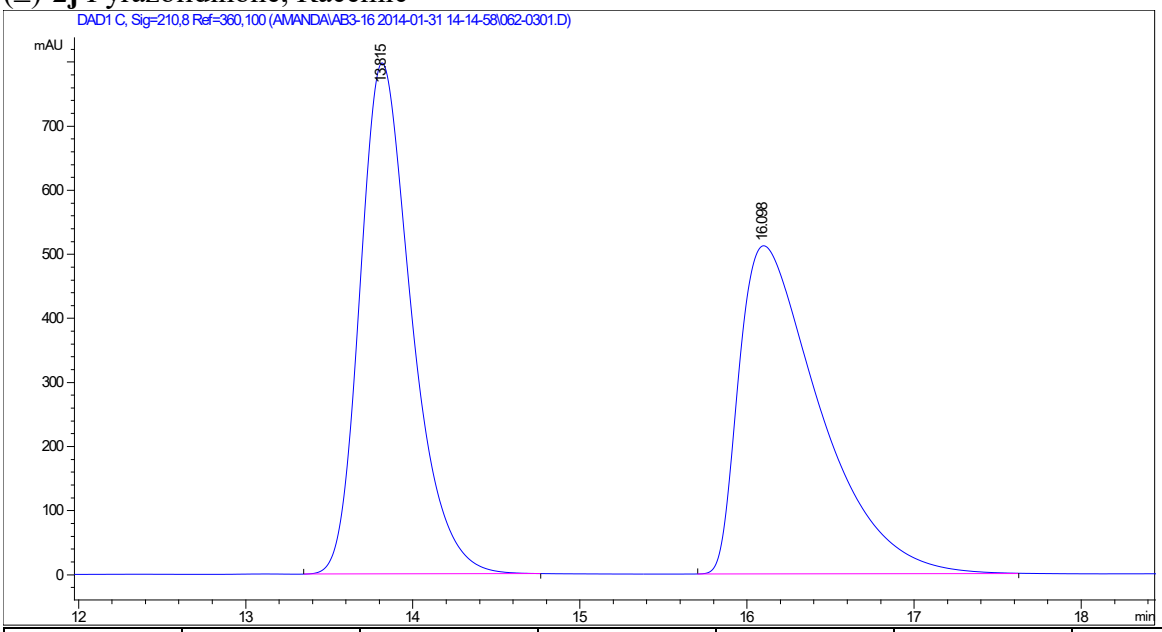

#	Time	Area	Height	Width	Area%	Symmetry
1	13.815	17118.8	797.5	0.3284	49.863	0.71
2	16.098	17212.8	512	0.5082	50.137	0.408

2j Pyrazolidinone

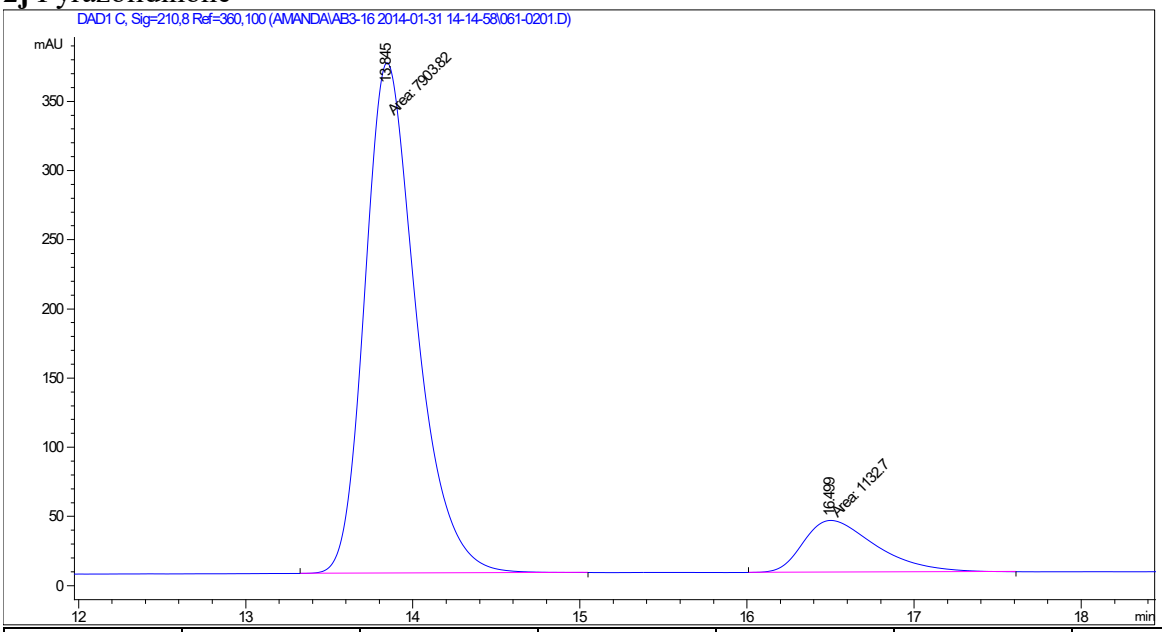

#	Time	Area	Height	Width	Area%	Symmetry
1	13.845	7903.8	369	0.357	87.465	0.736
2	16.499	1132.7	37.5	0.5037	12.535	0.588

(±)-**1k** Azomethine Imine, Racemic

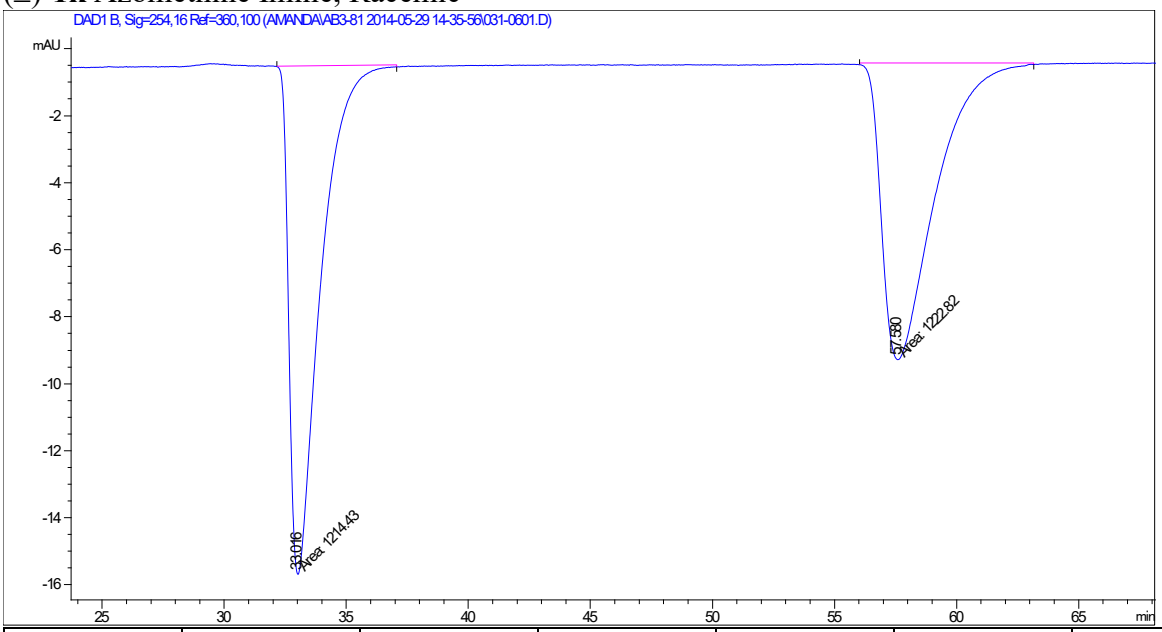

#	Time	Area	Height	Width	Area%	Symmetry
1	33.016	1214.4	15.2	1.3351	49.828	0
2	57.58	1222.8	8.8	2.3042	50.172	0

1k Azomethine Imine, Recovered

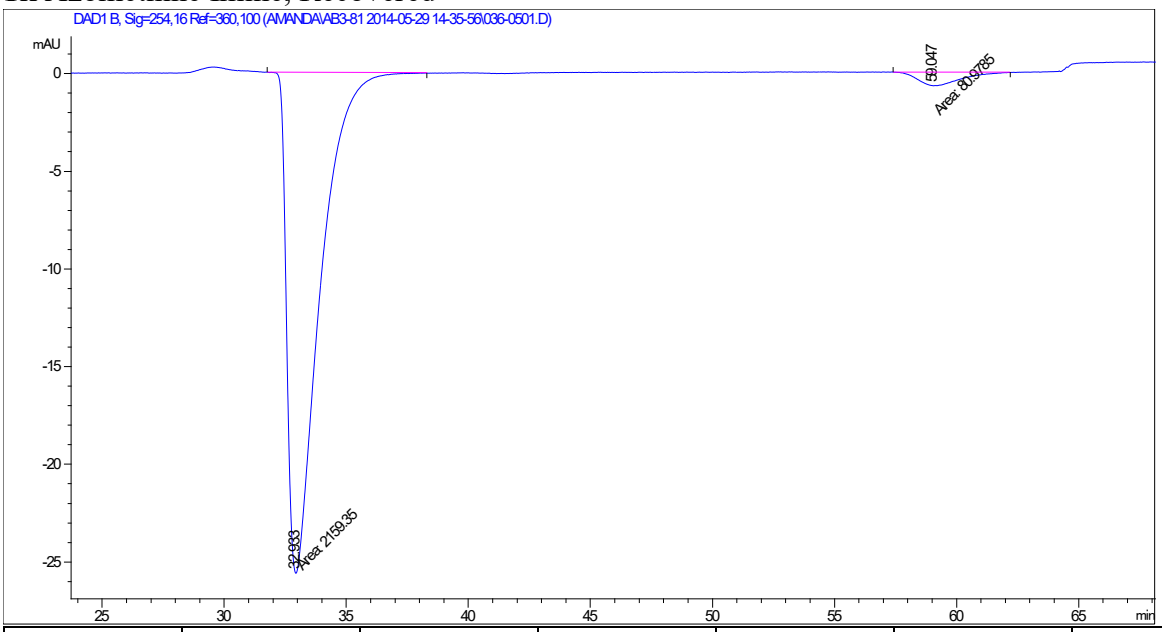

#	Time	Area	Height	Width	Area%	Symmetry
1	32.933	2159.4	25.6	1.4034	96.385	0
2	59.047	81	6.9E-1	1.9432	3.615	0

(±)-**2k** Pyrazolidinone, Racemic

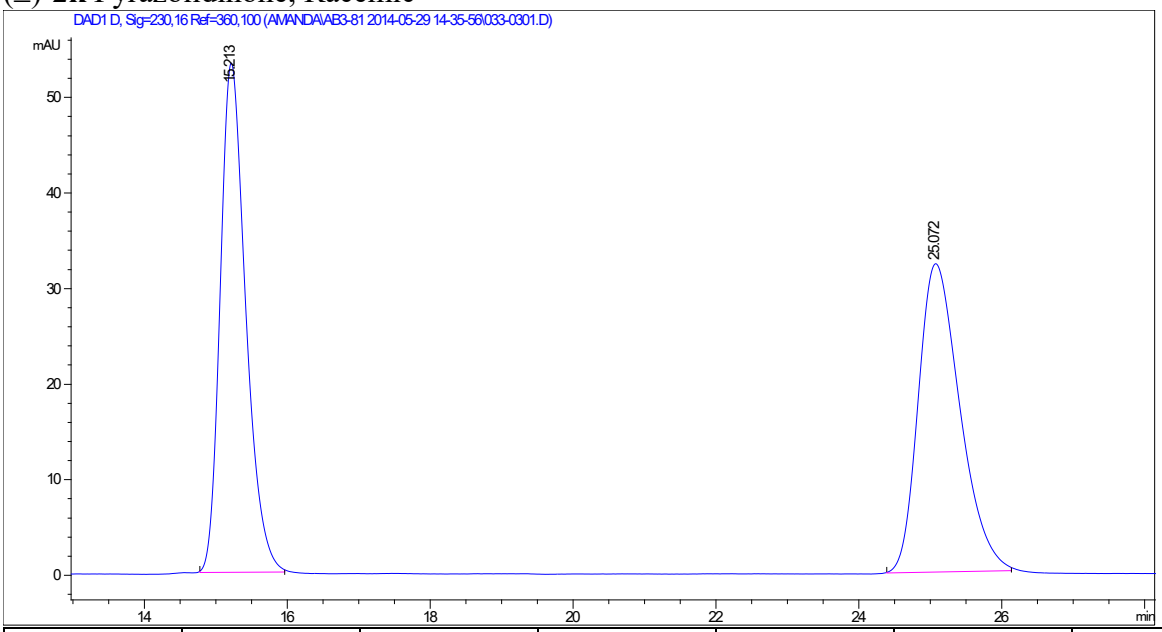

#	Time	Area	Height	Width	Area%	Symmetry
1	15.213	1319.7	53.3	0.3788	50.259	0.715
2	25.072	1306.1	32.3	0.622	49.741	0.681

2k Pyrazolidinone

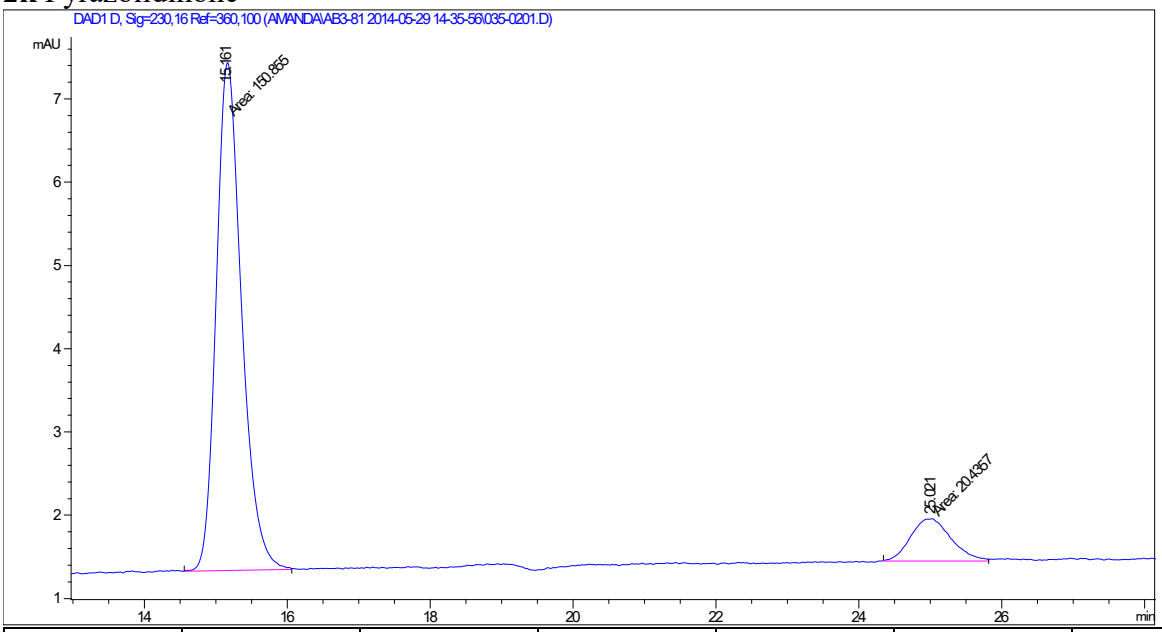

#	Time	Area	Height	Width	Area%	Symmetry
1	15.161	150.9	6.1	0.412	88.070	0.77
2	25.021	20.4	5.1E-1	0.664	11.930	0.7

(±)-**1k** Azomethine Imine, Racemic

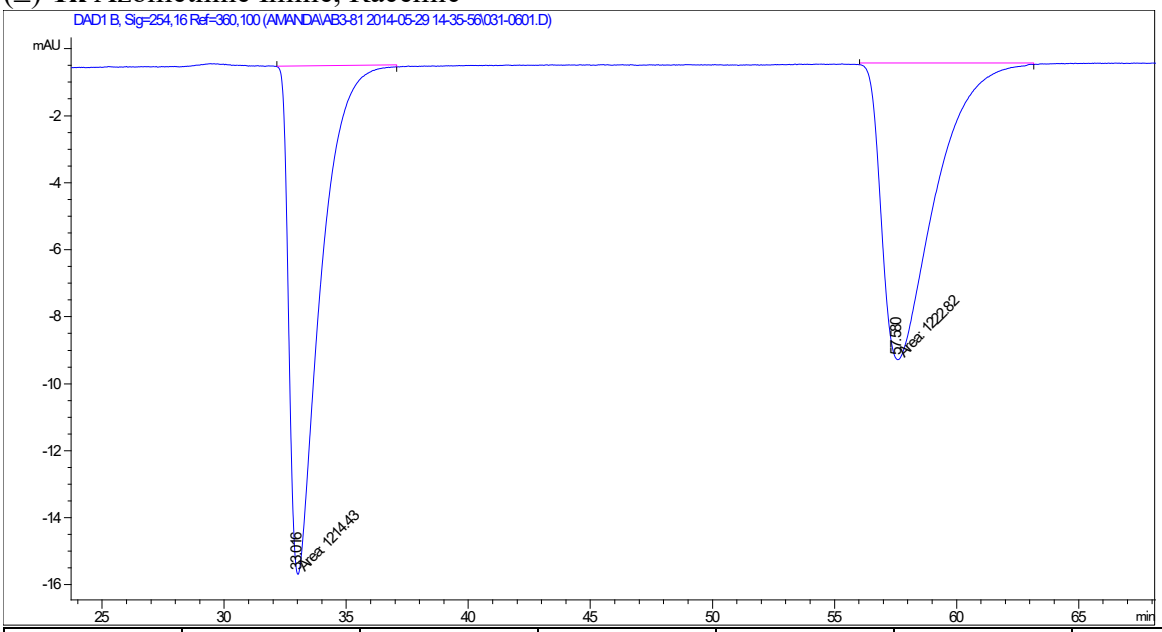

#	Time	Area	Height	Width	Area%	Symmetry
1	33.016	1214.4	15.2	1.3351	49.828	0
2	57.58	1222.8	8.8	2.3042	50.172	0

1k Azomethine Imine, Recovered

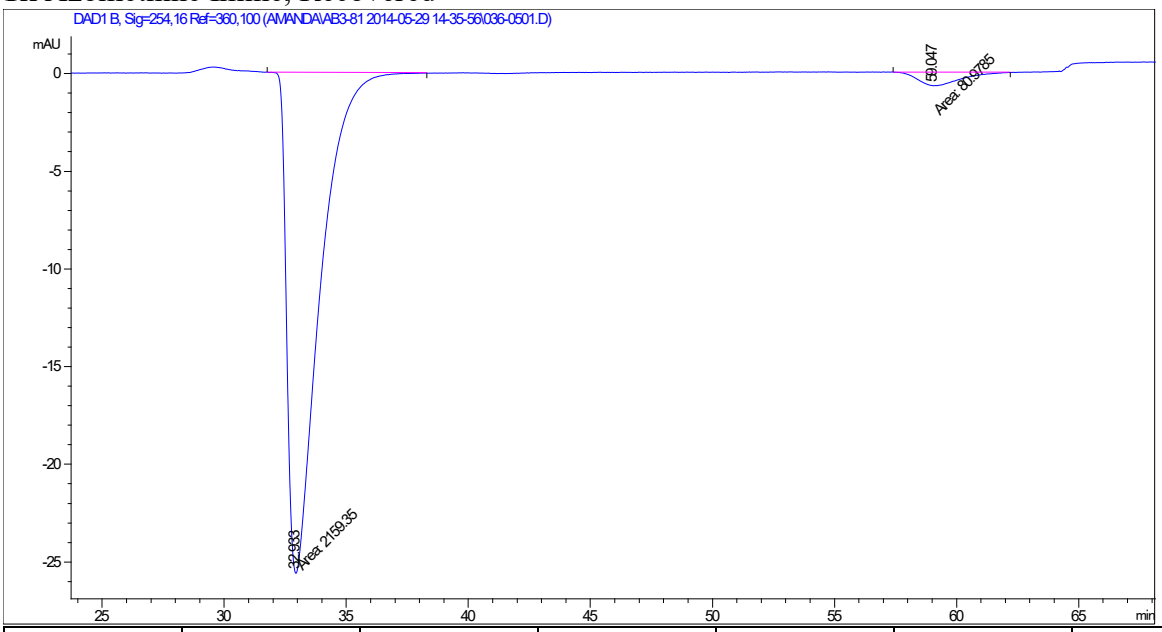

#	Time	Area	Height	Width	Area%	Symmetry
1	32.933	2159.4	25.6	1.4034	96.385	0
2	59.047	81	6.9E-1	1.9432	3.615	0

(±)-**2k** Pyrazolidinone, Racemic

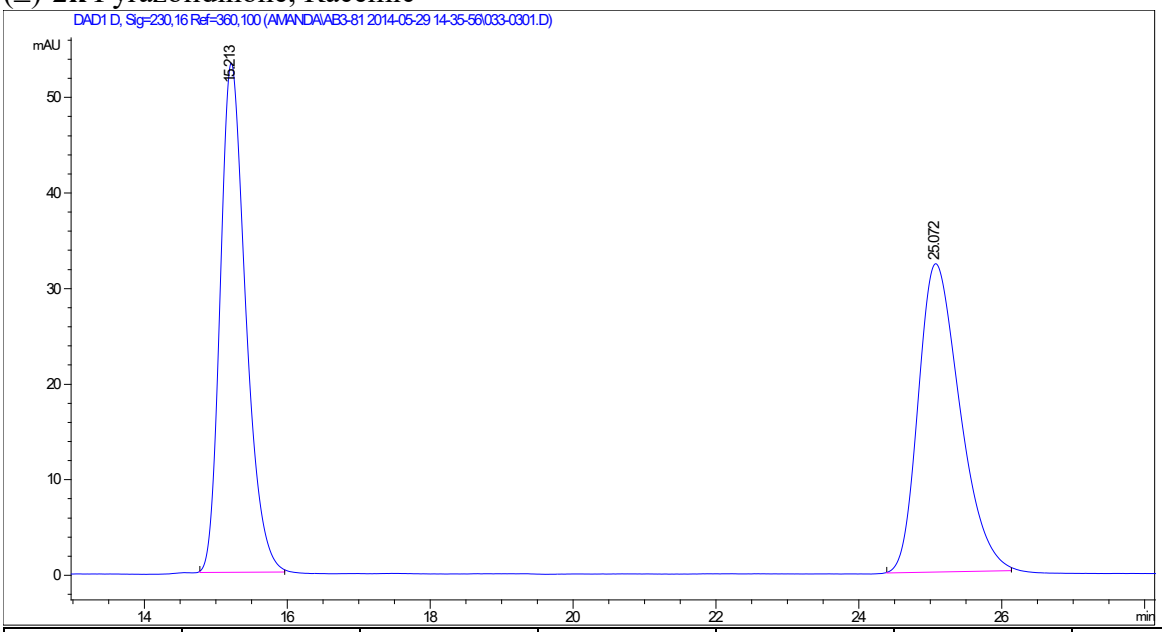

#	Time	Area	Height	Width	Area%	Symmetry
1	15.213	1319.7	53.3	0.3788	50.259	0.715
2	25.072	1306.1	32.3	0.622	49.741	0.681

2k Pyrazolidinone

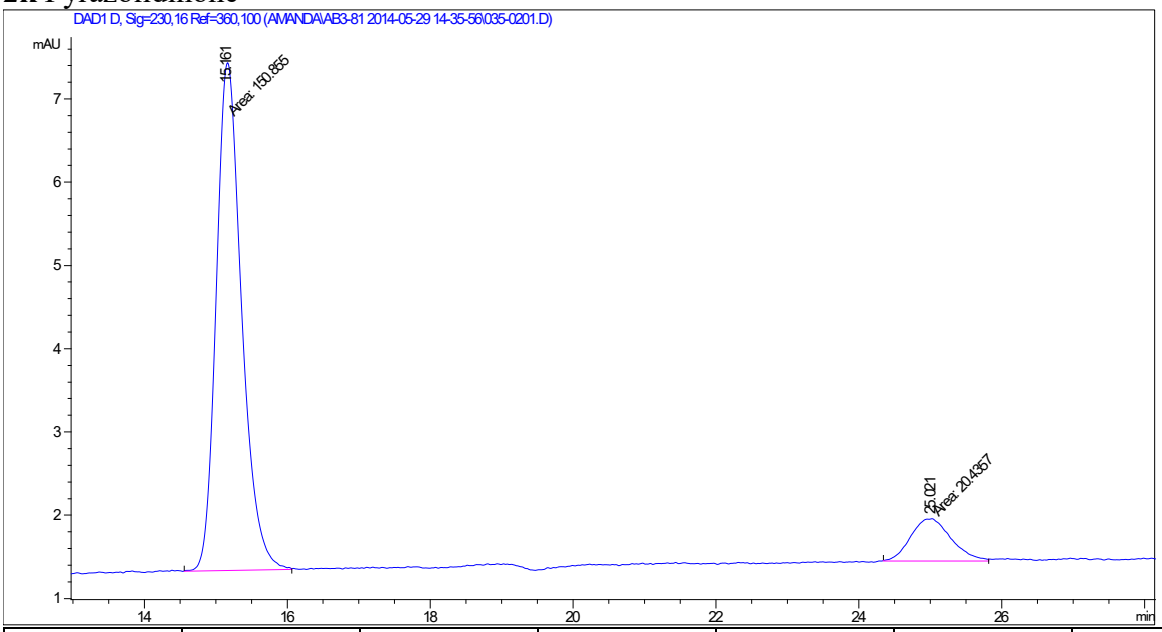

#	Time	Area	Height	Width	Area%	Symmetry
1	15.161	150.9	6.1	0.412	88.070	0.77
2	25.021	20.4	5.1E-1	0.664	11.930	0.7

(±)-**1l** Azomethine Imine, Racemic

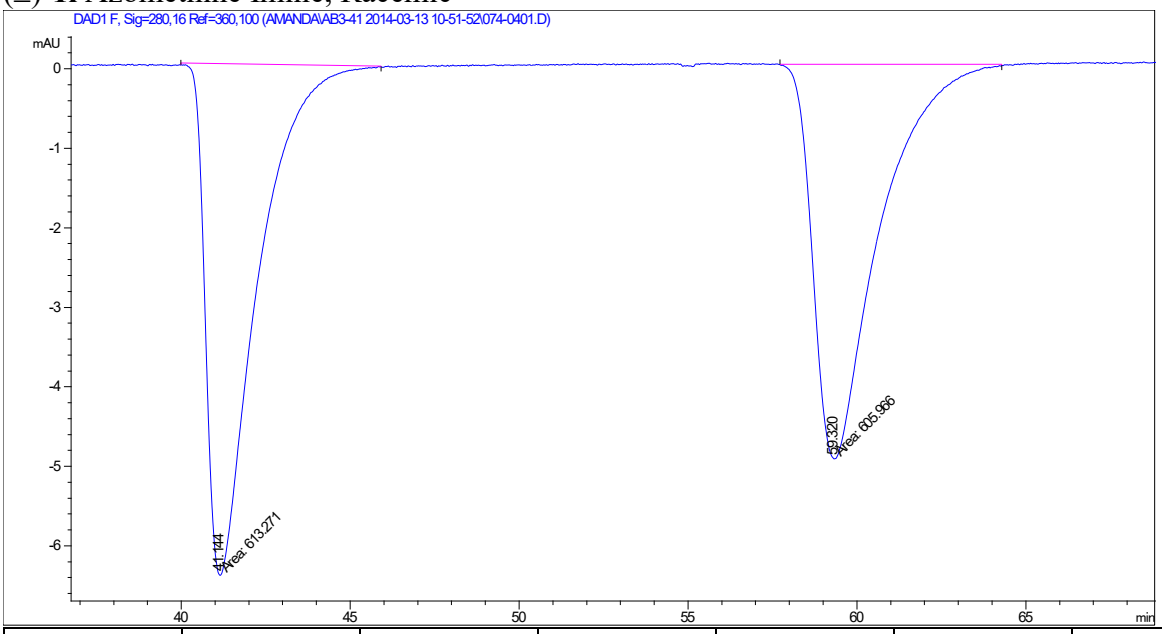

#	Time	Area	Height	Width	Area%	Symmetry
1	41.144	613.3	6.4	1.5884	50.300	0
2	59.32	606	5	2.0371	49.700	0

1l Azomethine Imine, Recovered (entry 4)

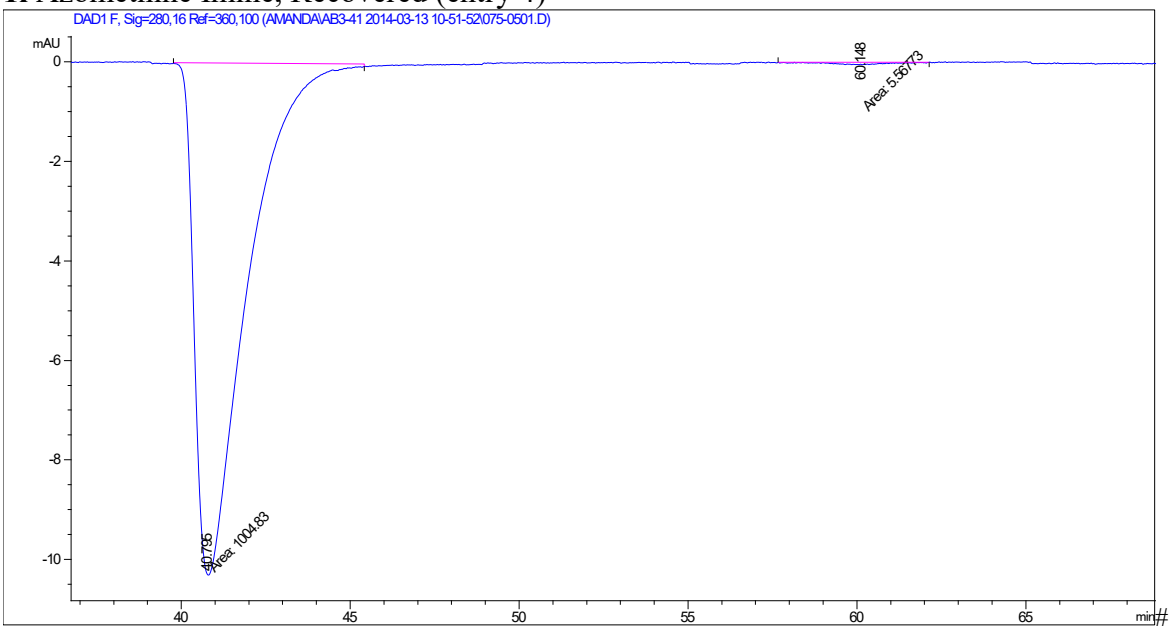

#	Time	Area	Height	Width	Area%	Symmetry
1	40.795	1004.8	10.3	1.6278	99.449	0
2	60.148	5.6	4.9E-2	1.9133	0.551	0

(±)-**2l** Pyrazolidinone, Racemic

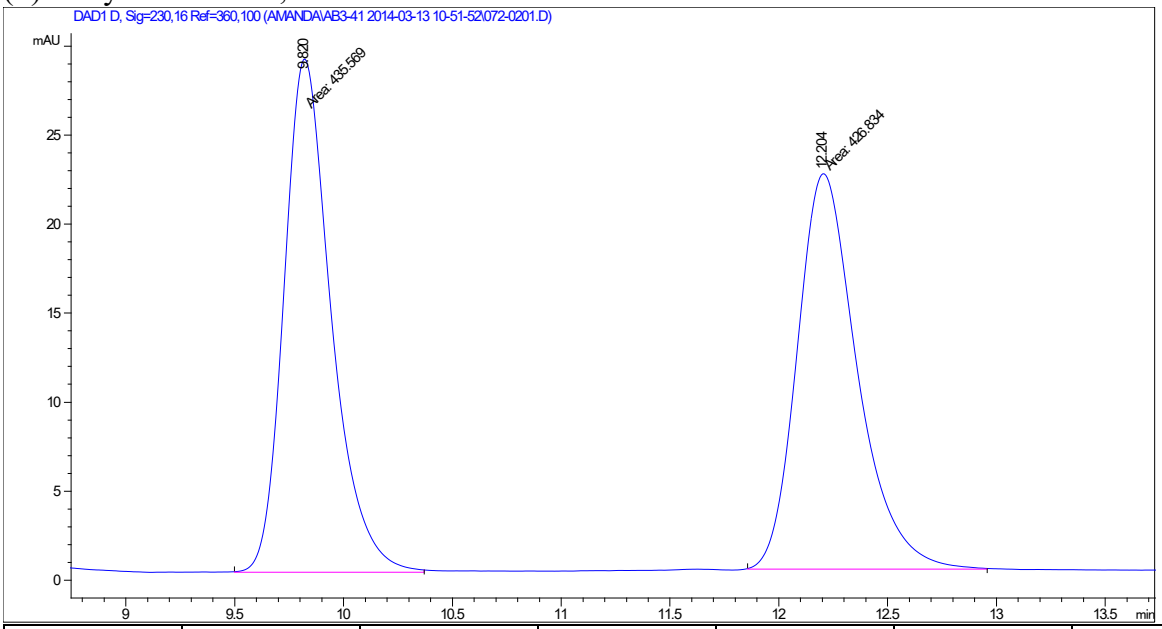

#	Time	Area	Height	Width	Area%	Symmetry
1	9.82	435.6	28.8	0.2517	50.506	0.743
2	12.204	426.8	22.2	0.3202	49.494	0.748

2l Pyrazolidinone (entry 4)

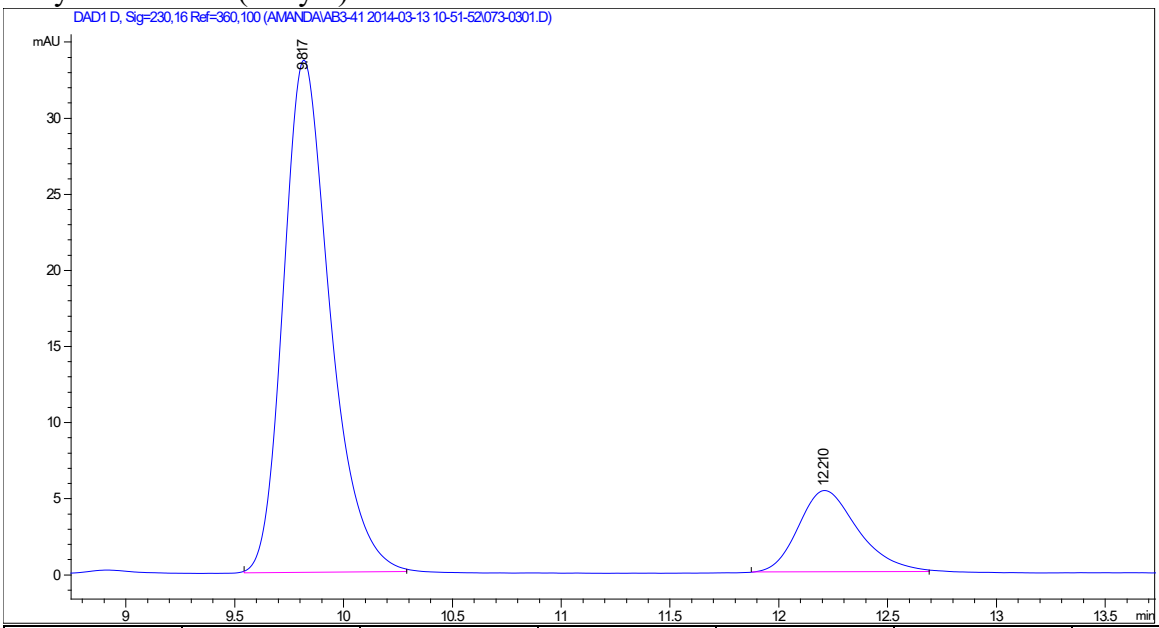

#	Time	Area	Height	Width	Area%	Symmetry
1	9.817	508.1	33.7	0.2511	82.756	0.743
2	12.21	105.9	5.4	0.3265	17.244	0.744

1l Azomethine Imine, Recovered (entry 5)

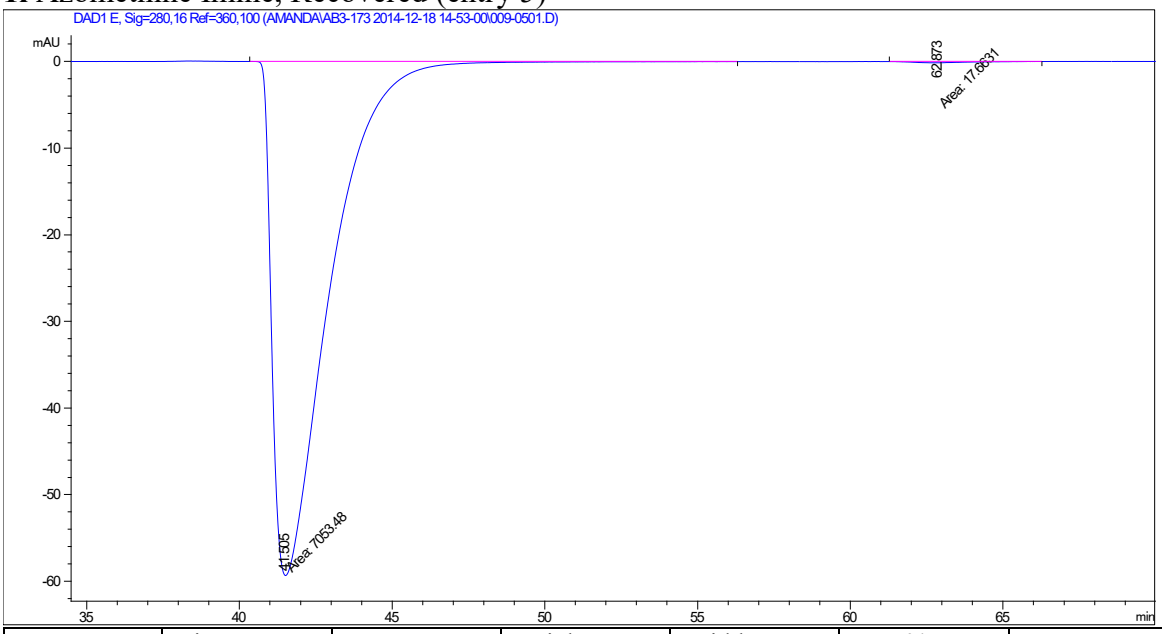

#	Time	Area	Height	Width	Area%	Symmetry
1	41.505	7053.5	59.3	1.9815	99.750	0
2	62.873	17.7	1.5E-1	2.0075	0.250	0

2l Pyrazolidinone, before recrystallization (entry 5)

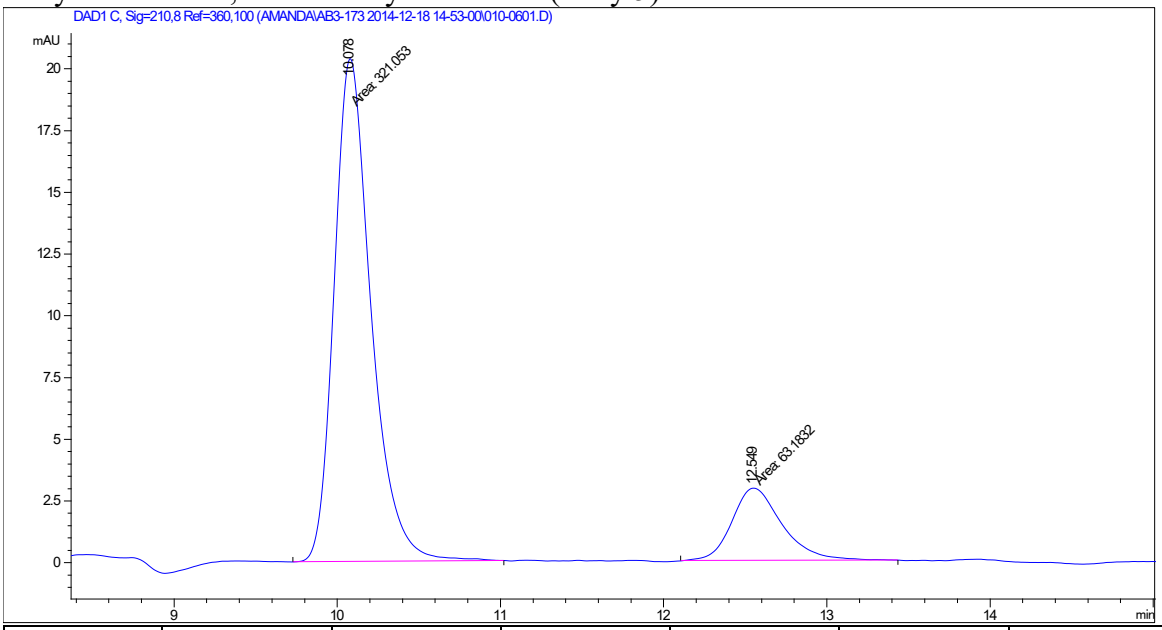

#	Time	Area	Height	Width	Area%	Symmetry
1	10.078	321.1	20.4	0.2626	83.556	0.728
2	12.549	63.2	2.9	0.3586	16.444	0.733

(±)-**2m** Pyrazolidinone - Racemic (3:1 Mixture of Diastereomers)

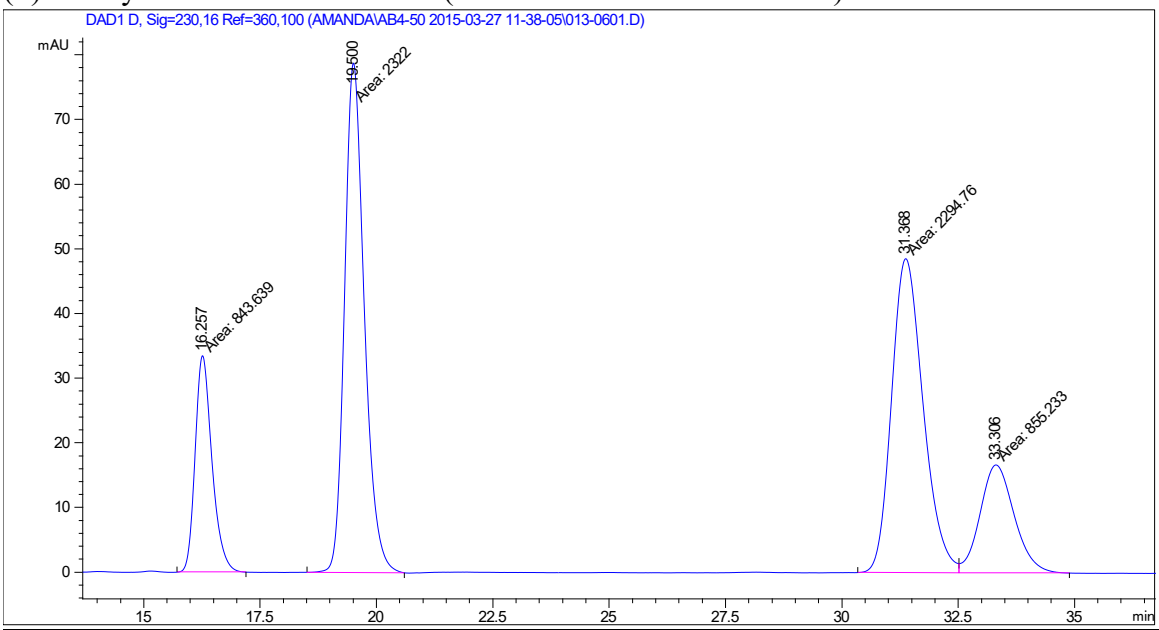

#	Time	Area	Height	Width	Area%	Symmetry
1	16.257	1150.8	45.6	0.4206	13.257	0.749
2	19.5	3218.7	108.6	0.4939	37.079	0.784
3	31.367	3168.4	67	0.7887	36.500	0.782
4	33.305	1142.8	22.5	0.8452	13.165	0.842

1m Azomethine Imine, reduced to pyrazolidinone

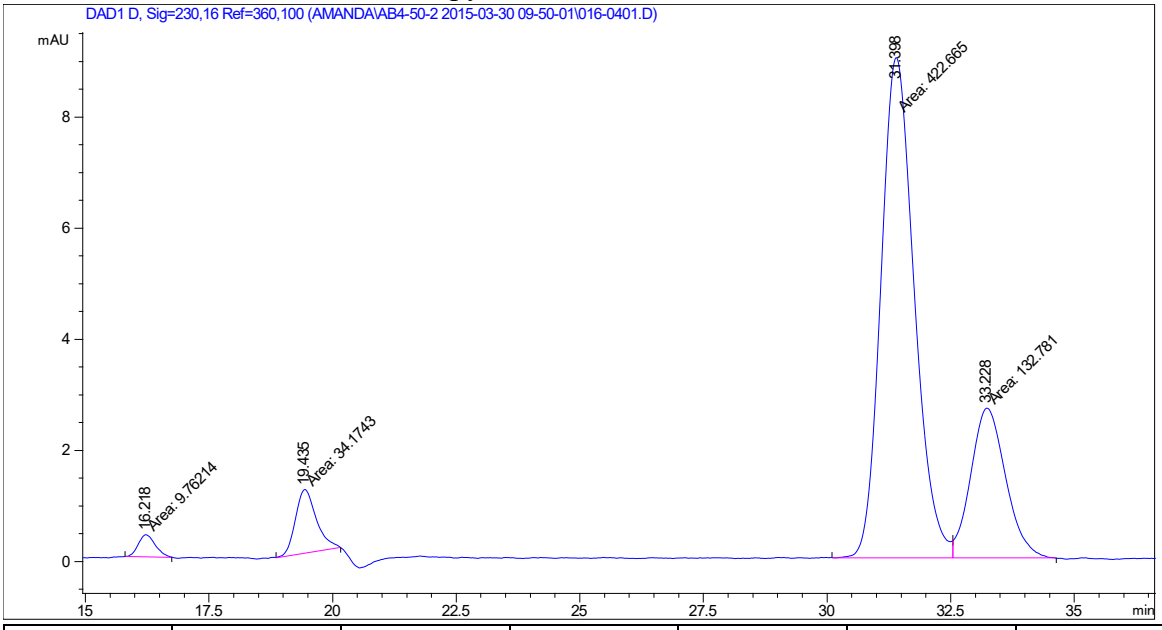

#	Time	Area	Height	Width	Area%	Symmetry
1	16.218	9.8	4E-1	0.4039	1.629	0.77
2	19.435	34.2	1.2	0.4946	5.702	0.793
3	31.398	422.7	9	1.0128	70.517	5.23E-3
4	33.228	132.8	2.7	0.82	22.153	0.83

2m Pyrazolidinone (2:1 Mixture of Diastereomers)

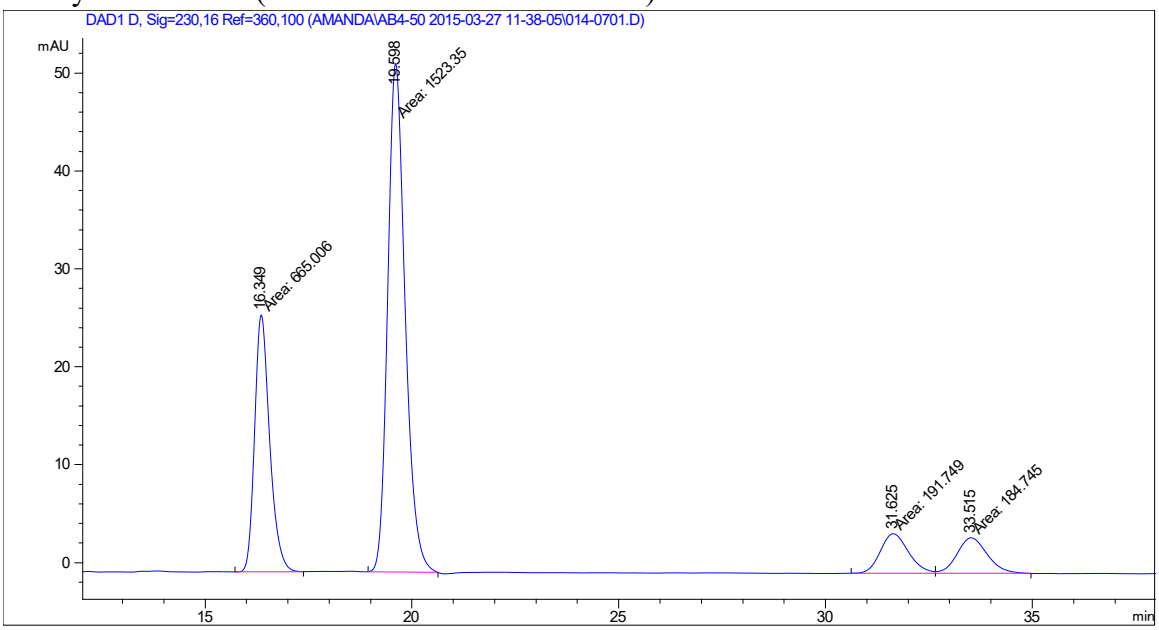

#	Time	Area	Height	Width	Area%	Symmetry
1	16.349	665	26.3	0.4221	25.928	0.753
2	19.598	1523.3	51.9	0.4889	59.393	0.789
3	31.625	191.7	4	0.7916	7.476	0.8
4	33.515	184.7	3.6	0.8481	7.203	0.851

1n Azomethine Imine, reduced to pyrazolidinone

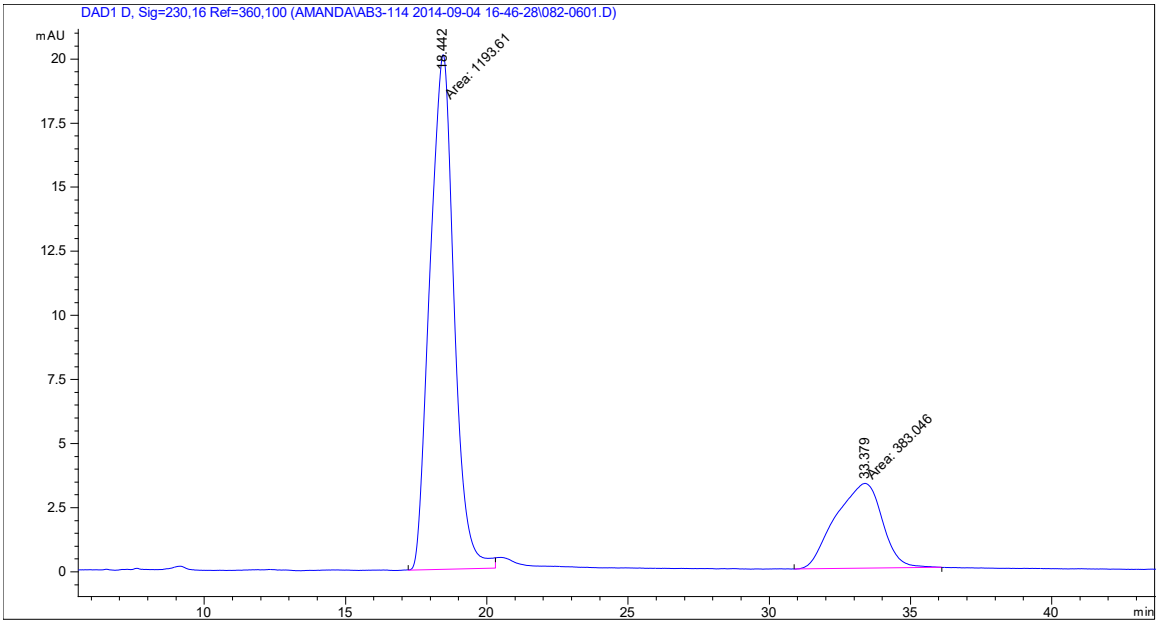

#	Time	Area	Height	Width	Area%	Symmetry
1	18.442	1193.6	20.1	0.9911	75.705	0
2	33.379	383	3.3	1.9258	24.295	1.6

2n Pyrazolidinone

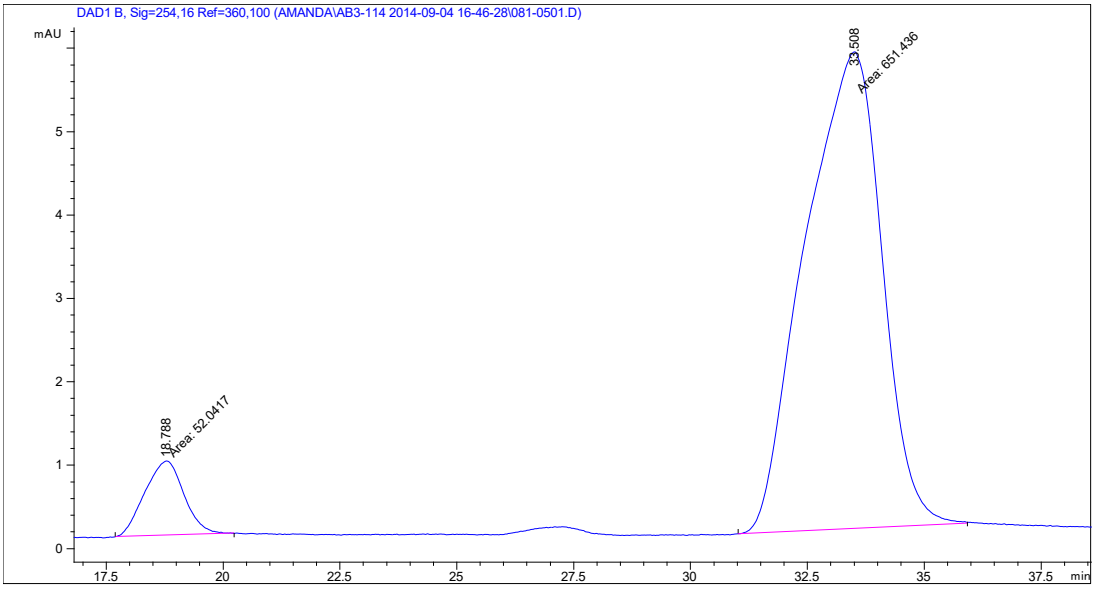

#	Time	Area	Height	Width	Area%	Symmetry
1	18.788	52	8.9E-1	0.9729	7.398	1.19
2	33.508	651.4	5.7	2.0884	92.602	1.48E-3

(±)-2n Racemic Pyrazolidinone

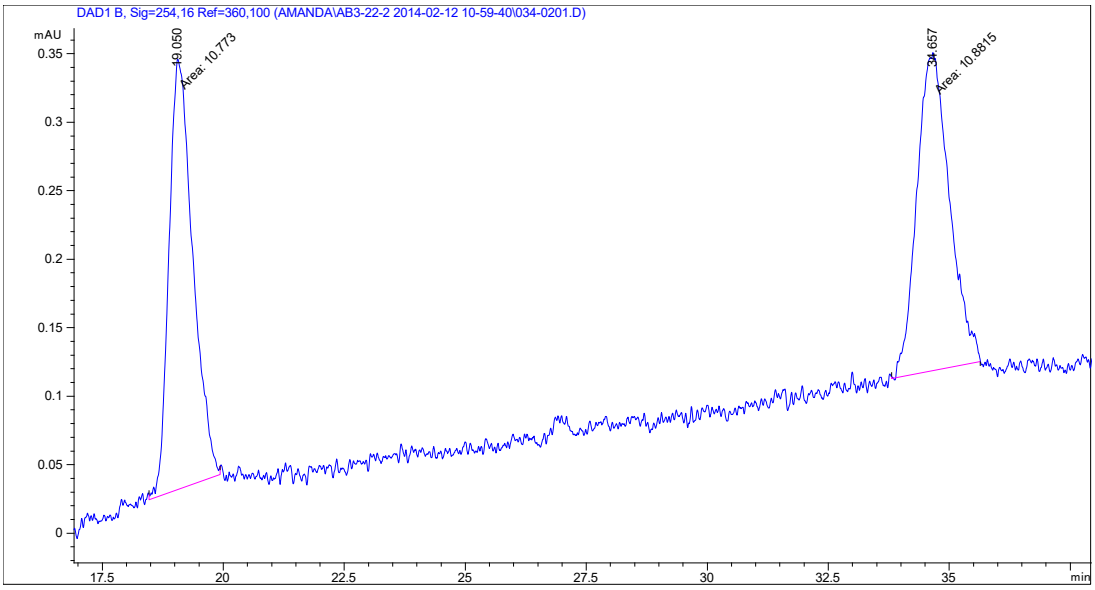

#	Time	Area	Height	Width	Area%	Symmetry
1	19.05	10.8	3.1E-1	0.571	49.749	2.29E-3
2	34.657	10.9	2.3E-1	0.7999	50.251	1.76E-2

(±)-**3l** β-Amino Amide, Racemic

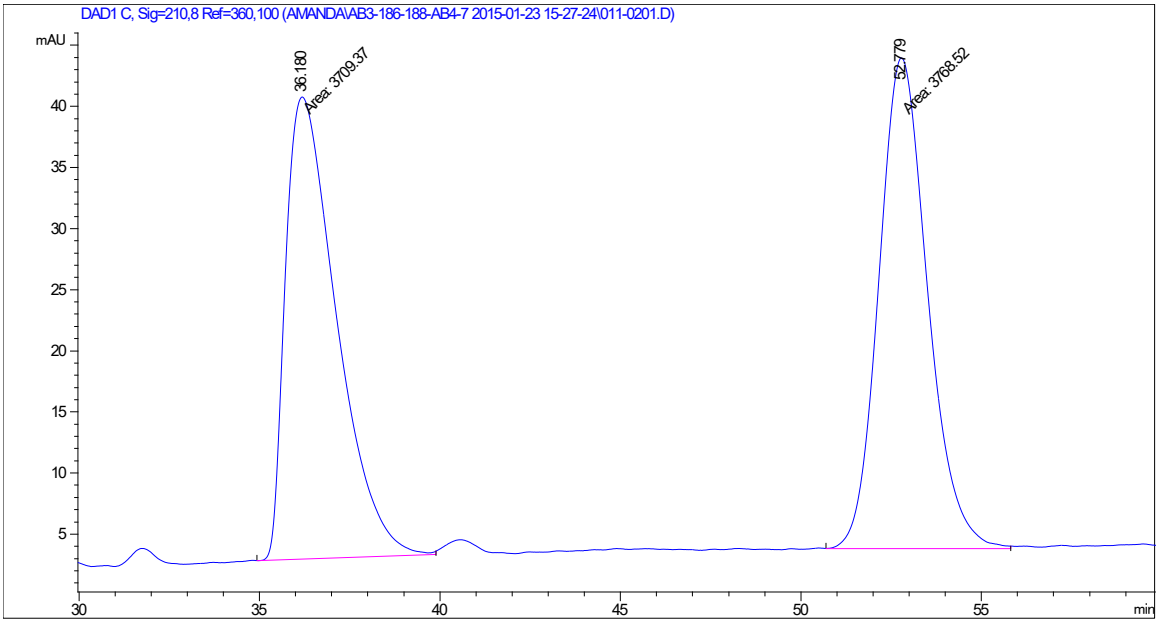

#	Time	Area	Height	Width	Area%	Symmetry
1	36.18	3709.4	37.8	1.6346	49.605	0
2	52.779	3768.5	40.2	1.5642	50.395	0.828

(+)-**3l** β-Amino Amide, from Azomethine Imine **1l**

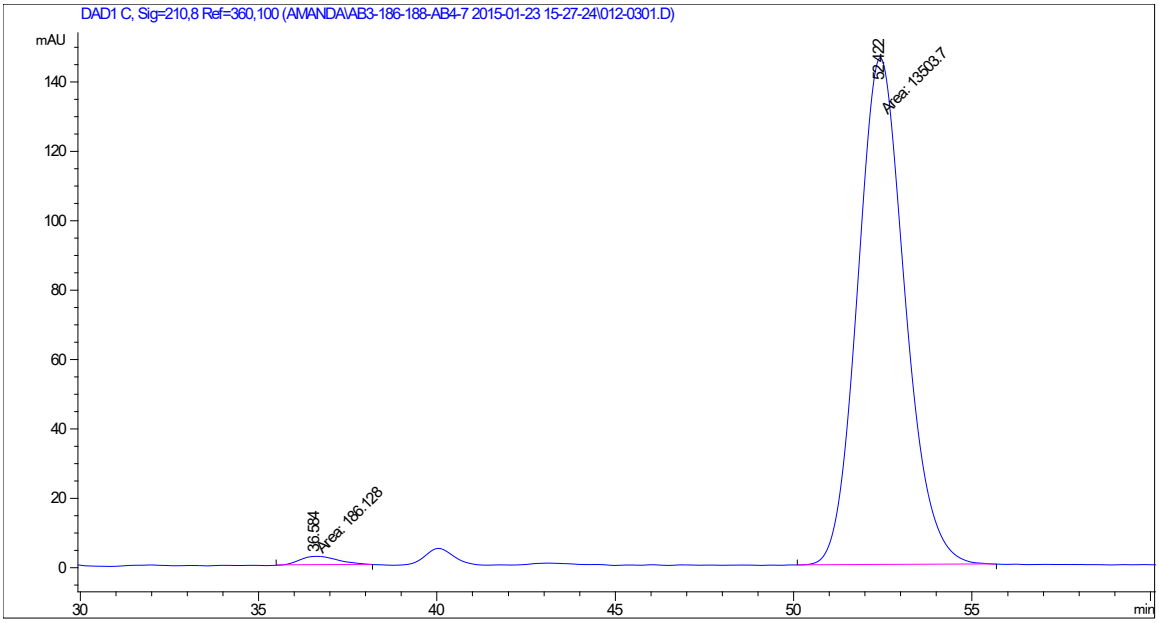

#	Time	Area	Height	Width	Area%	Symmetry
1	36.584	186.1	2.5	1.2561	1.360	0.658
2	52.422	13503.7	146.1	1.5401	98.640	2.1E-6

(–)-**3l** β-Amino Amide, from Pyrazolidinone **2l**

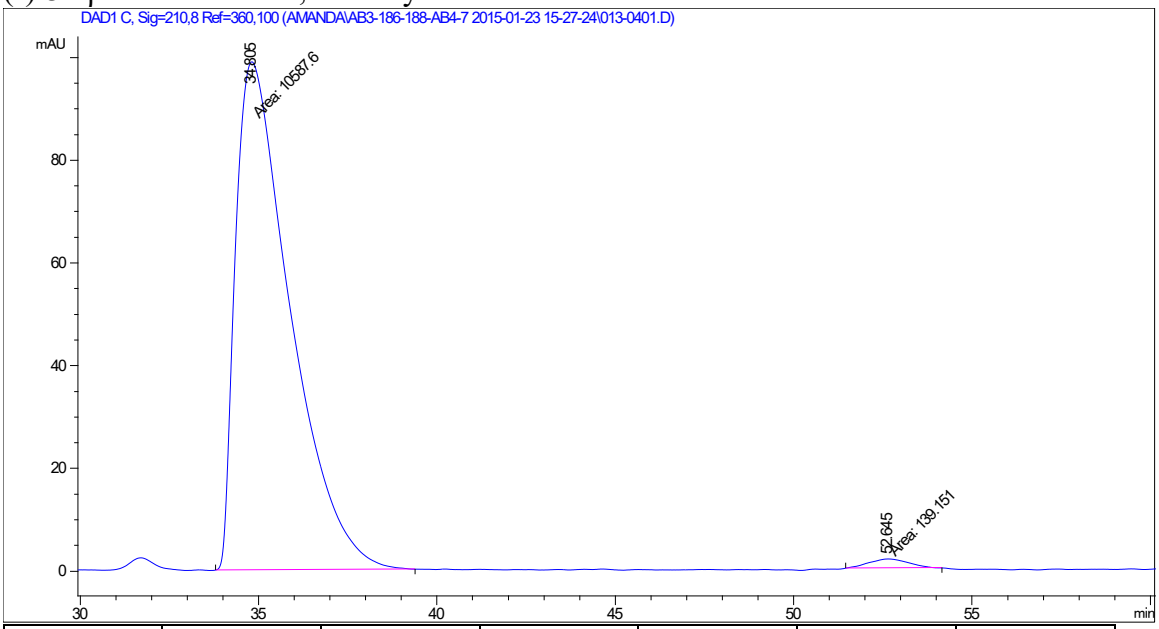

#	Time	Area	Height	Width	Area%	Symmetry
1	34.805	10587.6	98.9	1.7834	98.703	0.408
2	52.645	139.2	1.8	1.2973	1.297	0.942